

# **222nd ECS Meeting Abstracts 2012**

**Meeting Abstracts 2012-02**

**Honolulu, Hawaii, USA  
7-12 October 2012**

**Volume 1 of 7**

**ISBN: 978-1-62276-625-3  
ISSN: 1091-8213**

**Printed from e-media with permission by:**

Curran Associates, Inc.  
57 Morehouse Lane  
Red Hook, NY 12571



**Some format issues inherent in the e-media version may also appear in this print version.**

Copyright© (2012) by The Electrochemical Society  
All rights reserved.

Printed by Curran Associates, Inc. (2013)

For permission requests, please contact The Electrochemical Society  
at the address below.

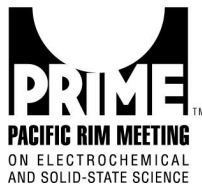
The Electrochemical Society  
65 South Main Street  
Pennington, New Jersey 08534-2839

Phone: (609) 737-1902  
Fax: (609) 737-2743

[www.electrochem.org](http://www.electrochem.org)

**Additional copies of this publication are available from:**

Curran Associates, Inc.  
57 Morehouse Lane  
Red Hook, NY 12571 USA  
Phone: 845-758-0400  
Fax: 845-758-2634  
Email: [curran@proceedings.com](mailto:curran@proceedings.com)  
Web: [www.proceedings.com](http://www.proceedings.com)



## Meeting Abstracts — MA 2012-02

### PRiME 2012 — Joint International Meeting Honolulu, Hawaii — October 7-12, 2012

### 222nd Meeting of ECS — The Electrochemical Society 2012 Fall Meeting of The Electrochemical Society of Japan (ECSJ)

and with the technical co-sponsorship of the Japan Society of Applied Physics, the Korean Electrochemical Society, the Electrochemistry Division of the Royal Australian Chemical Institute, and the Chinese Society of Electrochemistry

Published by The Electrochemical Society © 2012

## Table of Contents

To use this table of contents, scroll down the page or use the bookmarks in the left-hand frame to move to a new location. Click on the number or the title of the abstract you wish to view.

### A0 - Special Lectures

*All ECS Divisions*

- 1 (Edward Goodrich Acheson Award Presentation) Plasmas for Thin Film Processing and Surface Modification  
*D. Hess*
- 2a (Charles W. Tobias Young Investigator Award Presentation) Past, Current, and Future Research in Polymer Electrolyte Fuel Cells  
*B. S. Pivovar*
- 2b (Charles W. Tobias Young Investigator Award Presentation) Mechanochemistry at Oxide Thin Film Interfaces  
*B. Yildiz*

### A1 - General Student Poster Session

*All ECS Divisions, ECSJ*

- 3 Analysis of Carbon Electrode and Organic Electrolyte of Electric Double Layer Capacitors after Aging Test  
*H. Yoshitama, Y. Tanaka, and D. Tashima*
- 4 Atomic Layer Deposition of Vanadium Oxide on Carbon Nanotubes for High-Power Supercapacitor Electrodes  
*S. Boukhalfa, K. Evanoff, and G. Yushin*
- 5 Growth and Fabrication of GaN Light Emitting Diode on Patterned-Sapphire Substrate  
*B. Tran, K. Lin, C. Wang, C. Chen, C. Huang, C. Chung, and E. Yi Chang*
- 6 Conversion Reaction of Methane with Carbon Dioxide in Glow Discharge at Atmospheric Pressure  
*D. Nguyen, J. Park, and W. Lee*

- 7 Surface Treatment for Sterilization of Microorganism with Plasma Plume in Atmospheric Pressure  
*J. Park, H. Kwon, and W. Lee*
- 8 Indium Tin Oxide-Coated Glass Modified with Reduced Graphene Oxide Sheets and Gold Nanoparticles for Dopamine Sensing  
*J. Yang and S. Gunasekaran*
- 9 Electrochemical Detection of Phenol and Phenol Derivatives Modified with TiO<sub>2</sub>, ZrO<sub>2</sub>, and Mixed Metal Oxides (TiO<sub>2</sub> + ZrO<sub>2</sub>)  
*M. K. Hughes, V. Nguyen, and S. K. Lunsford*
- 10 Characteristics of Low-Temperature( $\leq 200$  °C) PECVD Silicon Nitride for Gate Dielectric of TFTs by Using N<sub>2</sub> Highly Diluted SiH<sub>4</sub>  
*K. Keum, K. No, J. Park, S. Kang, T. Song, and W. Hong*
- 11 Charge Induced Closing of *Dionaea Muscipula* Ellis Trap  
*C. Mitchell, N. E. Williams, and A. G. Volkov*
- 12 Lithium-Sulfur Batteries with Glyme-Li Salt Equimolar Complexes  
*A. Yamazaki, M. Tsuchiya, K. Yamauchi, K. Ueno, N. Tachikawa, K. Dokko, and M. Watanabe*
- 13 Effect of Hydrothermal Synthesis Condition on LiMnPO<sub>4</sub> Particle Size  
*S. Yanaka, K. Yoshida, K. Dokko, and M. Watanabe*
- 14 Design of Catalyst Layer of Non-Humidified Intermediate Temperature Fuel Cells  
*Y. Honda, R. Tataro, S. Nakamura, T. Yasuda, K. Dokko, and M. Watanabe*
- 15 Color Changes during Voltammograms of Prussian Yellow on ITO Electrode  
*J. Agrisuelas, J. García-Jareño, C. Moreno-Guerrero, A. Roig, and F. Vicente*
- 16 Effective Hydrogen Generation and Resource Circulation from Photocatalytic Decomposition of H<sub>2</sub>S Aqueous Solution  
*H. Takahashi, T. Mabuchi, T. Hayashi, S. Yokoyama, and K. Tohji*
- 17 Control Method for the Amount of Cu Site on the ZnS Stratified Photocatalysts  
*Y. Kajino, H. Takahashi, and K. Tohji*
- 18 Synthesis of Cu Supported Stratified Photocatalysts and Its Application for the CO<sub>2</sub> Conversion into Alcohol  
*Y. Kajino, H. Takahashi, and K. Tohji*
- 19 Improvement of Efficiency of Photo-Excited Electrons Transfer from Thin Film Consisted by the Semiconductor Particles on Electrode Surface to Developing Electrons Pathway  
*T. Mabuchi, T. Hayashi, H. Takahashi, and K. Tohji*
- 20 Relation between the Condition of Pd and Te Metal Complexes in the Aqueous Solution and Reduction Mechanism of Pd<sub>20</sub>Te<sub>7</sub> Alloy  
*T. Mabuchi, S. Yokoyama, H. Takahashi, and K. Tohji*

- 21 Oxidation of Bulk Amorphous  $\text{Ni}_{57}\text{Ti}_{18}\text{Zr}_{20}\text{Si}_3\text{Sn}_2$  Coating  
*S. Kim, S. Bong, M. Kim, and D. Lee*
- 22 Sodium-Sulfur Batteries with Room-Temperature Ionic Liquid Electrolytes  
*R. Nozawa, R. Harimoto, M. Tsuchiya, K. Yoshida, N. Tachikawa, K. Dokko, and M. Watanabe*
- 23 Single-Crystal Field-Effect Transistors of 21DNTT Derivatives  
*A. Maeda, T. Arakawa, M. Tsutsui, K. Okamoto, and Y. Kunugi*
- 24 Conductivity of Ceria Based Composite Electrolytes for Intermediate-Temperature-Solid Oxide Fuel Cells  
*S. Baek, T. Lee, and J. Park*
- 25 Effect of Synthesis Method and  $\text{Fe}_2\text{P}$  Phase on the Electrochemical Properties of  $\text{LiFexMn}_{1-x}\text{PO}_4$ -C Electrode  
*J. P. Välikangas, S. Tuomaala, M. T. Andersson, S. Manner, P. A. Tanskanen, T. Kallio, M. Karppinen, and U. Lassi*
- 26 Co-Ionic Neodymium-Doped Ceria/Carbonate Composite Electrolytes  
*J. Kim, N. Kim, and J. Park*
- 27 Fabrication of High Performance  $\text{BaLaIn}_2\text{O}_{5.5}$  Electrolyte Single Chamber Solid Oxide Fuel Cell by Using Sublimation Materials as Pore Former in Electrode Preparation  
*X. Shen, K. Takasu, and T. Yao*
- 28 Morphology Control of Palladium Nanostructures by Potential Adjustment  
*X. Pham, M. Bui, C. Li, K. Han, and G. Seong*
- 29 Preparation of Organoboron Ion-Gels Using PVA and Their Ion Conductive Properties  
*H. Tsutakawa and N. Matsumi*
- 30 Structure and Electrochemistry of  $\text{NaNiO}_2$   
*R. I. Fielden and M. N. Obrovac*
- 31 Fabrication of Ruthenium Oxide Nanosheet Electrodes by Electrophoretic Deposition  
*S. Ikuta, N. Ishigaki, K. Fukuda, T. Sato, and W. Sugimoto*
- 32 Characterization Attributes of Metal Oxide Nanocomposites  
*M. Hockey, Q. Lin, and E. Calderas*
- 33 Improvement in ORR Performance of 1-1.5 nm Pt Nanoparticles by Modification with Ruthenium Oxide Nanosheets  
*D. Takimoto, M. Ohuchi, L. Koodlur, C. Chauvin, and W. Sugimoto*
- 34 Pt/TiO<sub>2</sub> Nanohybrid Structures on Single-Walled Carbon Nanotubes: Preparation and Electrocatalytic Characteristics  
*K. Han, C. Li, M. Bui, X. Pham, and G. Seong*

- 35 Direct Synthesis of Nanostructures in a Microfluidic Device for Electrochemical Analysis  
*C. Li, K. Han, M. Bui, X. Pham, and G. Seong*
- 36 Influence of Surface Structure and Ion Type on the Capacitance of Doped SWCNTs Electrode of Electrochemical Capacitors  
*A. Al-zubaidi, Y. Ishii, T. Matsushita, and S. Kawasaki*
- 37 Electrochemical Study on Oxygen Reduction in a Pt/Nafion/Humidified Air System  
*Y. Sugiyama, E. Tada, A. Nishikata, and T. Tsuru*
- 38 Solid Phase Growth of Nickel Silicides in Polycrystalline Si Film on SiO<sub>2</sub> with Cl Plasma Containing NiCl  
*K. Kanomata, K. Momiyama, S. Kubota, T. Suzuki, and F. Hirose*
- 39 Enhancement of Dye-Sensitized Photocurrents by Gold Nanoparticles: Effects of Particle Size and Density  
*T. Kawakami, Y. Takahashi, and T. Tatsuma*
- 40 The Synthesizing Process and Electrochemical Characteristics of Si Active Material Particles Covered with Silicon Oxide as Anode Electrodes in a Lithium-Ion Battery  
*N. Shimoi and Y. Tanaka*
- 41 Electrochemical Property of the Composition by Ground Process of Active Materials Based on Silicon and Oxides  
*N. Shimoi, Q. Zhang, and Y. Tanaka*
- 42 Characterizations of Al<sub>2</sub>O<sub>3</sub>/Zn<sub>O</sub> Grown on Si Substrate by Plasma Enhanced Atomic Layer Deposition  
*C. Chung, B. Tran, K. Lin, C. Wang, C. Chen, C. Huang, S. Lee, and E. Yi Chang*
- 43 Preparation of π -Conjugated Polycarbazole - Boron Complexes as Fluoride Anion Sensor  
*Y. Hosono and N. Matsumi*
- 44 Preparation of Marimo Carbon Supported PtCo Bimetal Catalyst by the Nanocolloidal Solution Method  
*K. Sato, T. Onuma, K. Komatsu, M. Kobori, K. Iwasawa, M. Eguchi, Y. Kobayashi, M. Nishitani-Gamo, and T. Ando*
- 45 Changes in the Conduction Properties of LaBaGaO<sub>4</sub> Based Proton Conductor by Liquid-Phase Synthesis  
*N. Hamao, N. Kitamura, and Y. Idemoto*
- 46 The effect of the Relationship between Ionomer and Carbon in the PEFC Catalyst Layer  
*K. Baba, T. Onuma, K. Iwasawa, M. Eguchi, Y. Kobayashi, K. Komatsu, M. Kobori, M. Nishitani-Gamo, and T. Ando*
- 47 Effects of Misaligned Electrode for Measurement in PEFC with Reference Electrode  
*K. Baba, S. Ueda, M. Eguchi, Y. Kobayashi, and Y. Tsutsumi*

- 48 Low-Temperature Synthesis and Study of Apatite-Type Lanthanum Silicates  
*N. Kitamura, K. Kaneko, and Y. Idemoto*
- 49 Anodic Oxidation of Alcohols on Ni-Sn Electrocatalysts Prepared by Electrodeposition  
*K. Maruyama, N. Yoshimoto, M. Egashira, and M. Morita*
- 50 A New 4.3 V Aqueous Hybrid Capacitor Based on Manganese Dioxide Positive and Lithium Negative Electrode  
*Y. Shinohara, S. Makino, W. Shimizu, and W. Sugimoto*
- 51 Synthesis and Characteristics of Novel Boric Ester Type Ionic Liquids  
*Y. Toyota and N. Matsumi*
- 52 Aqueous Electrolytes for Ultracapacitor Devices Using Manganese Oxide as Electrode Material  
*A. Boisset, L. Athouël, J. Jacquemin, T. Brousse, and M. Anouti*
- 53 Molecular Weight Dependence of P-Type Semiconductive Polymer on High Efficiency Thin Film Organic Photovoltaic Cells  
*M. Sugimoto, H. Nakamura, K. Yamada, and H. Yamane*
- 54 Effect of Gold Nano-Seed Particles on Electrochemical Characteristics of Conducting Substrates  
*Y. Nakayama and M. Oyama*
- 55 Sn-CNT Fabric for Multifunctional Anodes in Li-ion Batteries  
*J. Benson, Y. Zhao, B. Hertzberg, M. Schauer, D. Lashmore, and G. Y. Yushin*
- 56 High Temperature Protonic Conduction and Crystall Structure of Eulytite-Type Phosphates  
*N. Kitamura, Y. Yamada, and Y. Idemoto*
- 57 Composition Dependence of Average and Local Structure and Thermodynamic Stability for  $x\text{Li}(\text{Li}_{1/3}\text{Mn}_{2/3})\text{O}_2-(1-x)\text{Li}(\text{Mn}_{1/3}\text{Ni}_{1/3}\text{Co}_{1/3})\text{O}_2$  as a Cathode Active Material for Li-Ion Batter  
*M. Inoue, N. Kitamura, and Y. Idemoto*
- 58 Non-Pacman Type Co-Porphyrin Bilayers for Oxygen Reduction Reaction  
*S. Satoh, K. Murakoshi, and K. Ikeda*
- 59 Stress Durability of Electrolyte Structure in Flexible Sheet Type Direct Methanol Fuel Cell (FS-DMFC)  
*Y. Sakurai and A. Kawai*
- 60 Fabrication of TiO<sub>2</sub> Layers for Dye Sensitized Solar Cells using Electrostatic Inkjet Printing Method  
*A. Ishii, S. Umezawa, and Y. Kunugi*
- 61 Construction of the Copper (I) Oxide/C<sub>60</sub> Hybrid Photovoltaic Devices  
*T. Saitoh, T. Ohata, F. B. Mohamad, J. Sasano, and M. Izaki*

- 62 Electrochemical Oxidation of Ammonia by Multi-Walled Carbon Nanotubes-Supported Pt-Core/Ir-Shell and Pt-Core/Pd-Shell Nanoparticles  
*S. Morita, S. Azuma, H. Shiroishi, M. Yonekawa, and K. Nagai*
- 63 A Study of Photochemical Proton Reduction and Oxidation of Water Using  $\text{Pb}_2\text{Ru}_2\text{O}_{7-\delta}$  Synthesized by Neutralization Method  
*S. Hanyu, H. Shiroishia, T. Hatai, Y. Ayato, and J. Kuwano*
- 64 Performance of Proton Conductive Intermediate Temperature Fuel Cell Using  $\text{ZrO}_2\text{-}1.6\text{P}_2\text{O}_5$  Electrolyte with 1% CO-H<sub>2</sub> and Methanol as Fuels  
*Y. Houshi, M. Yonekawa, H. Shiroishi, M. Kunimatsu, K. Matsushima, Y. Ayato, M. Saito, and J. Kuwano*
- 65 Electrochemical Studies of Epoxy Based Lignosulfonate Doped Double Stranded Polyaniline-Montmorillonite Nanocomposite Coatings on AA 2024 Alloy  
*G. Gupta, A. Khanna, and N. Birbilis*
- 66 Carbon Nanotube Synthesis over Nickel-Ferrite Loaded Oxidized Diamond Catalyst  
*G. Tsujino, K. Nakagawa, T. Ando, and H. Oda*
- 67 Cycle Performance of Nano Inclusion containing  $\text{LiMn}_2\text{O}_4$  Cathode Material  
*J. Harada, H. Tsubouchi, Y. Kawai, and T. Yao*
- 68 Peeling Force of Polymer Micro Pattern by Direct Peeling by using AFM Tip (DPAT)  
*T. Aiba and K. Akira*
- 69 Monitoring and Modeling for Response Time of Biopotential in Plant Cells  
*Y. Noguchi and A. Kawai*
- 70 A New High Energy Density Aqueous Hybrid Capacitor Based on Lithium Negative and Ruthenium Oxide Positive Electrode  
*T. Ban, S. Makino, W. Shimizu, and W. Sugimoto*
- 71 Construction and Photovoltaic Performance of Hybrid ZnO:CuPc Bulk Heterojunction Solar Cells  
*H. Ryo, K. Murata, J. Sasano, S. Watase, and M. Izaki*
- 72 VOC Sensing Characteristics of  $\text{SmFeO}_3$  Film Covered with SiC Powder  
*J. Iseda, M. Mori, and Y. Sadaoka*
- 73 Adsorption States and Reactivity of Nitric Oxide on Pd and Pd-based Binary Electrodes as Studied by Infrared Absorption Spectroscopy  
*K. Yamaki, A. Okubo, S. Notani, K. Nakata, M. Osawa, and K. Shimazu*
- 74 Platinum Nanodot and Nanohoneycomb Structures: Construction Using a Cyclodextrin Monolayer as a Molecular Template  
*R. Saito, Y. Domi, T. Kawaguchi, and K. Shimazu*
- 75 Design of Polymer Inclusion Complex of Curcumin Using Amylose  
*Y. Morita and N. Matsumi*

- 76 Electrochemical Quartz Crystal Microbalance Studies on Pt and Pd Ultra-Thin Films on Gold  
*A. Kurokawa, M. Shibata, T. Wada, and T. Kondo*
- 77 Change of Crystal and Electronic Structure of Layered Cathode Material 0.4Li<sub>2</sub>MnO<sub>3</sub>-0.6LiMn<sub>1/3</sub>Ni<sub>1/3</sub>Co<sub>1/3</sub>O<sub>2</sub> by Charge and Discharge Process  
*R. Yamamoto, N. Kitamura, and Y. Idemoto*
- 78 Structural Studies on Self-Assembled Monolayer of Porphyrin Derivative on Au(111)  
*N. Aoki, B. Zhang, R. Kuwana, T. Wada, and T. Kondo*
- 79 Electrocatalytic Activity for Oxygen Reduction of Pseudomorphic Pt Monolayer Electrochemically Prepared on a Au(111) Surface  
*T. Wada, M. Shibata, M. Kawabuchi, I. Yagi, and K. Toshihiro*
- 80 Performance of Nb and Mo Alloyed Ferritic Stainless Steel for SOFC Interconnect by Using Button Cell Configuration  
*D. Yun, H. Seo, J. Jun, and K. Kim*
- 81 Development of 4 V-class Aqueous Hybrid Electrochemical Capacitor with Porous Positive Electrode and Li Negative Electrode  
*S. Makino, Y. Shinohara, T. Ban, W. Shimizu, and W. Sugimoto*
- 82 Electrochemical Properties of Reduced Graphite Oxide Nanosheet Electrodes Prepared by Layer-by-Layer Assembly  
*T. Mitsui, K. Higurashi, J. Sato, K. Fukuda, and W. Sugimoto*
- 83 A Comparison of Steam and CO<sub>2</sub> Activation of Boron Doped Diamond Electrodes  
*J. Zhang and W. Sugimoto*
- 84 Electrochemical Properties of Nanocarbon Produced from Organic Waste and its Application in Electric Double-Layer Capacitor  
*D. Mishima, Y. Hamasuna, D. Tashima, S. Kumagai, and J. Madden*
- 85 Amorphous Titanium Oxide Prepared from Peroxo-Polytitanic Acid and Its Electrochemical Properties  
*K. Kobayashi and I. Tsuyumoto*
- 86 One Dimensional Silver/Silver Halide Nanocomposites: Synthesis and Electrocatalytic Activity  
*S. Kim, J. Shim, C. Lee, and Y. Lee*
- 87 Terminal Redox Moiety effects on the Long-Range Electron Conduction of  $\pi$ -Conjugated Bis(Terpyridine) Metal Complex Oligomer Wires on Electrode  
*S. Katagiri, R. Sakamoto, and H. Nishihara*
- 88 Pyrimidine Ring Motion Correlated with Electron Transfer at the Copper(II)/(I) Coordination Site Immobilized on Au Electrode Surface  
*Y. Takara, M. Nishikawa, S. Kume, and H. Nishihara*

- 89 Preparation of Glass-Coated CdSe/CdZnS Quantum Dots and Their Photostability  
*T. Gunshi, C. Li, K. Ogasawara, M. Ando, and N. Murase*
- 90 Development and Application of an Electrochemical Dual Microsensor for Simultaneous O<sub>2</sub>/pH Measurements  
*Y. Ha, S. Park, J. Shim, and Y. Lee*
- 91 Electrochemical Impedance Analysis for Corrosion on Current Collecting Electrodes in Dye-sensitised Solar Cells  
*K. Inoue, I. Shitanda, Y. Hoshi, and M. Itagaki*
- 92 Preparation of Polymer Nanoparticles Composite Coating Films for Investigation of the Co-Deposition Theory  
*K. Iwasaki, I. Shitanda, Y. Hoshi, and M. Itagaki*
- 93 Glancing Angle Sputter-Deposition of Titanium Dioxide Films with Rotating Substrate Holder for Photocatalytic Application  
*Y. Yasuda, N. Kitahara, and Y. Hoshi*
- 94 The Synthesis of SnO<sub>2</sub>-TiO<sub>2</sub> Core-Shell Nanotubes Using PAN Fiber and Its Cycling Performance for the Anode of Lithium-Ion Batteries  
*J. Jeun, W. Kim, D. Kim, K. Park, B. Lee, K. Kang, W. Yu, and S. Hong*
- 95 An InGaP Sub-Wavelength Structure (SWS) Realized by Colloidal Lithography for Solar Cell Applications  
*D. Kim, S. Eo, and J. Jang*
- 96 LbL Film with PtNPs as a Sensor of the Dopamine Encapsulated in Liposomes  
*V. dos Santos, M. dos Santos, B. Sandrino, C. de Jesus, J. R. Garcia, S. T. Fujiwara, C. A. Pessôa, and K. Wonhrath*
- 97 Effect of Lateral Size of Reduced Graphite Oxide Nanosheet on the Electrochemical Capacitance  
*Z. Lei, T. Sakai, and W. Sugimoto*
- 98 A Model for the Influence of Steel Corrosion Products on Nuclear Fuel Corrosion under Permanent Disposal Conditions  
*L. Wu, Y. Beauregard, Z. Qin, S. Rohani, and D. W. Shoesmith*
- 99 CO<sub>2</sub> Reduction at Glassy Carbon Electrode in the Presence of Pyridine  
*J. Agullo, M. Morin, and D. Bélanger*
- 100 Utilizing a Rotating Ring Disk Electrode (RRDE) to Simultaneously Measure Contaminant Species Adsorption effects on Two Different Catalyst Surfaces  
*J. M. Christ, K. Neyerlin, H. Wang, R. M. Richards, and H. N. Dinh*
- 101 Carbon Deposition and Gasification over Ni-YSZ Cermet during Methane Reforming Reaction  
*K. SONG and J. Jung*

- 102 Influence of Relaxation Time on the Lifetime of Commercial Lithium-Ion Cells  
*M. J. Reichert, H. Bremes, S. Passerini, and M. Winter*
- 103 3-D Electrochemical Impedance Spectroscopy Calculated by Wavelet Transformation -Influence of Scale and Time Parameters on Impedance Spectra-  
*K. Isobe, Y. Hoshi, I. Shitanda, and M. Itagaki*
- 104 In Situ ATR-IR Analysis of Graphite/Electrolyte Interface in Li-Ion Batteries  
*Y. Akita, H. Munakata, and K. Kanamura*
- 105 Sol-Gel Synthesis of  $\text{Li}_2\text{MnO}_3$ - $\text{LiMO}_2$  Cathode with Good Cycle Performance  
*K. Ando, Y. Jin, T. Nishioka, H. Munakata, and K. Kanamura*
- 106 Electrochemical Evaluation of  $\text{Li}_4\text{Ti}_5\text{O}_{12}$  Single Particle at Various Temperatures  
*K. Annaka, H. Munakata, and K. Kanamura*
- 107 3DOM Polyimide Separator for Rechargeable Lithium Batteries with High Rate Performance  
*K. Miyahara, Y. Jin, H. Munakata, and K. Kanamura*
- 108 A Semi-Empirical Model of Ammonia Electrolysis in Comparison to Water Electrolysis  
*A. Estejab, D. A. Daramola, and G. G. Botte*
- 109 RRDE Studies on Oxygen Reduction Reaction of Pd Single Crystal Electrodes  
*M. Kawabuchi, T. Wada, M. Shibata, and T. Kondo*
- 110 Synthesis and Characterization of Core-Shell Structured  $\text{Ni-Ce}_{0.8}\text{Gd}_{0.2}\text{O}_{1.9}$  SOFC Anodes by Ultrasonic Spray Pyrolysis  
*C. Lim and K. Lee*
- 111 Broadband Terahertz Antireflection Structure Fabricated By Utilizing Stamping Method  
*D. Kim, D. Kim, and J. Jang*
- 112 Fabrication of GDC Electrolyte Thin Films on NiO-GDC Anode Support by Electrophoretic Deposition for Solid Oxide Fuel Cells  
*S. Yu and K. Lee*
- 113 Characterization of  $\text{Ca}_{1-x}\text{La}_x\text{TiO}_3$  Anode Materials for Hydrocarbon-Fueled Solid Oxide Fuel Cells  
*J. Koo and K. Lee*
- 114 Design of Ion-gel Electrolytes Using Non-flammable Organoboron Bio-based Polymer as Polymer Support  
*Y. yoshinaga and N. Matsumi*
- 115 Enhanced Photocurrent Generation of Porphyrins - Ag Nanoparticles Composite Layers on an Electrode  
*S. Yagyu, M. Ishizaki, K. Kanaizuka, M. Kurihara, and M. Sakamoto*

- 116 Electrochemical behavior of Spin-coated Hybrid Thin Film of Prussian-blue Analog Nanoparticles  
*S. Soma, M. Ishizaki, K. Ono, K. Kanaizuka, M. Sakamoto, and M. Kurihara*
- 117 Electrochemical Intercalation of Bis(Fluorosulfonyl)Amide Anion into Graphite  
*F. Yamane, K. Miyazaki, T. Fukutsuka, and T. Abe*
- 118 Preparation of Perovskite Type Oxide Thin-Films as Bi-Functional Air Electrodes by Pulsed Laser Deposition Method and Their Electrochemical Properties  
*Y. Miyahara, K. Miyazaki, T. Fukutsuka, and T. Abe*
- 119 MgBr<sub>2</sub>/Ether-Based Electrolyte Solutions for Mg-Rechargeable Batteries  
*K. Asaka, K. Miyazaki, T. Fukutuka, T. Abe, K. Nihio, and Y. Uchimoto*
- 120 Electrochemical Properties of LiCoPO<sub>4</sub> in the Anion Receptor-Based Organic Electrolyte Solution  
*T. Nakagawa, K. Miyazaki, T. Fukutsuka, and T. Abe*
- 121 Anisotropic Anion Conduction of MgAl-CO<sub>3</sub><sup>2-</sup> Layered Double Hydroxides with Different Cation Ratios  
*Y. Asada, K. Miyazaki, T. Fukutsuka, and T. Abe*
- 122 Redox Reaction of Metal Cations on the Surface of LiCoO<sub>2</sub> Thin-Film Electrodes  
*J. Inamoto, K. Miyazaki, T. Fukutsuka, and T. Abe*
- 123 Electrochemical Behavior of Magnesium Metal in Alkaline Aqueous Solutions  
*Y. Taniguchi, K. Miyazaki, T. Fukutsuka, and T. Abe*
- 124 Frequency-Tunable Multicolor Light-Emitting Cell Based on AC-Driven Electrochemiluminescence  
*M. Nakakomi, T. Nobeshima, K. Nakamura, and N. Kobayashi*
- 125 Electrochemical Properties of Graphite Electrode in Ionic Liquid Containing Bis(Fluorosulfonyl) Amide Anion  
*K. Ono, K. Miyazaki, T. Fukutsuka, and T. Abe*
- 126 A Study on Electrochemical Performance of Hard Carbon / Na<sub>x</sub>[Fe<sub>1/2</sub>Mn<sub>1/2</sub>]O<sub>2</sub> Cells as Rechargeable Na-Ion Batteries  
*M. Kajiyama, N. Yabuuchi, J. Iwatake, and S. Komaba*
- 127 Fabrication of Electroless Cu/CNT Composite Plating Films Containing Different Sized CNTs  
*T. Osaki and S. Arai*
- 128 Electrochemical Properties of AZO Films Functionalized with Redox-Active Molecules  
*H. Kaneko, T. Tsuda, K. Kanaizuka, M. Kurihara, and M. Sakamoto*
- 129 Fabrication of Silicon Composite Films for Lithium-Ion Batteries by Electrodeposition  
*T. Kitamura and S. Arai*

- 130 Molecular Assembly of Porphyrin Derivative on a Substrate by Polymerization Reaction and Its Electrochemical Properties  
*A. Izumi, M. Ishizaki, K. Kanaizuka, M. Kurihara, and M. Sakamoto*
- 131 Surface Modification of Vapor Grown Carbon Nanofibers by Plasma Treatment  
*D. Shimizu, Y. Suzuki, M. Endo, and S. Arai*
- 132 Newly Developed Carbon-Nanocoating of Si Nanoparticles  
*Y. Sasaki, H. Tabuchi, H. Furukawa, K. Urita, and I. Moriguchi*
- 133 Study on the Formation of Self-Assembled Monolayers on Anodized Aluminum  
*H. Satoh, T. Fujii, E. Tsuji, and H. Habazaki*
- 134 Synthesis and Charge-Discharge Property of Si/Carbon Nanocomposites  
*H. Tabuchi, T. Enjoji, K. Kiyota, Y. Sasaki, K. Urita, H. Yamada, and I. Moriguchi*
- 135 Electrochemical Hybrid Capacitor Using Closest-Packed Ferrocene Terminated Monolayer on Carbon Electrode  
*Y. Sato, T. Kawaguchi, and K. Shimazu*
- 136 Electrochemical Properties of Zinc Oxide Electrodes Coated with Anion-Conducting Ionomer in Alkaline Solutions  
*Y. Lee, K. Miyazaki, T. Fukutsuka, and T. Abe*
- 137 Field Emission Properties of Nickel/Carbon Nanotube Composite Films Electrodeposited from a Citrate Bath  
*S. Tanabe and S. Arai*
- 138 Effects of Interferents on H<sub>2</sub>O<sub>2</sub> Quantification by Electrochemical Reduction on IrO<sub>2</sub> Electrodes  
*M. Ueda, T. Zhang, and M. Morimitsu*
- 139 Electrochemical Features of Nanoporous Electrodes and Their Applications  
*J. Han, J. Bae, and T. Chung*
- 140 All-Solid-State Chloride Ion-Selective Electrodes Using Polycation-Doped Manganese Oxides  
*T. Akatsuka, C. Suzuki, N. Yabuuchi, and S. Komaba*
- 141 Development of Titanium Wire-based Dye-sensitized Solar Cells and the Enhancement of the Performance by Surface Plasmon Resonance of Ag Nanoparticles  
*Y. Kawakami, M. Takeuchi, Y. Horiuchi, and M. Matsuoka*
- 142 Study on Deterioration of Electric Double-Layer Capacitor Cells  
*A. Haruta, Y. Suenaga, D. Tashima, T. Kawaji, and H. Toyama*
- 143 Electrochemical Construction of Pt Nanoparticles As a Catalyst for Oxygen Reduction Reaction  
*H. Aso, T. Wada, and T. Kondo*

- 144 Segmented Electrode Developed for Complementary Use of Small-Angle Neutron Scattering Measurement  
*S. Ueda, K. Baba, M. Eguchi, Y. Kobayashi, S. Koizumi, and Y. Tsutsumi*
- 145 Fundamental Research on Development of Novel Analysis Method for Hyaluronan Production with Use of Human Dermal Fibroblasts  
*M. Naruoka, Y. Nakamura, and Y. Iida*
- 146 Electrodeposition of Zn-Mg Alloy in Ethylene Glycol-ZnCl<sub>2</sub>-MgCl<sub>2</sub> Non-Aqueous Solution  
*H. Yamamoto, M. Morishita, T. Miwa, and K. Isono*
- 147 Relaxation Structure Analysis for Li Inserted  $\alpha$ -Fe<sub>2</sub>O<sub>3</sub>  
*K. Takasu, S. Park, and T. Yao*
- 148 GroEL Mutant Can Encapsulates Metal Nano Particles in Each Cavity  
*H. Yoda, O. Yamamoto, and A. Koike-Takeshita*
- 149 EIS and CV Characteristics of Pt Cathode Catalyst in PEMFC  
*S. Kanazawa, E. Tada, A. Nishikata, and T. Tsuru*
- 150 Pt-Loaded Carbon Nanofilament as an Electrocatalyst for Direct Methanol Fuel Cell  
*T. Toriyama, K. Nakagawa, T. Ando, and H. Oda*
- 151 Fabrication of Sexithiophene/Zr(IV) Hybrid Thin Films and Their Photofunctional Properties  
*A. kodaira, T. Harada, C. Pac, H. Moriyama, G. Sahara, T. Yui, and O. Ishitani*
- 152 Corrosion Behavior and Sacrificial Ability of Hot-Dip Al-Mg-Si Coated Steel  
*K. Chihara, Y. Kyo, E. Tada, A. Nishikata, and T. Tsuru*
- 153 Morphology of Self-ordered Nano Oxide Coatings for Oxygen and Chlorine Evolution  
*N. Ohnishi, M. Matsuda, T. Zhang, and M. Morimitsu*
- 154 Selection of B16 Melanoma Cells by Single Cell Manipulation and Analysis of Tyrosinase Gene Expression and Epigenetic Regulation  
*M. Hillary, K. Makoto, and Y. Iida*
- 155 Co-Electrolysis of CO<sub>2</sub> and H<sub>2</sub>O for Syngas Production  
*S. Nakamura, Y. Tanaka, K. Sato, K. Nozaki, A. Yamamoto, and T. Kato*
- 156 Detailed Observation and Analysis of the Reaction Distribution in LiFePO<sub>4</sub> Composite Electrodes  
*Y. Gogyo, H. Yamashige, M. Katayama, Y. Orikasa, Y. Inada, T. Ota, H. Arai, Y. Uchimoto, and Z. Ogumi*
- 157 Metal-Semiconductor-Metal Photodetectors on Flexible Substrats  
*T. Oh, W. Shin, J. Park, S. Chang, K. Choi, H. Ha, K. Lee, and B. Ju*

- 158 Effects of Gas Diffusion Electrodes with Hydrophilic Layer on Cold Start Behavior and Cell Performance of Polymer Membrane Fuel Cells  
*S. Hirakata, T. Mochizuki, M. Uchida, H. Uchida, and M. Watanabe*
- 159 Surface Oxidization Diamond for Dye-Sensitized Solar Cell  
*M. Mori, K. Nakagwa, T. Andou, and H. Oda*
- 160 Dynamics of Phase Transition in Li<sub>x</sub>FePO<sub>4</sub> Using Time-Resolved X-Ray Diffraction  
*T. Maeda, Y. Koyama, Y. Orikasa, H. Murayama, H. Tanida, H. Arai, E. Matsubara, Y. Uchimoto, and Z. Ogumi*
- 161 Hydrogen Starvation Tests on PEMFCs Using Segmented Cell Hardware  
*M. Geymayer, A. Stadlhofer, and V. Hacker*
- 162 Effect of SiO<sub>2</sub> on the Properties of Sulfonated Polyimide and Poly(Arylene Ether) Block Copolymer Membranes  
*M. Sakamoto, S. Nohara, K. Miyatake, M. Uchida, H. Uchida, and M. Watanabe*
- 163 Electrochemical Quartz Crystal Microbalance Analysis of Degradation Reactions of Pt/C Cathode Catalysts for Polymer Electrolyte Fuel Cells  
*J. Omura, H. Yano, M. Watanabe, and H. Uchida*
- 164 Relaxation Phase Analysis of Li-Co-O Cathode for Secondary Lithium-ion Battery  
*S. nagashima, S. Park, T. Iwai, and T. Yao*
- 165 Evaluation of Corrosion Resistance of Galvanized Steel under Wet-Dry Cyclic Condition  
*T. Okazaki, E. Tada, A. Nishikata, and T. Tsuru*
- 166 The Detection of Odor Vapors, H<sub>2</sub>S and CH<sub>3</sub>SH, by the Planar-Type Zirconia Sensor  
*Y. Nagai, M. Mori, and Y. Sadaoka*
- 167 Electrochemical Reaction Mechanism of FeS<sub>2</sub> Cathode Material in AlCl<sub>3</sub> - EMIC Ionic Liquids  
*T. Mori, Y. Orikasa, K. Nakanishi, T. Ohta, and Y. Uchimoto*
- 168 ZrO<sub>2</sub> coating Effect of LiCoO<sub>2</sub> Thin-film Model Electrode prepared by PLD  
*S. mori, D. Takamatsu, Y. Orikasa, Y. Koyama, H. Tanida, T. Uruga, H. Arai, Z. Ogumi, and Y. Uchimoto*
- 169 Novel Gel Polymer Electrolytes Based on Ethylene Oxide Containing Block-Copolymers for Lithium-Ion Batteries  
*M. Schaefer, P. Isken, M. Winter, S. Passerini, and A. Lex-Balducci*
- 170 Phase Transformation Mechanism during Cycling of Li<sub>2</sub>FeSiO<sub>4</sub>  
*T. N. Masese, H. Arai, Y. Orikasa, T. Ina, C. Tassel, K. Nakanishi, T. Ohta, K. Hiroshi, Y. Uchimoto, and Z. Ogumi*
- 171 in situ XAS Study on Effect of Platinum Catalyst on Cathodic Reaction in Nonaqueous Li - Air Batteries  
*J. Oyama, Y. Orikasa, and Y. Uchimoto*

- 172 Bioelectrocatalytic Conversion of Atmospheric CO<sub>2</sub> into Extracellular Organic compounds by Acidithiobacillus ferrooxidans  
*T. ISHII, T. Mogi, K. Hashimoto, and R. Nakamura*
- 173 Newly Found Electrochemical Oscillations during Reduction of Nitrate ions  
*S. Yamamoto, Y. Mukouyama, R. Nakazato, S. Nakanishi, and H. Okamoto*
- 174 Electrochemical and Surface Properties of Mg - Li Alloys  
*H. Endo, Y. Sugawara, I. Muto, and N. Hara*
- 175 Evaluation of Influence of Activated Carbon on Plant Growth  
*K. Oino and Y. Iida*
- 176 Relaxation Structure Analysis for Li Inserted LiNi<sub>1/3</sub>Mn<sub>1/3</sub>Co<sub>1/3</sub>O<sub>2</sub> Cathode Material  
*I. Seo, S. Park, and T. Yao*
- 177 Performance Evaluation of an Anode-supported Honeycomb Solid Oxide Fuel Cell  
*A. Fukushima, H. Nakajima, and T. Kitahara*
- 178 Synthesis of Co-Doped LaP<sub>3</sub>O<sub>9</sub> by Precipitation in Phosphoric Acid Solutions  
*Y. Adachi, N. Hatada, T. Onishi, A. Kuramitsu, and T. Uda*
- 179 Effect of Particle Size on the Relaxation of LiFePO<sub>4</sub> Cathode  
*S. Park, K. Kameyama, and T. Yao*
- 180 Electrical Performance Change by the Difference in the Production Methods of the Anode for SOFC  
*G. Watanabe, N. Takahashi, T. Takatsuka, and H. Fukunaga*
- 181 Structure and Electrochemical Properties of La<sub>2</sub>Li<sub>2x</sub>(CO)<sub>1-x</sub>O<sub>4</sub> with Layered Structure  
*M. Iqbal, G. Kobayashi, H. Masaaki, R. Kanno, and M. Yonemura*
- 182 Li-Air Battery Using Stabilized Acetonitrile Electrolyte  
*K. Furukawa, Y. Yamada, M. Yaegashi, F. Li, H. Zhou, and A. Yamada*
- 183 Control of Growth Density of Multi-walled Carbon Nanotubes Array and Its Gas Sensing Properties  
*M. Omae, T. Hashishin, K. Kojima, and J. Tamaki*
- 184 Electrochemical Stability of Au sub-ML on Pt/QC Electrode  
*T. KOBAYASHI, A. Kawamura, K. Katakura, and H. YAMADA*
- 185 A Novel Gas and Flow Sensor of Penetrating a Porous Polypyrrole Nanofiber Mat  
*T. jun and Y. Kim*
- 186 Hydrogen in Platinum Films Electrodeposited from Dinitrosulfatoplatinate Solution  
*N. Hisanaga, N. Fukumuro, S. Yae, and H. Matsuda*

- 187 Evaluation of Stress Condition of Operated Anode Supported-Type SOFC under Operating Conditions Based on Raman Scattering Spectroscopy  
*S. Onodera, M. Nagai, F. Iguchi, N. Sata, T. Kawada, and H. Yugami*
- 188 Development of Low-Temperature Operating Micro-SOFC with Perovskite-Type Proton Conductive Electrolytes  
*Y. Inagaki, F. Iguchi, K. Kubota, S. Tanaka, N. Sata, M. Esashi, and H. Yugami*
- 189 Study on Phase Diagram of Li-Rich Layered  $\text{Li}[\text{Li}_{0.2}\text{Ni}_{0.18}\text{Co}_{0.03}\text{Mn}_{0.58}] \text{O}_2$   
*Y. Irii, G. Kobayashi, T. Kataoka, T. Ikebara, F. Matsumoto, A. Ito, Y. Ohsawa, M. Hatano, and Y. Sato*
- 190 Preparation and Photoluminescence Properties of Sn/Mn Phosphate Zirconium Phosphor  
*T. Nishizaki, S. Takase, and Y. Shimizu*
- 191 Synthesis and Electrochemical Properties of Organogel Electrolytes Based on Low Molecular Weight Molecules  
*M. Miura, A. Iuchi, Y. Morita, K. Kasatani, and H. Okamoto*
- 192 Electrochemical Characterization of Lanthanum Calcium Titanium Manganite as Potential Dual Electrode Material in Symmetrical Solid Oxide Fuel Cell  
*H. Yoon, J. Zou, and J. Chung*
- 193 Depth-Resolved XAFS Study on Surface Segregation of  $\text{La}_{1-x}\text{Sr}_x\text{CoO}_{3-\delta}$  Electrode  
*S. Sakou, Y. Orikasa, E. J. Crumlin, Y. Shao-Horn, K. Amezawa, and Y. Uchimoto*
- 194 Synthesis and Physical Properties of Ionic Liquid Gels Based on Novel Low Molecular Weight Gelators  
*T. Yoshida, T. Hirakawa, T. Nakamura, Y. Yamada, H. Tatsuno, Y. Morita, and H. Okamoto*
- 195 Single Crystal Silicon based Sensor-Transistor Circuit by Thin Film Transfer Process  
*S. Jeong, T. Oh, S. Chang, K. Choi, K. Lee, Y. Kim, H. Ha, and B. Ju*
- 196 The effect of Au Nanoparticle on Metal Organic Semiconductor Field effect Transistor on Plastic Substrate by Transfer Method  
*H. Ha, S. Jeong, T. Oh, S. Chang, Y. Kim, K. Lee, K. Choi, and B. Ju*
- 197 Increasing Both Anodic and Cathodic Stability of Ether-Based Electrolyte for Li-Air and Li-Ion Batteries  
*M. Yaegashi, Y. Yamada, S. Nishimura, T. Abe, and A. Yamada*
- 198 Solvent Extraction Using Microchannel System for High Purification of Silica  
*N. Matsuo, Y. Matsui, Y. Fukunaka, and T. Homma*
- 199 Control of the Morphology of Si Nanostructure Using Single-Step Metal Assisted Etching Method  
*T. Yamaguchi, T. Shimizu, F. Inoue, C. Wang, S. Otsuka, Y. Tada, M. Inada, and S. Shingubara*

- 200 Maintaining Proper Hardness and Frictional Properties as a Noncyanide Gold Bath is Aged  
*J. R. Pillars and W. Yelton*
- 201 Polyoxometalates in Asymmetric Supercapacitors  
*J. Suarez-Guevara, V. Ruiz, and P. Gomez-Romero*
- 202 Electrochemical Construction and Characterizations of P-Copper(I) Oxide/N-Zinc Oxide Nano-Pillar Photovoltaic Device  
*T. Ohta, M. Kondo, J. Sasano, T. Shinagawa, T. Pauperté, and M. Izaki*
- 203 A Kinetic Study of Hydroxide, Bicarbonate and Carbonate Ion Inter-Conversion in Anion Exchange Membranes for Fuel Cells Using FT-IR Microscope  
*T. P. Pandey, J. L. Horan, M. Liberatore, and A. Herring*
- 204 Effect of Dissolved Gas in an Ionic Liquid Electrolyte for Lithium and Lithium/Sodium Metal Anode  
*J. K. Stark and P. Kohl*
- 205 Effect of Doping on the Ionic Conductivity and Bonding of Reactively Sputter Deposited Lithium Phosphorus Oxynitride Thin Films  
*P. Mani, V. Singh, M. Real-Robert, S. Duranceau, S. Seal, and K. Coffey*
- 206 Room Temperature Fabrication of Crystalline Germanium Nanowires by Electrochemical Deposition and its Application as Li Ion Battery Anode  
*J. Gu, S. Collins, A. Carim, X. Hao, B. Bartlett, and S. Maldonado*
- 207 Wet-Chemical Preparation of  $\text{Li}_{1.5}\text{Al}_{0.5}\text{Ti}_{1.5}(\text{PO}_4)_3$  Lithium Ionic Ceramic Thin-Films  
*C. Kubo, R. Aono, S. Takase, and Y. Shimizu*
- 208 Synthesis of Pt-Ir Catalysts by Coelectrodeposition: Application to Ammonia Electrooxidation in Alkaline Media  
*S. Le Vot, L. Roué, and D. Bélanger*
- 209 Direct Evaluation of Oxygen Chemical Potential in an SOFC Cathode by In Situ Micro XAS  
*Y. Fujimaki, H. Watanabe, Y. Kimura, K. Amezawa, Y. Terada, S. Hashimoto, and T. Kawada*
- 210 An Entirely Printed, Rechargeable Zinc-based Battery  
*Z. Wang, B. Kim, J. W. Evans, and P. K. Wright*
- 211 The effect of the Deposition Conditions on the Electrodeposition of Si Nanopillars in TMHATFSI  
*Y. Ishibashi, T. Akiyoshi, J. Komadina, Y. Fukunaka, and T. Homma*
- 212 Construction of Zinc Oxide/Phthalocyanine Hybrid Photovoltaic Device  
*R. Chizaki, K. Murata, J. Sasano, T. Shinagawa, S. Watase, and M. Izaki*

- 213 Novel Surface Modification Technique Based on the Liquid Phase Deposition Using Solid Fluorine Scavenger  
*T. Hasegawa, S. Matsumoto, and M. Mizuhata*
- 214 Electro-Oxidation of CO on Pt in Alkaline Media Studied by In Situ Surface-Enhanced Infrared Absorption Spectroscopy  
*J. Joo, T. Uchida, M. T. Koper, and M. Osawa*
- 215 Ultra-Strong Silicon-Coated Carbon Nanotube Fabric as Multi-Functional Lithium Ion Battery Anodes  
*K. Evanoff, J. Benson, M. Schauer, I. Kovalenko, D. Lashmore, J. Ready, and G. Y. Yushin*
- 216 Modification effects on Structural Changes of LiMn<sub>2</sub>O<sub>4</sub> Electrode during the Electrochemical Process  
*K. Suzuki, K. Kim, S. Taminato, M. Komo, A. Hagiwara, J. Son, T. Inami, H. Konishi, K. Tamura, J. Mizuki, M. Hirayama, and R. Kanno*
- 217 Variation of Crack Voltage in Anodic Aluminum Oxide/Aluminum Sheet for High Power LED Applications  
*H. Lee, H. Shin, and H. Lee*
- 218 Visualization of Bubble Behavior in Water Electrolyzer with High-Speed Camera  
*Y. Maeda, S. Tsukamoto, and K. Ito*
- 219 Memory Effect on Charge Storage in Layer-By-Layer Films of Rod-Shaped Multinuclear Complexs on Electrodes  
*T. Suzuki, T. Ryo, and M. Haga*
- 220 Nanoporous  $\alpha$ -Alumina Membrane with High Chemical Resistance Prepared by Anodizing  
*T. Masuda, H. Asoh, and S. Ono*
- 221 Biocompatibility and Corrosion Resistance of Magnesium Coated with Hydroxyapatite using Alternative Immersion Method  
*D. Kobayashi, H. Asoh, and S. Ono*
- 222 Application of Argon (70) + Nitrogen (30) Plasma Coagulation in Swine Mucosa  
*K. Ou and M. M. Colley*
- 223 Preparation of Flexible Micro-Glucose Sensor  
*T. Toba, N. Shiba, H. Matsuki, K. Edagawa, and M. Yasuzawa*
- 224 Preparation of Nonspecific Adsorption Eliminating Surface Using Perhydropolysilazane  
*N. Shinsuke, K. Ikebata, K. Rikitake, S. Nomoto, T. Koike, and M. Yasuzawa*
- 225 Stability of Different Bis-Terpyridine Metal Cations under Alkaline Solution  
*Y. Liu, M. Liberatore, and A. Herring*

- 226 Physical and Electrolytic Properties of Partially Fluorinated Chain Ethers as Solvents for Lithium Secondary Batteries  
*T. Satoh, N. Nambu, M. Takehara, M. Ue, and Y. Sasaki*
- 227 Positive-Tone, Aqueous-Developable, Polynorbornene Dielectric  
*B. K. Mueller, A. Grillo, E. Elce, and P. Kohl*
- 228 Fabrication of Nano-Structured  $(\text{La},\text{Sr})(\text{Zn},\text{Fe})\text{O}_3$  Cathodes for Intermediate-Temperature SOFC  
*S. Hwang, J. Jang, G. Choi, S. Lee, O. Kwon, D. Lee, S. Mukherjee, and S. Park*
- 229 Shape Selective Formation and Growth of High Index Polyhedral Gold Nanoparticles and Their Activity to Oxygen Evolution  
*B. C. Solomon, F. Ke, and X. Zhou*
- 230 Study of Optical and Structural Properties of SRSN Fabricated by Cat-CVD below 200 °C  
*S. Kang, K. Keum, J. Park, T. Song, J. Kim, and W. Hong*
- 231 The Structure, Thermal Expansion Property and Polymorphism of Solid Solution  $\text{Ho}_2\text{Mo}_3\text{-xW}_x\text{O}_{12}$   
*X. Liu, G. Yu, and Y. Liu*

#### A2 - Nanotechnology General Session

*All Divisions, ECS New Technology Subcommittee, ECSJ, CSE*

- 232 Growth of Pt Subnano-Clusters on Surface Limited Areas of Prussian-Blue Nanoparticles  
*M. Ishizaki, S. Tsuruta, K. Kananizuka, M. Kurihara, and M. Sakamoto*
- 233 Novel Synthesis Method of Copper Nanoparticles by Controlling Metal Complexes in Aqueous Solution  
*S. Yokoyama, H. Takahashi, and K. Tohji*
- 234 Characterization Attributes of Metal Oxide Nanocomposites  
*M. Hockey, Q. Lin, and E. Calderas*
- 235 Fabrication and Optical Characteristics of Ordered Crystalline  $\text{ZrO}_2$  Nanowires and Nanoporous Films on Glass  
*S. Chu, Y. Hitoshi, H. Segawa, S. Inoue, and K. Wada*
- 236 Electrochemical Synthesis of Crystalline and Compositionally-Uniform  $\text{Bi}_{1-x}\text{Sb}_x$  Nanowire Arrays  
*W. Yelton, S. Limmer, M. P. Siegal, D. Medlin, J. L. Lensch-Falk, M. Hekmaky, D. L. Overmyer, and J. M. Rivera*
- 237 Effects of Thermal Annealing on Conducting  $\text{ZnO}$  Nanowires: Conductor-To-Semiconductor Transition and Its Device Applications  
*P. Jeon, Y. Lee, R. Ha, H. Choi, and S. Im*

- 238 Oxygen Activation on Nanometer-Size Gold Nanoparticles  
*A. T. Staykov, K. Yoshizawa, and T. Ishihara*
- 239 Synthesis of Tailored Intermetallic Nanoparticles with Core-Shell Structure by Electrochemical Selective Phase Dissolution  
*G. Pigozzi, D. Mukherji, and P. Schmutz*
- 240 Annealing-Induced Interfacial Fracture Energy of Silver Nanoparticle Films on Substrate for Reliable Printed Electronics  
*I. Lee, S. Kim, J. Yun, I. Park, and T. Kim*
- 241 Atomistic Simulation Studies on Oxidation of Metal Nanoparticles  
*R. Subbaraman, S. A. Deshmukh, and S. Sankaranarayanan*
- 242 Photoinduced Spectral and Morphological Changes of Single Plasmonic Silver Nanoparticles on TiO<sub>2</sub>: Towards Single Particle Photochromism  
*T. Tatsuma and I. Tanabe*
- 243 Electooptic Study of Charge Carriers in Aligned Liquid Crystalline Polymers Transistors via Polarized Charge Modulation Spectroscopy  
*M. Lee, Z. Chen, J. Lee, and H. Sirringhaus*
- 244 Use of Förster Resonance Energy Transfer (FRET) as a New Characterization Method for the Interface in Sustainable Nanocomposites  
*J. W. Gilman, M. Zammarano, P. H. Maupin, L. Sung, E. McCarthy, Y. S. Kim, D. Fox, A. J. Berro, and I. Sacui*
- 245 Nanoimaging and Analysis of Localized Surface Plasmon-Induced Charge Separation and Application to Versatile Photochromism  
*E. Kazuma and T. Tatsuma*
- 246 Characterization of TiO<sub>2</sub> Particles Irradiated with N<sub>2</sub> Plasma by Newly Developed Plasma-Treatment System  
*K. Matsubara, M. Inoue, Y. Honda, and T. Abe*
- 247 Mapping of Electrochemical Interfaces at Nanoscale Dimensions Using Atom Probe Tomography  
*A. C. Hillier and Y. Zhang*
- 248 Measurements of Hydrogen Solubility in PdCu Thin Films  
*J. Galipaud, M. H. Martin, L. Roué, and D. Guay*
- 249 Graphene Nanocomposites for Electrochemical Applications  
*L. Niu*
- 250 Three Dimensional PtRh Alloy Porous Nanostructures: Tuning the Atomic Composition and Controlling the Morphology for the Application of Direct Methanol Fuel Cell  
*Y. Zhang, C. Liu, M. Janyasupab, J. Xu, and C. Liu*

- 251 Cesium Transfer from Granule Conglomerate Using Water Containing Nano-Sized Air Bubbles  
*Y. Ueda, Y. Tokuda, S. Fujimura, and T. Oka*
- 252 Scalable Non-Volatile Memory and Switch Device for High-Density Bipolar ReRAM Applications  
*D. Lee, M. Lee, and U. Chung*
- 253 Storage Properties of Surfaces and Interfaces: Enhanced Nonstoichiometry of Thin Silver Sulfide and Gold/Silver Sulfide Films  
*A. Rein, B. Luerßen, and J. Janek*
- 254 Fabrication of Hollow Spheres with Ordered Porous Structures by Anodizaiton of Small Metal Particles  
*T. Yanagishita, S. Ueno, K. Nishio, and H. Masuda*
- 255 Building 3D Nanostructured Supports for Pt Nanoparticles Used in Electrocatalytic Applications  
*C. Hu*
- 256 Molecular Electronic Devices Based on Self-Assembled Multilayer Films Bearing Redox-Active Ru Complexes  
*M. Haga, T. Nakabayashi, H. Ozawa, T. Suzuki, T. Joke, and K. Nakazato*
- 257 Micropatterned MnO<sub>2</sub>/CNT MEA Ultracapacitors  
*S. Raina, S. Hsu, W. Kang, and J. Huang*
- 258 Formation of a Vertically Oriented Anodic TiO<sub>2</sub> Nanotube Film on a Transparent Conductive Oxide Layer and Its Application to a Dye-Sensitized Solar Cell  
*R. Kojima, T. Ma, Y. Kimura, and M. Niwano*
- 259 Synthesis of ZnO Nano-Sheets and Their Application in UV-Detector  
*S. Sahoo, S. Barik, A. Gaur, R. Katiyar, and R. Katiyar*
- 260 Colloidal Synthesis of Semiconducting Ag<sub>2</sub>ZnSnS<sub>4</sub> Nanoparticle and Their Visible-Light-Driven Photoresponse  
*T. Sasamura, T. Osaki, T. Kameyama, K. Okazaki, A. Kudo, S. Kuwabata, and T. Torimoto*
- 261 A Novel Surface Nano-Structure Design for SiGe/Si Type-II Hetero-Junction Solar Cell with Superior Performance  
*M. Liao, C. Chen, L. Chang, C. Yang, C. Hsieh, and M. Lee*
- 262 Evolution of Germanium Quantum Dots Migration in Si Bearing Layer Mediated by Thermal Oxidation  
*K. Chen, I. Chen, C. Chien, C. Wang, T. George, and P. Li*
- 263 Fe-Co Alloy Nanoparticles and Nanowires Prepared by Electroless Deposition  
*M. Kawamori, S. Yagi, and E. Matsubara*

- 264 Adhesion Energy and Etching-Free Renewable Transfer of Graphene As-Grown on Copper  
*T. Yoon, W. Shin, T. Kim, J. Mun, B. Cho, and T. Kim*
- 265 Preparation and Characteristics of Proton Conducting Oxide Nano-Particles Using Planetary Bead-Mill  
*T. Sakai, Y. Okuyama, T. Ishihara, and H. Matsumoto*
- 266 Low Temperature Synthesis of Nanoscaled Carbon Thin Films by Chemical Vapor Deposition Using Solid Carbon Source  
*S. Vijapur, D. Wang, and G. G. Botte*
- 267 Deterministic Placement of Doping Atoms on Silanol Surfaces  
*L. Mathey, L. Veyre, H. Fontaine, V. Enyedi, K. Yckache, J. Guerrero, F. Martin, J. Barnes, F. Bertin, C. Thieuleux, and C. Copéret*
- 268 Optimization of Electrochromic Materials by Molecular Design: The Naphthalenediimide-Functionalized EDOT  
*R. Ruffo, M. Sassi, M. M. Salamone, and L. Beverina*
- 269 Functionalized Nanoporous Membrane Electrodes for ASV Analysis of Water  
*H. Bessbousse, T. Wade, and M. Clochard*
- 270 Silicon Nanowire Based Thermoelectric Device  
*M. Jang, Y. Park, Y. Hyun, W. Choi, and T. Zyung*
- 271 Studies of Boron Diffusivities on (001) and (110) Substrate Orientation in Si and Ge along Vertical/Out-Of Plane and Lateral/In-Plane Directions by SIMS and C-V Measurement on the Designed Test Pattern  
*M. Liao, C. Chen, L. Chang, C. Yang, C. Hsieh, and M. Lee*
- 272 Measurement of the Band Gap of Amorphous Silicon Based Thin Film with STEM-EELS  
*T. Motoya, T. Furuhata, and H. Kurata*
- 273 Electrical Properties and Microstructures of ZnO:Ga Films Formed by Magnetron Sputtering  
*N. Yamamoto, K. Morisawa, H. Makino, and T. Yamamoto*
- 274 Size effect on Photocatalytic Activity of Magnetite Nanoparticles under Visible-Light Irradiation  
*Y. Chen*
- 275 Liquid Phase Synthesis of Quantum Dots without Rare Metals and Toxic Elements  
*T. Makimura, S. Takeshita, and T. Isobe*
- 276 Diameter-Dependent Performance of the Metal Oxide Nanowire Lithium-Ion Battery Anodes Controlled by a Simple Contact Printing Method  
*S. Lee, J. Kim, and W. Kim*

- 277 Quantum Chemical Molecular Dynamics Simulations of Mechano-Chemical Reactions during Copper Chemical Mechanical Polishing Processes  
*K. Kawaguchi, T. Ishikawa, Y. Higuchi, N. Ozawa, T. Shimazaki, and M. Kubo*
- 278 Surface Potential Measurement of PCBM/CuPc Films on Indium Tin Oxide Electrode by DFM/KPFM  
*N. Satoh, S. Katori, K. Kobayashi, K. Matsushige, and H. Yamada*
- 279 Template-Free Electrochemical Growth of One-Dimensional Metal Nanostructures  
*S. Park, H. Shin, Y. Kim, H. Park, and J. Song*
- 280 First-Principles Calculations on the Chemical Mechanical Polishing Mechanism of SiO<sub>2</sub> Glasses by CaZrO<sub>3</sub> and SrFeO<sub>3</sub> Abrasive Particles  
*M. Nakamura, T. Ishikawa, Y. Higuchi, N. Ozawa, T. Shimazaki, and M. Kubo*
- 281 Synthesis and Characterization of Mesoporous Silica-Magnetite Nanocomposites  
*J. Lee, M. Yoon, and H. Hwang*
- 282 Nitrogen Incorporated Ultrananocrystalline Diamond/Nonhydrogenated Amorphous Carbon Composite Films Prepared by Pulsed Laser Deposition  
*S. S. Al-Riyami and T. Yoshitake*
- 283 Development of High Efficient Sulfur-Doped TiO<sub>2</sub> Photocatalysts Hybridized with Graphitic Carbon Nitride  
*K. Kondo, N. Murakami, and T. Ohno*
- 284 Tight-Binding Quantum Chemical Molecular Dynamics and First-Principles Molecular Dynamics Studies of Super-Low Friction Mechanism on Carbon Nitride Coatings  
*S. Sato, S. Bai, T. Ishikawa, Y. Higuchi, N. Ozawa, T. Shimazaki, K. Adachi, J. Martin, and M. Kubo*
- 285 Preparation of Au Nano or Micro Pattern on Hydrogels for Optical Applications  
*N. Shimamoto, Y. Tanaka, H. Mitomo, R. Kawamura, K. Ijiro, K. Sasaki, and Y. Osada*
- 286 Polymer-Nanocrystal Composites for Electrochromic Devices  
*E. Runnerstrom, G. Garcia, R. Buonsanti, A. Llordes, T. Pick, B. Helms, and D. Milliron*
- 287 Visible Light Response of Shape Controlled Rutile TiO<sub>2</sub> Nanorod Photocatalyst by LSPR Absorption  
*A. Tanibata, N. Murakami, and T. Ohno*
- 288 Effect of Sintering Temperature on the Microstructure of Nanocrystalline Ni-yttria Stabilized Zirconia Cermetts  
*K. Park, J. Kim, C. Kim, S. Nam, K. Cho, and J. Choi*
- 289 Synthesis, Characterization and Electrochemical Property of Graphene-Doped LiFePO<sub>4</sub> Cathode Material  
*H. V. Nguyen, E. Jin, and H. Gu*

- 290 Electrochemical Characteristics of Zn Doped TiO<sub>2</sub> for Dye-Sensitized Solar Cells  
*E. Jin, X. Zhao, H. V. Nguyen, and H. Gu*
- 291 Electrochemical Properties of Quasi-Solid Electrolyte Containing Graphene Oxide Dye Sensitized Solar Cell  
*X. Zhao, E. Jin, and H. Gu*
- 292 Electrochemical Characteristics of ZrO<sub>2</sub> Nanofiber added TiO<sub>2</sub> for Dye-Sensitized Solar Cells  
*E. Jin, W. Wang, J. Park, and H. Gu*
- 293 Fabrication of Dye-Sensitized Solar Cell with Community of Electrolyte and Pt Counter Electrode  
*X. Zhao, E. Jin, and H. Gu*
- 294 New Prepared TiO<sub>2</sub> was used in Photoelectrode with High Efficiency on Dye-Sensitised Solar Cells  
*W. Wang, E. Jin, and H. Gu*
- 295 Densification and Crystallization of Conducting La<sub>0.7</sub>Sr<sub>0.3</sub>VO<sub>3</sub> Nanopowder Derived from Hydrothermal Process  
*K. Fung, C. Cho, C. Liu, C. Ni, and S. Tsai*
- 296 Gallium Phosphide Nanowires for Solar Energy Conversion  
*W. Wen and S. Maldonado*
- 297 In Situ Monitoring of Photodegradation of Methylene Blue on Recyclable Gold Modified TiO<sub>2</sub> Nanotube (TiO<sub>2</sub>-NTs) Arrays by Using Surface-Enhanced Raman Scattering  
*R. Li and A. Zhou*
- 298 Controllable Variable Memory States Using Capacitive Coupling of Trapped Electrons  
*M. Lee, Y. Kim, and J. Lee*
- 299 Electrical Conductivity and Microstructure of NiO-CGO Composites Prepared By One Step Synthesis  
*D. A. Macedo, F. M. Figueiredo, S. G. Patrício, R. M. Nascimento, A. E. Martinelli, C. A. Paskocimas, and F. M. Marques*
- 300 Toxicity Assay-On-Chip for Engineered Nanomaterials  
*K. Garde and S. Aravamudhan*
- 301 n-Type Ultrananocrystalline Diamond/Hydrogenated Amorphous Carbon Composite Films Prepared by Pulsed Laser Deposition  
*S. Al-Riyami, H. Setoyama, K. Sumitani, Y. Hirai, and T. Yoshitake*
- 302 Active Targeting, Fluorescence Imaging, and NIR Photothermal Therapy of Malignant Tumors  
*H. Green, E. Rosenthal, C. Rodenburg, D. Martyshkin, S. Mirov, and W. Grizzle*

**A3 - Contemporary Issues and Case Studies in Electrochemical Innovation**  
*All ECS Divisions, ECS New Technology Subcommittee*

- 303 (Invited) Addressing a Medical Need: Introduction of the Battery for the Implantable Cardiac Defibrillator  
*E. S. Takeuchi, A. C. Marschilok, and K. J. Takeuchi*
- 304 Fuel Cell Technology Readiness  
*S. Petrovic*
- 305 Catalysis Research for Polymer Electrolyte Fuel Cell (CaRPE-FC): A Case Study on an Academic Led, Tri-Party Research Program in Canada  
*T. Navessin and S. Holdcroft*
- 306 (Invited) Next Generation Heavy Duty Bus Fuel Cells: An Industry-Academic Collaboration  
*S. Knights, E. Kjeang, S. Holdcroft, K. Malek, J. Kolodziej, M. Lauritzen, M. Watson, and J. DeVaal*
- 307 (Invited) Academia-Industry Synergy for Innovative PEFC Catalyst Layer and its Materials  
*A. Ohma*
- 308 Creating a Sustainable Business in the Hydrogen and Fuel Cell Market  
*K. E. Ayers, E. B. Anderson, C. B. Capuano, L. T. Dalton, and A. Roemer*
- 309 DMFC Power Modules for Materials Handling Vehicles  
*J. Mergel*
- 310 Technology Transfer between University and Industry in Uzbekistan: Techno Park Model  
*N. Mahamatov*
- 311 Electrochemical Discrimination of Ascorbic Acid Diastereomers Using Dihydroxyalkanedithiol-modified Au Electrode  
*M. Komatsu, T. Ando, and S. Suzuki*
- 312 Through the Looking Glass: A Journey into Innovation  
*R. Jalan*
- 313 (Invited) From Lab Bench to Marketplace: Building New Electrochemical Technologies  
*Y. Chiang*
- 314 Turning the Tides: New Mexico Materials for Japanese Cars  
*P. Atanassov*
- 315 A Case Study of Technological Innovation Related to ElectroPolishing of Stainless Steel Valves and Fittings  
*E. J. Taylor and M. Inman*

- 316 Electrochemical Cesium Recovery Using Nanoparticle Film of Copper Hexacyanoferrate  
*H. Tanaka, R. Chen, C. Fukushima, M. Asai, T. Kawamoto, M. Kurihara,  
M. Arisaka, T. Nankawa, and M. Watanabe*
- 317 Integration of a New Electroplated Magnetic Alloy with Power Semiconductor Wafer Manufacturing Processes  
*T. Liakopoulos, A. Panda, M. Wilkowski, and A. Lotfi*
- 318 A Novel Technique of Quantifying Micro Insulation Defects on Grain-Oriented Electrical Steel Using the Scanning Vibrating Electrode Technique  
*L. T. Cassemis, J. H. Sullivan, and D. Power*
- 319 Role of Dimensional Parameters for Determination of Diffusion Coefficient (D) and Surface Exchange Coefficient (K) Case Study for Oxygen Storage Materials, Electrode Materials for SOFCs, and Materials for Li-Ion and Na Batteries  
*K. Zheng, D. Baster, J. Molenda, and K. Swierczek*

**B1 - Batteries and Energy Technology Joint General Session - In Honor of James McBreen**

*ECS Battery, ECS Energy Technology, ECSJ Battery, CSE*

- 320 A Wonderful Life Dedicated to Energy Research In Memery of James McBreen  
*X. Yang, K. Nam, S. Mukerjee, M. Balasubramanian, W. Yoon, and K. Chung*
- 321 Recent Advances in Neutron Imaging for Battery Characterization  
*D. S. Hussey, J. Kahn, O. Zilcha, D. Jacobson, B. Khaykovich, M. V. Gubarev,  
J. Gagliardo, and J. Owejan*
- 322 Application of Synchrotron-Based X-Ray Techniques to Study Thermal Behavior of Electrode Materials for Lithium Rechargeable Batteries  
*W. Yoon, K. Nam, K. Chung, M. Balasubramanian, D. Jang, J. Hanson,  
and X. Yang*
- 323 Solid-State Batteries: A Fifty Year Perspective  
*B. B. Owens and O. Yamamoto*
- 324 Rechargeable Lithium Battery Electrodes Using a Multifunctional Polymer Binder  
*A. E. Javier, S. N. Patel, and N. P. Balsara*
- 325 An Empiric Approach to the Estimation of State of Charge of Lithium Cells and Range of an Electric Vehicle  
*G. Davolio, R. Giovanardi, and C. Lanciotti*
- 326 Designing Advanced Hybrid Materials for Rechargeable Lithium Batteries  
*Y. Guo*
- 327 Substation Installations of Electrovaya's MWh-Scale Lithium-Ion SuperPolymer Batteries for Smart Grid Applications  
*R. DasGupta*

- 328 Nanostructured Composites for Energy Storage Applications  
*D. Wang, S. Chen, Z. Song, T. Xu, J. Song, R. Yi, F. Dai, and M. Gordin*
- 329 Polymer Gel Electrolytes for Lithium-Ion Batteries  
*M. Gnanavel, M. Patel, and A. J. Bhattacharyya*
- 330 Nanostructured  $\beta$ -Li<sub>3</sub>PS<sub>4</sub> for All-Solid Lithium-Sulfur Batteries  
*C. Liang, Z. Lin, Z. Liu, N. J. Dudney, A. J. Rondinone, and E. Payzant*
- 331 Kinetically Asymmetric Reaction Pathways on Charging and Discharging LiNi<sub>0.5</sub>Mn<sub>1.5</sub>O<sub>4</sub> Electrodes  
*K. Sato, H. Arai, Y. Orikasa, H. Murayama, Y. Koyama, Y. Uchimoto, and Z. Ogumi*
- 332 High-Capacity 0.4Li<sub>2</sub>MnO<sub>3</sub>·0.6LiNi<sub>2/3</sub>Mn<sub>1/3</sub>O<sub>2</sub> with Excellent Cyclability for Lithium-Ion Batteries  
*Y. Jiang, Z. Yang, and Y. Huang*
- 333 Fabrication of Macroporous Li<sub>2</sub>FeSiO<sub>4</sub>/Carbon Monoliths for a Lithium-Ion Battery  
*G. Hasegawa, M. Sannohe, K. Kanamori, K. Nakanishi, and T. Abe*
- 334 Ag<sub>x</sub>V<sub>y</sub>O<sub>z</sub>PO<sub>4</sub>: Silver Vanadium Phosphorous Oxides as Cathode Materials in Lithium Batteries  
*E. S. Takeuchi, A. C. Marschilok, and K. J. Takeuchi*
- 335 Selenium and Selenium Sulfide – A New Class of Positive Electrode Material for Room Temperature Lithium and Sodium Rechargeable Batteries  
*A. Abouimrane, D. Dambournet, K. W. Chapman, P. J. Chupas, W. Weng, Y. Cui, H. El Tayeb, and K. Amine*
- 336 Open Framework Electrodes for Stationary Storage Devices  
*C. D. Wessells, M. Pasta, R. A. Huggins, and Y. Cui*
- 337 Solid State Lithium Sulfur Batteries Using a Nanostructured Block Copolymer Electrolyte  
*A. A. Teran and N. P. Balsara*
- 338 Spherical Carbon/Sulfur Composite Cathodes for Rechargeable Lithium Batteries  
*M. A. Loth, F. Rogers, R. Chen, C. Swartz, U. Graham, and S. M. Lipka*
- 339 SnS<sub>2</sub>-Graphene Nanocomposite for Advanced Lithium-Ion Battery  
*L. Ji, H. L. Xin, T. R. Kuykendall, S. Wu, H. Zheng, M. Rao, E. J. Cairns, V. Battaglia, and Y. Zhang*
- 340 V<sub>2</sub>O<sub>5</sub> Network Structure as Cathode for Lithium-Ion Batteries  
*Y. Xu, M. Dunwell, and H. Luo*
- 341 Enhancement of Li Insertion Capacity of Carbon Anode on the Basis of Faradaic Adsorption Combined with Nano-Ionics Mechanism  
*T. Takamura, J. Suzuki, K. Sumiya, and K. Sekine*

- 342 Microwave Synthesis of Graphene/Sn Nanocomposite Anodes for Lithium-Ion Batteries  
*F. R. Beck, R. Epur, A. Manivannan, and P. N. Kumta*
- 343 Understanding Cycle Life Failure Mechanisms in Graphite-Silicon Alloy Composite Electrodes by Electrochemical Calorimetry  
*L. J. Krause, L. Liu, L. Jensen, V. L. Chevrier, and J. Singh*
- 344 Tough Solid Composite Electrolytes to Enable Lithium Metal Anodes  
*W. E. Tenhaeff, K. A. Perry, E. Herbert, S. Kalnaus, and N. J. Dudney*
- 345 Study of Conversion Reactions in NiO Using Transmission Electron Microscopy and Electron Energy Loss Spectroscopy  
*A. K. Shukla, U. Boesenberg, and J. Cabana*
- 346 Electrochemical Versatility of Carbon for Energy Storage Application  
*L. A. Riley, H. Constantino, and A. Feaver*
- 347 Combined Experimental and Theoretical Study of Nitrogen Reduction on Novel Mo-N Catalyst Material  
*I. Matanović, K. Armstrong, L. Daemon, J. Eckert, F. H. Garzon, A. H. Mueller, and N. J. Henson*
- 348 Challenges in Water Electrolysis and Its Development Potential as a Key Technology for Renewable Energies  
*J. Mergel and D. Stolten*
- 349 Electrochemical Modeling of Anode Supported Solid Oxide Electrolyzer Cells (SOEC) in Electrolysis of Carbon Dioxide  
*J. Njodzeffon, A. Weber, and E. Ivers-Tiffée*
- 350 Novel Fluorine Doped Transition Metal Oxide ( $\text{Ru}_x\text{Sn}_{1-x}\text{O}_2:\text{F}$ ) Oxygen Evolution Electro-Catalysts for Hydrogen Generation from PEM Based Water Electrolysis  
*K. Kadakia, M. Datta, O. Velikokhatnyi, and P. N. Kumta*
- 351 Nanostructured Nickel Hydroxides for Urea Electrolysis  
*D. Wang, W. Yan, S. Vijapur, and G. G. Botte*
- 352 Synthesis of Active Fibrous Perovskite Catalyst and Its Application for Hydrogen Production  
*Y. Jeon, D. Park, M. Park, G. Lee, J. Park, and Y. Shul*
- 353 Electrochemical Behavior of Nanocrystalline  $\text{MgMnO}_3$  Cubic Defect Spinel Cathode for Rechargeable Magnesium Battery  
*P. Saha, M. Datta, A. Manivannan, and P. N. Kumta*
- 354 A Novel Boron-Based Electrolyte System for Rechargeable Mg Batteries  
*Y. Guo, J. Yang, F. Zhang, and F. Wang*

- 355 Electrochemical Stability of Metal Electrodes for Reversible Magnesium Deposition/Dissolution in Tetrahydrofuran  
*S. Yagi, A. Tanaka, T. Ichitsubo, and E. Matsubara*
- 356 Electrochemical Performances of Tetrathiafulvalene Polymer (TTF) as a Cathode Material for Nonaqueous Secondary Batteries  
*N. Hojo, T. Tsukagoshi, Y. Inatomi, and H. Yoshizawa*
- 357 A Review of Secondary Magnesium Battery R&D at The Dow Chemical Company  
*T. D. Gregory*
- 358 Magnesium Electrolyte Based on EMImBF<sub>4</sub> and δ-[MgCl<sub>2</sub>]<sub>n</sub> for Secondary Magnesium Batteries  
*V. Di Noto, F. Bertasi, E. Negro, and S. Lavina*
- 359 Beta-Battery Based on <sup>63</sup>Ni/Macroporous Silicon  
*A. Dolgyi, S. Redko, H. Bandarenka, A. Shapet, and V. Bondarenko*
- 360 Developing Novel Electrolytes for Rechargeable Mg Batteries  
*J. Muldoon and C. B. Bucur*
- 361 Improvement of Sulfone-Based Electrolyte for Aluminum Rechargeable Battery  
*Y. Nakayama, Y. Senda, H. Kawasaki, S. Chung, N. Koshitani, S. Hosoi, Y. Kudo, and H. Morioka*
- 362 A Conjugated Sulfidepolymer Battery with Variable Capacitance Controlled by Redox Reaction  
*J. Sakata*
- 363 Building a Robust Liquid Metal Battery  
*P. J. Burke, B. H. Chung, A. D. LaDelpha, and D. R. Sadoway*
- 364 Electrode Kinetics of Low Cost, High-Rate Tolerant, Engineering-Scale Liquid Metal Batteries  
*B. H. Chung, A. D. LaDelpha, and D. R. Sadoway*
- 365 Barium Hydroxide and the Rechargeable Performance of the Alkaline γ-MnO<sub>2</sub> Electrode  
*M. R. Bailey and S. W. Donne*
- 366 Optimizing Heat Treatment Environment and Atmosphere of Electrolytic Manganese Dioxide for Primary Li/MnO<sub>2</sub> Batteries  
*W. M. Dose and S. W. Donne*
- 367 Current Collectors for Secondary Zinc Electrodes  
*P. J. Bonnick and J. Dahn*
- 368 Comparison of Pocket Plate and Sintered Plate Ni Electrodes Used in NiFe Cells for PV Back up Applications  
*I. Mabbett, J. Malone, and D. A. Worsley*

- 369 Development of a Zinc-Based Battery System for Grid-Scale Energy Storage and Application of Flexographic Printing for the Fabrication  
*Z. Wang, R. Winslow, B. Kim, J. W. Evans, and P. K. Wright*
- 370 Effect of Substitution of Cobalt by Manganese on the Properties of Calcium-Doped Lanthanum Cobalt Oxide for Oxygen Evolution Reaction in Alkaline Medium  
*P. Trinh, S. Malkhandi, N. Moreno, A. Manohar, G. Prakash, S. Narayanan, and A. Manivannan*
- 371 Mechanism of Formation of Carbonyl Iron Electrodes in Alkaline Batteries  
*A. Manohar, C. Yang, S. Malkhandi, B. Yang, G. Prakash, and S. Narayanan*
- 372 Exploring the Role of Ionic Interfaces of the High Voltage Lead Acid-Metal Hydride Hybrid Battery  
*G. Weng, C. V. Li, and K. Chan*
- 373 Zinc Electrodeposition in Zinc-Nickel Flow-Assisted Batteries  
*X. Wei, A. Couzis, and S. Banerjee*
- 374 Modeling and Simulation of an Aqueous Li-Ion Battery with a Complex Electrolyte  
*A. Yermukhambetova, J. H. Pu, and Z. Bakenov*
- 375 A High Voltage Grid-Tied Stationary Energy Storage Demonstration Based on The Aqueous Hybrid Ion Battery System  
*J. F. Whitacre, S. Shanbhag, D. Blackwood, W. Campbell, W. Yang, J. Gulakowski, A. Mohamed, M. Sibenac, J. Weber, and T. Wiley*
- 376 Elucidating Failure Mechanisms in the Soluble Lead- Acid Flow Battery - Formation of PbO<sub>2</sub> at the Cathode  
*M. Verde, K. Carroll, D. Keogh, A. Sathrum, and Y. Meng*
- 377 Measurements of Effective Electronic and Ionic Conductivities in Porous Li-Ion Electrodes  
*S. Harris, N. Zacharias, C. Skelton, K. Knackstedt, D. Stephenson, Y. Wen, and D. R. Wheeler*
- 378 Nanostructured CFx Provides Breakthrough in Performance of Li-CFx Cells  
*D. Meshri, E. Shembel, S. Meshri, N. C. Mathur, R. Adams, V. Redko, T. Pastushkin, I. Maksyuta, A. Markevich, L. Neduzko, V. Mitkin, and L. Levchenko*
- 379 Structure and Electrochemistry of Olivine-Inorganic Composites for Lithium Batteries  
*I. Belharouak, G. Koenig, and R. R. Shahbazian-Yassar*
- 380 Graphene as a Conductive Additive to Improve the Performance of Layered LiNi<sub>0.66</sub>Co<sub>0.17</sub>Mn<sub>0.17</sub>O<sub>2</sub> Cathode for Lithium-Ion Batteries  
*C. Venkateswara Rao, J. Shojan, and R. Katiyar*
- 381 Olivine type LiMn<sub>1/3</sub>Co<sub>1/3</sub>Ni<sub>1/3</sub>PO<sub>4</sub> Cathode for Secondary Battery Applications  
*M. Minakshi and P. Singh*

- 382 Effects of LLTO Coating on High Temperature Cycle Life Performance of LiMn<sub>2</sub>O<sub>4</sub> Cathode Material  
*M. Reddy, M. Prabu, S. Selvasekarapandian, G. Subba Rao, and B. Chowdari*
- 383 Damage Evaluation of Solid Cells by Intelligent Information Processing on Acoustic Emission Events  
*D. Inaba, K. Fukui, K. Sato, J. Mizusaki, N. Kuwata, J. Kawamura, and M. Numao*
- 384 Advanced Proton Conducting Membrane for Solid Electrochemical Capacitors  
*H. Gao and K. Lian*
- 385 Nanostructured Transition Metal Nitride Supercapacitors: Effects of Composition, Structure, and Electronic Properties on Supercapacitor Response  
*P. Jampani Hanumantha, A. Manivannan, and P. N. Kumta*
- 386 Influence of Chemical Composition of the Electrolyte and Room-Temperature Ionic Liquids on the Electrical Double Layer Structure and Supercapacitor Characteristics  
*E. Lust, H. Kurig, A. Laheäär, I. Tallo, V. Ivaništšev, L. Siinor, C. Siimenson, A. Jänes, T. Thomberg, K. Lust, and J. Eskusson*
- 387 Carbon /MnO<sub>2</sub> Core-Shell Nanofibers for Supercapacitors  
*M. Zhi, A. Manivannan, F. Meng, and N. Wu*
- 388 Distortion of Solvated Structures by Microporous Structures of Carbon Materials  
*N. Ide, J. Nishioka, K. Urita, H. Furukawa, H. Yamada, and I. Moriguchi*
- 389 Bio-Enabled, Nanostructured Electrodes for Electrochemical Energy Storage Devices  
*M. Song and M. Liu*
- 390 Polymorphic Behavior and Morphology of Electrospun Poly(Vinylidene Fluoride) Separator Materials for Non-Aqueous Based Electric Double Layer Capacitors  
*K. Tõnurist, T. Thomberg, T. Romann, A. Jänes, and E. Lust*
- 391 Conducting Polymers Based on Natural Membranes and Eu<sup>3+</sup>  
*R. Leones, M. Fernandes, R. A. Ferreira, F. Sentanin, A. Pawlicka, L. D. Carlos, V. de Zea Bermudez, and M. M. Silva*
- 392 Performance Improvement of a Hydrogen-Bromine Flow Battery  
*K. Cho, A. Weber, Q. He, P. Ridgway, V. Battaglia, and V. Srinivasan*
- 393 Recent Progress in Redox Flow Battery Research and Development at Pacific Northwest National Lab  
*W. Wang, Q. Luo, Z. Nie, M. Vijayakumar, X. Wei, B. Li, F. Chen, B. Chen, Y. Shao, G. Xia, L. Li, and Z. Yang*
- 394 New Discharge/Charge Performance Data for a H<sub>2</sub>-Br<sub>2</sub> Flow Battery  
*V. Yarlagadda and T. V. Nguyen*

- 395 Halogen Flow Batteries for Grid-Scale Electricity Storage  
*B. Huskinson, S. Mondal, J. Rugolo, and M. J. Aziz*
- 396 Grid-Scale Energy Storage Requirements and the Potential for Halogen-Based Flow Batteries  
*J. Rugolo, B. Huskinson, and M. J. Aziz*
- 397 Aqueous Semi-Solid Flow Cell  
*Z. Li, P. Limthongkul, W. Carter, and Y. Chiang*
- 398 Hydrogen Bromine Redox Flow Battery Cell Performance Study  
*Y. Bai, A. B. Papandrew, and T. A. Zawodzinski*
- 399 Characterization of Vanadium Redox Flow Batteries: An AC Impedance Spectroscopy Study  
*C. Sun, D. S. Aaron, A. Papandrew, and T. A. Zawodzinski*
- 400 Performance Enhancement, Limitations, and Diagnostics of Vanadium Redox Flow Batteries  
*J. T. Clement, A. M. Pezeshki, Q. Liu, A. B. Papandrew, A. Turhan, T. A. Zawodzinski, and M. M. Mench*
- 401 Coulombic Efficiency of a Vanadium Redox Flow Cell  
*X. Gao, R. Lynch, M. Leahy, and D. Buckley*
- 402 Polymer Membrane for Redox Flow Battery Application  
*D. Kim, E. Mi Choi, E. Kang, and K. Kang*
- 403 Role of Membrane Properties on Species Crossover and Capacity Loss of a Vanadium Redox Flow Battery  
*K. W. Knehr, E. Agar, C. R. Dennison, A. R. Kalidindi, D. Chen, M. Hickner, and E. C. Kumbur*
- 404 Redox Flow Battery in Combination with Hydrogen Evolution/Oxidation Electrode  
*Z. Siroma, S. Yamazaki, M. Yao, N. Fujiwara, M. Asahi, and T. Ioroi*
- 405 Nonaqueous Redox Flow Battery Development at Pacific Northwest National Laboratory  
*W. Wang, W. Xu, L. Cosimescu, D. Choi, L. Li, and Z. Yang*
- 406 Effect of Porous Electrode Configuration on Redox Flow Battery Performance  
*S. Kim, D. Stephenson, G. Xia, Z. Nie, and V. Sprenkle*
- 407 Vanadium Redox Flow Battery Efficiency and Durability Studies of Sulfonated Diels Alder Poly(Phenylene)s  
*C. H. Fujimoto, S. Kim, R. Stanis, and M. Hickner*
- 408 Direct Measurement of Vanadium Crossover in an Operating Vanadium Redox Flow Battery  
*D. C. Sing and J. P. Meyers*

- 409 Component Optimization for High Performance Redox Flow Batteries  
*S. Kim, D. Chen, Z. Nie, M. Hickner, C. H. Fujimoto, and V. Sprenkle*
- 410 Redox-Active Organic Molecules for Non-Aqueous Flow Batteries  
*F. R. Brushett, L. Zhang, J. T. Vaughney, and A. N. Jansen*
- 411 Crossover Measurements for Vanadium Redox Flow Batteries Using Electron Spin Resonance  
*J. S. Lawton, A. M. Jones, D. S. Aaron, Z. Tang, A. Papandrew, and T. A. Zawodzinski*
- 412 Cationic Uptake Influence on PFSA Membrane Performance in Vanadium Redox Flow Battery  
*Z. Tang, J. S. Lawton, D. S. Aaron, A. Papandrew, and T. A. Zawodzinski*
- 413 Fabrication and Performance Evaluation of Direct Methane Fueled Ni-GDC Anode-Supported SOFC Unit Cells Operated at Intermediate Temperature (650 °C)  
*H. Ko, J. Myung, J. Lee, and S. Hyun*
- 414 Effects of Sn-Doped Ni-Based Anodes on Performance and Durability of CH<sub>4</sub>-Fueled SOFCs  
*J. Myung, H. Ko, J. Lee, and S. Hyun*
- 415 Enhanced Densification of SDC Barrier Layers on Anode Supported Solid Oxide Fuel Cells  
*J. W. Templeton, Z. Lu, J. S. Hardy, and J. W. Stevenson*
- 416 Tubular Segmented-in-Series Solid Oxide Fuel Cell with Metallic Interconnect Films: Performance Study through Mathematical Modeling  
*J. Lee, B. Son, S. Park, S. Lee, T. Lim, and R. Song*
- 417 Anode-Supported Flat-Tubular SOFCs with Ag-Infiltrated Cathodes: Performance and Durability  
*R. Song, J. Lee, S. Lee, T. Lim, and S. Park*
- 418 Non Noble Metal Thin Film Solid Oxide Fuel Cell  
*I. Chang, S. Ji, Y. Lee, and S. Cha*
- 419 Sputtered Thin Film Pt vs LSCF for Low Temperature Solid Oxide Fuel Cells  
*Y. Lee, I. Chang, S. Ji, and S. Cha*
- 420 Enhanced Oxide Ion Kinetics in Low-Temperature Solid Oxide Fuel Cells by Atomic Layer Deposited Cermet Interlayer  
*J. An, Y. Kim, T. M. Gür, and F. B. Prinz*
- 421 Performance and Stability of Zn-Doped BSCF Cathode for IT-SOFCs  
*D. Jung, H. Park, J. Kim, K. Moon, S. Seo, and C. Kwak*

- 422 Fabrication of Ni-YSZ Nano-Composite Electrode for Solid Oxide Fuel Cells via Thin Film Technique  
*G. Cho, Y. Lee, J. Choi, and S. Cha*
- 423 A New-Style Energy Conversion Scheme: Photo-Assist Fuel Cell Based on Titania Nanotube Arrays  
*P. Xiao, H. He, F. Liu, and Y. Zhang*
- 424 CdS/CdSe Co-Sensitized Quantum Dots Solar Cells with Different Density of ZnO Nanowire Arrays  
*J. Tian, Z. Liang, R. Gao, Q. Zhang, and G. Cao*
- 425 Regenerative Fuel Cells for Grid Applications  
*V. Yufit and N. Brandon*
- 426 The Hydrogen Fuel Cell Vehicles Powertrain Possible Roles in the Post Kyoto Perspective in the Pacific RIM Area  
*M. Romeri*
- 427 Preparation and Characterization of Ti Based Supports for Electrochemical Energy Conversion Devices  
*S. Siracusano, A. Stassi, E. Modica, V. Baglio, and A. Aricò*
- 428 Understanding Oxygen Reduction in Complex Metal Organic and Inorganic Composites for Fuel Cell, Electrolyzer and Energy Storage Applications  
*S. Mukerjee, T. M. Arruda, K. Abraham, M. Trahan, and N. Ramaswamy*
- 429 Electrochemical Reactions on Oriented Pt-V and Pt-Ni-V Metal Alloy Thin Films  
*C. C. Hays, M. A. Johnson, P. Bahrami, J. G. Kulleck, and H. Greer*
- 430 Remote Performance Monitoring of Photovoltaic Systems with Battery Storage  
*S. Petrovic, G. Kirby, J. Bockelman, M. Payne, J. Fuscaldo, N. Oester, J. Belanger, and P. Lackey*
- 431 Electrical Explosion Synthesis of Si/C Nanocomposites for Li Secondary Batteries  
*D. Kim, Y. Ha, C. Cho, H. Choi, S. Choi, and C. Doh*
- 432 Modifications in Nernst-Planck Equation for Solid State Electrochemistry in the 21<sup>st</sup> Century  
*T. Miyashita*
- 433 Composite Cathodes Based on  $\text{Sm}_{0.5}\text{Sr}_{0.5}\text{CoO}_{3-\delta}$  for Anode Supported Solid Oxide Fuel Cells  
*H. Kim and Y. Park*
- 434 Surface Modification of Si/C Composite Materials for Improving Distribution of Si Nano-Particles  
*H. Seo, K. Kim, and C. Yi*

- 435 Fe-Substituted  $\text{Li}_3\text{V}_2(\text{PO}_4)_3$  as High Rate Cathode Materials for Li-Ion Batteries  
*S. Wu, M. Chen, W. Pang, and F. Liu*
- 436 Lithium-Sulfur Battery Development  
*S. Urbonaite, A. Garsuch, and P. Novák*
- 437 Effect of Synthesis Method on the Activity of Carbon-Supported Copper Catalysts toward  $\text{CO}_2$  Electrocatalysis  
*B. Spigarelli, Z. Wang, W. Li, and O. A. Baturina*
- 438 The Comparative Performance of Carbon Felt Electrodes for Vanadium-Redox Flow Batteries According to Surface Treatment and Heat Treatment Conditions  
*T. Jung, S. Kim, H. Jeon, K. Kwon, and H. Lee*
- 439 Performance Test of a Direct Methanol Fuel Cell and  $\text{LiFePO}_4$  Battery Hybrid Electric Vehicles  
*B. Lee, D. Peck, S. Kim, S. Lim, and D. Jung*
- 440 Tape Casting, Lamination and Sintering of Calcium-Doped Lanthanum Chromite for SOFC Interconnects  
*D. Hernandez Rubio, A. C. Hoffmann, E. Dorolli, and C. Suciu*
- 441 Three-Dimensional Modeling on the effect of Active Cooling for a Lithium-Ion Battery Pack  
*J. Yi, C. Shin, Y. Hong, and C. Kim*
- 442 A Novel SOFC Anode Material: Cu Doped  $\text{La}_{0.75}\text{Sr}_{0.25}\text{Cr}_{0.5}\text{Mn}_{0.5}\text{O}_{3-\delta}$   
*L. Sun, Y. Yin, T. Ze, and Z. Ma*
- 443 Performances of Aqueous Lithium-Ion Battery with Hydrogel Electrolyte  
*K. Nakamoto, S. Park, S. Okada, and S. Mitsui*
- 444 Synthesis of Highly Redox Stable Double-Perovskite Oxide  $\text{Sr}_2\text{MgMoO}_{6-\delta}$  in Air  
*J. Yin, Y. Yin, Z. Tong, and Z. Ma*
- 445 Atomic Layer Deposition of Platinum Electrodes for LT-SOFCs  
*Y. Kim, J. An, and F. B. Prinz*
- 446 Physico-Chemical and Electrochemical Properties of Ni Perovskite Solid Oxide Fuel Cell Anode for Glycerol Oxidation  
*G. Monforte, M. Lo Faro, M. Minutoli, V. Antonucci, and A. Aricò*
- 447 Application of Anion-Exchange Membranes for Vanadium Redox Flow Battery  
*J. Shim, J. Jeon, S. Park, B. Lee, and K. Shin*
- 448 Synthesis and Physical Properties of Proton Conductors,  $A\text{-Mg}(\text{PO}_3)_3 \cdot y\text{H}_2\text{O}$  ( $A : \text{Li}^+$ ,  $\text{Na}^+$ ,  $\text{K}^+$ ,  $\text{Rb}^+$ ,  $\text{Cs}^+$  and  $\text{NH}_4^+$ )  
*M. Hirayama, Y. Matsuda, M. Yonemura, and R. Kanno*

- 449 Acetylene Black Modified 3D SnS<sub>2</sub> Nanoflowers with High Electrochemical Performance for Lithium-Ion Battery  
*M. He, L. Yuan, and Y. Huang*
- 450 Electrochemical Properties of NAFION Coated Hydriding Combustion Synthesized Mg Based Alloy  
*S. Kim, M. Chourashiya, C. Park, and C. Park*
- 451 Preparation of Ni(OH)<sub>2</sub> Nanowall/Ni Electrode and Its Application in Lithium-Ion Battery  
*T. Li, S. Ni, and X. Yang*
- 452 A One-Dimensional Model for Air-Breathing Direct Methanol Fuel Cells  
*J. Park, S. Ha, and S. Cha*
- 453 Novel Synthesis of SnO<sub>2</sub>/Graphite Composite as Anode Material for Lithium-Ion Batteries  
*Y. Zhou, X. Yang, and S. Ni*
- 454 Preparation of 3D Porous Silicon Powders with Fluoride-Free Technology  
*C. Shi, X. Yang, D. Yu, and L. Zhang*
- 455 Preparation of Chitosan /GPTMS Anion-Exchange Membranes via the Sol-Gel Routes for Vanadium Redox Flow Battery Applications  
*Y. Huang, S. Huang, K. Hsueh, and B. Wong*
- 456 Electrochemical Properties of MnO<sub>2</sub>/Carbon Composites by Microwave Heating  
*Y. Chun*
- 457 Study of the Kinetics of Vanadium (II)/(III) Redox Reaction  
*H. Yang, K. Hsueh, C. Hsieh, and J. Hung*
- 458 Membrane Permeability Measurement of Vanadium Ions  
*C. Wu, Y. Huang, Y. Chiu, S. Huang, and K. Hsueh*
- 459 Function and Performance of the Separator Membrane in Red-Ox Flow Batteries and Why Proton Exchange Based Membrane Might Not Be the Best Choice  
*K. A. Lewinski*
- 460 A Numerical Study of the Electrochemical Performance with the Electrolytic Flow Conditions in Vanadium Redox Flow Battery  
*J. Kim and H. Lee*
- 461 A Novel High Power - Long Cycle Life Energy Storage System for Large-Scale Applications  
*H. Jin, D. Ren, G. H. Brilmyer, and M. T. Nispel*
- 462 The Development of MT-HF-SOFCs Using New Fabrication Techniques  
*N. Droushiotis and G. H. Kelsall*
- 463 Performance Enhancement of Solid Oxide Storage Battery  
*X. Zhao, N. Xu, X. Li, Y. Gong, and K. Huang*

- 464 Research and Development Activities of SOFC in Pohang, Korea  
*N. M. Sammes and J. Chung*
- 465 A Novel High Temperature Metal - Air Battery  
*W. W. Drenckhahn, M. Kuehne, T. Soller, K. Litzinger, J. Shull, A. Iyengar, H. Greiner, H. Landes, A. Leonide, and C. Schuh*
- 466 Preparation of Ashless Coal and Its Oxidation in a Coin Type Direct Carbon Fuel Cell  
*C. Lee and W. Kim*
- 467 Oxide Solid/Melt Composites as Ion Transport Membranes for Oxygen Separation from Air  
*V. V. Belousov*
- 468 Synthesis and Characterization of Functional Ceramic Nanopowders by Thermal Oxidation of Metal-Alginate Gels  
*Z. Wang, G. Kale, and M. Ghadiri*
- 469 A Novel BaCo<sub>0.4</sub>Fe<sub>0.4</sub>Zr<sub>0.2</sub>O<sub>3-δ</sub> Cathode for Intermediate Temperature Proton-Conducting SOFC  
*M. Shang, J. Tong, and R. O'Hayre*
- 470 A Study of Anode -Supported Solid Oxide Fuel Cell with YSZ/GDC Bilayer Electrolyte Using Dry Press Process  
*H. Choi and S. Cha*
- 471 Dynamic Response Analysis of a Molten Carbonate Fuel cell Using a Sinusoidal Impedance Approach  
*M. Yousef Ramandi, P. Berg, and I. Dincer*
- 472 In-Operando X-ray Diffraction of LSCF Cathodes on Anode-Supported Solid Oxide Fuel Cells  
*J. S. Hardy, J. W. Templeton, and J. W. Stevenson*
- 473 3D Coupled Thermofluid-Thermomechanical Modelling and Experimental Validation of a Whole Solid Oxide Fuel Cell System  
*M. Peksen, A. Al-MASRI, L. Blum, and D. Stolten*
- 474 Reverse Breakdown in Bipolar Membranes  
*N. Craig and J. Newman*
- 475 Electrochemical and Mechanical Reliability of Three Dimensionally Reconstructed Electrode Microstructures  
*D. Chung, D. Ely, P. Shearing, N. Brandon, S. Harris, and E. García*
- 476 Application of the Molecular Interaction Volume Model (MIVM) to Ca-Based Liquid Alloys  
*S. Poizeau and D. R. Sadoway*

- 477 Electrochemical-Thermal Coupled Simulation of Lithium-Ion Secondary Batteries Using New Lumped Model  
*N. Baba, H. Yoshida, M. Nagaoka, C. Okuda, and S. Kawauchi*
- 478 Lattice Boltzmann Modeling of Advection-Diffusion Transport with Electrochemical Reactions in a Porous SOFC Anode Structure  
*H. Paradis and B. Sundén*
- 479 Synthesize Battery Degradation Modes via a Diagnostic Model  
*M. Dubarry, C. Truchot, and B. Liaw*
- 480 Modeling of Heat Transfer in a Fluidized Bed Carbon Fuel Cell  
*G. J. Armstrong, B. R. Alexander, R. E. Mitchell, and T. M. Gür*
- 481 Influences of Cells Assembling on Energetic Models and Simulations of Li-Ion Packs for Electric Vehicles Applications  
*K. Mamadou, T. Delaplagne, S. Hing, and F. Karoui*
- 482 The Impact of Diffusion-Induced Convection on Transference Number Measurements  
*J. Liu and C. W. Monroe*
- 483 A Model for Energy Storage Systems in the Frequency Domain  
*E. M. Krieger and C. B. Arnold*
- 484 Study of Energy Storage Materials Using Multi-Length Scale 3D Electron Microscopy  
*A. K. Shukla, P. Ercius, N. Krins, A. Gautam, S. Wu, J. Cabana, G. Chen, T. J. Richardson, V. Srinivasan, and U. Dahmen*
- 485 Modeling of Volume Change Behavior of Porous Electrodes  
*K. Kanneganti, J. Moraveji, and J. Weidner*
- 486 Towards Onboard Battery Management Systems Using Physics-Based Efficient Reformulated Models  
*B. Suthar, V. Ramadesigan, P. Northrop, W. Sung, and V. Subramanian*

## B2 - Electrochemical Capacitors

*ECS Battery, ECS Physical and Analytical Electrochemistry, ECSJ Capacitor Technology, CSE, KECS*

- 487 A Critical View on Graphene-Metal Oxide Based Electrochemical Supercapacitors  
*P. Gao, S. Baek, N. Pinna, F. Moser, T. Brousse, and F. Favier*
- 488 Tuning the Electrolytic Manganese Oxide/Graphene Oxide Nanocomposites for High-Energy Asymmetric Electrochemical Capacitors in Aqueous Electrolytes  
*K. I. Ozoemena, C. J. Jafta, M. K. Mathe, and S. Chen*
- 489 Pseudocapacitive Behavior of Hierarchical Porous Carbide-Derived Carbon with Integrated Niobium Pentoxide Nanoparticles  
*V. Presser, E. Perre, M. Lukatskaya, B. Dunn, and Y. Gogotsi*

- 490 MnO<sub>2</sub>/Carbon Nanocomposite Electrode Prepared Via Molecular Bridging  
*C. Ramirez Castro, R. Retoux, A. Morel, O. Crosnier, L. Athouël, P. Guillemet, F. Moser, C. Martin, D. Bélanger, and T. Brousse*
- 491 Hydrous Ruthenium Oxide: A Pseudocapacitance Champ with Lessons of Relevance for the Redesign of Energy-Storage Architectures  
*D. R. Rolison*
- 492 An Investigation of Nanostructured Thin Film α-MoO<sub>3</sub> Based Supercapacitor Electrodes in an Aqueous Electrolyte  
*B. Mendoza Sanchez, T. Brousse, C. Ramirez Castro, V. Nicolosi, and P. Grant*
- 493 Kinetic and Mass Transport Phenomena in Different Phases of Manganese Dioxide for Application in Electrochemical Capacitors  
*M. Dupont and S. W. Donne*
- 494 Transition Metal Nitrides Thin Films for Supercapacitor Applications  
*S. Bouhriyya, R. Lucio-Porto, J. Ducros, P. Boulet, F. Capon, T. Brousse, and J. Pierson*
- 495 New Developments in Colloidal Fabrication of Manganese Dioxide-Carbon Nanotube Electrodes of Supercapacitors  
*I. Zhitomirsky*
- 496 Research on Conducting Polymer/Carbon Composite Supercapacitors: Toward Enhanced Cycle Stability and Power Performance  
*N. N. Wu and Y. Weng*
- 497 Polyaniline-MnO<sub>2</sub> Nanocomposite Supercapacitor Electrodes Prepared by Galvanic Pulse Polymerization  
*G. Pandey and A. Rastogi*
- 498 Electrochemical Codeposition of Polyaniline and Tungsten Oxide for Supercapacitor  
*B. Zou and X. Liu*
- 499 Aqueous Hybrid Capacitor Based on Doping/Dedoping of Lithium- Ion into Conducting Polymer  
*J. Ahn, Y. Shul, and H. Kim*
- 500 Binder Free Thick Electrodes of Polyaniline Nanofibers/ Multiwalled Carbon Nanotubes  
*M. Hyder, S. Lee, Y. Shao-Horn, and P. Hammond*
- 501 Electrochemical Characteristics and Application of Linear Carbon for Electrochemical Capacitors  
*S. Park, J. Yang, H. Kim, and H. Kimm*
- 502 Chemical Modification of Carbons with Quinones by the Diazonium Chemistry for Application in Electrochemical Capacitors  
*M. Weissmann, A. Le Comte, G. Pognon, C. Cougnon, T. Brousse, and D. Bélanger*

- 503 Nitrogen Doped Graphene a High Efficient Electrode for Next Generation Supercapacitors  
*A. Yu, F. M. Hassan, Z. Chen, and V. Chabot*
- 504 Fine-Tuning the Carbon - Electrolyte Interface for Designing High Energy Density Double Layer Capacitors  
*P. Simon, B. Daffos, R. Lin, P. Taberna, and Y. Gogotsi*
- 505 Performance Limits of 2 V C/C Supercapacitors in Alkali Sulfate Aqueous Media  
*F. Béguin, K. Fic, P. Ratajczak, K. Jurewicz, Q. Abbas, G. Lota, G. Gao, L. Demarconnay, E. Raymundo, and E. Frackowiak*
- 506 Diameter Dependent Doping of Single-Walled Carbon Nanotube Used as Electrical Double Layer Capacitor Electrode  
*A. Al-zubaidi, Y. Ishii, T. Matsushita, and S. Kawasaki*
- 507 Three Dimensional Graphene-MWNTs Foam Architectures for Electrochemical Capacitors  
*W. Wang, S. Guo, M. Ozkan, and C. Ozkan*
- 508 Effect of Additives on the Hydrothermal Synthesis of Carbon Nano- and Micro-Spheres and Their Performance in Double-Layer Capacitors  
*I. Kunadian, R. Chen, S. M. Lipka, C. R. Swartz, and F. Rogers*
- 509 First Principles-Inspired Design Strategies for Carbon Aerogel Supercapacitors  
*B. C. Wood, T. Ogitsu, J. Lee, M. Otani, T. Baumann, M. Stadermann, M. A. Worsley, A. Wittstock, M. Merrill, and J. Biener*
- 510 Temperature effects in Activated Carbon Supercapacitors  
*D. W. Kirk*
- 511 Redox Active Electrolytes for Electrochemical Capacitors  
*E. Frackowiak, K. Fic, M. Meller, and G. Lota*
- 512 Mixed Ionic Liquid Electrolytes and Electrochemical Double Layer Capacitors  
*E. T. Fox, J. S. Dickmann, J. E. Weaver, J. L. Allen, and W. A. Henderson*
- 513 Electrochemical Capacitor Using a Highly Conductive Ionic Plastic Crystal  
*R. Taniki, K. Matsumoto, T. Nohira, and R. Hagiwara*
- 514 Influence of the Organic Solvent Additives on the Properties of 1-Ethyl-3-Methylimidazolium Tetrafluoroborate as Supercapacitor Electrolyte  
*R. Palm, H. Kurig, A. Jänes, and E. Lust*
- 515 Advanced Capacitors for Next Generation and Their R&D of Material in Nippon Chemi-Con  
*K. Tamamitsu, S. Suematsu, S. Ishimoto, and H. Uchi*
- 516 Electrochemical Capacitor Usable Power for Hybrid Electric Vehicle Applications as Determined from Transient Electrical Response  
*D. A. Corrigan, C. Fortin, and A. Zabik*

- 517 Characteristics of Electric Double Layer Capacitor Based on an Electrode Utilizing SWCNT on "Three-Dimensional Porous Aluminum" - Improvement of Electric Performance at Low Temperature  
*D. Iida, T. Noguchi, M. Kuramoto, K. Okuno, A. Hosoe, M. Majima, and Y. Nakai*
- 518 A New Aqueous Hybrid Electrochemical Capacitor with a 4 V Operating Voltage  
*W. Sugimoto, T. Ban, Y. Shinohara, S. Makino, and W. Shimizu*
- 519 The Next Generation "Nanohybrid" and "SuperRedox" Capacitors  
*K. Naoi*
- 520 Development and Evaluation of an Asymmetric Capacitor with a Nickel/Carbon Foam Positive Electrode  
*B. C. Cornilsen, J. Wang, P. Sasthan Kuttipillai, T. N. Rogers, W. Yeo, M. B. Chye, and A. Singh Bhatia*
- 521 Asymmetric Supercapacitors Consisting of a Graphene-Based Anode and Oxide-Based Cathodes in Aqueous Electrolytes  
*C. Hu, C. Liu, C. Chen, T. Wu, and K. Chang*
- 522 Testing of MnO<sub>2</sub> Aqueous Hybrid Supercapacitors under Extreme Climatic Conditions  
*A. J. Roberts and R. Slade*
- 523 Structured EDLC Electrode with Through-Plane Microchannel  
*T. Okura, A. Morimoto, G. Inoue, and M. Kawase*
- 524 Tailoring Carbons for Energy Storage Via Hydrogen Evolution and Capture under Anodic Biasing Conditions in Neutral pH Aqueous Electrolytes  
*S. Chun, S. Shanbhag, and J. F. Whitacre*
- 525 Understanding the Charging Mechanism of Nanoporous Carbon Electrodes from Molecular Dynamics Simulations  
*M. Salanne, C. Merlet, B. Rotenberg, P. Madden, P. Taberna, P. Simon, and Y. Gogotsi*
- 526 A Powerful Approach for Preparing Single-Phase Unitary/Binary Oxides-Graphene Composites  
*K. Chang and C. Hu*
- 527 Nanoporous Carbon Materials for Electrical Double Layer Capacitors  
*G. Y. Yushin*
- 528 High Voltage Electrochemical Double Layer Capacitors Containing Adiponitrile-Based Electrolytes  
*A. Balducci, A. Brandt, P. Isken, and A. Lex-Balducci*
- 529 Dramatic Improvements in Electric Double-Layer Capacitors by Using Polysaccharides  
*M. Yamagata, S. Ikebe, Y. Kasai, K. Soeda, and M. Ishikawa*

- 530 NMR Studies on the Mechanism of Electrochemical Double Layer Capacitors  
*H. Wang, T. K. Köster, N. Trease, J. Ségalini, P. Taberna, P. Simon, Y. Gogotsi, and C. P. Grey*
- 531 Nanohybrid Capacitor Utilizing Li<sub>4</sub>Ti<sub>5</sub>O<sub>12</sub> Composited with Single-Walled Carbon Nanotube  
*J. Miyamoto, S. Suematsu, K. Tamamitsu, K. Hata, S. Iijima, and K. Naoi*
- 532 Double Templates Synthesis of Mesoporous Nanowires  
*J. Lee*
- 533 Influence of Organic Solvents on Carbon-Layer Structure in Electrical-Double-Layer Capacitors  
*A. Banerjee, P. Suresh Kumar, and A. K. Shukla*
- 534 Polypyrrole-Covered MnO<sub>2</sub> as Electrode Material for Hydrid Supercapacitor  
*A. Bahloul, B. Nessark, E. Briot, H. Groult, A. Mauger, and C. M. Julien*
- 535 3-D Graphene/Metal Oxide Composite Material for Supercapacitors  
*S. Guo, W. Wang, C. Ozkan, and M. Ozkan*
- 536 Influence of Electrode Mass on the Electrochemical Performance of Asymmetric Supercapacitors with Nano-Ni(OH)<sub>2</sub> and Activated Carbon Electrodes  
*Y. Tian, J. Yan, R. Xue, H. Lixing, and B. Yi*
- 537 A General Model for Porous Layer Pseudo-Capacitive Impedance Spectrum  
*P. Guillemet, O. Crosnier, and T. Brousse*
- 538 Promising Bio-Carbon for Oxygen Reduction and Supercapacitor  
*X. Yang and H. Zhu*
- 539 Nitrogen-Enriched Metallophthalocyanine/Graphene Oxide Nanocomposites for High-Energy Asymmetric Electrochemical Capacitors in Aqueous Electrolytes  
*K. I. Ozoemena, J. Lekitima, K. Makgopa, C. J. Jafra, and S. Chen*
- 540 Ar<sup>+</sup> Plasma Enhanced Vertically Oriented Graphene Supercapacitors  
*M. Cai, R. A. Outlaw, S. M. Butler, and J. R. Miller*
- 541 Graphene Nanowall Supercapacitors with Ultra-High Performance  
*H. Yen, Y. Horng, M. Hu, W. Yang, Y. Tai, L. Chen, and K. Chen*
- 542 Polyacrylonitrile and 1-Ethyl-3-Methylimidazolium Thiocyanate Based Gel Polymer Electrolyte for Solid-State Supercapacitors with Graphene Electrodes  
*G. Pandey and A. Rastogi*
- 543 Cathodic Synthesis of Birnessite Films for Pseudocapacitor Application  
*T. Tanimoto, H. Abe, K. Tomono, and M. Nakayama*

- 544 EQCM Investigation on Electrodeposition and Charge Storage Behavior of Birnessite-Type MnO<sub>2</sub>  
*M. Shamoto, T. Tanimoto, K. Tomono, and M. Nakayama*
- 545 Study of Storage Capacity in Electrochemical Double Layer Capacitor Using Graphene and Blends of Graphene with Carbon  
*C. Subramaniam, T. Maiyalagan, G. Velayutham, and S. Bollepalli*
- 546 Ordered Mesoporous/Microporous Carbon Sphere Arrays Derived from Chlorination of Mesoporous TiC/C Composite and Their Application for Supercapacitors  
*D. D. Zhou, H. Liu, Y. Wang, C. Wang, and Y. Xia*
- 547 Ion-Exchange/Activation Combination Method to Synthesize 3D Hierarchical Porous Graphitic Carbon with Interconnected Pore Structure as Electrode Material for Supercapacitors  
*Y. Li and P. Shen*
- 548 Designing Porous Microstructures of NiCo<sub>2</sub>O<sub>4</sub> Spinel Nanoparticles by Using CTAB-Assisted Dispersion  
*C. Hsu, K. Chang, and C. Hu*
- 549 Effect of Manufacturing Factors on Electrochemical Performance of Carbon-PTFE Electrode for EDLC  
*I. Kim, S. Yang, and S. Lee*
- 550 A New Porous Anode Material Electrochemically Synthesized from Polycyclic Aromatic Hydrocarbons  
*M. Wagner, C. Kvarnström, A. Ivaska, and J. Bobacka*
- 551 NaClO<sub>4</sub> and NaPF<sub>6</sub> as Potential Non-Aqueous Electrolyte Salts for Electrical Double Layer Capacitor Application  
*A. Laheäär, A. Jänes, and E. Lust*
- 552 Gel-Based Activated Carbon Electrode for EDLC Supercapacitors  
*V. Jouille, C. Galindo, M. Paté, P. Le Barny, and M. Pham Thi*
- 553 Alginate Binder for High Power EDLC  
*S. Ikebe, S. Yamazaki, M. Yamagata, and M. Ishikawa*
- 554 The effect of Electrolyte on the Hybrid Capacitor of LiMn<sub>2</sub>O<sub>4</sub>/AC and LiCoO<sub>2</sub>/AC Prepared by Chemical Activation  
*J. Lee and H. Yoon*
- 555 Quinone-Functionalized Carbon Nano-Onion for Pseudocapacitor Applications  
*D. M. Anjos, V. Presser, J. McDonough, Y. Gogotsi, G. M. Brown, and S. Overbury*
- 556 Electrochemical Characteristic of CNT Sphere by Aggregation of W/O Emulsion Process  
*H. Kim, J. Yang, H. Kim, and S. Park*

- 557 Nonaqueous Proton Conducting Gel Electrolyte for Supercapacitors  
*A. A. Ojrzyńska, I. Rukowska, P. Simon, P. J. Kulesza, and W. Wieczorek*
- 558 The Electrochemical Behavior of CNFs by Liquid Phase Carbonization Using Polyethylene Oxide(PEO)  
*S. Ahn, J. Yang, H. Kim, H. Habazaki, and S. Park*
- 559 Activated Mesophase Pitch for High Performance Electric Double Layer Capacitors  
*C. Huang, M. Hsueh, and H. Teng*
- 560 Comparative Study of Using Chlorine and Hydrogen Chloride for Synthesis of Titanium Carbide Derived Carbon  
*I. Tallo, T. Thomberg, A. Jänes, and E. Lust*
- 561 The Contribution of N-Containing Functional Groups on Graphene for EDLC in Acidic and Alkaline Electrolytes  
*Y. Lee, K. Chang, and C. Hu*
- 562 A 3.9 V Lithium/Activated Carbon Hybrid Capacitor Based on an Aqueous Electrolyte  
*W. Shimizu, S. Makino, and W. Sugimoto*
- 563 Chemical Vapor Deposition Synthesis of Carbon Coated Graphite for Hybrid Capacitor  
*Y. Kim*
- 564 Performance of Supercapacitors Based on Graphene Oxide and Mesoporous Carbon by Screen Printing  
*I. Carrera Leon, J. Baas López, and D. Pacheco Catalán*
- 565 Potential Control with AC Electrode Capacity for Hybrid Capacitor  
*J. Yang, Y. Yuk, H. Kim, and S. Park*
- 566 Fabrication and Optimization of Nanoparticulate Manganese Dioxide Thin-Film Electrochemical Capacitor Prototypes  
*S. Pang, B. Wee, and S. Chin*
- 567 Electrochemical Properties of Electrochemical Capacitors Using NiO Electrode  
*M. Chiku, M. Toda, E. Higuchi, and H. Inoue*
- 568 N-Butyl-N-Methylpyrrolidinium-Dicyanamide Ionic Liquid as the Electrolyte for Manganese Oxide Pseudo-Capacitor  
*H. Cheng, I. Sun, C. Su, M. Lee, W. Tsai, J. Chang, and Y. Fu*
- 569 Capacitance Enhancement of Anodic ZrO<sub>2</sub> Films by Simultaneous Incorporation of Silicon and Yttrium Species  
*M. Ishizuka, E. Tsuji, Y. Aoki, and H. Habazaki*
- 570 N-doped Graphite Oxide Synthesized from Photocatalytic Reduction for Electrochemical Capacitors  
*H. Huang and H. Teng*

- 571 Organic-Inorganic Hybrid Materials for Supercapacitors  
*V. Ruiz, J. Suarez-Guevara, and P. Gomez-Romero*
- 572 Electrochemical Properties of Layered (Ni<sub>x</sub>Co<sub>y</sub>Mn<sub>z</sub>) Oxide Prepared by Co-Precipitation Method as Electrodes for Electrochemical Capacitors  
*M. Yano, S. Suzuki, and M. Miyayama*
- 573 Substrate effects on the Supercapacitive Behavior of Electrodeposited Manganese Oxides  
*M. Glenn and S. W. Donne*
- 574 Li Distribution in Carbon Anode with Li Pre-Doping for Li-Ion Capacitor  
*T. Toki, M. Yamagata, and M. Ishikawa*
- 575 Study of Polypyrrole-Manganese Oxide Composites as Supercapacitor Electrode Materials  
*P. Ningsih, C. Z. Holdsworth, and S. W. Donne*
- 576 Aqueous Asymmetric Electrochemical Capacitors: From Fundamental Electrode Design to Practical Considerations  
*J. W. Long, M. B. Sassin, B. Willis, C. Hoag, D. R. Rolison, A. Mansour, S. G. Greenbaum, J. M. Wallace, and K. Pettigrew*
- 577 Pulse-Electropolymerization of Polypyrrole on Free-Standing Graphene Films for Efficient Flexible Supercapacitors  
*F. M. Hassan, Z. Chen, A. Davies, J. Choi, and A. Yu*
- 578 Optimization of Activated Carbon Materials for Lithium-Ion Capacitor Applications  
*D. A. Totir, S. Letaj, D. Carruthers, M. Petruska, M. King, and M. Wodjenski*
- 579 Double Layer Capacitor Performances of Porous Carbon Electrodes Derived from Cyclic Oligosaccharide  
*M. Tokita, M. Egashira, N. Yoshimoto, and M. Morita*
- 580 Selective Adsorption of Ions into Nanoporous Carbons: A View Beyond Just the Mere Ion Size  
*S. Sigalov, M. Levi, G. Salitra, D. Aurbach, A. Jänes, E. Lust, and I. C. Halalay*
- 581 An Asymmetric Electrochemical Capacitor with Activated Carbon Electrodes in Organic Electrolyte  
*X. Tian, S. Dsoke, C. Täubert, and M. Wohlfahrt-Mehrens*
- 582 Addressing the Conductivity Issue in Electrochemical Supercapacitor Electrodes  
*X. Pétrissans, D. Giaume, J. Badot, and P. Barboux*
- 583 Electrochemically Reduced Graphene Oxide Sheets as High Performance Supercapacitors  
*J. Yang and S. Gunasekaran*
- 584 Exploring the Cycle Behavior of Electrodeposited Vanadium Oxide Supercapacitor Electrodes in Various Aqueous Environments  
*A. M. Engstrom and F. M. Doyle*

- 585 Fabrication of Graphite Oxide/ PEDOT-PSS/ Carbon Nanotubes Composite Paper Via One Step Solution-Casting Synthesis for High Performance Flexible Electrode  
*Y. Weng and N. N. Wu*
- 586 Synthesis and Characterization of N-Methylacetamide/LiBF<sub>4</sub> Complex as an Ionic Liquid Electrolyte for Supercapacitor  
*B. Bang and T. Yeu*
- 587 In Situ Electrochemical Deposition of MnO<sub>2</sub> on CNTs for Ultracapacitor Applications  
*S. Raina, S. Hsu, W. Kang, J. Huang, and M. Yilmaz*
- 588 Highly Conductive Activated Carbon for the Application of Supercapacitor  
*Y. Lin, W. Wang, and C. Cheng*
- 589 Characterization of LiNi<sub>1/3</sub>Mn<sub>1/3</sub>Co<sub>1/3</sub>O<sub>2</sub>/C Composite Positive Electrodes for Non-Aqueous Supercapacitors  
*B. Bang and T. Yeu*
- 590 Enhanced Electrochemical Supercapacitors Integrated with Polythiophene Using Oxidative Chemical Vapor Deposition  
*S. Nejati, C. Tran, T. E. Minford, V. Kalra, and K. K. Lau*
- 591 Comparative Study of Electrode Stabilization Technique for Graphene-Polyaniline Nanocomposite Electrodes Using Dielectrics for Supercapacitor Applications  
*S. A. Ketkar, M. Ram, A. Kumar, T. Weller, and A. M. Hoff*
- 592 Pseudo-Capacitive Performance of Sol-Gel Manganese Oxide/Graphene Electrodes with Various Heat-Treatments  
*M. Lee, C. Lin, C. Wu, C. Wang, C. Chen, and J. Chang*
- 593 Electrochemical Behavior of Electrolytes at Porous Electrode Investigated with Transmission-Line Model  
*N. Nambu and T. Satoh*
- 594 Advances in Solid Electrochemical Capacitors  
*K. Lian, H. Gao, H. Wu, K. Hu, and S. Katabi*
- 595 Planar Electrochemical Capacitor with Gelled Electrolyte  
*J. R. Miller, R. A. Outlaw, M. Cai, and S. M. Butler*
- 596 Soft Carbon as Anode Material in Lithium Ion Capacitors with a Propylene Carbonate Based Electrolyte  
*M. Schroeder, M. Winter, S. Passerini, and A. Balducci*
- 597 Development of Solid-State Photo-Supercapacitor by Coupling Dye-Sensitized Solar Cell Utilizing Conducting- Polymer Charge Relay with Proton-Conducting Membrane Based Electrochemical Capacitor  
*P. J. Kulesza, M. Skunik, K. Grzejszczak, N. Vlachopoulos, L. Yang, L. Häggman, and A. Hagfeldt*

- 598 Specific Performance of Electrical Double Layer Capacitors Based on Different Separator Materials in Room Temperature Ionic Liquid  
*K. Tõnurist, T. Thomberg, A. Jänes, and E. Lust*
- 599 Hybrid Supercapacitor Using Mesoporous Carbon and Ti-Based Material  
*Y. Xia, H. Liu, G. Zhu, and Y. Wang*
- 600 Surface Characterization of Supercapacitor Electrodes after Long-Lasting Constant Current Tests  
*A. Jänes, R. Kanarbik, J. Eskusson, and E. Lust*
- 601 Ultrahigh Rate Solid-State Supercapacitors with Graphene Additives  
*Y. Chen, K. Chiu, H. Lin, and C. Tsai*
- 602 Electrochemical Flow Capacitors: A New Concept for High-Power Scalable Energy Storage  
*C. R. Dennison, V. Presser, J. Campos, K. W. Knehr, E. C. Kumbur, and Y. Gogotsi*
- 603 Nanoscale Characterization of CDC Supercapacitors by In Situ Scanning Probe Microscopy Methods  
*T. M. Arruda, M. Heon, V. Presser, Y. Gogotsi, and N. Balke*
- 604 Pseudocapacitance of MnO<sub>2</sub> Originates from Reversible Insertion/Desertion of Li-Ion Studied Using In Situ XAS in Novel Ionic Liquid  
*M. Deng, J. Chang, C. Wang, J. Chen, and K. Lu*
- 605 Measuring Ion Transport in Energy Storage Devices Using In Situ Time-Resolved Infrared Spectroscopy  
*F. W. Richey, B. Dyatkin, Y. Gogotsi, and Y. A. Elabd*
- 606 ASAXS Measurements as a Powerful Technique for Structural Investigation of MnO<sub>2</sub>-Carbon Hybrid Supercapacitor Electrodes  
*C. Weber, V. Lorrman, G. Reichenauer, and J. Pflaum*
- 607 In Situ Characterization of Transition Metal Nitride Supercapacitor Electrodes  
*P. Pande, A. E. Sleightholme, P. Rasmussen, A. Deb, J. Penner-Hanh, and L. T. Thompson*
- 608 Thermodynamics in Porous Electrodes: A Monte Carlo Simulation Study  
*K. Kiyohara and K. Asaka*
- 609 Capacitance and Electric Double Layer Structure in Ionic Liquid-Based Supercapacitors with Nanopatterned and Nanostructured Electrodes  
*D. Bedrov, L. Xing, and J. Vatamanu*
- 610 Interaction Nature of Molecular Oxides with Keggin Structure with Carbon Matrices to Improve Capacitance and Cycling Performance in Supercapacitor Cells  
*A. CUENTAS-GALLEGOS, T. Brousse, H. Mosqueda, C. Martin, and D. Baeza Rostro*

**B3 - Grand Challenges for Energy Conversion and Large Scale Energy Storage**

*ECS High Temperature Materials, ECS Battery, ECS Energy Technology, ECS Industrial Electrochemistry and Electrochemical Engineering, ECSJ Energy Technology*

- 611 Grid Scale Energy Storage; Applications, Technology Demonstrations, and a US Perspective  
*I. Gyuk*
- 612 The Application and Development of Large-scale Energy Storage Technology in China  
*X. Lai*
- 613 National Energy Technology Developing Strategy in Korea  
*K. Nahm and S. Chung*
- 614 Challenges in Commercialization of Energy Storage Systems within the Electric Enterprise  
*D. Rastler*
- 615 Issues and Challenges for Implementation of Large-Scale Energy Storage in Australia  
*M. Syllas-Kazacos*
- 616 Status and Development of Energy Storage System In Korea  
*J. Lee*
- 617 Realities of Economic Screening for Energy Conversion and Storage Technologies  
*E. McFarland*
- 618 Energy Security with Clean and Green Energy  
*G. Ka'iliwai*

**B4 - Intercalation Compounds for Rechargeable Batteries**

*ECS Battery, ECSJ Battery, KECS*

- 619 Iron and Manganese Based Cathode Materials for Electrochemical Energy Storage  
*K. J. Takeuchi, A. C. Marschilok, and E. S. Takeuchi*
- 620 Electrochemical and Structural Properties of Li-Rich Layered Cathode Material  $\text{Li}_{1.2}\text{Ni}_{0.2}\text{Mn}_{0.6}\text{O}_2$   
*T. Sasakawa, Y. Harada, H. Inagaki, N. Takami, N. Kitamura, and Y. Idemoto*
- 621 Electrochemical Property of Nano Size Multiple Transition Metal Oxides Synthesized from Layered Double Hydroxide  
*N. Sonoyama, S. Hayashi, T. Toba, and Z. Quan*
- 622 Ion-Exchange Synthesis and Intercalation Process of  $\text{Li}_{1.05}\text{Na}_{0.02}\text{Ni}_{0.21}\text{Mn}_{0.63}\text{O}_2$  Cathodes for Li-Ion Batteries  
*M. Slater, S. Rood, D. Kim, S. Kang, E. Lee, V. Maroni, D. Bass, A. DeWahl, S. Hackney, and C. S. Johnson*

- 623 Li<sub>2</sub>MnO<sub>3</sub>-Based Positive Electrode Materials; Materials Design, Synthesis, and Structural Stability  
*N. Yabuuchi, Y. Aoki, R. Hara, and S. Komaba*
- 624 Change of Local, Average and Electronic Structures, and Property by Heat-Treatment under Vacuum Reducing Condition and Charge-Discharge Process in Li<sub>1.2</sub>Mn<sub>0.567</sub>Ni<sub>0.167</sub>Co<sub>0.067</sub>O<sub>2</sub>  
*Y. Idemoto, T. Kashima, and N. Kitamura*
- 625 Surface Control and Multi-Composite Cathodes  
*A. Mauger, K. Zaghib, H. Groult, and C. M. Julien*
- 626 Improvement in Electrochemical Performances of Li[Ni<sub>x</sub>Mn<sub>y</sub>Co<sub>z</sub>]O<sub>2</sub> Upon Cycling and Storage  
*J. Kim*
- 627 Structural and Electrochemical Properties of LiNi<sub>1/3</sub>Co<sub>1/3</sub>Mn<sub>1/3</sub>O<sub>2</sub> Positive Electrode Material Modified by Coating with Al Oxides (2)  
*Y. Sasaki, Y. Kikuzono, N. Fukuya, N. Taguchi, K. Araki, K. Okamura, K. Kojima, F. Kita, T. Takeuchi, H. Sakaebe, K. Tatsumi, and Z. Ogumi*
- 628 Epitaxial Growth of LiCoO<sub>2</sub> Thin Film on Single Crystal Substrate by Sol-Gel Method  
*T. Kwon, T. Ohnishi, K. Akatsuka, R. B. Cervera, and K. Takada*
- 629 Simulations of Charge-Discharge Processes in an Intercalation Compound at the Nanoscale  
*B. Orvananos, H. Yu, R. Malik, C. P. Grey, G. Ceder, and K. Thornton*
- 630 First-Principles Calculations on Defect Chemistry in Layered Lithium Transition-Metal Oxides  
*Y. Koyama, H. Arai, I. Tanaka, Y. Uchimoto, and Z. Ogumi*
- 631 First-Principles Study of Two-Phase Interface in LiFePO<sub>4</sub>  
*Y. Asari, Y. Suwa, T. Hamada, V. Dinh, J. Nara, and T. Ohno*
- 632 Design Criteria for Electrochemical Shock Resistant Battery Electrode Particles  
*W. H. Woodford, W. Carter, and Y. Chiang*
- 633 Electronic Model of Intercalation of Alkaline Ions into Transition Metal Oxides  
*J. Molenda*
- 634 High Resolution Chemical Imaging of Phase Transformations during Intercalation Reactions  
*J. Cabana*
- 635 Time Resolved XRD and XAFS Study on Phase Transition Dynamics in Li<sub>x</sub>FePO<sub>4</sub>  
*Y. Orikasa, T. Maeda, Y. Koyama, H. Murayama, H. Tanida, H. Arai, E. Matsubara, Y. Uchimoto, and Z. Ogumi*

- 636 Scanning Near-Field Infrared Microscopy of a  $\text{Li}_x\text{FePO}_4$  Single Particle  
*I. T. Lucas, J. S. Syzdek, S. F. Lux, N. S. Norberg, A. S. McLeod, Z. Fei, D. N. Basov, and R. M. Kostecki*
- 637 Nanoscale Single Crystal Electrochemistry as a Diagnostic Tool for Li-Ion Batteries  
*J. S. Syzdek, I. T. Lucas, J. Elangbam, A. Bagnato, and R. M. Kostecki*
- 638 In Situ TEM-EELS Studies of Degradation and Thermal Stability of High-Energy Cathodes for Li-Ion Batteries  
*F. Wang, S. Bo, L. Zhang, C. Ma, G. Clare, P. Khalifah, Y. Zhu, and J. Graetz*
- 639 In Situ TEM Studies of Capacity Fading Mechanisms of Nano-Structured Anode and Cathode for Lithium-Ion Battery  
*C. Wang, M. Gu, Z. Wang, X. Li, S. Hu, W. Xu, F. Gao, J. Liu, J. Zhang, S. Thevuthasan, and D. Baer*
- 640 In Situ Small-Angle Neutron Scattering Studies of Electrodes for Lithium-Ion Batteries  
*C. A. Bridges, X. Sun, J. Zhao, M. Paranthaman, and S. Dai*
- 641 Interest of Auger Electron Spectroscopy to Study Silicon Electrodes Used in Li-Ion Batteries  
*E. Radvanyi, E. De Vito, W. Porcher, and S. Jouanneau*
- 642 Local Probing of Activation Energy of Ionic Transport in Cathode Materials for Li-Ion Batteries  
*N. Balke, S. Kalnaus, S. Jesse, N. J. Dudney, C. Daniel, and S. Kalinin*
- 643 Use of In Situ XAS to Elucidate Surface Structural Changes and Capacity Loss during Electrochemical Cycling of nanoscale  $\text{LiCoO}_2$   
*C. J. Patridge, C. T. Love, and D. E. Ramaker*
- 644 Toward Safe and Long-Cycle Life Li-Ion Batteries: New Polyanion-Cathode and Their Reaction Mechanism  
*Y. Yang*
- 645 Bimetallic Sulfates  $\text{A}_x\text{M}_y(\text{SO}_4)_z \cdot x\text{H}_2\text{O}$  ( $\text{A} = \text{Li, Na}$  and  $\text{M} = 3\text{d Metal}$ ): New Electrode Materials for Li- and Na-Ion Batteries  
*M. Reynaud, M. Ati, M. Sougrati, B. Melot, G. Rousse, J. Chotard, and J. Tarascon*
- 646 Revisiting the Lithium Metal Borate ( $\text{LiMBO}_3$ ;  $\text{M} = \text{Fe, Mn, Co}$ ) Cathode Systems: Synthetic and Electrochemical Findings  
*Y. Yamashita, P. Barpanda, S. Chung, Y. Yamada, S. Nishimura, and A. Yamada*
- 647 Reaction Mechanism of Pyrophosphate Cathode Material  $\text{Li}_2(\text{Mn}_y\text{Fe}_{1-y})\text{P}_2\text{O}_7$   
*S. Nishimura, N. Furuta, D. Shimizu, P. Barpanda, Y. Yamada, and A. Yamada*
- 648 A Cooperative Mechanism for the Diffusion of  $\text{Li}^+$  Ions in  $\text{LiMgSO}_4\text{F}$   
*D. Marrocchelli, M. Salanne, and G. W. Watson*

- 649 Novel Electrode Materials for Li-Ion Batteries  
*M. Reddy and B. Chowdari*
- 650 Tracking Disorder in LiFePO<sub>4</sub> with Electrochemical Lithium Insertion/Extraction  
*C. T. Love, A. Korovina, D. E. Ramaker, and K. Swider-Lyons*
- 651 Distinct Configuration of Antisite Defects in Olivine Phosphates: Comparison between LiFePO<sub>4</sub> and LiMnPO<sub>4</sub>  
*S. Chung and S. Choi*
- 652 Rechargeable Batteries: From Hybrid Materials to Hybrid Electrodes and Devices  
*P. Gomez-Romero*
- 653 Novel Fabrication of Highly Conductive Titania/Carbon Electrodes for Lithium-Ion Batteries and Supercapacitors  
*M. J. Sussman and G. P. Demopoulos*
- 654 Improvement of Cycle Performance of Lithium-Ion Batteries at Elevated Temperature of 60°C Using Graphite Coated with Metal Oxide  
*N. Inoue, K. Kimura, S. Kataniwa, J. Momo, T. Moriwaka, M. Takahashi, and S. Yamazaki*
- 655 MXenes - A New Family of Two Dimensional Transition Metal Carbides Used as Intercalation Compounds  
*M. Naguib, J. Come, O. Mashtalir, V. Presser, P. Taberna, P. Simon, M. W. Barsoum, and Y. Gogotsi*
- 656 Characterization of Graphitic Nano-Onions as Lithium-Ion Anodes  
*J. D. Cardema, G. Radhakrishnan, and P. M. Adams*
- 657 Preparation of Reduced Graphene Oxide -Sn Composite Through Electroless Deposition and Its Use as an Anode Material in Lithium-Ion Battery  
*H. Noguchi, G. Kido, and W. Zhao*
- 658 Improved Electrochemical Performance of Graphite Negative Electrodes by Covalently Bound Surface Coatings  
*H. Meyer, T. Placke, S. Lux, F. Homeyer, F. Jöge, C. Engelhardt, M. Binnewies, K. Wirth, S. Passerini, and M. Winter*
- 659 Anion Intercalation into Graphitic Carbon from Ionic Liquid based Electrolytes for High Performance Dual-Ion Batteries  
*T. Placke, O. Fromm, R. Klöpsch, G. Schmülling, P. Bieker, S. Lux, H. Meyer, S. Passerini, and M. Winter*
- 660 Kinetic Behavior of Anion Intercalation into Graphite Electrodes in Organic Solutions  
*F. Sagane, K. Miyazaki, T. Fukutsuka, and T. Abe*
- 661 Carbon Coated  $\alpha$ -Fe<sub>2</sub>O<sub>3</sub> Nano-Particles as High Performance Anodic Material for Lithium-Ion Batteries  
*A. Brandt and A. Balducci*

- 662 Enhanced Electrochemical Ion Insertion/Extraction Reaction in Cyano-Bridged Coordination Polymer Electrodes for Rechargeable Battery  
*M. Okubo, Y. Mizuno, D. Asakura, T. Kudo, and H. Zhou*
- 663 Intercalation of  $\alpha$ -MnO<sub>2</sub> as Mg battery cathode  
*L. Chen, T. S. Arthur, R. Zhang, and F. Mizuno*
- 664 Towards the Development of Calcium-Ion Batteries  
*J. Rogosic and D. R. Sadoway*
- 665 Electrochemical Properties of Li<sub>5</sub>FeO<sub>4</sub>/C Composite Positive Electrode Materials  
*T. Okumura, M. Shikano, and H. Kobayashi*
- 666 New Fe-Based Oxyfluorides as Rechargeable Lithium-Ion Battery at High Voltage (Average > 3V vs. Li<sup>+</sup>/Li)  
*A. Demourgues, N. Penin, A. Wattiaux, D. Carlier-Larregaray, L. Bourgeois, E. Durand, A. Tressaud, H. Groult, D. Dambouronet, C. M. Julien, and K. Zaghib*
- 667 Splash Combustion Synthesis and Exploration of Lithium Metal Pyrophosphate (Li<sub>1</sub>{plus minus}y MP<sub>2</sub>O<sub>7</sub>) Cathodes  
*P. Barpanda, T. Ye, J. Lu, Y. Yamada, S. Chung, S. Nishimura, and A. Yamada*
- 668 Oxalic Dihydrazide Assisted Novel Combustion Synthesized Pyrophosphate Compounds for Rechargeable Batteries  
*N. Kalidoss, K. Nallathamby, and M. Minakshi*
- 669 LiTi<sub>2</sub>(PO<sub>4</sub>)<sub>3</sub>/Reduced Graphene Oxide Hybrids for High Performance Cathode Materials in Lithium-Ion Batteries  
*C. Lim, A. G Kannan, H. Lee, and D. Kim*
- 670 An Energy Storage Principle Delivered by Bipolar Porous Polymeric Frameworks  
*K. Sakaushi, G. Nickerl, F. Wissner, E. Hosono, H. Zhou, S. Kaskel, and J. Eckert*
- 671 LiNi<sub>1/3</sub>Mn<sub>1/3</sub>Co<sub>1/3</sub>O<sub>2</sub> Synthesized by Sol-Gel Method: Structure and Electrochemical Properties  
*A. M. Hashem, A. Abdel-Ghany, H. M. Abuzeid, H. Ehrenberg, A. Mauger, and C. M. Julien*
- 672 Electronic Properties of Olivine Materials for Positive Electrodes in Li-Ion Batteries  
*C. M. Julien, A. Mauger, K. Zaghib, and H. Groult*
- 673 LiMn<sub>y</sub>Fe<sub>1-y</sub>PO<sub>4</sub> Cathode Materials Grown by Hydrothermal Route: Structure and Morphology  
*M. Mathieu, J. Trottier, P. Hovington, A. Guerfi, K. Zaghib, M. Trudeau, A. Mauger, and C. M. Julien*
- 674 LiMn<sub>y</sub>Fe<sub>1-y</sub>PO<sub>4</sub> Cathode Materials Grown by Hydrothermal Route: Electrochemical Performance  
*J. Trottier, M. Mathieu, A. Guerfi, K. Zaghib, A. Mauger, and C. M. Julien*

- 675 Synthesis, Structural and Electrochemical Properties of  $\text{LiNi}_{1/3}\text{Mn}_{1/3}\text{Co}_{1/3}\text{O}_2$  Prepared by Sol-Gel Method Using Table Sugar as Chelating Agent  
*A. M. Hashem, H. M. Abuzeid, N. Kiziltas, M. Herklotz, H. Ehrenberg, A. Mauger, and C. M. Julien*
- 676 Surface and Bulk Properties of LiFePO<sub>4</sub>: The Magnetic Analysis  
*A. Mauger, H. Groult, K. Zaghib, and C. M. Julien*
- 677 MnO<sub>2</sub> Nano-Rods Prepared by Redox Reaction as Cathodes in Lithium Batteries  
*A. M. Hashem, H. M. Abuzeid, A. Abdel-Latif, H. Abbas, H. Ehrenberg, S. Indris, A. Mauger, and C. M. Julien*
- 678 Orthorhombic MoO<sub>3</sub> Nanofibers as Cathode Materials for Li Batteries  
*C. V. Ramana, A. M. Hashem, H. Groult, A. Mauger, and C. M. Julien*
- 679 Carbon-Coated Nano-Structured MoO<sub>3</sub> as Cathode Materials for Lithium Batteries: Synthesis, Structure and Electrochemical Performance  
*C. V. Ramana, H. Groult, A. Mauger, and C. M. Julien*
- 680 Single Crystal  $\text{Li}_{1.2}\text{Mn}_{0.56}\text{Ni}_{0.12}\text{Co}_{0.12}\text{O}_2$  Hexagonal Nanoplates with Lateral {010} Facets Exposed as cathode of Lithium-Ion Batteries with Excellent Cycleability  
*F. Fu, Y. Deng, X. Li, J. Li, L. Huang, and S. Sun*
- 681 Synthesis and Electrochemical Characterization of Carbonophosphates; A New Family of Intercalation Compounds Discovered by Ab Initio Computing  
*I. L. Matts, H. Chen, G. Hautier, and G. Ceder*
- 682 Improved Initial Coulombic Efficiency of Spinel Battery Cathode by Fluorine-Doping  
*J. Kim, C. Nguyen, Y. Bae, K. Lee, J. Song, J. Min, H. Ko, T. Kim, Y. Paik, and S. Song*
- 683 Investigation on the (de)Lithiation Mechanism of Li<sub>2</sub>MoO<sub>3</sub>  
*J. Lee, S. Kim, J. Kim, and G. Ceder*
- 684 Cathode Properties of P-Doped Li<sub>2</sub>MnO<sub>3</sub>  
*H. Komaki, A. Kitajo, and S. Okada*
- 685 Synthesis and Electrochemical Performance of a Lithium-Transition Metal-Fluoride as a New Cathode Material for Lithium-Ion Batteries  
*N. Twu, L. Liu, and G. Ceder*
- 686 The Electrical Properties of Amorphous TiO<sub>2</sub>-B Prepared from Lepidocrocite Type Precursors as an Anode Material in Lithium-Ion Battery  
*Y. Furuya, T. Iida, and H. Noguchi*
- 687 Structural and Magnetic Studies on Initial Cycling of Li-Excess Type Layered Rock-Salt Oxide Cathode  
*T. Nakamura, K. Nakao, H. Takahara, H. Yashiro, Y. Oka, and Y. Yamada*

- 688 Relation between Synthesis Conditions and Electrochemical Properties of Lithium Excess Li-Ni-Mn-O Compounds  
*H. Yamada, M. Oyama, H. Nakamura, and H. Noguchi*
- 689 Facile Synthesis of FeF<sub>3</sub> and Its Application to Positive Electrode for Rechargeable Lithium Batteries  
*S. Myung, S. Kim, and Y. Hitoshi*
- 690 Electrochemical Properties of Mg<sub>0.22</sub>MnO<sub>2</sub> as a Cathode Material for Mg Rechargeable Batteries  
*T. Kakibe, K. Miyazaki, T. Fukutsuka, T. Abe, and Y. Uchimoto*
- 691 Micro-Sized NaNi<sub>0.5</sub>Mn<sub>0.5</sub>O<sub>2</sub> Layered Materials as a Cathode Material for Rechargeable Na Batteries  
*M. Jang, S. Myung, S. Oh, and Y. Sun*
- 692 Crystal and Electronic Structures of Layered Li<sub>2</sub>MnO<sub>3</sub>-LiMO<sub>2</sub> Materials during Stepwise Pre-Cycling Treatment  
*H. Kobayashi, T. Okumura, M. Shikano, Y. Arachi, and H. Nitani*
- 693 LiCoO<sub>2</sub> Cathode Nanosheets with Enlarged Surface Area Induced by Hydrothermal Process  
*K. Fung, C. Ni, C. Liu, and S. Tsai*
- 694 Diffusion of Lithium-Ion and Polaron in Pyrophosphate Li<sub>2</sub>FeP<sub>2</sub>O<sub>7</sub>:First-Principles Study  
*Y. Asari, Y. Suwa, and T. Hamada*
- 695 Crystal Structure and Electrochemical Properties of Ni-Substituted Li<sub>2</sub>CuO<sub>2</sub> as a Positive Electrode  
*T. Ide, T. Nakagawa, Y. Arachi, and Y. Nakata*
- 696 Synthesis and Electrochemical Property of CuO-Containing Li<sub>2</sub>MnO<sub>3</sub>  
*S. Akiyama, Y. Arachi, K. Hinoshita, and Y. Nakata*
- 697 Kinetics and Stability Studies on Li<sub>1+x</sub>M<sub>1-x</sub>O<sub>2</sub> Single Crystals  
*H. Duncan, B. Hai, A. K. Shukla, and G. Chen*
- 698 Stability and Performance of High-Voltage Cathodes with Pure and Doped Lipon Coatings  
*Y. Kim, N. J. Dudney, M. Chi, G. M. Veith, S. K. Martha, and J. Nanda*
- 699 Controlled Synthesis of High Tap Density LiMn<sub>1.5</sub>Ni<sub>0.5</sub>O<sub>4</sub> with Tunable Shapes  
*A. Cao and A. Manthiram*
- 700 Impact of LiMn<sub>1.5</sub>Ni<sub>0.5</sub>O<sub>4</sub> Crystal Surface Facets  
*G. Chen, B. Hai, A. K. Shukla, and H. Duncan*
- 701 Unique Electrochemical Cycling Behaviour of Structurally Integrated Layered-Spinel Lithium Nickel Manganese Oxides  
*A. W. Rowe, C. L. White, and J. Dahn*

- 702 Fabrication of Hollow Wires of  $\text{LiNi}_{0.5}\text{Mn}_{1.5}\text{O}_4$  and 0.5  $\text{Li}_2\text{MnO}_3$ -0.5  $\text{LiNi}_{1/3}\text{Co}_{1/3}\text{Mn}_{1/3}\text{O}_2$  by the Electrospinning Method  
*E. Hosono, T. Saito, Y. Mizuno, M. Okubo, D. Nishio-Hamane, T. Kudo, and H. Zhou*
- 703 Microstructural Comparison of  $\text{LiNi}_{0.5}\text{Mn}_{1.5}\text{O}_4$  After 1000 Cycles  
*X. Song, Y. Fu, and V. Battaglia*
- 704 Electrochemistry Driven Structural Transition in High Voltage Lithium-Rich Composite Cathodes  
*S. K. Martha, J. Nanda, W. Zhou, J. Idrobo, and N. J. Dudney*
- 705 5-V System  $\text{LiMn}_{1.5-x}\text{Ni}_{0.5-y}\text{M}_{x+y}\text{O}_4$  for High-Energy Lithium Batteries: Post-Annealing and Coating Effect  
*D. Liu, A. Guerfi, P. Hovington, J. Trottier, M. Dontigny, J. Hamel-Paquet, M. Trudeau, A. Vijh, A. Mauger, C. Julien, and K. Zaghib*
- 706 Effect of the Crystal Chemistry of  $\text{LiNi}[1/2]\text{Mn}[3/2]\text{O}[4]$  Spinels On Its Electrochemical Properties  
*C. Kim, M. Leskes, E. Castillo, C. P. Grey, and J. Cabana*
- 707 Do You Really Want an Unsafe Battery  
*R. A. Huggins*
- 708 Reaction Mechanism of  $\text{Li}_x\text{FePO}_4$  Analyzed by Potential-Step Chronoamperometry  
*G. Oyama, Y. Yamada, S. Nishimura, and A. Yamada*
- 709 Iron substitution to increase energy density of lithiated phosphates  
*L. Daniel, S. Martinet, T. Gutel, C. Bourbon, E. Radvanyi, M. Amuntencei, and S. Patoux*
- 710 Synthesis and Morphology Control of Novel Nanostructured  $\text{LiFePO}_4$  Cathode Materials for Li-Ion Battery  
*O. Ayyad and P. Gomez-Romero*
- 711 Electrochemical Kinetics Studies on  $\text{LiMn}_{1-x}\text{Fe}_x\text{PO}_4$  during Lithium Insertion and Extraction  
*K. Hoshina, H. Inagaki, N. Takami, H. Munakata, and K. Kanamura*
- 712 Chemically Partly Delithiated Lithium Manganese Phospho Olivines: Investigations of Lattice and Atomic Structure and Electrochemistry  
*M. Köntje, G. Greco, P. Axmann, and M. Wohlfahrt-Mehrens*
- 713 Tailored Electrode Morphologies for Insertion Electrodes  
*M. Wagemaker, D. Singh, A. George, J. ten Elshof, and F. Mulder*
- 714 Measuring Electrode Tortuosity and Optimizing Electrode Performance  
*R. D. Deshpande, S. Harris, and V. Battaglia*

- 715 Vitreous Materials as Electrodes for Lithium Batteries  
*G. Delaizir, V. Seznec, P. Rozier, P. Lecante, C. Surcin, P. Salles, and M. Dollé*
- 716 Surface Coating of Vanadium Pentoxide Nanowires for Improved Cathodic Stability  
*F. Gittleson, J. Hwang, R. C. Sekol, and A. D. Taylor*
- 717 Structural and Electrochemical Characterization of Thermally Treated Vanadium Oxide Nanotubes for Li-Ion Batteries  
*D. McNulty, D. Buckley, and C. O'Dwyer*

**B5 - Interfaces and Interphases in Battery Systems**

*ECS Battery, ECS Energy Technology, ECSJ Battery*

- 718 Studies on Reactions and Structures at Electrode/Electrolyte Interface Using Epitaxial Model Electrodes  
*R. Kanno, M. Hirayama, and K. Tamura*
- 719 In Situ XAS and XRD Studies on Electrode/Electrolyte Interface of  $\text{Li}_x\text{CoO}_2$  Thin-Film Electrode  
*D. Takamatsu, S. Mori, K. Shimada, Y. Oriksa, T. Kawaguchi, H. Murayama, T. Hirano, M. Sato, H. Tanida, Y. Koyama, H. Arai, E. Matsubara, Y. Uchimoto, and Z. Ogumi*
- 720 Revealing Positive Electrode Oxide Changes on Electrochemical Cycling by In Situ Electron Microscopy  
*D. J. Miller, C. Proff, J. Wen, and D. P. Abraham*
- 721 Lithium Depletion in the Solid Electrolyte Adjacent to Cathode Materials  
*H. Yamada, K. Suzuki, Y. Oga, I. Saruwatari, and I. Moriguchi*
- 722 Advanced Characterization and First Principles Modeling of Surface and Interfaces of Lithium Intercalation Compounds  
*Y. Meng*
- 723 Electrochemical Impedance Analysis and Applications of Porous Electrodes for Lithium-Ion Batteries  
*N. Ogihara, Y. Itou, S. Kawauchi, C. Okuda, Y. Takeuchi, and Y. Ukyo*
- 724 In Situ Atomic Force Microscopy Studies of Surface Layer Formation on  $\text{LiMn}_2\text{O}_4$  Thin Films  
*N. Missert, R. Garcia, and J. M. Rivera*
- 725 The Effect of  $\text{ZrO}_2$  Coating on Nano Size  $\text{LiCoO}_2$  Cathode for Lithium-Ion Batteries  
*Y. Kusachi, T. Shimizu, Y. Oriksa, and Y. Uchimoto*
- 726 Phosphate-Based Additives for High Voltage Li-Ion Batteries and Their Derivatives  
*A. V. Cresce and K. Xu*

- 727 Two-Layer/Two-Mechanism Model of Li-Ion Diffusion in Solid Electrolyte Interphase  
*S. Shi, Y. Qi, P. Lu, Z. Liu, L. G. Hector Jr., and S. J. Harris*
- 728 Effect of Graphite Orientation on Solid-Electrolyte-Interphase Formation and Characterization  
*M. Tang, K. Miyazaki, J. Newman, and T. Abe*
- 729 Real-Time Dynamics during Recharging Cycles  
*J. Keist, B. El Dasher, S. Torres, J. W. Evans, P. K. Wright, F. Ross, D. Steingart, and C. Orme*
- 730 Simultaneous Coupling of Kinetic Monte-Carlo Simulations with Continuum Models to Examine Capacity Fade  
*P. Northrop, R. Braatz, and V. Subramanian*
- 731 Diffusion Limitations of the Liquid Metal Battery  
*G. A. Thompson, S. A. Barriga, U. P. Muecke, and D. R. Sadoway*
- 732 Ionic and Electronic Transport in Metal Fluoride Conversion Electrodes  
*J. Graetz, F. Wang, Y. Zhu, H. Yu, A. Van Der Ven, K. Thornton, N. Pereira, and G. G. Amatucci*
- 733 In Situ Neutron Reflectometry Analysis of  $\text{Li}_4\text{Ti}_5\text{O}_{12}$ /Electrolyte Interface Using Two-Dimensional Model Electrode  
*M. Hirayama, K. Suzuki, K. Kim, S. Taminato, R. Kanno, N. Yamada, and M. Yonemura*
- 734 Electrode Architectures for Conversion-Based Cathodes: Case of Iron Fluorides and Oxyfluorides  
*S. K. Martha, J. Nanda, J. Idrobo, S. Pannala, S. Dai, N. J. Dudney, J. Wang, and P. V. Braun*
- 735 Time-Dependent Determination of HF Formation in  $\text{LiPF}_6$ -Containing Electrolytes by Spectroscopic Ellipsometry  
*S. F. Lux, I. T. Lucas, J. Chevalier, T. J. Richardson, and R. M. Kostecki*
- 736 In Situ ECAFM and Raman Study on Interfacial Reactions between Graphite and PC-Based Solutions in Lithium Secondary Batteries  
*S. Jeong, H. Song, T. Abe, M. Inaba, and Z. Ogumi*
- 737 Polyimide Gel Polymer Electrolyte-Directed Nanoscale Wrapping of High-Voltage  $\text{LiNi}_{1/3}\text{Co}_{1/3}\text{Mn}_{1/3}\text{O}_2$  Cathode Active Materials for Lithium-Ion Batteries  
*J. Park, J. Cho, and S. Lee*
- 738 In Situ Raman Imaging Applied to the Observation of Li Transport in a  $\text{LiCoO}_2$  Cathode  
*T. Nishi, H. Nakai, and A. Kita*
- 739 In Situ Electrochemical X-ray Absorption Spectroscopy of Mg Deposition  
*T. S. Arthur, P. Glans-Suzuki, M. Matsui, R. Zhang, J. Guo, and F. Mizuno*

- 740 In Situ Observation of Sn Thin-Film Anode / Electrolyte Interface by X-ray Reflectivity  
*K. Shimada, T. Kawaguchi, T. Ichitsubo, E. Matsubara, K. Fukuda, Y. Uchimoto, and Z. Ogumi*
- 741 Spectroscopic and Spectrometric Studies of the SEI and Its Interaction with Anode Electrode Surfaces  
*A. A. Gewirth, H. Tavassol, B. R. Long, J. W. Buthker, and L. Huff*
- 742 Porous Silicon Impregnated Carbon Nano-Spheres for S-Block Metal Ion Battery Negative Electrodes  
*S. Polisski and T. Abe*
- 743 Study on Solid Electrolyte Interphase Layer on Si Anode by Surface Modification  
*C. Jung, W. Jeon, H. Han, H. Choi, and S. Jeong*
- 744 Inelastic Shape Changes in Contacting Silicon Particles and Binder Failure in Composite Lithium-ion-battery Electrodes  
*H. wang, V. A. Sethuraman, P. R. Guduru, and V. B. Shenoy*
- 745 Studies of Interfacial Reactions on Silicon-Based Film Electrode in Ionic Liquid Battery Electrolyte  
*C. Nguyen, S. Woo, and S. Song*
- 746 Mechanism of SEI Layer Formation on the Si Electrodes Studied by XPS and ToF-SIMS  
*C. Pereira-Nabais, J. Swiatowska, A. Chagnes, P. Tran-Van, M. Cassir, and P. Marcus*
- 747 In Situ Stress Measurements in Composite Lithium-Ion-Battery Electrodes during Charge/Discharge Processes  
*V. A. Sethuraman, A. Nguyen, S. P. Nadimpalli, D. P. Abraham, A. F. Bower, V. B. Shenoy, and P. R. Guduru*
- 748 Interface Modification for Advanced 5V-Class All-Solid-State Lithium Batteries  
*A. Omori, C. Yada, H. Yamasaki, F. Sagane, and Y. Iriyama*
- 749 Reduction of the Interfacial Resistance at the Li<sub>7</sub>La<sub>3</sub>Zr<sub>2</sub>O<sub>12</sub>/LiCoO<sub>2</sub> by Interface Modification  
*T. Kato, T. Hamanaka, F. Sagane, K. Yamamoto, T. Hirayama, and Y. Iriyama*
- 750 Enhanced Electrochemical Properties of Li<sub>4</sub>Ti<sub>5</sub>O<sub>12</sub> Epitaxial Thin Film Electrode with Surface Modification  
*K. Kim, K. Suzuki, S. Taminato, K. Tamura, J. Mizuki, J. Son, M. Hirayama, and R. Kanno*
- 751 Silicon and Porous Silicon/Carbon Nanocomposites for Rechargeable Li- and Mg-Ion Batteries  
*S. Polisski and T. Abe*

- 752 Effects of Initial Charging Temperature on Electrochemical Properties if Solid Electrolyte Interphase Formed upon Graphite Anodes  
*J. Choi, T. Lee, S. Kim, J. Ko, and Y. Lee*
- 753 Interfacial Reaction on Li<sub>3</sub>PO<sub>4</sub>/Li<sub>2</sub>RuO<sub>3</sub> Thin-Film Electrode  
*S. Taminato, K. Suzuki, K. Kim, J. Son, K. Tamura, J. Mizuki, M. Hirayama, and R. Kanno*
- 754 Fundamental Investigations of Mechanical and Chemical Degradation Mechanisms in Lithium-Ion Battery Materials  
*V. A. Sethuraman, V. B. Shenoy, A. F. Bower, L. Wang, B. L. Lucht, A. Bose, W. Euler, and P. R. Guduru*
- 755 Capacity Fading Mechanism of Graphite Negative-Electrodes in Electrolytes Containing Trialkyl Phosphates  
*H. Nakagawa, M. Ochida, S. Tsubouchi, Y. Domi, T. Yamanaka, T. Doi, T. Abe, and Z. Ogumi*
- 756 Depth-Resolved X-ray Absorption Spectroscopic Study on Nanoscale Observation of the Electrode-Electrolyte Interface for All Solid State Lithium-Ion Batteries  
*T. Ina, T. Okumura, T. Nakatsutsumi, Y. Orikasa, H. Arai, Y. Iriyama, T. Uruga, H. Tanida, Z. Ogumi, and Y. Uchimoto*
- 757 In Situ Analysis of Interfacial Reactions between Edge Plane Graphite Negative-Electrodes and EC-Based Electrolyte Solutions  
*T. Doi, Y. Domi, H. Nakagawa, S. Tsubouchi, M. Ochida, T. Yamanaka, T. Abe, and Z. Ogumi*
- 758 Ultrafast Laser Spectroscopy of Electrode/Electrolyte Interfaces  
*J. S. Syzdek, V. Zorba, X. Mao, R. E. Russo, and R. M. Kostecki*
- 759 Effects of Electrolyte Additives on the Suppression of Mn Deposition on the Edge Plane of HOPG for Lithium-Ion Battery  
*M. Ochida, S. Tsubouchi, H. Nakagawa, Y. Domi, T. Yamanaka, T. Doi, T. Abe, and Z. Ogumi*
- 760 Studies of Interfacial Processes of Lithium-Ion Batteries by In Situ Fourier Transform Infrared Spectroscopy  
*J. Li, X. Zheng, H. Su, X. Zeng, L. Huang, and S. Sun*
- 761 Materials Design and Analysis of Electrode/Solid Electrolyte Interface by In Situ Methods  
*Y. Iriyama*
- 762 Investigation of the Solid Electrolyte Interphase (SEI) with Pre-Lithiated Graphite  
*N. J. Dudney, L. A. Adamczyk, R. R. Unocic, G. M. Veith, P. Ganesh, and P. R. Kent*

- 763 Transport Properties and Chemical Stability of LISICON-Based Glass Ceramics in Contact with Lithium  
*P. Hartmann, M. Reich, T. Leichtweiss, M. Schneider, W. Schmidbauer, and J. Janek*
- 764 Bias Imposed Interface between Solid Li-Ion Conductor LiBH<sub>4</sub> and Li Metal: First Principles Molecular Dynamics Simulations  
*T. Ikeshoji, E. Tsuchida, M. Otani, S. Takagi, M. Matsuo, and S. Orimo*
- 765 Investigation of the Interface Between Li<sub>2</sub>S-P<sub>2</sub>S<sub>5</sub> Solid Electrolyte and Li Metal Electrode by Using Electrochemical Methods with Microelectrodes  
*M. Chiku, W. Tsujiwaki, E. Higuchi, and H. Inoue*
- 766 Studies on the Formation and Stability of Solid Electrolyte Interphase on the Surface of Anode and Cathode of Lithium-Ion Batteries  
*X. Yu, H. Li, K. Xu, K. Nam, H. Lee, X. Huang, L. Chen, A. von Cresce, and X. Yang*
- 767 Artificial Solid Electrolte Interface (SEI) for Improving Cycle-Ability on Lithium-Ion Battery  
*F. Wang*
- 768 Ultrathin Multifunctional Coatings as the Artificial Solid Electrolyte Interphases to Improve Performance of Lithium-Ion Batteries  
*X. Xiao, D. Ahn, P. Lu, and M. W. Verbrugge*
- 769 Li-Ion Transfer at the Interface between Solid Electrolyte/Ionic Liquid  
*Y. Ishihara, K. Miyazaki, T. Fukutsuka, T. Abe, and Z. Ogumi*
- 770 Atomistic Mechanisms of the Phase Boundary Evolution during Initial Lithiation into Crystalline Silicon  
*S. Kim, D. Datta, M. J. Chon, V. A. Sethuraman, P. R. Guduru, and V. B. Shenoy*
- 771 In Situ Optical Microscopic Observation of Lithium Electrodeposited in Room Temperature Ionic Liquids Containing Quaternary Ammonium Cation  
*H. Sano, H. Sakaebi, and H. Matsumoto*
- 772 Analytical Studies of Flow Battery Redox Reaction Electrokinetics on a Thin Fiber Film Rotating Disk Electrode  
*K. L. Hawthorne, J. S. Wainright, and R. F. Savinell*

## B6 - Lithium-Ion Batteries

*ECS Battery, ECS Energy Technology, ECSJ Battery, CSE, KECS*

- 773 Phase Transition Behavior of LiFePO<sub>4</sub> Based Cathode Materials  
*Y. Zhou, X. Wang, X. Yu, K. Nam, E. Hu, J. Liu, and X. Yang*
- 774 Multi-Scale, Multiphase Mathematical Modeling of LiFePO<sub>4</sub> Cathodes  
*T. W. Farrell and S. Dargaville*

- 775 Phase Transition Study of LiFePO<sub>4</sub> Nanowires in Li-Ion Battery  
*J. Niu, A. Kushima, L. Qi, J. Huang, and J. Li*
- 776 Thermal Stability of Binary Olivine Li<sub>1-y</sub>Fe<sub>1-x</sub>Mn<sub>x</sub>PO<sub>4</sub> [0 ≤ x, y ≤ 1] for Li Rechargeable Battery  
*J. Kim, K. Park, I. Park, J. Yoo, J. Hong, and K. Kang*
- 777 A Novel Double-Structured LiMn<sub>0.85</sub>Fe<sub>0.15</sub>PO<sub>4</sub>: LiFePO<sub>4</sub> Core-Shell Materials for Rechargeable Lithium-Ion Batteries  
*S. Oh, S. Myung, J. Park, B. Scrosati, K. Amine, and Y. Sun*
- 778 3D Nanoporous Current Collectors for Advanced Thin Film Microbatteries  
*S. Gowda, A. Reddy, and P. Ajayan*
- 779 High Energy Cells: Lithium-Sulfur and Lithium-Sulfur-Silicon  
*M. Hagen, S. Dörfler, E. Quiroga-González, H. Althues, J. Tübke, and H. Föll*
- 780 Effect of Initial Sulfur Morphology on Capacity and Cycle-Life of Lithium-Sulfur Batteries  
*H. Jha, A. Eberle, S. Eckstein, H. A. Gasteiger, C. Poggi, and O. Gröger*
- 781 Large Self-Weaving Sulfur-MWCNT Composite Cathodes for High Rate Lithium-Sulfur Batteries  
*Y. Su and A. Manthiram*
- 782 Hollow Carbon Balls-Sulfur Composite in Advanced Configuration Lithium Battery  
*D. Lee, J. Hassoun, J. Park, B. Scrosati, and Y. Sun*
- 783 Experimental Observation of Coherent Strain Effects on Phase Separation in LiFePO<sub>4</sub> Electrode  
*K. Tokuda, T. Kawaguchi, T. Ichitsubo, E. Matsubara, K. Fukuda, Y. Uchimoto, and Z. Ogumi*
- 784 Hydro Thermal Synthesized LiFePO<sub>4</sub> Modified by Li<sub>4</sub>P<sub>2</sub>O<sub>7</sub> and Carbon Coatings  
*J. Chong, S. Xun, X. Song, G. Liu, and V. Battaglia*
- 785 Comparison of Charge Transfer Resistance for Different LiFePO<sub>4</sub>-Electrodes  
*J. Illig, M. Ender, and E. Ivers-Tiffée*
- 786 A Comparative Study on A<sub>2</sub>MnPO<sub>4</sub>F (A = Na and Li) Cathodes for Rechargeable Batteries  
*S. Kim, D. Seo, H. Kim, K. Park, H. Kim, and K. Kang*
- 787 Olivine Type Cathodes for Stationary Lithium-Ion Batteries  
*D. Choi, Y. Choi, Q. Huang, W. Wang, J. Liu, J. Zhang, L. Pederson, and V. Sprenkle*
- 788 Nanosized Effect on Charge-Discharge Property of LiMnPO<sub>4</sub> Embedded in Porous Carbons  
*S. Aono, K. Urita, H. Yamada, and I. Moriguchi*

- 789 Synthesis and Characterization of Hybrid Organic-Inorganic Composite Electrodes for Li-Based Batteries  
*C. M. Lopez, P. Sánchez-Fontecoba, S. Pérez-Villar, V. Roddatis, and T. Rojo*
- 790 Modeling Failure due to Redistribution in Lithium-metal Batteries  
*A. Ferrese and J. Newman*
- 791 Solid State Fluoride Ion Batteries  
*A. Munnangi, R. Witter, and M. Fichtner*
- 792 Rechargeable, Lithium-ion Molten Salt Battery for High Temperature Applications  
*J. Caja, T. J. Dunstan, and M. Caja*
- 793 Fabrication of  $\text{Li}_{1+x}\text{Ti}_{2-x}\text{O}_4$  Electrode for All-Solid-State Lithium-Ion Rechargeable Batteries Using a Novel Flux Coating Method  
*H. Kojima, K. Teshima, H. Wagata, Y. Mizuno, and S. Oishi*
- 794 In Operando, Naked, and Hot: High Temperature Batteries Without Packaging  
*C. F. Petersburg, K. Bogaert, and F. M. Alamgir*
- 795 (ECS Battery Division Research Award) High Capacity Intercalation Materials for Li-Ion and Na-ion Batteries  
*S. Passerini*
- 796 Improvement of Battery Performances of  $\text{LiCoPO}_4$  as Cathode Material for Lithium Ion Batteries  
*J. Yoshida, S. Nakanishi, and H. Iba*
- 797 Combined First-Principle Calculations and Experimental Study of Doping Effect in  $\text{LiFe}_{0.95}\text{M}_{0.05}\text{PO}_4$  ( $\text{M} = \text{Na, Mg, Zn, Mn, Ni}$ )  
*Z. Wang, L. Yuan, and Y. Huang*
- 798 Lithium Iron Phosphate Wired by Carbon Nanotubes for High Rate Capability Lithium-ion Batteries  
*A. J. Bhattacharyya and M. Gnanavel*
- 799 Rapid Charge and Discharge Property of High Capacity Lithium Ion Battery applying 3D-Patterned Electrode  
*M. sanada, K. Furuichi, K. Teraki, T. Matsuda, K. Hiramatsu, D. Ueda, A. Izumi, H. Munakata, and K. Kanamura*
- 800 Advances in 3D Lithium Battery Technology  
*J. Prochazka*
- 801 High Power 3D Lithium Battery  
*J. Prochazka*
- 802 Lithium Ion Batteries: 3-D Multi-scale Tomography  
*F. Tariq, P. Shearing, V. Yusuf, J. Gelb, R. Bradley, P. Withers, and N. Brandon*

- 803 Effect of Binder Distribution in LIB Electrode on Mass Transport Performance  
*G. Inoue, T. Matsuoka, Y. Matsukuma, and M. Minemoto*
- 804 Synthesis of  $0.5\text{Li}_2\text{MnO}_3 \bullet 0.5\text{LiMO}_2$  (M = Mn, Ni, Co) Layered-Layered Integrated Cathode Electrode Materials with Mechanochemical Process  
*S. Kim, K. Chung, and B. Cho*
- 805 Composition Optimization of  $x\text{Li}_2\text{MnO}_3 \cdot (1-x)\text{LiMO}_2$  Electrodes (M= Mn, Ni, Co) Prepared via Spray Pyrolysis Process  
*M. Lengyel, X. Zhang, G. Atlas, D. Elhassid, I. Belharouak, and R. Axelbaum*
- 806 Structure Evolution and Its Relation to the Voltage Fade Behavior in Li-Rich Layered  $\text{Li}_{1.2}\text{Ni}_{0.15}\text{Co}_{0.1}\text{Mn}_{0.55}\text{O}_2$  Cathode Material during Cycling: X-ray Diffraction and Absorption Spectroscopy Study  
*X. Yu, K. Nam, E. Hu, D. P. Abraham, and X. Yang*
- 807 Effect of Precursor Synthesis Atmosphere on Morphology and Electrochemical Performance of  $\text{Li}_{1.20}\text{Ni}_{0.16}\text{Mn}_{0.56}\text{Co}_{0.8}\text{O}_2$  and  $\text{Li}_{1.17}\text{Ni}_{0.25}\text{Mn}_{0.58}\text{O}_2$   
*J. Camardese, R. Shunmugasundaram, and J. Dahn*
- 808 Synthesis and Morphological Analysis of Carbonate Based Precursors for Lithium-Ion Battery Cathode Materials  
*R. Shunmugasundaram, T. Byrne, and J. Dahn*
- 809 Development of All-Solid-State Lithium-Ion Rechargeable Battery Using Quasi-Solidified Glyme - Li-Salt Complexes as Electrolytes  
*A. Unemoto, T. Matsuo, Y. Gambe, and I. Honma*
- 810 Nanocrystalline Solid Electrolyte:  $\beta\text{-Li}_3\text{PS}_4$   
*Z. Liu, W. Fu, Z. Lin, N. J. Dudney, E. Payzant, and C. Liang*
- 811 Development of Li-Ion Technology Based on Aqueous Electrolytes  
*S. Martinet, L. Crepel-Marchal, F. Alloin, and J. Lepretre*
- 812 Topological Analysis of Lithium Migration Paths: Application to Solid Electrolytes  
*L. Miara, M. Aryanpour, S. Ong, Y. Mo, G. Ceder, and H. Lee*
- 813 The Effect of Microstructure on the Lithium Ion Conduction of the  $\text{LiBH}_4\text{-LiI}$  Solid Solution  
*D. Sveinbjornsson, D. Blanchard, M. Mogensen, P. Norby, and T. Vegge*
- 814 The Effect of  $\text{LaMeO}_3$  as Stabilizer Phase in  $0.5[\text{Li}_{0.33}\text{Mn}_{0.67}]\text{O}_2 \bullet 0.5\text{Li}[\text{Ni}_{0.33}\text{Co}_{0.33}\text{Mn}_{0.33}]\text{O}_2$  Cathode Material  
*M. Kim, K. Park, J. Yoon, M. Park, J. Park, W. Yoon, and S. Doo*
- 815 Effect of Carbon Coating on  $\text{Li}[\text{Li}_{1/3}\text{Mn}_{2/3}]\text{O}_2\text{-LiMO}_2$  Cathode Materials for Lithium Ion Batteries  
*Y. Wu, X. Wang, and Z. Liu*

- 816 Transition Metal Dissolution on Mixed LiNi<sub>1/3</sub>Co<sub>1/3</sub>Mn<sub>1/3</sub>O<sub>2</sub>-LiMn<sub>2</sub>O<sub>4</sub> Cathodes for Li-ion Batteries  
*L. Liu, A. Drews, and R. Kudla*
- 817 Optimizing LiNi<sub>1/3</sub>Mn<sub>1/3</sub>Co<sub>1/3</sub>O<sub>2</sub> Capacity by Controlling Cathode Porosity through Calendering  
*J. Li, J. Kiggans, C. Daniel, and D. L. Wood*
- 818 Root Cause for Rapid Growth of Cell Impedance in Li-Ion High Energy Cells Having Overlithiated Cathodes and Graphite Negatives  
*C. Ma, R. Staniewicz, B. Deveney, S. Hafner, R. Bugga, W. C. West, M. C. Smart, and J. Soler*
- 819 Structure Studies of Reaction Mechanism for Surface-Modified LiNi<sub>1/3</sub>Co<sub>1/3</sub>Mn<sub>1/3</sub>O<sub>2</sub> Epitaxial Thin-Film Electrode  
*M. Abe, K. Suzuki, H. Minamishima, M. Hirayama, R. Kanno, K. Tamura, and J. Mizuki*
- 820 Improvement of Elevated Temperature Performance of Li-Rich Cathode Material with Ionic Liquids Electrolyte for Lithium-Ion Batteries  
*J. Li, S. Jeong, R. Klöpsch, M. Winter, and S. Passerini*
- 821 Electrochemical Intercalation of Lithium-Ion in Propylene Carbonate Based Electrolytes — Effect of Addition of Bivalent-Ions —  
*S. Takeuchi, F. Sagane, K. Miyazaki, T. Fukutsuka, and T. Abe*
- 822 Investigation of Temperature Dependent Stability of Ethylene Carbonate and Propylene Carbonate in multicomponent Electrolytes for Lithium Ion batteries  
*C. L. Foss, A. Svensson, E. Sheridan, S. Sunde, and F. Vullum-Bruer*
- 823 Advanced Electrolytes for Lithium Ion Batteries in High Voltage Systems  
*J. Li and M. Payne*
- 824 Examination of Applying Fluorinated Phosphate Ester to Electrolyte Solvent of the Batteries with LiNi<sub>0.5</sub>Mn<sub>1.5-x</sub>TixO<sub>4</sub> Cathode  
*T. Noguchi, M. Uehara, Y. Katoh, H. Sasaki, and K. Utsugi*
- 825 Effect of Electrolyte Solvents on Low-Temperature Performance of Li-Ion Batteries  
*J. Eom, L. Cao, and C. Wang*
- 826 Influences of Molecular Interactions on Battery Electrolyte Properties and Processes  
*K. L. Gering*
- 827 Novel IL Based Electrolytes for Secondary Lithium Ion Batteries  
*H. Srour, H. Rouault, and C. Santini*
- 828 (ECS Battery Division Technology Award Presentation) Case Studies in Developing Battery Technologies  
*Y. Chiang*

- 829 Relaxation Phase Analysis for Li inserted Li-Mn-O Cathode Material  
*I. Seo, S. Park, and T. Yao*
- 830 Study on the Transport Properties of  $\text{LiNi}_{0.8}\text{Co}_{0.15}\text{Al}_{0.05}\text{O}_2/\text{LiMn}_2\text{O}_4$  Blends with Different Compositions  
*H. Tran, C. Taeubert, and M. Wohlfahrt-Mehrens*
- 831 Structural Modification and Electrochemical Characteristics of Co-substituted Hollandite-type Manganese Oxides using a Hydrothermal Method  
*Y. Kadoma, H. Watanabe, K. Ui, and N. Kumagai*
- 832 Conformal Electrodeposition of Copolymer Electrolyte into Self-Organized Titania Nanotubes for Lithium Ion Microbatteries  
*T. Djenizian*
- 833 Gelled Polymer Electrolyte Thin Films with Mechanical Integrity and Persistent Structure for Lithium Ion Batteries  
*S. Wang, C. Huang, P. Kuo, and H. Teng*
- 834 Intensive Dry and Wet Mixing Enhancing the Electrochemical Performance of Secondary Lithium-Ion Battery Electrodes  
*H. Bockholt, L. Kleinfeldt, W. Haselrieder, and A. Kwade*
- 835 Structure, Disorder, and Crystallization; Lessons Learned from Analysis of Lithium Trifluoromethanesulfonate  
*M. P. Foley, C. Worosz, L. M. Haverhals, K. Sweely, W. A. Henderson, H. De Long, and P. Trulove*
- 836 Synthesis and Characterization of Ionic Liquid for Lithium-Ion Batteries  
*X. Sun, C. Liao, and S. Dai*
- 837 Flux Growth of High-Quality  $\text{LiCoO}_2$  Crystals for All-Crystal-State Lithium-Ion Rechargeable Batteries  
*Y. Mizuno, H. Wagata, T. Ishizaki, T. Sakaguchi, K. Kohama, K. Yubuta, T. Shishido, S. Oishi, and K. Teshima*
- 838 The effects of Carbon Additive on Electrochemical Performance of High Voltage Spinel  $\text{LiNi}_{0.5}\text{Mn}_{1.5}\text{O}_4$   
*J. Zheng, J. Xiao, W. Xu, X. Li, and J. Zhang*
- 839 First Principles Calculation of Electronic Structures and Thermal Stability of Spinel  $\text{LiNi}_2\text{O}_4$   
*A. Kuwabara, C. Fisher, Y. Ikuhara, H. Moriwake, H. Oki, and Y. Ikuhara*
- 840 Investigations of the Phase Diagram of the Lithium-Manganese-Nickel Oxide System obtained at 800°C  
*E. McCalla and J. Dahn*

- 841 Production of Manganese Oxide Nanowire Powders and Their Characterization for Li Ion Batteries and Capacitors  
*V. Vendra, A. Thapa, S. Sunkara, T. Nguyen, and M. K. Sunkara*
- 842 Designing Long-Life, High Energy Lithium-Ion Cells  
*D. P. Abraham, Y. Li, M. Bettge, and Y. Zhu*
- 843 Electrochemical Characterization of Semi-Solid Li-Ion Electrodes  
*N. Baram, W. Carter, and Y. Chiang*
- 844 Influence of Anode/Cathode Balancing on Cycling Stability of Lithium Ion Cells  
*M. D. Wilka, A. Hoffmann, R. Stern, and M. Wohlfahrt-Mehrens*
- 845 Evaluation of Effective Electrical Conductivity of Carbon Electrode with Porous Metal Collector  
*G. Inoue, S. Abe, Y. Fan, Y. Matsukuma, and M. Minemoto*
- 846 VGCF Cloth for Thin, Flexible Electrodes for Advanced Conformal Batteries  
*D. J. Burton, N. J. Dudney, G. Nazri, S. K. Martha, G. Nazri, and J. Howe*
- 847 Effects of Volume Expansion and Fluid-Solid Stress Interaction within Lithium-Ion Batteries  
*C. Zhang, A. Conlisk, G. Rizzoni, and J. Marcicki*
- 848 Preparation and Electrochemical Performances of Sn<sup>4+</sup> Doped V<sub>2</sub>O<sub>5</sub> as Cathode material for Li Ion Battery  
*Y. Li and G. Cao*
- 849 V2O5 Network Structure as Cathode for Lithium Ion Batteries  
*Y. Xu, M. Dunwell, and H. Luo*
- 850 Developing 1400 Wh/kg Graphene-V2O5 Aerogel Composites as Cathodes for Li-Ion Batteries  
*Q. Liu, Y. Liu, and J. Xie*
- 851 Synthesis of FeOF Using Roll-Quench Method and the Charge-Discharge Mechanism  
*A. Kitajou, R. Nagano, and S. Okada*
- 852 Investigation of Graphite Foil as Current Collector for Cathodes of Li-Ion Batteries  
*B. Ziv, O. Haik, E. Zinigrad, M. Levi, D. Aurbach, and I. C. Halalay*
- 853 Electrochemical Properties of C<sub>60</sub> Coated Silicon Nanowires as Anodes in Lithium Secondary Batteries  
*A. Arie and J. Lee*
- 854 In Situ TEM Studies of Silicon Nanostructures for Li-Ion Batteries  
*K. Karki, C. Sun, E. Epstein, J. Cho, T. Picraux, C. Wang, Y. Wang, and J. Cumings*

- 855 Silicon Nitride Thin Film Electrode for Lithium-Ion Batteries  
*N. Suzuki, R. B. Cervera, T. Ohnishi, and K. Takada*
- 856 Investigation on Si Anode Materials for Lithium-Ion Batteries Using X-ray Absorption Spectroscopy  
*X. Yu, K. Nam, C. Ma, E. Hu, Y. Zhou, H. Li, and X. Yang*
- 857 Negatively and Positively Nanopatterned Silicon for Use in Lithium-ion Batteries  
*S. Nam, D. Park, J. Lee, J. Lee, and W. Kim*
- 858 Retardation of Phase Transformation of  $\text{Li}_x\text{CoO}_2$  in Fast Discharge  
*T. Kawaguchi, T. Ichitsubo, E. Matsubara, Y. Uchimoto, and Z. Ogumi*
- 859 Low Temperature Synthesis of Manganospinel Based Cathodes for Li-ion Batteries  
*X. Hao and B. Bartlett*
- 860 Effects of Heat Treatment on the Electrochemical Performance of  $\text{LiNi}_{0.5}\text{Mn}_{1.5}\text{O}_4$  Cathode Materials via Spray Pyrolysis Method  
*J. Shiu, W. Pang, and S. Wu*
- 861 Electrochemical Properties of High-Voltage  $\text{LiNi}_{0.5}\text{Mn}_{1.5}\text{O}_4$  and High-Capacity  $\text{Li}_{1.5}\text{Ni}_{0.25}\text{Mn}_{0.75}\text{O}_{2.5}$  Blends  
*X. Zhang, L. Li, and I. Belharouak*
- 862 Combined In Situ X-ray Absorption Spectroscopy and First-Principle Calculation Studies on Local Structural and Electronic Structural Alternations of  $\text{LiNi}_{1/3}\text{Co}_{1/3}\text{Mn}_{1/3}\text{O}_2$   
*H. Imai, K. Kubobuchi, M. Mogi, M. Matsumoto, M. Nishijima, T. Yamamoto, T. Matsumoto, and Y. Nitta*
- 863  $^6\text{Li}$  NMR Spectroscopic Investigation on Local Structures and Battery Properties of  $\text{Li}_2\text{MnO}_3$  Cathode Materials  
*H. Imai, K. Hashi, T. Sanada, K. Kamiguchi, A. Ito, M. Watanabe, K. Kubobuchi, M. Mogi, M. Matsumoto, N. Chiba, S. Ohki, T. Shimizu, M. Hatano, and T. Matsumoto*
- 864 Impact of the Calendering Process on the Interfacial Structure and the Related Electrochemical Performance of Secondary Lithium-Ion Battery Electrodes  
*W. Haselrieder, H. Seeba, and A. Kwade*
- 865 Si-C and  $\text{SiO}_x$  Versus Lithium Metal Anodes for High-Energy Rechargeable Batteries  
*A. Guerfi, D. Leblanc, P. Hovington, M. Lagacé, J. Trottier, J. Hamel-Paquet, M. Dontigny, A. Vijh, and K. Zaghib*
- 866 Implementation and Characterization of Silicon Anode with Metal Alloy Inactive Matrix for Lithium-Ion Secondary Batteries  
*C. Lee, S. Kwon, J. Kim, S. Suh, J. Cho, J. Moon, J. Choi, S. Kang, and Y. Kim*
- 867 First Principles Studies of the Electrochemical Lithiation and Delithiation of Crystalline Silicon  
*M. K. Chan, C. Wolverton, and J. Greeley*

- 868 Novel Nanostructured Si anode Behavior on Nanorod Array Polymer Substrate  
*M. Jung, M. Moon, Y. Joo, and I. Choi*
- 869 Well Controlled Array of Si Nanopillar with Metal Core as Negative Electrode for Lithium Ion Batteries  
*T. Oguri, R. Tajima, T. Osada, T. Muraoka, M. Kurata, S. Sasagawa, S. Adachi, T. Takeuchi, T. Kakehata, J. Momo, T. Moriwaka, M. Takahashi, and S. Yamazaki*
- 870 Cycling Behavior of a High Voltage Spinel Using an Original Three Electrodes  
 $\text{Li}_{1-x}\text{Ni}_{0.4}\text{Mn}_{1.6}\text{O}_4/\text{Li}/\text{LiNi}_{0.4}\text{Mn}_{1.6}\text{O}_4$  Symmetric Cell: Application to  
 $\text{LiNi}_{0.4}\text{Mn}_{1.6</s}$  Symmetric Cell: Application to  $\text{LiNi}_{0.4}\text{Mn}_{1.6}\text{O}_4$  Electrolyte Interface Degradation Studies  
*J. Demeaux, M. Caravanier, H. Galiano, B. Montigny, and D. Lemordant*
- 871 A Study of the High Rate Performance Polypyrrole-TiC Nanocomposite Anode Materials for Lithium-ion Battery  
*Y. Weng and N. N. Wu*
- 872 Enhanced High Temperature Stability of  $\text{LiMn}_2\text{O}_4$  Cathodes by Prussian Blue Coatings  
*C. Chen and K. Chiu*
- 873 Spinel Manganese Based Cathode Materials: A Thermal Stability Study  
*S. El Khakani and D. MacNeil*
- 874 Effect of Cr-Oxide Partial Coating on the Electrochemical Behavior of Thin Film High-Voltage Spinel  
*E. Garcia Tamayo, J. Ros, A. Kaas, R. Fredon, and E. M. Kelder*
- 875 Carbon - Silicon Nanocomposite Anodes for Lithium-Ion Batteries  
*G. Y. Yushin*
- 876 Thin-film Nanoporous Silicon Coated with PEO Polymer Electrolyte for Lithium-Ion Battery Anodes  
*C. R. Becker, J. Read, J. Wolfenstine, J. Allen, and C. Lundgren*
- 877 Real-Time Measurements of Stress and Damage Evolution during Initial Electrochemical Lithiation and Delithiation of Crystalline Silicon  
*M. Chon, V. A. Sethuraman, and P. R. Guduru*
- 878 High Performance Silicon Freestanding Anodes Fabricated by Low Pressure and Plasma-Enhanced Chemical Vapor Deposition onto Carbon Nanotube Electrodes  
*M. W. Forney, R. DiLeo, A. Raisanen, M. Ganter, J. Staub, R. Rogers, and B. Landi*
- 879 Impact of Electrolytes on Solid Electrolyte Interphase (SEI) Formation and Electrochemical Performance of a Silicon Anode in Lithium-Ion Cells  
*J. J. Wu*
- 880 TEM Study of Surface Region of Sol-Gel Coated Cathode Materials for Li Ion Battery  
*N. Taguchi, H. Sakaebi, T. Akita, T. Takeuchi, K. Tatsumi, and Z. Ogumi*

- 881 Electronic and Transport Properties of High-Capacity Silicate Cathode Materials for Li-Ion Batteries  
*R. Longo Pazos, K. Xiong, and K. Cho*
- 882 High-Performance Lithium-ion Battery Cathodes Based on Porous FeF<sub>3</sub> Nanowires  
*L. Li and S. Jin*
- 883 Scale Bridging via Surrogate Modeling for Multi-Scale Analysis of Li-Ion Cathodes  
*W. Du, N. Xue, A. Sastry, J. Martins, and W. Shyy*
- 884 Metal Oxide/Graphene Hybrid Nanostructured Electrodes for High Performance Lithium Batteries  
*H. Gullapalli, A. Reddy, and A. Pulickel*
- 885 Thermal Aging on the Cycleability of Cells Made of {LiMn<sub>1/3</sub>Ni<sub>1/3</sub>Co<sub>1/3</sub>O<sub>2</sub> + LiMn<sub>2</sub>O<sub>4</sub>} Composite Electrodes  
*B. Lochner, E. Wong, M. Dubarry, C. Truchot, B. Liaw, K. L. Gering, S. V. Sazhin, D. Jamison, and C. Michelbacher*
- 886 Electrochemical Characterization of Sn as an Alternative Anode Material in Li-Ion Batteries  
*D. X. Liu, J. Black, and A. Co*
- 887 R<sub>t</sub>qf w<sub>v</sub>q<sub>p</sub>"qh'EwUp"Vj kp Films qp Eqr r gt Uwdutcvg Xlc'Grgetqp'Dgco 'F gr qu<sub>k</sub>q<sub>p</sub>"Vgej pls wg  
*B. Polat, N. Sezgin, O. Keles, K. Kazmanli, A. Abouimrane, and K. Amine*
- 888 Investigating the Performance of Si- and Sn-Based Anode Materials in Electrovaya's Lithium Ion SuperPolymer Cells  
*L. Davis and R. DasGupta*
- 889 Large Scale Production of Titanate and Tin Oxide Nanowire Powders and Arrays for Anodes  
*A. K. Thapa, T. Nguyen, V. Vendra, G. Sunkara, and M. K. Sunkara*
- 890 Porous SnO<sub>2</sub> Helical Nanotubes and Sheets for Lithium-Ion Batteries  
*H. Luo, L. Fei, and Y. Xu*
- 891 XPS Depth Profiling of Tin Anodes for Lithium Ion Batteries  
*J. M. Black and A. Co*
- 892 Feedback Controlled Multistage Constant Current (FCMCC) Charging Protocol for Improving Performance on Lithium-Ion Battery  
*H. Wang, Y. Chen, and F. Wang*
- 893 The Effect of Oxy-Nitride Formation in Lithium-Ion Conductivity for LiMe(Ge, Si and Ti)PS  
*S. Lee, D. J. Kalita, S. Woo, K. Lee, and Y. Yoon*
- 894 Investigation of High-Temperature Endurance Test for Lithium-Ion Batteries in Vehicles  
*K. Maeda, K. Komatsu, and M. Takahashi*

- 895 Electron Energy Loss Structures in the Oxygen *K*-edge Spectra of Li-Inserted  $\text{Li}_4\text{Ti}_5\text{O}_{12}$   
*M. Kitta, T. Akita, S. Tanaka, and M. Kohyama*
- 896 Synthesis and Electrochemical Properties of Carbon-Coated  $\text{Li}_2\text{FeP}_2\text{O}_7$  for Li-Ion Batteries  
*M. Saito, S. Yano, A. Tasaka, and M. Inaba*
- 897 Structure-Related Electrochemistry of Sulfur-Poly(Acrylonitrile) Composite Cathode Materials for Rechargeable Lithium Batteries  
*J. Fanous, M. Wegner, J. Grimminger, M. Rolff, Å Andresen, and M. Buchmeiser*
- 898 Electrochemical Properties and Morphology of  $\text{Li}[\text{Fe}_{1-x}\text{Mn}_x]\text{PO}_4$  ( $x = 0, 0.1, 0.3$ ) Cathode Materials by Electrospinning Process  
*C. Kang, C. Kim, G. Yoo, and J. Son*
- 899 Structural-Tunable Graphene Anode via Controlling Oxidation Processes for Li-Ion Batteries Applications  
*W. Liu, S. Kuo, Y. Chen, and H. Wu*
- 900 Improvement of Tap Density of  $\text{TiO}_2(\text{B})$  Powder as High Potential Negative Electrode  
*Y. Nakano, M. Takagi, N. Honda, M. Saitou, A. Tasaka, and M. Inaba*
- 901 The Binary  $\text{Li}_4\text{Ti}_5\text{O}_{12}$ - $\text{Li}_2\text{Ti}_3\text{O}_7$  Nanocomposite as Anode for Improving the SOC Estimation of Li-Ion Batteries  
*G. Zhu and Y. Xia*
- 902 Electrochemical Test Cell Using Diamond Windows for In Situ XRD Measurement  
*S. Kawasaki, A. Alzubaidi, Y. Ishii, and T. Matsushita*
- 903 Improvement of Electrochemical Properties of Silicon Negative Electrode Prepared with Polyimide Binder  
*S. Uchida, M. Mihashi, M. Yamagata, and M. Ishikawa*
- 904 Correlation between Polydopamine Coating Effects and Separator-Types for High Power Lithium Ion Batteries  
*Y. Lee, M. Seo, B. Kim, M. Ryou, J. Choi, and Y. Lee*
- 905 Surface Modification of  $\text{Li}[\text{Ni, Co, Mn}]\text{O}_2$  Cathode Using  $\text{FeF}_3$  Coating  
*C. Kim, S. Kim, and Y. Park*
- 906 Electrochemical Properties of Graphite-Silicon Milled Nanocomposite as a Lithium Battery Anode Material  
*K. Kang, D. Shin, Y. Lee, and K. Kim*
- 907 Which One is the More Severe Test Method, Cycling or Storage at High Temperatures?  
*H. Lee, J. Jeong, B. Son, J. Choi, Y. Kim, and Y. Lee*
- 908 Study on Phase Transformation Characteristics of  $\text{LiFePO}_4$  during Charge-Discharge Process of Graphite/Lithium Iron Phosphate Battery  
*Y. Lou, Q. Wang, J. Zhang, C. Yang, and B. Xia*

- 909 Poly(Hydroquinone) Cathodes for a Sustainable Lithium-Ion Battery  
*K. Takeshi, J. Kadokawa, and H. Morioka*
- 910 TiO<sub>2</sub>/Marimo Carbon Composite as a New Material for Lithium Ion Battery  
*K. Iwasawa, S. Ueda, M. Eguchi, Y. Kobayashi, M. Kobori, M. Nishitani-Gamo, and T. Ando*
- 911 Effect of Ionic Liquid Electrolytes on Anode Properties of LaSi<sub>2</sub>/Si Composite Thick-Film Electrodes for Li-Ion Battery  
*M. Shimizu, H. Usui, and H. Sakaguchi*
- 912 Sandwiched MWCNT@TiO<sub>2</sub>-C Nanocables for Ultrafast Lithium Storage  
*J. Cheng and J. Kerr*
- 913 Modified SiO as a High Performance Anode for Li-Ion Batteries  
*Y. Hwa, C. Park, and H. Sohn*
- 914 Simple Preparation of Nanoporous Si/C Composites with Naphthalene for Li-Ion Batteries  
*B. Yu and H. Sohn*
- 915 Enhanced Electrochemical Performance of LiFePO<sub>4</sub> Cathode Material Promoted by CdO and Carbon Co-Coating  
*G. Peng, X. Yang, G. Liang, and L. Zhang*
- 916 Sub-Nano Tunnel-Structured Manganese Oxide Exhibiting Extremely Large Reversible Lithium Storage  
*D. Yonekura, Y. Igarashi, M. Hiraga, N. Ota, J. Miyamoto, and K. Naoi*
- 917 Nanohybridization of nc-SnO<sub>2</sub> with Hollow-Structured Carbon for High Performance Li-Ion Battery Anode  
*K. Kisu, M. Iijima, Y. Nagano, J. Miyamoto, and K. Naoi*
- 918 Cycling Stability of Li<sub>2</sub>MnO<sub>3</sub> Composite Materials by Co-Precipitation for Lithium Ion Battery  
*K. Kim, J. Kang, D. Chang, and K. Kim*
- 919 Electrochemical Performance of Li-Rich Based Cathode Materials for Lithium Ion Battery  
*K. Kim, J. Kang, S. Boo, and K. Kim*
- 920 High-Rate Capability of Hollow Carbon Microspheres as Anode Materials for Lithium-Ion Batteries  
*J. Hwang, H. Lim, T. Kang, Y. Sun, and K. Suh*
- 921 Hollow Fe<sub>3</sub>O<sub>4</sub> Microspheres as Anode Materials for Lithium-Ion Batteries  
*H. Lim, Y. Sun, and K. Suh*
- 922 Facile Synthesis of a Unique Interleaved Graphene-Embedded Sulfur Nanocomposite as Cathode of Li-S Batteries with Excellent Lithium Storage Performance  
*Y. Wang, L. Huang, Y. Xu, J. Li, and S. Sun*

- 923 In-situ Separating Layer Coating upon the Wire-type Electrode for Flexible Lithium Batteries  
*K. V. Luu, Y. Lee, S. Song, C. Kim, and Y. Lee*
- 924 Improvement of High-Capacity Behavior of Layered  $\text{Li}_{1.23}\text{Ni}_{0.13}\text{Co}_{0.14}\text{Mn}_{0.56}\text{O}_2$  Cathodes by Fluorine Substitution for Li-Ion Batteries  
*J. Min, J. Gim, J. Song, J. Kim, and W. Im*
- 925 First-Principles Study of K-edge XANES for Li-Rich Solid-Solution Layered Cathode Material  
*T. Tamura, R. Kobayashi, S. Ogata, T. Ohwaki, A. Ito, and Y. Ohsawa*
- 926 Novel 3-Dimensional Electrochemical Energy Storage Systems  
*F. Roumi, C. Cid, J. Roumi, and M. Hoffmann*
- 927 Highly Interconnected Silicon Nanowires Embedded in Porous Graphite as Anodes in Li-ion Batteries  
*S. Jeong, J. Lee, D. Yoon, H. Hwang, J. Kim, S. Kim, H. Sun, S. Park, and J. Cho*
- 928 A Study on Structural and Electrochemical Properties of Overcharged Ni-based Cathode Materials for Li-Ion Batteries  
*W. Chang, D. Kim, H. Chang, B. Cho, J. Lee, and K. Chung*
- 929 Anode Performance of Ni-P-coated Si Thick-film Electrodes for Li-ion Battery  
*M. Narita, H. Usui, N. Uchida, and H. Sakaguchi*
- 930 Electrochemical Property of Anderson-Type Polyoxometalates as Cathode Material of Lithium Battery  
*S. Uematsu, E. Ni, and N. Sonoyama*
- 931 Microstructure Study of Si Thin Film Anode with Different Adhesion Layers for Li-Ion Batteries  
*M. Oh, Y. Song, T. Yoon, C. Woo, J. Jeong, H. Lee, and S. Hyun*
- 932 Hydrothermal Synthesis of  $\text{LiCoPO}_4$  in the Presence of Carboxymethylcellulose  
*Y. Namiki, H. Munakata, and K. Kanamura*
- 933 Fabrication of  $\text{Li}_7\text{La}_3\text{Zr}_2\text{O}_{12}$ -Based All-Solid-State Rechargeable Li-Metal Battery  
*J. Wakasugi, T. Nishioka, H. Munakata, and K. Kanamura*
- 934 Preparation and Conductivity of Novel Ionic Liquid using Dianionic Hexacoordinated Silicates  
*M. Nanjo, Y. Nakano, and T. Esaka*
- 935 Structure and Electrochemical Properties of Oxygen-Deficient  $\text{Li}_2\text{MnO}_{3-x}$   
*K. Kubota, M. Hirayama, R. Kanno, M. Yonemura, Y. Imanari, K. Nakane, M. Cuisinier, N. Dupré, and D. Guyomard*

- 936 A Study on the Thermal Behavior of LiMnPO<sub>4</sub> Cathode for Li Secondary Battery by Using Synchrotron Based X-ray Techniques  
*H. Kim, J. Kim, S. Lee, D. Jang, S. Muhammad, W. Yoon, Y. Choi, and K. Park*
- 937 Analysis of Solid Electrolyte Interphase by Glow Discharge Optical Emission Spectroscopy for Li-Ion Battery Electrodes  
*H. Takahara, H. Miyauchi, H. Kobayashi, Y. Kobayashi, and T. Nakamura*
- 938 Investigation of the Irreversible Reaction Mechanism on SiO Anode Material for Li-Ion Batteries  
*H. Yamamura, K. Nobuhara, S. Nakanishi, and H. Iba*
- 939 SiOx Nanoparticles Preparation by an Evaporation and Condensation Process Using Induction Melting  
*J. Kim, B. Jang, and J. Lee*
- 940 Copper Nanofiber-embedded Cobalt Oxide Thin-Film for High Performance Lithium-Ion Batteries  
*D. Park, S. Nam, J. Lee, J. Lee, and W. Kim*
- 941 LiMPO<sub>4</sub> (M = Fe, Mn) for High Energy Rechargeable Lithium Battery by Solid State Reaction  
*T. Mahara, H. Miyauchi, H. Tomita, and Y. Sakaguchi*
- 942 Surface Modified High Capacity Li-Excess Transition Metal Oxide by Metal Phosphates  
*J. Lim, J. Yeon, S. Lee, H. Sun, and H. Lee*
- 943 Morphological, Structural and Electrochemical Study of Layered-Spinel Mixed Structure of Li-Mn-Ni-O as Cathode for Lithium ion Batteries  
*Y. Hwang, J. Choi, M. Christy, A. Zahoor, S. Park, P. Kim, and K. Nahm*
- 944 Density Functional Theory Studies of Lithium Diffusion on the Step Edge of Graphene Sheets  
*Y. Kubota*
- 945 Novel Flux Growth of Li<sub>1+x</sub>Mn<sub>2-x</sub>O<sub>4</sub> Crystals and Films for All-Crystal-State Lithium Ion Rechargeable Batteries  
*H. Wagata, H. Inagaki, T. Ishizaki, T. Sakaguchi, K. Kohama, S. Oishi, and K. Teshima*
- 946 Electrochemical Fabrication of Si Nanoparticles on Carbon Nanofiber for High Capacity Anodes of Lithium Ion Battery  
*S. Choi, S. Woo, J. Park, S. Hwang, and D. Whang*
- 947 Lithium Extraction Reaction for the Thin Films of Titanium Dioxide under UV Irradiation  
*S. Suzuki and M. Miyayama*
- 948 Structural Analysis and Electrochemical Property of Trance Metal Substituted Calcium Ferrite-Type Li(Mn<sub>x</sub>M<sub>1-x</sub>)<sub>2</sub>O<sub>4</sub> (M= Ni, Ti)  
*M. Mamiya, K. Kataoka, J. Akimoto, S. Kikuchi, Y. Terajima, and K. Tokiwa*

- 949 Graphene Oxide: Corrosion Inhibitor on LIB Cathode Current Collector  
*R. Prabakar and M. Pyo*
- 950 Silicon Nanowires Prepared by Zinc-Thermal Reduction of Silicon Tetrachloride and Their Application to Lithium Ion Batteries  
*R. han, M. Yamagata, T. Nohira, R. Hagiwara, and M. Ishikawa*
- 951 LiNi<sub>0.6</sub>Co<sub>0.2</sub>Mn<sub>0.2</sub>O<sub>2</sub>/LiMn<sub>0.8</sub>Fe<sub>0.2</sub>PO<sub>4</sub> Blends as Cathode Materials for High Energy Density Li Ion Battery  
*G. Choi, N. Kim, H. Lim, and S. Cho*
- 952 A Study on Synthesis and Properties of Nano-Sized Metal Oxide Coated on Carbonnanotubes  
*Y. Kim, J. Yoon, A. Choi, S. Choi, K. Palanisamy, and W. Yoon*
- 953 Electrochemical Performance of LiNi<sub>0.5</sub>Mn<sub>1.5</sub>O<sub>4</sub> Cathode Material Fabricated from Nanothorn Sphere Structured MnO<sub>2</sub>  
*S. Lim, W. Ryu, W. Kim, and H. Kwon*
- 954 Electrochemical Characteristics of Structure-modified Soft Carbon as an anode in Lithium Ion Batteries  
*Y. Jo, E. Lee, H. Jeong, Z. Lee, K. Hong, S. Lee, and Y. Kim*
- 955 Exploration of Manganese Oxide Based Cathodes for Alkali Metal Ion Batteries  
*X. Hao and B. Bartlett*
- 956 Electrochemical Lithiation and Delithiation of Stoichiometric Cu<sub>3</sub>Sn and Cu<sub>6</sub>Sn<sub>5</sub> Prepared Using Reduction-Diffusion Method  
*N. Fukuda, A. Kitada, K. Murase, T. Ichii, and H. Sugimura*
- 957 Preparation of LiNi<sub>0.5</sub>Ni<sub>1.5</sub>O<sub>4</sub> Cathode Material through Spray Drying Assisted Annealing Process and Its Electrochemical Performance  
*J. Li, M. Lu, X. Liao, and Z. Ma*
- 958 Highly Dispersed Sulfur in Porous Aromatic Framework as Cathode for Lithium-Sulfur Batteries  
*B. Guo, X. Sun, and S. Dai*
- 959 In-Plane Ionic Conductivity of Li(3x)La(2/3-x)TiO<sub>3</sub> Thin Films Deposited on Perovskite Substrates  
*F. Aguesse, T. Rojo, and J. A. Kilner*
- 960 Structural and Electrochemical Studies of Mesoporous Li<sub>4</sub>Ti<sub>5</sub>O<sub>12</sub>-TiO<sub>2</sub> Composite Spheres as Anode Material for Lithium Ion Batteries  
*S. Ting, C. V. Li, and K. Chan*
- 961 Method for Mitigating the Effects of Manganese Dissolution in Li-Ion Batteries  
*N. Levi, M. Levi, D. Aurbach, Z. Li, L. Zou, T. Fuller, and I. C. Halalay*

- 962 Local Structure Investigations on  $\text{Li}[\text{Li}_{0.2}\text{Mn}_{0.4}\text{Co}_{0.4}]\text{O}_2$  via In Situ X-ray Absorption Spectroscopy  
*R. Kloepsch, J. Rana, J. Li, G. Schumacher, J. Banhart, S. Passerini, and M. Winter*
- 963 Electrochemical Properties of Silicon 1D Nanostructures Prepared by Means of Electrochemical Deposition  
*D. Kim, H. Seo, and Y. Kang*
- 964 Capacity Fading Research on High Voltage Spinel  $\text{LiNi}_{0.5}\text{Mn}_{1.5}\text{O}_4$  Coupled with Graphite  
*Y. Fu, X. Song, P. Ridgway, G. Liu, and V. Battaglia*
- 965 Development of Thin Films Si Based Anode Materials for  $\text{Li}^+$  Ion Batteries Application  
*S. T. Hossain and S. Mitra*
- 966 Stabilized Lithium Metal Powder (SLMP®) - Performance Improvement of Silicon Based Anodes  
*B. Fitch, Y. Li, and M. Yakovleva*
- 967 Cu-Sn Thin Film Production on Copper Substrate  
*B. Polat, N. Sezgin, O. Keleş, K. Kazmanlı, A. Abouimrane, and K. Amine*
- 968 Use of Cu-Sn/C Multilayered Thin Film in Lithium Ion Batteries  
*B. D. Polat, N. Sezgin, O. Keleş, K. Kazmanlı, A. Abouimrane, and K. Amine*
- 969 The Synthesis and Electrochemical Characterization of Tin Encapsulated by Highly Graphitic Carbon Nanospheres as Anodes for Li-Ion Batteries  
*K. A. Hays, M. Li, K. Osea-Kwapong, R. P. Kopreski, N. A. Banek, and M. Wagner*
- 970 In Situ Energy Dispersive X-ray Diffraction Study of Prototype  $\text{LiMnO}_4$  and  $\text{LiFePO}_4$ -Based Coin Cell Batteries  
*G. Liang, M. Croft, and Z. Zhong*
- 971 Hollow Carbon Nanosphere with Germanium Nanoparticles Anode Material for Li-ion Battery  
*M. Li, K. Hays, R. P. Kopreski, N. Banek, and M. Wagner*
- 972 The Synthesis and Electrochemical Characterization of Silicon Encapsulated by Highly Graphitic Carbon Nanospheres as Anodes for Li-ion Batteries  
*R. P. Kopreski, K. Hays, M. Li, N. A. Banek, and M. Wagner*
- 973 Preparation of Manganese Oxide Cathodes for Lithium Secondary Batteries  
*J. Moon, H. Munakata, and K. Kanamura*
- 974 Structural and Optical Properties Study of Porous Silicon Membrane Filled with Lithium Bromide  
*M. Jaouadi, M. Khardani, W. Dimassi, and H. Ezzaouia*

- 975 Synthesis of Coherent SnO<sub>2</sub>/Carbon Cryogel Nanocomposites at Large-Scale for Efficient Lithium Ion Storage  
*M. Zhang, L. Shen, E. Uchaker, T. Wang, and G. Cao*
- 976 Mesoporous Thin Films: Model Structures to Assess the Role of Porosity in Composite Electrodes  
*N. Krins, R. Buonsanti, A. K. Shukla, G. Chen, B. Helms, D. Milliron, and T. J. Richardson*
- 977 Effects of Maleic Anhydride Electrolyte Additive on Silicon Anode for Lithium-Ion Battery  
*M. Suguro, M. Yamashiro, K. Nakahara, and K. Nakano*
- 978 Cycle Life Characterization of Lithium-Ion Batteries with Artificial Solid-Electrolyte Interphase Coating on Both Electrodes  
*Y. Eun, S. Woo, D. Kim, and W. Lee*
- 979 Long-term Cycling of High Energy Li-Ion Battery with NCM Electrode and High Voltage Electrolyte  
*W. Zhang, G. Liu, and V. Battaglia*
- 980 Electrochemical Properties of Delithiated Li<sub>2</sub>MnO<sub>3</sub>-LiMO<sub>2</sub>  
*S. Yamahara, A. Mineshige, Y. Daiko, and T. Yazawa*
- 981 Direct Observation of Battery Reaction Inhomogeneity in Operating Electrode  
*H. Murayama, T. Fujimoto, T. Kawaguchi, Y. Orikasa, H. Arai, E. Matsubara, Y. Uchimoto, and Z. Ogumi*
- 982 The Effects of the Slurry Mixing Procedure on Silicon Based Composite Electrodes for Li-Ion Batteries  
*M. Wu, K. Eberman, and G. Liu*
- 983 LiFePO<sub>4</sub> Cathode Materials prepared by Spray Pyrolysis and Its Electrical Characteristics as a Cathode Material  
*C. Lee, S. Eun, and S. Kim*
- 984 Fabrication of NCM (LiNi<sub>x</sub>Co<sub>y</sub>Mn<sub>z</sub>O<sub>2</sub>)Cathode Materials Prepared by Spray Pyrolysis  
*J. Park, C. Lee, and S. Kim*
- 985 Synthesis and Performance of Anode Material Li<sub>4</sub>Ti<sub>5</sub>O<sub>12</sub> by Sol-Gel Method for Lithium Ion Batteries  
*B. Na and S. Kim*
- 986 Encapsulation of Rechargeable Solid-State Lithium Batteries  
*J. Ribeiro, R. Sousa, J. Sousa, B. Pereira, M. Silva, L. Goncalves, M. M. Silva, and J. Correia*
- 987 Influence of Fe<sup>3+</sup> Ions Content for Electrochemical Properties of Nano-Sized Phospho-Olivine as Cathode Material for Li-Ion Batteries  
*D. Baster, W. Zajac, and J. Molenda*

- 988 Ac Impedance Analysis of Low Frequency Region for Commercial Lithium Ion Battery under Temperature Control  
*D. Mukoyama, T. Yokoshima, H. Nara, T. Momma, and T. Osaka*
- 989 AC Impedance Study of the Active Materials Reactions in a Three Electrode Lithium-Ion Secondary Cell  
*O. S. Mendoza, Y. Nishikawa, H. Ishikawa, Y. Sone, and M. Umeda*
- 990 Direct Determination of the Thickness and Composition of Electrode-Electrolyte Interface during Electrochemical Reaction  
*G. M. Veith, J. Browning, L. Baggetto, W. E. Tenhaeff, J. Keum, and N. J. Dudney*
- 991 Chronopotentiometric Investigation of Anode Deterioration in Lithium-Ion Secondary Cell Incorporating Reference Electrode  
*O. S. Mendoza, H. Ishikawa, Y. Nishikawa, Y. Maruyama, Y. Sone, and M. Umeda*
- 992 In Situ Detection of Lithium Plating on Graphite Electrodes Using Electrochemical Microcalorimetry  
*L. E. Downie, V. L. Chevrier, J. Dahn, and L. J. Krause*
- 993 A Novel Green Approach to Synthesis of  $\text{Li}_4\text{Ti}_5\text{O}_{12}$  Nanoparticulate Anode material  
*H. Chiu and G. P. Demopoulos*
- 994 Limitation of Rate Capability of  $\text{Li}_4\text{Ti}_5\text{O}_{12}$  Single-Particle  
*K. Dokko, K. Yoshida, R. Nozawa, and M. Watanabe*
- 995 Carbon Free  $\text{Li}_4\text{Ti}_5\text{O}_{12}$  Electrode with Exceptionally High Electrode Capacity and Outstanding Rate Capability  
*M. Song, A. Benayad, Y. Choi, J. Choi, and K. Park*
- 996 Microwave-Induced Solid-State Synthesis of  $\text{Li}_4\text{Ti}_5\text{O}_{12}$  Nanocrystallites with Enhanced Lithium-Storage Properties  
*Y. Qiao, X. Hu, Y. Liu, and Y. Huang*
- 997 Relaxation Behavior of  $\text{Li}_{4/3}\text{Ti}_{5/3}\text{O}_4$  Electrode for Li-ion Secondary Battery  
*S. Park, S. Uraki, and T. Yao*
- 998 Thermal and Electrical Characterization of Nonflammable Electrolytes\* in 18650 Full Cells  
*G. Nagasubramanian, K. Fenton, and C. Orendorff*
- 999 Safety and Long-Term Performance of Lithium-Ion Cells in a Pouch Format  
*J. A. Jeevarajan*
- 1000 Electrochemical-Calorimetric Studies on Safety Fundamentals of Lithium Ion Battery Pouch Cells  
*E. Schuster, C. Ziebert, and H. J. Seifert*

- 1001 Thermal and Overcharge Abuse Analysis of a Redox Shuttle for Overcharge Protection of LiFePO<sub>4</sub>  
*J. H. Lamb, C. Orendorff, K. Amine, G. Krumdick, Z. Zhang, L. Zhang, and A. Gozdz*
- 1002 Materials Development for Improved Lithium-Ion Battery Safety  
*K. Fenton, G. Nagasubramanian, M. T. Brumbach, and C. Orendorff*
- 1003 Process Optimisation by the Application of Cylindrical Cells (18650) and Pouch Cells with Reference Electrodes  
*M. D. Wilka, A. Hoffmann, R. Stern, and M. Wohlfahrt-Mehrens*
- 1004 Impedance Analysis of Anode and Cathode Separated by Using Micro Reference Electrode on Li-ion Battery  
*H. Nara, T. Yokoshima, D. Mukoyama, T. Hirabaru, T. Momma, and T. Osaka*
- 1005 Reference Electrodes for Impedance Measurements in Lithium Ion Cells  
*J. Illig, M. Ender, A. Weber, and E. Ivers-Tiffée*
- 1006 Studies of SDXTM on the Boundary Resistance between Aluminum Current Collectors and Cathode Active Material Layers  
*Y. Arai, M. Kunisawa, T. Yamaguchi, H. Yokouchi, A. Matsuo, and M. Ohmori*
- 1007 Application of Adiabatic and Isothermal Calorimetry in Studying Battery Material Properties and Small Cells  
*P. Ralovsky*
- 1008 Understanding the Performance of Rechargeable Lithium-Ion Batteries for HEV and PHEV Using a New Isothermal Calorimeter  
*S. Chippett, J. Ireland, M. Keyser, J. Mauger, A. Pesaran, P. Ralovsky, and G. Widawski*
- 1009 Study of Generative Gas Species from Lithium-Ion Battery Component under Abuse Conditions  
*S. Koike, M. Shikano, H. Sakaebi, and H. Kobayashi*
- 1010 Prelithiated Graphite Anode SEI Formation by Stabilized Lithium Metal Powder in Li-Ion Batteries  
*L. Wang, V. Battaglia, and G. Liu*
- 1011 Graphene Nanosheets as Negative Electrode for Lithium Ion Battery  
*A. N. Gildea, S. Vijapur, and G. G. Botte*
- 1012 The Rate of Active Lithium Loss from a Soft Carbon Negative Electrode as a Function of Temperature, Time and Electrode Potential  
*N. N. Sinha, T. H. Marks, H. M. Dahn, A. J. Smith, J. Burns, D. J. Coyle, J. J. Dahn, and J. Dahn*
- 1013 Meta-stable Mesographite Anodes  
*J. Fang, A. Kelarakis, W. Wu, H. Huang, Y. Lin, E. Giannelis, and L. Tsai*

- 1014 High Performance Lithium Ion Battery Using Graphene Net Electrode  
*H. Todoriki, T. Ikenuma, Y. Saito, M. Yukawa, R. Yatabe, M. Yamakaji, J. Momo, T. Moriwaka, K. Nanba, M. Takahashi, and S. Yamazaki*
- 1015 Theoretical Study of Hybrid Bundle of (5,0) Carbon Nanotube on Li-Ion Battery Anode  
*Y. Wen, B. Shan, X. Liu, X. Duan, and R. Chen*
- 1016 Effect of Anode Binders on Low-Temperature Performance of Li-Ion Batteries  
*J. Eom, L. Cao, and C. Wang*
- 1017 Development of Heat Resistant Lithium-ion Batteries and Safety Evaluation  
*M. Morishita, T. Mukai, T. Sakamoto, T. Miyuki, and T. Sakai*
- 1018 Composition Ratio-Dependent Structural Evolution of SiO<sub>2</sub>/Poly(Vinylidene Fluoride Hexafluoropropylene)-Coated Poly(Ethylene Terephthalate) Nonwoven Composite Separators for Lithium-Ion Batteries  
*H. Jeong, E. Choi, and S. Lee*
- 1019 Transport Properties of Strained Lithium-Ion Battery Separators  
*J. Cannarella and C. B. Arnold*
- 1020 Polymer Particle Layer Coated on Separator to Improve Lithium-Ion Battery Performance  
*T. Kaneda, H. Takamatsu, T. Murase, J. Akiike, N. Yasuda, T. Herai, T. Ooishi, and M. Tada*
- 1021 Development of Water-Borne Nanoparticle Ceramic Slurry to Improve Lithium-Ion Batteries Performance  
*Y. Toyoda, H. Takamatsu, T. Murase, J. Akiike, N. Yasuda, T. Kaneda, T. Herai, T. Ooishi, and M. Tada*
- 1022 Layer-by-Layer Deposition for Improved Performance of Separators for Lithium Ion Batteries  
*B. El-Zahab, N. Baram, D. Liu, W. Carter, Y. Chiang, and P. T. Hammond*
- 1023 Why Do We Need Polarization and Impedance Measurements of Lithium Insertion Electrodes?  
*T. Ohzuku, F. Ohgaki, and K. Ariyoshi*
- 1024 A Method to Measure the Rate of Side Reactions at the Positive and Negative Electrodes in LTO/LiNiMO Cells for the Second-Generation 12 V Lead-Free Batteries  
*K. Ariyoshi, H. Okada, H. Nishi, and T. Ohzuku*
- 1025 In Situ Fluorescence Spectroscopy of Interfacial Processes in High-Energy Li-ion Batteries  
*N. S. Norberg, S. F. Lux, I. T. Lucas, J. S. Syzdek, and R. M. Kostecki*
- 1026 Neutron Powder Diffraction Studies of Li-Ion Battery Materials  
*S. Lee*
- 1027 Reducing Coulombic Efficiency Noise in High-Precision Coulometry  
*T. M. Bond, J. Burns, A. Smith, and J. Dahn*

- 1028 Lithium Titanate Prepared from Mesoporous TiO<sub>2</sub> Fiber as Anode Material for Lithium Ion Batteries  
*S. Ting, Z. Yang, C. V. Li, W. Zhuang, W. Yao, X. Lu, and K. Chan*
- 1029 Nanosized Mixed Transition Metal Oxides as Superior Anode Material for Li-Ion Batteries  
*D. Bresser, E. Paillard, F. Mueller, M. Winter, and S. Passerini*
- 1030 Multi-Component effects on the Crystal Structures and Electrochemical Behaviors of Spinel-Structured M<sub>3</sub>O<sub>4</sub> (M=Fe, Mn, Co) Anodes in Lithium-Ion Batteries  
*H. Kim, D. Seo, H. Kim, I. Park, J. Hong, K. Park, and K. Kang*
- 1031 Hollow Single-Crystalline Mn<sub>3</sub>O<sub>4</sub> Nanotubes as a High Capacity Anode Material for Lithium-Ion Batteries  
*G. Xu, Y. Xu, H. Sun, X. Peng, J. Li, S. Yang, L. Huang, and S. Sun*
- 1032 Porous MnO@C Nanotubes and Their High Lithium-Storage Performances  
*W. Chen, L. Qie, L. Yuan, W. Zhang, and Y. Huang*
- 1033 Battery Durability Evaluation Using Load Data of Commercially Available Electric Vehicle  
*K. Koshika and T. Niikuni*
- 1034 Cycle Life Estimation of Lithium-ion Battery Using for PV Power Leveling Operation  
*Y. Mita, Y. Kobayashi, and H. Miyashiro*
- 1035 Lifetime Evaluation and Modelling of Li-Ion Modules and Cells  
*P. J. Vie and R. Fotedar*
- 1036 Constant-Potential Aging of Commercial Li-Ion Batteries  
*P. Albertus, J. Christensen, V. Peng, M. Hess, R. Klein, and J. Newman*
- 1037 Correlating Accelerated Tests to Long-term Data for Li-Ion Batteries  
*G. Jain, H. Ye, P. A. Tamirisa, P. Gomadam, E. Scott, and C. Schmidt*
- 1038 In-Situ Reference Electrode Testing of Lithium Ion Cells  
*J. R. Belt, C. Ho, and R. Bewley*
- 1039 Insight into Thermal Instability of Charged Cathode Materials for Lithium-Ion Batteries: Combined in situ Synchrotron X-ray and Mass Spectroscopy Study  
*S. Bak, K. Nam, E. Hu, X. Yu, K. Chung, S. Cho, F. Bonhomme, K. Kim, and X. Yang*
- 1040 Effect of Low Cell Voltages on the Performance of MCMB Anode and LiNi<sub>0.8</sub>Co<sub>0.2</sub>O<sub>2</sub> Cathode  
*R. V. Bugga, M. C. Smart, F. C. Krause, C. Hwang, P. Degrosse Jr., S. Santee, and F. Puglia*
- 1041 Impedance Diagnostic for Overcharged Lithium-Ion Batteries  
*C. T. Love, K. Swider-Lyons, and C. J. Patridge*

- 1042 Zero-Volt SPEC Cells to Measure the Rates of Side Reactions on the Positive and Negative Electrodes for Long-Life Lithium-Ion Batteries  
*K. Ariyoshi, H. Nishi, and T. Ohzuku*
- 1043 Study on the Electrochemical Properties of SnO<sub>2</sub>-Polypyrrole Hybrid Nanowires for Li-Ion Batteries Anode  
*D. Nam, S. Lim, M. Kim, and H. Kwon*
- 1044 High Capacity Li-Ion Batteries Based on Hetero-Nanostructured SnO<sub>2</sub>-Sn/CMK-3 Materials  
*F. M. Hassan, A. Yu, H. Park, Z. Chen, X. Xiao, and Z. Chen*
- 1045 Visualisation of Li Diffusion Pathways in Lithium Lanthanum Titanates  
*E. E. Jay, I. Seymour, M. Rushton, R. Grimes, and J. A. Kilner*
- 1046 Effect of Pattern Shape of Sn Anode on Charge-Discharge Performance for Lithium Secondary Batteries  
*T. Yokoshima, H. Nara, T. Momma, and T. Osaka*
- 1047 Poly(ethylene oxide)-Coated Graphite as an Anode Material for Lithium Ion Batteries  
*S. Park and G. Liu*
- 1048 PeakForce Tapping AFM Outfitted in a Glove-box for in-situ Real-time Visualization of SEI formation on Lithium Battery Anodes  
*C. Li*
- 1049 Electrochemical-Thermal Coupled Modeling for Battery Pack Design  
*G. Luo, C. Shaffer, and C. Wang*
- 1050 Design Optimization of a Battery Pack for Plug-in Hybrid Vehicle Applications  
*N. Xue, W. Du, T. Greszler, J. Martins, and W. Shyy*
- 1051 Nanowire Energy Storage Device: Fabrication and Electrochemical Studies  
*S. Gowda, A. Reddy, and P. Ajayan*
- 1052 Advanced Materials Processing for Lithium Ion Battery Applications  
*D. L. Wood, J. Li, D. Mohanty, S. Kalnaus, B. Armstrong, and C. Daniel*
- 1053 Lithium Battery Internal Temperature Sensor and SoC Monitor  
*R. Srinivasan, B. G. Carkhuff, and A. Q. Rogers*
- 1054 Dual-Scale Porosity Distribution for Maximizing Power At High Energy Densities  
*C. K. Erdonmez, C. Bae, Y. Chen, J. Wang, J. Halloran, and Y. Chiang*
- 1055 Cycling Fatigue Induced on Electrochemical Energy Storage Cells as a Result of High C Pulsed Charging  
*P. M. Novak, D. A. Wetz, and B. Shrestha*

- 1056 The Impact of High Pulsed Loading on the Fatigue of Electrochemical Energy Storage Devices  
*B. Shrestha, D. A. Wetz, and P. M. Novak*
- 1057 Heating Strategies for Li-Ion Batteries Operated from Subzero Temperatures  
*Y. Ji and C. Wang*
- 1058 Thermal Management for Startup of Li-Ion Batteries  
*C. Shaffer and C. Wang*
- 1059 Rechargeable Lithium-ion Batteries For Wireless Smart Designs & Extreme Conditions  
*F. Fusalba, H. Rouault, L. Daniel, M. Chami, D. Mourzag, and G. Moreau*
- 1060 Negative Electrode Properties of Carbon-Coated Si Leaf Powder for Lithium-Ion Batteries  
*M. Saito, T. Okubo, T. Yamada, C. Yodoya, A. Kamei, M. Hirota, T. Takenaka, A. Tasaka, and M. Inaba*
- 1061 Temperature Dependence of Cycle Performance at Various Cut-Off Voltages of Li-Ion Batteries Using SiO Anode  
*T. Kajita, J. Iriyama, H. Takahashi, R. Kasahara, T. Numata, S. Serizawa, and K. Utsugi*
- 1062 Anodic Compatibility of LiTDI Based Electrolytes with MPCVD Manufactured Si/C Nanostructured Electrodes  
*P. Wieczorek, A. Bitner, L. Niedzicki, A. Plewa-Marczewska, E. Zero-Sasim, G. Zukowska, M. Kasprzyk, F. Lindgren, K. Edström, W. Wieczorek, and M. L. Marcinek*
- 1063 Microstructural Evolution during Battery Charge and Discharge in Si Alloy Anode  
*J. Cho, J. Moon, C. Kang, S. Kim, S. Son, C. Lee, S. Kang, Y. Kim, S. Lee, and K. Oh*
- 1064 Ultra-Strong Silicon-Coated Carbon Nanotube Fabric as Multi-Functional Lithium Ion Battery Anodes  
*K. Evanoff, J. Benson, M. Schauer, I. Kovalenko, D. Lashmore, J. Ready, and G. Y. Yushin*
- 1065 Determination and Evaluation of Charge Distribution in Lithium Battery Electrodes  
*T. J. Richardson, C. Sirisopanaporn, V. Srinivasan, J. Liu, and V. Zorba*
- 1066 Multiscale Multiparadigm in Silico Design of New Materials for Li-ion Batteries  
*W. Goddard III, B. V. Merinov, A. Jaramillo-Botero, H. Kim, D. Seo, H. Kim, and K. Kang*
- 1067 Computational Framework for Modeling Multi-Physics Phenomenon of Li-Ion Batteries across Various Hierarchies  
*S. Allu, S. Pannala, P. Mukherjee, W. Elwasif, and J. Turner*
- 1068 Evaluation Model for Used Lithium-Ion Battery Life  
*K. Kaji, K. Tanaka, K. Maeda, H. Akimono, J. Zhang, and H. Horie*

- 1069 Parameterizing Li-Ion Cell Models Supported by Microstructure Reconstructions  
*M. Ender, J. Illig, and E. Ivers-Tiffée*
- 1070 Electrothermal Simulation of Spirally-Wound Lithium Ion Cells  
*R. Spotnitz, G. Yeduvaka, D. Schad, V. Gudimetta, J. Votteler, G. Damblanc, C. Lueth, E. Oxenham, and S. Hartridge*
- 1071 Ab Initio Study of Li Interaction with Graphene, Multi-Layer Graphene and Graphite Relevant for Li-Ion Electrode Materials  
*K. A. Persson and E. Lee*
- 1072 Binder Assisted Stabilization of Pure Sn Based Anode for Lithium Ion Batteries  
*S. Xun, X. Song, J. Chong, V. Battaglia, and G. Liu*
- 1073 Porous Sn-C Composite Synthesized by Electrochemical Method for the Binder-free Anode of Li-ion Battery  
*J. Jeun, W. Kim, K. Park, K. Kang, and S. Hong*
- 1074 SnO Microcrystals vs. Nanoparticles as Anode for Lithium Ion Batteries  
*C. T. Cherian, M. Reddy, C. Sow, and B. Chowdari*
- 1075 Electrochemical Analysis of Sn Electrodeposition to Optimize Preparation Process of SnOC Anode Material  
*M. Jeong, H. Nara, T. Yokoshima, T. Momma, and T. Osaka*
- 1076 Multi-scaled Sn Dispersed in Ni-Ti Shape Memory Alloy as High Performance Anode for Li-ion Battery  
*R. Hu, H. Liu, and M. Zhu*
- 1077 Autogenically-Prepared Spherical Carbon Particles (SCPs) and SCP-Sn Composites as Anodes for Li-Ion Batteries  
*V. G. Pol, K. C. Lau, L. A. Curtiss, and M. M. Thackeray*
- 1078 Effect of Particle Morphology on Stress in a Lithium-Ion Battery Using an Integrated Model in 2-D  
*R. T. Purkayastha and R. M. McMeeking*
- 1079 Simulation-Based Prediction of Residual Performance of Lithium-Ion Batteries  
*K. Maeda, W. Imamura, K. Tanaka, H. Akimoto, and H. Horie*
- 1080 Modeling of Fracture Initiation and Propagation in Lithium Ion Battery Electrodes  
*P. Barai, S. Simunovic, and P. Mukherjee*
- 1081 Modeling of the Interactions of Uniformly Sized Nanoparticles  
*B. Orvananos, H. Yu, T. Ferguson, M. Bazant, and K. Thornton*
- 1082 Dynamic Optimization Using Efficient Reformulated Models for Maximizing Energy Storage and Life of Lithium-Ion Batteries  
*V. Ramadesigan, P. Northrop, R. Braatz, and V. Subramanian*

- 1083 Synthesis of  $\text{Co}_3\text{O}_4$ - $\text{SnO}_2$  Multi-Layered Hollow Sphere and Their High Reversible Capacity for Anode of Li-Ion Battery  
*W. Kim, Y. Hwa, J. Jeun, H. Sohn, and S. Hong*
- 1084 Development of Li-Ion Rechargeable Battery Using Glassy  $\text{SnO-P}_2\text{O}_5$  Anode and Glass-Ceramic  $\text{LiFePO}_4$  Cathode and Their Safety Evaluation  
*A. Yamano, M. Morishita, H. Yamauchi, T. Nagakane, A. Sakamoto, M. Ohji, and T. Sakai*
- 1085 Development of Li-Ion Rechargeable Battery Using Glassy  $\text{SnO-P}_2\text{O}_5$  Anode and Glass-Ceramic  $\text{LiFePO}_4$  Cathode Materials  
*T. Nagakane, H. Yamauchi, A. Sakamoto, M. Ohji, A. Yamano, M. Morishita, and T. Sakai*
- 1086 Study of the Factors that Enable Carbon-Free Insulating Li-Ion Battery Electrodes  
*C. Kim, C. Alexander, N. S. Norberg, R. M. Kostecki, and J. Cabana*
- 1087 Single-Crystalline Porous Indium Phosphide as Novel Anode Material for Li-Ion Batteries  
*M. Gerngross, E. Quiroga-González, J. Carstensen, and H. Föll*
- 1088 A Thermodynamics-based Approach to Predicting Path Dependence of Aging in Electrochemical Cells: Part 2. Large-scale Simulation of Cell Aging Across Multiple US Cities  
*K. L. Gering*
- 1089 Cycle-Life Study and Aging Mechanism Diagnosis of NCM Composite/Graphite Cells  
*J. Wang, P. Liu, J. Hicks-Garner, L. Westman, E. Sherman, S. Soukiasian, M. W. Verbrugge, and H. Tataria*
- 1090 Characterization of Cycle-Life Aging in Automotive Lithium-Ion Pouch Cells  
*J. Marcicki, A. Bartlett, M. Canova, A. Conlisk, G. Rizzoni, Y. Guezenne, X. Yang, and T. Miller*
- 1091 A Common Capacity Loss Trend:  $\text{LiFePO}_4$  Cell's Cycle and Calendar Aging  
*Y. Miyaki, K. Hayashi, T. Makino, K. Yoshida, M. Terauchi, T. Endo, and Y. Fukushima*
- 1092 Capacity Fading of Mechanically Stressed Lithium-Ion Pouch Cells  
*J. Cannarella and C. B. Arnold*
- 1093 Battery Cycle Life Prediction with Coupled Chemical Degradation and Fatigue Mechanics  
*R. D. Deshpande, M. W. Verbrugge, Y. Cheng, J. Wang, and P. Liu*
- 1094 Lithium Storage Properties of Defect-Introduced Graphene Sheets  
*W. Lee, S. Suzuki, and M. Miyayama*
- 1095 Study of Solid Electrolyte Interface (SEI) on Graphite Anodes  
*J. Benson, J. Lee, N. Nitta, A. Magasinski, I. Kovalenko, T. Joshi, T. Fuller, and G. Yushin*

- 1096 Origin of Voltage Hysteresis of the Li-Cu-TiS<sub>2</sub> Displacement Reaction System: A Multi-Scale Simulation Based on Thermodynamics and Kinetics  
*H. Yu, J. Bhattacharya, C. Ling, A. Van Der Ven, and K. Thornton*
- 1097 The Effect of the Active Material of Lithium battery to the Contact Resistance between Carbon and Aluminum Current Collector  
*C. Honda, S. Onodera, K. Tachibana, and T. Nishina*
- 1098 Entangled Structures of Germanium Nanowires & Graphite Nanofibers for the Anode of Lithium Ion Batteries  
*S. Woo, S. Choi, J. Park, S. Hwang, and D. Whang*

### B7 - Metal-Air Batteries

*ECS Battery, ECS Energy Technology, ECS Fullerenes, Nanotubes, and Carbon Nanostructures, ECSJ Battery*

- 1099 (Invited) Metal-Air Batteries: A Reality Check  
*S. Whittingham*
- 1100 Very High Specific Surface Area Capacity Lithium-Air Battery  
*P. Stevens, G. Toussaint, P. Vinatier, and L. Puéch*
- 1101 A Versatile Composite Electrode Design for Metal-Air Batteries  
*A. C. Marschilok, E. S. Takeuchi, and K. J. Takeuchi*
- 1102 Comparison of Air Cathodes and Aluminium Anodes for High-Power Density Alkaline Aluminium-Air Batteries  
*D. MacAodhagáin, C. Ponce-de-Leon-Albarran, R. J. Wood, K. R. Stokes, and F. C. Walsh*
- 1103 (Invited) Cycling Stability and Charging Behavior of Carbon Nanotube Electrodes for Li-O<sub>2</sub> Batteries  
*B. M. Gallant, R. R. Mitchell, C. V. Thompson, and Y. Shao-Horn*
- 1104 N-Doped Graphene Nanosheet for Li-Air Fuel Cell under Acidic Conditions  
*E. Yoo, J. Nakamura, and H. Zhou*
- 1105 Structure of Li<sub>2</sub>O<sub>2</sub> Discharge Products on Free-Standing Aligned Carbon Nanotube Electrodes for Li-Air Batteries  
*R. R. Mitchell, B. M. Gallant, Y. Shao-Horn, and C. V. Thompson*
- 1106 Graphene and N-Doped Graphene as Cathodes for Li-Air Batteries  
*Y. Li, J. Wang, X. Li, D. Geng, R. Li, and X. A. Sun*
- 1107 (Invited) Promoting Ideal Reaction Processes in the Rechargeable Non-Aqueous Li-Air Battery  
*F. Bardé, Y. Chen, S. A. Freunberger, and P. Bruce*

- 1108 (Invited) Fundamental Electrochemistry in Non-Aqueous Li-air  
*B. McCloskey, A. Speidel, R. Scheffler, V. Viswanathan, J. S. Hummelshøj,  
J. K. Nørskov, and A. Luntz*
- 1109 (Invited) Metal-Air Technologies-- Reversibility of Zinc Electrode  
*J. Yamaki, A. Nakata, T. Yamane, T. Hirai, and Z. Ogumi*
- 1110 Electrochemistry of Cathode Materials for Lithium-Oxygen Batteries Using  
Microelectrode Voltammetry  
*E. Nemanick*
- 1111 Decomposition Kinetics of Li-Air Cell Discharge Products in Non-Catalyzed and  
Catalyzed Carbon Cathodes  
*S. Meini, H. Beyer, N. Tsiovaras, M. Piana, and H. A. Gasteiger*
- 1112 Toward Efficiently Rechargeable Li-O<sub>2</sub> Batteries: Freely Diffusing Catalysts and O<sub>2</sub>  
Electrode-Stable Solvents  
*W. Walker, V. Giordani, V. S. Bryantsev, J. Uddin, S. Zecevic, D. Addison,  
and G. V. Chase*
- 1113 (Invited) Dual-Electrolyte Lithium-Air Batteries with Buffer Catholytes  
*A. Manthiram, L. Li, and Y. Fu*
- 1114 Investigations of Li-O<sub>2</sub> Batteries Using Polyethylene Oxide in Structured Three-Phase  
Electrodes  
*J. R. Harding, Y. Lu, P. T. Hammond, and Y. Shao-Horn*
- 1115 Recent Developments in Solid Li-Ion Electrolytes  
*V. Thangadurai*
- 1116 The Effects of Electrolyte Salts on the Performance of Li-Air Batteries  
*E. Nasybulin, W. Xu, M. H. Engelhard, Z. Nie, J. Hu, J. Xiao, M. Gross,  
and J. Zhang*
- 1117 (Invited) A Reversible Lithium-Air Battery with Low Charge Polarization using  
Ether-Based Electrolytes  
*K. Amine, J. Lu, H. Jung, K. C. Lau, Z. Zhang, J. Schlueter, P. Du, R. Assary,  
J. Greeley, G. Ferguson, H. Wang, J. Hassoun, H. Iddir, Y. Sun, B. Scrosati,  
and L. A. Curtiss*
- 1118 A Long Life, High Capacity, High Rate Lithium-Air Battery Using a Stable Glyme  
Electrolyte  
*H. Jung, J. Park, H. Kim, J. Hassoun, C. Yoon, B. Scrosati, and Y. Sun*
- 1119 Stability of Li-Salts during the Discharge Reaction in a Li-O<sub>2</sub> Cell  
*G. M. Veith, J. Nanda, and N. J. Dudney*
- 1120 Stability of Pyr<sub>14</sub>TFSI Ionic Liquid in Li-O<sub>2</sub> Cells and Its effect on the Cycling Behavior  
*M. Piana, N. Tsiovaras, S. Meini, I. Buchberger, J. Wandt, H. A. Gasteiger,  
and A. Garsuch*

- 1121 Electrochemical Performance of All-Solid-State Lithium-Air Batteries  
*H. Kitaura and H. Zhou*
- 1122 (Invited) Investigation of ORR and OER in Non-Aqueous (and Aqueous) Li-O<sub>2</sub> Cells Using Metal Oxide Catalysts  
*B. D. Adams, S. Oh, R. W. Black, A. Baran- Harper, and L. F. Nazar*
- 1123 Metal Nitrides as Alternative Catalyst for Air Cathodes  
*C. Pozo-Gonzalo, A. A. Torriero, P. Howlett, M. Forsyth, A. M. Glushenkov, O. Kartachova, and Y. Chen*
- 1124 Role of Manganese Oxides in the Oxygen Electrode for Li-Air Batteries  
*I. Bae and K. Nam*
- 1125 Highly Performance and Stable Core-corona Bifunctional Catalyst for Rechargeable Metal-air Batteries  
*Z. Chen, Z. Chen, D. Higgins, and A. Yu*
- 1126 Graphene-Metal Oxide Catalysts for Li-O<sub>2</sub> Batteries  
*R. W. Black, J. Lee, B. D. Adams, A. Baran- Harper, and L. F. Nazar*
- 1127 The effect of the Surface Area of LaNiO<sub>3</sub> Support on the Oxygen Reduction/Evolution Activity of Air Electrode for Rechargeable Metal-Air Batteries  
*M. Yuasa, H. Imamura, T. Kida, and K. Shimanoe*
- 1128 Graphene/Metal Oxide Catalyst Based High Capacity Cathode for Li-O<sub>2</sub> Batteries  
*R. S. Kalubarme, C. Ahn, and C. Park*
- 1129 Activated and Nitrogen Doped Carbon Nanofibers as Oxygen Reduction Electrode Materials for Zinc-Air Batteries  
*D. C. Higgins, Y. Liu, Z. Chen, and Z. Chen*
- 1130 Nickel Cobalt Oxide Nanostructures on Graphene as an Active Bifunctional Electrocatalyst  
*D. Lee, A. Yu, H. Park, and Z. Chen*
- 1131 Cyclic Voltammetry of Zn/Zn(II) Couple in Dycyanamide Anion and Bis-(trifluoromethylsulfonyl)Imide Anion Based Ionic Liquids  
*M. Xu, D. Ivey, Y. Bing, Z. Xie, and W. Qu*
- 1132 Carbon Air Electrodes for Alkaline Aqueous Electrolyte Lithium/Air Secondary Batteries  
*H. Ohkuma, I. Uechi, N. Imanishi, Y. Takeda, and O. Yamamoto*
- 1133 Microwave-Assistanted Synthesis of Ag-MnO<sub>2</sub>/SWNT Electrocatalyst for Metal-Air Cells  
*G. Zhang and Y. Jiang*
- 1134 Carbon Sphere Dotted with Co<sub>3</sub>O<sub>4</sub> and RuO<sub>2</sub> Nano Particles for Rechargeable Li/Air Batteries  
*C. Park and Y. Park*

- 1135 Synthesis and Properties of Garnet-Type  $\text{Li}_{7-x-y}\text{La}_3\text{Zr}_{2-y}\text{Nb}_y\text{O}_{12-0.5x}$   
*K. Ishiguro, Y. Nakata, N. Imanishi, A. Hirano, Y. Takeda, and O. Yamamoto*
- 1136 Air Electrode with Oxide Catalyst for Aqueous Lithium-Air Rechargeable Batteries  
*S. Sunahiro, H. Ohkuma, I. Uechi, N. Imanishi, Y. Takeda, and O. Yamamoto*
- 1137 Lithium Nitride Formation on Lithium Metal  
*N. Futamura, T. Ichikawa, N. Imanishi, Y. Takeda, and O. Yamamoto*
- 1138 Role of Metal Decoration in the Catalytic Activity of Urchin-Like  $\text{MnO}_2$  for Oxygen Reaction in Aqueous Lithium-Oxygen Batteries  
*K. Jung, J. Lee, A. Riaz, S. Lee, T. Lim, S. Park, R. Song, and K. Shin*
- 1139 Tape-Cast Lithium Conducting Solid Electrolyte  $\text{Li}_{1.4}\text{Ti}_{1.6}\text{Al}_{0.4}(\text{PO}_4)_3$  for Aqueous Lithium-Air Batteries  
*K. Takahashi, N. Imanishi, Y. Takeda, and O. Yamamoto*
- 1140 Rechargeable, All-Solid Li-Air Battery  
*W. Chang, D. Hallinan, Y. Lee, T. Yen, and C. Yang*
- 1141 Mesoporous Nitrogen Doped Carbon as Cathode Materials for High Capacity Lithium-Air Batteries  
*A. Zahoor, M. Christy, Y. Hwang, J. Choi, and K. Nahm*
- 1142 An Effort to Understand the Basic Characteristics of Hybrid Li-air Cell Performance  
*D. Yoon, K. Kim, M. Park, S. Kim, and H. Sun*
- 1143 Electrodeposited Manganese Oxide Catalysts for Oxygen Reduction Aqueous Alkaline Media  
*S. H. Pulukadang and S. W. Donne*
- 1144 Electrochemical Properties of Graphene Based Catalyst for Rechargeable  $\text{Li}/\text{O}_2$  Batteries  
*C. Ahn, R. S. Kalubarme, and C. Park*
- 1145 Effects of  $\text{Nb}_2\text{O}_5$  Addition on the Electrochemical Properties of  $\text{Li}_{1.5}\text{Al}_{0.5}\text{Ge}_{1.5}\text{P}_3\text{O}_{12}$  Glass Ceramic for Li-Air Batteries  
*T. Kim, R. S. Kalubarme, and C. Park*
- 1146 Rechargeable  $\text{Li}/\text{O}_2$  Cell Based on a LiTFSI-DMMP/PFSA-Li Composite Electrolyte  
*H. Wang, X. Liao, L. Li, and Z. Ma*
- 1147  $\text{MnO}_2$ -Based Nanostructures as Catalysts for Oxygen Oxidation-Reduction Reaction in Rechargeable Lithium-Oxygen Battery  
*B. Huang, X. Liao, and Z. Ma*
- 1148 Multifunctional Carbon Nanoarchitectures as Air-Breathing Cathodes for Rechargeable Zn-Air and Li-Air Batteries  
*C. N. Chervin, J. W. Long, M. J. Wattendorf, N. W. Kucko, and D. R. Rolison*

- 1149 Modeling of Bifunctional Electrode in Metal Air Battery  
*D. Chan, K. Hsueh, C. Wu, and W. Chang*
- 1150 Inhibiting Ability of Chelating Agent on Aluminum Corrosion in Alkaline Solution and Testing of Aluminum-Air Single Cell  
*C. Wu, C. Chung, K. Hsueh, and W. Chang*
- 1151 The Kinetic Reaction of Aluminum-Air Battery in Different Aqueous Solution  
*C. Wang, K. Hsueh, and C. Hsieh*
- 1152 Manganese Oxide Nanosheets: Applications in High Energy Density Zn-Air Batteries  
*Y. Korenblit, G. Yushin, and J. Cho*
- 1153 (Invited) Protective Layers for the Lithium Electrode Based on Ceramic Phases  
*J. Cabana*
- 1154 (Invited) Factors Affecting the Cycle Life of a Nonaqueous Li-Air Cell with a Protected Anode  
*D. Im, D. Lee, T. Kim, V. Roev, S. Ma, and S. Doo*
- 1155 Lithium Dendrite Formation between PEO<sub>18</sub>LiTFSI and Lithium Metal  
*H. Wang, N. Imanishi, Y. Takeda, and O. Yamamoto*
- 1156 (Invited) Ultra-High Energy Density Lithium-Air Batteries Based on Protected Lithium Electrodes (PLEs)  
*S. J. Visco, E. Nimon, B. Katz, M. Chu, and L. De Jonghe*
- 1157 Ionic Conductivity of Garnet-Type Li<sub>7-x</sub>La<sub>3</sub>Zr<sub>2</sub>O<sub>12-0.5x</sub> Solid Electrolyte for Lithium Metal Electrode  
*Y. Nakata, K. Ishiguro, N. Imanishi, Y. Takeda, and O. Yamamoto*
- 1158 Nickel Foam, a Probable Current Collector in Rechargeable Li-Air Batteries  
*X. Liu and D. Wang*
- 1159 Degradation Products on Li-Negative Electrode and the Carbon Cathode in Li-O<sub>2</sub> Batteries  
*R. Younesi, M. Hahlin, and K. Edström*
- 1160 Metal-Free "Li-Ion" Air Battery Realized by Controlling Solvation State in Electrolyte  
*Y. Yamada, M. Yaegashi, K. Furukawa, F. Li, H. Zhou, and A. Yamada*
- 1161 (Invited) Investigation of Rechargeable Li-Air Battery  
*D. Zheng, Q. Wang, D. Qu, and X. Yang*
- 1162 Effect of Substitution of Cobalt by Manganese on the Properties of Calcium-Doped Lanthanum Cobalt Oxide for Oxygen Reduction Reaction in Alkaline Medium  
*S. Malkhandi, P. Trinh, A. Manohar, G. Prakash, S. Narayanan, and A. Manivannan*

- 1163 Towards Understanding the Mechanism of the Electrochemical Oxygen Reduction: DFT Modeling and Spectroelectrochemical Validation  
*P. Biedermann, S. Nayak, and A. Erbe*
- 1164 Predictive Modeling of Size-Dependent Dendritic Growth in Dilute-Electrolyte Lithium Metal Batteries with Potentiostatic Cycling  
*A. Aryanfar, M. Hoffmann, and A. Colussi*
- 1165 Computational Investigations of the Electronic Transport in Lithium-Air Battery Materials  
*T. Vegge, J. Garcia-Lastra, J. Myrdal, and K. Thygesen*
- 1166 A Transient Model of an Aqueous Li/Air Battery Forming LiOH (aq) and LiOH•H<sub>2</sub>O  
*P. Albertus, V. Viswanathan, and J. Christensen*
- 1167 Oxygen Reduction Catalyst Selection for Lithium Air Batteries via Rotating Ring Disc Electrode Voltammetry and In Situ X-ray Absorption Spectroscopy  
*M. Trahan, S. Mukerjee, and K. Abraham*
- 1168 Probing Reaction Mechanisms of Li-O<sub>2</sub> Batteries via In Situ Ambient Pressure X-ray Photoelectron Spectroscopy  
*Y. Lu, E. J. Crumlin, G. M. Veith, J. R. Harding, E. Mutoro, L. Baggetto, N. J. Dudney, Z. Liu, and Y. Shao-Horn*
- 1169 Electrochemistry and Transport Limitations of Non-Aqueous Li-Air Batteries from First-Principles  
*V. Viswanathan, J. S. Hummelshøj, A. C. Luntz, and J. K. Nørskov*
- 1170 Electrochemical Strain Spectroscopy: Monitoring Partially Reversible Electrochemical Processes In Situ on Li-Air Battery Electrolytes  
*T. M. Arruda, A. Kumar, S. Jesse, and S. V. Kalinin*
- 1171 (Invited) Critical Components of Rechargeable Li-Air Batteries  
*J. Zhang, W. Xu, J. Xiao, E. Nasybulin, Y. Shao, D. Mei, and J. Zhang*
- 1172 A High Energy Density Rechargeable Zinc-Air Battery for Automotive Application  
*G. Toussaint, P. Stevens, R. Rouget, and F. Fourgeot*
- 1173 Examining the Interplay of Electrolyte, Electrocatalyst, and Cathode Architecture En Route to High-Capacity, Rechargeable Li-O<sub>2</sub> Batteries  
*C. N. Chervin, J. W. Long, M. J. Wattendorf, N. W. Kucko, and D. Rolison*
- 1174 Air Dehydration Membranes for Ambient Operation of Non-Aqueous Lithium-Air Batteries  
*J. Zhang, W. Xu, J. Xiao, X. Chen, E. Nasybulin, and J. Zhang*
- 1175 (Invited) Understanding the Cathode Processes in the Non-Aqueous Li-O<sub>2</sub> Battery  
*O. Fontaine, Y. Chen, S. A. Freunberger, Z. Peng, and P. Bruce*

- 1176 The effect of Layered Structures of Perovskite Oxide Catalyst on Activity for Oxygen-Reduction Reaction  
*M. Matsuda, T. Murota, and T. Takeguchi*
- 1177 Understanding of Electrolyte Stability and Its Impact to Lifespan of Li-O<sub>2</sub> Battery  
*J. Shui, J. Okasinski, D. Zhao, J. Almer, and D. Liu*
- 1178 Electrospun Nanofibrous Bifunctional LaNiO<sub>3</sub> Catalysts for Oxygen Reduction Reaction and Oxygen Evolution Reaction  
*J. Wu and Z. Chen*
- 1179 Synthesis and Oxygen Reduction Catalytic Properties of La<sub>0.6</sub>Ca<sub>0.4</sub>CoO<sub>3</sub> Fine Powders by Sintering with Carbonate  
*S. Takase, Y. Kanda, and Y. Shimizu*
- 1180 (Invited) Recent Progress in as Highly Efficient Non-Precious Catalysts for Oxygen Reduction Reactions in Alkaline Solutions  
*J. Cho*
- 1181 (Invited) Secondary Li-Air Batteries with Acidic Aqueous Catholytes  
*O. Crowther and M. Salomon*
- 1182 (Invited) Aqueous Electrolyte-Based Metal-Air Batteries: Challenges for Rechargeable Zinc Electrodes and Reversible Air Electrodes  
*T. Abe and K. Miyazaki*
- 1183 Enhancement of Oxygen Transport in the Storage Electrode of a High Temperature Secondary Metal-Air Battery Based on an Oxygen Ion Conducting Electrolyte  
*H. Landes, R. Reichenbacher, C. Schuh, T. Soller, G. Zhang, and C. Lu*
- 1184 Hybrid Li-air Battery with Sulfuric Acid Electrolyte and Buckypaper Air Cathode  
*Y. Li, K. Huang, and Y. Xing*
- 1185 Improvement in Discharge Performance of an MH/Air Secondary Battery with Multiple Electrodes  
*M. Mizutani, M. Morimitsu, and Y. Wada*
- 1186 Comparison of Room Temperature Sodium/Oxygen- and Lithium/Oxygen-Batteries with Liquid Electrolyte  
*P. Hartmann, C. Bender, A. Garsuch, A. Dürr, J. Janek, and P. Adelhelm*
- 1187 Effect of Bismuth Additives on the Performance of Iron Electrodes in Alkaline Batteries  
*A. Manohar, C. Yang, S. Malkhandi, B. Yang, G. Prakash, and S. Narayanan*

## B8 - Non-Aqueous Electrolytes for Lithium Batteries

*ECS Battery, ECS Energy Technology, ECS Physical and Analytical Electrochemistry, ECSJ Battery*

- 1188 Development of Sulfide Glass Electrolytes for All-Solid-State Lithium Batteries  
*A. Hayashi and M. Tatsumisago*
- 1189 Suppression of H<sub>2</sub>S Gas from Li<sub>2</sub>S-P<sub>2</sub>S<sub>5</sub> Glass Electrolytes by the Addition of Li<sub>2</sub>O  
*T. Ohtomo, K. Kawamoto, A. Hayashi, and M. Tatsumisago*
- 1190 New Lithium Superionic Conductor and Its Application to All Solid-State Batteries  
*R. Kanno, M. Hirayama, M. Yonemura, Y. Kato, and K. Kawamoto*
- 1191 Interface Structures in Solid-State Lithium Batteries with Sulfide Electrolytes  
*K. Takada, X. Xu, K. Fukuda, K. Kumagai, K. Watanabe, K. Akatsuka, B. Hang, M. Osada, I. Sakaguchi, T. Ohnishi, T. Sekiguchi, and T. Sasaki*
- 1192 Enlarged Lithium-Ions Migration Pathway by Substitution of B<sup>3+</sup> for P<sup>5+</sup> in Li<sub>3</sub>PS<sub>4</sub>  
*K. Homma, T. Yamamoto, S. Watanabe, and T. Tanaka*
- 1193 First Principles Investigations of the Li<sub>10</sub>GeP<sub>2</sub>S<sub>12</sub> Superionic Conductor and Related Materials  
*S. Ong, Y. Mo, W. D. Richards, and G. Ceder*
- 1194 First-Principles Molecular Dynamics Simulations for Li<sup>+</sup> Diffusion in Li<sub>3</sub>PO<sub>4</sub> and Li<sub>3</sub>PS<sub>4</sub> Electrolytes  
*M. Ikeda, T. Yamasaki, C. Kaneta, K. Homma, T. Yamamoto, and T. Tanaka*
- 1195 Analysis of Lithium-Ion Conduction in LISICON-Based Solid Electrolytes by First-Principles Molecular Dynamics Simulation  
*K. Fujimura, A. Kuwabara, H. Moriwake, A. Seko, Y. Koyama, and I. Tanaka*
- 1196 Research on Electrode-Electrolyte Interfaces of Innovative New Generation Batteries  
*F. Mizuno and H. Iba*
- 1197 The Preparation of Li<sub>7</sub>La<sub>3</sub>Zr<sub>2</sub>O<sub>12</sub> by Sol-Gel Method and Its Electrochemical Performance  
*T. Nishioka, J. Wakasugi, N. Saito, H. Munakata, and K. Kanamura*
- 1198 Flux Growth of Idiomorphic Garnet-Type Solid Electrolyte Crystals for All-Solid-State Lithium-Ion Rechargeable Batteries  
*H. Onodera, K. Teshima, H. Wagata, Y. Mizuno, K. Yubuta, T. Shishido, and S. Oishi*
- 1199 High Lithium-Ion Conducting Garnet-type Oxide; Li<sub>7+x</sub>La<sub>3-y</sub>A<sub>y</sub>Zr<sub>2-z</sub>Nb<sub>z</sub>O<sub>12</sub> (A = Alkali Earth Metals)  
*Y. Kihira, S. Ohta, H. Imagawa, and T. Asaoka*
- 1200 Electrochemical Performance of an All-Solid-State Lithium-Ion Battery with Garnet-Type Oxide Electrolyte  
*S. Ohta, T. Saeki, S. Morishita, J. Seki, and T. Asaoka*

- 1201 Nanostructured Solid Electrolytes for Lithium Batteries  
*N. P. Balsara*
- 1202 Block Copolymer-Ceramic Nanocomposites as Solid Electrolytes for Lithium Batteries  
*I. Gurevitch, J. Cabana, and N. P. Balsara*
- 1203 Conductivity of Electronic and Ionic Conducting Block Copolymer Electrolytes through Electrochemical Doping in the Solid-State  
*S. N. Patel, A. E. Javier, and N. P. Balsara*
- 1204 High Temperature Cycling of Solid Polymer Lithium Batteries  
*Q. Hu, A. Caputo, and D. R. Sadoway*
- 1205 Preparation, Performance in Various Cell Configurations and Limitations of Novel Electrolyte Components for Liquid and Gel Polymer Electrolytes  
*R. Schmitz, E. Krämer, R. Müller, R. W. Schmitz, J. Kasnatscheew, R. Wagner, M. Amereller, P. Janßen, P. Bieker, T. Placke, O. Fromm, H. Meyer, P. Isken, A. Lex-Balducci, I. Profatilova, T. Langer, A. Schmitz, C. Stock, U. Vogl, T. S*
- 1206 Organoboron Ion-Gel Electrolytes as Lithium-Ions Transport Media  
*N. Matsumi*
- 1207 Design of Borosilicate Type Organic-Inorganic Hybrid Ion-Gel Electrolytes  
*K. S. Smaran and N. Matsumi*
- 1208 3D Hybrid Clay-CNT Nanofillers for Polymer Electrolytes in Lithium-Ion Batteries  
*H. Ardebili, C. Tang, K. Hackenberg, Q. Fu, and P. Ajayan*
- 1209 Electrochemical Characterization of Ionic Liquid Based Composite Electrolytes for Lithium-Ion Batteries  
*N. Krawczyk, K. Sann, S. Kraas, A. Schlifke, J. Vogel, B. Luerßen, M. Fröba, and J. Janek*
- 1210 FSI-Based Ionic Liquid Electrolyte and Its Specific Effects with Other Component Materials on Li Battery Performance  
*M. Ishikawa and M. Yamagata*
- 1211 Lithiated Block Copolymer Electrolytes with Ionic Liquids for Batteries  
*A. S. Fisher, M. B. Khalid, and P. Kofinas*
- 1212 Improving the Cathode/Electrolyte Interface Using Ionic Liquids  
*A. Caputo, Q. Hu, and D. R. Sadoway*
- 1213 Cycle Performance of Lithium-Ion Batteries Containing Ionic Liquids with Improved Reduction Stability  
*T. Itakura, K. Ito, R. Yokoi, J. Ishikawa, H. Inoue, H. Kadoma, J. Momo, T. Moriwaka, K. Nanba, M. Takahashi, and S. Yamazaki*
- 1214 Application of Electroactive Ionic Liquids to Improve the Safety of Lithium-Ion Batteries  
*J. C. Forgie, D. Rochedfort, S. El Khakani, and D. MacNeil*

- 1215 Transport Properties for Ionic Liquids and Implications for Li-Ion Battery Design  
*V. L. George and T. F. Fuller*
- 1216 Exploring Solvents toward Stable Electrolyte for Li-Air Battery  
*K. Takechi, T. Shiga, S. Higashi, H. Nakamoto, F. Mizuno, H. Nishikoori, H. Iba, and T. Asaoka*
- 1217 Li<sup>+</sup> Cation Diffusion in Ionic Liquid Electrolyte and Rate Capability of Lithium Secondary Battery  
*K. Yoshida, N. Tachikawa, K. Ueno, K. Dokko, and M. Watanabe*
- 1218 Compatibility of Room Temperature Ionic Liquid Electrolytes with Sulfur Cathode for Lithium Secondary Batteries  
*J. Park, N. Tachikawa, K. Ueno, K. Dokko, and M. Watanabe*
- 1219 First-Principles Study on Li Diffusion in Solid Electrolyte Lithium Lanthanum Titanates(LLTO)  
*Y. Tanaka and T. Ohno*
- 1220 Application of Nonflammable Gel Electrolytes Containing Fluorinated Alkylphosphates to Lithium-Ion Batteries  
*N. Yoshimoto, Y. Abiru, M. Egashira, M. Aoki, H. Mimura, H. Eguchi, and M. Morita*
- 1221 Ion Transport Behavior in Polymerized Imidazolium Ionic Liquids  
*J. Lee, M. Kim, J. Lee, S. Hong, and C. Koo*
- 1222 Highly Stable Cycling of Si-C Composite Anode for Lithium-Ion Batteries by Using FSI-Based Ionic Liquid  
*K. Koga, T. Sugimoto, M. Kikuta, T. Higashizaki, M. Kono, M. Yamagata, and M. Ishikawa*
- 1223 Ionic Liquid-Lithium Salt-Glyme Mixtures: Understanding the Thermophysical and Transport Properties of Ternary Mixtures  
*J. E. Weaver, E. T. Fox, E. Parrish, W. A. Henderson, and R. A. Mantz*
- 1224 Electrochemical Performance of Vitreous Eutectic Electrolytes for Li-Ion Batteries  
*Y. Shilina, M. Levi, D. Aurbach, O. Geiculescu, D. DesMarteau, and I. C. Halalay*
- 1225 Electrolyte Performance of LiFTA-CsFTA Molten Salt for Lithium Secondary Battery  
*K. Kubota and H. Matsumoto*
- 1226 Ionic Liquid-In-Salt: Characterization of Electrolytes for High Temperature Lithium Batteries  
*M. J. Marczewski, Y. Choi, J. Scheers, A. Matic, P. Jacobsson, and P. Johansson*

- 1227 Joint Theoretical and Experimental Study of Novel Electrolytes Based on Eutectic Mixtures of DMMSA with LiFSI and LiTFSI Salts  
*D. Bedrov, L. Xing, J. Hooper, Y. Shilina, M. Levi, D. Aurbach, O. Geiculescu, D. DesMarteau, and I. C. Halalay*
- 1228 Development of Electrolytes for Stable Operation and Highly Safe Lithium-Ion Batteries  
*H. Tokuda*
- 1229 Concentrated Electrolytes: Improving Oxidative Stability for Use in High Voltage Li-Ion Batteries  
*D. W. McCowan, J. L. Allen, D. M. Seo, and W. A. Henderson*
- 1230 Polyfluorinated Electrolyte Solutions and Additives for High Voltage Non-Flammable Lithium Batteries  
*H. Sun and Q. Wei*
- 1231 Effect of Electrolyte and Additives on Performance of  $\text{LiNi}_{0.5}\text{Mn}_{1.5}\text{O}_4$   
*M. Xu, D. Lu, A. Garsuch, and B. L. Lucht*
- 1232 Electrochemical Stability of an Electrolyte of  $\text{LiPF}_6$  in Carbonate Ester Containing Trialkoxyboroxine with  $\text{LiNi}_{0.5}\text{Mn}_{1.5}\text{O}_4$  Cathode  
*Y. Tanaka, K. Yamashita, S. Onoda, Y. Iriyama, and T. Fujinami*
- 1233 Tailored Redox Shuttle Additives for Overcharge Protection of Lithium-Ion Batteries  
*Z. Zhang, L. Zhang, W. Weng, and K. Amine*
- 1234 Perfluoronated Phosphazene Based Additives for Improvement of Safety and Battery Lifetimes in Lithium-Ion Batteries  
*M. K. Harrup, K. L. Gering, H. W. Rollins, S. V. Sazhin, M. T. Benson, D. Jamison, and C. Michelbacher*
- 1235 Wide Operating Temperature Range Electrolytes for High Voltage and High Specific Energy Li-Ion Cells  
*M. C. Smart, C. Hwang, F. C. Krause, J. Soler, W. C. West, B. Ratnakumar, and K. Amine*
- 1236 Initial Decomposition of  $\text{LiPF}_6$ -Based Lithium Battery Electrolytes with Additives  
*S. Wilken, M. Treskow, J. Scheers, P. Johansson, and P. Jacobsson*
- 1237 Structure of the Graphite Anode Solid Electrolyte Interphase in Lithium-Ion Batteries  
*B. L. Lucht, M. Nie, D. P. Abraham, Y. Chen, and A. Bose*
- 1238 The Electrochemical Performance Improvement of Water as an Additive to Graphene-Based Anode Materials  
*C. Cheng, W. Liu, and F. Wang*
- 1239 Highly Quantitative Electrochemical Characterization of Non-Aqueous Electrolytes and Solid Electrolyte Interphases  
*S. V. Sazhin, K. L. Gering, M. K. Harrup, and H. W. Rollins*

- 1240 A Study of the Solid/Liquid Li<sup>+</sup>-Electrolytes Interface  
*C. O'Laoire, J. S. Syzdek, and R. M. Kostecki*
- 1241 Formulation and Properties of Vitreous Eutectic Electrolytes for Li-Ion Batteries  
*O. Geiculescu, D. DesMarteau, S. Creager, D. Hirschberg, O. Haik, Y. Shilina, E. Zinigrad, M. Levi, D. Aurbach, and I. C. Halalay*
- 1242 Synthesis and Electrochemical Performance of Fluorinated Orthoborate Salts as Additives for Li-Ion Battery Electrolytes  
*O. Geiculescu, D. DesMarteau, S. Creager, V. Borgel, M. Levi, D. Aurbach, and I. C. Halalay*
- 1243 Enhanced the Safety of the Lithium-Ion Batteries by the Electrolyte Additive  
*T. Yeh, J. Chen, S. Liao, M. Shen, and C. Liu*
- 1244 Effects of LiNO<sub>3</sub> Additive on the Electrochemical Properties of Lithium-Sulfur Batteries  
*H. Kim*
- 1245 Solvent-Dependent Solid Electrolyte Interphases on Nongraphite Electrodes  
*M. Ihara, H. Nakai, A. Kita, K. Kawase, and T. Kubota*
- 1246 Electrolytes with Improved Safety Developed for High Specific Energy Li-Ion Cells with Si-Based Anodes  
*M. C. Smart, F. C. Krause, C. Hwang, J. Soler, W. C. West, B. Ratnakumar, and G. Prakash*
- 1247 Enhanced Morphology and Cycling Efficiency of Li Metal Anode by Electrolyte Additives for Rechargeable Li Batteries  
*W. Xu, F. Ding, J. Zhang, X. Chen, M. H. Engelhard, M. Sushku, E. Nasybulin, J. Xiao, G. L. Graff, and J. Zhang*
- 1248 Investigation of the Electrolyte Composition in a Li-S Cell upon Long-Term Cycling  
*R. Schmidt, H. Schneider, J. Tomforde, and T. Weiss*
- 1249 Electrolyte Solvation and Ionic Association: Cyclic Carbonate and Ester-LiTFSI and -LiPF<sub>6</sub> Mixtures  
*W. A. Henderson, D. M. Seo, J. L. Allen, L. A. Gardner, S. Han, and P. D. Boyle*
- 1250 Thermal Phase Behavior and Electrochemical/Physicochemical Properties of Carbonate and Ester Electrolytes with LiBF<sub>4</sub>, LiDFOB and LiBOB  
*J. L. Allen, S. Han, D. W. McOwen, B. A. Knight, D. M. Seo, P. D. Boyle, and W. A. Henderson*
- 1251 Delving into the Properties and Solution Structure of Nitrile-Lithium Difluoro(Oxalato)Borate (LiDFOB) Electrolytes for Li-Ion Batteries  
*S. Han, J. L. Allen, P. D. Boyle, and W. A. Henderson*
- 1252 Ion Transport in Non-Aqueous Liquid Electrolytes Containing Oxide Inclusions  
*S. K. Das and A. J. Bhattacharyya*

- 1253 The Influence of Molecular Interactions on Battery Electrolyte Properties and Processes  
*K. L. Gering*
- 1254 Insight into Electrolyte Stability, Decomposition and Transport Properties from DFT and MD Simulations  
*O. Borodin, L. Xing, and T. Jow*
- 1255 Electrolyte Structure Near Charged Electrode Surfaces: A Molecular Dynamics Simulation Study  
*D. Bedrov, L. Xing, J. Vatamanu, and O. Borodin*
- 1256 Properties of Fluoro-Free Non-Aqueous Electrolytes: Computational Predictions and Experimental Results  
*J. Scheers, W. A. Henderson, P. Johansson, and P. Jacobsson*
- 1257 Stability of Aprotic Solvents in Li-Air Batteries: Theoretical Investigation of Nucleophilic Substitution by Superoxide, C-H Acidity, and Autoxidation  
*V. S. Bryantsev, J. Uddin, W. Walker, V. Giordani, S. Zecevic, D. Addison, and G. V. Chase*
- 1258 Ab Initio Study on Reduction Mechanisms of Vinylene Carbonate Using Global Reaction Route Mapping Method  
*K. Miyamoto, R. Asahi, and K. Ohno*
- 1259 DFT Study on Reduction Reactions of Ethylene Carbonate and Propylene Carbonate as Co-Solvents inside Graphite in Lithium-Ion Battery Cells  
*K. Tasaki and A. Goldberg*

### **B9 - Polymer Electrolyte Fuel Cells 12 (PEFC 12)**

*ECS Energy Technology, ECS Corrosion, ECS Physical and Analytical Electrochemistry, ECS Battery, ECS Industrial Electrochemistry and Electrochemical Engineering, ECSJ Fuel Cells, CSE, KECS*

- 1260 Development of PEFCs with Nanostructurally Controlled Electrocatalysts  
*A. Hayashi and K. Sasaki*
- 1261 Graphitized Aerogel Supported PEMFC catalysts for Oxygen Reduction Reaction  
*P. Kolla, Y. Normah, K. Kerce, and A. Smirnova*
- 1262 Influence of Chemistry and Structure on the ORR Activity of Pt Supported on N-Doped Mesoporous Carbon  
*S. Shrestha, S. Ashegi, J. Timbro, and W. E. Mustain*
- 1263 Low Pt-Loaded Nanofiber Electrodes for Hydrogen/Air Fuel Cells  
*M. Brodt and P. N. Pintauro*
- 1264 Electrospinning : A Promising Pathway in the Design of Carbon Nanotubes-Based Electrodes for Hydrogen Fuel Cells  
*S. Zils and M. Michel*

- 1265 Durability of the Electrocatalyst Fabricated based on Carbon Nanotubes  
*T. Fujigaya, B. Mohamad, and N. Nakashima*
- 1266 Cathode Thickness Dependency of Oxygen Reduction Rate in PEFC  
*M. Kawase, S. Chin, G. Inoue, K. Sato, and M. Kageyama*
- 1267 Investigation of Solvent Effects on Dispersion of Carbon Agglomerates and Nafion Ionomer Particles in Catalyst Inks Using Ultra Small Angle X-Ray Scattering and Cryo-TEM  
*L. Sun, H. Zhang, L. Stanciu, J. Ilavsky, and J. Xie*
- 1268 Structural Control and Evaluation of PEMFC Catalyst Layers by Blending Platinum-Supported/Stand-Alone Carbon Black  
*T. Suzuki, S. Tsushima, and S. Hirai*
- 1269 Influence of Nafion on the Electrochemical Activity of Pt-based Electrocatalysts  
*S. S. Kocha, J. W. Zack, K. Neyerlin, and B. S. Pivovar*
- 1270 Analysis of Oxygen Transport Resistance of Nafion Thin Film on Pt Electrode  
*K. Kudo and Y. Morimoto*
- 1271 Effect of High Oxygen Permeable Ionomers on MEA Performance for PEFC  
*K. Yamada, S. Hommura, and T. Shimohira*
- 1272 Evaluation of Anion Adsorption on Pt Surface in MEA  
*Y. Furuya, T. Mashio, A. Ohama, and K. Shinohara*
- 1273 Elemental and Morphological Analysis of Novel Pt Catalysts Synthesized by Galvanic Displacement  
*K. A. Perry, B. A. Larsen, K. Neyerlin, B. S. Pivovar, and K. L. More*
- 1274 Hyundai's FCEVs: A Pathway to New Possibilities  
*T. Lim and B. Ahn*
- 1275 Development of Advanced Materials and Devices for Cost Reduction of PEFC CHP System  
*H. Ohara and T. Omura*
- 1276 Polymer Electrolyte Fuel Cell Lifetime Limitations: The Role of Electrocatalyst Degradation  
*D. J. Myers, X. Wang, N. N. Kariuki, S. DeCrane, T. Nowicki, S. Arisetty, R. Subbaraman, R. K. Ahluwalia, J. Gilbert, B. Puchala, E. Holby, D. Morgan, S. Ball, J. Sharman, B. Theobald, G. Hards, M. Gummalla, Z. Yang, S. Zhitnik, D. Groom, S. Rajasekhara,*
- 1277 Membrane Fuel Cells - Options for Bipolar Plate Materials and Production Technology  
*A. Heinzel, L. Kühnemann, T. Derieth, T. Grimm, and P. Butzen*
- 1278 Limiting Current as a Tool to Study Oxygen Transport in PEM Fuel Cells  
*D. R. Baker and D. Caulk*

- 1279 Ionomer in the Catalyst Layer  
*S. Holdcroft*
- 1280 Development of Thin, Reinforced PEMFC Membranes through Understanding Structure-Property-Performance Relationships  
*W. Liu, T. Suzuki, H. Mao, and T. Schmiedel*
- 1281 Development of Highly Active and Durable Pt Core-Shell Catalysts for Polymer Electrolyte Fuel Cells  
*M. Inaba and H. Daimon*
- 1282 Modeling and Diagnostics in Biological Fuel Cells  
*H. Wen, D. Chakraborty, P. Kar, and S. Calabrese Barton*
- 1283 Modelling of Water Droplet Dynamics in PEM Fuel Cell Flow Channels  
*T. Wu and N. Djilali*
- 1284 Modeling Oxygen Concentration Oscillation in the Gas Channel of Polymer Electrolyte Fuel Cells: A Comparison between Numerical and Analytical Approaches  
*P. Guillemet, G. Maranzana, J. Mainka, O. Lottin, J. Dillet, and A. Lamibrac*
- 1285 A Two-Phase Pressure Drop Model Incorporating Local Water Balance in PEM Fuel Cell Gas Channels  
*E. J. See and S. G. Kandlikar*
- 1286 Diffusive - Kinetic Evaporation Models for Fuel Cells  
*E. F. Médici, D. Frtiz, and J. S. Alllen*
- 1287 A Map to Start PEFC under Freezing Temperature -Theoretical Analysis of Super-cooled State in Cell-  
*Y. Ishikawa, K. Ito, M. Shiozawa, and M. Kondo*
- 1288 Numerical Modeling of a Non-Flooding Hybrid Polymer Electrolyte Fuel Cell  
*B. E. McNealy and J. L. Hertz*
- 1289 Statistical Simulation of the Performance and Degradation of a PEMFC Membrane Electrode Assembly  
*D. A. Harvey, A. Bellemare-Davis, K. Karan, B. Jayansankar, J. G. Pharoah, V. Colbow, A. Young, and S. Wessel*
- 1290 Multi-Scale First-Principles Modeling of Three-Phase System of Polymer Electrolyte Membrane Fuel Cell  
*G. Brunello, J. Choi, S. Jang, and D. A. Harvey*
- 1291 Missions and Progressions of Impurities WG under NEDO's PEFC Residential CHP System Project  
*K. Kobayashi, Y. Oono, and M. Hori*

- 1292 Characterizing Leachant Contaminants from Fuel Cell Assembly Aids, a Prelude to Effects on Performance  
*C. S. Macomber, J. Christ, H. Wang, B. S. Pivovar, and H. N. Dinh*
- 1293 Understanding the Effects of Contaminants from Assembly Aids Materials used as Balance of Plant Materials on PEMFCs -In-situ Studies  
*M. S. Opu, M. Ohashi, H. Cho, C. S. Macomber, H. N. Dinh, and J. W. Van Zee*
- 1294 The Impact of Operating Conditions on the Performance effect of Selected Airborne PEMFC Contaminants  
*Y. Zhai, M. S. Angelo, and J. St-Pierre*
- 1295 The Contamination Behavior of Organic Compounds on PEMFC  
*H. Cho, M. S. Opu, M. Ohashi, and J. W. Van Zee*
- 1296 Liquid Water Scavenging of PEMFC Contaminants  
*B. Wetton and J. St-Pierre*
- 1297 The Poisoning and Recovery of Pt/VC Electrocatalysts Contaminated with Glycol-Based Coolant Formulations  
*Y. Garsany, S. Dutta, and K. Swider-Lyons*
- 1298 Evaluation of PEMFC System Contaminants on the Performance of Pt Catalyst via Cyclic Voltammetry  
*H. Wang, C. S. Macomber, J. Christ, G. Bender, B. S. Pivovar, H. N. Dinh, R. Reid, B. Lakshmanan, K. O'Leary, M. Das, M. Ohashi, and J. Van Zee*
- 1299 The Influence of NaCl Aerosol on the Performance of a PEM Fuel Cell Cathode  
*O. A. Baturina, P. Northrup, and K. Swider-Lyons*
- 1300 Effect of Cationic Contaminants on PEM Fuel Cell Performance  
*J. Qi, X. Wang, U. Pasaogullari, L. Bonville, and T. Molter*
- 1301 The Impact of Low Levels of NH<sub>3</sub> in an Operating Polymer Electrolyte Fuel Cell as the Platinum Loading/Ionomer is Varied  
*T. Rockward, C. Quesada, K. C. Rau, and F. H. Garzon*
- 1302 Advances in Proton Exchange Membrane Technology  
*S. Banerjee, D. N. Prugh, and S. Frisk*
- 1303 Nanofiber Composite Membranes Using Low EW PFSA  
*J. B. Ballengee and P. N. Pintauro*
- 1304 Novel System for Characterizing Electro-Osmotic Drag Coefficient of Proton Exchange Membranes  
*H. Xu, J. Ma, and C. Mittelsteadt*
- 1305 Mechanism of Perfluorsulfonic Acid Membrane Chemical Degradation Under Low RH Conditions  
*F. D. Coms, H. Xu, T. McCallum, and C. Mittelsteadt*

- 1306 Challenges to High-Volume Production of Fuel Cell Materials: Quality Control  
*M. Ulsh, B. Sopori, N. V. Aieta, and G. Bender*
- 1307 Polymer Electrolyte Membrane Durability -Local degradation at pinholes  
*S. Kreitmeier, A. Wokaun, and F. Büchi*
- 1308 Nafion Polymer Backbone Degradation Mechanism in PEM Fuel Cell from Quantum Mechanics Calculations  
*T. Yu, Y. Sha, W. Liu, B. V. Merinov, P. Shirvanian, and W. Goddard III*
- 1309 Modeling of Side Chain Degradation in PEMFC Membranes  
*K. Wong, P. Melchy, M. Eikerling, M. Lauritzen, and E. Kjeang*
- 1310 Investigation of PEM Degradation Kinetics and Degradation Mitigation Using In Situ Fluorescence Spectroscopy and Real-Time Monitoring of Fluoride-Ion Release  
*V. Prabhakaran, C. G. Arges, and V. Ramani*
- 1311 Imaging Catalyst Degradation at the Atomic Scale  
*D. A. Muller, Y. Yu, H. Xin, D. Wang, and H. D. Abruña*
- 1312 3-D Tracking and Visualization of Hundreds of Fuel Cell Nanocatalysts during Electrochemical Aging  
*Y. Yu, H. Xin, R. Hovden, D. Wang, J. Mundy, D. A. Muller, and H. D. Abruña*
- 1313 Correlating Catalyst and Catalyst-Support Structures with Observed Degradation in PEM Fuel Cell  
*K. L. More, D. A. Cullen, J. Idrobo, K. A. Perry, and K. Reeves*
- 1314 Quantifying Catalyst Losses in Polymer Electrolyte Membrane Fuel Cells  
*D. A. Cullen and K. L. More*
- 1315 Catalyst Degradation: Nanoparticle Population Dynamics and Kinetic Processes  
*S. G. Rinaldo, W. Lee, J. Stumper, and M. Eikerling*
- 1316 Study of the Cathode Catalyst Layer Degradation Mechanisms in PEM Fuel Cell  
*P. Urchaga, S. Goli, and C. A. Rice*
- 1317 In Situ Anomalous Small-Angle X-ray Scattering Study of Fuel Cell Catalyst Degradation in Aqueous and Membrane Electrode Assembly Environments  
*J. A. Gilbert, N. N. Kariuki, A. Kropf, D. Morgan, D. J. Myers, S. Ball, J. Sharman, B. Theobald, and G. Hards*
- 1318 Cathode Catalysts Degradation Mechanism from Liquid Electrolyte to Polymer Electrolyte Membrane Fuel Cells  
*A. A. Marcu and G. Toth*
- 1319 Rotating Disk Electrode Techniques Designed to Simulate Fuel Cell Startup/Shut-Down Transient Conditions  
*D. A. Stevens, J. Harlow, R. J. Sanderson, T. J. Crowtz, J. Dahn, G. D. Vernstrom, L. L. Atanasoska, G. M. Haugen, and R. T. Atanasoski*

- 1320 The Influence of Experimental Conditions on the Catalyst Degradation in the Accelerated Durability Test using a Rotating Disk Electrode  
*T. Nagai, H. Murata, and Y. Morimoto*
- 1321 Electrocatalysis of Small Organic and Inorganic Molecules for Direct Oxidation Fuel Cells  
*E. A. Baranova, A. Allagui, and B. Middleton*
- 1322 Reaction Mechanism of Ethanol Oxidation over Gold Catalyst under Alkaline Environment  
*M. Koyama, Y. Amano, S. Liu, and T. Ishimoto*
- 1323 Rh Porphyrin-Based Electrocatalysts for the Oxidation of Alcohols  
*S. Yamazaki, M. Yao, N. Fujiwara, Z. Siroma, M. Asahi, and T. Ioroi*
- 1324 Ethanol Electro-Oxidation on Pt/C and Pd/C Catalysts in Alkaline Media  
*L. Ma, H. He, A. Hsu, D. Chu, and R. Chen*
- 1325 Enhanced O<sub>2</sub> Reduction Kinetics by Tuning Electrochemical Interface of Carbon or Ag/C Electrodes with Metallophthalocyanine Molecules in Alkaline Media  
*R. Chen, J. Guo, H. He, J. Zhou, and D. Chu*
- 1326 Catalysts for Alkaline Direct Ethanol and Direct Formate Fuel Cells  
*A. M. Bartram, G. Ognibene, J. Ta, J. Tran, and J. L. Haan*
- 1327 Development of Electrocatalyst for Anion-type Polymer Electrolyte Fuel Cell using KOH-doped Polybenzimidazole  
*T. Fujigaya and N. Nakashima*
- 1328 Pt-Free Catalysts for Alkaline Direct Ethanol Membrane Electrode Assemblies  
*A. Stadlhofer, M. Bodner, H. Schröttner, and V. Hacker*
- 1329 High Performance Pt on Composite Ni-Pb / C Support for Methanol Oxidation in Alkaline Media  
*M. Lee, B. Mikes, D. Abbott, and S. Mukerjee*
- 1330 Network Formation and Ion Conduction in Ionomer Membranes  
*K. Promislow, A. Christlieb, J. Jones, Z. Xu, and N. Gavish*
- 1331 On Water Transport in Polymer Electrolyte Membranes during the Passage of Current  
*T. Berning*
- 1332 Molecular Simulation of Proton and Water Transport in Hydrated Nafion Membrane  
*T. Mabuchi and T. Tokumasu*
- 1333 Understanding Water Management as a Function of Catalyst-Layer Thickness  
*P. K. Das and W. Adam*
- 1334 Numerical Simulation of the Interfacial Oxygen Transport Resistance for a PEMFC Cathode Incorporating Water Coverage  
*M. Koz and S. G. Kandlikar*

- 1335 Molecular Dynamics Study of Water Transport Property in Micro Hydrophobic Pore  
*A. Fukushima, T. Mima, I. Kinoshita, and T. Tokumasu*
- 1336 3D Modeling of One and Two Component Gas Flow in Fibrous Microstructures in Fuel Cells by Using the Lattice-Boltzmann Method  
*J. Brinkmann, D. Froning, U. Reimer, V. Schmidt, W. Lehnert, and D. Stolten*
- 1337 Lattice Boltzmann Modeling of the Effective Thermal Conductivity of an Anisotropic PEMFC GDL with Residual Water  
*J. Yablecki and A. Bazylak*
- 1338 Numerical Determination of Transport Properties of Gas Diffusion Layers in Wet Conditions  
*Z. TAYARANI YOOSEFABADI, D. A. Harvey, and E. Kjeang*
- 1339 A Case Study of Validation of Multiphase PEMFC Computer Models Using Through-Plane Liquid Water Measurements  
*B. Carnes, K. Chen, D. Spernjak, G. Luo, L. Hao, and C. Wang*
- 1340 Effect of N-doping on Performance and Durability of Supported PtRu Direct Methanol Fuel Cell Catalyst  
*S. Pylypenko, A. Corpuz, T. Olson, A. Dameron, K. Wood, P. Joghee, K. Hurst, S. Christensen, D. Ginley, B. S. Pivoar, R. M. Richards, H. N. Dinh, T. Gennett, and R. O'Hayre*
- 1341 Performance and Durability of HT-PEFCs with Customized Flow Field Plates  
*F. Liu, M. Kvesić, K. Wippermann, U. Reimer, and W. Lehnert*
- 1342 Impact of Polymer Electrolyte Membrane Degradation Products on the Activity of the Oxygen Reduction Reaction on Platinum Catalysts  
*J. M. Christ, K. Neyerlin, H. Wang, R. M. Richards, and H. N. Dinh*
- 1343 Internal Currents, CO<sub>2</sub> Emissions and Decrease of the Pt Electrochemical Surface Area during Fuel Cell Start-Up and Shut-Down  
*A. Lamibrac, J. Durst, D. Spernjak, G. Maranzana, J. Dillet, S. Didierjean, O. Lottin, F. Maillard, L. Dubau, M. Chatenet, R. Mukundan, and R. L. Borup*
- 1344 MEA Design for Improved Cathode Durability under Startup Shutdown Automotive Conditions  
*J. Roberts, F. Berretta, H. Haas, A. Yang, S. Ronasi, S. Kundu, A. Leow, Z. Moreland, G. Orha, Y. Hsieh, and N. Barsan*
- 1345 Relation between Local Loss of Performances in a Segmented PEMFC and Local Degradations of the Pt/C Cathode Catalyst  
*J. Durst, A. Lamibrac, L. Dubau, F. Maillard, M. Chatenet, J. Dillet, G. Maranzana, and O. Lottin*
- 1346 Study on Protocols for Evaluating Mechanical and Chemical Durability of PEFC Electrolyte Membranes  
*Y. Oono, Y. Yamaguchi, K. Kobayashi, A. Daimaru, and M. Hori*

- 1347 Membrane Durability Testing for Heavy Duty Bus Fuel Cells  
*N. MACAULEY, M. Watson, M. Cruickshank, C. Lim, A. Tavassoli, G. Wang, X. Feng, M. Lauritzen, J. Kolodziej, S. Knights, and E. Kjeang*
- 1348 Cross-linked Aromatic Polymers for High Durability PEM Membranes: Materials and Methods  
*M. Di Vona*
- 1349 Cross-Linked poly(arylene Ether Ketone) Membranes Sulfonated on both Backbone and Pendant Position for High Proton Conducting and Low Water Uptake  
*H. Dang and D. Kim*
- 1350 Poly(Arylene Ether Sulfone) Ionomers with Different Acidity Strengths and Fuel Cell Membrane Properties  
*Y. Chang, G. Brunello, M. Disabb-Miller, M. Hawley, Y. Kim, M. Hickner, S. Jang, and C. Bae*
- 1351 Synthesis and Characterization of Sulfonated Poly(Arylene Ether-1,3,4-Oxadiazole) Derivatives  
*I. Hajdok and J. A. Kerres*
- 1352 Effect of Humidity and Temperature on Durability of Sulfonated Poly(arylene ether sulfone ketone) Multiblock Copolymer Membranes in PEFC Operation  
*Y. Sakiyama, H. Uchida, M. Kondo, K. Miyatake, M. Uchida, M. Watanabe, and Y. Nakagawa*
- 1353 Proton Mobility in Hydrated Acidic Polymers: Consequences for Optimization of Proton Conductivity  
*P. Knauth and M. Di Vona*
- 1354 PFG-NMR and SANS Studies in Cation Exchange Membranes based on Sulfonated Polyphenylene Multiblock Copolymers  
*M. Yoshida, Y. Zhao, M. Yoshizawa-Fujita, A. Ohira, Y. Takeoka, S. Koizumi, and M. Rikukawa*
- 1355 Proton Conductive Paths on Polymer Electrolyte Membranes Detected by AFM under Controlled Hydrogen Atmosphere  
*J. Inukai, M. Hara, D. Hattori, B. Bae, K. Miyatake, and M. Watanabe*
- 1356 Synthesis of Polyethylene-Based Proton Exchange Membranes Containing PE Backbone and Sulfonated Poly(arylene ether sulfone) Side Chains for Fuel Cell Applications  
*H. Kim, S. N. Lvov, and T. Chung*
- 1357 New Ionically and Covalently Cross-Linked Polyaromatic Membranes for Fuel Cells and Electrolysis  
*J. A. Kerres*
- 1358 Studies on the Platinum Dissolution Reaction in PEMFC Electrocatalysts - The Effect of Temperature on catalyst degradation  
*P. Sivasubramanian and R. Mohtadi*

- 1359 Degradation of Platinum Cathode Electrocatalysts in Sulphuric Acid Solution under Thermal Stress Induced by Linear Sweep Cyclic Thermammetry  
*G. T. Burstein and G. Smith*
- 1360 A Study of Electrochemical Ostwald Ripening in Pt and Ag Catalysts Supported on Carbon  
*P. Parthasarathy and A. V. Virkar*
- 1361 Particle Size Effect on Electrocatalyst Stability  
*C. Wang, N. M. Markovic, and V. R. Stamenkovic*
- 1362 Performance, Degradation and Structural Changes Associated with Pt Cathode Catalyst Layer Design  
*V. Colbow, M. Dutta, A. Young, Z. Ahmad, E. Rogers, D. A. Harvey, and S. Wessel*
- 1363 Mitigation of Catalyst Layer Degradation under Automotive Fuel Cell Operations  
*J. Li, K. Wang, Y. Yang, Y. Zou, and R. Vohra*
- 1364 PtCo Alloy Stability in PEMFCs under Automotive Cyclic Conditions  
*C. Chuy, M. Davis, M. Guenther, H. Haas, D. Susac, C. Talpalaru, and H. Zhang*
- 1365 Durable, OER-Active Compositions of Pt, Ir, and Ru for PEM Fuel Cell Start-Stop Protection  
*J. E. Harlow, D. A. Stevens, R. Sanderson, T. J. Crowtz, J. Dahn, G. M. Haugen, L. L. Atanasoska, G. D. Vernstrom, and R. T. Atanasoski*
- 1366 Effect of Nanosheet Size on Activity and Durability of RuO<sub>2</sub> Nanosheet Pt/C Catalyst  
*C. Chauvin, T. Saida, K. S. Lokesh, and W. Sugimoto*
- 1367 Time Resolved Corrosion of Electrode Supports in PEM Fuel Cells  
*J. D. Fairweather, D. Spernjak, R. Mukundan, R. K. Ahluwalia, S. Arisetty, and R. L. Borup*
- 1368 Alkaline Membrane Fuel Cell (AMFC) materials and system improvement - State-of-the-Art  
*D. R. Dekel*
- 1369 A Raman Spectroscopy Investigation into the Alkaline Stabilities of Hydrated Anion-Exchange Head-Groups Relevant to Alkaline Membrane Fuel Cells  
*J. R. Varcoe, H. Herman, and D. K. Whelligan*
- 1370 Engineering the van der Waals Interaction in Cross-Linking-Free Hydroxide Exchange Membranes for Low-Swelling and High-Conductivity  
*S. Gu, J. Skovgard, and Y. Yan*
- 1371 Catalytic Advances and Electrolyte Stability for Carbonate Exchange Membrane Fuel Cells  
*W. E. Mustain*

- 1372 Molecular Dynamics Simulations of Hydroxide Solvation and Transport in Anionic Exchange Membranes  
*G. E. Lindberg, C. Knight, and G. A. Voth*
- 1373 Anion Conducting Pore-Filling Membranes for Solid Alkaline Fuel Cells  
*Y. Choi, M. Lee, C. Kim, T. Yang, and S. Park*
- 1374 Evaluating the Contribution of Direct vs. Indirect Carbonate Production in Anion Exchange Membrane Fuel Cells  
*M. Ignatowich, G. Crettol, M. Chhiv, and W. E. Mustain*
- 1375 Fundamental Studies of Alkaline Exchange Membranes Towards Optimization in a Fuel Cell Environment  
*A. Herring, E. Coughlin, D. Knauss, G. A. Voth, T. Witten, M. Liberatore, and Y. Yan*
- 1376 Development of Alkaline Exchange Ionomers for use in Alkaline Polymer Electrolyte Fuel Cells  
*S. D. Poynton, R. Zeng, J. Kizewski, A. Ong, and J. R. Varcoe*
- 1377 Electrochemical Performance of Pt Extended Network Catalysts from Spontaneous Galvanic Displacement in MEAs  
*K. Neyerlin, B. A. Larsen, S. S. Kocha, and B. S. Pivovar*
- 1378 Effect and Development of Cathode Catalyst on PEFC Cell Performance under Low and High Relative Humidity  
*H. Nakajima and K. Matsutani*
- 1379 Subzero Degradation Analysis of Membrane Electrode Assemblies Fabricated Using Two Common Techniques  
*A. Pistono, C. A. Rice, J. Lewis, and V. Ramani*
- 1380 Application of Electrospinning Technique in the Fabrication of a Composite Electrode for PEMFC  
*J. J. Sightler, E. McPherson, W. A. Rigdon, and X. Huang*
- 1381 Verification of Durability Test Methods of an MEA for Automotive Application  
*Y. Hashimasa, T. Shimizu, Y. Matsuda, D. Imamura, and M. Akai*
- 1382 Structural Change of the Pt/C Electrocatalyst in Humidified Air Observed by In Situ TEM  
*T. Shimizu, D. Imamura, T. Yaguchi, T. Kanemura, and T. Kamino*
- 1383 Effects of Pt Loading in Anode Electrode on the Degradation of MEA for PEMFCs during Startup/Shutdown Cycling  
*E. Cho, K. Eom, T. Lim, J. Jang, and H. Kim*
- 1384 Evaluation of Pt/C Catalysts and MEA's Fabricated by Carbon Materials with Different Nanostructures for Polymer Electrolyte Fuel Cells  
*X. Zhao, Z. Noda, A. Hayashi, and K. Sasaki*

- 1385 Real-time CO<sub>2</sub> Detection from Carbon Support Oxidation in PEM Fuel Cell Cathodes During Potential Cycling  
*E. Niangar, T. Han, N. Dale, and K. Adjeman*
- 1386 Investigation of Role of Cathode Microporous Layers in PEMFC  
*E. Nishiyama, M. Hara, and T. Murahashi*
- 1387 Multi-Analytical Study of Gas Diffusion Layers PTFE Content Variation  
*K. Artyushkova, P. Atanassov, T. V. Reshetenko, and J. St-Pierre*
- 1388 Using Plasmas to Modify Gas Diffusion Layers to Enhance the Long Term Stability of PEMFCs  
*C. Walter, V. Brüser, A. Quade, and K. Weltmann*
- 1389 Dynamic SIMS Analysis of PEMFC Catalyst Layer/Solid Electrolyte Membrane Interface  
*T. Ebihara, M. Nojima, T. Kondo, and M. Yuasa*
- 1390 Numerical Investigation of effect of Oxygen and Water Distribution on PEM Fuel Cell Performance  
*M. Yoneda and H. Motegi*
- 1391 Reactive Molecular Dynamics Simulations of Proton Exchange Membranes  
*J. Savage and G. A. Voth*
- 1392 Thermo-Fluid Dynamics Simulation of Passive Type PEFC by COMSOL Multiphysics  
*Y. Nakajima, J. Otsuka, and E. Ejiri*
- 1393 The Mechanism of the Improvement in Catalytic Activity of Ir Modified by V Compared to Pure Ir/C  
*B. Li, D. Yang, R. Lin, Z. Yu, and J. Ma*
- 1394 Analysis of Non-Steady State Electrochemical Gas Permeability Measurements for PEM Fuel Cells and Electrolysers  
*D. Bessarabov, I. Beckman, and I. Buntseva*
- 1395 Interfacial Contact Resistance of Tantalum Coated Construction Materials for High Temperature Steam Electrolysers and Fuel Cells  
*A. H. Jensen, E. Christensen, and J. von Barner*
- 1396 Hydrogen Generation from Aluminum Corrosion in Aqueous Solutions  
*Y. Chiu, C. Chen, K. Hsueh, and J. Hung*
- 1397 Fabrication of Mg-Ni Alloys for the Purpose of Fast Hydrogen Generation from the Hydrolysis in Neutral Aqueous NaCl solution  
*S. Oh, K. Eom, J. Kyung, D. Kim, and H. Kwon*
- 1398 Computer Modeling of a kW Combined Heat and Power Fuel Cell Unit  
*P. Ho, W. Wang, C. Dai, Y. Chang, W. Chang, K. Hsueh, and J. Hung*

- 1399 Maximum Efficiency Point Tracking Type Power Control System for a Fuel Cell Power Generation System  
*K. Itako and H. Takahashi*
- 1400 A 3D Two-Phase Model for a Membraneless Fuel Cell Using Decomposition of Hydrogen Peroxide with Y-Shaped Microchannel  
*J. Peng, Z. Zhang, and H. Niu*
- 1401 A Study of Electrochemical Recycle for Noble Metals in PEFCs  
*H. Shiroishi, H. Matsumoto, M. Yonekawa, R. Shoji, I. Kato, and M. Kunimatsu*
- 1402 Effects of Atmospheric Trace Species on Polymer Electrolyte Fuel Cell Performance: Analysis of Performance Deterioration Mechanism by Current Distribution Measurement  
*D. Imamura and K. Ohno*
- 1403 Development of Methods to Estimate the Effects of Impurities on PEFC Performance II. Impact of Acrylonitrile Poisoning on Oxygen Reduction Reaction at Pt/C Catalysts  
*M. El-Deab, F. Kitamura, and T. Ohsaka*
- 1404 Ammonium Polyphosphate Composite Based Electrolytes for Intermediate Temperature Fuel Cells  
*N. Kluy, B. B. Reeb, O. Paschos, F. Maglia, O. Schneider, U. Stimming, S. Angioni, and P. P. Righetti*
- 1405 Flow Field Design for a Polymer Electrolyte Unitized Reversible Fuel Cell  
*C. Hwang, H. Ito, T. Maeda, A. Nakano, A. Kato, and T. Yoshida*
- 1406 A New Design of PEMFC Bipolar Plate for Corrosion Study  
*Y. Hitoshi, T. Ichikawa, S. Chu, M. Kumagai, and S. Myung*
- 1407 DMFC Performance of Cross-Linked Sulfoethylcellulose/Poly(Vinyl Alcohol) Blend Electrolyte Membranes  
*Y. Kasai, T. Okayama, G. Guan, and A. Abudula*
- 1408 Investigation of Power Efficiency from the Microbial Biofuel Cell System with the Photosynthetic Bacteria, Rhodopseudomonas Sphaeroides  
*M. Syu and Y. Chang*
- 1409 Immobilization of Enzymes onto the Carbon Paper Electrode by the Conducting Polymer/Carbon Nanotubes Composite for the Investigation of the Biofuel Cell System  
*M. Syu and C. Lin*
- 1410 Designing a Highly Ordered Nanowire with High Proton Conductivity for Polymer Membrane and Catalyst Layer of PEFC  
*T. Kim, Y. Choi, and S. Yim*
- 1411 Electrochemical and Raman Spectroscopic Evaluation of Pt/GCB Durability for the Start/Stop Operating Condition  
*M. Hara, M. Lee, Y. Yamashita, M. Uchida, H. Uchida, and M. Watanabe*

- 1412 Investigation of Carbon Corrosion Resistance of CNT Containing Electrode  
*D. Larrabee, W. A. Rigdon, E. McPherson, J. J. Sightler, and X. Huang*
- 1413 Investigation of the Corrosion of Carbon Supports in Polymer Electrolyte Fuel Cells Using Simulated Start-Up/Shut-Down Cycling  
*Y. Park, K. Kakinuma, M. Hara, M. Uchida, H. Uchida, and M. Watanabe*
- 1414 Durability of Arc Plasma Synthesized Pt/C Nano-Catalyst  
*H. Joo, J. Park, and H. Choi*
- 1415 Kinetics and Mass Transport Investigation of Pt/Carbon Electrocatalyst by Rotating Disk Electrode  
*C. Wang, N. Dale, and K. Adjemian*
- 1416 Oxygen Reduction Reaction Activity and Durability of Electrocatalysts Supported on SnO<sub>2</sub>  
*T. Tsukatsune, Y. Takabatake, Z. Noda, S. Taniguchi, Y. Shiratori, A. Hayashi, and K. Sasaki*
- 1417 Effects of Tin Dioxide Loading on ORR Activity and Durability of Pt/C Catalyst  
*N. Eguchi, T. Kinumoto, T. Tsumura, and M. Toyoda*
- 1418 Durability Enhancement of Pt/C Catalysts via Support Functionalization with Silicotungstic Acid  
*K. S. Mason, K. Neyerlin, M. Kuo, K. Horning, S. S. Kocha, J. A. Turner, and A. Herring*
- 1419 Performance Evaluation of Pt-Deposited SiO<sub>2</sub> Composite Catalyst under Low Humidity Conditions  
*J. Yoo, I. Choi, S. Ahn, J. Kim, and O. Kwon*
- 1420 Durability of Au Core/Pt Shell Structured Catalyst  
*E. Maki, Y. Ikehata, T. Nishikawa, Y. Kirihata, N. aoki, H. Inoue, H. YAMADA, H. Daimon, and M. Inaba*
- 1421 Electrochemical Stability of Pt ML on Au/QC Electrode  
*H. YAMADA, A. Kawamura, T. Kobayashi, K. Katakura, and M. Inaba*
- 1422 Electrochemical Stability for Pt-Enriched Ni/Pt(111) Topmost Surface Prepared by Molecular Beam Epitaxy  
*N. Todoroki, Y. Iijima, R. Takahashi, K. Matsumoto, Y. Yamada, T. Hayashi, and T. Wadayama*
- 1423 Platinum Dissolution in Nitrogen Oxides-Containing HClO<sub>4</sub> Solution Studied by Electrochemical Quartz Crystal Microbalance  
*Y. Uchiyama, T. Abe, T. Morita, and S. Imabayashi*
- 1424 Poly(Benzimidazole)-Functionalized Graphene Supported Pt Electrocatalyst and Its Application in High Temperature PEM Fuel Cells  
*A. A. Permyakova, J. Jensen, Q. Li, and N. Bjerrum*

- 1425 Evaluation of the Pt/C Catalyst for Fuel Cells Prepared by a Nano Particle Formation Technique Using a Pulsed Arc Plasma Source  
*Y. Agawa, S. Endo, M. Matsuura, and Y. Ishii*
- 1426 Controlled Pt Coverage for Extended Thin Film Catalyst ORR Studies via Templated Gas Phase Synthesis  
*J. Bult, K. Neyerlin, S. Christensen, A. Dameron, B. S. Pivovar, and K. Hurst*
- 1427 Synthesis and Characterization of Au-Decorated Pt Surface for Oxygen Reduction Reaction  
*J. Ahn, H. Lee, H. Kim, Y. Shul, and H. Kim*
- 1428 Synthesis of Alkanetiol Stabilized Au/C and Durability of Au Core/Pt Shell Structured Catalyst  
*N. aoki, H. Inoue, T. Kirihata, E. Maki, H. Daimon, and M. Inaba*
- 1429 Various Types of Tubular Carbon Nanofibers as a Support Material of Catalysts for Fuel Cell  
*J. Kim, S. Lim, M. Seo, B. Kim, S. Yoon, and D. Jung*
- 1430 High-Performance Pt catalysts Supported on High-Surface-Area Graphene Composites for PEFCs  
*L. Sun, H. Zhang, L. Stanciu, J. Ilavsky, and J. Xie*
- 1431 Platinum Yttrium Alloy Nanocrystals as Oxygen Reduction Reaction Electrocatalysts  
*Z. Zhuang, Y. Zhang, and Y. Yan*
- 1432 Oxygen Reduction on Pt-Pd Electrode for PEFC Cathode  
*A. Hyono, Y. Sugawara, M. Ueda, and T. Ohtsuka*
- 1433 Improvement in Activity of Highly Durable Silica-Coated Pd/CNT Cathode Catalysts for PEFC by Addition of Cu  
*S. Takenaka, H. Miyata, T. Tsukamoto, H. Matsune, and M. Kishida*
- 1434 Preparation of Highly Active Zr Oxide-Based Oxygen Reduction Electrocatalysts as PEFC Cathode  
*S. Yin, A. Ishihara, M. Matsumoto, M. Arao, H. Imai, K. Matsuzawa, S. Mitsushima, and K. Ota*
- 1435 Highly Active Titanium Oxide-Based Electrocatalyst for Oxygen Reduction Reaction for PEFC  
*K. Suito, A. Ishihara, M. Matsumoto, M. Arao, H. Imai, K. Matsuzawa, S. Mitsushima, and K. Ota*
- 1436 Surface Reaction Analysis of Tantalum-Oxide Oxygen-Reduction Catalysts by Using X-ray Photoelectron Spectroscopy  
*M. Matsumoto, H. Imai, T. Miyazaki, S. Fujieda, A. Ishihara, and K. Ota*

- 1437 Development of Tantalum Boride Thin Film Catalysts for Oxygen Reduction Reaction  
Using an RF Magnetron Sputtering Deposition  
*K. Kushibe, K. Iyatani, Y. Horiuchi, and M. Matsuoka*
- 1438 Preparation and Electrochemical Performance of Nitrogen-doped Graphene by Intermittent  
Microwave-assisted Heating for Fuel Cells  
*J. Liu, Y. Xin, Y. Zhou, and Z. Zou*
- 1439 Characteristics of Oxygen Adsorption on Nitrogen Doped HOPG Revealed by X-ray  
Absorption Spectroscopy  
*H. Kiuchi, T. Kondo, M. Sakurai, H. Niwa, M. Kobayashi, Y. Harada, T. Ikeda,  
K. Terakura, J. Nakamura, and M. Oshima*
- 1440 Nitrogen-doped Graphene for Oxygen Reduction Reaction in Air Electrodes  
*D. Lee, A. Yu, and Z. Chen*
- 1441 NH<sub>3</sub>-Pyrolyzed Fe-Impregnated Polyaniline for the use as a Cathode Catalyst for Polymer  
Electrolyte Fuel Cells  
*K. Nahm, S. Kim, and P. Kim*
- 1442 Characterization of High-Performance Non-precious Metal Catalysts for Oxygen  
Reduction Reaction (ORR)  
*N. Ranjbar Sahraie, D. Wilhelm, and P. Strasser*
- 1443 Highly Active Tetracyanoethylene Derived Non-precious Metal Catalyst for Oxygen  
Reduction Reaction in PEM Fuel Cell  
*J. Choi and Z. Chen*
- 1444 Carbon Supported Copper Phthalocyanine (CuPc/C) as Novel Cathode Catalyst for  
Polymer Electrolyte Membrane Fuel Cells ---Effect of Nafion Ionomer as for Alkaline  
Electrolyte  
*L. Ding, L. Xu, B. Tian, S. Ibrahim, Y. Liu, and J. Qiao*
- 1445 RRDE Studies of Oxygen Reduction Reaction at Various Catalysts in Alkaline Solution  
*J. Choi and H. Jung*
- 1446 Analysis of Mechanism of Oxygen Reduction Reaction on Non-Noble Metals in Alkaline  
Solution by Scanning Electrochemical Microscopy  
*R. Teranishi, E. Higuchi, M. Chiku, and H. Inoue*
- 1447 FePc/C and CoPc/C Catalysts for the Oxygen Reduction Reaction as Cathode Catalysts for  
Alkaline Direct Methanol Fuel Cell  
*J. Jang, S. Kim, S. Lim, D. Peck, and D. Jung*
- 1448 New Manganese Oxide-based Cathode Catalysts for Anion-Exchange Membrane Fuel  
Cells  
*T. Kenko, M. Hagiwara, T. Takakuwa, M. Saito, H. Daimon, A. Tasaka,  
M. Inaba, Y. Kadoma, N. Kumagai, H. Shiroishi, T. Hatai, and J. Kuwano*

- 1449 Enhanced Electrocatalytic Performance for Methanol Oxidation via Insertion of Ruthenium Oxide Particles into Pt and Polyamine-Poly(Acrylic Acid-co-Maleic Acid) Composite Electrode  
*C. Kuo, Z. Kuo, T. Wu, J. Chen, and W. Li*
- 1450 Methanol Oxidation Performance of Electrocatalysts Prepared by the Polygonal Barrel-Sputtering Method  
*M. Inoue, C. Hiromi, K. Hirakawa, and T. Abe*
- 1451 Quantitative Analysis of CO<sub>2</sub> Generation during Ethanol Electrooxidation on Pt-Sn/C and Pt-SnO<sub>2</sub>/C  
*S. Kaneda, K. Matsuzawa, and S. Mitsushima*
- 1452 The Distribution of Products of Ethanol Electrooxidation on Carbon-Supported Noble Metals Catalysts in Direct Ethanol Fuel Cell  
*J. Seweryn and A. Lewera*
- 1453 The Graphene-Supported Palladium and Palladium-yttrium Nanoparticles for the Ethanol Oxidation Reactions: Experimental and Theoretical Modeling  
*M. Seo, S. Choi, J. Seo, S. Noh, W. Kim, and B. Han*
- 1454 Studies of the Catalytic Activity of Unsupported Pt-Based Anodes Modified with CeO<sub>2</sub> for the Electro-Oxidation of Ethylene Glycol in Acid Electrolyte  
*A. Chávez Villanueva, A. Ramírez, G. Vargas Gutiérrez, and F. Rodríguez Varela*
- 1455 Investigation of Electrocatalytic Activity of the Nanostructured Au-Cu Catalyst Deposited on the Titanium Surface towards Borohydride Oxidation  
*L. Tamašauskaitė-Tamašiūnaitė, A. Balčiūnaitė, A. Vaiciukevičienė, I. Stankevičienė, A. Selskis, and E. Norkus*
- 1456 Catalytic Activity of Pt/MWCNT for the Electro-Oxidation of Ethylene Glycol in Alkaline Media  
*Y. Verde-Gomez, B. Escobar, A. Chávez Villanueva, and F. Rodríguez Varela*
- 1457 Chemisorption Studies of Dissolved Pt Species on RuO<sub>2</sub> nanosheet  
*L. K. Sannegowda, C. Chauvin, and W. Sugimoto*
- 1458 Electro-Oxidation of Borohydride by Rh Porphyrins  
*S. Yamazaki, H. Senoh, N. Fujiwara, M. Yao, Z. Siroma, K. Yasuda, and T. Ioroi*
- 1459 Enhanced Performance of MEAs Using Non-Platinum Catalyst for Direct Alcohol Alkaline Fuel Cell  
*T. Mizukami, S. Suzuki, J. Kawaji, O. Taigo, and K. Yamaga*
- 1460 Fabrication and Electrochemical Properties of Electro-Spun RuO<sub>2</sub>-Carbon Nanofibers Supported Pt Nanoparticles  
*G. An and H. Ahn*

- 1461 Synthesis and Characterization of Cross-Linked Polyethyleneimine Based Membranes for Alkali Anion Exchange Fuel Cells  
*A. M. Maes, M. Vandiver, A. Krosovski, J. L. Horan, and A. Herring*
- 1462 Alkaline Membrane Fuel Cells with Several Alternative Fuels  
*K. Fukuta, T. Negishi, Y. Kikkawa, K. Oda, S. Watanabe, and H. Yanagi*
- 1463 Synthesis and Characterization of Perfluoro Quaternary Ammonium Ion Exchange Membranes for Fuel Cell Applications  
*M. A. Vandiver, M. Liberatore, and A. Herring*
- 1464 Transport properties of Plasma Polymerized Anion Exchange Membrane for Direct Methanol Alkaline Fuel Cells  
*T. Kurozumi, Y. Okajima, H. Nagai, and M. Sudoh*
- 1465 Investigation of Mechanical Properties of Alkaline Exchanges Membranes for Fuel Cell Applications  
*B. R. Caire, M. A. Vandiver, S. Lustgraaf, A. Herring, and M. Liberatore*
- 1466 Preparation and Characterization of Anionic Binder Based Electrodes for Anion-Exchangeable Membrane Fuel Cells  
*M. Shin, Y. Byun, J. Park, M. Kang, and Y. Kim*
- 1467  $^{13}\text{C}$  PGSTE NMR Diffusion and Conductivity Measurements on Tetraalkyl Ammonium Cations  
*H. N. Sarode and A. Herring*
- 1468 Chemical Degradation Mechanism of Membranes for Alkaline Membrane Fuel Cells  
*Y. Choe, N. J. Henson, and Y. Kim*
- 1469 Novel Nanostructured High-Performance Anion Exchange Ionomers for Anion Exchange Membrane Fuel Cells  
*J. Zhou, L. Sun, J. Guo, D. Chu, and R. Chen*
- 1470 Radio-Chemically Pore-Filled Anion Exchange Membranes for Solid Alkaline Fuel Cells (SAFC)  
*T. Sherazi, D. Hwang, J. Sohn, M. D. Guiver, and Y. Lee*
- 1471 Ionic Conductivity of [dema][TfO]/Solid Acid-Base Composite Membrane  
*A. Fujisawa, K. Matsuzawa, and S. Mitsushima*
- 1472 A Proton Conductive Silicate-Nanoencapsulated Polyimide Nonwoven as a Novel Porous Substrate for a Reinforced Sulfonated Poly(Arylene Ether Sulfone) Composite Membrane  
*J. Seol, J. Won, M. Lee, Y. Hong, and S. Lee*
- 1473 Relationship Between Morphology and Proton Conductivity of Aromatic Diblock Copolymer Electrolytes  
*T. Oshima, K. Umezawa, M. Yoshizawa-Fujita, A. Ohira, Y. Takeoka, and M. Rikukawa*

- 1474 Synthesis of Hydrocarbon Ionomer Materials and Evaluations of MEA  
*S. Miura, T. Oshima, K. Umezawa, M. Yoshizawa-Fujita, A. Ohira, Y. Takeoka, and M. Rikukawa*
- 1475 Nano-Composite Ion-Conducting Polymer Electrolytes (ICPEs) for Fuel Cell Application  
*H. Zarrin, M. Fowler, A. Yu, and Z. Chen*
- 1476 Polyvinyl Alcohol Based Nanocomposite Membranes Containing Aluminum Hydroxide Gel  
*O. I. Radionova, I. Y. Prokhorov, and G. Y. Akimov*
- 1477 Radiolytic Preparation and Characterization of Silane-Crosslinked ETFE-g-PSSA/PTMSPM Membrane for Proton Exchange Membrane Fuel Cell  
*J. Sohn, J. Song, Y. Nho, and J. Shin*
- 1478 Cross-Linked Poly(Arylene Ether Ketone) Membranes Containing Pendant Sulfonic Acid Groups for Fuel Cell Applications  
*H. Dang and D. Kim*
- 1479 Electron Beam-Induced Crosslinked SPEEK Membrane for PEMFC  
*J. Song, D. Shin, J. Sohn, Y. Nho, Y. Lee, and J. Shin*
- 1480 The Compatibility of the Composite Membrane Based on Sulfonated Poly(Ether Ether Ketone) (sPEEK) / Poly(Vinylidenefluoride) (PVdF) / Urethane Acrylate Non-Ionomer (UAN) for a Unitized Regenerative Fuel Cell (URFC)  
*H. Jung and J. Choi*
- 1481 Catalyst Coated PBI Membrane High Temperature Assemblies  
*N. Séphane, A. Kreisz, N. Donzel, J. Bernard d'Arbigny, D. J. Jones, and J. Rozière*
- 1482 Microelectrode Analysis of Oxygen Permeation through Nafion® Thin Films  
*A. Oda, H. Okada, H. Daimon, A. Tasaka, and M. Inaba*
- 1483 Water Uptake and Transport in Nafion®  
*G. Hwang, D. Parkinson, A. Kusoglu, A. MacDowell, and A. Weber*
- 1484 Theoretical Study on the Degradation Mechanism of Polymer Electrolyte Membrane  
*H. Motegi and M. Yoneda*
- 1485 Membrane Science for Liquid Organic Fuel Cells  
*K. T. Clark, L. Krishnan, G. W. Yeager, and J. Kerr*
- 1486 In Situ Water Distribution Visualization in MEA by Soft X-ray Radiography  
*S. Tsushima, P. Deevanhxay, T. Sasabe, and S. Hirai*
- 1487 Visualization of Liquid Water Accumulation in PEMFCs Operating at Different Temperatures by Soft X-ray Radiography  
*P. Deevanhxay, T. Sasabe, S. Tsushima, and S. Hirai*

- 1488 Visualized Liquid Water Evolution in a PEM fuel cell using Synchrotron Radiography  
*J. Hinebaugh, J. Lee, and A. Bazylak*
- 1489 Three-Dimensional Studies on Compressed Gas Diffusion Layers and the Water Distribution in Operating Fuel Cells Using Synchrotron X-ray Imaging  
*C. Tötzke, I. Manke, T. Arlt, H. Markötter, A. Hilger, F. Wieder, J. Bohner, W. Lehnert, G. Gaiselmann, V. Schmidt, J. Haufmann, J. Scholta, H. Riesemeier, A. Kupsch, and J. Banhart*
- 1490 Neutron Imaging PEMFCs with ~1 μm Spatial Resolution  
*D. S. Hussey, D. Jacobson, B. Khaykovich, M. V. Gubarev, D. Spernjak, J. D. Fairweather, R. Mukundan, R. Lujan, and R. L. Borup*
- 1491 3D-Visualization of Cathode Catalyst Layer in MEA of Polymer Electrolyte Membrane Fuel Cell by X-ray Computed Laminography XAFS  
*T. Saida, O. Sekizawa, N. Ishiguro, K. Uesugi, M. Hoshino, T. Uruga, S. Ohkoshi, T. Yokoyama, and M. Tada*
- 1492 Electron Tomography Based 3D Reconstruction of Fuel Cell Catalysts and Catalyst Layers  
*J. Jankovic, D. Susac, T. Soboleva, and J. Stumper*
- 1493 3D Chemical Mapping of PEM Fuel Cell Cathodes by Scanning Transmission Soft X-ray Spectro-Tomography  
*V. Berejnov, D. Susac, J. Stumper, and A. P. Hitchcock*
- 1494 Heterogeneous Porosity Distribution Under Compression of Gas Diffusion Layer Using Synchrotron X-Ray Tomography  
*J. Je, S. Doh, J. Kim, and M. Kim*
- 1495 Effects of Channel Structure and Wettability on Liquid Water Transport in Cathode of PEFC  
*Y. Ishizaki, R. Taniguchi, K. Nishida, S. Tsushima, and S. Hirai*
- 1496 Higher Current Density Operation in PEMFC for Automobile applications  
*Y. Tabuchi, T. Shiomi, Y. Fukuyama, K. Sato, and N. Kubo*
- 1497 Missions and Progressions of NEDO's Cell Evaluation Project  
*M. Hori, K. Kobayashi, Y. Oono, and A. Daimaru*
- 1498 A 2 kW Power System Based on an Alkaline Membrane Fuel Cell Stack Developed at Cellera Technologies  
*S. Gottesfeld*
- 1499 Investigation on Effect of PTFE Treatment on GDL Micro-structure by High-resolution X-ray CT  
*T. Sasabe, G. Inoue, S. Tsushima, S. Hirai, T. Tokumasu, and U. Pasaogullari*
- 1500 Dynamic Analysis and Diagnostics of a High Temperature PEM Fuel Cell Stack  
*Y. Zhu, W. H. Zhu, and B. J. Tatarchuk*

- 1501 Fabrication and Optimization Membrane Electrode Assembly with Support-Less Platinum Catalysts for Space Applications  
*X. Huang, W. A. Rigdon, K. J. Billings, and T. I. Valdez*
- 1502 Novel Metallic Glass Micro Fuel Cell Architecture  
*R. C. Sekol, G. Kumar, M. Carmo, S. Mukherjee, F. Gittleson, N. Hardesty-Dycke, J. Schroers, and A. D. Taylor*
- 1503 Screening Balance of Plant Materials to Understand their effect on Fuel Cell Performance  
*H. N. Dinh, M. Das, K. Neyerlin, M. S. Opu, H. Wang, C. S. Macomber, M. Ohashi, and J. Van Zee*
- 1504 Investigating the Performance of Catalyst Layer Micro-Structures with Different Platinum Loadings  
*M. Khakbaz Baboli, D. A. Harvey, and J. G. Pharoah*
- 1505 Development of Ultra-Low Pt Alloy Cathode Catalyst for PEM Fuel Cells  
*B. N. Popov, T. Xie, T. Kim, W. Jung, A. Kriston, P. Ganesan, and H. Kim*
- 1506 Synthesis and Properties of High Temperature Proton Exchange Membranes Based on Polybenzimidazoles Containing Hydroxypyridine  
*L. Zhou and R. He*
- 1507 Polymer Electrolyte Membranes for Fuel Cells of Graft-type sulfonated Polybenzimidazoles  
*J. Park, M. Asano, Y. Maekawa, and K. Kudo*
- 1508 Performance of the HT-PEM Membrane Electrode Assembly  
*H. Hjuler, T. Steenberg, C. Terkelsen, T. Holst, H. Garcia, and K. Cooper*
- 1509 Performance Analysis of a HT-PEM Fuel Cell under Mechanical Compression Control  
*A. Diedrichs and P. Wagner*
- 1510 Thermogravimetric and Spectroscopic Investigation of the Interaction between Polybenzimidazole and Phosphoric Acid  
*A. Majerus, F. Conti, C. Korte, W. Lehnert, and D. Stolten*
- 1511 Sulfonated-Nanocomposites Incorporated Polybenzimidazole Based Polymer Electrolyte Membranes for Fuel Cells  
*K. A. Stewart and H. Pal Singh Missan*
- 1512 Novel Polybenzimidazole-Phosphoric Acid Membranes for Fuel Cell Applications  
*G. W. Yeager, L. Krishnan, E. Thomas, and T. Zhang*
- 1513 A Novel, Easy to Synthesize, Anhydrous Derivative of Phosphoric Acid for Use as Electrolyte in H<sub>2</sub>/O<sub>2</sub> Fuel Cells  
*Y. Ansari, T. Tucker, and A. Angell*
- 1514 Non-Humidified Fuel Cells Using a Protic Ionic Liquid as Electrolyte  
*T. Yasuda, Y. Honda, R. Tatara, K. Dokko, and M. Watanabe*

- 1515 A Non-humidified Fuel Cell Using Fluorohydrogenate Ionic Liquid-Polymer Composite Membrane Prepared by Living Radical Polymerization  
*P. Kiatkittikul, J. Yamaguchi, T. Nohira, R. Hagiwara, Y. Tsujii, and T. Sato*
- 1516 Intermediate-Temperature Fuel Cells Using an Anhydrous Proton Conductor  $\text{A}^{\text{III}}_{0.5}\text{B}^{\text{V}}_{0.5}\text{P}_2\text{O}_7$   
*P. Heo, Y. Shen, M. Nagao, K. Kim, C. Pak, K. Choi, H. Chang, and T. Hibino*
- 1517 U.S. Department of Energy Polymer Electrolyte Membrane Fuel Cell Catalyst Development Activities  
*T. G. Benjamin, K. Epping-Martin, N. L. Garland, D. L. Ho, J. P. Kopasz, D. C. Papageorgopoulos, and W. F. Podolski*
- 1518 Performance and Durability Benchmark of Advanced Cathode Catalysts, and Development Target for Platinum Reduction in PEM Fuel Cell Vehicles  
*R. Makharia, T. Greszler, and N. Subramanian*
- 1519 Theoretical Study on Particle Size effect of Oxygen Reduction Reaction on Pt Catalyst  
*Y. Kawamura and R. Jinnouchi*
- 1520 The Particle Size Effect on the Oxygen Reduction Reaction Activity of Pt Catalysts: Influence of Electrolyte and Relation to Single Crystal Models  
*M. Nesselberger*
- 1521 Synthesis of Platinum Catalyst Clusters and Electrochemical Investigation of Stability  
*R. A. Hackendorn and A. V. Virkar*
- 1522 Pt Nanoparticles Dispersion Influence on the Fuel Cell Performance  
*M. Darab, J. Gómez de la Fuente, M. Skinlo Thomassen, and S. Sunde*
- 1523 Electrocatalytic Behavior of Tailored Shape Platinum Nanoparticles  
*S. Baranton, P. Urchaga, C. Coutanceau, and G. Jerkiewicz*
- 1524 First-Principles Analysis of the Electrocatalytic Activity of Pt(100) Surface for Oxygen Reduction Reaction  
*B. Han, V. Viswanathan, and H. Pitsch*
- 1525 Analysis of Pt Oxide Formation on Working Cathode of PEFC by Operando-XAFS  
*T. Hatanaka, K. Hiroshima, Y. Nishimura, T. Nonaka, K. Dohmae, R. Jinnouchi, and Y. Morimoto*
- 1526 The effect of Platinum Oxide Growth on Platinum Stability in PEMFCs  
*E. L. Redmond, P. Trogadas, F. M. Alamgir, and T. F. Fuller*
- 1527 A Ternary Catalyst for Dimethyl Ether Electrooxidation  
*Q. Li, G. Wu, C. M. Johnston, and P. Zelenay*
- 1528 Pt Decorated Amorphous RuIr Alloys as High Efficiency Electrocatalyst for the Methanol Oxidation Reaction  
*B. G. Pollet*

- 1529 Ethanol Oxidation Reaction on Tandem-type Pt/Rh/SnO<sub>x</sub> Electrocatalysts  
*H. Inoue, A. Haze, M. Chiku, and E. Higuchi*
- 1530 Development of High Performance Direct Formic Acid Fuel Cell Using Hyper Branched Polymer as a Catalyst Stabilizer  
*T. Tsujiguchi, M. Kojima, T. Iwakami, N. Nakagawa, and K. Kojima*
- 1531 Carbon-TiO<sub>2</sub> Composite Nanofibers as a Promising Support for PtRu Anode Catalyst of DMFC  
*M. A. Abdelkareem, Y. Ito, T. Tsujiguchi, and N. Nakagawa*
- 1532 O<sub>2</sub>-Enhanced Methanol Oxidation at Pt-Ru-C Ternary Sputtered Electrode  
*S. Shironita, M. Ueda, and M. Umeda*
- 1533 Enhancement of Catalytic Properties for the Electrooxidation of Polyols on Bi-Modified Pt and Pd Nanoparticles  
*C. Coutanceau, S. Baranton, M. Simoes, and L. Demarconnay*
- 1534 Electrochemical Behavior and Morphology of Nano Catalyst for Fuel Cell: The effect of Ultrasonic and Microwave Techniques  
*V. Tran, T. Doan, N. Duong, M. Le, and T. Nguyen*
- 1535 Novel 3-D Graphite Oxide-Nanoribbon Supported Metal Catalysts for Methanol Oxidation Reaction  
*H. Wang, B. A. Kakade, T. Tamaki, H. Ohashi, and T. Yamaguchi*
- 1536 Reaction Analysis of Alcohol Electro-oxidation at Intermediate Temperatures  
*J. Otomo, I. Shimada, F. Kosaka, K. Ishiyama, and Y. Oshima*
- 1537 The Impact of Formaldehyde and Formic Acid on Methanol Electrooxidation at Pt-film Electrode: A Combined ATR-FTIRS/DEMS Study  
*R. Reichert, J. Schnaidt, Z. Jusys, and R. Behm*
- 1538 Application of Impedance Spectroscopy to Characterize PEM Fuel Cells  
*M. E. Orazem*
- 1539 Performance Characterization of PEM Fuel Cell Stacks Using AC impedance Spectroscopy  
*J. O. Park, J. Yi, J. Kim, T. Song, and J. Ko*
- 1540 Study on Protocols for Evaluating Reactant Gas Transport in Cathode Catalyst Layers of PEFC  
*H. Yasuda, K. Kobayashi, A. Daimaru, and M. Hori*
- 1541 An Oxygen Flux Interrupt Method and In Situ Micro-Sensor for Characterizing Oxygen Transport in PEFCs  
*W. K. Epting and S. Litster*

- 1542 Measurements of Water Vapor and Current Distributions and Prediction of Water Crossover in PEMFC under Low-Humidity Conditions  
*K. Nishida, M. Asa, S. Tsushima, and S. Hirai*
- 1543 In-plane Liquid Water Distribution at the Interface Between the Gas Diffusion Layer and Catalyst Layer in the Cathode of a Polymer Electrolyte Fuel Cell with a Hybrid Pattern Flow Field  
*H. Nakajima, T. Kitahara, Y. Takazono, S. Miyahara, and A. Shimizu*
- 1544 Segmented PEMFC with Sub-millimeter Resolution  
*U. Shrivastava, A. Sarkar, and K. Tajiri*
- 1545 Using a Novel Current Distribution Board to Understand Local Water Transport in PEMFCs  
*V. Lilavivat, S. Shimpalee, J. W. Van Zee, C. Mittelsteadt, and H. Xu*
- 1546 Design of An Optical Fiber Sensor for in-situ Measurement of Temperature and Water Droplet Detection in a PEM Fuel Cell  
*K. Inman and X. Wang*
- 1547 Calculating Hydrogen Mass Transport Coefficients in a PEMFC at Different Operating Conditions Using a Hydrogen Pump Configuration  
*M. S. Angelo, K. P. Bethune, and R. E. Rocheleau*
- 1548 Manufacturing All-Polymer Laminar Flow-Based Fuel Cells  
*A. Hollinger and P. J. Kenis*
- 1549 Fabricating and Measuring Low-Platinum Content HOR/HER Gas Diffusion Electrodes  
*Y. Zhang, J. Wang, Y. Hsieh, and R. R. Adzic*
- 1550 Fabrication of Bipolar Plates Based on Graphite Sheet via Stamping Method  
*T. Park, I. Chang, Y. Lee, and S. Cha*
- 1551 A Novel Lightweight Polymer Electrolyte Fuel Cell Stack for Robot Systems  
*S. Hwang, J. Jang, G. Choi, S. Lee, O. Kwon, D. Lee, A. Bates, R. M. Ench, and S. Park*
- 1552 Copolymeric Short-Long Side Chain PFSA/PTFE Composite Membranes with High Ion Exchange Capacities for Fuel Cell Applications  
*Y. Zhang and Y. Zhu*
- 1553 Effect of Thermal Treatment on the Properties of Ultra-Thin Nafion Film  
*D. K. Paul and K. Karan*
- 1554 Role of Chemical-Mechanical Energies in Understanding Structure and Properties of Aged and Degraded Membranes  
*A. Kusoglu and A. Weber*
- 1555 Numerical Validation of Water Transport in Polymer Electrolyte Membranes  
*R. S. Fu, N. Khajeh-Hosseini-Dalasm, and U. Pasaogullari*

- 1556 On the Diffusion Coefficient of Water in Polymer Electrolyte Membranes  
*T. Berning, A. Olesen, and S. K. Kær*
- 1557 A Study on Structural Property of Ionomer as A Model for Catalyst Layer  
*A. Ohira, S. Kuroda, M. Yamaguchi, M. Barique, and H. Mohamed*
- 1558 Accelerated Testing of Carbon Corrosion and Membrane Degradation in PEM Fuel Cells  
*R. Mukundan, G. James, D. Ayotte, J. R. Davey, D. Langlois, D. Spernjak, D. Torraco, S. Balasubramanian, A. Weber, K. L. More, and R. L. Borup*
- 1559 Degradation of Perfluorosulfonic Acid Membrane Water Permeance via Formation of Sulfonic Acid Anhydrides  
*S. M. Clapham, F. D. Coms, T. J. Fuller, and L. Zou*
- 1560 High-Fidelity Simulations of Nano-Structured Thin Film (NSTF) Catalysts  
*S. Kim, Z. Zhou, and K. Moriyama*
- 1561 DFT Study of Pt Alloy and Pt Thin Film Catalysts for the Cathode Oxygen Reduction Reaction in PEM Fuel Cells  
*W. Goddard III, Y. Sha, T. Yu, H. Tsai, B. V. Merinov, and P. Shirvanian*
- 1562 Development of Alternated Catalyst Layer Structure for PEM Fuel Cells  
*W. Mei, T. Fukazawa, Y. Nakano, Y. Akasaka, and K. Naito*
- 1563 Theoretical Study of the Structure, Stability and Oxygen Reduction Activity of Ultrathin Platinum Nanotubes  
*I. Matanović, F. H. Garzon, P. R. Kent, and N. J. Henson*
- 1564 Oxygen Reduction Activity of Vapor-Grown Platinum Nanotubes  
*A. B. Papandrew, R. W. Atkinson, G. A. Goenaga, D. L. Wilson, S. S. Kocha, K. Neyerlin, J. W. Zack, B. S. Pivovar, and T. A. Zawodzinski*
- 1565 Activity and Durability of Pt Extended Network Electrocatalyst Structures Made from Spontaneous Galvanic Displacement  
*K. Neyerlin, B. A. Larsen, S. S. Kocha, and B. S. Pivovar*
- 1566 Important Role of Cerium Oxide in Oxygen Reduction Reaction at Pt-CeO<sub>x</sub> Nanocomposite Electrocatalyst Studied by in situ Electrochemical XAFS  
*T. Masuda, H. Fukumitsu, K. Fugane, H. Togasaki, D. Matsumura, K. Tamura, Y. Nishihata, H. Yoshikawa, K. Kobayashi, T. Mori, and K. Uosaki*
- 1567 Effect of Silicotungstic acid on Cathode Performance in Proton Exchange Membrane Fuel Cells  
*P. Baker, H. R. Kunz, and L. Bonville*
- 1568 Analyzing the effect of Ultra-Low Pt Loading on Mass and Specific Activity of PEM Fuel Cells  
*A. Kriston, T. Xie, T. Kim, W. Jung, P. Genesan, and B. N. Popov*

- 1569 Impact of Platinum Loading and Catalyst Layer Structure on PEMFC Performance  
*J. Owejan, J. Owejan, and W. Gu*
- 1570 Multi-Step Oxygen Reduction Reaction (ORR) Kinetics on Pt including Water Activation  
*B. Jayasankar, K. Karan, and D. A. Harvey*
- 1571 Borohydride Electrooxidation: New Insights Based on an Old Paradigm  
*S. Sun, Z. Jusys, and R. Behm*
- 1572 Hydrazine Electrooxidation of Ni-La Catalysts for Anion Exchange Membrane Fuel Cells  
*T. Sakamoto, K. Asazawa, U. Martinez, B. Halevi, P. Atanassov, K. Yamaguchi, N. Mizuno, D. Matsumura, Y. Nishihata, and H. Tanaka*
- 1573 Effect of Carbonate Ion Species on Power Generation Characteristics of Anion Exchange Membrane Fuel Cell  
*S. Suzuki, H. Muroyama, T. Matsui, and K. Eguchi*
- 1574 Investigations of the Anodic Oxidation of Ethanol under Forced Convection and Ambient Conditions  
*J. O. Meier, C. Cremers, U. Stimming, and J. Tübke*
- 1575 Development of a Swiss-Roll Mixed-Reactant Feed Direct Borohydride Fuel Cell  
*A. Aziznia, C. W. Oloman, and E. L. Gyenge*
- 1576 Direct Borohydride Fuel Cells: A Progress Review from Electrocatalysis to Novel Mixed Reactant Fuel Cell Design  
*E. L. Gyenge*
- 1577 Improvement of Properties of Anion Exchange Membranes for Fuel Cell Applications by Controlling Water State  
*H. Jung, H. Ohashi, T. Tamaki, and T. Yamaguchi*
- 1578 Boron and Phosphorus Co-Doped Graphene as Metal-Free Catalysts for Oxygen Reduction Reaction in Alkaline Medium  
*G. Jo and S. Sangaraju*
- 1579 Hydroxide Based Decomposition of Functionalized Benzyltrimethylammonium Cations  
*C. S. Macomber, H. Long, E. Gjersing, C. Engrakul, C. Lyiza, Y. Yang, D. Knauss, and B. S. Pivovar*
- 1580 Determination of CL Ionomer Conductivity  
*K. Karan*
- 1581 STXM Characterization of PEM Fuel Cell Catalyst Layers  
*D. Susac, V. Berejnov, A. P. Hitchcock, and J. Stumper*
- 1582 Analysis and Experiments of Major Parameters in Catalyst Layer Structure Affecting on PEFC Performance  
*M. Kobayashi, Y. Tabe, and T. Chikahisa*

- 1583 Performance Characteristics of PEFCs with Patterned Electrodes Prepared by Piezo-electric Printing  
*D. Malevich, M. S. Saha, E. Halliop, B. A. Peppley, J. G. Pharoah, and K. Karan*
- 1584 Ice-Crystallization Kinetics and Water Movement in Gas-Diffusion and Catalyst Layers  
*T. J. Dursch, M. Ciontea, G. Trigub, C. Radke, and A. Weber*
- 1585 The effect of Pt Particle Distribution of Various Supported Electrocatalyst on Pt Utilization of Membrane-Electrode Assembly  
*M. Uchida, K. Kakinuma, H. Uchida, and M. Watanabe*
- 1586 Temperature Sensitivity of Polymer-Electrolyte Fuel Cells with Ultra-Low Catalyst Loadings  
*M. L. Perry, C. Shovlin, and R. Zaffou*
- 1587 Effects of Through-plane Thermal Gradients of Anode and Cathode Electrodes on PEMFC Performance  
*K. Inman and X. Wang*
- 1588 The Spatial Performance Effect of Electrode Defects in PEMFC  
*G. Bender, W. Felt, and M. Ulsh*
- 1589 Design of Al-Fe Alloys for Fast On-board Hydrogen Production from Hydrolysis, and Its Application to PEMFC  
*K. Eom, J. Kwon, M. Kim, and H. Kwon*
- 1590 Influences of Various Recycled Fuel Conditions on the Stability of Direct Methanol Fuel Cells  
*K. Park, M. Yang, and J. Park*
- 1591 Immobilized Viologen Polymers for Carbohydrate Fuel Cell  
*Y. Pan, J. Stockton, D. Hansen, W. Pitt, and D. R. Wheeler*
- 1592 In Situ and Ex Situ Characterization of Bipolar Plates for PEM Fuel Cells  
*S. Ladre, O. Kongstein, A. Oedegaard, F. Seland, and H. Karoliussen*
- 1593 Spatially Resolved Characterization of DMFCs Aged under Critical Conditions  
*A. Löhmer, K. Wippermann, M. Müller, and D. Stolten*
- 1594 The Effect of Gas Diffusion Media on AMFC performance  
*T. Isomura, K. Fukuta, H. Yanagi, S. Ge, and C. Wang*
- 1595 Development of High Performance MEA by CS-AFM (Current Sensing - Atomic Force Microscopy)  
*S. Lee, O. Kwen, D. Lee, B. Han, S. Hwang, J. Jang, G. Choi, A. Bates, and S. Park*
- 1596 Comparison of H<sub>2</sub>S Effects: Using Two Different Ultra-Low Platinum Anode Loadings under Different PEFC Operating Conditions  
*C. Quesada, T. Rockward, K. C. Rau, and F. H. Garzon*

- 1597 Novel Anion Conductive Block Copolymers for Alkaline Fuel Cells and Water Electrolysis  
*P. Kohl, J. Zhou, D. Park, K. Joseph, J. Ahlfeld, and H. Beckham*
- 1598 Advanced Hybrid Super Acidic Inorganic-Organic PEMs for Hotter and Drier Operation  
*A. Herring, J. L. Horan, M. Kuo, J. Jessop, G. Schlichting, and Y. Yang*
- 1599 Anhydrous Novel Acid-Base Binary and Ternary Systems for Fuel Cell Applications  
*M. Singh and H. Missan*
- 1600 New Composite PEM for High Temperature Fuel Cells  
*M. E. Cordova, A. Slezcka, E. M. Kelder, and S. J. Picken*
- 1601 Zeolite 4A-Methane Sulfonic Acid-Sulfonated Poly (Ether Ether Ketone) Based Mixed Matrix Membranes for Direct Methanol Fuel Cells  
*S. Meenakshi, S. D. Bhat, A. Sahu, P. Sridhar, and S. Pitchumani*
- 1602 Polymer Inorganic Composite (PIC) Nanofiber Proton Exchange Membrane for Direct Methanol Fuel Cells  
*G. Arumugam, V. Kamavaram, V. Veedu, and K. Cheung*
- 1603 Nanofiber Composite Membranes for a Regenerative H<sub>2</sub>/Br<sub>2</sub> Fuel Cell  
*J. Park and P. N. Pintauro*
- 1604 Composite Sulfonated Polyether Ether Ketone (SPEEK) Membranes with 3-(Trihydroxysilyl)-1-Propanesulfonic Acid for a Direct Methanol Fuel Cell (DMFC)  
*S. Yun, J. Parrondo, and V. Ramani*
- 1605 Dispersed PtCo Alloy Catalyst Synthesized by Modified Polyol Reduction Method for PEM Fuel Cells  
*T. Kawamura and S. Matsumoto*
- 1606 Enhanced ORR and MOR Activities by Bimetallic CoPt and PdPt Electrocatalysts  
*B. A. Kakade, T. Tamaki, H. Ohashi, and T. Yamaguchi*
- 1607 Development of Highly Active Pt<sub>2</sub>Ni/C Catalyst for PEM Fuel Cell  
*T. Xie, T. Kim, W. Jung, A. Kriston, P. Ganesan, and B. N. Popov*
- 1608 Subsurface Enrichment in Highly Active Dealloyed Pt-Ni Catalyst Nanoparticles for Oxygen Reduction  
*L. Gan, M. Heggen, and P. Strasser*
- 1609 Core-Shell Fine Structure and Size-Dependent Morphology of Dealloyed Pt Bimetallic Nanoparticle Fuel Cell Electrocatalysts  
*M. Oezaslan, M. Heggen, and P. Strasser*
- 1610 Anion-Exchange Membrane Fuel Cell for Platinum-free Liquid Fuel Car  
*K. Asazawa, H. Tanaka, U. Martinez, B. Halevi, A. Serov, K. Artyushkova, P. Atanassov, and B. Kiefer*

- 1611 Alkaline Durable Anion Exchange Membranes Based on Graft-type Fluoropolymer Films for Hydrazine Hydrate Fuel Cell  
*K. Yoshimura, H. Koshikawa, T. Yamaki, Y. Maekawa, K. Yamamoto, H. Shishitani, K. Asazawa, S. Yamaguchi, and H. Tanaka*
- 1612 Stringing Cations in Hydroxide Exchange Membranes for Low Water-Uptake and High Hydroxide-Conductivity  
*J. Wang, S. Gu, and Y. Yan*
- 1613 Highly Anion-Conducting Porous Polymer Electrolyte Membrane for Alkaline Fuel Cells  
*H. Zarrin, M. Fowler, and Z. Chen*
- 1614 Modeling and Analysis of Ion Transport Through Anion Exchange Membranes Used in Alkaline Fuel Cells  
*S. Castañeda Ramírez and C. Sánchez Sáenz*
- 1615 Synthesis of Triarylsulfonium Functionalized Polysulfone for Hydroxide Exchange Membrane Fuel Cells  
*B. Zhang, S. Gu, J. Wang, Y. Yan, and A. Herring*
- 1616 Polymer Backbone Stability of Quaternized Fluorinated Poly(arylene ether)s and Its Impact on AMFC Performance  
*D. Kim, C. H. Fujimoto, M. Hibbs, D. Wroblewski, and Y. Kim*
- 1617 Alkaline Stability and AMFC Performance of Perfluorinated Polymer Electrolytes  
*D. Kim, C. H. Fujimoto, M. Hibbs, and Y. Kim*
- 1618 The Performance of Anionic Ionomers in Direct Methanol Fuel Cells  
*K. Joseph, J. Ahlfeld, J. Zhou, and P. Kohl*
- 1619 Oxygen Reduction Reaction on Electrodeposited Pt<sub>100-x</sub>Ni<sub>x</sub>: Influence of alloy composition and dealloying  
*Y. Liu, C. Hangarter, U. Bertocci, and T. Moffat*
- 1620 High Activity De-alloyed PtMn (M = Co and Ni) Cathodic Catalysts showing OO(H) or O(H) coverage on Pt Consistent with the Sabateir Model  
*D. E. Ramaker, K. Caldwell, S. Mukerjee, Q. Jia, and J. Ziegelbauer*
- 1621 PEMFC Nanoparticle Catalyst Dealloying from Kinetic Monte Carlo Simulations  
*B. Puchala, S. Lin, L. Wang, and D. Morgan*
- 1622 Dealloying of Nanoparticles  
*X. Li, I. McCue, J. Snyder, J. Erlebacher, and K. Sieradzki*
- 1623 Correlation between Local Structure and Catalytic Activity of Monolayer Pt Catalysts for Oxygen Reduction  
*X. Wang, Y. Orikasa, M. Inaba, and Y. Uchimoto*

- 1624 Influence of Hydrophilic and Hydrophobic Double MPL Coated GDL on PEFC Performance  
*T. Kitahara, H. Nakajima, K. Mori, and M. Inamoto*
- 1625 Observation of Water Transfer Phenomena in Micro-Porous Layer of PEFC  
*Y. Aoyama, K. Kadowaki, Y. Tabe, and T. Chikahisa*
- 1626 The Effect of Microporous Layer on PEFC Dryout  
*D. Malevich, E. Halliop, J. Suryana, B. A. Peppley, J. G. Pharoah, and K. Karan*
- 1627 Understanding Mechanism of PTFE Distribution in Fibrous Porous Media  
*G. Inoue, N. Ishibe, Y. Matsukuma, and M. Minemoto*
- 1628 Hydrophobic Gas Diffusion Media for PEM Fuel Cells by Direct Fluorination  
*T. V. Nguyen, A. Ahosseini, and X. Wang*
- 1629 Measurement of Capillary Pressure Curves in GDLs at Elevated Temperatures  
*J. Gostick and K. P. Shrestha*
- 1630 Water Distribution in GDL at Optimum Humidification  
*J. Eller, J. Roth, R. Gaudenzi, S. Irvine, F. Marone, M. Stampatori, A. Wokaun, and F. Büchi*
- 1631 Three-Dimensional Morphological Characterization of Micro Porous Layers  
*A. Sadeghi Alavijeh, A. Nanjundappa, M. El Hannach, and E. Kjeang*
- 1632 Investigation of Water Breakthrough and Flow in Gas Diffusion Layers and Relavance to Fuel Cell Water Management  
*Z. Lu and J. Patterson*
- 1633 Effect of Channel Materials on the Behavior of Water Droplet Emerging from GDL into PEMFC Gas Channels  
*P. Gopalan and S. G. Kandlikar*
- 1634 Microstructure-Driven Analysis of Two-Phase Transport in Dual-Layer Diffusion Media of PEFCs  
*E. A. Wargo, V. P. Schulz, A. Cecen, S. R. Kalidindi, and E. C. Kumbur*
- 1635 Nanoscale Transport Phenomena in PEM of PEFC by Large Scale Molecular Dynamics Simulations  
*T. Tokumasu*
- 1636 A Direct DME High Temperature PEM Fuel Cell  
*A. Vassiliev, J. Jensen, Q. Li, C. Pan, L. Cleemann, T. Steenberg, H. Hjuler, and N. Bjerrum*
- 1637 Percolation in Catalyst Layer of PEMFC  
*S. A. Stacy and J. S. Allen*

- 1638 Impact of Structural Plastics as Balance of Plant Components on Fuel Cell Performance  
*B. Lakshmanan, K. O'Leary, and R. Reid*
- 1639 Electrochemical Characterization of Non-Precious Metal Catalysts Based on Copper-Triazole Complexes for Oxygen Reduction Reaction in PEM Fuel Cells  
*C. Zhang, G. A. Goenaga, C. Dabke, A. Belapure, A. Papandrew, S. Foister, and T. A. Zawodzinski*
- 1640 Synthesis and Electrochemical Characterization of Co, Fe and Cu-based Catalysts For ORR In PEM Fuel Cells  
*G. A. Goenaga, J. Brooksbank, C. Dabke, C. Zhang, A. Belapure, A. Papandrew, S. Foister, and T. A. Zawodzinski*
- 1641 Non-PGM Electrocatalysts for ORR: Structure and Reactivity of Dinuclear Heterometallic Catalysts  
*K. Strickland and S. Mukerjee*
- 1642 Group 4 and 5 Metal Oxide-Based Compounds as New Non-Platinum Cathode for PEFC  
*A. Ishihara, S. Yin, K. Suito, K. Hara, K. Matsuzawa, S. Mitsushima, K. Ota, M. Matsumoto, and H. Imai*
- 1643 ORR Activity of Nb Oxide Based Catalyst Prepared from Nb Compound Including C and N  
*K. Hara, A. Ishihara, M. Matsumoto, M. Arao, H. Imai, K. Matsuzawa, S. Mitsushima, and K. Ota*
- 1644 Oxygen Reduction on TiO<sub>2</sub>-Coated Carbon Nanofibers Decorated with Graphene Platelets  
*J. P. McClure, C. Devine, A. Loebl, R. Jiang, D. Chu, J. Cuomo, G. Parsons, and P. S. Fedkiw*
- 1645 Highly-dispersed Nanoscale Tantalum-based Catalysts Prepared by Electrodeposition as Novel Non-platinum Cathodes for PEFCs  
*J. SEO, K. Takanabe, J. Kubota, and K. Domen*
- 1646 Bio-inspired Electrocatalysts for ORR: The Case for Structured Mixed Metal Oxides  
*B. Halevi, C. Harrison, A. Serov, C. Lau, K. Artyushkova, B. Kiefer, and P. Atanassov*
- 1647 Coaxial TiN-CNT Composites as Effective Low Temperature Fuel Cell Electrocatalyst Supports  
*D. C. Higgins and Z. Chen*
- 1648 Electrospun Iron/Polyacrylonitrile Derived Nanofibrous Catalysts for Oxygen Reduction Reaction  
*J. Wu, H. Park, D. C. Higgins, and Z. Chen*
- 1649 Nitrogen-doped Activated Graphene Supported Platinum Electrocatalyst for Oxygen Reduction Reaction in PEM Fuel Cells  
*J. Choi, D. Lee, and Z. Chen*

- 1650 Advanced Electrocatalysts for PEM Fuel Cells  
*C. Wang, D. van der Vliet, D. Tripkovic, D. Strmcnik, D. Li, N. M. Markovic, and V. R. Stamenkovic*
- 1651 In Situ Pt K-Edge XAFS Study on Pt/Au Nanoclusters for Fuel Cell Catalysts  
*T. Kaito, H. Mitsumoto, S. Sugawara, K. Shinohara, H. Uehara, H. Ariga, S. Takakusagi, and K. Asakura*
- 1652 Evaluation of Electrocatalytic Activity and Durability for Oxygen Reduction Reaction of Au Core/Pt Shell Catalysts with Small Core  
*E. Higuchi, K. Okada, M. Chiku, and H. Inoue*
- 1653 Improvement of Durability of Au core/Pt Shell Structured Catalyst  
*H. Daimon, N. aoki, H. Inoue, T. Nishikawa, Y. Ikehata, E. Maki, H. YAMADA, and M. Inaba*
- 1654 Synthesis of Pt-Au Nanoparticle Netlike Assembly as High Active and Durable Catalysts for ORR  
*Z. Zhou, H. Wang, L. Song, C. Chen, N. Tian, and S. Sun*
- 1655 In Situ XAFS Study on the Structure and Behavior of PEFC Core-Shell Pt-M/C (M = Au, Pd) Catalysts under Stepwise Voltage Operation Conditions  
*S. Nagamatsu, T. Arai, M. Yamamoto, H. Oyanagi, T. Ishizaka, H. Kawanami, T. Uruga, M. Tada, and Y. Iwasawa*
- 1656 Enhanced Oxygen Reduction Performance and Durability for Titanium Dioxide Modified PtAu/C Nanoparticles  
*C. Liu, M. Janyasupab, Y. Zhang, C. Lai, J. Lin, L. Tsai, C. Liu, and K. Wang*
- 1657 PtPd Areogels as a New Class of High Surface Area Catalysts towards the Oxygen Reduction Reaction  
*W. Liu, A. Rabis, A. Foeslke, R. Kötz, J. Yuan, A. Hermann, P. Rodriguez, A. Eychmüller, and T. J. Schmidt*
- 1658 Pt-Sn(Oxidized Shell)/C and Pt-Sn(Reduced)/C as Cathode Catalysts for the Oxygen Reduction Reaction in Polymer Electrolyte Fuel Cells: Catalyst Performances and Characterization  
*G. Samjeské, S. Nagamatsu, K. Nagasawa, Y. Imaizumi, S. Takao, O. Sekizawa, T. Yamamoto, T. Uruga, and Y. Iwasawa*
- 1659 PtSc Alloy Nanocrystals as Electrocatalysts with High Specific and Mass Activity for Oxygen Reduction Reaction  
*Y. Zhang, Z. Zhuang, and Y. Yan*
- 1660 Hydrogen Oxidation at Small Amount of Pt on TiO<sub>2</sub>-SiO<sub>2</sub>  
*W. Zhang, S. Shironita, and M. Umeda*
- 1661 Hydrocarbon Electrolytes with Nitrile Groups for Direct Methanol Fuel Cells  
*S. Hürter, M. Müller, D. Stolten, and M. D. Guiver*

- 1662 Meso-Structured Aluminosilicate-Nafion Hybrid Membranes for DMFCs  
*S. Meenakshi, A. Sahu, S. D. Bhat, P. Sridhar, S. Pitchumani, and A. K. Shukla*
- 1663 Mechanistic Studies of Palladium Based Catalysts in the Reactions of Alcohols Electrooxidation  
*A. Serov, U. Martinez, K. Artyushkova, B. Halevi, and P. Atanassov*
- 1664 Multiscale modeling for Direct Ethanol Fuel Cells  
*R. Ribadeneira, D. C. Orozco, and J. Molina*
- 1665 Tungsten Carbide on Multiwalled Carbon Nanotube as a Co-Catalyst for Methanol Oxidation  
*M. Rahsepar, P. Nikolaev, and H. Kim*
- 1666 Electrode Degradation of Direct Methanol Fuel Cells Evidenced by X-ray Tomography  
*Q. Li, D. Spernjak, and Y. Kim*
- 1667 Catalysts for Direct Formic Acid Fuel Cells  
*C. A. Rice and A. Bauskar*
- 1668 Effect of Nanometallic Catalysts on Electrochemical Oxidation of Glycerol  
*V. Tran, T. Nguyen, T. Lam, T. Co, and T. Nguyen*
- 1669 Product Distribution on Ethylene Glycol Oxidation Reaction for Carbon Neutral Energy Cycle System  
*T. Takeguchi, H. Arikawa, K. Sato, M. Yamauchi, and R. Abe*
- 1670 Ex Situ Characterization of Degradation Mechanisms of MEAs by Imaging XPS and SEM  
*K. Artyushkova, A. Patel, P. Atanassov, M. Dutta, V. Colbow, and S. Wessel*
- 1671 PEMFC Gas Diffusion Media Degradation Determined by Acid-Base Titrations  
*J. Chlistunoff, K. C. Rau, R. Mukundan, and R. L. Borup*
- 1672 Influence of In Situ and Ex Situ Aging of Gas Diffusion Layers on Fuel Cell Performance Degradation  
*D. Spernjak, J. D. Fairweather, T. Rockward, K. C. Rau, R. L. Borup, and R. Mukundan*
- 1673 Subzero Degradation Analysis of Membrane Electrode Assemblies Modified with Additives  
*A. Pistono, C. A. Rice, J. Lewis, and V. Ramani*
- 1674 PEM Fuel Cell Performance and Durability with Different Treatments of Microporous Layer  
*D. Spernjak, R. Mukundan, P. Wilde, R. Schweiss, K. L. More, D. Langlois, J. D. Fairweather, and R. L. Borup*
- 1675 Effects of Pt Concentration of Carbon Supported Catalysts on High Temperature PEMFC Performance  
*J. O. Park, J. Ha, S. Hong, Y. Lee, M. Takezawa, and K. Choi*

- 1676 Improvement of PEFC Performance by Removing GDLs  
*K. Takeuchi*
- 1677 Effect of Gas Diffusion Layer Design on PEM Fuel Cell MEA Water Removal in an Under Humidified Environment  
*J. Bellerive and A. Bellemare-Davis*
- 1678 PEMFC GDE Oxygen Mass Transport Coefficient Separation with Different Gas Diluents  
*T. V. Reshetenko and J. St-Pierre*
- 1679 The Dew Point Temperature as a Criterion for Optimizing PEMFC Operating Conditions  
*T. Berning*
- 1680 Handheld Characterization Probe for Catalytic Assessments of Electrodes and MEAs  
*D. Carr, B. Slote, K. Jayne, and M. C. Kimble*
- 1681 The Potential of Non-Carbon Supported Electrocatalyst for Automotive Fuel-Cells  
*J. Suchsland, B. Klose-Schubert, D. Herein, and M. Lennartz*
- 1682 Microstructure and Durability of Non-Carbon Supported Cathode Prepared by a Direct Dry Deposition Technique  
*R. Maric, J. Roller, M. Arellano-Jiménez, W. E. Mustain, and C. Carter*
- 1683 Corrosion-Resistant PEFC Cathode Catalysts Based on Sub-Stoichiometric Titanium Oxide Supports  
*T. Ioroi, M. Asahi, S. Yamazaki, Z. Siroma, N. Fujiwara, and K. Yasuda*
- 1684 Alternative Electrocatalyst Support Materials for Polymer Electrolyte Fuel Cells  
*K. Sasaki, S. Hayashi, K. Kanda, Y. Takabatake, T. Tsukatsune, T. Higashi, F. Takasaki, Z. Noda, and A. Hayashi*
- 1685 Electrochemical Characterization of Pt Catalysts Supported on  $\text{Sn}_{0.96}\text{Nb}_{0.04}\text{O}_{2-\delta}$  and  $\text{Sn}_{0.96}\text{Sb}_{0.04}\text{O}_{2-\delta}$  with Aggregated Structure in Rotating Disk Electrode and Membrane Electrod  
*K. Kakinuma, Y. Chino, M. Uchida, H. Uchida, S. Deki, and M. Watanabe*
- 1686 Mixed Metal Oxides as Corrosion-Resistant Catalyst Supports for Polymer Electrolyte Fuel Cells  
*A. Kumar and V. Ramani*
- 1687 Titania and Carbon Nanotube Composite Catalyst Supports for Durable Electrocatalyst Performance  
*W. A. Rigdon, J. J. Sightler, D. Larrabee, E. McPherson, and X. Huang*
- 1688 Conductive Nanostructured Materials for Supported Metal Catalysts  
*J. Sansiñena, M. Wilson, and F. H. Garzon*
- 1689 Molybdenum Carbide as Support for Platinum Catalysts for Oxygen Reduction in Fuel Cells  
*L. Elbaz, J. Philips, N. J. Henson, and E. L. Brosha*

- 1690 Vanadium Carbide Derived Carbon as a Possible Catalyst Support for PEMFC  
*E. Härk, J. Nerut, K. Vaarmets, S. Sepp, P. Valk, R. Jäger, and E. Lust*
- 1691 Catalytic Activity and Stability of Ta Compounds for Oxygen Reduction Reaction  
*S. Mitsushima, Y. Fujita, A. Ishihara, Y. Ohgi, K. Matsuzawa, M. Matsumoto, M. Arao, H. Imai, and K. Ota*
- 1692 Non-Precious Metal Oxygen-Reduction Catalysts for PEM Fuel Cells Based on N-Doped Ordered Porous Carbon  
*A. Dorjgotov, J. Ok, Y. Jeon, S. Yoon, and Y. Shul*
- 1693 Evaluation of Nitrogen Species and Microstructre of Silk-Derived Activated Carbon as Non-Precious Metal Catalyst for PEFC Cathode  
*H. Fukunaga, T. Shimoyama, N. Takahashi, T. Takatsuka, and H. Kishimoto*
- 1694 Insight into the Possible Nature of the Active Catalytic Site in Non-Precious Metal Fuel Cell ORR Catalysis  
*P. Zelenay, G. Wu, H. T. Chung, M. Blair, E. F. Holby, C. D. Taylor, and M. Neidig*
- 1695 Active Site Modeling: Non-Precious Metal Based Catalysts for ORR  
*E. F. Holby, C. D. Taylor, G. Wu, and P. Zelenay*
- 1696 Using a Dual Plasma Process to Produce Cobalt-Polypyrrole Catalysts for the Oxygen Reduction Reaction in Fuel Cells  
*C. Walter, K. Kummer, D. Vyalikh, A. Quade, V. Brüser, and K. Weltmann*
- 1697 Low-Cost, High-Efficiency Non-PGM Cathode Catalysts Using MOFs as Precursors  
*D. Zhao, J. Shui, C. Chen, S. Comment, B. Reprogla, and D. Liu*
- 1698 Basicity of Non-precious Metal Catalysts for Oxygen Reduction  
*N. D. Leonard and S. Calabrese Barton*
- 1699 Templated Non-PGM Electrocatalysts for Polymer Electrolyte Fuel Cells  
*P. Atanassov, A. Serov, B. Halevi, K. Artyushkova, and B. Kiefer*
- 1700 Investigation of Fe-N-C Cathode Catalysts in Laminar Flow Fuel Cells  
*M. Naughton, N. D. Leonard, S. Calabrese Barton, and P. J. Kenis*
- 1701 Development of Hybrid Cathode Catalyst for PEM Fuel Cells  
*T. Kim, W. Jung, T. Xie, A. Kriston, P. Ganesan, and B. N. Popov*
- 1702 High Temperature Electrochemical Hydrogen Pump Cell Using a PBI Membrane at High Current Densities  
*T. J. Petek, J. S. Wainright, and R. F. Savinell*
- 1703 Testing of 17-Cell Dimensionally Stable Membrane (DSA) High-Pressure Electrolysis Stack  
*A. K. Kisor, M. Errico, T. I. Valdez, M. Hamdan, J. Willey, T. Norman, C. Mittelsteadt, and M. Hoberecht*

- 1704 Optimization of Clamping Pressure for High Pressure (Proton Exchange Membrane) PEM Electrolyzers  
*O. F. selamet, M. Acar, M. Ergoktas, and M. Mat*
- 1705 Comparing Platinum and Palladium as Hydrogen Oxidation/Evolution Electrocatalysts in Alkaline Medium  
*J. Herranz, P. Rheinländer, S. Henning, and H. A. Gasteiger*
- 1706 Carbonate and Bicarbonate Ion Transport in Alkaline Anion Exchange Membranes  
*A. M. Kiss, T. D. Myles, K. N. Grew, A. A. Peracchio, G. J. Nelson, and W. K. Chiu*
- 1707 Alkaline Stability and Ion Conductivity of Polysulfone Anion Exchange Membranes (AEMs) with Different Cation Chemistries  
*C. G. Arges and V. Ramani*

#### **B10 - Renewable Fuels from Sunlight and Electricity**

*ECS Energy Technology, ECS High Temperature Materials, ECS Physical and Analytical Electrochemistry, ECS New Technology Subcommittee, ECSJ, KECS*

- 1708 Electron- and (In Situ) Soft X-ray Spectroscopy of Materials for Photo-Electrochemical Water Splitting  
*L. Weinhardt*
- 1709 Analysis of Functional and Dysfunctional Defects in Photoelectrode Materials for Solar Water Splitting  
*A. Braun, N. M. Gaillard, Y. Chang, D. K. Bora, K. Gajda-Schrantz, J. Guo, Z. Liu, K. Sivula, M. Grätzel, and E. Constable*
- 1710 Hybrid Photovoltaic/Photoelectrochemical Device Design Using I-III-VI<sub>2</sub> Copper Chalcopyrite-Based Photocathodes  
*J. M. Kaneshiro, Y. Chang, and N. M. Gaillard*
- 1711 Silicon Microwires Coupled to Earth Abundant Catalysts as Photocathodes for the Hydrogen Evolution Reaction  
*E. L. Warren, J. R. McKone, M. R. Shaner, H. A. Atwater, H. B. Gray, and N. S. Lewis*
- 1712 Photoelectrochemical Hydrogen Production from Water Using p-type Calcium Ferrite and n-type Semiconducting Electrodes  
*S. Ida, K. Yamada, H. Hagiwara, and T. Ishihara*
- 1713 Band Structure Controls of SrTiO<sub>3</sub> towards Visible-Light Induced Two-Step Overall Water-Splitting  
*H. Irie*
- 1714 Development of Metal-Oxide-Semiconductor (MOS) Electrodes for Photoelectrochemical Water Splitting  
*D. V. Esposito, A. Talin, and T. Moffat*

- 1715 Optimum Conditions for Efficient Water Splitting in an Electrolyzer Powered by Solar Cells or Power Supply  
*M. Frites and S. U. Khan*
- 1716 Development of High Throughput Experimentation Capabilities for Accelerated Discovery of PEC Materials  
*X. Liu, M. Marcin, S. Mitrovic, J. Gregoire, S. Lin, E. Cornell, C. Xiang, J. Fan, G. D. Stucky, and J. Jin*
- 1717 Adiabatic Free Energy Surface of Hydrogen Evolution Reaction on GaInP<sub>2</sub>  
*W. Choi, B. C. Wood, E. Schwegler, and T. Ogitsu*
- 1718 Growth of GaAs Array Assisted-TiO<sub>2</sub> Heterojunction Nanostructure for Solar Hydrogen Production  
*S. Huang, C. Kei, and T. Perng*
- 1719 Hydrogen Production from Photoelectrochemical Cells: Economic and Theoretical Considerations and Experimental Results  
*J. A. Turner*
- 1720 Critical Assessment of Research and Development Needs in Solar to Hydrogen Production Technologies  
*E. L. Miller, S. Dillich, E. Sutherland, and S. Studer*
- 1721 Materials for Photocatalytic and Photoelectrochemical Water Splitting  
*A. Kudo*
- 1722 Solar Energy Conversion and Environmental Remediation Using Semiconductor-Liquid Interfaces: Design Paradigms for the Photocatalyst Material and Progress Update  
*K. Rajeshwar*
- 1723 Solar Energy Materials for High Efficiency Photoelectrochemical Sensitized Solar Cell  
*N. Park*
- 1724 Photoelectrochemical Energy Conversion Using Earth-Abundant Semiconductor Nanomaterials  
*S. Jin*
- 1725 All-Oxide Quantum-Confining Heteronanostructures for Solar Hydrogen Generation  
*L. Vayssières*
- 1726 Plasmon-Enhanced Photocatalytic Activity of Metal/Metal Oxide Composites  
*S. Cushing, J. Li, A. Bristow, and N. Wu*
- 1727 Photooxidation of Water at Nanostructured Hybrid Materials Utilizing Polyoxometallate-Decorated Tungsten Oxide and Gold Nanoparticles  
*P. J. Kulesza, R. Solarska, K. Miecznikowski, S. Zoladek, and S. Fiechter*

- 1728 Plasmonic-Enhancing Efficiency of Water Splitting in Au/Quantum Dots Sensitized ZnO Nanowires-Array Photoelectrodes  
*R. Liu, H. Chen, C. Chen, D. Tsai, and S. Hu*
- 1729 The Electrocatalytic Conversion of CO<sub>2</sub> to Fuels and Chemicals  
*T. F. Jaramillo, K. P. Kuhl, E. R. Cave, and D. N. Abram*
- 1730 Graphene-Supported Copper Catalysts for Electrochemical Reduction of Carbon Dioxide  
*S. Huang and P. S. Fedkiw*
- 1731 Room Temperature Electrochemical Conversion of CO<sub>2</sub> to Fuels  
*X. Zhou, J. Wu, and F. Risalvato*
- 1732 Photoreduction of CO<sub>2</sub> over Morphology Controlled TiO<sub>2</sub> or Nanocomposite System of g-C<sub>3</sub>N<sub>4</sub> and WO<sub>3</sub>  
*T. Ohno and N. Murakami*
- 1733 Photoelectrochemical Enzyme Biofuel Cell with the Function of CO<sub>2</sub> Conversion to Formic Acid  
*Y. Amao, Y. Sakai, and N. Shuto*
- 1734 Upconversion Nanocrystals: A New Class of Energy Materials  
*X. Liu*
- 1735 Photoelectrochemical Water Splitting Using Electrodes Prepared by Particle Transfer Method  
*T. Minegishi, N. Nishimura, J. Kubota, and K. Domen*
- 1736 Graphite Oxide Modified by Ammonia as Photocatalyst for Water Oxidation under Visible Light Illumination  
*T. Yeh and H. Teng*
- 1737 Hydrogen Production Promoted by Visible Light-Responsive MOF (Metal-Organic Framework) Photocatalyst  
*T. Toyao, M. Saito, Y. Horiuchi, K. Mochizuki, M. Iwata, H. Higashimura, and M. Matsuoka*
- 1738 Electrospun Ceria-Based Fibers for Renewable Fuel Production from Concentrated Sunlight  
*W. T. Gibbons and G. S. Jackson*
- 1739 Role of Electrocatalysts in Photoelectrochemical Water Oxidation of Oxide Semiconductor Electrodes  
*S. Choi, T. Jeon, U. Kang, H. Jeong, and H. Park*
- 1740 Fabrication of Efficient Nanostructured Photoelectrodes for Photoelectrochemical Hydrogen Production from Water  
*J. Lee*

- 1741 Performance and Limits of 2.2 eV Copper Tungstate ( $\text{CuWO}_4$ ) Mineral for Photoelectrochemical Hydrogen Production  
*N. M. Gaillard*
- 1742 Performance Limiting Factors in Co-Pt Catalyzed, Spray-Deposited  $\text{BiVO}_4$  Photoanodes  
*F. F. Abdi, N. Firet, and R. van de Krol*
- 1743 Photoelectrolysis on p-GaInP<sub>2</sub>; Extended Durability by Nitrogen Ion Implantation  
*T. G. Deutsch, A. Welch, M. Bär, L. Weinhardt, M. G. Weir, K. E. George, C. Heske, and J. A. Turner*
- 1744 Development of Nanostructured Photocatalysts for Hydrogen Generation by Water Splitting under Visible Light  
*Y. Wang, J. Hong, S. Goh, and R. Xu*
- 1745 Co-Alloying Approach for Bandgap Engineering of Metal Oxides for Improved Photoelectrochemical Water Splitting  
*Y. Yan*
- 1746 Corrosion Protection of p-GaInP<sub>2</sub> for Durable Photoelectrochemical Water Splitting  
*H. Wang, T. G. Deutsch, A. Welch, and J. A. Turner*
- 1747 Photoelectrochemical Modeling of a Multi-Junction Architecture for Artificial Photosynthesis  
*A. Berger and J. Newman*
- 1748 Toward a General Strategy for Chemical Stabilization of Non-Oxide Photoanodes for Water Oxidation  
*N. C. Strandwitz and N. S. Lewis*
- 1749 Photocatalytic Hydrogen Production from Sunlight via Tuning the Band Gaps Using Impurities-Doping Techniques  
*H. Yun, S. Yu, and J. Yi*
- 1750 Fueling Vehicles with Sun and Water  
*K. E. Ayers, E. B. Anderson, K. Dreier, and K. W. Harrison*
- 1751 Photobiological H<sub>2</sub> Production: Theoretical Maximum Light Conversion Efficiency and Strategies to Achieve it  
*M. L. Ghirardi*
- 1752 Vectorial Enzyme Activation at Illuminated Semiconductor-Enzyme-Electrolyte Junctions  
*K. Skorupska, H. Lewerenz, and P. J. Kulesza*
- 1753 ITO Nanowire-Based Photoelectrodes for Extremely Fast Charge Collection  
*J. Noh, J. Kim, G. Han, H. Shin, and H. Jung*
- 1754 Straightforward Measurement of Photoelectrode Minority Carrier Diffusion Length  
*A. J. Leenheer, R. A. Pala, and H. A. Atwater*

- 1755 Silicon Based Tandem Cells: A Novel Photocathode for Efficient PEC Water Splitting  
*E. Murugesen, W. Calvet, B. Kaiser, and W. Jaegermann*
- 1756 Enhancement of Photoactivity in Hematite Film with Controlled Morphology and Texture from Direct Spray Pyrolysis for Solar Water Splitting  
*T. Yang, H. Kang, J. Lee, B. Koo, K. Nam, and Y. Joo*
- 1757 Photoelectrochemical Hydrogen Production: Insights on Disrupting the Stability/Efficiency Trade-Off  
*T. Schiros, J. Leisch, H. Ohldag, H. Ogasawara, M. Toney, A. Nilsson, T. G. Deutsch, W. Choi, M. Mayer, and J. Turner*
- 1758 Photoelectrosynthetic Hydrogen Evolution from Free-Standing Silicon Microwire Arrays  
*S. Ardo, E. L. Warren, S. Park, B. S. Brunschwig, H. A. Atwater, and N. S. Lewis*
- 1759 Visible-Light-Absorbing Polyoxometalates as Building Blocks for All-Inorganic Photosynthetic Assemblies  
*R. Nakamura, T. Takashima, A. Yamaguchi, and K. Hashimoto*
- 1760 Reversible Fuel Cells for Power Generation and Fuel Production  
*A. V. Virkar*
- 1761 Integrative Multiphysics Development of Material Systems for a Renewable Future: The HeteroFoAM Story  
*K. Reifsnider, Y. Du, W. K. Chiu, and K. Brinkman*
- 1762 Solid Oxide Fuel Cell Systems for Small Scale Power Generation  
*S. C. Singhal and X. Zhou*
- 1763 Design and Preparation of Pt Nanocatalysts of High Surface Energy for Efficient Energy Conversion of Small Organic Molecule Fuels in Direct Fuel Cells  
*S. Sun, R. Huang, S. Chen, Z. Liu, Z. Zhou, L. Huang, N. Tian, Y. Jiang, and Y. Cai*
- 1764 Reversible Solid Oxide Fuel Cells: Status and Technology Development Challenges  
*N. Q. Minh*
- 1765 Microscopic Properties of III-V Semiconductor Photocathodes at the Interface with Water  
*B. C. Wood, W. Choi, E. Schwegler, and T. Ogitsu*
- 1766 Structural and Photoelectrochemical Evaluation of Nano-Textured Sn-Doped AgInS<sub>2</sub> Films Prepared by Spray Pyrolysis  
*Q. Cheng and C. K. Chan*
- 1767 Photoelectrochemical Hydrogen Production from Silicon Nanostructures  
*S. Hwang, J. Kye, and I. Oh*
- 1768 Lowering Overpotential of Electrochemical Reduction of CO<sub>2</sub>  
*W. Shin, D. Saravanakumar, and J. Song*

- 1769 Synthesis and Electrochemical Properties of Platinum-Based Films Used as Cathode Materials in the Dye-Sensitized Solar Cells  
*P. Hien, L. M. Phung, N. T. Hoang, and N. T. Thoa*
- 1770 The Properties According to Pore Former with SOFC Unit Cell Using Decalcomania Method  
*M. Lee, B. Kim, B. Choi, and S. Kim*
- 1771 Solar Hydrogen Generation at Pre-Structured Silicon Photocathodes Activated by Bimetallic Nanoparticles  
*M. Lublow, C. Merschjann, and T. Schedel-Niedrig*
- 1772 Understanding the Reaction Mechanism in the Sugar-Air Flow Battery  
*S. Li, D. Scott, and B. Liaw*
- 1773 Catalytic Reduction of Carbon Dioxide to Carbon Monoxide Using the Rhenium(I) Complex (5,5'-Bisphenylethynyl-2,2'-Bipyridyl)Re(CO)<sub>3</sub>Cl  
*E. Portenkirchner, K. Oppelt, C. Ulbricht, D. A. Egbe, H. Neugebauer, G. Knör, and N. Sariciftci*
- 1774 New Polyethylene Based Anion Exchange Membranes (PE-AEMs) with High Ionic Conductivity  
*M. Zhang, H. Kim, E. Chalkova, F. Mark, S. N. Lvov, and T. Chung*
- 1775 Ruthenium-Based Materials for Oxygen and Hydrogen Evolution Catalysis in Photoelectrochemical Applications  
*Y. Chang, J. M. Kaneshiro, and N. M. Gaillard*
- 1776 Membranes for Solar Water Splitting Devices  
*S. Ardo, M. McDonald, S. Park, M. DiFranco, M. Freund, and N. S. Lewis*
- 1777 A Non-Combustible Process for Generating Energy from Bio-Waste  
*A. Kumar, V. Kamavaram, V. Veedu, and K. Cheung*
- 1778 Electrochemistry of Molybdenum and Its Oxides for CIGS Solar Cells  
*V. S. Saji, S. Lee, Y. Yeon, and C. Lee*
- 1779 Interhalogen-Based Binary-Redox Couples for High-Voltage Solar Cells  
*N. C. Deb Nath, S. Sarker, H. Lee, and J. Lee*
- 1780 Development of an Artificial Co-Enzyme for Formate Dehydrogenase with the Function of CO<sub>2</sub> Reduction  
*S. Ikeyama and Y. Amao*
- 1781 Photoelectrochemical Dehydrogenation of Ammonia Borane with Pt/n-Si  
*H. Inoue, C. Matsuda, M. Shimada, M. Chiku, and E. Higuchi*
- 1782 The Activity of Ash-free Coal in Direct Carbon Fuel Cells  
*H. Ju, J. Kim, J. Lee, S. Lee, R. Song, and J. Lee*

- 1783 In-situ FTIR Analysis of CO<sub>2</sub> Electrochemical Reduction at Copper Electrodes  
*M. Ren, E. Andrews, and J. Flake*
- 1784 Theoretical Characterization of Ammonia Oxidation Intermediates and Products on Platinum Clusters  
*D. A. Daramola and G. G. Botte*
- 1785 Evaluation of Current Efficiency of SOEC Using Precise On-Line Gas Analysis  
*Y. Tanaka, S. Nakamura, K. Sato, K. Nozaki, T. Kato, and A. Yamamoto*
- 1786 Metal Tungstates as Oxygen Evolution Catalysts  
*H. Jia, T. Sekito, J. Stark, L. Zhou, and L. Chen*
- 1787 Modified Fe<sub>2</sub>O<sub>3</sub> Photoanodes Prepared by Pulse Electrodeposition  
*W. J. Lee, P. Shinde, and G. Go*
- 1788 Polycrystalline Cu(In, Ga)Se<sub>2</sub> Thin Films and PV Devices Sputtered from a Binary Target without Additional Selenization  
*P. Liu, B. B. Jheng, and M. Wu*
- 1789 Theoretical Investigations of Transition Metal Nano-Clusters for Electrochemical NH<sub>3</sub> Production  
*J. G. Howalt and T. Vegge*
- 1790 Choline Chloride Enhancement of Carbon Dioxide Reduction on Platinum Catalysts  
*W. Zhu, B. Rosen, A. Salehi-Khojin, and R. Masel*
- 1791 Structure Sensitivity of CO<sub>2</sub> Conversion on EMIM-BF<sub>4</sub> Silver Co-Catalyst System  
*A. salehi-khojin, B. Rosen, W. Zhu, and R. Masel*
- 1792 Basic Study of Alkaline Water Electrolysis  
*A. Manabe, T. Hashimoto, M. Kashiwase, M. Kuroasaki, T. Hayashida, K. Hirao, I. Shimomura, and I. Nagashima*
- 1793 CO<sub>2</sub> Reduction at Glassy Carbon Electrode in the Presence of Pyridine  
*J. Agullo, M. Morin, and D. Bélanger*
- 1794 Cu Monolayer on Au/C and Pt/C for the Electrochemical Reduction of CO<sub>2</sub> to Hydrocarbons  
*I. L. Escalante-Garcia, J. S. Wainright, and R. F. Savinell*
- 1795 Ti-Doped Hematite Nanostructures for Solar Water Splitting with High Efficiency  
*J. Deng, J. Zhong, A. Pu, D. Zhang, and X. Sun*
- 1796 Electrochemical Synthesis of Disordered Three-Dimensional Cuprous Oxide (Cu<sub>2</sub>O) Film and Its Photoelectrochemical Properties  
*S. Yoon, M. Kim, J. Lim, K. Lee, and B. Yoo*

- 1797 Impact of Nitrogen Treatment on the Electronic and Chemical Structure of GaInP<sub>2</sub> Thin-Film Surfaces  
*M. G. Weir, K. E. George, T. G. Deutsch, A. Welch, R. G. Wilks, D. C. Hanks, M. Blum, W. Yang, M. Bär, L. Weinhardt, J. A. Turner, and C. Heske*
- 1798 A Ceramic-Anode Supported Low Temperature Solid Oxide Fuel Cell  
*H. Ding, J. Ge, and X. Xue*
- 1799 Electrochemical Decomposition of Urea with Ni-Based Catalysts  
*W. Yan, D. Wang, and G. G. Botte*
- 1800 Transport Phenomena in Acid-Alkaline Membrane Bi-Cell Configurations for Portable Power Sources  
*K. N. Grew and D. Chu*
- 1801 Effect of Photodeposited Metal Catalysts on Oxygen Evolution at Well-Defined TiO<sub>2</sub> (110) Surfaces  
*M. A. Rigsby, G. E. Alliger, and G. M. Brown*
- 1802 Renewable Fuels for SOFCs: Fuel Flexibility by Gradual Internal Reforming  
*S. Georges, N. Bailly, M. Steil, F. Fonseca, S. D. Nobrega, J. Viricelle, A. Hadjar, and P. Gélin*
- 1803 The Co2p Oxidation State in Co-PI Catalysts  
*M. Richter and D. Schmeißer*
- 1804 Quasi Fermi Energy Tuning of Carbon Nanotubes for Solar Cells  
*N. C. Deb Nath, S. Sarker, H. Lee, and J. Lee*
- 1805 Photocatalytic Reduction of CO<sub>2</sub> Using Shape Controlled Anatase TiO<sub>2</sub> with Co-Catalyst Loading  
*D. Saruwatari, N. Murakami, and T. Ohno*
- 1806 CO<sub>2</sub> Reduction on Tin Oxide-Based Catalysts  
*Y. Chen and M. Kanan*
- 1807 Fabrication and Characterization of Metal/Ceramic Composite Electrodes for New Electrochemical Cells  
*A. Lapina, C. Chatzichristodoulou, P. Holtappels, and M. Mogensen*
- 1808 Photoelectrochemical Activity of Hematite Nanowire Arrays Synthesized Using Plasmas  
*H. B. Russell, U. Cvelbar, J. B. Jasinski, T. G. Deutsch, and M. K. Sunkara*
- 1809 Mechanistic Studies during Electro-Oxidation of Urea on Ni-Co Catalyst in Alkaline Medium  
*V. Vedharathinam and G. G. Botte*
- 1810 Development of Methanol Electrolysis System for Hydrogen Production  
*T. I. Valdez, K. J. Billings, and A. K. Kisor*

- 1811 Electrochemical Reduction of CO<sub>2</sub> to Value-Added Products: The effect of Electrode Structure and Electrolyte  
*H. Jhong, M. R. Thorson, S. Ma, A. Salehi, and P. J. Kenis*
- 1812 Carbon Dioxide Decomposition and Oxygen Generation Via SOEC  
*H. Guo and B. Kang*
- 1813 Low Overpotential CO<sub>2</sub> Reduction on Nanostructured Copper Electrodes  
*C. W. Li and M. Kanan*
- 1814 Room Temperature Electrochemical Synthesis of Oxygenates through a Carbonate Anion Pathway  
*N. Spinner and W. E. Mustain*
- 1815 Degradation of Solid Oxide Electrolysis Cells Applied for H<sub>2</sub>O/CO<sub>2</sub> Co-Electrolysis  
*Y. Tao, S. D. Ebbesen, and M. Mogensen*
- 1816 Hydrogen Production Via Electrolysis in Cu-Cl Thermochemical Cycle  
*S. N. Lvov, R. Schatz, S. Kim, S. Khurana, A. Morse, M. Chung, and M. Fedkin*
- 1817 Nanostructured Molybdenum Carbide as Pt-Free Catalysts for Hydrogen Evolution  
*W. Chen, C. Wang, K. Sasaki, N. Marinkovic, W. Xu, J. Muckerman, Y. Zhu, and R. R. Adzic*
- 1818 Reverse Combustion: The Efficient Electrochemical Conversion of Carbon Dioxide and Water to Organic Fuels Using an Aromatic Amine Catalyst  
*A. B. Bocarsly, T. Shaw, E. Zeitler, K. Liao, Y. Hu, Z. Detweiler, M. Baruch, J. Herb, and J. White*
- 1819 Reactive Molecular Dynamics Modeling of Interfacial Phenomena in Solid Oxide Fuel Cells  
*B. V. Merinov, A. C. van Duin, and W. Goddard III*
- 1820 Modeling the Behavior of a Solar-Hydrogen Generator  
*S. Haussener, C. Xiang, A. Berger, J. Newman, N. S. Lewis, and A. Weber*
- 1821 Renewable Liquid Fuels from Sunlight  
*P. G. Hoertz, J. Bittle, A. Miller, D. Murry, C. Bonino, J. Newman, and J. Trainham*
- 1822 Low-Cost Renewable Hydrogen from Sunlight and Water  
*S. Y. Reece*
- 1823 Thermochemical Water Splitting with Zirconium-Substituted Cerium Oxides  
*Y. Hao, W. Chueh, and S. M. Haile*
- 1824 Heterogeneous Nanostructures: Fast Electrochemistry for High-To-Ultrahigh Power Electrical Energy Storage  
*S. Lee*

- 1825 Kinetics of Oxidation of CO and H<sub>2</sub> and Reduction of CO<sub>2</sub> and H<sub>2</sub>O in Ni/YSZ Based Solid Oxide Cells  
*S. D. Ebbesen and M. Mogensen*
- 1826 Understanding Trends in Electrocatalytic Activity for CO Evolution  
*H. A. Hansen, J. Varley, A. A. Peterson, and J. K. Nørskov*
- 1827 The Status of Direct Methanol Fuel Cell System Lessons Learned and the Road Ahead  
*D. Chu and R. Jiang*
- 1828 X-ray Absorption Measurements on Perovskite Electrodes for the Oxygen Evolution Reaction  
*M. Risch, K. Stoerzinger, K. May, A. Mansour, and Y. Shao-Horn*
- 1829 Crossover in a Homogeneous-Catalyst Reactor  
*J. Newman*
- 1830 Proton Conductive Niobium Phosphates as Electrolytes for Fuel Cells Operating with Renewable Biofuels  
*Y. Huang, Q. Li, T. Anfimova, A. H. Jensen, J. Jensen, E. Christensen, and N. Bjerrum*

### B11 - Sodium Batteries

*ECS Battery, ECS Energy Technology, ECS High Temperature Materials, ECSJ Battery*

- 1831 Sodium Ion Batteries for Grid Applications  
*M. M. Doeff, M. Shirpour, and J. Cabana*
- 1832 Towards the Development of the Na-Ion Technology: In Search of Suitable Electrodes and Electrolytes  
*A. Ponrouch, P. Senguttuvan, E. Marchante, M. Courty, J. Tarascon, and M. Palacin*
- 1833 Understanding the Difference in Intercalation Behavior between Layered Na- and Li-Transition Metal Oxides  
*S. Kim, X. Ma, S. Ong, and G. Ceder*
- 1834 P2-type Na<sub>2/3</sub>[Fe<sub>1/2</sub>Mn<sub>1/2</sub>]O<sub>2</sub> Made from Earth-Abundant Elements for High-Energy Na-Ion Batteries  
*N. Yabuuchi, M. Kajiyama, Y. Yamada, and S. Komaba*
- 1835 Structure and Electrochemistry of Na<sub>x</sub>Fe<sub>x</sub>Mn<sub>1-x</sub>O<sub>2</sub> Na-Ion Cathode Materials  
*J. S. Thorne, R. A. Dunlap, and M. N. Obrovac*
- 1836 Layered Na<sub>1-x</sub>Li<sub>x</sub>Ni<sub>0.5</sub>Mn<sub>0.5</sub>O<sub>2</sub> Electrodes with O3- and P2- Composite Structure for Na-Ion Batteries  
*E. Lee, D. Kim, M. Slater, S. Rood, V. Maroni, D. Bass, S. Hackney, and C. S. Johnson*

- 1837 A Study of the Reactivity of De-Intercalated  $\text{NaNi}_{0.5}\text{Mn}_{0.5}\text{O}_2$  with Non-Aqueous Solvent and Electrolyte by Accelerating Rate Calorimetry  
*X. Xia and J. Dahn*
- 1838 Cathode Properties of Disodium Rhodizonate for Sodium Secondary Battery  
*K. Chihara, N. Chujo, A. Kitajou, E. Kobayashi, and S. Okada*
- 1839 Electrochemical Behavior of Olivine  $\text{FePO}_4$  Cathode Material for Na-Ion Batteries  
*P. Kubiak, M. Casas-Cabanas, V. Roddatis, J. Carretero-Gonzalez, D. Saurel, and T. Rojo*
- 1840 First Principles Investigations of the Electrochemical Properties of Sodium-Ion Cathode Materials  
*A. J. Toumar, W. D. Richards, S. Kim, X. Ma, X. Li, S. Ong, and G. Ceder*
- 1841 Development of High Capacity Positive Electrode Material for Sodium Ion Battery  
*R. Kataoka, T. Mukai, K. Nakatani, A. Yoshizawa, and T. Sakai*
- 1842 Na-Ion Intercalation Cathode with High Rate and Excellent Structural Stability  
*D. Lee, J. Xu, and Y. Meng*
- 1843 Nanostructured Na-Ion Full-Cells  
*S. Tepavcevic, H. Xiong, C. J. Johnson, and T. Rajh*
- 1844 Sodium Manganese Oxide Thin Film Cathodes: Characterization of a Na-Ion Intercalation Model System  
*L. Baggetto, C. A. Bridges, R. R. Unocic, F. Delnick, N. J. Dudney, and G. M. Veith*
- 1845 Phase Change of  $\text{NaFeO}_2$  during Electrochemical Na Intercalation and Deintercalation: An In Situ X-ray Diffraction Study  
*N. Takeichi, K. Kuratani, M. Yao, M. Tabuchi, and T. Kiyobayashi*
- 1846 Microstructure Evolution with Electrochemical Desodiation Process in  $\text{Na}_x\text{MnO}_2$   
*X. Li, X. Ma, A. J. Toumar, S. Ong, and C. Gerbrand*
- 1847 Novel Cathode Materials of Sodium-Containing Metal Phosphates as Highly Voltage Sodium-Ion Batteries  
*M. Nose, H. Nakayama, K. Nobuhara, S. Nakanishi, and H. Iba*
- 1848 Structural Investigation of  $\text{NaCrO}_2$  as a Positive Electrode for Rechargeable Sodium Battery Using Molten NaFSA-KFSA  
*C. Chen, K. Matsumoto, T. Nohira, R. Hagiwara, K. Numata, E. Itani, A. Fukunaga, S. Sakai, K. Nitta, and S. Inazawa*
- 1849 Electrochemical Properties of Sn-Based Electrodes for Na-Ion Batteries  
*Y. Matsuura, T. Ishikawa, W. Murata, N. Yabuuchi, S. Kuze, and S. Komaba*

- 1850 Na Insertion Mechanism in Alpha NaFeO<sub>2</sub> as Positive Electrode Materials for Na-Ion Batteries  
*H. Yoshida, N. Yabuuchi, and S. Komaba*
- 1851 Synthesis, Characterizations and Electrochemical Studies of Na<sub>2</sub>Ti<sub>6</sub>O<sub>13</sub> for Sodium Ion Batteries  
*N. Trinh, O. Crosnier, S. Schougaard, and T. Brousse*
- 1852 High Capacity Negative Electrodes for Na-Ion Batteries: Insertion Mechanism and SEI Layer  
*S. Komaba, T. Ishikawa, Y. Matsuura, W. Murata, N. Yabuuchi, S. Shimazu, J. Son, Y. Cui, H. Oji, K. Gotoh, and K. Takeda*
- 1853 Reversible Insertion of Sodium in Tin  
*L. D. Ellis, T. D. Hatchard, and M. N. Obrovac*
- 1854 First-Principles Study on Alkali Metal-Graphite Intercalation Compounds  
*K. Nobuhara, H. Nakayama, S. Nakanishi, and H. Iba*
- 1855 Electrochemical Properties of Titanium-Based Anode Materials for Rechargeable Na Ion Battery  
*H. Nakayama, M. Nose, K. Nobuhara, S. Nakanishi, and H. Iba*
- 1856 GaV<sub>4</sub>S<sub>8</sub> : A New Class of Anode Material for Sodium-Ion Batteries  
*C. Michelet, O. Crosnier, T. Brousse, P. Moreau, and D. Guyomard*
- 1857 Electrochemical Insertion of Na Ion into Nanocarbon Materials for Sodium Ion Batteries  
*T. Matsushita, Y. Ishii, and S. Kawasaki*
- 1858 Reaction of Li and Na with Iron Oxide/ Carbon Nanotube Composite Electrode in Ionic Liquid Electrolyte  
*M. Egashira, Y. Tsubouchi, D. Ogawa, N. Yoshimoto, and M. Morita*
- 1859 Microwave Synthesized NaTi<sub>2</sub>(PO<sub>4</sub>)<sub>3</sub> Anode Materials For Rechargeable Aqueous Electrolyte Sodium-Ion Battery  
*W. Wu, A. Mohamed, and J. F. Whitacre*
- 1860 Na<sub>3</sub>V<sub>2</sub>(PO<sub>4</sub>)<sub>3</sub>/C : A Novel Porous Sodium Ion Insertion Host For Sodium Ion Battery Applications  
*K. Saravanan, L. Bing, and P. Balaya*
- 1861 Quinone-Based Organic Active Materials for Use in Sodium and Magnesium Batteries  
*M. Yao, H. Senoh, H. Sano, K. Kuratani, T. Kiyobayashi, and H. Sakaeb*
- 1862 Na-Ion Capacitor Using Activated Carbon and Na Pre-Doped Hard Carbon  
*K. Kuratani, M. Yao, H. Senoh, N. Takeichi, T. Sakai, and T. Kiyobayashi*
- 1863 Synthesis and Characterization of Na<sub>3+x</sub>M<sub>x</sub>Zr<sub>2-x</sub>Si<sub>2</sub>PO<sub>12</sub> for Solid State Na-Ion Battery Applications  
*G. Hitz, K. Lee, and E. D. Wachsman*

- 1864 Electrochemical Sodium Ion Intercalation Property of  $\text{Na}_{2.7}\text{Ru}_4\text{O}_9$  in Nonaqueous and Aqueous Electrolytes  
*Y. Jung, S. Hong, and D. Kim*
- 1865 Charge and Discharge Properties of Sodium Secondary Batteries Using Molten NaFSA-KFSA  
*A. Fukunaga, T. Yamamoto, T. Nohira, R. Hagiwara, K. Numata, E. Itani, S. Sakai, K. Nitta, and S. Inazawa*
- 1866 New Sodium Imidazolium Salts for Battery Electrolytes  
*A. Plewa-Marczewska, T. Trzeciak, L. Niedzicki, J. S. Syzdek, E. Sasim, M. Dranka, G. Z. Zukowska, M. Marcinek, and W. Wieczorek*
- 1867 Conductivity and Viscosity of Perchlorate Salts Dissolved in Nonaqueous Solvents  
*N. Uemura, K. Kuratani, T. Kiyobayashi, and H. T. Takeshita*
- 1868 Low-Temperature, Low-Cost Liquid Metal Batteries  
*B. L. Spatocco, P. J. Burke, and D. R. Sadoway*
- 1869 In Situ Measurements to Extract Potential, Local Current and Charging Current Distributions in the Electric and Electrolyte Phases of an EDL Capacitance Electrode  
*K. C. Hess, J. F. Whitacre, and S. Litster*
- 1870 Advanced Electrochemical Energy Storage Development at Pacific Northwest National Laboratory for Renewable Integration and Smart Grid Applications  
*V. Sprenkle, S. Kim, W. Wang, G. Xia, J. Kim, and D. Choi*
- 1871 The Effect of Discharge Duration Distribution on Sodium Metal Halide Battery Cycle Life for Uninterruptible Power Supplies  
*D. B. Hall*
- 1872 Solid Electrolytes for Sodium Batteries  
*J. W. Fergus*
- 1873 Novel Sodium-Zinc Chloride Battery  
*X. Lu, G. Li, J. Kim, J. Lemmon, V. Sprenkle, and Z. Yang*
- 1874 Development of Sodium-Metal Halide Batteries for Energy Storage  
*G. G. Tao, N. Weber, and A. V. Virkar*
- 1875 Molten Sodium Battery with NaSICON Ceramic Membrane  
*A. Eccleston, M. Robins, S. V. Bhavaraju, Y. Kim, W. Koh, J. Chae, and J. Kim*
- 1876 Effects of Nickel Content and Operating Conditions on Cathode Degradation of Sodium-Nickel Chloride (Zebra) Battery  
*G. Li, X. Lu, J. Kim, and V. Sprenkle*
- 1877 Development of a Brass Supported Zinc-Chloride Sodium Cell  
*D. C. Bogdan Jr., M. Vallance, K. Gourishankar, H. Seshadri, G. Sundararajan, and A. Viswanathan*

- 1878 Influence of Sulfur Concentration on Low Temperature Operation of the Cell  
Na/ $\beta$ "-Alumina/S(IV) in AlCl<sub>3</sub>-NaCl Melt  
*T. J. Dunstan and J. Caja*

**B12 - Solid State Ionic Devices 9 - Ion Conducting Thin Films and Multilayers**  
*ECS High Temperature Materials, ECSJ Solid-State Chemistry*

- 1879 Innovative Oxides Materials for Electrochemical Energy Conversion  
*E. D. Wachsman*
- 1880 Study of Crystal Growth in Oxide Thin Films Fabricated by Pulsed Laser Deposition  
*N. Sata, S. Tamura, Y. Fujiwara, Y. Shibata, F. Iguchi, H. Yugami, Y. Nagao, H. Kageyama, and K. Nomura*
- 1881 Probing Pr<sub>x</sub>Ce<sub>1-x</sub>O<sub>2-d</sub> Thin Film Defect Concentrations Using In Situ Optical Absorption and Impedance Spectroscopy Techniques  
*S. R. Bishop, D. Chen, J. Kim, N. Thompson, and H. L. Tuller*
- 1882 Metastable Thin Films for Energy Applications: On Structural Lattice Anomalies and Electrical Transport  
*J. L. Rupp, S. Bishop, E. Fabbri, J. Han, D. Marrochelli, E. Traversa, H. L. Tuller, and B. Yildiz*
- 1883 Relating Nanostructures of Yttria-Stabilized-Zirconia Thin Films to Their Proton Conductivity  
*J. Martynczuk, M. V. Schlupp, B. Scherrer, D. Stender, R. Tölke, A. Evans, M. Prestat, and L. Gauckler*
- 1884 Ion Conduction in BaZr<sub>0.85</sub>Y<sub>0.15</sub>O<sub>3- $\delta$</sub>  Films Fabricated by Pulsed Laser Deposition in Various Conditions  
*D. Jang, K. Bae, and J. Shim*
- 1885 Do Oxygen-Ion Conductors Feel the Strain  
*D. Pergolesi, E. Fabbri, S. N. Cook, V. Roddatis, E. Traversa, and J. A. Kilner*
- 1886 Epitaxial Zirconia and Ceria Based Thin Films and Multilayers with Arbitrary Composition  
*W. Shen, J. Jiang, and J. L. Hertz*
- 1887 Electric Conductivity in Cu- and Ga-Doped Pr<sub>2</sub>NiO<sub>4</sub> Nano Film Laminated with Sm-Doped CeO<sub>2</sub>  
*J. Hyodo and T. Ishihara*
- 1888 Electronic Activation in the (La<sub>0.8</sub>Sr<sub>0.2</sub>)CoO<sub>3</sub>/(La<sub>0.5</sub>Sr<sub>0.5</sub>)<sub>2</sub>CoO<sub>4</sub> Superlattices at High Temperature  
*Y. Chen, Z. Cai, Y. Kuru, H. L. Tuller, and B. Yildiz*

- 1889 Low Energy Ion Scattering (LEIS) Analysis of SrTiO<sub>3</sub> (100) and NdGaO<sub>3</sub> (110) Single Crystal Surface Terminations  
*A. Cavallaro and J. A. Kilner*
- 1890 Enhanced Oxygen Surface Exchange Kinetics in Surface Modified Yttria Stabilized Zirconia by Atomic Layer Deposition  
*J. Park, C. Chao, X. Tian, J. Shim, and F. Prinz*
- 1891 Thin Film Electrolyte Membranes of Yttria-Stabilized Zirconia Prepared by Aerosol Assisted Chemical Vapor Deposition  
*M. V. Schlupp, J. Courbat, D. Briand, N. de Rooij, M. Prestat, and L. Gauckler*
- 1892 Ion Conduction in Nanoscale Yttria-Stabilized Zirconia Thin Films Fabricated by Atomic Layer Deposition  
*K. Son, M. Bae, K. Bae, J. Ha, and J. Shim*
- 1893 Atomic Resolution Imaging of Oxygen Columns in Oxide Ion Conductor Using HRTEM  
*J. An, A. Koh, J. Park, H. Jung, T. M. Gür, and F. B. Prinz*
- 1894 Detecting Li-Ion Currents on the Nanoscale through a Thin Film Battery  
*N. Balke, S. Jesse, A. Tselev, N. J. Dudney, and S. Kalinin*
- 1895 Lateral Oxygen Tracer Diffusion in a Multilayered SDC/PNCG Film Displaying Enhanced Electrical Conductivity  
*S. N. Cook, J. Druce, T. Ishihara, and J. A. Kilner*
- 1896 Analysis of Lateral Diffusion of Oxide Ions along YSZ-MgO(100) Interface  
*K. Bae, J. Park, F. B. Prinz, J. Son, and J. Shim*
- 1897 Electrochemical Performance of Free-standing Micro-Solid Oxide Fuel Cell Membranes using De-alloyed Pt-Y-Al Electrodes  
*R. Tölke, M. Prestat, H. Galinski, J. Martynczuk, and L. Gauckler*
- 1898 Thin Pulsed Laser Deposited Bilayer Electrolytes in Anode-Supported SOFCs  
*J. S. Hardy, Z. Lu, J. W. Templeton, and J. W. Stevenson*
- 1899 Morphological and Compositional Changes on YSZ/GDC Bi-layered SOFC Electrolytes in Various Temperature and Reducing Environments  
*Y. Jee, J. An, J. Choi, T. Park, G. Cho, M. Lee, F. B. Prinz, and S. Cha*
- 1900 Cation Interdiffusion Model for Enhanced Oxygen Kinetics at Oxide Heterostructure Interfaces  
*M. Gadre, Y. Lee, and D. Morgan*
- 1901 Nanostructured La<sub>0.6</sub>Sr<sub>0.4</sub>CoO<sub>3-δ</sub> Cathodes Prepared by Spray Pyrolysis for Thin Film SOFC  
*M. Prestat, Z. Yáng, O. Pecho, L. Holzer, J. Martynczuk, A. Evans, L. Gauckler, T. Hocker, J. Hwang, and J. Son*

- 1902 Cation Segregation and Electrochemical Activity of Ruddlesden Popper Phase Cobalt Oxides in Oxygen Reduction and Oxygen Evolution  
*Z. Cai, Y. Chen, and B. Yildiz*
- 1903 In Situ Ambient Pressure X-ray Photoelectron Spectroscopy of Epitaxial Strontium Substituted Lanthanum Cobalt Oxides Near Operating Conditions Under Applied Potentials  
*E. J. Crumlin, E. Mutoro, Z. Liu, M. D. Biegalski, W. T. Hong, H. M. Christen, H. Bluhm, and Y. Shao-Horn*
- 1904 Hard X-ray Surface Composition and Electronic Structure Measurements of Heteroepitaxial Solid Oxide Fuel Cell Cathode Material  
*J. N. Davis, L. Saraf, T. Kaspar, S. Gopalan, U. B. Pal, J. Woicik, S. Basu, and K. F. Ludwig*
- 1905 Spray Pyrolysis Deposition and Electrochemistry of  $\text{La}_{0.5}\text{Sr}_{0.5}\text{Mn}_{0.5}\text{Co}_{0.5}\text{O}_{3-\delta}$  Thin Film Anodes for Solid Oxide Fuel Cells  
*Z. Yáng, S. Bisig, M. Prestat, and L. Gauckler*
- 1906 Synthesis and Characterization of Ruthenium - Gadolinia-doped Ceria Composite Thin Film Anode for Direct Methane SOFCs  
*Y. Takagi and S. Ramanathan*
- 1907 Nanostructured Vanadium Oxide Anodes for Thin Film Solid-Oxide Fuel Cells  
*Q. Van Overmeere and S. Ramanathan*
- 1908 Atomistic Investigation of Oxygen Vacancy Induced Volume Changes in  $\text{CeO}_2$  Grain Boundaries  
*S. Kim and V. B. Shenoy*
- 1909 Obtaining Mixed Ionic/Electronic Conductivity in Perovskite Oxides at Anodic Solid Oxide Fuel Cell Conditions: A Computational Approach  
*S. Suthirakun, S. C. Ammal, and A. Heyden*
- 1910 Electrochromic Films Produced by Ultrasonic Spray Deposition of Mesoporous Tungsten Oxide  
*C. Li, F. Lin, R. M. Richards, R. Tenent, A. Dillon, and C. Wolden*
- 1911 Development of Safe All Inorganic Li-Ion Batteries  
*L. Castro, G. Jouan, A. Kubanska, V. Seznec, L. Tortet, M. Morcrette, V. Viallet, R. Bouchet, and M. Dollé*
- 1912 Stabilization of NASICON-Type  $\text{LiZr}_2(\text{PO}_4)_3$  at Room Temperature  
*L. Castro, A. Kubanska, L. Tortet, R. Bouchet, and M. Dollé*
- 1913 Open-Circuit Voltage Anomalies in Dense Bilayered Electrolytes: Explanation and Implications  
*K. Duncan and E. D. Wachsman*

- 1914 Conductivity of New Electrolyte Material  $\text{Pr}_{1-x}\text{M}_{1+x}\text{InO}_4$ (M=Ba,Sr) with Related Perovskite Structure for Solid Oxide Fuel Cells  
*X. Li, H. Shimada, and M. Ihara*
- 1915 Fabrication and Characterization of Nanosized  $(\text{DyO}_{1.5})_x(\text{WO}_3)_y(\text{BiO}_{1.5})_{1-x-y}$  for Lower Temperature SOFC Application  
*A. A. Lidie, K. Lee, and E. D. Wachsman*
- 1916 Investigation of Electrolyte and Electrode Effects on GDC Electrolyte by Electrochemical Impedance Spectroscopy  
*L. Zhang, F. Liu, and A. V. Virkar*
- 1917 Mapping Thermodynamics and Kinetics of Oxygen Vacancies in Fuel Cell Electrolytes on the Nanoscale  
*S. Jesse, A. Kumar, M. D. Biegalski, A. Morozovska, E. Eliseev, F. Ciucci, and S. Kalinin*
- 1918 Effect of Sulfur Poisoning on Exchange Current Density of SOFC Anodes  
*T. Hosoi, T. Yonekura, T. Yoshizumi, Y. Tachikawa, S. Taniguchi, Y. Shiratori, and K. Sasaki*
- 1919 Thin Film Ceria Based Anodes for a Single Direct Carbon Fuel Cell  
*M. G. Werhahn, O. Schneider, and U. Stimming*
- 1920 Anode Materials and Design for Lower Temperature, Hydrocarbon-Fueled Solid Oxide Fuel Cells  
*C. Gore, K. Lee, H. Yoon, and E. D. Wachsman*
- 1921 Degradation Induced by Sintering of Ni-YSZ Anode in SOFCs  
*Y. Lee, H. Muroyama, T. Matsui, and K. Eguchi*
- 1922 Electrical Performance of La-Substituted  $\text{SrTiO}_3$  Anode Material with Deficient in A-Site  
*G. Chen, H. Kishimoto, K. Yamaji, K. Kuramoto, and T. Horita*
- 1923 Infiltrated Ni-ScYSZ Fuel-Electrodes with Improved Carbon and Sulfur Tolerance  
*C. Graves, S. Ricote, and T. Ramos*
- 1924 Synergy Effects of  $\text{Pr}_2\text{NiO}_4$  and  $\text{Ba}(\text{La})\text{CoO}_3$  on Cathodic Activity for Intermediate Temperature Solid Oxide Fuel Cells  
*T. Ishihara, J. Xie, Y. Ju, and S. Ida*
- 1925 Electrochemical Study on LSCF Cathode Reaction as a Function of Microstructure, Temperature and Oxygen Partial Pressure  
*D. Marinha, L. Dessemond, and E. Djurado*
- 1926 Effects of Strontium Dopant Concentration on the Oxygen Reduction Reaction Rate Limiting Steps in  $\text{La}_x\text{Sr}_{1-x}\text{Co}_{0.2}\text{Fe}_{3-\delta}$  Cathodes  
*A. Dynkin, S. Basu, U. B. Pal, and S. Gopalan*

- 1927 Control of Activity and Stability by Tailoring Microstructure of Electrocatalyst-Modified Composite Cathode of SOFC  
*S. Lee, P. Ohodnicki, and K. Gerdes*
- 1928 Characterization and Modeling of Infiltrated SOFC Cathode  
*X. Liu, Y. Li, M. Gong, K. Gerdes, R. Gemmen, R. Pakalapati, I. Celik, and T. Horita*
- 1929 Ab Initio Based Modeling of  $\text{LaMnO}_3\{\text{plus minus}\}^\delta$  Defect Chemistry for Solid Oxide Fuel Cell Cathodes  
*Y. Lee and D. Morgan*
- 1930 A-Site Diffusion in  $\text{La}_{1-x}\text{Sr}_x\text{MnO}_3$ : Ab Initio and Kinetic Monte Carlo Calculations  
*B. Puchala, Y. Lee, and D. Morgan*
- 1931 Influence of Water Vapor on Sulfur Distribution Within  $\text{La}_{0.6}\text{Sr}_{0.4}\text{Co}_{0.2}\text{Fe}_{0.8}\text{O}_3$  Cathode  
*F. Wang, K. Yamaji, D. Cho, T. Shimonosono, M. Nishi, H. Kishimoto, M. Brito, T. Horita, and H. Yokokawa*
- 1932 Electrochemical Operation of  $\text{La}(\text{Ni},\text{Fe})\text{O}_3$  under Cr-Poisoning Conditions  
*M. K. Stodolny, B. A. Boukamp, D. H. Blank, and F. P. van Berkel*
- 1933 Nonlinear Electrochemistry Impedance Spectroscopy and Its Applications  
*N. Xu, J. Riley, and J. A. Kilner*
- 1934 Ultra Small Angle X-ray Scattering Studies of Solid Oxide Fuel Cell Cathode Powders  
*K. Chang, B. Ingram, M. Hopper, J. Ilavsky, and H. You*
- 1935 In Situ Examination of Oxygen Kinetics in  $\text{La}_{1-x}\text{Sr}_x\text{CoO}_{3-\delta}$  Thin Films at Intermediate and Low Temperatures by X-ray Diffraction  
*M. D. Biegalski and S. V. Kalinin*
- 1936 Preparation of  $\text{A}_2\text{BB}'\text{O}_6$  Oxides by Pechini Method for Solid Oxide Fuel Cells  
*S. Kim, A. Dorai, D. Seo, I. Han, J. Yu, S. Kim, J. Joo, and S. Woo*
- 1937 Crystal Structure and Electrical Properties of Al-Doped Lanthanum Silicate Solid Electrolytes  
*T. Funahashi, A. Mineshige, H. Mieda, Y. Daiko, H. Yoshioka, and T. Yazawa*
- 1938 Power Generation of Rechargeable Direct Carbon Fuel Cells with Batch-type Charging System  
*H. Tanaka, A. Yabuki, X. Li, and M. Ihara*
- 1939 A Comparative Study on Microstructural Change of LSM/SDC and LSCF/SDC Interfaces  
*M. Komoto, H. Muroyama, T. Matsui, and K. Eguchi*
- 1940 Study of  $\text{La}_{0.1}\text{Sr}_{0.9}\text{Co}_{0.8}\text{Fe}_{0.2}\text{O}_{3-\delta}$  for Ceria-Based IT-SOFC Cathode  
*M. Choi, H. Im, K. Lee, and S. Song*

- 1941 Evaluation of Y and Fe Co-Doped SrTiO<sub>3</sub> as Anode Material for SOFC  
*H. Im, M. Choi, S. Jeon, and S. Song*
- 1942 Resistivity and Interfacial Properties of CGO-YSZ Bilayers in Solid Oxide Fuel Cells  
*J. Hjelm, P. Hjalmarsson, K. Brodersen, and S. Foghmoes*
- 1943 Cathode Performance and Deposited Cr under Cr Poisoning Condition in the (La<sub>0.6</sub>Sr<sub>0.4</sub>)(Co<sub>0.2</sub>Fe<sub>0.8</sub>)O<sub>3</sub> Cathode  
*D. Cho, T. Horita, M. Brito, K. Yamaji, H. Kishimoto, M. Nish, T. Shimonosono, F. Wang, and H. Yokokawa*
- 1944 Performance Degradation and Microstructural Change of Ni-YSZ Anode upon Thermal and Redox Cycles  
*M. Kubota, H. Muroyama, T. Matsui, and K. Eguchi*
- 1945 Electrochemical Studies of LSCF Powder Prepared using Pechini Process for IT-SOFC Unit Cell  
*H. Jeon, H. Kim, T. Kim, and H. Kim\**
- 1946 Correlation between Protonic Conductivity and Structure of Phosphate Glasses for Intermediate Temperature Fuel Cells  
*H. Sumi, Y. Fujishiro, T. Oine, and T. Kasuga*
- 1947 Proton Conduction in CsH(PO<sub>3</sub>H) under Dry or Humid Conditions  
*M. Nagao, A. Ikeda, and S. M. Haile*
- 1948 Structure and Electrochemical Property of Various Valence Metal Ion Co-doped Scandia Stabilized Zirconia  
*N. Sonoyama, M. Ikeda, Y. Ota, N. Imanishi, A. Hirano, Y. Takeda, and O. Yamamoto*
- 1949 Fabrication of a Micro-tubular Bi-Layered Membrane by Electrophoretic Deposition  
*K. Lee, J. Seo, J. Yoon, and H. Hwang*
- 1950 Analysis of Electrical Conduction Mechanism of LaNi<sub>1-x</sub>M<sub>x</sub>O<sub>3-δ</sub> (M = Fe, Mn)  
*E. Niwa, H. Maeda, C. Uematsu, and T. Hashimoto*
- 1951 Oxygen Transport Properties of Al doped La<sub>2</sub>NiO<sub>4+δ</sub>  
*S. Jeon, M. Choi, H. Im, and S. Song*
- 1952 Transport Properties of the Proton Conducting BaCe<sub>0.45</sub>Zr<sub>0.4</sub>Y<sub>0.15</sub>O<sub>3-δ</sub>  
*D. Lim, M. Choi, H. Im, K. Lee, and S. Song*
- 1953 Performance of BaCe<sub>0.85</sub>Y<sub>0.15</sub>O<sub>3-δ</sub> Electrolyte for the Proton Conducting Ceramic Fuel Cells  
*K. Lee, M. Choi, D. Lim, and S. Song*
- 1954 Molecular Dynamics Simulation on Oxygen Ion Diffusion in LaInO<sub>3-δ</sub> Perovskite Structure Doped with Ba and Sr  
*S. Jeong, K. Hwang, M. Yoon, and H. Hwang*

- 1955 Hydrothermal Synthesis and 3D-Arrangement of CeO<sub>2</sub> Nanocrystals  
*K. Kobayashi, M. Haneda, and M. Ozawa*
- 1956 Thin Film Electrodes for Li-Ion Batteries: Improved Electrochemical Properties and Mechanism Study  
*Z. Cui, P. Yu, and X. Guo*
- 1957 A Novel All-Solid-State Lithium-Ion Battery with In Situ Formed Negative Electrode Material  
*Y. Amiki, F. Sagane, and Y. Iriyama*
- 1958 Ionic and Electronic Conductivity in Telluride Glass Systems: Interfacial Materials for All-Solid-State Devices  
*I. Alekseev, E. Bychkov, D. Le Coq, M. Kassem, M. Fourmentin, and T. Usuki*
- 1959 Mechanistic Study of the Electrochemical Promotion of Catalysis Using Isotopic Exchange  
*M. Tsampas, F. Sapountzi, A. Boréave, and P. Vernoux*
- 1960 Defect Chemistry and Transport Properties in MnO<sub>2</sub> Nanowires  
*B. C. Solomon, J. Wu, E. Thomsen, J. Yang, and X. Zhou*
- 1961 Enhanced Proton Conductivity by Hydrogenation in Anodic ZrO<sub>2</sub>-WO<sub>3</sub>-SiO<sub>2</sub> Nanofilms  
*K. Ye, Y. Aoki, E. Tsuji, S. Nagata, and H. Habazaki*
- 1962 Water-Absorbing Porous Electrolyte Based on Sulfated Hydrous Titania and Application to Water Electrolysis  
*S. Kim, T. Sakai, J. Hamagami, Y. Okuyama, H. Oda, T. Ishihara, and H. Matsumoto*
- 1963 Current-Voltage Relation in (La,Ce)PO<sub>4</sub> Mixed-Conducting Ceramics  
*H. L. Ray and L. De Jonghe*
- 1964 Proton Conductivity and Stability of In<sup>3+</sup> Doped SnP<sub>2</sub>O<sub>7</sub> with Varying P:M  
*C. R. Kreller, M. Wilson, R. Mukundan, E. L. Brosha, and F. H. Garzon*
- 1965 Simulations of Proton Conduction in Tin Pyrophosphates  
*N. J. Henson, F. H. Garzon, and R. Mukundan*
- 1966 First-Principles Defect Equilibrium Calculations in Rare-Earth Phosphate Electrolytes with Mixed Conductivity  
*N. Adelstein, H. L. Ray, M. Asta, and L. De Jonghe*
- 1967 Effect of Multi-Site Doping on The Conductivity of ABO<sub>3</sub> Perovskite Mixed Proton/Electron Conductors  
*K. Pan and E. D. Wachsman*
- 1968 Nanoionics Applied to Proton Conducting Ceramics  
*J. Tong, D. Clark, S. Nikodemski, M. Shang, A. Herring, C. Wolden, A. Bunge, and R. O'Hayre*

- 1969 Functional Relationships between Structure and Transport in the BZY and BCY Proton Conductors  
*A. Braun and Q. Chen*
- 1970 Improving the Performance of Solid Oxide Fuel Cells with BaZrO<sub>3</sub> Electrolyte by Using Sinteractive Anodic Powders  
*L. Bi, E. Fabbri, and E. Traversa*
- 1971 Magnesium Manganese Spinel Coatings for Solid Oxide Fuel Cell Interconnects  
*S. Joshi, C. Silva, and A. Petric*
- 1972 Increased Performance Stability of SOFC Cathodes by Use of Protective Coatings on Metallic Interconnectors  
*M. Kornely, N. Menzler, A. Weber, and E. Iver-Tiffée*
- 1973 Imaging of Oxide Ionic Diffusion at Cathode/Interlayer/Electrolyte Interfaces for Solid Oxide Fuel Cells: long-term operation effects  
*T. Horita, D. Cho, T. Shimonosono, M. Nishi, H. Kishimoto, K. Yamaji, and H. Yokokawa*
- 1974 Novel Anode Material for Direct Hydrocarbon Solid Oxide Fuel Cells  
*C. Yang, Z. Yang, G. Xiao, L. Zhang, M. Han, and F. Chen*
- 1975 Efficient High Power Density SOFCs with Zirconia/Bismuth Oxide Bilayered Electrolytes  
*K. Lee and E. D. Wachsman*
- 1976 Process Integration for Scale-Up of Ce<sub>0.9</sub>Gd<sub>0.1</sub>O<sub>1.95</sub> Electrolyte-Based LT-SOFCs  
*H. Yoon, C. M. Gore, A. A. Lidie, K. Lee, and E. D. Wachsman*
- 1977 Performance of Solid Oxide Fuel Cells on H<sub>2</sub>, NH<sub>3</sub> and Hydrocarbon Fuels  
*M. Han, J. Xiong, and S. C. Singhal*
- 1978 Improved Power Density by (Mn, Fe) Doped CeO<sub>2</sub> as a Oxide Anode for Ni-Fe Metal Support SOFC  
*Y. Ju, S. Ida, and T. Ishihara*
- 1979 Effect of Co Addition on Sintering and Electrical Properties of La-Doped CeO<sub>2</sub> as a Buffer Layer for Doped LaGaO<sub>3</sub> Electrolyte Films of Solid Oxide Fuel Cells  
*J. Hong, S. Ida, and T. Ishihara*
- 1980 Effect of Fuel Utilization on the Performance of Nickel/Zirconia Anode-Supported SOFCs  
*O. A. Marina, C. Coyle, D. Edwards, and J. Stevenson*
- 1981 Durability of SOFC Against Thermal and Redox Cycling  
*M. Hanasaki, C. Uryu, S. Taniguchi, Y. Shiratori, and K. Sasaki*
- 1982 Sulfur-Poisoning in Reformate Fuelled Anode Supported Solid Oxide Fuel Cells  
*A. Kromp, S. Dierickx, A. Leonide, A. Weber, and E. Ivers-Tiffée*

**C1 - Organic and Biological Electrochemistry General Poster Session**  
*All ECS Divisions, ECSJ Organic and Biological Electrochemistry*

- 1983 The Electrolytic Dissociation of 1,3-Cyclobutanedicarboxylic Acids  
*E. Kvaratskhelia and R. Kvaratskhelia*
- 1984 Propagation and Collision of Nonlinear Electrical Responses in *Aloe Vera* L. and *Arabidopsis Thaliana*  
*L. O'Neal, M. I. Volkova, V. S. Markin, and A. G. Volkov*
- 1985 Effect of Surfactants on the Voltammetric Response and Determination of an Antihypertensive Drug Phentolamine at Boron Doped Diamond Electrode  
*R. Shrivastav, S. Satsangee, and R. Jain*
- 1986 Potential-Induced Conformational Changes in Self-Assembled Monolayers of L-Cysteine at p-GaAs(100) Electrodes  
*M. Enache, L. Preda, V. Lazarescu, C. Negrila, and M. Lazarescu*
- 1987 Effect of Humidity of Atmosphere on Characteristics of Cathodic Film Formed on Ti in Ca<sup>2+</sup>/Ethanol Solution  
*T. Haruna and A. Nonaka*
- 1988 Evolution of Cathode Surface Hydrophobicity in Microbial Fuel Cell Using Sessile Drop Technique  
*C. Santoro, M. Cremins, A. Mackay, U. Pasaogullari, M. Guilizzoni, A. Casalegno, and B. Li*
- 1989 Electrodeposition of Poly (Ethyleneglycol) for Constructing the Artificial Scaffold onto Titanium  
*S. Migita, S. Okada, Y. Tsutsumi, H. Doi, N. Nomura, and T. Hanawa*
- 1990 Monitoring of the Processes of Proliferation and Differentiation of Immunocytes by the Impedance Measurement Method  
*S. Kasai, K. Shoji, M. Tada, H. Kiri, R. Ishii, and H. Kodama*
- 1991 Photocurrent Characteristics of Thin Films Produced from Aqueous Colloidal Dispersion of Indolino[60]Fullerene by Using Electrospray Deposition Method  
*H. Matsutaka, Y. Shigemitsu, T. Orii, T. Aoyama, H. Takaku, and Y. Tajima*
- 1992 Electrochemical Characteristics of Vinylferrocene-Terminated Si(111) Prepared in Diethyl Ether and Dibutyl Ether Grafting Media  
*M. U. Herrera, T. Ichii, K. Murase, and H. Sugimura*
- 1993 A Green Electrochemical Method to Remove Protein Surface Fouling and Industrial Dye Wastes  
*J. Yang and S. Gunasekaran*
- 1994 Effects of Cathodic Platinum Loadings and Organic Substrate Concentrations on the Performance of Single Chamber Microbial Fuel Cells Fed with Raw Wastewater  
*C. Santoro, B. Li, U. Karra, A. G. Agrios, G. Squadrato, and P. Cristiani*

- 1995 Electrosynthesis of Polypyrrole in Low-Viscosity Ionic Liquids  
*K. Tsunashima, T. Matsabayashi, Y. Ono, and M. Matsumiya*
- 1996 Disc-Like and Bent-Shape Semiconducting Liquid Crystals for Organic Electronics  
*F. Ely, M. O. da Silva, R. Cristiano, A. Vieira, and H. Gallardo*
- 1997 Irreversible Thermodynamics Microbial Fuel Cell Anode Model  
*J. E. Velez and C. Sanchez*
- 1998 Graphene Nanohybrids based on Genetically Engineered Protein for Agrichemical Biosensing  
*N. Heo, S. Lee, K. Lee, and T. Park*

## C2 - Bioengineering Based on Electrochemistry

*ECS Organic and Biological Electrochemistry, ECS Sensor, ECSJ Bioengineering*

- 1999 Electrochemical-Based Bioprocessing Device Composed of Recombinant Protein/DNA Conjugate  
*J. Choi*
- 2000 Fabrication of Multilayer Cell Structure Using Electro-Deposited Alginate Gel  
*F. Ozawa, K. Ino, H. Shiku, and T. Matsue*
- 2001 Metabolism Feature of Multicellular Tumor Spheroids Assessed by a Comprehensive System  
*Y. Zhou, T. Arai, Y. Horiguchi, K. Ino, H. Shiku, and T. Matsue*
- 2002 Development of Voltage Switching Mode Scanning Electrochemical Microscopy for Topographical and Electrochemical Nanoscale Imaging of Living Cells  
*Y. Takahashi, A. I. Shevchuk, P. Novak, Y. Matsumae, B. Babakinejad, J. V. Macpherson, P. R. Unwin, K. Ino, H. Shiku, J. Gorelik, D. Kleinerman, Y. E. Korchev, and T. Matsue*
- 2003 Electrochemically Modulated Release of Nitric Oxide through Polymers to Inhibit Bacterial Biofilm Formation and Prevent Platelet Activation  
*M. E. Meyerhoff, L. Höfner, D. Koley, H. Ren, T. C. Major, J. Wu, and C. Xi*
- 2004 Engineering of Catalytic Domain of Cellobiose Dehydrogenase and Its Application for the Direct Electron Transfer Type Enzyme Electrode  
*S. Ando, S. Ferri, W. Tsugawa, and K. Sode*
- 2005 Aptameric Sensor for Detection of VEGF Based on Labeling Technique Using GDH Fused Zinc Finger Protein  
*A. Tatsumi, K. Abe, T. Fukaya, K. Sode, and K. Ikebukuro*
- 2006 Evolution of Cathodic Characteristics (Water and Oxygen Transport) in Microbial Fuel Cell (MFC)  
*C. Santoro, M. Cremins, A. Mackay, U. Pasaogullari, M. Guilizzoni, A. Casalegno, and B. Li*

- 2007 Turning Oxidase into Dehydrogenase for Application to the Electrochemical Measurement  
*S. Saito, Y. Horaguchi, T. Endo, S. Ferri, K. Mori, K. Kojima, W. Tsugawa, and K. Sode*
- 2008 Peroxidase Activity of G-Quadruplex Hemin-Binding DNA Aptamers Determined by Electrochemical Measurement  
*I. Kubo, Y. Hoshino, M. Liu, H. Abe, and Y. Ito*
- 2009 Electron Transfer between Cytoplasm and Electrode via Redox-Active Phospholipid Polymer  
*K. Nishio, R. Nakamura, S. Nakanishi, X. Lin, T. Konno, K. Ishihara, and K. Hashimoto*
- 2010 In Situ Observation of Direct Electron Transfer Reaction between Cytochrome c and ITO Electrode with Electrochemically Controlled Slab Optical Waveguide Spectroscopy  
*N. Matsuda and H. Okabe*
- 2011 Recent R&D on Disposable Electrochemical Biosensors  
*H. Nam, G. Cha, M. Kim, M. Lee, and S. Chung*
- 2012 Floated Electrochemical Cell for On-Line Electrospray Mass Spectrometry for Detection of Biological Radical Reactions  
*D. Looi, I. Iftikhar, G. Garbellini, and A. Brajter-Toth*
- 2013 High Efficient Glucose Oxidation by Ordered Molecular Assembly inside Carbon Nanotube Forests  
*S. Yoshino, T. Miyake, H. Kaji, T. Yamada, K. Hata, and M. Nishizawa*
- 2014 Evaluation of Electrochemical Disinfection of Feline Calicivirus in Aqueous Conditions  
*N. Shionoiri, T. Tanaka, T. Sato, Y. Fujimori, T. Nagao, T. Nakayama, and T. Matsunaga*
- 2015 Electrochemistry-Based and Signal-Amplified Sensing Strategies for DNA-Based Point-of-Care Biosensors  
*I. Hsing*
- 2016 Electrochemical and Physical Assessment on Electrode Coating Materials for Neuromodulation Application  
*A. Shi, B. Li, P. Cong, and D. Seeley*
- 2017 Mechanical Force-Based Probing of Cytoskeletal Proteins in Living Cells Using Antibody-Immobilized Nanoneedles  
*C. Nakamura, Y. R. Silberberg, R. Kawamura, S. Mieda, Y. Amemiya, T. Kihara, K. Fukazawa, K. Ishihara, N. Nakamura, and J. Miyake*
- 2018 A Spatio and Temporal Gaseous Ethanol Visualization System for Real-Time Analysis from Human Breath and Body  
*T. Arakawa, X. Wang, T. Kajiro, K. Miyajima, H. Kudo, K. Yano, and K. Mitsubayashi*

- 2019 Development of Human-Environment Interface by Sensing and Multivariate Analysis of Bio-Ecosystem  
*M. Koshiba, G. Karino, A. Seno, Y. Shirakawa, K. Mimura, T. Sagawa, W. Tsugawa, K. Sode, and S. Nakamura*
- 2020 Electrochemical Impedance Spectroscopy on Nanomaterial-Modified Surfaces  
*A. J. Veloso, X. Chen, V. Hung, N. Li, and K. Kerman*
- 2021 Second Generation Continuous Glucose Sensing System Employing Direct Electron Transfer Principle  
*W. Tsugawa, K. Kojima, and K. Sode*
- 2022 Engineering Fungi Derived FAD Glucose Dehydrogenase and Its Application for Glucose Sensor Strip Employing Screen Printed Carbon Electrode  
*Y. Onishi, M. Nakajima, W. Tsugawa, K. Mori, K. Kojima, and K. Sode*
- 2023 Profile of IgE and IgG4 Binding Epitopes in Cow's Milk Allergens Using Peptide Array  
*M. Okochi, Y. Yoshida, and H. Honda*
- 2024 Fiber-Optic Fluoroimmunoassay System for *On-Site* Determination of the Indoor Allergen  
*K. Miyajima, K. Tamari, E. Kiyomiya, M. Hayashi, T. Arakawa, H. Kudo, K. Shiba, and K. Mitsuabayashi*
- 2025 Self-Assembled Synthetic Protein Scaffolds: Biosynthesis and Applications  
*W. W. Su and Z. Han*
- 2026 Use of High Surface Area Electrodes for Safe Delivery of Direct Current for Nerve Conduction Block  
*T. Vrabec, J. Wainright, N. Bhadra, N. Bhadra, and K. Kilgore*
- 2027 Electrochemical Approach to Fabricate Stacked Thick Cell Sheets  
*N. Mochizuki, H. Suzuki, and J. Fukuda*
- 2028 Electrical Bioassay System Using a Hydrogel-Supported Skeletal Muscle Cells  
*K. Nagamine, H. Kaji, M. Kanzaki, and M. Nishizawa*
- 2029 Fabrication of Semi-Invasive Micro-Needle Array Using Gradation Exposure  
*M. Yamaguchi, Y. Sasaki, Y. Kimura, and M. Sasaki*
- 2030 Higher Catalytic Activity by Fluctuation effect of Captured Enzyme Molecules in Designed Self-Organized Membrane on an Electrode Surface  
*Y. Takatsuji, R. Yamasaki, A. Iwanaga, M. Lienemann, M. Linder, and T. Haruyama*
- 2031 Nano-Structured Protein Layer on an Electrode Surface Taking Advantage of Self-Organized HFBI and Its Electrochemical Property  
*R. Yamasaki, Y. Takatsuji, A. Iwanaga, M. Lienemann, M. Linder, and T. Haruyama*

- 2032 Analysis of Cell Exfoliation Specifically Observed during the Formation of Spermine-Induced Multilayer Muscle Fiber Sheet  
*A. Ishida, N. Abe, H. Matsuoka, and M. Saito*
- 2033 Quantitative Analysis of Cell Death Observed during the Formation of Spermine-Induced Multilayer Muscle Fiber Sheet  
*N. Abe, A. Ishida, H. Matsuoka, and M. Saito*
- 2034 In Vivo Delivery of RNAi Reagents into a Mouse  
*M. Kaburagi, Y. Kakutani, H. Matsuoka, and M. Saito*
- 2035 Surface Modification of Titanium Dioxide Nanoparticles with Gold Nanoparticles for Bio Fuel Cell Application  
*H. Park, S. Pyo, D. Lee, S. Kim, and H. Park*
- 2036 Optimizing Functionalized Carbon Nanotube Matrix for Enhancing Direct Ethanol Fuel Cell Performance  
*L. Q. Hoa, H. Yoshikawa, M. Saito, and E. Tamiya*
- 2037 Evaluation of Activity of RNAi Against Diabetes Related Genes in MIN6 Cells  
*Y. Kakutani, M. Kaburagi, H. Matsuoka, and M. Saito*
- 2038 Electrochemical Detection of Cell Membrane Proteins using Scanning Electrochemical Microscopy  
*Y. Matsumae, Y. Takahashi, K. Ino, H. Shiku, and T. Matsue*
- 2039 Electrochemical Monitoring of Loop-Mediated Isothermal Amplification for Influenza Virus Detection  
*K. Yamanaka, M. Saito, N. Nagatani, K. Ikuta, and E. Tamiya*
- 2040 Cell-Based Assay Using Cells Adjusted at a Specific Stage during Differentiation to  $\beta$ -Cells  
*N. Hanata, H. Matsuoka, and M. Saito*
- 2041 Development of High-Throughput Toxicity Assay System Integrated with a Chemical Gradient Generator  
*Y. Sugamura, M. Hosokawa, A. Arakaki, T. Tanaka, and T. Matsunaga*
- 2042 Detection of *E. coli* Using Electrochemical and Immunochromatographic Assay for Amplified Gene by PCR  
*Y. Ogido, H. Ushijima, K. Yamanaka, M. Saito, E. Tamiya, S. Katayama, T. Miyahara, and N. Nagatani*
- 2043 Suppression of an Oct3/4 Transcription Activity in ES Cells by Decoy DNA Femtoinjection  
*S. Oura, H. Funabashi, M. Saito, and H. Matsuoka*
- 2044 Production of a Differentiation Regulating Protein to Be Femtoinjected into ES Single-Cells  
*T. Tanaka, H. Funabashi, M. Saito, and H. Matsuoka*

- 2045 PEDOT Microelectrodes Anchored to Hydrogel for Efficient Cellular Electrical Stimulation  
*D. Takahashi, M. Sasaki, R. Suzuki, K. Nagamine, T. Miyake, H. Kaji, and M. Nishizawa*
- 2046 Development of a Patch-Type Gel Sheet Sensor for Detection of Extracellular Metabolites  
*S. Otani, S. Ito, K. Nagamine, H. Kaji, and M. Nishizawa*
- 2047 Dynamic Properties of Fluorescent Reporter Proteins Femtoinjected into ES Single-Cells  
*S. Hisatomi, H. Funabashi, M. Saito, and H. Matsuoka*
- 2048 Development of Cell Analysis Method by Using CMOS Sensor for High-Throughput Blood Cell Profiling  
*T. Saeki, M. Hosokawa, T. Lim, K. Tomita, M. Harada, T. Yoshino, T. Tanaka, and T. Matsunaga*
- 2049 Flexible Biofuel Cell Using Enzyme-Modified Nanoengineered Carbon Fabric  
*T. Yamada, S. Yoshino, T. Ofuji, T. Miyake, H. Kaji, and M. Nishizawa*
- 2050 Evaluating the Insertion Efficiencies of Silicon Nanoneedles into Living Single Cells  
*S. Ryu, R. Kawamura, T. Kitagawa, N. Nakamura, and C. Nakamura*
- 2051 Development of a Method to Modify Nanoneedle Arrays with Molecular Probes for the Analysis of Living Cells  
*M. Shimooku, S. Ramachandra Rao, R. Kawamura, K. Ishihara, K. Fukazawa, and C. Nakamura*
- 2052 Feasibility Study of Dual-FRET Molecular Beacon for the Dynamic Analysis of Oct3/4 mRNA in ES Cells  
*H. Koike, H. Funabashi, M. Saito, and H. Matsuoka*
- 2053 Effect of Particle Size on the Electrochemical Responses of Cytocochrome *c* and Pyrroloquinoline Quinone Immobilised on Gold Nanoparticle-Modified Electrodes  
*M. Suzuki, K. Murata, N. Nakamura, and H. Ohno*
- 2054 Hydrophilicity and Osteoconductivity of Ti Anodized in Various Aqueous Solutions  
*D. Yamamoto, K. Kuroda, R. Ichino, and M. Okido*
- 2055 Effect of a Carbohydrate-Binding Domain on Electron Transfer between Proteins and Carbon Electrodes  
*H. Shimofusa, M. Inukai, M. Yoshida, K. Igaraqshi, M. Samejima, N. Nakamura, and H. Ohno*
- 2056 Comparison of Quantitative Imaging Analysis and Electrochemical Sensing for the Beatings of Cardiomyocyte Derived from Mouse Embryonic Stem Cells  
*Y. Yamaguchi, E. Shimizu, T. Ikeuchi, A. Hashimoto, M. Saito, and E. Tamiya*
- 2057 Turning Glucose Oxidase into Essentially Dehydrogenase  
*Y. Horaguchi, S. Saito, S. Ferri, K. Mori, K. Kojima, W. Tsugawa, and K. Sode*

- 2058 Enhancement of Wettability on Titanium Substrates by Femtosecond Laser Micron/Nano Machining  
*K. Fung, Y. Su, C. Liu, C. Ni, C. Lin, P. Wu, and C. Cheng*
- 2059 Correlation between Spectroscopic Absorbance and Biofilm to Anode Microbial Fuel Cell  
*R. J. Marassi, J. M. Santos, C. E. Teodoro, F. S. Santos, and G. C. Silva*
- 2060 Assessment of Cell Behaviors on TiO<sub>2</sub> Nanotube Arrays by Using Atomic Force Microscopy, Raman Spectroscopy, Fluorescence Microscopy  
*R. Li, Q. Li, L. Xiao, S. Williams, E. Suasnavas, C. Isom, D. Larson, L. Rickards, and A. Zhou*
- 2061 Sucarcane Waste as Substrate for Microbial Fuel Cell  
*J. M. Santos, R. J. Marassi, C. E. Teodoro, F. S. Santos, and G. C. Silva*
- 2062 Development of a POCT Diagnostic System for Periodontal Disease Using a Printed Electrode  
*T. Uenoyama, K. Yamanaka, M. Saitou, Y. Yamaguchi, M. Wada, and E. Tamaiya*
- 2063 Implantable Nerve Cuff Electrode Deposited with Electrospun Nanofiber to Control Drug Release for Long-Term Implantation  
*S. Lee, S. Park, S. Lim, K. Hwang, and J. Kang*
- 2064 Amino Acid Sensing Based on 2D-SPR Imaging  
*Y. Hida and H. Shinohara*
- 2065 Non-FET Electrochemical DNA Detection Using Metal-Gap-Oxide-Silicon Structures  
*K. Kawai, Y. Doi, T. Furukawa, J. Uchikoshi, K. Arima, and M. Morita*

**C4 - New Synthetic and Mechanistic Approaches to Molecular Electroorganic Chemistry**  
*ECS Organic and Biological Electrochemistry, ECSJ Electroorganic Chemistry*

- 2066 Anodic Oxidation of *gem*-Diaryl Ketones in the Presence of Alcohols  
*A. J. Fry and B. Sheludko*
- 2067 Oxidative Dechlorination of Chlorinated Organic Compound Catalyzed by Vitamin B<sub>12</sub>-TiO<sub>2</sub>  
*H. Shimakoshi and Y. Hisaeda*
- 2068 Controlling and Improvement of Electrosynthetic Reaction by Using Microreactor: Application to Intermolecular Coupling Reaction of Phenol Derivatives  
*T. Kashiwagi, S. R. Waldvogel, and M. Atobe*
- 2069 Site-Controlled Modification of Conducting Polymer Films Based on Bipolar Electrochemistry  
*S. Inagi, Y. Ishiguro, and T. Fuchigami*

- 2070 Electrochemical Dehalogenation of Persistent Organic Pollutants with a Silver Cathode in Aqueous Media  
*A. A. Peverly and D. G. Peters*
- 2071 Electrochemical Fluorination Using Alkali-Metal Fluorides  
*T. Fuchigami, T. Sawamura, and S. Inagi*
- 2072 Development of Regioselective Electrochemical Glycosylation Oriented Natural Products Synthesis  
*K. Kawa, T. Saitoh, E. Kaji, and S. Nishiyama*
- 2073 Direct Reduction of 6-Halo-1-Phenyl-1-Hexynes at Silver Cathodes  
*L. M. Strawsine and D. G. Peters*
- 2074 Application of Methoxy Radical Generation on a Boron-Doped Diamond Electrode  
*T. Sumi, T. Saitoh, K. Natsui, T. Yamamoto, M. Atobe, Y. Einaga, and S. Nishiyama*
- 2075 Electrocatalytic Reduction of 1,1,2-Trichloro-1,2,2-Trifluoroethane (CFC-113) at a Silver Cathode  
*E. R. Wagoner and D. G. Peters*
- 2076 Coordination Programming of Photo- and Electro-Functional Molecular Materials  
*R. Sakamoto, M. Hayashi, S. Kusaka, M. Tsuchiya, J. Kakinuma, and H. Nishihara*
- 2077 Evaluation of Bioluminescence Activity of Firefly Luciferin Nucleotide Derivatives  
*S. Iwano, S. Kojima, T. Hirano, S. Maki, and H. Niwa*
- 2078 Synthesis of Multinuclear Metalladithiolenes and Control of Their Internuclear Electronic Communication  
*S. Tsukada, Y. Shibata, T. Kambe, R. Sakamoto, and H. Nishihara*
- 2079 Redox Active Dendronized Polymers Equipped with Peripheral Triarylaminies  
*T. Nokami, N. Musya, T. Morofuji, K. Takeda, and J. Yoshida*
- 2080 Synthesis of Alkaloids Skeletons Using the Hyper-Valent Iodobenzene Oxidant  
*D. Kajiyama, T. Saitoh, S. Yamaguchi, and S. Nishiyama*
- 2081 Rapid Access to the Pyrene Cored Dendrimers Using Dendritic Diarylcarbenium Ion Pools  
*K. Takeda, T. Nokami, and J. Yoshida*
- 2082 Preparation of Nanoemulsion Using Tandem Acoustic Emulsification and Its Application to Templated Electropolymerization  
*K. Nakabayashi, T. Fuchigami, and M. Atobe*
- 2083 Electrochemical Nickel-Induced Fluoroalkylation  
*D. Y. Mikhaylov, Y. H. Budnikova, Y. B. Dudkina, T. V. Gryaznova, and O. G. Sinyashin*

- 2084 Synthesis and Properties of Nitrogen-Bridged Terthiophenes  
*K. Mitsudo, S. Shimohara, and S. Suga*
- 2085 Regioselective Cross-Coupling Reaction of Azulene and  $\alpha$ ,  $\beta$ -Unsaturated Ketone by Electron Transfer from Magnesium  
*H. Maekawa, J. Honda, and R. Akaba*
- 2086 Prediction of Reduction Potentials from Calculated Electron Affinities for Metal-Salen Compounds  
*J. A. Miranda, J. M. Yates, and B. F. Gherman*
- 2087 Anodic Oxidation of Carbamates in the Presence of Solid-Supported Acids and Its Application to Carbon-Carbon Bond Forming Reactions  
*T. Tajima, A. Takabayashi, and K. Yamazaki*
- 2088 Paired Electrochemical Reaction of a Poly(Fluorenol) Derivative  
*H. Nagai, S. Inagi, and T. Fuchigami*
- 2089 Fabrication of Gradient Surface Using Bipolar Electrochemistry  
*N. Shida, Y. Ishiguro, S. Inagi, and T. Fuchigami*
- 2090 Synthetic Study of O-Methylthalbrane Using Anodic Oxidation  
*Y. Kawabata, Y. Naito, T. Saitoh, Y. Ishikawa, and S. Nishiyama*
- 2091 Preparation and Reaction of Titania Particles Encapsulated in Hollow Silica Shells as an Efficient Photocatalyst for Stereoselective Synthesis of Pipecolinic Acid  
*S. Chandren and B. Ohtani*
- 2092 Electrochemical Oxidation of Poly(*p*-phenylene-vinylene) Derivatives Containing Tetraphenylethylene Units  
*S. Wakana, S. Inagi, T. Fuchigami, and I. Tomita*
- 2093 Voltammetry of Nitrofluorenes: Simulation  
*I. U. Haque and A. Dar*
- 2094 The Electrochemical Oxidation of Pyrogallol: Formation of Long-Lived Oxygen Radicals and Application to Assess the Radical Scavenging Abilities of Antioxidants  
*S. Mu*

**D1 - Corrosion General Poster Session**

*All ECS Divisions, ECSJ Corrosion*

- 2095 Corrosion Protection of Steel by Conducting Polypyrrole Film Doped with Poly-acids of Mo and W  
*M. Sasaki, A. Hyono, M. Ueda, and T. Ohtsuka*
- 2096 Corrosion under Water-Repellent Coating  
*H. Saito*

- 2097 Monolayer and Bilayer Conducting Polymer Coatings for Corrosion Protection of Copper in Various Aggressive Media  
*F. Branzoi, V. Branzoi, and Z. Pahom*
- 2098 Local Bond Structure of BaZrO<sub>3</sub> Doped with Various Dopant Probed by Raman Spectroscopy  
*D. Kim, E. Patrik, S. Miyoshi, T. Tsuchiya, and S. Yamanguchi*
- 2099 Analysis of Nickel Electrodeposition Process by Using Quartz Crystal Microbalance  
*M. Shiina, T. Tanabe, and K. Noda*
- 2100 Analysis of Corrosion Behavior of Zn Thin Film by Using QCM  
*R. Inoue, T. Tanabe, and K. Noda*
- 2101 Passivation of AA5083 Aluminium Alloy by Anodic Pre-Treatments in Ionic Liquids  
*P. Huang, P. Howlett, D. MacFarlane, and M. Forsyth*
- 2102 Passivity and Local Activation of Aluminum in Borate Buffer Solution under Action of Bromide-Ions Additives  
*A. Chikova, T. A. Minakova, and S. A. Kaluzhina*
- 2103 Material Performance of Alloys in NaNO<sub>3</sub>/KNO<sub>3</sub> at 600°C  
*A. M. Kruizenga and D. Gill*
- 2104 Determination of Current Efficiency of Anodic Film Formation in the Molten Melt by ICP-AES  
*S. Han and H. Kim*
- 2105 Electron Beam Induced Texture Change of the Anodic Films Formed in the Molten Melt  
*S. Han and H. Kim*
- 2106 Evaluation of Zinc Rich Paint (ZRP) Efficiency on Mild Steel in Seashore Environment  
*A. H. Sofian and K. Noda*
- 2107 Evaluation of Degradation of High Performance Organic Coatings under Outdoor Salt Spray Test  
*D. Ito, Y. Akira, Y. Miyata, T. Yokoyama, and S. Okazaki*
- 2108 A Novel Nanomaterial Hybrid Corrosion Resistant Coating for Marine Applications  
*V. Kamavaram, G. Arumugam, V. Veedu, and K. Cheung*
- 2109 Electrochemical and Microstructural Characterization of Cr(VI) Free Passivation Layers Applied on Electrogalvanized Steel  
*V. E. Hernandez, M. P. Segundo, C. R. Tomachuk, and H. G. de Melo*
- 2110 Evaluation of Corrosion Protection of Zinc Rich Paint Coated Steel  
*A. Tanaka, A. H. Sofian, and K. Noda*

- 2111 Evaluation of Corrosion Protection Property on Galvanized Steels in Atmospheric Environment  
*K. Ito and K. Noda*
- 2112 Effect of Alloy Element in Low Alloy Steels on Corrosion Behavior  
*A. Sunahara, T. Ohmori, K. Noda, H. Katayama, and H. Masuda*
- 2113 Potential Measurement of High Corrosion Resistance Metals Surface in Atmospheric Environment  
*Y. Hirohata, K. Noda, H. Katayama, and H. Masuda*
- 2114 Corrosion Inhibition of Carbon Steel in Cooling Water Systems by New Organic Polymers as Green Inhibitors  
*F. Branzoi, V. Branzoi, M. Iordoc, and Z. Pahom*
- 2115 In Situ Electrochemical Detection of Molybdate in an Absorption Refrigerator  
*Y. Hitoshi, Y. Hatakeyama, H. Inabe, K. Sekiguchi, T. Hishinuma, M. Itoh, and N. Ohnaka*
- 2116 Sodium Nitrite-Based Corrosion Inhibitor for Reinforcing Steel in Simulated Concrete Pore Solutions  
*R. Du, Y. Guo, Y. Zhu, W. Chen, X. Wang, and C. Lin*
- 2117 Effect of Stress on Oxide Film Growth on SUS 316L Stainless Steel under High Pressure-High Temperature Water  
*Y. Hamaguchi and T. Ohtsuka*
- 2118 The effect on Impurities of the Properties of Passive Oxides on Stainless Steels  
*M. Abe, A. Hyono, M. Ueda, T. Ohtsuka, and T. Ishii*
- 2119 Synthesis and Characterization of Modified Nano-TiO<sub>2</sub> Films for Corrosion Protection of Stainless Steel  
*Y. Zhu, J. Zhang, R. Du, H. Qi, L. Xu, and C. Lin*
- 2120 Effects of Tritiated Water on Passivation Behavior of SUS304 Stainless Steel  
*M. Oyaizu, K. Isobe, and T. Yamanishi*
- 2121 Localized Corrosion Behavior of Austenitic Stainless Steel Containing Martensitic Phases in NaCl Solution  
*S. Abe, T. Saito, K. Noda, and Y. Watanabe*
- 2122 Analysis of Localized Corrosion Behavior of Stainless Steel in Atmospheric Environment  
*Y. Nakajima, T. Saito, and K. Noda*
- 2123 Analysis of Passivation Behavior of Stainless Steel in Na<sub>2</sub>SO<sub>4</sub> Solutions  
*A. Moriyasu, T. Saito, and K. Noda*
- 2124 Low Temperature Deposition of SiO<sub>2</sub> Matrix onto the Surface of Stainless Steel as Protective Coating  
*T. M. Abdel-Fattah and H. Elsayed-Ali*

- 2125 The Electrochemical Properties of the Main Constituent Phases in Magnesium Alloys  
*Y. Chou, H. Yang, S. Pan, S. Chung, and W. Tsai*
- 2126 Corrosion Resistance of Mg(OH<sub>2</sub>/Mg-Al LDH Film Formed on Magnesium alloy by Steam Coating Method  
*T. Ishziaki and K. Teshima*
- 2127 Characterization of a New Polypropylene+Graphite+Zinc Ternary Composite  
*J. Agrisuelas, J. García-Jareño, M. Llop, M. Piedras, and F. Vicente*
- 2128 Non-Destructive Evaluation for Corroded Metal Surface Using Terahertz Wave  
*H. Kariya, A. Sato, T. Tanabe, K. Saito, K. Nishihara, A. Taniyama, and Y. Oyama*
- 2129 The Influences of Roughness of Ti Substrate and Thickness of IrO<sub>2</sub> Intermediate Layer on Oxygen Evolution Anode Performance in Seawater Electrolysis  
*Z. Kato, K. Izumiya, N. Kumagai, and K. Hashimoto*
- 2130 Electrochemical Impedance Spectroscopy to Characterize Different Materials in Soybean Biodiesel Medium  
*A. H. Akita, C. Fugivara, I. Aoki, and A. Benedetti*
- 2131 Graphite Layer on Metal Plates for PEMFC Applications  
*W. Wang and C. Lan*
- 2132 Surface Morphology Changes during Dealloying  
*F. U. Renner, G. Ankah, and A. Pareek*
- 2133 Using LEIS to Evaluate Local Electrochemical Activity of Al 7475 T761/Cu Model Electrodes  
*J. Ferrari, H. G. de Melo, N. Pébère, B. Tribollet, and V. Vivier*
- 2134 Triboelectrochemical Characterization of Copper Surface  
*S. Joo and H. Liang*
- 2135 Application to Non-Destructive Inspection of Copper Corrosion via Coherent Terahertz Light Sources  
*K. Saito, T. Yamagata, H. Kariya, T. Tanabe, and Y. Oyama*
- 2136 Effect of Alloying Elements on Corrosion Behavior of Zr-Based Binary Alloys in Simulated Body Fluid  
*Y. Tsutsumi, S. Yalatu, S. Migita, H. Doi, N. Nomura, K. Noda, and T. Hanawa*
- 2137 Corrosion Behavior of Nanocrystalline Hydroxyapatite Coating on New Ti Alloy Surface in Ringer Solution  
*M. Popa, J. Calderon Moreno, C. Vasilescu, and S. Drob*
- 2138 Corrosion Study of Ni-Ti Orthodontic Archwires: An In Vitro Study  
*K. M. Britto, D. A. Macedo, R. M. Nascimento, A. E. Martinelli, and H. S. Júnior*

- 2139 A Three-Electrode Implantable Micro-Chip for Obtaining Real Time Corrosion Rates during Small Animal Testing  
*B. A. Shaw, E. Sikora, M. W. Horn, H. A. Basantani, A. Hartsock, D. R. Cook, B. J. Gluckman, and B. A. Bimber*
- 2140 In Vitro Galvanic Corrosion of Metallic Biomaterials  
*N. Shida, S. Miyabe, and S. Fujimoto*
- 2141 Analysis of Electrochemical Impedance Spectroscopy Results and Ion Release In Vitro of Si<sup>+</sup> Ion Implanted Medical 316 LVM Steel  
*J. C. Galván, M. Larrea, M. Multigner, I. Bráceras, L. Saldaña, N. Vilaboa, and J. González-Carrasco*
- 2142 Electrochemical Behavior of Ti-6Al-7Nb in Simulated Physiological Body Fluid Environment  
*N. A. Al-Mobarak, A. Al-Swayih, and F. Al-Rashoud*
- 2143 Evaluation of Corrosion Resistance of Co-Cr Alloy in NaCl Solution  
*R. Suzuki, K. Noda, Y. Tsutsumi, and T. Hanawa*

**D2 - Materials Degradation in Energy Systems: Corrosion and Hydrogen-Material Interactions**

*ECS Corrosion, ECS Battery, ECS Energy Technology, ECSJ Corrosion*

- 2144 First-Principles Molecular Dynamics Simulation of the Chemical Degradation of Polymer Electrolyte Membranes  
*A. Kobayashi, T. Ishikawa, Y. Higuchi, N. Ozawa, T. Shimazaki, and M. Kubo*
- 2145 Molecular Dynamics Study for Sintering Characteristics of Solid Oxide Fuel Cell Anode  
*K. Nakao, T. Ishimoto, and M. Koyama*
- 2146 Density Functional Theory Study and Model Development on Pt Nano-Particles  
*G. Brunello, J. Choi, S. Jang, and D. A. Harvey*
- 2147 Density Functional Theory Study of Pt Dissolution at Water-Pt Interface  
*J. Choi, G. Brunello, S. Jang, and D. A. Harvey*
- 2148 Degradation Mechanisms in PEM Fuel Cells  
*R. L. Borup, R. K. Ahluwalia, K. L. More, C. M. Johnston, and R. Mukundan*
- 2149 Regarding the Enhanced Durability of Platinum Monolayer Electrocatalysts for the Oxygen Reduction Reaction  
*K. Sasaki, H. Naohara, K. A. Kuttyiel, Y. Choi, D. Su, P. Liu, and R. R. Adzic*
- 2150 Dissolution Mechanism of Platinum in Simulated PEFC Conditions  
*Y. Sugawara, T. Okayasu, A. P. Yadav, A. Nishikata, and T. Tsuru*
- 2151 Selective Dissolution of Binary Pt Alloys in Sulfuric Acid Solution  
*Y. Hoshi, R. Ozawa, T. Yoshida, E. Tada, A. Nishikata, and T. Tsuru*

- 2152 Influence of Cathode Polarization on the Chromium Poisoning of SOFC Cathode Materials LSM, LSCF and LNF  
*E. Park, S. Taniguchi, Y. Tachikawa, Y. Shiratori, and K. Sasaki*
- 2153 Micro Modeling Study of Cathode/Electrolyte Interfacial Stresses for Solid Oxide Fuel Cells  
*X. Jin, J. Shi, and X. Xue*
- 2154 High Temperature Oxidation of Ferritic Steels for Solid Oxide Electrolysis Stacks  
*S. Molin, M. Chen, J. J. Bentzen, and P. Hendriksen*
- 2155 On the Shape of Stress Corrosion Cracks in Water-Cooled Nuclear Power Reactor Piping  
*D. Kramer, S. Lee, and D. D. Macdonald*
- 2156 Electrochemical Impedance Modeling of the Passivity of Iron in Simulated Concrete Pore Water  
*D. D. Macdonald, S. Sharifiasl, and G. R. Engelhardt*
- 2157 Comparative Study of Oxide Film Formation as a Function of Potential on High-Purity Co and Stellite-6  
*M. Behazin, X. Zhang, M. Biesinger, J. J. Noël, and J. Wren*
- 2158 Materials and Interfaces Degradation in High-Energy Cathodes for Li-ion Batteries  
*R. M. Kostecki, I. T. Lucas, N. S. Norberg, and J. S. Syzdek*
- 2159 Corrosion Behavior of Nitride Coatings for Anodic Protection in Liquid Metal Batteries  
*S. Phadke and D. R. Sadoway*
- 2160 Metal-Oxide-Semiconductor Nanocomposites for Photoelectrochemical Water Splitting  
*P. C. McIntyre*
- 2161 Materials Degradation in Solar Panels  
*H. G. Wheat*
- 2162 Degradation of Electrocatalysts Used in the Reduction of CO<sub>2</sub> - A Review  
*N. Sridhar, A. S. Agarwal, S. Guan, and E. Rode*
- 2163 Computational Study on Nickel Catalyst Degradation Mechanism by Carbon Deposit in Hydrogen Production  
*T. Ogura, H. Tsukikawa, and M. Tajima*
- 2164 Electrochemistry of Ferroelectric PbZr<sub>0.52</sub>Ti<sub>0.48</sub>O<sub>3</sub> Thin Films in Sulfuric Acid  
*L. J. Small, C. Apblett, J. Ihlefeld, G. Brennecka, and D. Duquette*
- 2165 Electrochemical Mechanism and Model of H<sub>2</sub>S Corrosion of Carbon Steel  
*Y. Zheng, B. Brown, and S. Nestic*
- 2166 Corrosivity Comparison between Petroleum and Blended Hydro-Refined Diesel and Jet Fuels  
*J. S. Lee, R. Ray, and B. Little*

- 2167 Electrochemical and Metal-Phase Processes Accompanying Hydrogen Absorption in Aluminum During Aqueous Corrosion  
*K. R. Hebert, O. O. Capraz, P. Shrotriya, and G. Zhang*
- 2168 Effect of Absorbed Hydrogen on Cavity Formation at High Temperature Water and Its Role on SCC Growth  
*K. Arioka*
- 2169 The Effects of Chromate, Molybdate, and other Selected Inhibitors on Surface and Crack Tip Corrosion Inhibition  
*S. B. Madden and J. R. Scully*
- 2170 Hydrogen Diffusion and Trapping in High Purity Al and Aluminum Alloy 5083-H131  
*J. Ai, M. Lim, and J. R. Scully*
- 2171 Lattice Defects Induced by Hydrogen Absorption in Metallic Materials  
*H. Suzuki, K. Takai, and M. Fujinami*
- 2172 The Hydriding of Uranium: Bulk Transport and Trapping of Hydrogen in Uranium  
*R. Lillard, C. D. Taylor, J. R. Wermer, N. A. Mara, and J. C. Cooley*
- 2173 The Influence of Hydrogen on Nuclear Fuel Corrosion Inside a Failed Waste Container  
*M. E. Broczkowski, L. Wu, Z. Qin, and D. W. Shoesmith*
- 2174 ZrO<sub>2</sub> Passive Layer Stability Loss in the Presence of Hydrogen Defects - Connections to Pit Initiation  
*M. Youssef and B. Yildiz*
- 2175 The effect of Thermal Hydrogenation Processing on the Oxide Layer Formation of Ti-6Al-4V Alloy  
*L. Wang, S. Yu, C. Shen, C. Chang, and C. Tsai*

**D3 - Corrosion, Passivity, and Energy: A Symposium in Honor of Digby Macdonald**  
*ECS Corrosion*

- 2176 The Semiconducting Properties and Impedance Analysis of Passive Films on Copper in Anaerobic Sulfide Solutions from the Viewpoint of the Point Defect Model  
*Y. Ling, M. L. Taylor, S. Sharifiasl, and D. D. Macdonald*
- 2177 Determining the Coupling Current as a Means of Detecting Crevice Activity and Inhibition  
*S. Lee, J. A. Mathews, and D. D. Macdonald*
- 2178 Influence of the Microstructure on the Passive Character of Titanium Oxide Films Characterized by EIS  
*N. Rodríguez de la Cruz, E. M. Arce, J. Torres, R. Luna Sánchez, J. G. Vazquez Arenas, J. Hallen, and R. Cabrera Sierra*
- 2179 Effects of Solution Temperature on the Kinetic Nature of Passive Film on Ni  
*K. Park, S. Ahn, and H. Kwon*

- 2180 Effect of Sour Environment pH on Crack Morphology in Ultra Strength Drilling Steel under Cyclic Stress  
*M. Ziomek-Moroz, J. Hawk, R. Thodla, and F. Gui*
- 2181 Electrochemical Reduction of Ethanol at Lead Electrodes  
*S. B. Hall, N. Wise, and M. Waterland*
- 2182 IGSCC Caused by Passive Film's Dielectrostrictive Stress  
*T. M. Devine*
- 2183 The Relationship between Nanostructure and Electronic Properties of Passive Films Studied by Scanning Tunneling Microscopy Combined with Scanning Tunneling Spectroscopy  
*P. Marcus, T. Massoud, and V. Maurice*
- 2184 Characterization of Repassivation Process on Fe-Cr Alloys Using Scratching Technique  
*M. Wada, A. Kawano, M. Saito, and S. Fujimoto*
- 2185 Coupling the Point Defect Model and the Density Functional Theory for Modeling Pit Nucleation  
*B. Malki, B. Baroux, O. Le Bacq, and A. Pasturel*
- 2186 Development of Base Electrocatalysts which are Passive towards Corrosion in Hot Acidic Electrolytes  
*G. T. Burstein, G. E. Haslam, and X. Y. Chin*
- 2187 Characterization of Bound Water in Passive Film of Titanium Formed in H<sub>2</sub>SO<sub>4</sub> Solution  
*T. Haruna, S. Ito, and K. Kimoto*
- 2188 Kinetic Stability of Aluminium and Its Alloys: The Role of "Structural" Features  
*X. Zhou, D. D. Macdonald, and N. Birbilis*
- 2189 Effect of Galvanostatic Condition on Growth Behavior and Repassivation Potential of Crevice Corrosion of Duplex Stainless Steels  
*S. Aoki, T. Ehashi, and J. Sakai*
- 2190 Metallographic Characterization of Transgranular Stress Corrosion Cracking on Type316L Stainless Steel in High Temperature and High Pressure Water Environment  
*S. Fujimoto, N. Okada, T. Saito, and H. Tsuchiya*
- 2191 Corrosion Inhibition of Localized Corrosion and Stress Corrosion Cracking of Steam/Gas Turbine Materials  
*B. Bavarian, J. Zhang, and L. Reiner*
- 2192 Comparison of Electrochemical Pitting Characteristics of Alloy 825, Alloy 690 and Titanium for a Concentrated Radioactive Waste Hold-Up Tank  
*H. Kim and K. Na*

- 2193 Studies of Pitting Initiation on High-Strength Pipeline Steel by Metallurgical Micro-Electrochemistry  
*Y. Cheng*
- 2194 Hydrogen Induced Passivity Degradation and Stress Corrosion Cracking  
*J. Luo, B. Lu, and S. Shi*
- 2195 Birth and Death Stochastic Process in Pitting Corrosion and Stress Corrosion Cracking  
*T. Shibata*
- 2196 Implications for the Initiation of Pitting Corrosion of Composition Changes around Sulphide Inclusions in Stainless Steels  
*D. E. Williams*
- 2197 Effect of Sulfate Ion on Pitting Corrosion Behavior of Type 420 Martensitic Stainless Steel in Chloride Solution  
*W. Ji, S. Pan, and W. Tsai*
- 2198 Intrinsic Vacancies and Their effect on Corrosion Reactivity at the FeS<sub>2</sub> (100) Surface  
*A. Krishnamoorthy, F. W. Herbert, and B. Yildiz*
- 2199 Predicting the Steady State Thickness of Passive Films with the Point Defect Model in Fretting Corrosion Experiments  
*J. Geringer, M. L. Taylor, and D. D. Macdonald*
- 2200 Optimization of Impedance Models with Differential Evolution  
*M. L. Taylor, S. Sharifi, and D. D. Macdonald*
- 2201 Neural Network as a Data Mining Tool for Prediction of Corrosion Behavior  
*M. ( Kamrunnahar and M. Urquidi-Macdonald*
- 2202 Vacancy Formation and Electronic Structure on FeS<sub>2</sub> Surfaces - Model System for Iron Sulfide Corrosion Films  
*F. W. Herbert, A. Krishnamoorthy, K. J. Van Vliet, and B. Yildiz*
- 2203 Deterministic Prediction of Localized Corrosion Damage in Oil and Gas Pipelines  
*G. R. Engelhardt, R. Wollam, and D. D. Macdonald*
- 2204 Application of the Kramers-Kronig Relations to Impedance Spectroscopy  
*M. E. Orazem*
- 2205 Microstructure-Influenced Numerical Modeling of Pitting Corrosion in 316 Stainless Steel  
*N. Kota, S. Qidwai, and V. DeGiorgi*
- 2206 The Role of MnS Inclusions and Passive Films in the Initiation of Pitting Corrosion of Stainless Steels  
*N. Hara, Y. Sugawara, and I. Muto*
- 2207 CPE Behavior of Oxide Layer Impedance  
*B. Tribollet, I. Frateur, M. Musiani, M. E. Orazem, and V. Vivier*

- 2208 A Spectroscopic and Electrochemical Investigation of the Structure of Ni(OH)<sub>2</sub> Materials  
*D. S. Hall, C. Bock, B. MacDougall, D. J. Lockwood, and S. Poirier*
- 2209 Electrochemical and Surface Study of the Oxide Growth and Conversion on 316L Stainless Steel  
*Q. W. Knapp, J. J. Noël, and J. Wren*
- 2210 Constant Phase Elements and Impedance of Rough Surfaces : A Numerical Study  
*M. Venkatraman, I. S. Cole, D. Sherwood, I. G. Bosco, and B. Emmanuel*
- 2211 Mathematical Models for Under-Deposit Corrosion  
*Y. Chang and M. E. Orazem*
- 2212 Weight Loss Model for Atmospheric Corrosion of Steel in Mexico Using Artificial Neural Networks  
*E. BOLAÑOS RODRIGUEZ and J. González Islas*
- 2213 Electrochemical Correlation Study of On-Line Corrosion Monitoring Probes  
*D. Bai, J. Wu, and F. Chen*
- 2214 (Corrosion Division H. H. Uhlig Award Presentation) Understanding of Passivity Due to the Application of Surface Methods, a Review  
*H. Strehblow*
- 2215 (Corrosion Division Morris Cohen Award Presentation) Evaluation of Thiosulfate as a Substitute of Hydrogen Sulfide in Sour Corrosion Fatigue Studies  
*M. Kappes, G. Frankel, R. Thodla, N. Sridhar, and R. Carranza*
- 2216 Marine Biofilms Mimic Metal/Air Battery Current Enhancement Strategies: A Study of Peroxide Degradation via Manganese Dioxide Catalysis in Seawater  
*M. J. Strom, G. W. Luther, and S. C. Dexter*
- 2217 Dissolution Behavior of Novel Lead Anodes for Copper Electrowinning  
*M. Clancy, C. Bettles, N. Birbilis, and A. Stuart*
- 2218 Corrosion Behavior of High Level Waste (HLW) Storage Tank Materials  
*J. Grant and D. Chidambaram*
- 2219 Nuclear Corrosion and Electrochemistry: Achievements and Challenges  
*D. Feron*
- 2220 Probabilistic Model for SCC: Integration of the Several Environment and Fracture Processes  
*S. Jain, F. Ayello, J. A. Beavers, and N. Sridhar*
- 2221 Chloride-Induced Stress Corrosion Cracking of Austenitic Stainless Steel for Dry Storage of Spent Nuclear Fuel  
*T. M. Ahn, G. Oberson, and S. DePaula*

- 2222 Dynamic Polarization Behaviors of Stainless Steels in Water Film Simulating the Water Treatment Plants  
*Y. Kim and Y. Park*
- 2223 Electrochemical Characterization of UNS S32760 and UNS S31603 Alloys in Presence of Fluoride and Bromide Solutions  
*E. Maya Visuet, A. Karayan, and H. Castaneda-Lopez*
- 2224 Determination of Kinetic Parameters for Water Reduction and Oxygen Reduction on Copper  
*S. Sharifiasl and D. D. Macdonald*
- 2225 In-Situ Spectroscopic Ellipsometry and Electrochemical Studies of the Barrier Layer on Iron in Borate Buffer Solutions  
*Z. Lu, S. Sharifiasl, and D. D. Macdonald*
- 2226 Copper Alloys Corrosion and Passivation Monitoring by Electrochemical Integrated Probes in Chlorinated Condenser Cooling Circuits  
*P. Cristiani, M. Carvalho, and G. Perboni*
- 2227 State of Health Estimation of LiFePO<sub>4</sub>/Graphite Cells  
*Y. Zhang and C. Wang*
- 2228 On the Stability of the Passive Film on Iron as Indicated by Electrochemical Impedance Spectroscopy  
*M. Urquidi-McDonald and D. D. Macdonald*
- 2229 Density Functional Theory Calculations of Defects Formation Energies in Cr<sub>2</sub>O<sub>3</sub>  
*B. Malki, B. Baroux, O. Le Bacq, and A. Pasturel*
- 2230 Electrical Microdischarge Characterization during Spark Anodization of Zirconium  
*J. S. Santos, S. G. Lemos, W. N. Gonçalves, O. M. Bruno, and E. C. Pereira*
- 2231 Preparation of Pt-Ru/CNT/Carbon Cloth Catalysts by Electrodeposition Method for Use in Fuel Cell  
*Y. Lin, T. Yeh, and M. Tsai*
- 2232 Effect of Passivation Potential on Amount of Bound Water in Passive Film on Titanium  
*T. Haruna and S. Ito*
- 2233 Prediction of Stress Corrosion Cracking of Type304 Stainless Steel Weld Components Exposed to Chloride Environments  
*G. Nakayama and Y. Sakakibara*
- 2234 Electrochemical Studies of the Alloy Ti6Al4V after Being Subjected to UV-C Irradiation Treatment  
*M. Pacha-Olivenza, A. Gallardo-Moreno, V. Vadillo-Rodríguez, M. González-Martín, C. Pérez Giraldo, and J. C. Galván*

- 2235 Effects of Cu on the Localized Corrosion and Repassivation kinetics of Ferritic Stainless Steels  
*S. Ahn, K. Oh, and H. Kwon*
- 2236 Electrochemical Corrosion Measurements in Supercritical CO<sub>2</sub> - Water Systems with and without Membrane Coating  
*J. Beck, M. Fedkin, and S. N. Lvov*
- 2237 Enhanced Corrosion Resistance of Interstitially Hardened 316L Stainless Steel: Gas Phase Nitridation under Paraequilibrium Conditions  
*N. R. Tailleart, F. Martin, R. Rayne, P. M. Natishan, H. Kahn, and A. Heuer*
- 2238 Corrosion Maps for Aluminium Alloys: Defining the Property Space and the Role of Microstructure and Chemistry in Corrosion  
*N. L. Sukiman, R. K. Gupta, R. G. Buchheit, and N. Birbilis*
- 2239 Corrosion Protection by Trivalent Chromium Process (TCP) Coatings on Aluminum Alloys  
*L. Li and G. Swain*
- 2240 Corrosion Resistance of Nanoporous Superhydrophobic Surfaces of Anodic Aluminum Oxide  
*C. Jeong, W. Xu, K. Du, and C. Choi*
- 2241 Enhanced Corrosion Resistance of Stainless Steels Interstitially Hardened with Carbon or Nitrogen under Paraequilibrium Conditions  
*P. M. Natishan, N. R. Tailleart, F. Martin, R. Bayles, R. Rayne, H. Kahn, and A. Heuer*
- 2242 Effect of Acetic Acid on the Cathodic Reaction of Carbon Steel Corrosion  
*T. Tran, B. Brown, and S. Nesić*
- 2243 Corrosion of Nickel and Iron Based Superalloys in High Temperature Gas Environments  
*H. Chang and T. Yeh*
- 2244 Investigation of the Corrosion Behavior of Zinc Magnesium Aluminium Alloys with a Novel Quaternary Addition Using SVET and Time-Lapse Microscopy  
*J. H. Malone, S. Mehraban, J. H. Sullivan, J. Elvins, and D. Penney*
- 2245 Redox Transformations in the Oxide Films on Ni-Cr-Mo Alloys and Their Influence on Corrosion Susceptibility  
*X. Zhang, A. Mishra, D. Zagidulin, J. J. Noël, and D. W. Shoesmith*
- 2246 Transition Metal Inhibition of Titanium Corrosion: Electrochemical Behavior of Titanium in Alkaline Electrolyte  
*W. B. Utomo and S. W. Donne*
- 2247 Overview of the Mg Corrosion Mechanism  
*A. Atrens*

- 2248 Investigation of Zinc Dimercaptothiadiazole as a Corrosion Inhibitor for Steel  
*R. L. Mercado, J. Fury, M. B. Kiely, D. Buhrmaster, C. E. Miller, and P. Zarras*
- 2249 In-Situ Electrochemical Measurement of Acid Dew Point Corrosion of Carbon Steel  
*T. Zhang*
- 2250 Incorporation of Modifiers to Improve the Anticorrosion Behavior of Organic-Inorganic Hybrid Coatings Applied to High Strength Al Alloys  
*R. P. Hernandez, B. M. Vasconcelos, V. R. Capelossi, M. Olivier, and H. G. de Melo*
- 2251 Effect of Halogen Ions and Inhibitors on Corrosion Behavior of 13 Cr Stainless Steel in Packer Fluid  
*M. Sakairi, R. Fujita, A. Kageyama, M. Kimura, and Y. Miyata*
- 2252 Hydration and Structural Transformations during Titanium Anodization under Alkaline Conditions  
*P. Acevedo Peña, J. G. Vazquez Arenas, R. Cabrera Sierra, and I. Gonzalez Martinez*
- 2253 The Palladium Hydrogen System; Corrosion Monitoring and Energy Production  
*M. C. McKubre, J. Bao, S. Crouch-Baker, P. Jayaweera, A. Sanjurjo, and F. Tanzella*
- 2254 A 12 V / Kilo-Farad Range Lead-Carbon Hybrid Ultracapacitor and Their Envisaged Applications  
*A. K. Shukla, A. Banerjee, A. Jalajakshi, and M. K. Ravikumar*
- 2255 In Situ Monitoring of Phosphate Inhibitor Surface Deposition in the Cathodic Region during Corrosion of a Zinc Magnesium Aluminium Alloy Using Time-Lapse Microscopy and Energy Dispersive X-ray Spectroscopy  
*S. Mehraban, J. H. Sullivan, and J. Elvins*
- 2256 An Investigation into the Individual and Synergistic effects of Organically Coated Steel Systems Using the Scanning Vibrating Electrode Technique (SVET)  
*A. W. Littlehales, J. H. Sullivan, D. A. Worsley, and J. Elvins*
- 2257 Inhibition of Corrosion-Driven Organic Coating Delamination on Hot Dip Galvanized Steel by Phenyl Phosphonic Acid  
*C. F. Glover and G. Williams*
- 2258 Self-organized Anodic Structures  
*P. Schmuki*
- 2259 Development of Zn-Mn Alloy Based Sacrificial Coatings  
*S. Ganesan, P. Ganesan, and B. N. Popov*
- 2260 Study of the Inhibition of Mild Steel Corrosion by Molybdate and Nitrite Anions  
*A. Al-Refaei*

- 2261 Oxygen Sensors for Accelerator Driven System (ADS) Reactors  
*A. Verdaguer, S. Colominas, and J. Abellà*
- 2262 Prussian Blue Films in Ammonium Aqueous Solution  
*J. Agrisuelas, C. Delgado, J. García-Jareño, and F. Vicente*
- 2263 Towards Tritium Electrochemical Sensors: Synthesis and Characterization of Proton Conducting Ceramic Elements  
*L. Llivina, S. Colominas, and J. Abellà*
- 2264 In Situ Coupling Current Studies in AA5083 and AA2024  
*K. Williams, R. Bayles, and D. D. Macdonald*
- 2265 On the Corrosion of Iron in Physically-Constrained Locations  
*D. D. Macdonald and G. R. Engelhardt*
- 2266 Mechanisms of Depassivation  
*D. D. Macdonald*
- 2267 Two Manifestations of the Passivity of the Metal in Aqueous Solution  
*H. Hua and H. Hua*
- 2268 Could this Fuel Replace Gasoline  
*J. O. Bockris*

**D4 - High Resolution Characterization of Corrosion Processes 3**  
*ECS Corrosion, ECSJ Corrosion*

- 2269 Kelvin Probe Force Microscopic Study on Galvanic Action between MnS Inclusions and Stainless Steel Matrix  
*Y. Sugawara, I. Muto, and N. Hara*
- 2270 Analysis of Pit Corrosion Using Temporal Series of Micrographs Coupled with Electrochemical Methods to Estimate the Three-Dimensional Evolution of Pits  
*A. M. Zimer, E. Rios, M. A. de Carra, L. H. Mascaro, and E. C. Pereira*
- 2271 Microscopic Polarization Behavior and Thermodynamic Stability of TiS and Ti<sub>4</sub>C<sub>2</sub>S<sub>2</sub> Inclusions in Stainless Steels  
*N. Shimahashi, I. Muto, Y. Sugawara, and N. Hara*
- 2272 Microelectrochemical Investigation of Pit Initiation and Selective Dissolution between MnS and Stainless Steel  
*A. Chiba, I. Muto, Y. Sugawara, and N. Hara*
- 2273 In Situ Ex-Polarized TEM Observation on Dissolution of MnS Inclusions and Metastable Pitting of Authentic Stainless Steel  
*B. Zhang, Y. Zhou, and X. Ma*

- 2274 Corrosion and Dealloying of Crystallized Amorphous Steel  
*F. U. Renner, M. Duarte, J. Lengsfeld, K. J. Mayrhofer, and P. Choi*
- 2275 Combining Microelectrochemical Methods with Electron Microscopy to Explore Pit Initiation in Aluminum  
*K. R. Zavadil*
- 2276 Observation of Metal Dissolution under LaminarFlow in a Microfluidic Channel - Copper with Chloride Solution -  
*S. Sakugawa, N. Kotake, and M. Hayase*
- 2277 The effect of Sulfate and Chloride Ions on the Rust Composition of Weathering Steel  
*T. Ohtsuka, S. Tanaka, M. Koya, A. Hyono, and M. Ueda*
- 2278 Marine Aerosol Drop Size Effects on the Corrosion Behavior of Plain Carbon Steel  
*E. schindelholz, B. Risteen, R. Kelly, and I. S. Cole*
- 2279 Corrosion Inhibition by Zinc Corrosion Products on Zinc-Coated Steel  
*Y. Sato and K. Azumi*
- 2280 Improving the Corrosion Protection Properties of Al<sub>2</sub>O<sub>3</sub> ALD Nanocoatings on Steel  
*J. Swiatowska, B. Díaz, V. Maurice, A. Seyeux, E. Häkkinen, M. Ritala, S. Tervakangas, J. Kolehmainen, S. E. Potts, W. Kessels, and P. Marcus*
- 2281 Environmental and Temporal Characterization of a Self-Healing Coating with Galvanic Protection  
*A. J. Maisano, R. Srinivasan, M. W. Patchan, L. M. Baird, E. D. LaBarre, and J. J. Benkoski*
- 2282 Application of Mg-Ion Selective and Antimony Electrodes for the Characterization of Corrosion Reactions by Scanning Electrochemical Microscopy  
*J. Izquierdo, L. Nagy, J. Santana, I. Bitter, G. Nagy, and R. M. Souto*
- 2283 High Resolution Characterization of Pitting Corrosion Using a Novel Environmental SVET and White Light Interferometry  
*S. Geary, H. N. McMurray, and A. de Vooy*
- 2284 Studies with the Three-Dimensional Scanning Vibrating Technique: Investigation into the effect of Spot Weld Electrode Life and Quality on the Corrosion Behavior of Galvanized Automotive Steel  
*B. P. Wilson, J. R. Searle, K. Yliniemi, D. A. Worsley, and H. McMurray*
- 2285 The Influence of Rare-Earth Doping and Non-Stoichiometry on the Corrosion of Uranium Dioxide  
*H. He, K. O'Neil, O. Semenikhin, and D. W. Shoesmith*
- 2286 EDTA as a Tool to Probe Cathodic Corrosion (Trenching) on AA2024-T3  
*H. N. McMurray, G. Williams, and A. Coleman*

- 2287 Localised SKP Studies of Cathodic Disbondment on Chromium/Chromium Oxide Coated Steel  
*D. J. Warren and H. N. McMurray*
- 2288 Investigation of Copper Corrosion Inhibition by Ethyl Xanthate with Frequency-Dependent Alternating-Current Scanning Electrochemical Microscopy  
*J. J. Santana and R. M. Souto*
- 2289 Damage Evolution Quantification of Hybrid Coatings on Aluminum Alloy by Surface and Electrochemical Techniques  
*I. Barraza-Fierro, T. Gao, M. Soucek, and H. Castaneda*
- 2290 Study of Electrochemical Corrosion Behavior of Nanocrystalline Thin Film by Electrochemical Techniques and In Situ AFM  
*L. Liu, Y. Li, and F. Wang*

**D5 - High Temperature Corrosion Materials Chemistry 10**  
*ECS High Temperature Materials, ECS Corrosion*

- 2291 In Situ Optical Studies of Electrochemically Induced Anode Degradation in High Temperature Solid Oxide Fuel Cells  
*R. A. Walker, J. D. Kirtley, D. M. Halat, and M. McIntyre*
- 2292 Mechanical Properties of Ni-YSZ Cermets under Simulated Environment of Redox Cycling  
*T. Miyasaka, S. Sukino, S. Watanabe, T. Kawada, K. Sato, and T. Hashida*
- 2293 Improved Sintering Property of Y-Doped BaZrO<sub>3</sub> by Mn Addition  
*D. Kim, E. Patrik, S. Miyoshi, T. Tsuchiya, and S. Yamaguchi*
- 2294 Non-Linear Doping effect on the Electrochemical Properties of BaZr<sub>1-x</sub>Pr<sub>x</sub>O<sub>3</sub>  
*M. Tamaru, S. Miyoshi, D. Kim, T. Higuchi, Y. Oyama, and S. Yamaguchi*
- 2295 Study on Electrode Reaction of Perovskite Oxide Electrodes on a Proton Conducting Electrolyte  
*K. Suzuki, S. Hashimoto, K. Amezawa, and T. Kawada*
- 2296 Mechano-Electrochemical effect on Materials Property of Ion Conducting Oxides  
*K. Yashiro, Y. Kawamura, S. Nakakawaji, K. Sato, K. Amezawa, and J. Mizusaki*
- 2297 Chemical Stability of Ba<sub>0.5</sub>Sr<sub>0.5</sub>Co<sub>0.8</sub>Fe<sub>0.2</sub>O<sub>3-δ</sub> (BSCF)  
*F. Wang, K. Yashiro, K. Amezawa, and J. Mizusaki*
- 2298 A Study of Nickel-Substituted Lanthanum Cobaltite as Cathode Materials for SOFCs  
*Y. Uzumaki, S. Hashimoto, K. Amezawa, and T. Kawada*
- 2299 La/Sr-Co Perovskite-Based Multi-Layered Super Cathode Fabricated by Sputtering Method  
*A. Takeshita, S. Miyoshi, and S. Yamaguchi*

- 2300 Oxygen Transport in Perovskite Type Oxide  $\text{La}_{0.6}\text{Sr}_{0.4}\text{Co}_{0.2}\text{Fe}_{0.8}\text{O}_{3-\delta}$   
*H. Kudo, K. Yashiro, S. Hashimoto, K. Amezawa, T. Kawada, and J. Mizusaki*
- 2301 Influence of Phase Crystallography on Precipitation Microstructures and Deformation Mechanisms in Tantalum Carbides  
*G. B. Thompson, R. A. Morris, N. De Leon, B. Wang, and C. Weinberger*
- 2302 Preparation and Characterization of Materials in the Ta-Hf-C System  
*J. A. Zaykoski, M. M. Opeka, and I. Talmy*
- 2303 Variability in Oxidation Resistance of  $\text{ZrB}_2\text{-SiC}$   
*K. N. Shugart and E. J. Opila*
- 2304 Effect of Silicon Addition on the Oxidation Kinetic and on the Structure of the Oxide Layer Formed on Transition Metal Nitride Coatings  
*J. Pierson, P. Steyer, A. Mège-Revil, and D. Pilloud*
- 2305 Oxidation of  $\text{Cr}_2\text{AlC}$  between 700 and 1300°C in Air  
*S. Kim, S. Bong, and D. Lee*
- 2306 Fabrication of Vertically Aligned Nano-Oxide Arrays via Internal Oxidation of Dilute Alloys  
*M. Nanko and D. T. Do*
- 2307 High-Temperature Oxidation Kinetics for Recovery of Mechanical Strength on Nano-Ni Dispersed  $\text{Al}_2\text{O}_3$  Hybrid Materials  
*D. Maruoka and M. Nanko*
- 2308 Early Oxidation Stages of Alumina Formers and the effect of the Additions: A Brief Survey  
*J. Jedliński*
- 2309 The Influence of KCl(s) on the Oxidation of a FeCrAl Alloy at 600 °C in Dry and Wet Environment  
*N. Israelsson, L. Johansson, and J. Svensson*
- 2310 Deposit-Induced Corrosion of Nickel-Base Alloys at Low Temperatures (650-750°C)  
*B. S. Lutz, M. N. Task, N. M. Yanar, F. S. Pettit, G. R. Holcomb, and G. H. Meier*
- 2311 High-Temperature Corrosion Behavior of Sputtered Ni-Based Nanocrystalline Coating with Yttrium Addition in Chloride at 900°C  
*P. Yu, W. Wang, F. Wang, and S. Zhu*
- 2312 Accelerated Corrosion of Low Alloy and Stainless Steel by  $\text{PbCl}_2$ -Containing Salt Mixtures  
*D. P. Bankiewicz, P. Yrjas, and M. Hupa*
- 2313 An Electrochemical Impedance Spectroscopy Study on the effect of Condensate on Oxides Formed on a 25Cr/20Ni Cast Stainless Steel in Exhaust Environments  
*M. Ekström, B. Zhu, P. Szakalos, and S. Jonsson*

- 2314 The effect of Water Vapor on the Distribution of Oxide Precipitates during Internal Oxidation of Ni-5Cr Alloy at 1073 K  
*M. Ueda, Y. Kurata, K. Kawamura, and T. Maruyama*
- 2315 Oxidation Behaviour of Sanicro 25 in CO<sub>2</sub> and H<sub>2</sub>O-Rich Environments  
*L. Intiso, L. Johansson, and M. Halvarsson*
- 2316 Behaviors of SOFC Interconnect Steels and Coatings with Contacting Electrodes and Seals in Single and Dual Atmosphere Exposures  
*R. Amendola, A. Weinstein, S. Sofie, and P. Gannon*
- 2317 Oxygen Activity Distribution from Atmosphere to Scale Surface on High Temperature Oxidation of Iron  
*K. Kawamura, S. Sonota, M. Ueda, and T. Maruyama*
- 2318 Kinetics and Mechanisms of Copper Catastrophic Oxidation in the Presence of Low-Melting Oxides  
*V. V. Belousov*
- 2319 The Activity of Rh<sub>2</sub>O<sub>3</sub> in Boro-Silicate Glass at 1373 K  
*H. Kimura, S. Yamamoto, M. Ueda, K. Kawamura, T. Maruyama, K. Minami, and E. Ochi*
- 2320 High Temperature Electrolysis for Liquid Iron Production  
*G. Haarberg, E. Kvalheim, A. Martinez, S. Rolseth, and H. Gudbrandsen*
- 2321 Corrosion Behavior of Construction Materials for Intermediate Temperature Steam Electrolysers  
*A. V. Nikiforov, I. M. Petrushina, J. Jensen, and N. Bjerrum*
- 2322 Evaluation of Electrode Materials for Electrolytic Reduction of Nuclear Fuels  
*A. Merwin and D. Chidambaram*
- 2323 Fabrication of Nano-Rod Array Structure Used Aluminizing and Internal Oxidation of Alloy for Micro-Channel  
*T. Ishizaki, D. T. Do, and M. Nanko*
- 2324 Measuring Cr Volatility from Ferritic Stainless Steels: Novel and Conventional Methods Compared  
*J. J. Eziashi, C. Key, R. Smith, and P. Gannon*
- 2325 Thermodynamic Modeling of Chromate Salt Mixtures in High-Temperature Corrosion of Superheater Materials  
*D. K. Lindberg, J. Lehmusto, and M. Hupa*
- 2326 Investigation of the effect the Polarisability of Dipoles on the Local Microstructures of Molten Slags Using Density Functional Theory Molecular Dynamics  
*A. A. Gray-Weale, J. Krahl, A. Jacob, and P. J. Masset*

- 2327 Thermodynamic Modeling for Liquid Phase Sintering and Joining of Silicon Carbide  
*H. J. Seifert*
- 2328 Multiscale Analysis on Gas Phase and Surface Chemistry of SiC-CVD Process  
*Y. Fukushima, K. Hotozuka, Y. Funato, N. Sato, T. Momose, and Y. Shimogaki*
- 2329 Study of  $\text{La}_2\text{Zr}_2\text{O}_7$  and  $\text{La}_2\text{Hf}_2\text{O}_7$  Melting by Thermal Analysis and X-ray Diffraction  
*S. V. Ushakov, P. Saradhi, A. Navrotsky, R. J. Weber, and C. J. Benmore*
- 2330 In Situ Investigation of a High Temperature Phase Transformation Using Laser Heating and Synchrotron Diffraction  
*P. Saradhi, S. V. Ushakov, A. Navrotsky, R. J. Weber, and C. J. Benmore*
- 2331 Hydration and Dehydration Behavior of Amorphous Tantalum Oxide with Various Oxygen Contents  
*T. Ozato, T. Tsuchiya, S. Miyoshi, and S. Yamaguchi*
- 2332 Determination of Vapor Pressures of Fe-Oxides in Humid Atmospheres  
*T. Markus, W. Quadakkers, and L. Singheiser*
- 2333 Reaction Syntheses with Carbon Materials Chemistry: Intragranular Nanocomposites and 'Carbon Copies'  
*D. W. Lipke and K. H. Sandhage*
- 2334 Thermochemical Interactions of Rare Earth Based TBCs with Molten CMAS Deposits  
*E. M. Zaleski, C. Ensslen, and C. G. Levi*
- 2335 Ceramic Dusting Corrosion of Yttria Stabilized Zirconia in Ultra-High Temperature Reverse-Flow Pyrolysis Reactors  
*C. Chun, S. Desai, and T. A. Ramanarayanan*
- 2336 Chemical Densification of Oxide Based Coatings for High Temperature Wear and Corrosion Resistance  
*P. J. Masset, M. Faulstich, K. Fehr, C. Weih, G. Wolf, and Y. Ye*
- 2337 Relationship between Electrical Properties and Stress Field in Solid Electrolyte Thin Films  
*F. Iguchi, Y. Osawa, and H. Yugami*
- 2338 Oxygen Gas Sealing between YSZ and Fe-Cr Alloy by Liquid-Phase-Oxidation Joining via  $\text{ZrO}_2$ -Dispersed Al Interlayer  
*Y. Hashimoto and T. Akashi*
- 2339 Microstructures and Phase Evolution in NiAl-Based Overlay Coatings  
*M. L. Weaver and J. P. Alfano*
- 2340 Transition Metal Spinel Oxide Coatings for Solid Oxide Fuel Cell Interconnects  
*J. W. Fergus, C. Dileep Kumar, Y. Liu, W. Tilson, A. Dekich, and H. Wang*

- 2341 Microstructural Investigation of Co- and RE-Nanocoatings on FeCr Steels  
*S. Canovic, J. Froitzheim, R. Sachitanand, M. Nikumaa, L. Johansson, and J. Svensson*
- 2342 Protection of Ferritic Steels by Nano-Structured Coatings: Supercritical Steam Turbines Applications  
*M. Mato, M. Hierro, S. Castañeda, G. Alcalá, I. Lasanta, M. Tejero, J. Sánchez, M. Brizuela, and F. J. Pérez*
- 2343 Improvement of the Resistance of Titanium Aluminides to Environmental Embrittlement  
*P. J. Masset, F. Bleicher, L. Bortolotto, G. Geiger, A. Kolitsch, C. Langlade, J. Paul, B. Pelic, F. Pyczak, D. Rafaja, P. Schumacher, M. Schütze, G. Wolf, and R. Yankov*

**D6 - Light Alloys 4**  
*ECS Corrosion, ECSJ Corrosion*

- 2344 High Resolution SEM Investigation of Intercrystalline Corrosion on 6000-Series Aluminum Alloy with Low Copper Content  
*K. Shimizu and K. Nisancioglu*
- 2345 Effect of Additive Elements on Corrosion Behavior for Aluminum in Weak Alkaline Solution at High Temperature  
*Y. Honkawa, T. Yaegashi, and Y. Kojima*
- 2346 Combined Role of Trace Elements Pb and Sn in Low Temperature Activation of Aluminum  
*K. Kurt, J. C. Walmsley, S. Diplas, and K. Nisancioglu*
- 2347 Interactions of Sulfide with Aluminum Alloys  
*J. S. Lee, R. Ray, and B. Little*
- 2348 The Role of Environmental Aspects and Atmospheric Contaminants on the Corrosion of 2024, 6061 and 7075 Aluminum Alloys  
*Y. Yoon and D. C. Hansen*
- 2349 Pitting Corrosion of Aluminum Alloy in Chloride Environment  
*Y. Oya and Y. Kojima*
- 2350 Effect of Surface Topography, Cleaning, and Conversion Coatings in the Adhesion Strength of Organic Polymers to AA2024-T3 using the Blister Test  
*B. C. Rincon Troconis and G. Frankel*
- 2351 Self-Healing Nature of Molybdate Conversion Coatings for Aluminum Alloys  
*D. Rodriguez, R. Misra, and D. Chidambaram*

- 2352 Organic-Inorganic Sol-Gel Coatings Modified with TiO<sub>2</sub> Nanoparticles for Corrosion Protection of a Powder Metallurgical Aluminum Alloy  
*A. Jiménez-Morales, F. García-Galván, D. Carbonell, D. Montoya, and J. C. Galván*
- 2353 The Role of Environmental and Atmospheric Conditions on the Corrosion of AA 2024-T3 with Various Pre-Treatments and Coating Systems  
*L. Petry and D. C. Hansen*
- 2354 Corrosion Control Studies of Aluminum-Composite Interfaces in Diverse Micro-Climates  
*R. Srinivasan and L. H. Hihara*
- 2355 Metal Dissolution and Repassivation Behavior of Ti6Al4V Alloy during Rapid Straining in Simulated Body Fluid  
*K. Doi, S. Miyabe, and S. Fujimoto*
- 2356 Investigation of the Corrosion of Magnesium and Titanium in Simulated Body Fluids  
*R. Feser, M. Ceylan, and S. Virtanen*
- 2357 Magnesium and Mg Alloys "Biocorrosion" in Protein Containing Body Fluids  
*P. Schmutz, N. Ott, R. Grisch, and P. Uggowitzer*
- 2358 Influence of Chemistry, Microstructure and Texture on the Durability of Mg-Alloys: An overview  
*K. Gusieva, C. H. Davis, and N. Birbilis*
- 2359 A Cumulative Approach to Tracking the Corrosion of Mg Alloys on the Microscale  
*R. M. Asmussen, P. Jakupi, and D. W. Shoesmith*
- 2360 Local, Time-Resolved and Element-Specific Investigations of Corrosion Processes for the Development of Biodegradable Mg Alloys  
*N. Ott, P. Schmutz, C. Ludwig, and A. Ulrich*
- 2361 Improvement in Corrosion Characteristics of AZ31 Mg Alloy by Square Pulse Anodizing between Transpassive and Active Regions  
*Y. Choi, S. Salman, K. Kuroda, and M. Okido*
- 2362 The Development of Ionic Liquid Generated Conversion Coatings for Magnesium Alloys  
*P. Howlett, J. Latham, D. MacFarlane, and M. Forsyth*
- 2363 Corrosion Inhibition of Mg Alloys by Inorganic and Organic Inhibitors  
*J. Hu, D. Huang, G. Song, and X. Guo*
- 2364 Biocompatible Coatings for Mg Alloys for Tailored Degradation Behavior  
*S. Virtanen*

**D7 - Pits and Pores 5: A Symposium in Honor of David Lockwood**  
*ECS Corrosion, ECS Luminescence and Display Materials, ECSJ Corrosion*

- 2365 Thinking Again of Porous Si Formation  
*Y. H. Ogata*
- 2366 Investigation of Pore Diameter Modulation in Depth in p-type Silicon  
*E. Ossei-Wusu, J. Carstensen, E. Quiroga-González, M. Amirmaleki, and H. Föll*
- 2367 Differential Photoacoustic Electrochemical Cell to Study In Situ the Porous Silicon Formation  
*D. G. Espinosa-Arbelaez and M. E. Rodriguez-Garcia*
- 2368 Spontaneous Groove Formation on Silicon during Anodic Dissolution Induced by Turing Instability  
*K. Fukami, T. Urata, T. Sakka, K. Krischer, and Y. H. Ogata*
- 2369 Anodic Dissolution of Si: Electrochemical Oscillations and Porous Silica Formation  
*F. Ozanam and J. Chazalviel*
- 2370 Stain Etching of Silicon with and without the Aid of Metal Catalysts  
*K. W. Kolasinski, J. Gogola, W. B. Barclay, and C. Somerville*
- 2371 Metal-Assisted Chemical Etching of Silicon Using Oxygen as an Oxidizing Agent  
*S. Yae, Y. Morii, M. Enomoto, N. Fukumuro, and H. Matsuda*
- 2372 On the Metal-Assisted Chemical Etching of Nanoporous Silicon  
*D. Goryachev, L. Belyakov, O. Yeltsina, J. Vainshtein, and O. M. Sreseli*
- 2373 Formation of Group IV Porous Semiconducting Nanowires and Nanotubes: The Role of Etching  
*X. Huang, R. Gonzalez, and J. L. Coffer*
- 2374 A "Cook's Tour" of Two Decades of Research into the Optical Properties of Nanostructured Materials  
*D. J. Lockwood*
- 2375 Magnetic Field Assisted Etching of Porous Silicon as a Tool to Enhance Magnetic Characteristics  
*P. Granitzer, K. Rumpf, T. Ohta, N. Koshida, P. Poelt, and M. Reissner*
- 2376 Structural and Morphological Study of Mesoporous Germanium Layers Formed by Bipolar Electrochemical Etching  
*S. Tutashkonko, A. Boucherif, T. Nyhyporuk, R. Arès, V. Aimez, and M. Lemiti*
- 2377 Morphological Development from Uniform Microporous Structure to Macropore-Like Structure  
*T. Urata, K. Fukami, T. Sakka, and Y. H. Ogata*

- 2378 Relaxation Processes and Functions of Blue Phosphorescent Porous Silicon  
*B. Gelloz, R. Mentek, and N. Koshida*
- 2379 Tuning of Optical Properties of Silicon Photonic-Crystal Devices by Infiltration of Grooves and Pores with Liquid Crystals  
*T. S. Perova, V. Tolmachev, and A. V. Baldycheva*
- 2380 Size-Dependent Assessment of Fe<sub>3</sub>O<sub>4</sub>-Nanoparticles Loaded into Porous Silicon  
*P. Granitzer, K. Rumpf, Y. Tian, G. Akkaraju, J. L. Coffer, P. Poelt, P. Morales, and M. Reissner*
- 2381 Magnetic Properties of an Iron Oxide/Porous Silicon System Controlled by Magnetic Interactions  
*K. Rumpf, P. Granitzer, P. Poelt, P. Morales, and M. Reissner*
- 2382 The effects of Confinement and Coulomb Blockade on the Transport in Ensembles of Si Quantum Dots  
*I. Balberg*
- 2383 Optical Characterization of Self-Assembled Systems: Nanoparticles and Monolayers  
*N. Rowell*
- 2384 XPS Analysis of Porous Silicon  
*D. Aureau, J. Chazalviel, F. Ozanam, and A. Etcheberry*
- 2385 Transient Surface Photovoltage Studies of Nano-Porous Silicon with Embedded Metal Nanoparticles  
*P. R. Chapagain, E. Davis, A. Nemashkalo, Y. Strzhemechny, P. Granitzer, K. Rumpf, and E. Nguyen*
- 2386 Enhanced Suppression of the Formation of Porous Silicon Based on Secondary Knocked-On effect in FIB  
*J. Wang, J. Jiao, P. Yan, M. Wang, W. Liu, D. Ge, and J. Xu*
- 2387 Conversion Kinetics and Characterisation of Pt/Pb Nanoparticles on Fluorine Doped Tin Oxide Glass  
*K. Yliniemi, D. Wragg, T. M. Watson, D. A. Worsley, H. McMurray, B. P. Wilson, P. Schmuki, and K. Kontturi*
- 2388 Low-Lying Electronic Excitations and Optical Absorption Spectra of the Black Dye Sensitizer: A First-Principles Study  
*A. Delgado, S. Corni, and G. Goldoni*
- 2389 Applications of Porous Silicon to Multicrystalline Silicon Solar Cells: State of the Art  
*C. Levy-Clement*
- 2390 Deposition of Ternary Alloys of Cadmium Seleno-Sulfide Thin Films on Nanoporous TiO<sub>2</sub> for Solar Cells Applications  
*A. Sepehrifard, A. Aushana, and S. Morin*

- 2391 Fabrication of Highly Ordered Porous Si and Its Application to Anodes in Lithium-Ion Battery  
*H. Masuda, S. Tagawa, and K. Nishio*
- 2392 Silicon and Porous Silicon/Carbon Nanocomposites for Rechargeable Li- and Mg-Ion Batteries  
*S. Polisski and T. Abe*
- 2393 Silicon Nanowires for Innovative Energy Applications  
*V. Sivakov, M. Kulmas, B. Hoffmann, F. Talkenberg, R. Kirchgeorg, C. Lee, P. Schmuki, and S. Christiansen*
- 2394 Transition Metal Oxide Particles Deposited onto Titania Nanotubes as High Performance Electrodes for Li-Ion Microbatteries  
*N. Kyeremateng and T. Djenizian*
- 2395 Designing Structure and Composition of Nanoporous Anodic Alumina for Optical Applications  
*D. Routkevitch*
- 2396 Deposition of LaF<sub>3</sub> to Passivate the Pore-Walls of Porous Silicon Using a Simple Single-Source Chemical Bath Technique  
*A. Ismail, M. Rahman, M. Hossain, M. Nain, and S. Mou*
- 2397 Preparation and Characteristics of Anodic Aluminum Oxide Membranes with Mesosponge Structure  
*T. N. Nguyen, M. Kim, J. Ahn, J. Kaewsuk, J. Kim, and D. Jeong*
- 2398 Fabrication of Flexible Alumina Microlens Array by Laser Irradiation and Aluminum Anodizing  
*T. Kikuchi, Y. Wachi, T. Takahashi, M. Sakairi, and R. O. Suzuki*
- 2399 Formation of Self-Organized Nanoporous Anodic Films on Carbon Steels  
*S. Yang, Y. Konno, E. Tuji, Y. Aoki, H. Shoji, P. Skeldon, G. E. Thompson, and H. Habazaki*
- 2400 Metal Assisted Etching of Silicon in a V<sub>2</sub>O<sub>5</sub> Plus HF Solution  
*W. B. Barclay and K. W. Kolasinski*
- 2401 Anodic Porous Etching of n-InP: A Chemical-Assisted Dissolution Process  
*L. Santinacci, M. Bouttemy, and A. Etcheberry*
- 2402 Mathematical Model for <111>A Pore Propagation and Relation to Current for InP in Aqueous KOH Electrolytes  
*R. Lynch, N. Quill, C. O'Dwyer, and D. Buckley*
- 2403 Differential Photoacoustic Electrochemical Cell to Study In Situ the Wetting Process in Different Materials  
*D. G. Espinosa-Arbelaez and M. Rodriguez-Garcia*

- 2404 Study of the Microstructural and Optical Properties of Porous Silicon Bragg Reflectors Obtained by Differential Photoacoustic Electrochemical Cell  
*M. Rodriguez-Garcia and D. G. Espinosa-Arbelaez*
- 2405 Solid-State Nanopores: Electronic Tools for Single-Molecule Analysis  
*V. Tabard-Cossa*
- 2406 Transport in Surface Passivated Porous Silicon Membranes  
*A. Kovacs, W. Kronast, A. Filbert, and U. Mescheder*
- 2407 New Cheap Composite Membranes Using Nanoporous Anodic Aluminum Oxide Films  
*M. Kim, T. N. Nguyen, J. Ahn, J. Kaewsuk, J. Kim, and D. Jeong*
- 2408 Importance of Pore Morphology for Super-Liquid Repellency of Solid Surfaces  
*H. Habazaki, T. Fujii, and E. Tsuji*
- 2409 Morphological Instability Leading to Formation of Porous Anodic Oxide Films  
*K. R. Hebert and A. Macrostie*
- 2410 A Continuum Model of Anodic Pore Growth in Alumina  
*S. J. DeWitt and K. Thornton*
- 2411 Controlled Fabrication of Ordered 3D Porous Alumina Nanostructures with Designed Cell Ratios by Stepwise Anodization  
*S. Chu, Y. Hitoshi, K. Wada, S. Inoue, and H. Segawa*
- 2412 Self-Ordered Sub-10 nm Nanoporous Anodic Alumina Membranes: A New Tool for Nanotechnology  
*E. Moyen, L. Assaud, K. Pitzschel, L. Masson, M. Hanbücken, and L. Santinacci*
- 2413 Electrochemical Formation of Ordered Pore Arrays on Metallic Substrates  
*H. Tsuchiya, M. Kim, Y. Terada, and S. Fujimoto*
- 2414 New Cheap Anodic Aluminum Oxide Composite Membranes by Lithography Technique  
*J. Kaewsuk, J. Kim, M. Kim, T. N. Nguyen, J. Ahn, and D. Jeong*
- 2415 Dependence of the Reactivity of Silicon Dioxide Layers on the Porous Structure  
*F. N. Dultsev*
- 2416 Nanostructure Modified Porous Interfaces for Enhanced Sensing and Directed Microcatalysis  
*J. Gole and W. Laminack*
- 2417 Miniaturization of Hydrogen Gas Sensors by Using Anodization Processes of Titanium  
*Y. Kimura, S. Kimura, R. Kojima, and M. Niwano*
- 2418 Photoelectric-conversion Devices Based on InP Porous Structure  
*T. Sato, R. Jinbo, and Z. Yatake*

- 2419 Multi-Functionality of Nanosilicon and Its Device Applications  
*N. Koshida*
- 2420 The Effect of Temperature and Electrolyte Concentration on Porous Layers Formed on InP in KOH  
*N. Quill, R. Lynch, C. O'Dwyer, and D. Buckley*
- 2421 Current-Line Oriented Pore Formation in n-InP Anodized in KOH  
*N. Quill, R. Lynch, C. O'Dwyer, and D. Buckley*
- 2422 Fabrication of a Single-Crystalline Porous InP Membrane by Electrochemical and Photoelectrochemical Etching  
*M. Gerngross, J. Carstensen, and H. Föll*
- 2423 SVET Analysis of Tinplate Flow Melted Using Resistance Heating and Induction Vs Novel Near Infrared Heat Treatment  
*I. Mabbett, D. J. Warren, S. Geary, J. H. Sullivan, D. Penney, T. M. Watson, and D. A. Worsley*
- 2424 Imaging Metastable Pits on Austenitic Stainless Steel In Situ at the Open-Circuit Corrosion Potential Using Scanning Electrochemical Microscopy  
*R. M. Souto, J. Izquierdo, and S. González*
- 2425 Porous Silicon as a Biomaterial  
*M. J. Sailor*
- 2426 Silicon Nanowires: A General Platform for Biosensing  
*R. Boukherroub*
- 2427 Innovative Applications of Porous Structures of Alumina and Silicon  
*R. B. Wehrspohn, S. Schweizer, B. Gesemann, P. Göring, and M. Lelonek*
- 2428 Three-Dimensional Structure of (110) Porous Silicon with In-Plane Optical Birefringence  
*M. Fujii, S. Shichi, T. Nishida, H. Yasuda, K. Imakita, and S. Hayashi*
- 2429 Formation of Area and Thickness Controlled Porous Type Aluminum Anodic Oxide Films by Sf-MDC  
*M. Sakairi, T. Yamaguchi, T. Murata, and K. Fushimi*
- 2430 Irregularity and Defects of Porous Anodic Oxide Films Formed on Metals  
*S. Ono and H. Asoh*
- 2431 Scan Rate and Fluoride Concentration effect on the Anodic Growth of Self-Aligned Titanium Dioxide Nanotubes in Phosphates  
*E. Krasicka-Cydzik, A. Kaczmarek, I. Glazowska, and K. Bialas Heltowski*
- 2432 Pit Initiation at MnS Nano-Inclusions in Carbon Steel under Exposure to Sulfate-Reducing Bacterium D. alkanexedens  
*B. H. Davis, Z. Suo, I. Beech, D. Paul, J. Hammond, and R. Avci*

- 2433 Bulk Diffusion Controlled Dealloying  
*Q. Chen and K. Sieradzki*
- 2434 The Strong Rashba Spin-Orbit Interaction in  $\text{Hg}_{0.77}\text{Cd}_{0.23}\text{Te}$  Inversion Layer  
*G. Yu, X. Liu, L. Wei, T. Lin, J. Chu, Y. Wei, and J. Yang*
- 2435 Pitting Corrosion Behavior and Grain Evolution of Shot Peened 304 Type Stainless Steel  
*T. D. Widodo and K. Noda*
- 2436 Formation of Interconnected Nano-Channels in Highly-Ordered Anodic Alumina  
*B. Huang, Y. Tian, B. Shan, and R. Chen*
- 2437 TiO<sub>2</sub> Nanotubes and Other Self-organized Anodic Structures: Formation and Applications  
*P. Schmuki*

### **E1 - Solid State Topics General Session**

*ECS Dielectric Science and Technology, ECS Electronics and Photonics, ECS Energy Technology, ECSJ Solid-State Chemistry, ECSJ Functional Ceramics*

- 2438 Characteristics of Zinc Oxide Films Grown on Sapphire Substrates Using High-Energy H<sub>2</sub>O Generated by a Catalytic Reaction on Platinum Nanoparticles  
*K. Yasui, H. Miura, S. Satomoto, and T. Kato*
- 2439 Dielectric Constant Studies of BCN Thin Films  
*K. B. Sundaram and V. Todi*
- 2440 Effect of Wet Surface Treatments on Amorphous Silicon Anneal and Gate Breakdown  
*C. S. Tiwari, T. Guo, C. Breyfogle, J. Zhang, H. Mitro, L. Olmer, V. Kumar, D. Pohlman, and M. Rutte*
- 2441 Ultrasonic Spray-Assisted Vapor-Deposition Method as a Cost-Effective and Environmental-Friendly Technology for Semiconductor and Dielectric Materials for Devices  
*S. Fujita, S. Katori, J. Piao, T. Ikenoue, and K. Kaneko*
- 2442 UV-Visible Faraday Rotators Based on Rare-Earth Fluoride Single Crystals: LiREF<sub>4</sub> (RE=Tb, Dy, Ho, Er and Yb), PrF<sub>3</sub> and CeF<sub>3</sub>  
*V. Vasyliev, E. G. Villora, Y. Sugahara, and K. Shimamura*
- 2443 The Characterization Study of Polycrystalline Silicon Grain Growth with Electron Backscatter Diffraction Patterns and Crystallinity  
*S. Yang, J. Chang, J. Lim, J. Shin, Y. Yoo, J. Kim, B. Chung, H. Choi, K. Hwang, and H. Kang*
- 2444 Electrical Breakdown of Anodic Aluminum Oxide Films for Electrowetting Systems  
*M. Mibus, E. Nein, A. Sapkota, C. Knospe, M. Reed, and G. Zangari*
- 2445 Ultrafast Carrier Dynamics in Green-Sensitive Organic Photodiodes  
*S. Sul, K. Lee, D. Leem, K. Kim, and H. Han*

- 2446 Single Chamber HFCVD Process for Growth of Diamond, Graphene and CNTs  
*S. Albin, R. Vispute, and A. Seiser*
- 2447 The Systematic Study and Simulation Modeling on Dislocation Edge Stress Effects for Si N-MOSFETs  
*M. Liao, C. Chen, L. Chang, C. Yang, C. Hsieh, and M. Lee*
- 2448 The Investigation on the Relaxation of Intrinsic Compressive Stress in CMOS Transistors by Additional N IMP Treatment and AFM-Raman Stress Extraction  
*M. Liao, C. Chen, L. Chang, C. Yang, C. Hsieh, and M. Lee*
- 2449 Plasmonic Color Filters for OLED by Laser Interference Lithography  
*J. Park, Y. Do, B. Hwang, K. Choi, and B. Ju*
- 2450 Hot Carrier effects by Gate Induced Drain Leakage Current  
*K. Kim, C. Han, J. Lee, D. Kim, H. Kim, H. Lee, and B. Choi*
- 2451 Development of Visual Inspection System for Metal Surface with Multivariate Pattern Analysis  
*K. Shigyo, T. Matsumoto, K. Sakiyama, and H. Kobayashi*
- 2452 Effects of Tungsten Composition Ratio on the Properties of W-In-Zn-O Films Deposited by RF Magnetron Sputtering  
*G. Heo, B. Oh, J. Park, Y. Lee, Y. Lee, and D. Shin*
- 2453 Fabrication of n-type Semiconductive Polycrystalline Diamond by Incorporating Phosphorous Atoms  
*A. Nakahara, H. Naragino, K. Yoshinaga, S. Tanaka, and K. Honda*
- 2454 Carrier Transport Mechanism at Metal/Amorphous Gallium Indium Zinc Oxide Interfaces  
*S. Kim, C. Choi, and H. Kim*
- 2455 Growth of AlN Single Crystals by Sublimation Method  
*Y. Oshima, M. Nakamura, Y. Masa, E. G. Villora, K. Shimamura, and N. Ichinose*

## E2 - Atomic Layer Deposition Applications 8

*ECS Dielectric Science and Technology, ECS Electronics and Photonics*

- 2456 Fabrication of Sb<sub>2</sub>Te<sub>3</sub> and Bi<sub>2</sub>Te<sub>3</sub> Multilayer Composite Films by Atomic Layer Deposition  
*K. Zhang, D. Nminibapiel, M. Tangirala, H. Baumgart, and V. Kochergin*
- 2457 Trimethylaluminum-Based Atomic Layer Deposition of Al:MO<sub>2</sub> (M=Zr, Hf): A Viable Route to Integrate High-Permittivity Oxides on In<sub>0.53</sub>Ga<sub>0.47</sub>As Substrates  
*A. Molle, E. Cianci, A. Lamperti, C. Wiemer, S. Baldovino, L. Lamagna, S. Spiga, M. Fanciulli, G. Brammertz, C. Merckling, and M. Caymax*

- 2458 Are Ions Good or Bad during Plasma-Assisted ALD  
*H. B. Profijt and W. Kessels*
- 2459 Atomic Layer Deposition of Mo: Al<sub>2</sub>O<sub>3</sub> Nanocomposites with Tunable Resistivity  
*A. U. Mane and J. W. Elam*
- 2460 In Situ Study of ALD Processes Using Synchrotron-based X-ray Fluorescence and Scattering Techniques  
*J. Dendooven, K. Devloo-Casier, M. Ide, K. Grandfield, K. F. Ludwig, S. Bals, P. Van Der Voort, and C. Detavernier*
- 2461 Reaction Mechanism of Non-Heating SiO<sub>2</sub> Atomic Layer Deposition by Using TDMAS and Plasma Excited Water Vapor  
*F. Hirose, K. Kanomata, M. Degai, and K. Momiyama*
- 2462 Crystallization Study by Transmission Electron Microscopy of SrTiO<sub>3</sub> Thin Films Grown by Plasma-Assisted ALD  
*V. Longo, M. A. Verheijen, F. Roozeboom, and W. Kessels*
- 2463 TiO<sub>2</sub>-Based Metal-Insulator-Metal Structures for Future DRAM Storage Capacitors  
*K. Fröhlich, B. Hudec, M. Tapajna, K. Hušeková, A. Rosová, J. Aarik, R. Rammula, A. Kasikov, T. Arroval, K. Murakami, M. Rommel, and A. J. Bauer*
- 2464 Application of the Plasma Surface Modification for Uniform Al<sub>2</sub>O<sub>3</sub> Films Grown by Atomic Layer Deposition on Polyethylene Blown Film  
*G. Lee, K. Son, S. Park, J. Shim, and B. Choi*
- 2465 Atomic Layer Deposition of Molybdenum Oxide Using Bis(Tert-Butylimido)Bis(Dimethylamido) Molybdenum  
*A. Bertuch, L. Lecordier, M. Dalberth, G. Sundaram, J. Becker, E. Deguns, M. Saly, D. Moser, and R. Kanjolia*
- 2466 Room-Temperature ALD of Metal Oxide Thin Films by Energy-Enhanced ALD  
*S. E. Potts, H. B. Profijt, R. Roelofs, and W. Kessels*
- 2467 Growth Characteristics and Properties of Yttrium Oxide Thin Films by Atomic Layer Deposition from Novel Y(iPrCp)<sub>3</sub> Precursor and O<sub>3</sub>  
*R. Xu, S. Selvaraj, N. Azimi, and C. G. Takoudis*
- 2468 Electrocatalytic Activity of Platinum Grown by Atomic Layer Deposition on Carbon Nanotubes for Si-Based DMFC Applications  
*A. Johansson, R. Yang, B. Dalslet, J. V. Larsen, K. Haume, L. H. Christensen, and E. V. Thomsen*
- 2469 Atomic Layer Deposition of Copper (I) Sulfide Using Commercially Produced Precursors  
*S. Christensen, A. Dameron, T. Gennett, and I. Repins*
- 2470 High Performance Core-Shell Nanowire Array Devices Prepared by Atomic Layer Deposition  
*H. Kim*

- 2471 Metal Oxide ALD Films for Low Power Sensor Applications  
*S. H. Brongersma*
- 2472 Enabling High Performance Detectors and Optics for Astronomy and Planetary Exploration with ALD  
*F. Greer*
- 2473 Nanomechanical Properties of Ultra Thin Films Synthesized by Atomic Layer Deposition  
*H. Baumgart*
- 2474 Study on Growth Characteristics of ALD RuO<sub>2</sub> Thin Films with Deposition Conditions  
*W. Kim, B. Kim, J. Chang, Y. Tak, H. Yang, S. Moon, O. Kwon, K. Cho, C. Yoo, and H. Kang*
- 2475 Atomic Layer Deposition of TiN/Al<sub>2</sub>O<sub>3</sub>/TiN Nanolaminates for Capacitor Applications  
*L. Assaud, M. Hanbücken, and L. Santinacci*
- 2476 Impact of Direct Plasma Densification on Resistivity and Conformality of PEALD Tantalum Nitride  
*O. van der Straten, X. Zhang, C. Penny, J. Maniscalco, S. Chiang, J. Ren, and P. Ma*
- 2477 Atomic Layer Deposition of Ruthenium in Various Precursor and Oxygen Doses  
*J. Kim, K. Son, B. Kim, and J. Shim*
- 2478 In Situ FTIR Characterization of Growth Inhibition in Atomic Layer Deposition Using Reversible Surface Functionalization  
*A. Yanguas-Gil, J. A. Libera, and J. W. Elam*
- 2479 Substrate Reactivity effects in the ALD of Al<sub>2</sub>O<sub>3</sub> Revealed by In Situ ALD  
*M. Tallarida, M. Michling, C. Das, and D. Schmeisser*
- 2480 New Reaction Chemistries for Late Transition Metal Atomic Layer Deposition  
*B. Vidjayacoumar, V. Ramalingam, R. Kleinberger, D. J. Emslie, J. Blackwell, and S. Clendenning*
- 2481 Tungsten Nitride Films Prepared by Cyclic-Pulsed Chemical Vapor Deposition for IC Metallization  
*E. Kim, H. Woo, and D. Kim*
- 2482 Highly Uniform Self-Assembled Gold Nanoparticles over High Surface Area ZnO Nanorods as Novel Catalysts  
*T. M. Abdel-Fattah, K. Zhang, W. Cao, and H. Baumgart*
- 2483 Characterization of Complex Magnetic Nanotubes  
*K. Pitzschel, J. Bachmann, S. Martens, J. Moreno Montero, J. Escrig, K. Nielsch, and D. Görilitz*

- 2484 Synthesis of VO<sub>2</sub> Thin Films by Atomic Layer Deposition with TEMA V as Precursor  
*K. Zhang, M. Tangirala, D. Nminibapiel, V. Pallem, C. Dussarrat, and H. Baumgart*

**E3 - Chemical Mechanical Polishing 12**  
*ECS Dielectric Science and Technology*

- 2485 Corrosion Inhibition Effect of Organic Additive on Ru Film in Colloidal Silica Based Slurry with Sodium Periodate  
*H. Cui, J. Lim, J. Cho, H. Hwang, J. Park, and J. Park*
- 2486 Electrochemical Characterizations on Chemical Mechanical Polishing Compositions of Polishing Ruthenium Films in CMP Processes  
*T. X. Shi, J. Henry, and J. Schlueter*
- 2487 Brush Scrubbing Scratches Reduction Methods in Post CMP Cleaning  
*H. Soondrum*
- 2488 Studies on Slurry Design Fundamentals for Advanced CMP Applications  
*G. Basim, A. Karagoz, L. Chen, and I. Vakarelski*
- 2489 Managing Corrosion during the Chemical Mechanical Polishing (CMP) of Metal Films  
*J. Schlueter, J. Henry, and T. X. Shi*
- 2490 Microstructure and Pattern Size Dependence of Copper Corrosion in Submicron-Scale Features  
*U. Lee, J. Choi, J. Won, H. Lee, H. Sohn, and T. Kang*
- 2491 Scratching of Patterned Composite Surfaces by Pad Asperities in Chemical-Mechanical Polishing  
*S. Kim, N. Saka, and J. Chun*
- 2492 Effect of Chelating Agent on Chemical Mechanical Polishing Performance for Polycrystalline Ge<sub>2</sub>Sb<sub>2</sub>Te<sub>5</sub> Film  
*J. Cho, J. Lim, S. Woo, E. Hwang, and J. Park*
- 2493 Metal Oxide Nano Film Characterization for CMP Optimization  
*G. Basim, A. Karagoz, and Z. Ozdemir*
- 2494 Novel Ru CMP Slurry Using TiO<sub>2</sub> Nano Particle as Abrasive and H<sub>2</sub>O<sub>2</sub> as Oxidizer  
*J. Park, H. Cui, J. Lim, J. Jo, H. Hwang, and J. Park*
- 2495 Metal Clearing Process Control in Metal CMP  
*K. Xu, I. Carlsson, T. Liu, S. Shen, B. Swedek, Y. Wang, X. Xia, D. Bennett, W. Tu, and L. Karupiah*
- 2496 Post-CMP Cleaning of Copper Interconnects at Sub-32nm Technology Node  
*T. Dnyanesh, M. Rao, and G. Banerjee*

- 2497 Effect of Iron(III) Nitrate Concentration on Tungsten Chemical-Mechanical-Polishing Performance  
*J. Lim, J. Cho, H. Hwang, H. Cui, J. Park, and J. Park*
- 2498 Effect of slurry on Vapor Deposition Polymerization (VDP)Chemical Mechanical Planarization (CMP) in Through-Silicon Via (TSV) Applications  
*I. Ali, B. Sapp, R. Quon, S. Kruger, K. Maekawa, K. Sugita, H. Hashimoto, M. Stender, J. Dysard, and S. Arkalgud*
- 2499 Effects of Polishing Parameters on the Evolution of 3-D Wafer Pattern during CMP  
*L. Wu*
- 2500 The Step Height Reduction in STI-CMP by Controlling the Adhesion Force between Abrasive and Polishing Pad  
*J. Seo, J. Moon, K. Kim, W. Sigmund, and U. Paik*
- 2501 Controls of Interactions among Polishing Pad, Abrasive, and Oxide Film by Modification of Polyethyleneimine(PEI) on Under 30nm Ceria Abrasive CMP Slurry  
*J. Moon, J. Bae, K. Park, K. Kim, H. Park, and U. Paik*
- 2502 Bottom Electrode Surface Treatment effect on MTJ in MRAM Device  
*C. Kim, J. Jung, I. Yoon, B. Yoon, J. Park, and S. Jung*
- 2503 Improved Removal Rate in Organic Additive Assisted Ceria Chemical Mechanical Planarization  
*J. Bae, J. Seo, K. Park, J. Moon, H. Park, and U. Paik*
- 2504 A Modeling Study on the Layout Impact of With-In-Die Thickness Range for STI CMP  
*S. Kincaid and G. Basim*
- 2505 Critical Cu Line Scaling Challenges  
*J. Lu, T. Tran, G. Herdt, N. Petrov, Y. Hu, V. Antonov, D. Collins, P. Murali, Z. Zhang, S. Kondoju, and S. Ireland*
- 2506 Development of SiN CMP Slurry with Selectivity Control  
*Y. Kim, K. Kim, J. Lee, I. Hwang, and S. Nam*
- 2507 Investigation of the Slurry for Poly Si Stopping CMP Process  
*Y. Pyon, C. Seong, J. Lim, K. Bae, K. Park, K. Kim, and Y. Shin*
- 2508 Combinational effect of Hydroplane and Alkaline Agent on Remaining Particle Reduction for Silicon Wafer Polishing  
*H. Hwang, H. Cui, J. Lim, J. Jo, J. Park, E. Choi, J. Ahn, and J. Park*
- 2509 Tribological, Thermal, and Kinetic Attributes of 300 vs. 450 mm Chemical Mechanical Planarization Processes  
*Y. Jiao, X. Liao, C. Wu, Y. Zhuang, S. Theng, Y. Sampurno, M. Goldstein, and A. Philipossian*

- 2510 Chemical Mechanical Polishing for Extreme Ultraviolet Lithography Mask Substrates  
*A. Hariprasad, R. Teki, and S. V. Babu*
- 2511 Effect of CMP Additives on the Agglomeration Rate of Alumina Nanoparticles  
*N. Brahma and J. B. Talbot*
- 2512 Microreplicated Pad Conditioner for Advanced CMP Applications  
*C. Gould, J. Zabasajja, and D. Le-Huu*

**E4 - Gallium Nitride and Silicon Carbide Power Technologies 2**  
*ECS Electronics and Photonics, ECS Dielectric Science and Technology*

- 2513 Overview of Three-Dimension Integration for Point-of-Load Converters  
*F. C. Lee and Q. Li*
- 2514 Development of High Power Density All-SiC Three-Phase Inverter  
*S. Sato, K. Matsui, Y. Zushi, Y. Murakami, and S. Tanimoto*
- 2515 Defect Electronics in SiC and Fabrication of Ultrahigh-Voltage Bipolar Devices  
*T. Kimoto*
- 2516 SiC Trench Devices with Ultra Low  $R_{on}$   
*T. Nakamura, M. Aketa, and Y. Nakano*
- 2517 Fabrication of a SiC Double Gate Vertical Channel JFET and It's Application in Power Electronics  
*A. Schöner and M. Bakowski*
- 2518 Recent Advances in VJFETs at SemiSouth  
*K. Chatty, D. C. Sheridan, V. Bondarenko, R. Schrader, K. Speer, and J. B. Casady*
- 2519 Optimization of 4.5kV Si IGBT/SiC Diode Hybrid Module  
*K. D. Hobart, E. Imhoff, T. Duong, and A. Hefner*
- 2520 Aspects on SIC Switches for Soft-Switching Converters in an Industrial Application  
*P. Ranstad and J. Linner*
- 2521 Fast High Voltage Switching With SiC Power Devices  
*T. Funaki*
- 2522 On the De-Rating of Silicon Carbide (SiC) Power Devices  
*K. Shenai*
- 2523 Managing Basal Plane Dislocations in SiC: Perspective and Prospects  
*D. Gaskill, R. Myers-Ward, V. Wheeler, R. Stahlbush, N. Mahadik, E. Imhoff, L. O. Nyakiti, and C. Eddy Jr*

- 2524 Growth and Characterization of Thick 4H-SiC Epilayers for Very High Voltage Bipolar Devices  
*H. Tsuchida, T. Miyazawa, X. Zhang, M. Nagano, R. Tanuma, I. Kamata, and M. Ito*
- 2525 Life-Time Killing Defects in Ion-Implanted 4H-SiC; Enhanced Annealing and Lateral Distribution  
*L. Sundnes Løvlie, L. Vines, I. Pintilie, and B. G. Svensson*
- 2526 Silicon Carbide Bulk Crystal Growth Modeling from Atomic Scale to Reactor Scale  
*S. Nishizawa*
- 2527 Modeling of SiC CVD Epitaxial Growth using CFD-ACE+  
*A. Bhoj, S. Tangli, and K. Shenai*
- 2528 Physics of GaN-based Power Field Effect Transistors  
*M. Shur*
- 2529 Recent Advances in III-N High-Power Electronics  
*R. Dupuis, Y. Lee, Z. Lochner, H. Kim, Y. Zhang, J. Ryou, and S. Shen*
- 2530 Quasi-Vertical GaN-on-Silicon Transistors for Compact Enhancement-mode Power Switches  
*B. Brar, D. Kim, C. Neft, C. Nguyen, and V. Mehrotra*
- 2531 Demonstration of Low ON-Resistance CAVETS with Ammonia MBE Grown Active p-GaN Layer as the Current Blocking Layer for High Power Applications  
*R. Yeluri, C. Hurni, S. Chowdhury, J. S. Speck, and U. Mishra*
- 2532 AlGaN/GaN Heterojunction FETs for High-Breakdown and Low-Leakage Operation  
*M. Kuzuhara and H. Tokuda*
- 2533 III-Nitride High Voltage Power Electronics  
*M. Spencer and W. Schaff*
- 2534 Hydrophobic Growth of GaN Material: Current Status and Future Potential  
*J. M. Mann, B. Wang, and D. Bliss*
- 2535 Electrochemical Solution Growth of Gallium Nitride  
*T. C. Monson, K. Waldrip, V. Krishnamoorthy, A. Mollo, and L. E. Johnson*
- 2536 Comparison of Si, Sapphire, SiC, and GaN Substrates for HEMT Epitaxy  
*M. Leszczynski, P. Prystawko, J. Plesiewicz, L. Dmowski, E. Litwin-Staszewska, S. Grzanka, E. Grzanka, and F. Roccaforte*
- 2537 GaN-on-Si for Power Technology  
*D. Visalli, J. Derluyn, S. Degroote, and M. Germain*
- 2538 Scalable GaN-On-Silicon Using Rare Earth Oxide Buffer Layers  
*M. Lebby, F. Arkun, R. Dargis, R. Roucka, R. S. Smith, and A. Clark*

- 2539 Recent Advances in Wide Bandgap Power Devices  
*K. Sheng*
- 2540 Advanced Driver and Control ICs for GaN and SiC Power Devices  
*S. P. Pendharkar and C. Chey*
- 2541 GaN-Based Wide-Bandgap Power Switching Devices: From Atoms to the Grid  
*S. Atcity, R. Kaplar, S. DasGupta, M. Marinella, A. Armstrong, L. Biedermann, M. Sun, T. Palacios, and M. Smith*
- 2542 Device Breakdown and Dynamic effects in GaN Power Switching Devices: Dependencies on Material Properties and Device Design  
*J. Würfl, E. Bahat-Treidel, F. Brunner, M. Cho, O. Hilt, A. Knauer, P. Kotara, M. Weyers, and R. Zhytnytska*
- 2543 Degradation Study of Single and Double-Heterojunction InAlN/GaN HEMTs by Two-Dimensional Simulation  
*V. Palankovski and J. Kuzmik*
- 2544 Temperature Dependence of Kink Effect for AlGaN/GaN/SiC High Electron Mobility Transistors  
*C. Cheng, T. Chang, S. Liao, H. Chang, W. Ho, Y. Shieu, and J. Sen*
- 2545 Band Diagrams and Trap Distributions in Metal-SiO<sub>2</sub>-SiC(3C) Structures with Different Metal Gates  
*H. M. Przewlocki, T. Gutt, K. Piskorski, and M. Bakowski*
- 2546 Angle-Resolved XPS Studies on Transition Layers at SiO<sub>2</sub>/SiC Interfaces  
*H. Okada, A. Komatsu, M. Watanabe, Y. Izumi, T. Muro, and H. Nohira*
- 2547 Effect of Stress and Measurement Conditions in Determining the Reliability of SiC Power MOSFETs  
*A. Lelis, R. Green, M. El, and D. Habersat*
- 2548 POCl<sub>3</sub> Annealing as a New Method for Improving 4H-SiC MOS Device Performance  
*H. Yano, T. Hatayama, and T. Fuyuki*
- 2549 Passivation in High-Power Si Devices - An Overview  
*U. Grossner, A. Mihaila, U. Vemulapati, and C. Corvasce*
- 2550 Broadband GaN Power Amplifiers  
*S. Leong and K. Shenai*
- 2551 A Promising New n<sup>++</sup>-GaN/InAlN/GaN HEMT Concept for High-Frequency Applications  
*V. Palankovski and J. Kuzmik*
- 2552 Achieving Low Doped (<10<sup>16</sup>) GaN with Large Breakdown Voltages (~1000 V)  
*K. A. Jones, R. P. Tompkins, M. A. Derenge, K. W. Kirchner, S. Zhou, R. Metzger, J. Leach, P. Suvana, M. Tungare, and F. Shahedipou-Sandvik*

- 2553 GaN Technology for Millimeter Wave Power Amplifiers  
*A. K. Oki, M. Wojtowicz, B. Heying, I. Smorchkova, B. Luo, and M. Siddiqui*
- 2554 A Simple and Accurate Physics-Based Circuit Simulation Model for Depletion-Mode GaN Power Transistors  
*K. Shenai and S. Leong*
- 2555 Current Status and Future Prospects of GaN HEMTs for High Power and High Frequency Applications  
*T. Kikkawa, M. Kanamura, T. Ohki, K. Imanishi, K. Watanabe, and K. Joshin*
- 2556 S-Band 300 W Output SiC MESFET  
*S. Cai, L. Li, J. Li, J. Mo, B. Liu, and Z. Feng*
- 2557 Low Dynamic ON-Resistance in AlGaN/GaN Power HEMTs Obtained by AlN Thin Film Passivation  
*K. Chen, S. Huang, and Q. Jiang*
- 2558 Thickness Dependent Electrical Characteristics of AlGaN/GaN MOSHEMT with La<sub>2</sub>O<sub>3</sub> Gate Dielectrics  
*J. Chen, K. Tsuneishi, K. Kakushima, P. Ahmet, Y. Kataoka, A. Nishiyama, N. Sugii, K. Tsutsui, K. Natori, T. Hattori, and H. Iwai*
- 2559 Field Control Energy-Band (FCE) Technology for GaN-Based Heterostructure Power Devices  
*W. Chen, Z. Wang, X. Deng, and B. Zhang*
- 2560 Electro-Thermal Circuit Modeling of Power Inductors  
*K. Shenai, J. Wu, and H. Cui*
- 2561 eGaN FETs in Low Power Wireless Energy Converters  
*M. A. de Rooij and J. T. Strydom*
- 2562 Ion Implanted 4H-SiC p-i-n Diodes: Comparison between 1600-1650°C and 1950°C Post Implantation Annealing  
*R. Nipoti*
- 2563 Thermal Behavior of SiC Power Diodes  
*J. Millán, P. Godignon, and V. Banu*
- 2564 Multilayer Epitaxial Growth and Fabrication of 4H-SiC BJT with Double Base Epilayers  
*Y. Zhang, L. Yuan, Y. Zhang, X. Tang, Q. Song, X. Zhang, and Q. Zhang*
- 2565 Merits of Buried Grid Technology for SiC JBS Diodes  
*M. Bakowski, J. Lim, and W. Kaplan*
- 2566 Towards Very High Voltage SiC Power Devices  
*D. Planson, P. Brosselard, D. Tournier, and C. Brykinski*

- 2567 GaN Technology for Energy Efficient Electronics  
*K. Boutros, R. Chu, B. Hughes, and S. Khalil*
- 2568 Nanoscale Probing of Interfaces in GaN for Devices Applications  
*F. Giannazzo, G. Greco, P. Fiorenza, R. Lo Nigro, F. Roccaforte, and A. Scuderi*
- 2569 Ti Silicide Electrodes Low Contact Resistance for Undoped AlGaN/GaN Structure  
*K. Tsuneishi, J. Chen, K. Kakushima, P. Ahmet, Y. Kataoka, A. Nishiyama, N. Sugii, K. Tsutsui, K. Natori, T. Hatorri, and H. Iwai*
- 2570 Fully Copper-Based Metallization for GaN High Electron Mobility Transistor Devices  
*E. Yi Chang, Y. Lin, L. Chang, Y. Chen, and Y. Wong*
- 2571 XPS analysis of AlGaN/GaN Surface after Chemical and N-Containing Plasma Treatments  
*R. Meunier, A. Torres, M. Charles, E. Morvan, C. Petit-Etienne, O. Renault, and T. Billon*
- 2572 Characterizations of GaN Films Grown on Si (111) Substrates under Various Growth Temperatures of Multiple AlN Buffer Layers  
*B. Tran, E. Chang Yi, K. Lin, T. Luong, H. Yu, M. Huang, C. Chung, H. Trinh, H. Nguyen, C. Nguyen, and Q. Luc*
- 2573 Characteristics of GaN Nanowires Produced Using VLS Method on the Growth Temperatures  
*J. Yoon, B. Oh, and J. Yang*

**E5 - Dielectric Materials and Metals for Nanoelectronics and Photonics 10**  
*ECS Dielectric Science and Technology, ECS Electronics and Photonics*

- 2574 Ultra-Low Switching Power RRAM Using Hopping Conduction Mechanism  
*A. Chin, Y. Chiu, C. Cheng, Z. Zheng, and M. Liu*
- 2575 ALD Grown Functional Oxide Layers for Nonvolatile Resistive Switching Memory Applications  
*S. Hoffmann-Eifert and R. Waser*
- 2576 Hafnium Oxide Based CMOS Compatible Ferroelectric Materials  
*U. Schroeder, J. Mueller, E. Yurchuk, S. Mueller, D. Martin, S. Slesazeck, and T. Mikolajick*
- 2577 HfO<sub>2</sub>-based RRAM for Embedded Nonvolatile Memory: From Materials Science to Integrated 1T1R RRAM Arrays  
*T. Bertaude, C. Walczyk, D. Walczyk, M. Sowinska, D. Wolansky, B. Tillack, G. Schoof, C. Wenger, S. Thiess, and T. Schroeder*
- 2578 Resistive Switching of Iron Oxide Nanoparticles in Patterned Array Structure on Flexible Substrate  
*J. Kim, J. Yoo, Y. Baek, H. Kim, Q. Hu, C. Kang, and T. Yoon*

- 2579 Theoretical Perspectives in Defect and Impurity Physics toward Materials Design for Oxides  
*N. Umezawa*
- 2580 Strain-induced effects on dielectric properties of thin, crystalline rare earth oxides on silicon  
*H. Osten and D. Schwendt*
- 2581 Epitaxial Si and Gd<sub>2</sub>O<sub>3</sub> Heterostructures - Distributed Bragg Reflectors with Stress Management Function for GaN on Si Light Emitting Devices  
*R. Dargis, A. Clark, E. Arkun, R. Roucka, D. Williams, R. S. Smith, and M. Lebby*
- 2582 Room Temperature Ferromagnetism Induced by Electric Field in Cobalt-Doped TiO<sub>2</sub>  
*T. Fukumura*
- 2583 Enhancement of Dielectric Properties and Magnetic Coupling of Pb(Fe<sub>0.5</sub>Nb<sub>0.5</sub>)O<sub>3</sub> by Doping Ni<sub>0.65</sub>Zn<sub>0.35</sub>Fe<sub>2</sub>O<sub>4</sub>  
*S. K. Barik, D. K. Pradhan, S. Sahoo, V. Pauli, and R. Katiyar*
- 2584 Conduction Band-offset in GeO<sub>2</sub>/Ge Stack Determined by Internal Photoemission Spectroscopy  
*W. Zhang, T. Nishimura, K. Nagashio, K. Kita, and A. Toriumi*
- 2585 Hydrogen Interaction with HfO<sub>2</sub> Films Deposited on Ge(100) and Si(100)  
*G. V. Soares, T. Feijó, I. J. Baumvol, C. Aguzzoli, C. Krug, and C. Radtke*
- 2586 MOS Interface Control of High Mobility Channel Materials for Realizing Ultrathin EOT Gate Stacks  
*S. Takagi, R. Zhang, R. Suzuki, N. Taoka, M. Yokoyama, and M. Takenaka*
- 2587 III-V/Oxide Interfaces Investigated with Synchrotron Radiation Photoemission Spectroscopy  
*M. Tallarida*
- 2588 Unit Cell by Unit Cell Cleaning and Nucleation for ALD Gate Oxide Deposition  
*W. Melitz, T. J. Kent, E. Chagarov, M. Edmonds, T. Kaufman-Osborn, J. Sung Lee, K. Kiantaj, and A. C. Kummel*
- 2589 Scaling and Interface Control of High-k/III-V Interfaces  
*S. Stemmer, V. Choppattana, Y. Hwang, and R. Engel-Herbert*
- 2590 Effect of In<sub>0.53</sub>Ga<sub>0.47</sub>As surface Nitridation on Electrical Characteristics of High-k/Capacitors  
*Y. Suzuki, D. H. Zadeh, K. Kakushima, P. Ahmet, Y. Kataoka, A. Nishiyama, N. Sugii, K. Tsutsui, K. Natori, T. Hattori, and H. Iwai*
- 2591 Interface Dipole Cancellation in SiO<sub>2</sub>/High-k/SiO<sub>2</sub>/Si Gate Stacks  
*S. Hibino, T. Nishimura, K. Nagashio, K. Kita, and A. Toriumi*

- 2592 Phenomena of Dielectric Capping Layer Insertion into High- $\kappa$  Metal Gate Stacks in Gate-First/Gate-Last Integration  
*H. Jagannathan, P. Jamison, and V. K. Paruchuri*
- 2593 Conformal Metal Gate Process Technology for 14nm Logic Node and Below  
*A. M. Noori, A. Brand, Y. Lei, M. Chen, W. Tang, X. Lu, X. Fu, S. Ganguli, J. Anthis, D. Thompson, N. Yoshida, M. Xu, M. Chang, and S. Gandikota*
- 2594 Investigation of Mg Diffusion in Ta(N) based Electrodes on HfO<sub>2</sub> for sub-32nm CMOS Gate-Last Transistors  
*R. Gassilloud, C. Maunoury, C. Leroux, P. Chevalier, C. Dressler, F. Aussénac, F. Martin, D. Bensahel, and S. Maitrejean*
- 2595 Device-Circuit Co-design of FinFETs in Scaled Technologies  
*S. Gupta and K. Roy*
- 2596 Independent-Double-Gate FinFET SRAM Technology  
*K. Endo, S. O'uchi, Y. Liu, T. Matsukawa, and M. Masahara*
- 2597 Electrical Characterization and Reliability Assessment of Double-gate FinFETs  
*C. D. Young, K. Akarvardar, K. Matthews, M. Baykan, J. Pater, I. Ok, T. Ngai, K. Ang, M. Minakais, G. Bersuker, C. Hobbs, P. Kirsch, and R. Jammy*
- 2598 Current Status of High- $\kappa$  and Metal Gates in CMOS  
*G. D. Wilk, M. Verghese, P. Chen, and J. Maes*
- 2599 Roles of Target Composition on the Dielectric Property of RF Sputtered Bi<sub>2</sub>O<sub>3</sub>-ZnO-Nb<sub>2</sub>O<sub>5</sub> Pyrochlore Thin Film  
*K. Ko, M. Lim, B. Lee, H. Lee, and J. Choi*
- 2600 Effect of Erbium Silicide Crystallinity for Low Barrier Contact Between Erbium Silicide and n-type Silicon  
*H. Tanaka, A. Teramoto, S. Sugawa, and T. Ohmi*
- 2601 Measurement and Identification of Three Contributing Charge Terms in Negative bias Temperature Instability  
*C. Mayberry, D. D. Nguyen, C. Kouhestani, K. E. Kambour, H. P. Hjalmarson, and R. A. Devine*
- 2602 Process to Etch Ni and Pt Residues during Silicide Contact Electrode Processing using Low Temperature Aqueous Solutions  
*A. N. Duong, C. Fitz, S. Metzger, O. Karlsson, J. C. Foster, G. Nowling, V. Sih, and P. Besser*
- 2603 Correlation between Electrical and Optical Properties of Tantalum Anodic Oxide and Electron Cyclotron Resonance Etching Studies of E-beam Deposited Ta<sub>2</sub>O<sub>5</sub> Films  
*A. Kulpa and N. Jaeger*

- 2604 Area Dependence of Reliability characteristics for Atomic Layer Deposition HfO<sub>2</sub> Film under Static and Dynamic Stress  
*Y. Cheng, Y. Chang, C. Hsieh, and J. Lin*
- 2605 Characterization of Sol-Gel-Derived Crystalline HfO<sub>2</sub> -Y<sub>2</sub>O<sub>3</sub> Thin Films on Si(001) Substrates  
*H. Shimizu and T. Nishide*
- 2606 Comparison on Physical and Electrical Properties of Sputtered Ru and RuO<sub>2</sub> Gate Electrodes Grown on HfO<sub>2</sub>/Si for p-MOSFET  
*H. Kim, S. Lee, I. Yu, J. Lee, T. Park, and C. Hwang*
- 2607 MOSFETs on InP Substrate with LaAlO<sub>3</sub>/HfO<sub>2</sub> Bilayer of Different LaAlO<sub>3</sub> Thickness and Single La<sub>x</sub>Al<sub>1-x</sub>O Layer with Different La Doping Level  
*Y. Wang, Y. Chen, F. Xue, F. Zhou, Y. Chang, and J. C. Lee*
- 2608 Thiol-Ene Reaction Derived Sol-Gel Hybrid Dielectric Layer for Organic Thin Film Transistors  
*J. Kim, Y. Kim, J. Ko, and B. Bae*
- 2609 Comprehensive Study on Chemical Structures of Compositional Transition Layer at SiO<sub>2</sub>/Si(100) Interface  
*T. Suwa, A. Teramoto, T. Muro, T. Kinoshita, S. Sugawa, T. Hattori, and T. Ohmi*
- 2610 Development of Ultrathin Gold Film Tensile Testing by Floating Specimen on Water Surface  
*J. Kim, A. Nizami, H. Lee, S. Hyun, and T. Kim*
- 2611 Characterization of Stress Transfer from Process Induced Stressor Layer to Substrate in MOSFETs  
*R. Thomas, D. Benoit, A. Pofelski, L. Clement, P. Morin, D. Cooper, and F. Bertin*
- 2612 Si Nanowire Technology  
*H. Iwai*
- 2613 Fabrication of High-Quality GOI and SGOI Structures by Rapid Melt Growth Method - Novel Platform for High-Mobility Transistors and Photonic Devices -  
*H. Watanabe, Y. Suzuki, S. Ogiwara, N. Kataoka, T. Hashimoto, T. Hosoi, and T. Shimura*
- 2614 A Study of Metal Gates on HfO<sub>2</sub> using Si Nanowire Field Effect Transistors as Platform  
*Q. Li, H. Zhu, H. Yuan, O. Kirillov, D. Ioannou, J. Suehle, and C. A. Richter*
- 2615 Aggressive SiGe Channel Gate Stack Scaling by Remote Oxygen Scavenging: pFET Performance and Reliability  
*M. M. Frank, E. A. Cartier, T. Ando, S. W. Bedell, J. Bruley, Y. Zhu, and V. Narayanan*

- 2616 Interface Properties La-Silicate MOS Capacitors with Tungsten Carbide Gate Electrode for Scaled EOT  
*K. Tuokedaerhan, R. Tan, K. Kakushima, P. Ahmet, Y. Kataoka, A. Nishiyama, N. Sugii, K. Tsutsui, K. Natori, T. Hattori, and H. Iwai*
- 2617 Remote Scavenging Technology using Ti/TiN Capping Layer Interposed in a Metal/High-k Gate Stack  
*X. Ma, X. Wang, K. Han, W. Wang, and T. Ye*
- 2618 Band Lineup Issues Related with High-k/SiO<sub>2</sub>/Si Stack  
*J. Xiang, X. Wang, T. Li, C. Zhao, W. Wang, Q. Liang, J. Li, D. Chen, and T. Ye*
- 2619 Schottky Barrier Height at TiN/HfO<sub>2</sub> Interface of TiN/HfO<sub>2</sub>/SiO<sub>2</sub>/Si Structure  
*K. Han, X. Wang, W. Wang, J. Zhang, J. Xiang, H. Yang, C. Zhao, D. Chen, and T. Ye*
- 2620 SiC MOS Interface States: Similarity and Dissimilarity from Silicon  
*T. Umeda, Y. Satoh, R. Kosugi, Y. Sakuma, M. Okamoto, S. Harada, and T. Ohshima*
- 2621 Controlled Lateral Etching of Titanium Nitride in a CMOS Gate Structure using DSP+  
*J. C. Foster, S. Metzger, and P. Besser*
- 2622 The Electrochemical Kinetics of Selectively Corroding Poly-Silicon in Generating Lonely Crater-Defects  
*L. Sheng and E. Glines*
- 2623 Local-Loading Effects for Pure-Boron-Layer Chemical-Vapor Deposition  
*V. Mohammadi, W. de Boer, T. Scholtes, and L. K. Nanver*

## **E6 - High Purity Silicon 12** *ECS Electronics and Photonics*

- 2624 Challenges for the Semiconductor Industry in the 21st Century  
*P. A. Gargini*
- 2625 Si Crystal Growth from a Melt: The Secrets Behind the v/G Criterion  
*J. Vanhellemont*
- 2626 FZ Crystal Growth of Si and Ge- Current Limitations and Approaches to Overcome  
*H. Riemann, H. Rost, M. Wuenscher, R. Menzel, and B. Hallmann-Seiffert*
- 2627 Electrolytic Deposition of Silicon for Solar Application  
*S. Sokhanvaran and M. Barati*
- 2628 A Study on Density Functional Theory of the effect of Pressure on the Formation and Activation Enthalpies of Intrinsic Point Defects in Growing Single Crystal Si  
*K. Sueoka, E. Kamiyama, and H. Kariyazaki*

- 2629 Surface and Gate-Oxide Properties of a Large-Scale, <110>-oriented High-Purity CZ-Si  
*J. Lee, W. Lee, J. Kim, D. Hwang, and H. Kang*
- 2630 Schottky Barrier Height Engineering for Low Resistance Contacts to Ge and III-V Devices  
*K. Saraswat, J. Lin, A. Nainani, A. Roy, B. Yang, and Z. Yuan*
- 2631 Challenges and Opportunities for Doping Control in Ge for Micro and Optoelectronics Applications  
*E. Bruno, G. Scapellato, E. Napolitani, S. Mirabella, A. La Magna, M. Mastromatteo, D. De Salvador, S. Boninelli, G. Fortunato, V. Privitera, and F. Priolo*
- 2632 Defect Engineering at the Nanoscale: Challenges and Trends  
*E. G. Seebauer*
- 2633 Long-Range Interaction between H and (B or P) Dopant Atoms in Silicon Crystals Investigated by First Principles Calculation  
*E. Kamiyama and K. Sueoka*
- 2634 Manufacturing of Ultra Thin SOI  
*O. Bonnin, W. Schwarzenbach, V. Barec, N. Daval, X. Cauchy, B. Nguyen, and C. Maleville*
- 2635 Hybrid-Formation of Ge-on-Insulator Structures on Si Platform by SiGe-Mixing-Triggered Rapid-Melting Growth --- A Road to Artificial Crystal ---  
*M. Miyao, M. Kurosawa, K. Toko, and T. Sadoh*
- 2636 The Pseudo-MOSFET: Principles and Recent Trends  
*S. Cristoloveanu, I. Ionica, A. Diab, and F. Liu*
- 2637 Interface and Border Traps in Ge pMOSFETs  
*D. M. Fleetwood, E. Simoen, S. Francis, X. Zhang, R. Arora, E. Zhang, R. D. Schrimpf, K. F. Galloway, J. Mitard, and C. Claeys*
- 2638 Radiation Influence on Biaxial+uniaxial Strained Silicon MuGFETs  
*C. Bordallo, P. G. Agopian, J. A. Martino, E. Simoen, and C. Claeys*
- 2639 Wafer Level Statistical Evaluation of the Proton Radiation Hardness of a High-k Dielectric/Metal Gate 45 nm Bulk CMOS Technology  
*C. Claeys, S. Iacovo, D. Kobayashi, A. Mercha, A. Griffoni, P. Roussel, F. Crupi, and E. Simoen*
- 2640 Transistor-Based Extraction of Carrier Lifetime and Interface Traps in Silicon-on-Insulator Materials  
*J. A. Martino, V. Sonnenberg, M. Galeti, M. Aoulaiche, E. Simoen, and C. Claeys*
- 2641 Physical Mechanisms of Charge Pumping and DCIV Currents in Floating-Body SOI MOSFETs  
*E. Zhang, D. M. Fleetwood, R. D. Schrimpf, E. Simoen, and D. Linten*

- 2642 Lifetime-Degrading Boron-Oxygen Centres in p-types and n-type Silicon  
*V. V. Voronkov, R. J. Falster, B. Lim, and J. Schmidt*
- 2643 Impact of Oxide Precipitates on Minority Carrier Lifetime in Silicon  
*J. D. Murphy, K. Bothe, R. Krain, M. Olmo, V. V. Voronkov, and R. J. Falster*
- 2644 Comparison of the Impact of Thermal Treatments on the Second and on the Millisecond Scales on the Precipitation of Interstitial Oxygen  
*G. Kissinger, D. Kot, and W. von Ammon*
- 2645 Thermal Budget of Hydrogen-Related Donor Profiles - Diffusion Limited Activation and Thermal Dissociation  
*J. G. Laven, R. Job, H. Schulze, F. Niedernostheide, W. Schustereder, and L. Frey*
- 2646 Difficulties in Characterizing High-Resistivity Silicon  
*P. Nayak, R. Richert, and D. K. Schroder*
- 2647 Investigation of Doping Type Conversion of Hydrogen Implanted Cz-Silicon by EBIC  
*S. Kirnstötter, M. Faccinelli, P. Hadley, J. G. Laven, H. Schulze, R. Job, and W. Schustereder*
- 2648 Characterization of Deep Levels Introduced by RTA and by Subsequent Anneals in n-Type Silicon  
*D. Kot, T. Mchedlidze, G. Kissinger, and W. von Ammon*
- 2649 Deep-Level Transient Spectroscopy of MOS Capacitors on GeSn Epitaxial Layers  
*E. Simoen, B. Vincent, C. Merckling, F. Gencarelli, L. Chu, and R. Loo*
- 2650 Low Temperature Fluorinated Silicon Film Synthesis  
*D. E. Milovzorov*
- 2651 Chemical Vapor Deposition of Silicon by the Reaction of Bromosilanes and Hydrogen  
*K. Tomono, H. Furuya, S. Miyamoto, T. Ogawa, Y. Okamura, R. Komatsu, and M. Nakayama*
- 2652 Diode Characteristics and Thermal Donor Formation in Germanium-Doped Silicon Substrates  
*J. Rafi, J. Vanhellemont, E. Simoen, J. Chen, M. Zabala, and D. Yang*
- 2653 Introduction of New Materials into CMOS Devices  
*H. Iwai*
- 2654 Cu Contamination Assessment and Control in 3-D Integration  
*M. Koyanagi, K. Lee, J. Bea, T. Fukushima, and T. Tanaka*
- 2655 Modeling of Boron and Phosphorus Diffusion Gettering of Iron in Silicon  
*A. Haarahiltunen, V. Vähänissi, H. Talvitie, M. Yli-Koski, and H. Savin*

- 2656 Defect Generation in Device Processing and Impact on the Electrical Performances  
*M. Polignano, I. Mica, G. P. Carnevale, A. Mauri, E. Bonera, and S. Speranza*
- 2657 Segregation Behavior of Copper and Tantalum in Oxide Film and Si Substrate after Device Heat-treatment  
*I. Lee, S. Baek, G. Lee, U. Paik, and J. Park*
- 2658 The Characteristics of Gettering Ability in Advanced Multi-Chip Packaging Thinned Wafer  
*J. An, J. Kim, J. Kim, K. Lee, H. Kang, S. Lee, B. Moon, Y. Shin, S. Hwang, and H. Park*
- 2659 Effects of Slow Diffusivity Metallic Contaminant on Electrical Characteristic Degradation for Silicon C-MOS Image Sensor  
*G. Lee, I. Lee, S. Baek, I. Kim, and J. Park*

#### **E7 - Low-Dimensional Nanoscale Electronic and Photonic Devices 5**

*ECS Electronics and Photonics, ECS Dielectric Science and Technology, ECS Sensor*

- 2660 Syntheses of a Variety of Silicide Nanowire and Nanosheet Bundles  
*H. Tatsuoka, W. Li, E. Meng, and D. Ishikawa*
- 2661 Bottom-up Process to Fabricate Periodic Arrays of  $\beta$ -FeSi<sub>2</sub> Nanopillars for Photonic Applications  
*Y. Kaneko, M. Suzuki, K. Nakajima, and K. Kimura*
- 2662 Mn Silicide Nanowires on the Si(001)-2×1 Surface Having Anisotropic Strain Fields with Bi Nanolines  
*K. Miki, H. Liu, and J. Owen*
- 2663 A Proposal of Schottky Barrier Height Tuning Method with Interface Controlled Ni/Si Stacked Silicidation Process  
*Y. Tamura, R. Yoshihara, K. Kakushima, P. Ahmet, Y. Kataoka, A. Nishiyama, N. Sugii, K. Tsutsui, K. Natori, T. Hattori, and H. Iwai*
- 2664 High-Performance Piezoelectric Nanogenerators Based on Piezoelectric and Semiconducting Coupled Properties  
*S. Kim*
- 2665 Novel Functional Materials and Characterizations for Highly Efficient Dye-Sensitized Solar Cells  
*E. W. Diau*
- 2666 WO<sub>3</sub> Nanotubes for Effective Photoelectrochemical Water-Splitting  
*X. Zheng*
- 2667 Fabrication of Silicon Groove/Pyramid Hierarchical Structures for Solar Cell Applications  
*Z. Lin, A. Li, H. Wang, and J. He*

- 2668 Large Scale Single-Crystal Cu(In,Ga)Se<sub>2</sub> Nanotip Arrays For High Efficiency Solar Cell  
*Y. Chueh*
- 2669 GaN-based Nanorods: From High-Gain Photoconductor to Solar Hydrogen Generation  
*Y. Huang, Y. Huang, W. Tu, K. Chen, and L. Chen*
- 2670 From Organic Powders to Geometrically Well Defined Low-Dimensional Structures: A way for Unprecedented Optical and Chemical Properties  
*J. Park, H. Moon, and H. Choi*
- 2671 Hybrid Silicon Solar Cells with Hierarchical Structure for Energy Harvesting  
*W. Wei, C. Ho, S. Tai, H. Wang, A. Li, R. Chung, and J. He*
- 2672 Three-dimensional Silicon Phononic Crystal  
*Y. Lin, H. Ting, L. Chou, and L. Chen*
- 2673 One-Dimensional Semiconductor Heterostructures: Challenges and Opportunities  
*S. A. Dayeh*
- 2674 Chemical Vapor Deposited MoS<sub>2</sub> Thin Layers and Their Applications  
*L. Li*
- 2675 Epitaxial Growth of Iron-Silicide Nanodots on Si Substrates Using Ultrathin SiO<sub>2</sub> Film Technique and Their Physical Properties  
*Y. Nakamura and M. Ichikawa*
- 2676 Au@SnO<sub>2</sub> Core-Shell Nanowires: Novel Material for Gas Sensor  
*W. Liu, C. Hsu, and L. Chou*
- 2677 DC and RF Characteristics of Ga<sub>2</sub>O<sub>3</sub>/GaN Single Nanowire MOSFET  
*J. Yu, C. Li, P. Yeh, Y. Wu, and L. Peng*
- 2678 Controllable Surface Plasmon Resonance Properties of Hexagonal Close-packed Metal Nanosphere Arrays  
*H. Ting, Y. Lin, L. Chou, C. Tsai, and L. Chen*
- 2679 Surface Plasmon-Enhanced Optical Properties of Composite Materials Containing Metal Nanoparticles: Birefringence and Laser Oscillation  
*K. Tanaka, K. Fujita, S. Murai, X. Meng, Y. Moriguchi, and T. Komine*
- 2680 Nanoheterostructures of Semiconducting Nanowires for Electronic Sensors and Photodetectors  
*P. Lee*
- 2681 Implantable and Bio-Integrated Flexible GaN LED  
*K. Lee*
- 2682 Photoacoustic Emission from Local Plasmon Resonators Nanostructured by Glancing Angle Deposition  
*K. Namura, M. Suzuki, K. Nakajima, and K. Kimura*

- 2683 Field Emission of Core-Shell  $\text{Ga}_2\text{O}_3$  Nanowires  
*K. Cheng, C. Hsu, C. Hsieh, and L. Chou*
- 2684 2D Oxide Nanosheets: Controlled Assembly and Applications  
*M. Osada and T. Sasaki*
- 2685 Optical Second Harmonic Generation of Pt Nanowires Created by Shadow Deposition on  $\text{MgO}(110)$  Facetted Templates  
*G. Mizutani and Y. Ogata*
- 2686 SiO<sub>2</sub> nano- cylinder structure for low-k dielectric layer  
*R. Maeno, T. Fujii, and M. Omiya*
- 2687 Synthesis and Characterization of the Core-Shell Au/ $\text{Ga}_2\text{O}_3$  Nanowires  
*B. Wu, C. Hsu, and L. Chou*
- 2688 Horizontal-Slot Disk Resonators Incorporating Nanocrystals for Low-Cost, On-Chip Bio-Sensors  
*S. Lee, G. Kim, and J. H. Shin*
- 2689 Study of the active volume for High Bright AlGaInP-based Light Emitting Diodes  
*H. Oh*
- 2690 Near-Infrared Light Detection of n-Type  $\beta\text{-FeSi}_2$ /i-Si/p- Type Si Heterojunction Photodiodes at Low Temperatures  
*R. Iwasaki, K. Yamashita, N. Promros, S. Izumi, and T. Yoshitake*
- 2691 Single-Nanowire CMOS Inverter based on Ambipolar Si Nanowire FETs  
*H. Yuan, Q. Li, H. Zhu, H. Li, D. Ioannou, and C. A. Richter*
- 2692 Visible Light-Induced Immobilization of Gold Nanoparticles on Silicon Substrates  
*S. Mo, T. Ichii, K. Murase, and H. Sugimura*
- 2693 Fabrication of Silicon Nanowire Arrays for Photovoltaic Applications  
*H. Li, J. Tseng, S. Chiou, H. Liu, and H. Cheng*
- 2694 Ultra-Compact Photonic Circuit Components based on Propagation of Exciton Polaritons in Organic Dye Nanofibers  
*K. Takazawa, J. Inoue, and K. Mitsuishi*
- 2695 Extremely Low Electron Density in a Modulation-Doped Si/SiGe 2DEG by Effective Schottky Gating  
*J. Li, C. Huang, and J. C. Sturm*
- 2696 Influences of Hydrogen Passivation on Near-Infrared Light Detection of n-Type  $\beta\text{-FeSi}_2$ /p-Type Si Heterojunction Photodiodes  
*R. Iwasaki, K. Yamashita, N. Promros, S. Izumi, and T. Yoshitake*

- 2697 Transparent Conductive CNT/PMMA Nanocomposite Via Electrostatic Adsorption Technique  
*H. Muto, N. Hakiri, G. Kawamura, and A. Matsuda*
- 2698 Transfer Printing of Compound Semiconductor Nanostructures on Heterogeneous Substrates  
*H. Ko*
- 2699 Electrochemical Growth of Vertically Standing Ni Nanorod Arrays on Si Substrate and the Low-Dimensional Effect on Their Enhanced Cold Field Electron Emission Properties  
*A. N. Banerjee and S. Joo*
- 2700 Formation of Ge-Nanodots Capped with SiC Layer by Gas-Source MBE Using MMGe and MMSi  
*K. Yasui, Y. Anezaki, K. Sato, A. Kato, T. Kato, M. Suemitsu, Y. Narita, and H. Nakazawa*
- 2701 Extremely Stretchable Electrodes beyond Intrinsic Limit Originated from Three Dimensional Nanonetworks  
*J. Park, C. Ahn, K. Hyun, and S. Jeon*
- 2702 Synthesis and Characterizations of InGaAs Nanowire Parallel Arrays for High Performance Electronic Devices  
*J. J. Hou, N. Han, F. Wang, S. Yip, F. Xiu, T. Hung, and J. C. Ho*
- 2703 Self-Assembly of Gold Nanoparticle Arrays Covalently Bonded to Silicon Surface  
*H. Sugimura*
- 2704 Carbon Nanotube Field Emitters: Fundamental Properties and Applications  
*Y. Saito*
- 2705 Optically Pumped Lasing in Gallium Nitride Nanorods Structure  
*Y. Hsu, S. Chang, K. Sou, M. Shih, H. Kuo, K. Hsu, and C. Chang*
- 2706 Three-Dimensional Nanowire Architectures for Highly-Efficiency Photoelectrochemical Electrodes  
*X. Wang*
- 2707 Piezoelectronics of Obliquely-Aligned InN Nanorod Array  
*C. Liu and N. Ku*
- 2708 Self-organized 3-D Nanostructures for Photon Management and Cost-effective Photovoltaics  
*S. Leung, M. Yu, Q. Lin, K. Kwon, K. Ching, K. Yu, and Z. Fan*
- 2709 Optical and Surface Recombination Properties of Compound Surface Textures for Heterojunction Solar Cells  
*H. Wang, C. Lin, and J. He*

- 2710 Gold Nanoparticle 2D-Arrays Chemically Immobilized as Large-Area Near-Field Light Source

*K. Miki, K. Isozaki, T. Ochiai, T. Taguchi, and K. Nittoh*

- 2711 Light- and Energy-Harvesting Scheme Employing the Nanoscale Photon Management in the Solar Cells and the Photodetectors

*J. He*

- 2712 Self-Powered Flexible Strain Sensor

*J. Zhou*

- 2713 Thermal Properties of  $\text{In}_2\text{O}_3$  Nanowires

*C. Hsu, C. Hung, and L. Chou*

- 2714 Optical Characterization of Si Quantum Dots

*S. Hu, T. Lin, D. Tsai, and R. Liu*

#### **E8 - Processing Materials of 3D Interconnects, Damascene and Electronics Packaging 4**

*ECS Dielectric Science and Technology, ECS Electrodeposition, ECS Electronics and Photonics, ECSJ Electronics*

- 2715 Innovation Through Industry and University Collaboration

*S. Johnston*

- 2716 Heterogeneous 3D Stacking Technology Developments

*H. Ikeda*

- 2717 Metallization for 3D interconnect processing

*H. Philipsen, Y. Civale, K. Vandersmissen, M. Honore, F. Inoue, and P. Leunissen*

- 2718 3D Wafer Stacking via Bonding of Recessed Cu Damascene Structures

*C. Tan*

- 2719 3D Integration Technologies Based on Surface-Tension Driven Multi-Chip Self-Assembly Techniques

*T. Fukushima, K. Lee, J. Bea, T. Tanaka, and M. Koyanagi*

- 2720 High Aspect Ratio Silicon Etch

*B. Wu*

- 2721 Through Silicon Via (TSV) Process Using DRIE and Cathode Coupled PE-CVD

*Y. Kusuda*

- 2722 Advances in Semiconductor Metallization Technologies for New Applications and Device Scaling

*R. Preisser*

- 2723 Opportunities for Electroless Copper Deposition in Semiconductor Manufacturing

*Y. Dordi*

- 2724 Cu Electroless Deposition on Ru Barrier - Investigation of Growth Phenomena and Film Properties  
*K. Kim, T. Lim, K. Park, H. Koo, M. Kim, and J. Kim*
- 2725 Control of Adhesion Strength and TSV Filling Morphology of Electroless Barrier Layer  
*R. Arima, F. Inoue, H. Miyake, T. Shimizu, and S. Shingubara*
- 2726 The Wire Grid Polarizer made by Electro- and Electroless- Deposition Processes  
*N. Okamoto, Y. Ikeda, Y. Koyama, Y. Kawazu, T. Saito, and K. Kondo*
- 2727 Bath Stability Monitoring for Electroless Cu Seed Formation in High Aspect Ratio TSV  
*F. Inoue, H. Philipsen, S. Armini, A. Radisic, Y. Civale, P. Leunissen, and S. Shingubara*
- 2728 Via Filling Electrodeposotion of 4 $\mu$ m Diameter via by Periodical Reverse Current  
*T. Hayashi, K. Kondo, M. Takeuchi, T. Saito, N. Okamoto, M. Bunya, and M. Yokoi*
- 2729 The Effect of Polymer Additives on TSV Filling by Copper Electroplating  
*C. Lin, W. Dow, J. Lin, W. Chang, and H. Lee*
- 2730 Periodic Pulse Reverse Cu Electroplating for Through Hole Filling  
*F. Shen, W. Dow, J. Lin, W. Chang, and H. Lee*
- 2731 Copper-free Through Silicon Via Filling by Ni-W Electrodeposition  
*H. Huang, W. Dow, J. Lin, W. Chang, and H. Lee*
- 2732 High Density Copper Nucleation on Ruthenium Using Commercial Plating Chemistry and Its Application to Metallization of High Aspect Ratio Through-Silicon Vias  
*P. Shi*
- 2733 Exploration of Process Window for Fill of Sub 30 nm Features by Direct Plating  
*M. Nagar, A. Radisic, K. Stubbe, and P. Vereecken*
- 2734 The Impact of Electrolyte Acidity on Bottom-up Metallization of Copper Interconnects  
*L. Boehme, J. Wu, X. Kang, R. Preisser, and U. Landau*
- 2735 Temperature Effects on Additives Induced Polarization in Copper Electroplating of Interconnects  
*L. Boehme and U. Landau*
- 2736 Effect of Additives on Direct Copper Electrodeposition on Transition Metal Diffusion Barriers for Silicon-based Integrated Devices  
*B. Im and S. Kim*
- 2737 Superconformal Film Growth  
*T. Moffat and D. Josell*

- 2738 Multi-Scale Modeling of Direct Copper Plating on Resistive Non-Copper Substrates  
*L. Yang, A. Radisic, M. Nagar, J. Deconinck, L. Leunissen, P. Vereecken, and A. West*
- 2739 Synergistic Effects of Additives on the Filling Process of High-Aspect-Ratio TSV - Kinetic Monte Carlo Simulation -  
*Y. Fukuiage, Y. Kaneko, K. Ohara, and F. Asa*
- 2740 Ultrathin Copper Layers Deposited by Galvanic Displacement: Characterization by Atom Probe Tomography  
*J. Ai, Y. Zhang, A. C. Hillier, and K. R. Hebert*
- 2741 Simulation of Shape Evolution in Through-Mask Electrochemical Deposition  
*G. J. Wilson, P. McHugh, S. Lee, and T. L. Ritzdorf*
- 2742 Inverse Analysis of Accelerator Distribution for Through Silicon Via Filling  
*M. Hayase, T. Matsuoka, K. Otsubo, Y. Onishi, and K. Amaya*
- 2743 Cu Electroplating for Through Silicon Vias (TSVs) Filling Using a Dimensionally Stable Anode (DSA)  
*W. Hsiung, W. Dow, J. Lin, W. Chang, H. Lee, and S. Lin*
- 2744 Lead Free Solder Deposited by ECD - Material Analysis  
*T. L. Ritzdorf, S. Lee, and I. Drucker*
- 2745 Evaluation of Grain Size Distributions of 50nm Wide Cu Interconnects by X-ray Diffraction Method  
*T. Inami and J. Onuki*
- 2746 A Novel Synthesis Method of Cu Nanoparticles with High Stability and Their Applications Acting as Seed Layer of TSV  
*C. Hsieh, W. Dow, and Y. Chang*
- 2747 Halide-Free Flux Activity at Copper and Tin Surface  
*S. Vegunta, G. Qu, K. Mai, J. Nguyen, and J. Flake*
- 2748 Investigation of the Mechanism of Cu Eruption-Induced Copper Void Defects in Memory Applications.  
*K. Chung, J. Park, T. Yoon, G. Oh, D. Park, S. Kim, D. Im, D. Lee, J. Kim, M. Park, D. Kim, Y. Chung, J. Baek, S. Kwon, H. Jeong, J. Kim, S. Nam, H. Kang, and C. Chung*
- 2749 Failure Mechanism of Copper Through-Silicon Vias Under Biased Thermal Stress  
*S. Seo, J. Hwang, J. Yang, and W. Lee*
- 2750 Stability of Glassy Ta-Rh Diffusion Barriers for Cu Metallization  
*N. Dalili, Q. Liu, and D. Ivey*

- 2751 Investigation of Tetrahedral Amorphous Carbon (ta-C) as Diffusion Barrier for Advanced Cu Metallization Technology  
*X. Ma, H. Yin, Z. Fu, X. Zhang, K. Du, J. Yan, C. Zhao, D. Chen, and T. Ye*
- 2752 Positive-Tone, Aqueous-Developable, Polynorbornene Dielectric  
*B. K. Mueller, A. Grillo, E. Elce, and P. Kohl*
- 2753 Ladder-like Polymethylsilsesquioxane (PMSQ) for Interlayer Dielectric (ILD) Application  
*H. Lee, S. Hwang, and K. Baek*
- 2754 Effect of Thermal Treatment on Physical, Electrical Properties and Reliability of Porogen-Containing and Porogen-Free Ultralow-k Dielectrics  
*Y. Cheng, W. Chang, Y. Chang, and J. Leu*
- 2755 System-in-Package concept for a Carbon Nanotube resonator  
*R. Gueye, S. Lee, T. Akiyama, D. Briand, M. Muoh, C. Roman, C. Hierold, and N. de Rooij*
- 2756 Concept of Spatially Divided Deep Reactive Ion Etching of Si using Oxide Atomic Layer Deposition in the Passivation Cycle  
*F. Roozeboom, B. Kniknie, R. Knaapen, M. Smets, A. Illiberi, P. Poodt, G. Dingemans, W. Keuning, and W. Kessels*
- 2757 Adhesion Reliability Enhancement of Silicon/Epoxy/Polyimide Interfaces for Flexible Electronics  
*S. Kim and T. Kim*
- 2758 The Effects of Levelers on Copper Via Filling in 3D SiP  
*M. Jung, K. Kim, and J. LEE*
- 2759 Direct Measurement and Enhancement of Adhesion Energy of Bi-Te Thermoelectric Thin Films  
*C. Kim, S. Jeon, H. Lee, S. Hyun, and T. Kim*

**E9 - Fundamentals and Applications of Microfluidic and Nanofluidic Devices**  
*ECS Electronics and Photonics, ECS Physical and Analytical Electrochemistry, ECS Sensor*

- 2760 Molecular Dynamics Simulation of Effects of Nanoparticles on Pulmonary Surfactant  
*G. Hu, B. Jiao, and Y. Zuo*
- 2761 Molecular Theory of Fluid Transport and Electrokinetic Potential for Microfluidics and Nanofluidics  
*A. Kovalenko*
- 2762 Effect of Solvent Polarization in Nano-Confining Electric Double Layer with Finite Ion Sizes  
*S. Das and S. Mitra*

- 2763 Influence of Slippage and Charge Leakage on the Electric Field Induced Patterns in Thin Bilayers  
*K. Mondal, S. Sen, P. Kumar, and D. Bandyopadhyay*
- 2764 Insulator-based Dielectrophoresis in Microfluidics  
*X. Xuan*
- 2765 Microfluidic Cell Electrofusion Chip based on Discrete Sidewall Microelectrodes  
*N. Hu, S. Qian, S. Joo, J. Yang, and X. Zheng*
- 2766 A Microfluidic Device for Dielectric Spectroscopy of Jurkat Cells  
*A. Beskok, A. C. Sabuncu, J. Zhuang, and J. Kolb*
- 2767 Triaxial Magnetic Fields Enable Mixing and Controlled Flows in Microfluidic Devices  
*J. Martin, K. Solis, and L. Rohwer*
- 2768 Novel Non-equilibrium Electrokinetic Micromixer with Nanoporous Membrane  
*S. Hwang and S. Song*
- 2769 Template-Based Synthesis of Aligned Carbon Nanotube Arrays for Microfluidic and Nanofluidic Applications  
*M. Golshadi and M. Schrlau*
- 2770 Sensing Performance of EGFET pH Sensors with CuO Nanowires Fabricated on glass substrate  
*T. Yang, S. Chang, C. Li, and S. Chang*
- 2771 Manipulation of DNA Translocation Through Polyelectrolyte Brushes-Functionalized Nanopores  
*L. Yeh, M. Zhang, S. Qian, J. Hsu, S. Joo, and S. Tseng*
- 2772 A Low Voltage Portable Nano-Pore Electroosmotic Pump with Passive Zeta Potential Control  
*D. Gu, S. Yalcin, H. Baumgart, S. Qian, A. Beskok, and O. Baysal*
- 2773 Hyphenating Capillary Isoelectric Focusing with Gas-phase Electrophoretic Mobility Molecular Analyzer for Determination of Proteins in Human Tear Fluids  
*T. Ma and Y. Fung*
- 2774 Micro-PIV Measurements of Induced-Charge Electroosmosis Around a Metal Rod  
*A. Beskok, C. Canpolat, and S. Qian*
- 2775 Thin-Film Heat Switch Based on Electrohydrodynamic Flow in a Dielectric Fluid  
*A. H. Mueller, N. Weisse-Bernstein, M. Yazdani, R. Eppstein, and M. Hehlen*
- 2776 Carbon Nanotubes Laden Hydrogel Microsphere Preparation Using Microfluidic Device  
*T. Dang, Y. Kim, G. Kim, and S. Joo*

- 2777 Superhydrophobicity and Graphene Oxide Nanosheets to Prevent Biofouling in EWOD based Lab-on-chip Devices  
*G. Perry, F. Lapierre, Y. Coffinier, V. Thomy, and R. Boukherroub*
- 2778 Influence of Lateral Confinement on the Dewetting Induced Patterns on Chemically Patterned Surfaces  
*D. Bandyopadhyay, A. Sharma, A. Sehgal, and A. Karim*
- 2779 Spreading of a Micro-Droplet on a Physicochemically Heterogeneous Porous Medium  
*A. Kumar, V. Prasad S, T. Banerjee, and D. Bandyopahdyay*
- 2780 The Flow Transitions of a Liquid-Liquid Multiphase Flow Inside Microchannels  
*S. Timung, V. Tiwari, T. Mandal, and D. Bandyopadhyay*
- 2781 Electrohydrodynamic and Electrokinetic Instabilities in Elastic Membranes Confined Between Electrolyte Films  
*M. Dey and D. Bandyopadhyay*

#### **E10 - More than Moore**

*ECS Dielectric Science and Technology, ECS Electronics and Photonics, ECS Sensor, ECS New Technology Subcommittee*

- 2782 More Moore or More than Moore  
*C. Hobbs, K. Ang, R. Hill, C. Kang, W. Loh, K. Hummler, S. Arkalgud, P. Kirsch, and R. Jammy*
- 2783 Technology Roadmapping of ICs "More than Moore" Functional Diversification  
*B. Bader and M. Gaitan*
- 2784 Emerging Research Devices and Architectures for More-Than-Moore Applications  
*A. Chen*
- 2785 Engineering the Bio-Abio Interface to Enable Next Gen Bionics  
*A. Guiseppi-Elie, C. Kotanen, O. Karunwi, and A. Wilson*
- 2786 Enabling Long-Term Dielectrophoretic Actuation for Cell Manipulation and Analysis in Microfluidic Biochips  
*D. R. Reyes*
- 2787 Microsystem Pathways to a Greener World Using Radioisotopes  
*A. Lal*
- 2788 Superconducting Fault Current Limiter with Fast Nanosecond Switching Time for Communication System Application  
*T. Chiu, C. Shih, C. Cheng, C. Cheng, T. Huang, and T. Chang*
- 2789 High-Speed Alkaline Etching for Backside Exposure of through Silicon Vias  
*K. Yoshikawa, T. Miyazaki, N. Watanabe, and M. Aoyagi*

- 2790 Development of Novel MOSFET with Front and Back Side Electrodes for 3D-Structured Image Sensors  
*M. Goto, K. Hagiwara, Y. Iguchi, H. Otake, T. Saraya, H. Toshiyoshi, and T. Hiramoto*
- 2791 Metrology to Enable "More than Moore" Applications of Resistive Switching Devices  
*C. A. Richter, J. Tedesco, H. Jang, H. Li, O. Jurchescu, and Q. Li*
- 2792 Measurement Science for "More-Than-Moore" Technology Reliability Assessments  
*Y. S. Obeng, C. Okoro, and J. J. Kopanski*
- 2793 Multi-physics Equivalent Circuit Models for MEMS Sensors and Actuators  
*T. Konishi, K. Machida, K. Masu, and H. Toshiyoshi*
- 2794 ThruChip Interface for Heterogeneous Chip Stacking  
*T. Kuroda*
- 2795 Energy-efficient Nonvolatile Logic systems based on CMOS/spintronics Hybrid technology  
*S. Sugahara, Y. Shuto, and S. Yamamoto*
- 2796 Programmable Cell Array using Rewritable Atom Switch  
*M. Miyamura, T. Sakamoto, M. Tada, N. Banno, K. Okamoto, N. Iguchi, and H. Hada*
- 2797 Wafer Processing Photoresist Stripping Requirements  
*C. L. Arvin and G. Banerjee*
- 2798 Graphene for Nanoelectronic Device Applications  
*L. Colombo*
- 2799 Improving  $I_{on}/I_{off}$  in Bilayer Graphene Transistors by Molecular Functionalization  
*M. Cantoro, A. Nourbakhsh, A. Klekachev, I. Asselberghs, C. Huyghebaert, M. M. Heyns, and S. De Gendt*
- 2800 Integration with Diverse Functionalities on Standard CMOS  
*K. Masu*
- 2801 Heterogeneous Integration of Alternative Materials and Devices on Silicon CMOS Integrated Circuits  
*T. S. Mayer*
- 2802 New Technology Trends: Expand and Extend  
*R. Rhoades*

## **E11 - Nonvolatile Memories**

*ECS Dielectric Science and Technology, ECS Electronics and Photonics, ECSJ Electronics*

- 2803 Scalable Non-volatile Memory and Switch Device for High-Density Bipolar ReRAM Applications  
*D. Lee, M. Lee, and U. Chung*
- 2804 A Two Terminal Vertical Selector Device for Bipolar RRAM  
*S. Chopra, P. Bafna, P. Karkare, S. Srinivasan, S. Lashkare, P. Kumbhare, Y. Kim, S. Srinivasan, S. Kuppurao, S. Lodha, and U. Ganguly*
- 2805 Forming-less Interfacial Resistive Switching Mechanism of Ultra-Thin HfO<sub>2</sub> Films  
*J. Kim, I. Mok, K. Lee, Y. Kim, and H. Sohn*
- 2806 Hf Cap Thickness Dependence in Bipolar-Switching TiN\HfO<sub>2\</sub>Hf\TiN RRAM Device  
*Y. Chen, G. Pourtois, S. Clima, B. Govoreanu, L. Goux, A. Fantini, R. Degreave, G. Groeseneken, D. Wouters, and M. Jurczak*
- 2807 Material Engineering of GexSbyTez and GaxSby Phase Change Materials for High Performance Phase Change Memory  
*H. Cheng, S. Raoux, T. Hsu, C. Wu, M. BrightSky, H. Lung, and C. Lam*
- 2808 Advances in ALD GST Process and Equipment for sub-20nm PCRAM Devices : Precursor delivery, GST Gapfill and Electrical Characterization  
*Z. Karim, L. Yang, J. Mack, M. Liu, U. Weber, P. Baumann, S. Ramanathan, B. Lu, W. Czubatyj, S. Hudgens, and T. Lowrey*
- 2809 Characterisation of GeTe Phase Change Material Deposited by Plasma Assisted MOCVD  
*L. Dussault, C. Vallée, M. Aoukar, D. Jourde, and P. Michallon*
- 2810 Supercritical Fluid Deposition of Bismuth Titanate for Embedded FeRAM Applications  
*Y. Zhao, K. Jung, T. Momose, and Y. Shimogaki*
- 2811 Deposition Mechanism of Metal Oxide for FeRAM Electrode using Flow Type Supercritical Fluid Deposition Reactor  
*K. JUNG, T. Momose, and Y. Shimogaki*
- 2812 Progresses on High Density MRAMs with perpendicular MTJs and Challenges to Realize Normally-Off systems  
*H. Yoda*
- 2813 Racetrack Memory 2.0  
*S. Parkin*
- 2814 STT-MRAM Development and Its Integration with BEOL Process for Embedded Applications  
*T. Sugii, Y. Iba, M. Aoki, H. Noshiro, K. Tsunoda, A. Hatada, M. Nakabayashi, Y. Yamazaki, A. Takahashi, and C. Yoshida*

- 2815 Ohmic and Non-Ohmic ON States in Pt/Ta<sub>2</sub>O<sub>5</sub>/Cu Memristive Switches  
*P. R. Shrestha, A. Ochia, K. Cheung, J. Campbell, H. Baumgart, and G. Harris*
- 2816 Resistive Switching Characteristics of N-doped ZnO Films Using Atomic Layer Deposition  
*T. Huang, W. Chang, J. Chien, C. Kang, P. Yang, M. Chen, and J. He*
- 2817 Current Status of NAND Memories and its Future Prospect with 3D NAND Technology  
*T. Endoh*
- 2818 Analysis of the Scaling Effect on NAND FLASH Memory Cell Operation  
*R. Shirota and H. Watanabe*
- 2819 The Development of the Novel High Speed Erase Scheme for 3D Stacked NAND Flash Memory  
*W. Lin, R. Shirota, T. Kuo, N. Mitiukhina, F. Li, and C. Chang*
- 2820 Temperature Effects on Performance of nc-MoO<sub>x</sub> Embedded ZrHfO High-k Nonvolatile Memories  
*C. Lin and Y. Kuo*
- 2821 Characteristics of Nano-Crystalline Ge<sub>2</sub>Sb<sub>2</sub>Te<sub>5</sub> Material for Phase Change Memory  
*T. Ohyanagi and N. Takaura*
- 2822 Oxygen Ion based Resistive Switching in Ta<sub>2</sub>O<sub>5-x</sub>/TiO<sub>2-x</sub> Bi-Layer Frameworks for the Nonvolatile Memory Applications  
*J. Hong, Y. Bae, and A. Lee*
- 2823 Effect of Post-Annealing on the Resistance Switching Characteristic of Oxygen Modulated HfO<sub>x</sub> Films  
*K. Lee, J. Kim, S. Park, and H. Sohn*
- 2824 Perpendicular Magnetic Dipolar Interaction of Co/Pt Nanodot Arrays on Carbon Nanopost Stamps  
*S. Yoon, S. Lee, and B. Cho*
- 2825 Low-Temperature Annealed Sol-Gel Derived SONOS-Type Flash Memory  
*C. Wu and Y. Yu*
- 2826 Large Resistive Switching Phenomenon Induced by Magnetic Field in Nano Conduction Path  
*T. Kato, T. Shimizu, S. Otuka, T. Kyomi, and S. Shingubara*
- 2827 Electrical Properties of Sol-Gel Derived PbLaZrTiO<sub>x</sub> Capacitors with Nonnoble Metal Oxide Top Electrodes  
*Y. Takada, T. Tsuji, N. Okamoto, T. Saito, K. Kondo, T. Yoshimura, N. Fujimura, K. Higuchi, A. Kitajima, and A. Oshima*

- 2828 Converse Magnetoelectric effect in a Room Temperature Multiferroic  $\text{Pb}(\text{Zr}_{0.53}\text{Ti}_{0.47})_{1-x}(\text{Fe}_{0.5}\text{Ta}_{0.5})_x\text{O}_3$  Ceramic System  
*D. A. Sanchez, R. Martinez, A. Kumar, N. Ortega, G. Srinivasan, R. Katiyar, and J. Scott*
- 2829 Electric Conduction Mechanism of Resistive Switching Memory using Anodic Porous Alumina  
*S. Otsuka, T. Shimizu, S. Shingubara, N. Iwata, T. Watanabe, Y. Takano, and K. Takase*
- 2830 Pulse Switching Property of Reset Process in Resistive Random Access Memory (ReRAM) Consisting of Binary-Transition-Metal-Oxides  
*T. Moriyama, K. Kinoshita, R. Koishi, and S. Kishida*
- 2831 Physical Properties Elucidation of Filaments in  $\text{HfO}_2$ -Conducting-Bridge Random Access Memory  
*S. Haswgawa, K. Kinoshita, S. Turuta, T. Fukuhara, and S. Kishida*
- 2832 Switching Phenomena in Iron-Oxide Thin Films Deposited through Chemical Vapor Deposition  
*S. Lee, Y. You, H. Yang, J. Hwang, T. Chung, C. Kim, S. Lee, and K. An*
- 2833 Physical Picture of Filaments in Reset Process of Resistive Random Access Memory Consisting of Pt/NiO/Pt Structure  
*M. Yoshihara, K. Kinoshita, R. Ogata, and S. Kishida*
- 2834 Recent Progress in Modeling the Operation of Resistive Switching Memory Devices  
*Y. Nishi and B. Magyari-Kope*
- 2835 ReRAM  $\text{SrTiO}_3\text{-La}_{0.7}\text{Sr}_{0.3}\text{O}_3$  Multilayer Oxide Structures: Playing with Space Charge Interfaces  
*J. L. Rupp, B. Yildiz, and H. L. Tuller*
- 2836 Nonvolatile Resistance Switching in Electrodeposited  $\text{Co}_3\text{O}_4$   
*J. A. Koza, Z. He, M. Willmering, and J. Switzer*
- 2837 Fully Transparent Non-Volatile Memory Using Multi-Layer Graphene Electrode  
*P. Yang, S. Jen, W. Chang, P. Chiu, and J. He*
- 2838 Atom Movement Controlled Devices: Atomic Switches and Atom Transistor  
*T. Hasegawa and M. Aono*
- 2839 Molecular Flash Memories  
*S. Pay davosi, K. Aidala, P. Brown, P. Hashemi, T. Osedach, J. Hoyt, and V. Bulovic*
- 2840 Self-rectifying Flexible Nonvolatile Small-molecule Memory-cell Embedded with Ni Nanocrystals Surrounded by NiO Tunneling Barrier  
*H. Seung, J. Lee, J. Lee, M. Song, J. Hong, and J. Park*

- 2841 Flexible Polymer Memory-cell with Au Nanocrystals Embedded in Polystyrene  
*K. Kwon, H. Seung, D. Yang, D. Park, J. Hong, and J. Park*
- 2842 Effect of Buffer LiF Layer on Nonvolatile Memory Characteristics for Polymer Memory-cell with Au Nanocrystals Embedded in Polystyrene  
*J. Lee, K. Kwon, D. Yang, D. Park, J. Hong, and J. Park*
- 2843 Crossbar Memory Using TiO<sub>2</sub> Thin Film-based Schottky Diode and Unipolar Switching Cell  
*G. Kim, J. Lee, J. Han, S. Song, J. Seok, J. Yoon, K. Yoon, and C. Hwang*
- 2844 Direct Observation of Redox Reactions during Resistance Switching by using Synchrotron Radiation Spectroscopy  
*H. Kumigashira*
- 2845 Direct Observation of Conducting Nanofilaments in BMO Resistive Switching Memory  
*C. Kang, W. Kuo, C. Huang, W. Chang, W. Wu, Y. Chu, and J. He*
- 2846 Conditions for Formation and Rupture of Multiple Conductive Filaments in a Cu/TaOx/Pt Device  
*Y. Kang, M. Verma, T. Liu, and M. Orlowski*
- 2847 De-Process and Physical Characterization of HfO<sub>2</sub> based Resistive Memory as Studied by C-AFM  
*U. Celano, Y. Chen, D. Wouters, M. Jurczak, and W. Vandervorst*
- 2848 Fabrication of a Vertical Nanogap for Nonvolatile Memories  
*S. Furuta, Y. Masuda, T. Takahashi, M. Ono, Y. Naitoh, and T. Shimizu*
- 2849 Physical Model of Nonvolatile Resistance Switching Using Simple Nanogap Electrode  
*Y. Naitoh, M. Horikawa, H. Suga, T. Shimizu, S. Furuta, Y. Masuda, T. Sumiya, T. Takahashi, and M. Ono*
- 2850 Impact of Air on Photo-Assisted Atomic Switch  
*T. Hino, T. Hasegawa, H. Tanaka, T. Tsuruoka, Y. Okawa, T. Ogawa, and M. Aono*
- 2851 Engineering Dielectric Stacks for Charge-Trapping Non-Volatile Memory  
*H. Zhu, Q. Li, H. Li, H. Yuan, D. Ioannou, and C. A. Richter*
- 2852 Ferroelectric Nonvolatile Nanowire Memory Circuit using Single ZnO Nanowire and Ferroelectric Polymer Top Layer  
*Y. Lee, P. Jeon, K. Lee, R. Ha, H. Choi, and S. Im*

## **E12 - Photovoltaics for the 21st Century 8**

*ECS Dielectric Science and Technology, ECS Electrodeposition, ECS Electronics and Photonics, ECS Energy Technology, ECS Industrial Electrochemistry and Electrochemical Engineering, ECSJ Photoelectrochemistry*

- 2853 Microstructural Controls of a Titania Electrode for Dye-Sensitized Solar Cells  
*A. Nakamura, T. Hyodo, and Y. Shimizu*
- 2854 Rapid Synthesis of High Performance TiO<sub>2</sub> Nanoparticles for Dye-Sensitized Solar Cells Employing Microwave and Supercritical Water  
*K. Manseki, Y. Kondo, D. Ishihama, T. Ban, T. Sugiura, and T. Yoshida*
- 2855 Protonated Carboxyl Anchor for Stable Adsorption of Ru N749 dye on TiO<sub>2</sub> Anatase (101) Surface  
*K. Sodeyama, M. Sumita, and Y. Tateyama*
- 2856 High Efficiency Dye-sensitized Solar Cells Using Thin TiO<sub>2</sub> Films Co-sensitized by Indoline Dyes  
*S. MORITA, M. Ikegami, A. Ishii, and T. Miyasaka*
- 2857 Preparation of Non-annealed Anatase TiO<sub>2</sub> Films on ITO substrates by Anodizing in Hot Phosphate/glycerol  
*E. Tsuji, N. Hirata, and H. Habazaki*
- 2858 Enhanced Hole Transport in Nickel Oxide Electrodes for Photoelectrochemical Sensitized Cells  
*K. Zhu, S. Kang, N. Neale, and A. Frank*
- 2859 Alkylation of Chlorin e6 for Higher Efficiency Dye-Sensitized Solar Cells  
*X. Wang, H. Tamiaki, and S. Sasaki*
- 2860 Tin Oxide Nanowires and Their Hybrid Architectures for Kinetically Fast Redox Couples in Dye-Sensitized Solar Cells  
*V. Vendra, T. Nguyen, D. Amos, T. Druffel, and M. K. Sunkara*
- 2861 Nano-Clay Electrolyte for High Performance Dye-Sensitized Solar Cells  
*S. Uchida, T. Kubo, and H. Segawa*
- 2862 Integration of Polymer Electrolytes in Nanostructured Electrodes of Dye Sensitized Solar Cells  
*S. Nejati, D. Martin, C. Prejean, J. Deshmukh, and K. K. Lau*
- 2863 Conductivity Enhanced CuSCN for Improved Performance in Dye-Sensitized Solid-state Solar Cells  
*A. Konno, E. Premalal, and N. Dematage*
- 2864 Dye-sensitized photocapacitors fabricated with ionic liquid electrolytes for power generation and storage  
*T. Miyasaka, H. Ina, and M. Ikegami*

- 2865 Immobilization of Polymer-Protected Platinum Nanocluster on Plastic Substrate for Highly Efficient Dye-Sensitized Plastic Solar Cell  
*T. Wei, M. Ikegami, and T. Miyasaka*
- 2866 Atmospheric Processing of Dye Sensitized Solar Cell Photoanode  
*T. Druffel, V. Vendra, and R. Lupitsky*
- 2867 Electrochemical Analysis for the Realization of Low Temperature Processed ZnO Dye-Sensitized Solar Cells  
*D. T. Bryant, M. Carnie, T. M. Watson, and D. A. Worsley*
- 2868 Nanostructured Photoelectrodes for Dye Sensitized Solar Cells  
*I. Turkevych, K. Matsubara, and M. Kondo*
- 2869 Study on Central Metal Ions and Electrolytes for Efficient Porphyrin-sensitized Solar Cells  
*F. AWAI, Y. Arai, S. Uchida, T. Kubo, and H. Segawa*
- 2870 In Situ Observation of Structural Change in N719 Dye Molecule in Dye Sensitized Solar Cells under a Visible Light Exposure  
*C. Yoshida, S. Nakajima, Y. Syoji, and F. Hirose*
- 2871 Gold Nanoparticles Embedded Single Crystalline ZnO (Au NPs@ZnO) Nanowire Arrays for Plasmonic Enhanced Dye-sensitized Solar Cells (DSSCs)  
*M. Lu, H. Chen, H. Chen, C. Peng, Y. Chueh, S. Gwo, and H. Chen*
- 2872 Zinc Oxide Nano-pillar Array prepared by a Microwave-assisted Process for an Organic Photovoltaic Cell  
*N. Murakami, Y. Imoto, and T. Ohno*
- 2873 Development of Inverted Organic Photovoltaic Cells Using Amorphous Niobium Oxide as Electron Collection Layer  
*K. Hamada, N. Murakami, and T. Ohno*
- 2874 Dye-Sensitized Solar Cell Prepared with TNO Transparent Conductive Film  
*S. Takemura, R. Muramoto, Y. Sekine, M. Okuya, S. Okazaki, E. Sakai, N. Yamada, T. Hitosugi, and T. Hasegawa*
- 2875 Reliable and Secure DSSC Sub-Module Assembled by One Drop Filling Method  
*C. Nishiyama, S. Uchida, T. Kubo, and H. Segawa*
- 2876 Cu<sub>2</sub>S Counter Photocathodes for Quantum-Dot Sensitized Solar Cells  
*S. Lee and K. Ahn*
- 2877 CdS Quantum Dots Deposited by Chemical Bath Deposition for the Application to Quantum Dot-Sensitized Solar Cells  
*D. Lee and K. Ahn*
- 2878 Effects of High Pressure Annealed for Electrodeposited CuInSe<sub>2</sub> Solar Cell  
*T. Chang, W. Lee, and Y. Su*

- 2879 Organic Photovoltaics by Using a Nanoscale Thin Film of Solution-based Titanium Sub-Oxide (Solution based Titanium sub-oxide Nanoscaled Thin Films for Passivation (or Sealant) of Organic Photovoltaic Cells)  
*K. Foe, V. Potturi, M. Samson, H. Baumgart, and G. Namkoong*
- 2880 The Effect of TiO<sub>2</sub> Microstructure and Introduction of Silver Nanoparticles on Conversion Efficiency of Sb<sub>2</sub>S<sub>3</sub> Sensitized Semiconductor Solar Cells  
*S. Yoshioka, T. Mishima, and M. Ihara*
- 2881 ZnS Films Deposited by ALD for Solar Cell Applications  
*Y. Erkaya, D. Nminibapiel, N. Hegde, K. Aryal, G. Rajan, P. Boland, K. Zhang, H. Baumgart, and S. Marsillac*
- 2882 Molecular Precursors and Their Application to Chalcogenide Solar Cell  
*C. Kim, J. Park, H. Choi, B. Park, J. Song, T. Chung, and D. Jeon*
- 2883 Effect of Post-Treatment for Colloidal PbS Quantum dots on Performance of Schottky Solar Cell  
*J. Kim, J. Song, H. An, K. Kim, and S. Jeong*
- 2884 Analysis of Degradation Products in Electrolyte of Dye Sensitized Solar Cell by High Mass Accuracy MS<sup>n</sup> and Multivariate Statistical Technique  
*T. Goda, D. Nakayama, T. Nishine, S. Satoshi, C. Nishiyama, S. Uchida, and H. Segawa*
- 2885 Application of Electrochemical Impedance Spectroscopy in Characterization of Mass- and Charge Transfer Processes in Dye-Sensitized Solar Cell  
*N. T. Hoang, H. Tran, and T. Nguyen*
- 2886 Photovoltaic Properties in Al-doped ZnO/non-doped Zn<sub>1-X</sub>Mg<sub>X</sub>O/Cu<sub>2</sub>O Heterojunction Solar Cells  
*T. Minami, Y. Nishi, T. Miyata, and S. Abe*
- 2887 Two-Step Anodization for TiO<sub>2</sub> Nanotube Arrays  
*Y. Lee, J. Kim, J. Lee, and W. Choi*
- 2888 Development of a Cu<sub>2</sub>OZnO Nanorod Heterojunction Solar Cell  
*D. Marui, N. Murakami, and T. Ohno*
- 2889 Fabrication of CZTS based Solar Cells Using Nanocrystals  
*S. Suehiro, M. Yuasa, T. Tanaka, K. Fujita, S. Hata, T. Kida, and K. Shimano*
- 2890 Electrochemically Self-Assembled ZnO/Rhodamine dye Hybrid 2D-Nanostructure towards One-Pot Synthesis of Solar Cells  
*S. Lina, T. Sekiya, Y. Kimikado, and T. Yoshida*
- 2891 Improved Conversion Efficiency of CdS Quantum Dot-Sensitized Solar Cells based on Nanoporous-Layer-Covered TiO<sub>2</sub> Nanotube Arrays  
*S. Jung and K. Ahn*

- 2892 Photovoltaic Performances of p-type Nickel Oxide as Photocathode in Photoelectrochemicalsolar Cells  
*M. Park and K. Ahn*
- 2893 The Effect of CuI Layer Deposited from Various Solutions on the Performance of Dye-Sensitized Solid-State Solar Cells  
*S. Endo, T. Yamamoto, and A. Konno*
- 2894 Fabrication of Silicon and Carbon based Wide-Gap Semiconductor Thin Films for High Conversion Efficiency  
*K. Yoshinaga, H. Naragino, A. Nakahara, S. Tanaka, and K. Honda*
- 2895 Improving the Efficiency of Polymer:Fullerene Bulk Heterojunction Solar Cells by Varying the Material Concentration in the Photoactive Layer  
*M. Samson, K. Latimer, P. Boland, K. Foe, G. Namkoong, H. Baumgart, and T. M. Abdel-Fattah*
- 2896 Optical Management by Localized Surface Plasmon of Metal Nanoparticles and Application to a Solar Cell  
*K. NAM, H. Hachimura, K. Hirano, M. Ihara, P. Sichanugrist, and M. Konagai*
- 2897 Novel Method of Synthesis of Zinc Oxide Doped with Nitrogen for photocatalytic Applications  
*J. Flores, J. Valladares, and P. Nandakumar*
- 2898 FTO Film with High Haze and Transmittance Prepared for Dye-Sensitized Solar Cell  
*R. Murakami, R. Muramoto, and M. Okuya*
- 2899 Dye-Sensitized Solar Cells Based on Polyaniline - Single Waller Carbon Nanotubes Composite  
*T. M. Abdel-Fattah, S. Ebrahim, and M. Soliman*
- 2900 Electrodeposited ZnO Morphological, Structural and Optical Properties Control by Potential Sweep Rate  
*E. Matei, M. Enculescu, C. Florica, and I. Enculescu*
- 2901 Photovoltaic R&D Status and Strategy of Korea  
*C. Park*
- 2902 Size-dependent Photoelectrochemical Properties of Semiconducting Cu<sub>2</sub>ZnSnS<sub>4</sub> Nanoparticles  
*T. Torimoto, T. Osaki, T. Nagano, T. Kameyama, S. Suzuki, and S. Kuwabata*
- 2903 A New Approach to Fabricate Selenide-based Absorber Layer Uusing Stoichiometric Single Target  
*T. Kim, J. Park, S. Lee, and J. Kim*
- 2904 Smooth and Dense CuInSe<sub>2</sub> Film Growth by Selenization of Sputtered Metallic Precursors  
*J. Suh*

- 2905 CIGS Electrodeposition from Improved Electrolytes: Electrochemical Characterization and Transport Effects  
*M. A. Saeed, O. Gonzalez, and U. Landau*
- 2906 Use of Surface Chemistry Control and Low Temperature Growth Methods for Overcoming Perceived Limitations in III-Nitride Epitaxy  
*W. Doolittle, M. Moseley, B. Gunning, and G. Namkoong*
- 2907 Controlled Synthesis of Chalcogenide Nanocrystal Inks for High-Performance Photodetectors and Solar Energy Conversion  
*J. Hu, Y. Guo, and L. Wan*
- 2908 CuInS<sub>2</sub>- and Cu<sub>2</sub>ZnSnS<sub>4</sub>-based Thin Film Solar Cells Prepared from Electrodeposited Metal Stacks  
*S. Ikeda, Y. Otsuka, A. Kyoraiseki, W. Septina, T. Harada, and M. Matsumura*
- 2909 Electrodeposition of In-S based Buffer Layers for High Efficiency Cu(In,Ga)Se<sub>2</sub> based Solar Cells  
*E. Chassaing, N. Naghavi, S. Galanti, G. Renou, M. Soro, M. Bouttemy, A. Etcheberry, and D. Lincot*
- 2910 Overview of Electrodeposition Based Copper Indium Gallium Selenide (CIGS) Solar Cell Fabrication  
*S. Aksu, S. Pethe, A. Kleiman-Shwarsctein, S. Kundu, and M. Pinarbasi*
- 2911 Electrodeposition of Cu<sub>2</sub>ZnSn(S,Se)<sub>4</sub> (CZTSSe) Thin Films for the Thin film Solar Cell Application  
*K. Lee, S. Seo, and J. Kim*
- 2912 Synthesis of Phase Pure Pyrite Nanowires/Nanotubes for Solar Energy Applications  
*D. R. Cummins, H. B. Russell, J. Jasinski, and M. K. Sunkara*
- 2913 Electrodeposition of Tin (II) Sulfide from 1-Butyl-3-methylimidazolium Dicyanamide at High Temperature for Thin Film Solar Cells  
*M. Steichen, R. Djemour, D. Regesch, L. Gütay, S. Siebentritt, and P. Dale*
- 2914 Multilayer Hybrid Solar Cell using Anodic TiO<sub>2</sub> Nanotubes  
*T. Ma, R. Kojima, D. Tadaki, J. Zhang, Y. Kimura, and M. Niwano*
- 2915 Optical Property of Random Inverted-Pyramid Textures on Si Surface by Etching with N-Fluoropyridinium Salts  
*M. Otani, J. Uchikoshi, K. Tsukamoto, T. Hirano, T. Nagai, K. Adachi, K. Kawai, K. Arima, and M. Morita*
- 2916 Enhancement of Thermal and Chemical Stabilities of Gold Nanorods Embedded in Titanium Oxide Film  
*Y. Takahashi, N. Miyahara, and S. Yamada*

- 2917 Development of Organic-Inorganic Hybrid Photovoltaic Cells with Metallocene Molecular Complexes  
*A. Ishii and T. Miyasaka*
- 2918 Effect of Ag Nano-crystals on Power-conversion-efficiency Enhancement for Polymer Photovoltaic Cells  
*J. Kim, D. Kim, Y. Hwang, J. Shin, J. Park, and J. Park*
- 2919 An Analysis on Electrorefining for Solar-Grade Silicon  
*M. Tao*
- 2920 Dislocation Analysis for a New Mushroom-Shaped Growth of Large-Size Monocrystalline Silicon by Seed Casting Technique  
*B. Gao, H. Harada, Y. Miyamura, S. Nakano, and K. Kakimoto*
- 2921 Effects of Metal Contamination on Power-conversion-efficiency Degradation for p-type Silicon Solar Cell  
*S. Baek, I. Lee, H. Yoon, M. Choi, G. Lee, and J. Park*

### **E13 - Plasma Processing 19**

*ECS Dielectric Science and Technology, ECS Electronics and Photonics*

- 2922 Direct SiGe BFFT Patterning by Dry Plasma Etching  
*A. Milenin, L. Witters, B. Deweerdt, C. Vrancken, and M. Demand*
- 2923 Hydrogen Plasma-Based Etching of Copper  
*F. Wu, G. Levitin, T. Choi, and D. Hess*
- 2924 Inductively Coupled Plasma Etching of InP with Cl<sub>2</sub>/H<sub>2</sub>/Ar Plasma  
*E. A. Douglas, J. Stevens, R. Shul, and S. Pearton*
- 2925 Extreme Nano Etching  
*D. L. Olynick, Z. Liu, S. Dhuey, C. Peroz, B. Harteneck, and S. Cabrini*
- 2926 Investigation of Synchronized Pulsed Plasma for High Selective Etching of Silicon Nitride Spacers  
*R. Blanc, O. Joubert, T. David, F. Leverd, and C. Vérove*
- 2927 Systematic Approach to TDM Process Development  
*C. W. Johnson, D. Pays-Volard, L. Martinez, and J. Plumhoff*
- 2928 Advanced Dual Hard Mask Patterning Scheme to Enable High Resolution Lithography for sub 30 nm Technology Nodes  
*J. Paul, M. Rudolph, S. Riedel, S. Wege, C. Hohle, and V. Beyer*
- 2929 Towards New Plasma Technologies for 22 nm Gate Etch Processes and Beyond  
*O. Joubert*

- 2930 Precision, Damage-Free Etching and Cleaning by Electron-Enhanced Reactions: Results and Simulations.  
*H. P. Gillis, S. Anz, S. Han, J. Su, and W. Goddard III*
- 2931 Simulations of Industrial Plasma Processes: SF<sub>6</sub> Etching  
*S. Lopez-Lopez, A. Williams, D. Brown, and J. Tennyson*
- 2932 Quantum Chemical Molecular Dynamics Simulation of GaN Etching Processes by Cl Radical  
*K. Yanagiya, H. Ito, T. Kuwahara, T. Ishikawa, Y. Higuchi, N. Ozawa, T. Shimazaki, and M. Kubo*
- 2933 Dry Etching Characteristics of Palladium Thin Films Using Inductive Coupled Plasma  
*J. Kim, D. Lee, J. Kwak, S. Lee, J. Yoon, J. Yang, and J. Lee*
- 2934 Improvement in Electric Property of ITO Films at Low Temperature  
*H. Lee, Y. Han, M. Lee, J. Hur, H. Kim, and H. Lee*
- 2935 Feature Profile 2D and 3D Simulation with Etching, Deposition and Implantation Processes  
*P. Moroz*
- 2936 Preparation of Zinc Oxide Films by Coplanar Plasma Discharge Technique  
*M. Okuya, T. Hanai, M. Iyoda, and K. Nabeta*
- 2937 Preparation of Polymer Particles Coated with a Diamond-like Carbon Film by a Polygonal Barrel-Plasma Chemical Vapor Deposition Method  
*Y. Honda, S. Akamaru, M. Inoue, and T. Abe*
- 2938 Enhanced Optical and Electrical Property of ITO by Hydrogen Plasma and Post-Wet Treatment  
*D. Lee, S. Yang, J. Kim, and J. Lee*
- 2939 Low Temperature TiC Coating Process by Plasma Enhanced Chemical Vapor Deposition  
*H. Masaoka, S. Matsumoto, N. Okamoto, T. Saito, K. Kondo, and T. Kan*
- 2940 Observation of Vacancy-Induced Resistance Change in AlGaN/GaN HEMT  
*C. Cheng, T. Chang, S. Liao, W. Ho, Y. Shiau, T. Chang, and J. Sen*
- 2941 Preparation of IZO Transparent Conductive Thin Film by Microwave Heating Technique  
*S. Muto, Y. Kawabata, and M. Okuya*
- 2942 Effect of Inductively Coupled Plasma on the Electrical and Optical Properties of Indium Tin Oxide Films Deposited by Ionized Physical Vapor Deposition  
*C. Hong, J. Shin, N. Park, K. Kim, B. Kim, B. Ju, and W. Cheong*
- 2943 Deep Silicon Etching with CCP based Process Approaches for Small and Medium Size TSV Applications  
*M. Rudolph, J. Paul, and S. Wege*

- 2944 The Chemical Reaction of IGZO Thin Film as the Effect of Inert Gas in CF<sub>4</sub>/Ar Plasmas  
*Y. Joo, J. Woo, Y. Chun, and C. Kim*
- 2945 Etching Characteristics of Top Metal Electrode and IGZO channel layer in Inductively Coupled Plasma System  
*Y. Chun, Y. Joo, J. Woo, and C. Kim*
- 2946 Interplay Between Plasma Modification of Surfaces and Atomic Layer Deposition for Semiconductor Applications  
*J. Swerts, C. Adelmann, S. Armini, A. Delabie, L. Nyns, M. Popovici, M. Schaekers, P. Verdonck, and S. Van Elshocht*
- 2947 Hybrid Sublimation ECR-PECVD System for Fabrication of Rare Earth Doped Silicon Based Thin Film Structures  
*R. Dabkowski, J. Wojcik, and P. Mascher*
- 2948 Characterization and Modelling of CH<sub>4</sub>-CO<sub>2</sub> Microwave Plasmas for Nano-Smooth Diamond Coatings and Homogeneous Nano-Diamond Grain Synthesis  
*L. Vandenbulcke, T. Gries, S. de Persis, and M. Vandenbulcke*
- 2949 Charge-based Delivery of Molecules to Skin Using Atmospheric Plasmas  
*A. M. Hoff, R. Connolly, T. Chapman, J. Llewellyn, R. Gilbert, and M. Jaroszeski*
- 2950 Analysis and Applications of Nonthermal Atmospheric Plasma: High Electric Field Plasma and Plasma Discharges/Jets  
*Y. B. Manga and K. Ou*
- 2951 Evaluation of Micro Plasma formed in the Narrow Gap in Electrolyte Solution  
*H. Tamai, M. Hafner, A. Hassel, H. Tachikawa, and K. Azumi*

**E14 - Semiconductor Wafer Bonding 12: Science, Technology, and Applications**  
*ECS Electronics and Photonics*

- 2952 Direct Bonding Energy Measurement Under Anhydrous Atmosphere  
*F. Fournel, L. Continni, C. Morales, J. Da Fonseca, H. Moriceau, C. Martin Cocher, F. Rieutord, A. Barthelemy, and I. Radu*
- 2953 Study of Hydrophilic Si Direct Bonding with Ultraviolet Ozone Activation for 3D Integration  
*J. Fan, G. Chong, and C. Tan*
- 2954 Hydrophilic Wafer Bonding - An Acid/Base Concept  
*M. Reiche*
- 2955 Surface Activation for Semiconductor Wafer Direct Bonding Using Polymer-Stripping Wet Chemicals  
*R. Knechtel, H. Wünschre, and H. Klingner*

- 2956 In-situ Observation of Formation of Bonded Interface using MEMS-in-TEM at the Nanoscale  
*T. Ishida*
- 2957 Structure of Directly Bonded Interfaces Between Si and SiC  
*M. Yoshimoto, R. Araki, T. Kurumi, and H. Kinoshita*
- 2958 Influence of Interfacial Particles on Unbonded Area in Semiconductor Wafer Bonding: an Experimental Approach  
*H. Kim-Lee, A. Kim, D. Kim, J. Jeon, K. Woo, and B. Park*
- 2959 Strain Characterization of Directly Bonded Germanium-to-Silicon Substrates  
*I. P. Ferain, N. Bennett, P. McNally, S. Holl, and C. Colinge*
- 2960 The Study on Defects of Germanium-on-Insulator Fabricated by a Low Temperature Smart-Cut Process  
*X. Zhang, F. Yang, Y. Ou, T. Ye, and S. Zhuang*
- 2961 Advanced III-V Multijunction Solar Cells Fabricated by Semiconductor Wafer Bonding  
*D. C. Law, D. Bhusari, S. Mesropian, S. Singer, P. Chiu, W. Hong, R. Woo, X. Liu, C. Fetzer, A. Palmer, E. Rehder, R. King, J. Boisvert, and N. Karam*
- 2962 Development of GaInP/GaAs/Si Solar Cells using Surface Activated Wafer Bonding  
*S. Essig, K. Derendorf, E. Oliva, A. Wekkeli, J. Benick, M. Hermele, G. Siefer, A. Bett, and F. Dimroth*
- 2963 Electrical Conductivity of Direct Wafer-Bonded GaAs/GaAs Structures for Wafer-Bonded Tandem Solar Cells  
*K. Yeung, J. Mc Kay, C. Roberts, and M. Goorsky*
- 2964 Cu Surface Passivation with Self-Assembled Monolayer (SAM) and Its Application for Wafer Bonding at Moderately Low Temperature  
*C. Tan and D. Lim*
- 2965 Evaluation of Titanium Direct Bonding Mechanisms  
*F. Baudin, L. Di Cioccio, P. Gergaud, N. Chevalier, V. Delaye, D. Mariolle, J. Fabbri, B. Imbert, and Y. Bréchet*
- 2966 A New Combined Process of Formic Acid Pretreatment for Low-temperature Bonding of Copper Electrodes  
*W. Yang, M. Akaike, M. Fujino, and T. Suga*
- 2967 Low-Temperature Cu-Cu Wafer Bonding  
*B. Rebhan, G. Hesser, J. Duchoslav, V. Dragoi, M. Wimplinger, and K. Hingerl*
- 2968 Advanced Heterogeneous Integration of InP HBT and CMOS/SiGeBiCMOS Technologies  
*A. Gutierrez-Aitken, P. Chang-Chien, B. Oyama, D. Scott, K. Hennig, E. Kaneshiro, P. Nam, K. Thai, B. Poust, A. K. Oki, and R. Kagiwada*

- 2969 Wafer Level 3D Stacking using Smart CutTM and Metal-Metal Direct Bonding Technology  
*L. Di Cioccio, F. Mazen, F. Baudin, A. Mounier, T. Lacave, V. Delaye, B. Imbert, N. Chevalier, M. Denis, G. Gaudin, I. Radu, S. Thieffry, and T. Signamarcheix*
- 2970 Cu-Sn Transient Liquid Phase Wafer Bonding: Process Parameters Influence on Bonded Interface Quality  
*C. Floetgen, K. Corn, M. Pawlak, and V. Dragoi*
- 2971 Laser Transmission Bonding of Silicon with Titanium and Copper Layer for Wafer-Level Packaging  
*A. Wissinger, M. Schmitz, A. Olowinsky, A. Gillner, and R. Poprawe*
- 2972 Mechanics of Wafer Bonding and Layer Transfer Processes  
*K. T. Turner*
- 2973 A Study of Factors Influencing Micro-Chevron-Testing of Glass Frit Bonded Interfaces  
*F. Naumann, S. Brand, D. Wiinsch, P. Czurratis, and M. Petzold*
- 2974 Failure Mechanisms and Mechanical Characterization of Reactive Bonded Interfaces  
*B. Boettge, F. Naumann, F. Schippel, and M. Petzold*
- 2975 Low Temperature Fusion Wafer Bonding Quality Investigation for Failure Mode Analysis  
*V. Dragoi, P. Czurratis, S. Brand, A. Graff, C. Patzig, and M. Petzold*
- 2976 Using of Different Nano Scale Energetic Material Systems for Reactive Bonding  
*J. Braeuer, J. Besser, M. Wiemer, and T. Gessner*
- 2977 Integrating Laser Diode and Optical Isolator by Photosensitive Adhesive Bonding  
*H. Yokoi, N. Ichishima, and I. Myouzenzono*
- 2978 Room Temperature Wafer Bonding by Surface Activated ALD- Al<sub>2</sub>O<sub>3</sub>  
*Y. Li, S. Wang, B. Sun, H. Chang, W. Zhao, X. Zhang, and H. Liu*
- 2979 Interface Morphology and Electrical Properties of Bonded GaAs/GaAs Wafers at Different Temperatures  
*S. Chang and Y. Wu*
- 2980 Multi-Wavelength High Resolution Micro-Raman and Optical Reflectance Characterization of Nano-Scale Strained Silicon-on-Insulator Substrates  
*T. Kim, T. Shim, W. Yoo, and J. Park*
- 2981 Advanced Process Control in Megasonic- Enhanced Pre-Bonding Cleaning  
*D. Dussault, F. Fournel, and V. Dragoi*
- 2982 Glass Direct Bonding  
*G. Kalkowski, C. Rothhardt, R. Eberhardt, P. Jobst, and M. Schürmann*
- 2983 Quality Control of Bond Strength in Low-Temperature Bonded Wafers  
*J. Siegert, C. Cassidy, F. Schrank, R. Gerbach, F. Naumann, and M. Petzold*

- 2984 Micro-Structural Analysis of AlN Wafer Bonding and Hydrogen Ion-Induced Splitting for Film Exfoliation  
*M. Mamun, K. Taplyi, O. Moutanabbir, D. Gu, H. Baumgart, and A. Elmustafa*
- 2985 The Effects of Composition and Design of Experiment on the Quality of Al-Ge Eutectic Bonding for Wafer Level Packaging  
*X. Huang, C. Cheng, P. Liu, Y. Hsieh, L. Chao, C. Tsai, D. Huang, and C. Colinge*
- 2986 High Resolution Double-Crystal X-ray Diffraction Imaging for Interfacial Defect Detection in Bonded Wafers.  
*S. Sharma and M. Goorsky*
- 2987 Optimization of H<sub>+</sub> Implantation Parameters for Exfoliation of 4H-SiC Films  
*V. P. Amarasinghe, L. Wielunski, A. Barcz, L. C. Feldman, and G. K. Celler*
- 2988 Plasma Activation as a Pretreatment Tool for Low-Temperature Direct Wafer Bonding Materials in Microsystems Technology  
*M. Eichler, P. Hennecke, K. Nagel, M. Gabriel, and C. Klages*
- 2989 Mechanisms for Ultra-Low Temperature Plasma Activated Direct Wafer Bonding  
*T. Plach, K. Hingerl, V. Dragoi, and M. Wimplinger*
- 2990 Treatments of Deposited SiO<sub>2</sub> Surfaces Enabling Low Temperature Direct Bonding  
*C. Rauer, H. Moriceau, F. Fournel, A. Charvet, C. Morales, N. Rochat, L. Vandroux, F. Rieutord, T. McCormick, and I. Radu*
- 2991 Room Temperature Bonding of Polymer to Glass Wafers using Surface Activated Bonding (SAB) Method  
*T. Matsumae, M. Nakano, Y. Matsumoto, R. Kondo, and T. Suga*
- 2992 Cost-effective layer transfer by Controlled Spalling Technology  
*S. W. Bedell, D. Shahrjerdi, K. Fogel, P. Lauro, B. Hekmatshoar, N. Li, J. Ott, and D. Sadana*
- 2993 Development of Porous InP for Subsequent Epitaxial Layer Transfer onto Flexible Substrates  
*X. Kou and M. Goorsky*
- 2994 Effect of Two-step Oxidation in Ge Condensation on Surface Roughness Property of Relaxed SiGe layer-on-insulator Substrates  
*T. Shim, T. Kim, D. LEE, R. Okuyama, and J. Park*
- 2995 Advanced Characterization of a Direct Wafer Bonding-compatible Germanium Exfoliation Process  
*I. P. Ferain, X. Kou, C. Moulet-Ventosa, M. Goorsky, and C. Colinge*
- 2996 Low-Temperature Bonding Technologies for Photonics Applications  
*E. Higurashi*

- 2997 Adhesive Wafer Bonding Applied for Fabrication of True-Chip-Size Packages for SAW Devices  
*T. Heuser, C. Bauer, V. Dragoi, and G. Mittendorfer*
- 2998 Distortion Free Wafer Bonding Technology for Backside Illumination Image Sensors  
*M. Broekaart, A. Castex, K. Landry, R. Fontaniere, and C. Lagache-Blanchard*
- 2999 Monitoring Inner Pressure of MEMS Devices Sealed by Wafer Bonding  
*R. Knechtel, S. Hering, and S. Dempwolf*
- 3000 Chemical-Mechanical Polishing YAG For Wafer Bonding  
*J. Mc Kay, C. Moulet-Ventosa, and M. Goorsky*

**E15 - State-of-the-Art Program on Compound Semiconductors 54 (SOTAPoCS 54)**  
*ECS Electronics and Photonics, ECS Luminescence and Display Materials*

- 3001 Progress in Nonpolar and Semipolar GaN Materials and Devices  
*J. S. Speck*
- 3002 Study of Protein-Peptide Binding Affinity Using AlGaN/GaN High Electron Mobility Transistors  
*C. Huang, G. Lee, J. Chyi, H. Cheng, C. Hsu, Y. Hsu, F. Ren, and Y. Wang*
- 3003 Science Challenges of Ultra-Efficient Solid-State Lighting  
*M. H. Crawford and J. Tsao*
- 3004 InGaN/GaN Nanostructure Arrays for LEDs  
*T. Yeh, Y. Lin, and P. D. Dapkus*
- 3005 Wide Bandgap Semiconductors for Sensing within Extreme Harsh Environments  
*D. G. Senesky*
- 3006 ZnS-based Nanostructures: An Unique UV-Light Sensor  
*X. Fang, L. Hu, and L. Wu*
- 3007 Detection of SARS Coronavirus Nucleocapsid Protein Using AlGaN/GaN High Electron Mobility Transistors  
*Y. Hsu, G. Lee, J. Chyi, C. Chang, C. Huang, C. Hsu, T. Huang, F. Ren, and Y. Wang*
- 3008 n-type Nanostructures / p- GaN or Si Thin Film Positioned by Non-Uniform Electric Field  
*J. Kim*
- 3009 Resistive Switching in Zinc-Tin-Oxide and Atomic Layer Deposition of Nanolaminates for Amorphous Oxide Semiconductor Thin Film Transistors  
*J. Conley Jr.*
- 3010 Impurity-Induced Disorder in Si- and Mg-doped AlGaN-AlN Superlattices  
*A. Allerman, J. Wierer, Q. Li, M. H. Crawford, and S. Lee*

- 3011 III-Nitride Growth by PAMBE and Characterizations Towards Green Energy Applications  
*L. Tu, Y. Lin, C. Chang, P. Wadekar, T. Chen, and T. Deng*
- 3012 Phosphor-Free Green and Yellow LEDs in Nano-Patterned and Polarization Controlled Epitaxy  
*C. Wetzel and T. Detchprohm*
- 3013 Improved Hydrogen Sensing Performance of AlGaN/GaN based sensor with Platinum Nanonetworks  
*S. Jang, H. Kim, S. Pearson, and F. Ren*
- 3014 Revisiting Impurity Doping of III-Nitride Materials for Optical and Magnetic Device Applications  
*J. M. Zavada*
- 3015 Effects of Proton Irradiation on the Reliability of InAlN/GaN High Electron Mobility Transistors  
*L. Liu, C. Lo, Y. Xi, Y. Wang, H. Kim, H. Kim, S. Pearson, O. Laboutin, Y. Cao, J. Johnson, I. Kravchenko, and F. Ren*
- 3016 Efficiency Droop in GaN-based Light-Emitting Diodes: Mechanisms and Solutions  
*J. Kim, S. Hwang, J. Park, D. Kim, J. Cho, and E. Schubert*
- 3017 GaN HEMT Degradation: Effect of RF Stress  
*E. A. Douglas, B. Gila, F. Ren, C. Abernathy, and S. Pearson*
- 3018 A Survey of Electrical Signatures Characteristic of Step-Stressed InGaP/GaAs HBTs  
*A. G. Baca, A. J. Scruggs, A. Gorenz, T. R. Fortune, J. F. Klem, R. D. Briggs, J. B. Clevenger, G. A. Patrizi, and C. T. Sullivan*
- 3019 Direct Die Solder of GaAs Power Amplifier Dies and Application of Electrolessly Plated Nickel Barrier  
*H. Shen and S. Maganti*
- 3020 Resistive Switching Characteristics of N-doped ZnO Films Using Atomic Layer Depsition  
*T. Huang, W. Chang, J. Chien, C. Kang, P. Yang, M. Chen, and J. He*
- 3021 Influence of Catalytic Effect on Transport Behaviors of InAs NWs For High Performance Nanoscale Transistors  
*Y. Chueh*
- 3022 Semiconductor Nanostructure Direct-Write Using Scanning Probes and Conducting Stamps  
*M. Rolandi*
- 3023 CMOS-Compatible Precise Placement of Ge Quantum Dots for Nanoelectronic, Nanophotonic, and Energy Conversion Devices  
*K. Chen, I. Chen, C. Wang, and P. Li*

- 3024 Why <111>A Pore Propagation Occurs in InP and the Mechanism that Dictates Pore Width  
*R. Lynch, N. Quill, C. O'Dwyer, S. Nakahara, and D. Buckley*
- 3025 TiC Electrode Formed by Multi-Stacking Process for Diamond Contact Metal  
*Y. Tanaka, K. Kakushima, P. Ahmet, Y. Kataoka, A. Nishiyama, N. Sugii, K. Tsutsui, K. Natori, T. Hattori, S. Yamasaki, and H. Iwai*
- 3026 Application of Inline X-ray Metrology for Defect Characterization of III-V/Si Heterostructures  
*P. Hung, M. Wormington, K. Matney, P. Ryan, K. Dunn, A. Wang, R. Hill, M. Wong, J. Price, W. Wang, and G. Bersuker*
- 3027 Advanced Compound Semiconductor and Silicon Fabrication Techniques for Next-Generation Solar Power Systems  
*G. N. Nielson*
- 3028 Improvement in Etching Rate of Epilayer Lift-Off for High Concentrated Solar Cell Applications with Low Surface Tension Fluid  
*R. Horng, F. Wu, and M. Tseng*
- 3029 Band Offsets in Dielectric/InGaZnO<sub>4</sub> Heterojunctions  
*H. Cho, K. Kim, E. A. Douglas, B. P. Gila, V. Craciun, E. S. Lambers, F. Ren, and S. Pearton*
- 3030 Anodic Formation of Porous InP in KCl Solutions  
*N. Quill, R. Lynch, C. O'Dwyer, and D. Buckley*
- 3031 Cytotoxicity Study of Zinc Oxide Nanoparticles Modified with Biological Coatings  
*R. Chung, W. Wei, R. Lin, W. Shih, and H. Wang*
- 3032 4H-SiC Lateral JFET for Low Power Operational Amplifier Applications  
*W. Lien, D. G. Senesky, and A. Pisano*
- 3033 Visible-Blind Ultraviolet Photodetector Fabricated on n-ZnO/LaAlO<sub>3</sub>/p-Si Heterojunction  
*D. Tsai, C. Kang, H. Wang, Y. Chu, and J. He*
- 3034 VCSELs for Atomic Clocks  
*D. K. Serkland, K. Geib, and G. Peake*
- 3035 Oxide-Semiconductor-Based TFTs for Displays and Flexible Electronics  
*C. Wu*
- 3036 Direct Observation of Conducting Nano filaments in BMO Resistive Switching Memory  
*C. Kang, W. Kuo, C. Huang, W. Chang, W. Wu, Y. Chu, and J. He*
- 3037 Bloch Oscillations in Two-Dimensional Antidot Arrays  
*W. Pan*

- 3038 Single Donor Devices for Quantum Computing  
*M. Carroll, E. Bielejec, N. Bishop, J. Dominguez, and M. Lilly*
- 3039 Sulfide Quantum Dots as a Sensitizer for Titanium Dioxide Photoanodes of Solar Cells  
*T. Li, C. Lin, and H. Teng*
- 3040 Multi-Shelled Metal Oxide Hollow Microsphere: Design, Preparation and Property  
*Z. Dong, R. Yu, and D. Wang*
- 3041 Fully Transparent Non-Volatile Memory Using Multi-Layer Graphene Electrode  
*P. Yang, S. Jen, W. Chang, P. Chiu, and J. He*
- 3042 Hybrid Silicon Solar Cells with Hierarchical Structure for Energy Harvesting  
*W. Wei, C. Ho, S. Tai, H. Wang, A. Li, R. Chung, and J. He*

**E16 - Thin Film Transistors 11 (TFT 11)**  
*ECS Electronics and Photonics*

- 3043 Transparent Amorphous Oxide Semiconductor TFTs: History and current status  
*H. Hosono*
- 3044 Top-Gate effects in Dual-Gate Amorphous InGaZnO<sub>4</sub> Thin-Film Transistors  
*K. Takechi, S. Iwamatsu, T. Yahagi, Y. Watanabe, S. Kobayashi, and H. Tanabe*
- 3045 Deposition of Low Stress Amorphous Zinc Tin Oxide at Ambient Temperature using a Remote Plasma Sputtering Process Suitable for Delicate Substrates  
*S. M. Pfaendler, G. Ercolano, J. Driscoll, and A. J. Flewitt*
- 3046 MgZnO/ZnO Heterostructure Field-Effect Transistors Fabricated by RF-Sputtering  
*B. Wang, I. Cheng, and J. Chen*
- 3047 a-InGaZnO Thin-Film Transistor with Non-Vacuum Processed InGaZnO/AlOx Gate Dielectric Stack  
*M. Furuta, T. Kawaharamura, T. Toda, and W. Dapeng*
- 3048 Simple Aqueous Solution Route for Fabrication of High Performance Oxide TFT  
*B. Bae, Y. Hwang, J. Seo, and G. Choi*
- 3049 Fabricating Multiple Channeled Zinc Oxide Thin Film Transistor via Sol-Gel Method  
*G. Chiou, S. Liu, S. Chen, and H. Chen*
- 3050 Improvement of Solution-Processed Oxide Thin-Film Transistors by Ultra-Violet Treatment  
*J. Lee, S. Song, D. Kang, Y. Kim, J. Kwon, and M. Han*
- 3051 Light and Bias Induced Defects in a-IGZO Thin Film Transistors  
*P. Migliorato, M. Seok, J. Um, M. Chowdhury, and J. Jang*

- 3052 Improvement of the Photo-Bias Stability of Zn-Sn-O Field effect Transistors by an Ozone Treatment  
*B. Yang, S. Oh, Y. Kim, and H. Kim*
- 3053 Improvement in the Photo-Induced Bias Instability of Oxide TFT by Controlling Sub-Gap States  
*K. Son, T. Kim, J. Park, H. Kim, S. Seo, J. Seon, K. Ji, J. Jeong, H. Lee, S. Im, M. Ryu, and S. Lee*
- 3054 Mixed Oxide Thin Film Transistors Under Combinatory Optical Irradiation and Electrical Bias  
*T. L. Alford, R. Vemuri, and W. Mathews*
- 3055 The effect of Zn/Sn Ratio on the Electrical Performance of Amorphous ZrZnSnO (ZZTO) Thin Film Transistors by RF Sputtering  
*I. Chiu, I. Cheng, and J. Chen*
- 3056 Twenty five Years of Improvement of the Silicon Based TFT: From As-Deposited Polycrystalline Silicon to Nanostructured Silicon Deposited at Very Low Temperature  
*T. Mohammed-Brahim and O. Bonnaud*
- 3057 Beyond the Current Horizontal of Silicon Thin Film Technology: Light-Soaking Free Nano-Crystal Embedded Polymorphous Silicon Thin Film and TFT by Neutral Beam Assisted CVD at Room Temperature  
*M. Hong and J. Jang*
- 3058 Impacts of Channel Thickness on the Characteristics of N-Type Planar Junctionless Poly-Si Thin-Film Transistors  
*C. Lin, H. Lin, and T. Huang*
- 3059 Grain Growth Control during Micro-Thermal-Plasma-Jet Irradiation Using Amorphous Si Strips and Slit Masks  
*Y. Fujita, S. Hayashi, K. Sakaike, and S. Higashi*
- 3060 Decreasing the Off-Current for Vertical TFT by Using an Insulating Layer between Source and Drain  
*P. Zhang, E. Jacques, R. Rogel, and O. Bonnaud*
- 3061 Thick Single Grain Silicon Formation with Microsecond Green Laser Crystallization  
*A. Arslan, H. Kahlert, P. Oesterlin, D. Mofrad, R. Ishihara, and C. Beenakker*
- 3062 Single-Grain Si TFTs Fabricated by Liquid-Si and Long-Pulse Excimer-Laser  
*R. Ishihara, J. Zhang, M. Trifunovic, M. van der Zwan, H. Takagishi, R. Kawajiri, T. Shimoda, and C. Beenakker*
- 3063 Materials, Processing, and Characterization for Printed Flexible Electronics  
*W. S. Wong*

- 3064 Investigation of Transfer Mechanism of Si Film with Mid-Air Structure Induced by Near-Infrared Semiconductor Diode Laser Irradiation  
*K. Sakaike, Y. Kobayashi, S. Nakamura, M. Akazawa, and S. Higashi*
- 3065 Modes of Operation and Optimum Design for Application of Source-Gated Transistors  
*R. A. Sporea, J. M. Shannon, and S. Silva*
- 3066 CVD Produced Graphene/Silicon Nitride TFTs  
*W. I. Milne, M. T. Cole, P. Kidambi, K. Ying, M. Drapeko, S. Hofmann, and A. Nathan*
- 3067 Characterization and Modeling of Organic Field-Effect Transistors  
*G. Horowitz*
- 3068 Carrier Behavior in a Highly-Doped P3HT Layer and Its Application to Organic Thin Film Transistors  
*D. Tadaki, T. Ma, J. Zhang, S. Iino, Y. Kimura, and M. Niwano*
- 3069 High Performance Low-Voltage Organic Phototransistors: Interface Modification and the Tuning of Electrical, Photosensitive and Memory Properties  
*X. Liu, G. Dong, L. Duan, L. Wang, and Y. Qiu*
- 3070 Influence of Annealing Conditions on the Bias Temperature Stability of MgZnO TFTs  
*Y. Tsai, J. Chen, and I. Cheng*
- 3071 Comparative Study of  $\text{In}_2\text{O}_3$ , ZnO and In-Zn-O Source Solutions for Oxide Channel Thin Film Transistors  
*E. Tokumitsu, T. Shimizu, K. Haga, and T. Shimoda*
- 3072 Thin-Film Transistor Using Dielectrophoretic Assembly of Single-walled Carbon Nanotubes  
*T. Toda, T. Kawaharamura, H. Furusawa, and M. Furuta*
- 3073 Degradation of p-Channel Low Temperature Poly-Si TFTs with Positive Source Pulse Stress  
*H. Liu, S. Chiou, P. Chan, C. Kung, F. Wang, and T. Kang*
- 3074 Simple Patterning Process of the Polymer Source/Drain electrodes for Organic Thin-Film Transistors  
*Y. Jang*
- 3075 Influence of Polymer Dielectric Surface Energy on Thin-Film Transistor Performance of Solution-Processed Triethylsilylethynyl Anthradithiophene (TES-ADT)  
*L. Chen, P. Lin, C. KIM, M. Chen, P. Huang, J. Ho, and C. Lee*
- 3076 Study of Electronic Structure and Film Composition at Back Channel Surface of Amorphous In-Ga-Zn-O Thin Films  
*A. Hino, T. Kishi, S. Morita, K. Hayashi, and T. Kugimiya*

- 3077 Performance Variations of Amorphous-In<sub>2</sub>Ga<sub>2</sub>ZnO<sub>7</sub> Thin-Film Transistors According to Thin Al<sub>2</sub>O<sub>3</sub> Passivation Layer Deposited by Atomic Layer Deposition  
*S. Rha, U. Kim, J. Jung, W. Jeon, Y. Yoo, E. Hwang, B. Park, and C. Hwang*
- 3078 Chemical-Structure Tailored, High Performance Indium Gallium Zinc Oxide Thin-Film Transistors  
*S. Jeong, J. Lee, Y. Seo, S. Choi, Y. Choi, and B. Ryu*
- 3079 Electrospray Deposited Semiconducting Oxide Thin Films For Display Backplane TFT Application  
*S. LEE and C. Hwang*
- 3080 Low-Temperature, Aqueous Solution Processed Amorphous Indium Oxide Thin Film Transistors  
*K. Choi, S. Chang, T. Oh, S. Jeong, K. Lee, Y. Kim, H. Ha, and B. Ju*
- 3081 Characteristics of Nanocrystalline Silicon Films Deposited by Cat-CVD Below 100 °C  
*T. Song, K. Keum, S. Kang, J. Park, J. Kim, and W. Hong*
- 3082 Influence of Thermal Stress and Kinetic Bias Stress on The Electrical Performance of Mixed Oxide Thin Film Transistors  
*T. L. Alford, S. Husein, and R. Vemuri*
- 3083 Composition Dependence of the Negative Bias Light Illumination Instability of Indium Zinc Oxide Transistors  
*S. Oh, B. Yang, Y. Kim, and H. Kim*
- 3084 SKPM Study on Oxide TFT  
*J. Park and H. Cha*
- 3085 The Change of Electrical Performance and Stability of Ti, B-doped In-Zn Oxide Thin Film Transistors Depending on Gate Insulators  
*B. Kim, J. Shin, C. Hong, K. Kim, N. Park, and W. Cheong*
- 3086 Aqueous Inorganic Inks for Low Temperature Fabrication of Metal Oxide-Based High-Mobility Transparent Thin-Film Transistors  
*C. Liu, W. Lee, and T. Shih*
- 3087 Channel Width and Channel Length Dependencies in Amorphous-Oxide-Semiconductor Thin-Film Transistors: From a Device Structure Perspective  
*M. Mativenga, J. Um, R. Mruthyunjaya, J. Chang, G. Heiler, T. Tredwell, and J. Jang*
- 3088 Ambipolar SnO Thin-Film Transistors and Inverters  
*L. Liang and H. Cao*
- 3089 Structure and Material Considerations for Thin Film Transistor Applications beyond LCD Driving  
*Y. Kuo*

- 3090 Issues of Backplane Technologies for AMOLED  
*S. Lee, J. Lee, and M. Han*
- 3091 A Novel LTPS TFT Pixel Circuit for Compensating IR Drop of Large Area AMOLED Display  
*S. Lee, S. Kuk, S. Song, M. Song, and M. Han*
- 3092 Memory Thin Film Transistor with Monolayered Nanoparticles through Chemical and Biological Bindings  
*H. Lee, H. Jung, M. Kim, Y. Kim, S. Oh, and T. Yoon*
- 3093 High Mobility Oxide TFT  
*S. K. Park, M. Ryu, H. Oh, C. Hwang, S. Yang, and S. Lim*
- 3094 Nanocrystal Floating Gate Memory with Indium-Gallium-Zinc-Oxide Channel and Pt-Fe<sub>2</sub>O<sub>3</sub> Core-Shell Nanocrystals  
*S. Lee, Q. Hu, J. Lee, Y. Baek, H. Lee, and T. Yoon*
- 3095 Transparent Amorphous Oxide Semiconductors for System on Panel Applications  
*P. Liu, L. Chu, L. Teng, Y. Fan, and C. Fuh*
- 3096 Thin-Film Transistors on Germanium-on-Glass Substrate  
*R. G. Manley and T. Chuang*
- 3097 Dual In-Plane-Gate Thin-Film Transistors Gated by Chitosan on Paper Substrates  
*Q. Wan and W. Dou*
- 3098 Highly Stable IGZO TFT with Electro-Less Ni Plated Cu Electrodes  
*S. Nam, T. Moon, K. Lee, K. Lee, S. Yoo, W. Shin, and S. Im*
- 3099 Laser Patterned Junctionless In-Plane-Gate Oxide Thin-Film Transistors Arrays  
*L. Zhu and Q. Wan*
- 3100 The Stability and Reliability of Mixed Oxide-Based Thin Film Transistors Under Gamma Irradiation  
*T. L. Alford, A. Indluru, and K. E. Holbert*

**E17 - SiGe, Ge, and Related Compounds: Materials, Processing, and Devices 5**  
*ECS Electronics and Photonics*

- 3101 Advanced CMOS Scaling and FinFET Technology  
*E. J. Nowak*
- 3102 FinFET--How to Make a Very Short Channel MOSFET  
*C. Hu*

- 3103 Effect of Fin Doping Concentration on the Electrical Characteristics of Germanium-on-Insulator Multi-Gate Field-Effect Transistor  
*B. Liu, X. Gong, C. Zhan, G. Han, N. Daval, C. Veytizou, D. Delprat, B. Nguyen, and Y. Yeo*
- 3104 Germanium Gate-All-Around FETs on SOI  
*H. Chang, S. Hsu, C. Chu, W. Tu, Y. Chen, P. Sung, G. Luo, and C. Liu*
- 3105 Selective Growth Of Strained Ge Channel On Relaxed SiGe Buffer In Shallow Trench Isolation For High Mobility Ge Planar And Fin p-FET  
*B. Vincent, L. Witters, O. Richard, A. Hikavyy, H. Bender, R. Loo, M. Caymax, and A. Thean*
- 3106 Stress Techniques and Mobility Enhancement in FinFET Architectures  
*G. Eneman, L. Witters, J. Mitard, G. Hellings, A. De Keersgieter, D. Bruno, A. Hikavyy, B. Vincent, E. Simoen, P. Favia, H. Bender, A. Veloso, T. Chiarella, G. Boccardi, M. Kim, M. Togo, R. Loo, K. De Meyer, N. Horiguchi, N. Collaert, and A. Thean*
- 3107 Advanced Transistor Architectures for Half-Terahertz SiGe HBTs  
*B. Heinemann, A. Fox, and H. Rücker*
- 3108 Understanding the Effects of Epitaxy Artifacts on SiGe HBT Performance through Detailed Process/Device Simulation  
*R. Camillo-Castillo, Q. Liu, P. Cheng, J. Adkisson, and D. Harame*
- 3109 Improved Frequency Response in a SiGe npn Device through Improved Dopant Activation  
*J. Adkisson, M. Khater, J. Gambino, P. Cheng, V. Jain, R. Camillo-Castillo, C. Lavoie, A. Sutton, O. Gluschenkov, Q. Liu, T. McDevitt, S. Engelmann, J. Pekarik, and D. Harame*
- 3110 Evaluation of RF Noise Source Relative Importance in SiGe HBTs Using Various Noise Representations  
*Z. Xu and G. Niu*
- 3111 Strained Silicon Heterojunction Bipolar Transistors  
*A. O'Neill*
- 3112 A Self-Aligned Sacrificial Emitter Process for High Performance SiGe HBT in BiCMOS  
*Q. Liu and D. Harame*
- 3113 Implant Free SiGe-Quantum Well: From Device Concept To High-Performing pFETs  
*J. Mitard, G. Hellings, L. Witters, G. Eneman, A. Hikavyy, B. Vincent, R. Loo, N. Collaert, N. Horiguchi, and A. Thean*
- 3114 Effective Condensation Process for Higher Ge Concentration and Thin SiGe layer-on-insulator Substrates in Advanced High Mobility MOSFETs  
*D. LEE, T. Shim, T. Kim, S. Song, S. Lee, R. Okuyama, and J. Park*

- 3115 SiGe Doped-Channel FET Formed by Sputter Epitaxy Method  
*M. Yoshikawa, H. Otsuka, A. Kasamatsu, N. Hirose, T. Mimura, T. Matsui, and Y. Suda*
- 3116 Hole Mobility Boost of Ge p-MOSFETs by Composite Uniaxial Stress and Biaxial Strain  
*H. Lan, Y. Chen, J. Lin, and C. Liu*
- 3117 Modeling of Field-Effect-Transistors with Strained and Alternative Channel Materials  
*F. Conzatti, D. Esseni, P. Palestri, and L. Selmi*
- 3118 Physical Mechanism of Enhanced Uniaxial Stress Effect on Carrier Mobility in ETSOI MOSFETs  
*T. Ohashi, O. Shunri, and U. Ken*
- 3119 Reliability of SiGe channel MOS  
*J. Franco, B. Kaczer, J. Mitard, M. Toledano-Luque, G. Eneman, P. Roussel, M. Cho, T. Kauerauf, T. Grasser, L. Witters, G. Hellings, L. Ragnarsson, N. Horiguchi, M. M. Heyns, and G. Groeseneken*
- 3120 Evaluation of Two contact Resistivity References on  $\text{Si}_{1-x}\text{Ge}_x$  for FDSOI 20nm pMOS  
*E. Bourjot, F. Nemouchi, V. Carron, Y. Morand, S. Bernasconi, M. Vinet, J. Damlecourt, F. Allain, O. Cueto, D. Lafond, and D. Mangelinck*
- 3121 Gate Stack and Source/Drain Junction Formations for High-Mobility Ge MOSFETs  
*H. Nakashima, K. Yamamoto, H. Yang, and D. Wang*
- 3122 Thermally Stable  $\text{NiSi}_2$  for Ge Contact with Schottky Barrier Height Modulation Capability  
*R. Yoshihara, Y. Tamura, K. Kakushima, P. Ahmet, Y. Kataoka, A. Nishiyama, N. Sugii, K. Tsutsui, K. Natori, T. Hattori, and H. Iwai*
- 3123 Effect of an Atomically Matched Structure on Fermi-level Pinning at Metal/p-Ge Interfaces  
*K. Kasahara, H. Yoshioka, S. Yamada, T. Nishimura, M. Miyao, and K. Hamaya*
- 3124 Understanding Diffusion, Activation, and Related Phenomena in SiGe Alloys: Models and Challenges  
*H. W. Kennel*
- 3125 Strain Control of Si and  $\text{Si}_{1-x-y}\text{Ge}_x\text{C}_y$  Layers in  $\text{Si}/\text{Si}_{1-x-y}\text{Ge}_x\text{C}_y/\text{Si}$  Heterostructures  
*J. Murota, T. Kikuchi, and M. Sakuraba*
- 3126 Phosphorus Profile Control in Ge by Si Delta Layers  
*Y. Yamamoto, P. Zaumseil, R. Kurps, J. Murota, and B. Tillack*
- 3127 Dopant Enhanced Diffusion for High n-typed Doped Ge  
*Y. Cai, R. E. Camacho-Aguilera, J. Bessette, L. Kimerling, and J. Michel*

- 3128 A Threading Dislocation Density Study of Ge Epitaxial Layer on Si and The Dependency on Various Post Growth Treatments  
*A. Silber and E. Ginsburg*
- 3129 Ge Optical Emitters Fabricated by Ge Condensation and Epitaxial Growth  
*K. Oda, K. Tani, S. Saito, and T. Ido*
- 3130 Group-IV Subcells in Multijunction Concentrator Solar Cells  
*R. R. King, C. Fetzer, P. Chiu, E. Rehder, K. Edmondson, and N. Karam*
- 3131 Substrate Design and Thermal Budget Tuning for Integration of Photonic Components in a High-Performance SiGe:C BiCMOS Process  
*D. Knoll, H. Richter, B. Heinemann, S. Lischke, Y. Yamamoto, L. Zimmermann, and B. Tillack*
- 3132 Direct Band-gap Electroluminescence from Strained n-Ge Light Emitting Diodes  
*P. Velha, K. F. Gallacher, D. C. Dumas, D. J. Paul, M. Myronov, and D. R. Leadley*
- 3133 Parameters Controlling Emission of Terahertz Frequency Electromagnetic Radiation from InAs and GaAs: An Ensemble Monte Carlo Simulation Study  
*D. Cortie and R. Lewis*
- 3134 Selective-Area Epitaxial Lateral Overgrowth of InGaAs Microdiscs on Si  
*M. Sugiyama*
- 3135 III-V/GaP Epitaxy on Si for Advanced Photovoltaics and Green Light Emitters  
*S. A. Ringel, T. Grassman, C. Ratcliff, A. Carlin, J. Carlin, L. Yang, and M. Mills*
- 3136 Controlling Epitaxial GaAsP/SiGe Heterovalent Interfaces  
*P. Sharma, T. Milakovich, M. Bulsara, and E. A. Fitzgerald*
- 3137 High Efficiency Low Temperature Pre-epi Clean Method for Advanced Group IV epi Processing  
*V. Machkaoutsan, K. D. Weeks, M. Bauer, J. Maes, J. Tolle, S. Thomas, A. Alian, A. Hikavy, and R. Loo*
- 3138 Heteroepitaxy of III-V Compound Semiconductors on Si for Logic Applications: Selective Area Epitaxy in Shallow Trench Isolation Structures vs. Direct Epitaxy mediated by Strain Relaxed Buffers  
*M. Cantoro, C. Merckling, S. Jiang, W. Guo, N. Waldron, H. Bender, J. Dekoster, R. Loo, W. Vandervorst, M. Caymax, and M. Heyns*
- 3139 Electrically Pumped Lasing from Ge-on-Si  
*J. Michel*
- 3140 Strain Engineering for Optical Gain in Germanium  
*P. Boucaud, M. El Kurdi, M. de Kersauson, A. Ghrib, S. Sauvage, R. Jakomin, G. Beaudoin, O. Mauguin, L. Largeau, I. Sagnes, G. Ndong, M. Chaigneau, and R. Ossikovski*

- 3141 Silicon Compatible High Performance Optical Interconnect Technology  
*B. Dutt*
- 3142 Optical Characterization of Ge-on-Si Grown by using RTCVD  
*T. Kim, Y. Kil, W. Hong, H. Yang, S. Kang, T. Jeong, and K. Shim*
- 3143 High Extinction Ratio, Low Energy Consumption Ge Quantum Well Electro-Absorption Modulator with 23 GHz Bandwidth  
*G. Isella, P. Chaisakul, D. Marris-Morini, M. Saïd Rouifed, D. Chrastina, J. Frigerio, X. Le Roux, S. Edmond, J. Coudeville, and L. Vivien*
- 3144 Effects of HCl on the Growth of Epitaxial Ge  
*D. Franca*
- 3145 Analysis of Local Electric Conductive Property for Si Nanowire Models  
*Y. Ikeda, M. Senami, and A. Tachibana*
- 3146  $\text{Ge}_{1-x}\text{Sn}_x$  Alloys Pseudomorphically Grown by R. F. Magnetron Sputtering  
*H. Pérez Ladrón de Guevara, A. Rodríguez Vázquez, H. Navarro Contreras, and M. Vidal Borbolla*
- 3147 High Quality Silicon Cap Layer for 28nm and Beyond PMOS Processes  
*C. I. Liao, T. Hsuan, C. Chien, M. Chan, C. Yang, J. Y. Wu, and B. Ramachandran*
- 3148 Accurate Reactive Ion Etching of Si, Ge and P Doped Ge in an  $\text{SF}_6\text{-O}_2$  Radio-Frequency Plasma  
*C. Wongwanitwattana, V. A. Shah, M. Myronov, E. H. Parker, T. E. Whall, and D. R. Leadley*
- 3149 Formation of Large Grain SiGe on Insulator by Si Segregation in Seedless-Rapid-Melting Process  
*R. Kato, M. Kurosawa, R. Matsumura, T. Sadoh, and M. Miyao*
- 3150 Direct Measurement of Silicon Strain Induced by Stressed TiNx Stripes Through Raman  
*Z. Fu, X. Ma, H. Yin, J. Niu, J. Yan, and C. Zhao*
- 3151 Nano-Engineered  $\text{Ge}_x\text{Si}_{1-x}$ -on Insulator for Heteroepitaxy  
*K. Hossain, O. Holland, M. Debnath, T. Mishima, and M. Santos*
- 3152 NMOS SiP Epitaxy Process - Optimizing Facet Growth  
*C. I. Liao, C. Chien, M. Chan, C. Yang, J. Y. Wu, C. Chung, and B. Ramachandran*
- 3153 Control of Schottky Barrier Height at Al/p-Ge Junctions by Ultrathin Layer Insertion  
*A. Ohta, M. Matsui, H. Murakami, S. Higashi, and S. Miyazaki*
- 3154 Characterization of Resistance-Switching Properties of SiO<sub>x</sub> Films Using Pt Nanodots Electrodes  
*K. Makihara, M. Fukushima, A. Ohta, M. Ikeda, and S. Miyazaki*

- 3155 X-ray and Raman Characterization of strained SiGe Layers Treated by Stain Etching  
*W. Zhou, R. Liang, and L. Yan*
- 3156 Ge-on-Si Bufferless Epitaxial Growth for Photonic Devices  
*R. E. Camacho-Aguilera, Y. Cai, J. Bessette, X. Duan, L. Kimerling, and J. Michel*
- 3157 Formation of Large-Grain Ge(111) Films on Insulator by Gold-Induced Layer-Exchange Crystallization at Low Temperature  
*J. Park, T. Suzuki, M. Kurosawa, M. Miyao, and T. Sadoh*
- 3158 Impedance Spectroscopy of GeSn/Ge Heterostructures by a Numerical Method  
*B. Baert, O. Nakatsuka, S. Zaima, and N. Nguyen*
- 3159 Improvements in Atomic Layer Deposition Nucleation on Ge(100) and SiGe(100) via HOOH dosing  
*T. Kaufman-Osborn, J. Lee, K. Kiantaj, and A. C. Kummel*
- 3160 Orientation Dependence of  $\text{Si}_{1-x}\text{C}_x:\text{P}$  Growth and the Impact on FinFET Structures  
*J. Tolle, K. D. Weeks, M. Bauer, V. Machkaoutsan, J. Maes, M. Togo, A. Hikavyy, S. Brus, and R. Loo*
- 3161 High Throughput SEG of Highly In-Situ Doped SiCP/SiP Layers for NMOS Devices Using a  $\text{Si}_3\text{H}_8\text{SiH}_3\text{CH}_3/\text{PH}_3/\text{Cl}_2$  based CDE Process  
*M. Bauer*
- 3162 Ge-on-Si: Single-Crystal Selective Epitaxial Growth in a CVD reactor  
*A. Sammak, W. de Boer, and L. K. Nanver*
- 3163 The Structural and Electrical Properties in  $\text{CeO}_2$  Dielectric on Ge Substrate for MOS Capacitors by Atomic Layer Deposition with  $\text{Ce}(\text{iPrCp})_3$   
*I. Oh, M. Kim, J. Park, J. Gatineaub, K. Changhee, and H. Kim*
- 3164 Point-of-Use Sampling and Organic Impurity Analysis for Bulk Gases in Semiconductor Processing  
*J. Park, S. Shin, Y. Lee, P. Jun, and J. Kim*
- 3165 Electronic Band Structure and Effective Masses of  $\text{Ge}_{1-x}\text{Sn}_x$  Alloys  
*K. Low, Y. Yang, G. Han, W. Fan, and Y. Yeo*
- 3166 Multi-Wavelength High Resolution Micro-Raman and Optical Reflectance Characterization of Nano-Scale Strained Silicon-on-Insulator Substrates  
*T. Kim, T. Shim, W. Yoo, and J. Park*
- 3167 Theoretical Calculation of Defects Formation Under Thermal Equilibrium in Heavily n-type Doped Germanium  
*K. Takinai, Y. Ishikawa, and K. Wada*
- 3168 Strain Engineering in GeSnSi Materials  
*H. Radamson, M. Noroozi, A. Jamshidi, and M. Ostling*

- 3169 Optimization of SiC:P Raised Source Drain Epitaxy for Planar 20nm Fully Depleted SOI MOSFET Structures  
*N. Loubet, T. Nagumo, T. Adam, Q. Liu, M. Raymond, K. Cheng, A. Khakifirooz, Z. Zhu, P. Khare, V. K. Paruchuri, B. Doris, and R. Sampson*
- 3170 Evidence of Boron Cluster Formation in Ultra-Shallow Ion Implanted Ge  
*B. R. Yates, B. L. Darby, N. Rudawski, D. H. Petersen, O. Hansen, R. Lin, P. F. Nielsen, A. Kontos, and K. S. Jones*
- 3171 Strain Evolution of  $\text{Si}_{1-x}\text{Ge}_x$  Selective Epitaxial Growth in Steps  
*S. Koo, S. Kim, and D. Ko*
- 3172 Formation of Silicene and 2D Si Sheets on Ag(111): Growth Mode, Structural and Electronic Properties  
*P. Vogt, T. Bruhn, A. Resta, B. Ealet, P. De Padova, and G. Le Lay*
- 3173 Investigations on GeO Disproportionation Using X-ray Photoelectron Spectroscopy  
*S. Wang, H. Liu, T. Nishimura, K. Nagashio, K. Kita, and A. Toriumi*
- 3174 The Oxidation of Germanium Surfaces Investigated at the Atomic Scale: Site-specific Atomic and Electronic Structure  
*C. Fleischmann, K. Schouteden, C. Merckling, S. Sioncke, M. Meuris, C. Van Haesendonck, K. Temst, and A. Vantomme*
- 3175 GeSn Photodetection and Electroluminescence Devices on Si  
*M. Oehme, E. Kasper, and J. Schulze*
- 3176  $\text{Ge}_{1-x-y}\text{Si}_x\text{Sn}_y$  Photodiodes with 1 eV Pptical Gaps Grown on Si(100) and Ge(100) Platforms  
*R. Beeler, J. Menendez, and J. Kouvetsakis*
- 3177 MBE Growth of GeSn and SiGeSn Heterojunctions for Photonic Devices  
*J. S. Harris, R. Chen, H. Lin, Y. Huo, E. Fei, and T. Kamins*
- 3178 Beyond Graphene: Silicene and Germanene Novel Two-Dimensional Electronic Materials  
*G. Le Lay, A. Resta, B. Ealet, P. De Padova, T. Bruhn, and P. Vogt*
- 3179 Epitaxial Growth of Low Defect SiGe Buffer Layers for Integration of New Materials on 300 mm Silicon Wafers  
*G. Kozlowski, T. Schroeder, and P. Storck*
- 3180 Synthesis of Monocrystalline Silicon-like (III-V)-Si Semiconductors: Structural and Optical Properties  
*A. Chizmeshya, J. Kouvetsakis, T. Watkins, R. Beeler, and J. Menendez*
- 3181 Strained Ge Core/Si(Ge) Shell Nanowires: Stability and Surface Defect Passivation  
*P. C. McIntyre*
- 3182 Spin Coherence in Si and Applications to Quantum Information Processing  
*S. Lyon, A. M. Tyryshkin, J. He, and R. M. Jock*

- 3183 Single-Shot Readout of Singlet-Triplet Qubit States in a Si/SiGe Double Quantum Dot  
*J. Prance, Z. Shi, C. Simmons, D. Savage, M. Lagally, L. Schreiber, L. Vandersypen, M. Friesen, R. Joynt, S. Coppersmith, and M. Eriksson*
- 3184 A Design Scheme for Topological Insulators based Bonds, Bands, Symmetry and Spin Orbit Coupling  
*C. Felser, L. Müchler, S. Chado, H. Zhang, and S. Zhang*
- 3185 Measurement and Control of Individual Electron Spins in Silicon MOS-based Quantum Dots  
*H. Jiang*
- 3186 Non Planar Non Si CMOS - Challenges and Opportunities  
*C. Hobbs, K. Ang, R. Hill, I. Ok, B. Min, D. Franca, H. Stamper, S. Vivekanand, M. Rodgers, S. Gausepohl, P. Kirsch, and R. Jammy*
- 3187 Phonon Dispersion in <100> Si Nanowire Covered with SiO<sub>2</sub> Film Calculated by Molecular Dynamics Simulation  
*T. Watanabe, T. Zushi, M. Tomita, R. Kuriyama, N. Aoki, and T. Kamioka*
- 3188 Electron Transport and Strain Mapping in Ge-SixGe1-x Core-Shell Nanowire Heterostructures  
*E. Tutuc*
- 3189 Liquid-Phase Deposition of Thin Si and Ge Films Based on Ballistic Electro-reduction  
*T. Ohta, R. Mentek, B. Geloz, N. Mori, and N. Koshida*
- 3190 Evidence of Layer-by-Layer Oxidation of Ge Surfaces by Plasma Oxidation Through Al<sub>2</sub>O<sub>3</sub>  
*R. Zhang, P. Huang, J. Lin, M. Takenaka, and S. Takagi*
- 3191 GOI substrates -Fabrication and Characterization-  
*A. Sakai, S. Yamasaka, J. Kikkawa, Y. Nakamura, Y. Moriyama, T. Tezuka, S. Takeuchi, and K. Izunome*
- 3192 Strained Nanoscaled Devices  
*D. Gruetzmacher, S. Mantl, Q. Zhao, S. Richter, L. Knoll, J. Moers, J. Gerharz, G. Mussler, D. Buca, and R. Minamisawa*
- 3193 Effect of Two-step Oxidation in Ge Condensation on Surface Roughness Property of Relaxed SiGe layer-on-insulator Substrates  
*T. Shim, T. Kim, D. LEE, R. Okuyama, and J. Park*
- 3194 Simple Fabrication of Suspended Germanium Structures and Their Electrical Properties from High Quality Ge on Si(001) Layers  
*V. A. Shah, M. Myronov, C. Wongwanitwatana, R. Morris, M. Prest, J. S. Richardson-Bullock, E. H. Parker, T. E. Whall, and D. R. Leadley*
- 3195 Formation of Graded SiGe on Insulator by Segregation-Controlled Rapid-Melting-Growth  
*R. Matsumura, Y. Tojo, H. Yokoyama, M. Kurosawa, T. Sadoh, and M. Miyao*

- 3196 Modeling Two Dimensional Solid Phase Epitaxial Growth for Patterned Ge Substrates  
*B. L. Darby, B. R. Yates, A. Kumar, A. Kontos, R. Elliman, and K. S. Jones*
- 3197 Germanium/Silicon Heterostructures for Terahertz Emission  
*R. W. Kelsall, V. Dinh, P. Ivanov, A. Valavanis, L. Lever, Z. Ikonik, P. Velha, D. Dumas, K. F. Gallacher, D. J. Paul, J. Halpin, M. Myronov, and D. R. Leadley*
- 3198 Ge Photodiodes for CMOS Photonics Optical Engines and Interconnects  
*S. Sahni and G. Masini*
- 3199 Long Wavelength {greater than or equal to} 1.9  $\mu\text{m}$  Germanium for Optoelectronics Using Process Induced Strain  
*P. Velha, D. J. Paul, M. Myronov, and D. R. Leadley*
- 3200 Single Photon Emitters on Si substrate  
*S. Bietti, L. Cavigli, M. Abbarchi, G. Isella, J. Frigerio, C. Frigeri, A. Vinattieri, M. Gurioli, and S. Sanguinetti*
- 3201 Advanced GE-ON-SI Telecommunication Receivers  
*C. R. Doerr*
- 3202 Heteroepitaxial Lattice Mismatch Stress Relaxation in Nonpolar and Semipolar GaN by Dislocation Glide  
*J. S. Speck*
- 3203 Channel Strain Evolution of Recessed Source/Drain  $\text{Si}_{1-x}\text{C}_x$  Structures by Modifying Scaling Factors  
*S. Kim, D. Byeon, M. Jung, I. Lee, D. Ko, Y. Kim, and H. Lee*
- 3204 High Ge Content SiGe Selective Processes for Manufacturing Source/Drain in the Next Generations of pMOS Transistors  
*A. Hikavyy, W. Vanherle, L. Witters, B. Vincent, J. Dekoster, and R. Loo*
- 3205 Formation of Uniaxially Strained Si/Ge Channels on SiGe Buffers Strain-Controlled with Selective Ion Implantation  
*K. Sawano, Y. Hoshi, S. Nagakura, K. Arimoto, K. Nakagawa, N. Usami, and Y. Shiraki*
- 3206 Coherent Manipulation of a Si/SiGe-based Singlet-Triplet Qubit  
*M. G. Borselli*
- 3207 Spin Generation and Relaxation in Ge/SiGe Quantum Wells  
*G. Isella, F. Bottegoni, S. Cecchi, A. Ferrari, F. Ciccacci, F. Pezzoli, A. Giorgioni, E. Gatti, E. Grilli, M. Guzzi, C. Lange, N. Koester, R. Woscholski, S. Chatterjee, D. Trivedi, P. Li, Y. Song, and H. Dery*
- 3208 Enhancement-Mode Buried Strained Silicon Channel Double Quantum Dot with Integrated Electrometer  
*M. Carroll, N. Bishop, T. Lu, T. Pluym, and P. Kotula*

- 3209 Local Quantity Analysis of Nanosize Electronics and Spintronics Material  
*M. Senami and A. Tachibana*
- 3210 (Panel Discussion) How Far Can We Push Si CMOS and What are the Alternatives for Future ULSI  
*D. Haraue*
- 3211 GeSn Materials: Challenges and Applications  
*R. Loo, V. Benjamin, F. Gencarelli, E. Geert, W. Liesbeth, C. Matty, H. Marc, and T. Aaron*
- 3212 GeSn Alloys on Si Using Deuterated Stananne and Higher-Order Germanes: Synthesis and Properties  
*G. Grzybowski, R. Beeler, L. Jiang, A. Chizmeshya, J. Kouvetakis, and J. Menendez*
- 3213 Crystalline Properties and Strain Relaxation Mechanism of CVD Grown GeSn  
*F. Gencarelli, B. Vincent, A. Kumar, J. Demeulemeester, A. Vantomme, A. Franquet, J. Meersschaut, W. Vandervorst, R. Loo, M. Caymax, K. Temst, and M. Heyns*
- 3214 Reduced Pressure CVD Epitaxial Growth of  $\text{Ge}_{1-x}\text{Sn}_x$  Using  $\text{SnCl}_4$  and  $\text{Ge}_2\text{H}_6$   
*S. Wirths, D. Buca, A. Tiedemann, P. Bernardy, B. Holländer, T. Stoica, D. Grützmacher, and S. Mantl*
- 3215 Thermal Chemical Vapor Deposition of Epitaxial Germanium Tin Alloys  
*Y. Huang, C. Wang, M. Jin, E. Sanchez, and Y. Kim*
- 3216 Growth and Optical Properties of  $\text{Ge}_{1-x}\text{Sn}_x$  Alloy Thin Films with a High Sn Content  
*S. Zaima, O. Nakatsuka, M. Nakamura, W. Takeuchi, Y. Shimura, and N. Taoka*
- 3217 Growth of  $\text{Ge}_{1-x}\text{Sn}_x$  Alloys Using Combined Sources of Solid Tin and Gaseous Germane  
*S. Su, B. Cheng, D. Zhang, G. Zhang, C. Xue, and Q. Wang*
- 3218 Growth and Characterization of Heteroepitaxial Layers of  $\text{Ge}_{1-x-y}\text{Si}_x\text{S}_y$  Ternary Alloy  
*T. Yamaha, O. Nakatsuka, S. Takeuchi, W. Takeuchi, N. Taoka, K. Araki, K. Izunome, and S. Zaima*
- 3219 Single Crystalline GeSn on Silicon by Solid Phase Crystallization  
*R. Lieten, S. Decoster, M. Menghini, J. Seo, A. Vantomme, and J. Locquet*
- 3220 Tin Deuteride ( $\text{SnD}_4$ ) Stabilization  
*R. F. Spohn and C. B. Richenberg*
- 3221 Tin-Incorporated Source/Drain and Channel Materials for Field-Effect Transistors  
*Y. Yeo, G. Han, X. Gong, L. Wang, W. Wang, Y. Yang, P. Guo, B. Liu, S. Su, G. Zhang, C. Xue, and B. Cheng*

- 3222 GeSn Channel n and p MOSFETs  
*S. Gupta, R. Chen, B. Vincent, D. Lin, B. Magyari-Kope, M. Caymax, J. Dekoster, J. S. Harris, Y. Nishi, and K. Saraswat*
- 3223 High Hole Mobility in Strained Germanium-Tin (GeSn) Channel pMOSFET Fabricated on (111) Substrate  
*G. Han, S. Su, Y. Yang, P. Guo, X. Gong, L. Wang, W. Wang, C. Guo, G. Zhang, C. Xue, B. Cheng, and Y. Yeo*
- 3224 Negative Bias Temperature Instability Study on  $\text{Ge}_{0.97}\text{Sn}_{0.03}$  P-MOSFETs with  $\text{Si}_2\text{H}_6$  Passivation,  $\text{HfO}_2$  High-k Dielectric and TaN Metal Gate  
*X. Gong, S. Su, B. Liu, L. Wang, W. Wang, Y. Yang, E. Kong, B. Cheng, G. Han, and Y. Yeo*
- 3225 Si/SiGe Thermoelectric Generators  
*D. J. Paul, A. Samarelli, L. Ferre Llin, Y. Zhang, J. Weaver, P. Dobson, S. Cecchi, J. Frigerio, F. Isa, D. Chrastina, G. Isella, T. Etzelstorfer, J. Stangl, and E. Müller Gubler*
- 3226 SiGe Band-to-Band Tunneling Calibration based on p-i-n Diodes: Fabrication, Measurement and Simulation  
*K. Kao, A. Verhulst, R. Rooyackers, A. Hikavyy, R. Loo, A. Milenin, J. Tolle, H. Dekkers, E. Simoen, V. Machkaoutsan, J. Maes, K. De Meyer, N. Collaert, M. Heyns, C. Huyghebaert, and A. Thean*
- 3227 Tunneling Field-Effect Transistor with Novel  $\text{Ge}/\text{In}_{0.53}\text{Ga}_{0.47}\text{As}$  Tunneling Junction  
*P. Guo, Y. Yang, Y. Cheng, G. Han, C. Chia, and Y. Yeo*
- 3228 Germanium Tin Tunneling Field Effect Transistor for Sub-0.4 V Operation  
*Y. Yang, K. Low, G. Han, and Y. Yeo*
- 3229 Si/SiGe Tunneling Static Random Access Memories  
*G. Ternent and D. J. Paul*
- 3230 Ge Surface-Energy-Driven Secondary Grain Growth for Vertical Channel in 3D NAND Flash Memories  
*S. Lee, Y. Son, and E. Yoon*
- 3231 Epitaxial Growth and Applications of Low-Resistivity Phosphorous-Doped  $\text{Si}_{1-x}\text{C}_x$   
*T. N. Adam, N. Loubet, A. Reznicek, V. K. Paruchuri, R. Sampson, and D. Sadana*
- 3232 Selective Epitaxial Growth of Heavily Boron-Doped Silicon with Uniform Doping Depth Profile  
*Z. Zhu, Z. Cong, and R. Balasubramanian*
- 3233 High Tensile Strained In-Situ Phosphorus Doped Silicon Epitaxial Film for nMOS Applications  
*Z. Ye, S. Chopra, R. Lapena, Y. Kim, and S. Kuppurao*

- 3234 Microstructure Development and Its Effects on the Electrical Properties in Epitaxially Grown In-Situ Boron and Carbon (co)-doped Highly Strained High Percentage Silicon-Germanium Layers  
*A. Reznicek, T. N. Adam, J. Li, Z. Zhu, H. Hovel, J. de Souza, S. W. Bedell, V. Paruchuri, and D. Sadana*
- 3235 In Situ Boron (B) Doped Germanium (Ge:B) Grown on (100), (110), and (111) Silicon: Crystal Orientation and B Incorporation Effects  
*G. Han, Q. Zhou, P. Guo, W. Wang, Y. Yang, and Y. Yeo*
- 3236 Materials Integration for III-V/SiGe+CMOS Integrated Circuit Platforms (Invited)  
*E. A. Fitzgerald, P. Sharma, M. Bulsara, T. Milakovich, S. Ringel, A. Pitera, J. Hennessy, and A. Malonis*
- 3237 Heterogeneous Integration of III-V Devices and Si CMOS on a Silicon Substrate  
*T. Kazior*
- 3238 Heterogeneous Integration of InP HBTs on CMOS: Leveraging and Providing Value to Conventional Silicon Technologies  
*J. C. Li, Y. Royter, P. Patterson, T. Hussain, J. Duvall, M. Montes, I. Valles, F. Ku, M. Boag-O'Brien, A. Lopez, D. Le, D. Zehnder, S. Kim, S. Chen, T. Oh, M. Akmal, E. Wang, D. Hitko, M. Sokolich, D. Chow, P. Brewer, and K. Elliott*
- 3239 Wafer-level Heterogeneous Integration of GaN HEMTs and Si (100) MOSFETs  
*H. Lee, Z. Li, M. Sun, K. Ryu, and T. Palacios*
- 3240 Scalable GaN-on-Silicon Using Rare Earth Oxide Buffer Layers  
*F. Arkun, M. Lebby, R. Dargis, R. Roucka, R. S. Smith, and A. Clark*
- 3241 Formation and Characterization of Nickel Germanosilicide on  $\text{Si}_{1-x}\text{Ge}_x/\text{Si}/\text{SiO}_2/\text{Si}$   
*W. Yoo, N. Hasuike, H. Harima, and M. Yoshimoto*
- 3242 Low Specific Ohmic Contacts to n-type Germanium Using a Low Temperature NiGe Process  
*K. F. Gallacher, P. Velha, D. J. Paul, I. Maclarens, M. Myronov, and D. Leadley*
- 3243 Formation of 1.7-nm-thick-EOT Germanium Dioxide Film with a High-Quality Interface Using a Direct Neutral Beam Oxidation Process  
*A. Wada, R. Zhang, S. Takagi, and S. Samukawa*

### **F1 - Bio-Enabled Materials, Processes, and Devices**

*ECS Electrodeposition, ECS Physical and Analytical Electrochemistry, ECS Sensor, ECSJ*

- 3244 (Invited) DNA-Translocation through a Solid-State Nanopore Coated with a Functionally Switchable Self-Assembled Monolayer  
*S. Harrer, D. Wang, B. Luan, G. Stolovitzky, H. Peng, and A. Afzali-Ardakani*
- 3245 (Invited) Electrochemical Biosensors for Detecting Pathogens  
*W. R. Heineman, X. Guo, A. Kulkarni, S. Iyer, and H. Halsall*

- 3246 Iridium Oxide Hybrids as Electrodes for the Neural System  
*N. M. Carretero, J. Moral, A. Cruz, and N. Casañ-Pastor*
- 3247 (Invited) Hierarchically Assembly of Materials Using Biological Building Blocks  
*S. Kim, M. Vasudev, J. Slocik, S. Jones, T. Bunning, and R. Naik*
- 3248 (Invited) Biologically Inspired Synthesis of a Photocatalytically Active Membrane for Water Treatment  
*N. Kinsinger, A. Dudchenko, A. Wong, D. Li, and D. Kisailus*
- 3249 Bio-Inspired Chemistry for Electrophoretic Nanotechnology  
*I. Zhitomirsky*
- 3250 (Invited) Rational Design of Proteins for Modulation of Materials Growth Processes  
*D. T. Schwartz*
- 3251 (Invited) Selective Metallization of Scaffolded DNA Origami to Form Self-Assembled Nanoelectronic Systems  
*A. T. Woolley, Y. Geng, E. Pound, M. Lydiksen, A. Pearson, J. Liu, B. Uprety, R. Davis, and J. N. Harb*
- 3252 DNA/Metal Nanoparticles Functionalized Single-Walled Carbon Nanotubes Based Gas Sensor Arrays  
*H. C. Su, M. Zhang, J. Lim, and N. Myung*
- 3253 Use of Galvanic Displacement to Fabricate DNA-Templated Tellurium and Bismuth Telluride Nanowires  
*J. Liu, B. Uprety, N. Myung, and J. N. Harb*
- 3254 (Invited) Modification of Solid Surface with Self-Assembled Monolayer for Chiral Sensing  
*T. Nakanishi and T. Osaka*
- 3255 Design of Molecular Recognition Interface for Detecting Carbohydrate and Lectin Weak Interactions  
*Y. SATO, K. Yoshioka, T. Murakami, and O. Niwa*
- 3256 Interfacial Structure and Function of Nano-Structured Membranes of Newly Synthesized Phosporylcholine Derivatives  
*T. Sawaguchi and M. Tanaka*
- 3257 A Study on the Effect of Novel Surface Treatments and Biodegradable Polymer Coatings on Corrosion and Surface Properties of Ternary Nitinol Alloys  
*C. Pulletikurthi and N. Munroe*
- 3258 Using Biocompatible Ionic liquid to Control the Corrosion of Mg Alloys in Simulated Body Fluid  
*Y. Zhang, B. Hinton, G. Wallace, X. Liu, and M. Forsyth*

- 3259 Development of Novel Guided Tissue Regeneration Membranes for Biomedical Applications  
*Y. C. Chen and K. Ou*
- 3260 Multifunctional Biodegradable Cross-Linked Polymer Research and Development and Clinical Application of Animal Experiments  
*W. Su and K. Ou*
- 3261 Investigating Phosphonate Monolayer Stability as Protective Coatings for Retinal-Neural Sensors  
*B. A. Branch, M. Dubey, A. Aaron, K. Baldwin, A. M. Dattelbaum, and D. Petsev*

**F2 - Electrodeposition General Session: Fundamentals and New Materials - Dieter M. Kolb Memorial Symposium**

*ECS Electrodeposition, ECSJ Nano-Micro Fabrication*

- 3262 On the Structure of the Helmholtz Layer at the Solid-Electrolyte Boundary and its Relation to Electrode Kinetics  
*H. J. Lewerenz*
- 3263 Metal Deposition on Metal, Semiconductor, Organic Layer - Common Interests with Prof. Dieter Kolb  
*K. Uosaki*
- 3264 Underpotential Deposition of Cu on Au(111) in Acid Sulfate Solution  
*N. Vasiljevic, L. Viyannalage, N. Dimitrov, and K. Sieradzki*
- 3265 Tuning the Driving Force in Underpotential Codeposition of Alloys via Selective Complexation: Application to Au-Cu Alloys  
*D. Liang and G. Zangari*
- 3266 Lead Underpotential Deposition on Sub-Monolayer Pt and Ru Modified Au(111) Surface  
*Q. Yuan, A. Tripathi, M. Slavkovic, and S. Brankovic*
- 3267 EC-STM Study of Two-Dimensional Complex Adlayer Directly Formed on Au(111)  
*S. Yoshimoto and K. Nishiyama*
- 3268 Characterisation of the Deposition of n-octanohydroxamate on Copper Surfaces  
*G. K. Parker, S. Holt, and G. Hope*
- 3269 Electrochemical Formation of Cu-Corronene Adlayer on Au(111) in Acidic Solution  
*T. Sawaguchi and S. Yoshimoto*
- 3270 E-ALD of Pd on Au Single Crystals  
*L. Sheridan, Y. Kim, J. Stickney, and D. B. Robinson*
- 3271 Layer-by-layer Pt Electrodeposition on Au Single Crystal Surfaces Studied by In situ Resonance Surface X-ray Scattering  
*T. Kondo, M. Shibata, T. Masuda, and K. Uosaki*

- 3272 The Evolution of Surface Morphology and Stress in Electrodeposited Copper Nanofilms  
*M. O'Grady, C. Lenihan, and D. Buckley*
- 3273 Electrochemical Impedance Spectroscopy Applied to Cantilever Curvature  
*M. C. Lafouresse, U. Bertocci, C. Beauchamp, and G. Stafford*
- 3274 Controlling Pt Nucleation and Growth by Solution Chemistry and Deposition Conditions  
*Y. Liu, D. Gokcen, U. Bertocci, and T. Moffat*
- 3275 XAS Study of Core-Shell PtRu Nanoparticles from Galvanic Pulse Current Deposition  
*Y. Hsieh, L. Chang, P. Wu, and J. Lee*
- 3276 Electroforming of Thick Film Bi<sub>2</sub>Te<sub>3</sub>-based Thermoelectrics  
*C. L. Arrington, P. Sharma, J. Coleman, E. Baca, A. Rowen, D. Banga, D. B. Robinson, and V. Stavila*
- 3277 Electrodeposition of Sb<sub>x</sub>Te<sub>y</sub> and Bi<sub>x</sub>Te<sub>y</sub> Thin Films for Thermoelectric application  
*J. Lim, I. Yoo, N. Myung, Y. Song, D. Chang, D. Lim, Y. Kim, and K. Lee*
- 3278 Wear and Corrosion Resistance of Cr-C Deposits Obtained from a Trivalent Chromium Electroplating Bath with the Addition of Nanosized Al<sub>2</sub>O<sub>3</sub> Powder  
*C. Huang, C. Chuang, and C. Lin*
- 3279 Effects of Sonication on Electrodeposited Nickel-based Carbon Nanotube Composites Coatings  
*T. Suzuki and M. Kato*
- 3280 Application of Artificial Neural Networks to Predict Chemical Composition of Electrodeposited Nanocrystalline Ni-Mo Thin Films  
*M. Allahyazadeh, A. Ashrafi, B. Rozbehani, and A. Seddighian*
- 3281 Stepwise Anodizing Processes for Hierarchical Nanoporous Structures  
*C. Jeong and C. Choi*
- 3282 Dependence of Fermi Level in Conducting Polymers Joined with Oxide Semiconductor on Its Crystal Plane  
*Y. Fujikawa, J. Kawakita, T. Chikyow, and Y. Sakamoto*
- 3283 Photoluminescence Properties of Electrodeposited Porous Silicon/ Cerium oxide Composite  
*M. Mizuhata and Y. Kubo*
- 3284 Superconformal Film Growth: Challenges and Opportunities  
*T. Moffat, G. Liu, S. Zou, L. Richter, L. Ou Yang, C. Lee, and D. Josell*
- 3285 Beyond Interfacial Anion/Cation Pairing: The Role of Cu(I) Coordination Chemistry for the Action of Leveler Additives in Copper Electroplating  
*M. Hai, F. Janser, T. Brunner, A. Fluegel, F. Simona, M. Cascella, K. Kraemer, D. Mayer, M. Arnold, and P. Broekmann*

- 3286 Influence of Glycine as Additive on Cobalt Electrodeposition  
*R. A. Critelli and P. Sumodjo*
- 3287 Mechanistic Studies of Zinc Electrodeposition from Deep Eutectic Electrolytes  
*L. Vieira, B. Gollas, and R. Schennach*
- 3288 Theoretical Analysis of the Solvent Effect on Hypophosphite Ion Adsorption on Pd and Cu Surfaces  
*M. Kunimoto, K. Seki, H. Nakai, and T. Homma*
- 3289 Electrodeposition of FeRh Alloys: Influence of Ag Underlayer  
*R. Della Noce, D. Cornejo, H. Kumar, and A. Benedetti*
- 3290 Surface Alloy Formation During Pb UPD on Cu(100) and Its Role in Cu-Pb Alloy Deposition  
*D. Gokcen, C. Hangarter, and T. Moffat*
- 3291 An Environmentally Friendly Process for Electroplating Copper on Zinc  
*C. Liao, F. Ernst, and U. Landau*
- 3292 Study of the Copper Electrodeposition Mechanism on Molybdenum Substrate  
*E. Delbos, H. El Belghiti, D. Mercier, J. Vigneron, M. Bouttemy, and A. Etcheberry*
- 3293 Deposition of Metallic Nanoparticles; Variations of Particle Size  
*T. Brüllle, O. Schneider, and U. Stimming*
- 3294 Electrodeposition of Arrays of Au/NiO/Au Nanowire Heterostructures for ReRAM Applications  
*D. Perego, S. Franz, M. Bestetti, S. Brivio, G. Tallarida, and S. Spiga*
- 3295 Crystal Orientation of Iron Produced by Electrodeoxidation of Hematite Particles  
*M. Tokushige, O. Kongstein, and G. Haarberg*
- 3296 Study of the Electrodeposition of Zn-TiO<sub>2</sub> Dispersion Coatings  
*M. K. Camargo, U. Schmidt, and A. Bund*
- 3297 Epitaxial Growth of Au on Pt (111) and Pt (poly) by Surface Limited Redox Replacement of Pb UPD Layer  
*N. Dimitrov, C. Mitchell, and M. Fayette*
- 3298 Implications on the Use of 1-D and 2-D Models for Metal Electrodeposition: Voltammetry and Impedance Analysis  
*J. G. Vazquez and M. Pritzker*
- 3299 Understanding the Mechanism of Functional Molecules in Shape-Controlled Synthesis of Nanomaterials -- In Situ FTIR Spectroscopic Study of Citrate Adsorption on Pt Polycrystalline and Single Crystal Electrodes  
*D. Chen, J. Ye, C. Xu, X. Li, J. Li, C. Zhen, and S. Sun*

- 3300 Fabrication of Low CTE Metal Masks by the Invar Fe-Ni Alloy Electroforming Process for Large and Fine Pitch OLED Displays  
*T. Nagayama, T. Yamamoto, T. Nakamura, and Y. Mizutani*
- 3301 Synthesis and Characterization of Electrodeposited Cu<sub>2</sub>O Thin Film for Photo-Electrochemical Cells  
*M. Kim, S. Yoon, D. Chang, N. Myung, D. Lim, I. Kim, B. Yoo, K. Lee, and J. Lim*
- 3302 Characterization of Zn-Ni-P alloys Electrodeposited in Alkaline Solutions  
*Y. Kamimoto, K. Yamamoto, S. Yamashita, and R. Ichino*
- 3303 The Electrodeposition of Zinc-Bismuth Alloys  
*A. Luegger, B. Gollas, and J. Zidar*
- 3304 Influence of Adatom Supersaturation on Real Activation Energy of Charge Transfer Stage during Metal Electrocristallization  
*I. Kryshko, N. Yurchenko, and V. Trofimenco*
- 3305 Electrochemical Assembly of Ruthenium Complexes during the Multilayering Process of MnO<sub>2</sub>  
*K. Tomono, R. Yamaguchi, and M. Nakayama*
- 3306 AFM Analysis for Initial Stage of Electroless Displacement Deposition of Silver on Silicon Surface  
*T. Ego, S. Yae, T. Hagiwara, N. Fukumuro, and H. Matsuda*
- 3307 Fabrication of Cu-Ag Film Using Electrodeposition and Characterization of Its Properties  
*H. Ko, M. Kim, J. Kim, and O. Kwon*
- 3308 Degradation of Additives and Its Influences on Copper Electrodeposition  
*S. Choe, M. Kim, H. Kim, T. Lim, A. Lee, S. Jun, K. Woo, and J. Kim*
- 3309 Electrodeposition of CoNiW Alloys: HCP-FCC Structural Transition  
*A. M. Sakita, R. Della Noce, C. Sadao Fugivara, and A. Vicente Benedetti*
- 3310 Electrochemical Formation of Functional Silver Coatings: Nanostructural Peculiarities  
*O. Bersirova and V. Kublanovsky*
- 3311 High Temperature Hardness of Electrodeposited Nickel-based Carbon Nanotube Composite Coatings  
*T. Suzuki, M. Kato, T. Matsuda, and S. Kobayashi*

**F3 - Electroless Deposition: Principles, Activation, and Applications 2**  
*ECS Electrodeposition, ECSJ, CSE*

- 3312 Influence of Added Elements on Electroless Ni-P  
*P. Cavallotti and L. Magagnin*

- 3313 Corrosion of Copper and Nickel During Electroless NiP/Pd Deposition  
*C. S. Tiwari and R. Nguyen*
- 3314 Electrochemical Evaluation of Electroless Ni-Zn-Cu-P Alloy Deposition  
*M. Zaimi and K. Noda*
- 3315 Deposition of Thin Metallic Films on Semiconductor Substrates  
*S. Djokic, N. Djokic, and T. Thundat*
- 3316 Copper Electroless Deposition on a Glass Substrate  
*P. Chan and W. Dow*
- 3317 Co-Ni Electroless Composite Plating of 20 nm Diamond particles on 10 micrometer Plastic Balls and the Application of thus prepared devices to Post CMP Processes  
*S. Yoshihara*
- 3318 Impact of the Silicon Substrates Cleaning and Activation in the Nickel Electroless Plating  
*M. Bouttemy, H. El Belghiti, D. Aureau, E. Delbos, and A. Etcheberry*
- 3319 Fluoride Free Galvanic Displacement of Copper and Silver as Surface Modifications for MEMS  
*D. Serrao, A. Raygani, and L. Magagnin*
- 3320 Solution-Source Vapor-Phase Mist Deposition Method for Future Roll-to-Roll Process in Semiconductor Device Fabrication  
*S. Fujita, S. Katori, T. Ikenoue, and J. Piao*
- 3321 Effect of Light/Heat on Fast Formation Reaction of Highly-Conductive Polymer with Metal Shell Structure  
*Y. Hashimoto, J. Kawakita, T. Chikyow, and Y. Sakamoto*
- 3322 Deposition Rate of Metal on Conducting Polymer Under Photo Irradiation  
*H. Fujihira, J. Kawakita, T. Chikyow, and Y. Sakamoto*
- 3323 On the Mechanism of Electroless Deposition of Ni-P: Electrochemical and Computational Investigations  
*L. Magagnin, C. Cavallotti, and P. Cavallotti*
- 3324 Electroless Deposition for Developing ATR Surface Enhanced IR Spectroscopy  
*W. Cai*
- 3325 Investigation of Reactions and Additive Effects in Electroless Deposition by In-Situ Transmittance Measurement  
*K. Park, T. Lim, M. Kim, and J. Kim*
- 3326 Factors Affecting Reaction Rates of Chemical Bath Deposition of Copper Oxide Thin Films  
*J. Sasano, Y. Adachi, and M. Izaki*

- 3327 The Interaction of Tantalum with Tellurite Ions in Basic Solution  
*C. Tsang and J. Stickney*
- 3328 Electroless Atomic Layer Deposition: a Scalable Approach to Tailored Surface Structures  
*D. B. Robinson, P. Cappillino, L. Sheridan, and J. Stickney*
- 3329 Electroless Deposition of Cu and Ag on Valve Metal Substrates  
*L. Nolan, S. Djokic, K. Cadien, and T. Thundat*
- 3330 Chemical Modification of Nano-Nonwoven Fabrics Using Electrochemical and Electroless Deposition  
*S. Ndzesse and C. Shannon*
- 3331 Miniature Fuel Cell with Monolithically FabricatedSi Electrodes -Reduction of Pt by UPD-SLRR-  
*D. Ogura, T. Honjo, and M. Hayase*
- 3332 Large Scale, Electroless Synthesis of Highly Stable Flower-like Silver Nanostructures by a Templateless Method for SERS Application  
*C. Desmonda and Y. Tai*
- 3333 SERS-Active Substrates Fabricated by Displacement Deposition of Metals on Porous Silicon  
*K. Artsemyeva, H. Bandarenka, A. Panarin, I. Khodasevich, S. Terekhov, M. Balucani, and V. Bondarenko*
- 3334 The Kinetic Parameter of the Ni-W Alloy Electrodeposition  
*H. Xiao, N. Yu, Y. Feng, and Z. Liu*
- 3335 Cohesion Property of Electroless Plated Ni-P Coating on Fiber Bragg Grating  
*L. Fang, P. Zhang, A. Tang, and S. Xue*
- 3336 Oxygen-Assisted Vacuum Ultra-Violet Surface Modification of Polymers as a Pretreatment for Electroless Nickel Platimg  
*A. Nakamura, N. Mukado, T. Ichii, and H. Sugimura*
- 3337 Enhanced Pd Distribution by Three-Step Activation Process for Electroless Cu Plating  
*C. Lee, H. Lee, M. Lee, J. Hur, and H. Lee*
- 3338 Preparation and properties of Ni-Co-P/nano-sized SiC electroless composite coatings  
*J. Hu, L. Fang, P. Zhong, and Y. Yang*
- 3339 Raman and DFT study of Reductant Adsorption on Metal Surfaces in Electroless Deposition Process  
*B. Jiang, M. Kunimoto, M. Yanagisawa, and T. Homma*

**F4 - Emerging Materials and Processes for Energy Conversion and Storage**  
*ECS Electrodeposition, ECS Battery, ECS Energy Technology, ECSJ*

- 3340 (Invited) The Battery of the Future: Using Computational Modeling to Understand the Limits of Intercalation Systems Across a Wide Range of Chemistries  
*G. Ceder*
- 3341 Single-Step and Low-Temperature Synthesis of Layered LiCoO<sub>2</sub> Thin Film Electrodes: An Electrochemical-Hydrothermal Route  
*H. Porthault, F. Le Cras, and S. Franger*
- 3342 (Invited) Fabrication of Rechargeable Micro Lithium-Ion Battery with 3D Anode and 3D Cathode  
*K. Kanamura, K. Yoshima, and H. Munakata*
- 3343 Energy Harvesting Device  
*Y. Garsany and K. Swider-Lyons*
- 3344 Fundamental Study of Li Dendrite Growth in Ionic Liquid  
*T. Nishida, K. Nishikawa, T. Homma, Y. Fukunaka, and M. Rosso*
- 3345 Effect of Dissolved Gas in an Ionic Liquid Electrolyte for Lithium and Lithium/Sodium Metal Anode  
*J. K. Stark and P. Kohl*
- 3346 Two-dimensionally Patterned Electrodeposition of Sn Film from Aqueous Acid Bath  
*S. Yagi, E. Takeda, T. Okada, D. Mu, N. Okamoto, T. Saito, and K. Kondo*
- 3347 Porous Li<sub>2</sub>MnO<sub>3</sub> as a High Capacity and High Rate Capability Cathode Material  
*M. Nookala, T. Penki, and S. Duraisamy*
- 3348 Synthesis and Electrochemical Properties of Cation Doped Spinel LiM<sub>x</sub>Mn<sub>2-x</sub>O<sub>4</sub> (M=Ni, Al; 0≤ x ≤ 0.5) Cathode Materials for Li-Ion Battery  
*M. A. Kebede, N. Kunjuzwa, K. I. Ozoemena, and M. K. Mathe*
- 3349 Improved Lithium Storage and Cyclability in Graphene/Graphene Oxide Wired Mesoporous SnO<sub>2</sub>  
*K. Shiva and A. J. Bhattacharyya*
- 3350 (Electrodeposition Division Research Award Presentation) Electrodeposition for the Synthesis of Thin Film Solar Cells  
*L. Deligianni*
- 3351 (Invited) New Paradigms for Cost-Effective III-V Photovoltaic Technology  
*D. Shahjerdi, S. W. Bedell, B. Hekmatshoar, C. Bayram, N. Li, K. Fogel, P. Lauro, J. Ott, M. Hopstaken, and D. Sadana*
- 3352 Silicon Bonding State in Films Electrodeposited from SiCl<sub>4</sub> in Ionic Liquid  
*J. Komadina, T. Akiyoshi, Y. Ishibashi, X. Wang, Y. Fukunaka, P. Pianetta, and T. Homma*

- 3353 Novel Front Side MetallizationPprocesses for Silicon based Solar Cells  
*A. Bund, M. Fritz, U. Schmidt, O. Luehn, and H. Kuehnlein*
- 3354 (Invited) CIGS-Based Solar Cells Prepared from Electrodeposited Precursor Films  
*R. N. Bhattacharya and Y. Kim*
- 3355 One-Step Electrochemical Deposition of Cu-In-Ga Mixed Oxide Thin Films for Low-Cost CIGS Solar Cells  
*E. Chassaing, A. Duchatelet, T. Sidali, G. Savidand, and D. Lincot*
- 3356 Electrophoretic Deposition: A Bottom-up Approach to Functional Nanocomposite Films  
*M. A. Worsley, A. Pascall, K. Sullivan, T. Olson, C. Orme, J. Satcher, and J. Kuntz*
- 3357 Electrodeposition of Elements for Thin Film, Photovoltaic Applications: Citrate Complexation and Partial Current Densities  
*S. S. Zahmi and E. Podlaha*
- 3358 Wet Clean Efficiency Monitor by SP3 SM  
*Y. Chang Chien, M. Yeh, C. Yang, S. Ku, C. Wan, C. Hu, E. Chen, J. Yan, E. Khuan, K. Joyce, and C. Hu*
- 3359 Tuning of Mesopore Size in  $\text{WO}_3$ -based Photoaodes for Enhanced Visible Light Driven Water Oxidation  
*D. Chandra and M. Yagi*
- 3360 CIS Thin Film Solar Cells from Electrodeposited Cu/In Stacked Precursors  
*Y. Kim, S. Chae, S. Yoon, M. Jeon, and R. N. Bhattacharya*
- 3361 Various Metal Oxides based Dye-Sensitized Solar Cells  
*S. Kang*
- 3362 Fabrication Mediated by Self-Assembly of Block Copolymer and Photoelectrochemical Properties of Mesoporous  $\text{WO}_3$  Films  
*D. Chandra, K. Ouchi, and M. Yagi*
- 3363 Preparation and Photoanodic Properties of a Chromium-Electrodeposited  $\text{TiO}_2$  Electrode  
*R. Tsuriya, M. Kajita, N. Abe, A. Shoji, and M. Yagi*
- 3364 Energy Storage Devices from Biomass Conversion Byproducts, Lignin  
*J. Yang, S. Gunasekaran, and S. Gunasekaran*
- 3365 Pore-Filling Anion-Exchange Membranes for Non-Aqueous Redox Flow Batteries (RFBs)  
*M. Kang, M. Lee, J. Kim, H. Cha, and J. Park*
- 3366 Novel Graphene - Polyethylene Oxide Composite Electrolyte for Highly Efficient Solid State Dye Sensitized Solar  
*M. Akhtar, Z. Li, J. Jang, and O. Yang*

- 3367 Designing the Far-red Sensitive Squaraine Dyes for Dye-Sensitized Solar Cells in the Light of Photo-Physical Investigations  
*S. S. Pandey, R. Watanabe, Y. Ogomi, G. Miguel, M. Marchena, A. Douhal, and S. Hayase*
- 3368 Graphene-Quantum Dots Composite for Photovoltaic Devices  
*S. Guo, W. Wang, C. Ozkan, and M. Ozkan*
- 3369 Electrodeposition of Zn-based Chalcogenide Materials  
*K. Park, D. Kim, and B. Yoo*
- 3370 Electrodeposition and Growth of Widegap Copper Indium Selenide Thin Films  
*S. Menezes and Y. Li*
- 3371 Possibility of Large-Size Single Crystal Growth in Seed Cast-Grown Monocrystalline Silicon  
*B. Gao, H. Harada, Y. Miyamura, S. Nakano, and K. Kakimoto*
- 3372 High Performance of "Intelligent" Conductive Ceramic Anodes for Solid Oxide Fuel Cells Based on Infiltration  
*L. Adijanto, V. Balaji Padmanabhan, R. Kuungas, J. Vohs, and R. Gorte*
- 3373 Synthesis and Characterization of Molybdenum Nitride for Electrosynthesis Applications  
*M. Sykora, A. H. Mueller, C. R. Kreller, E. L. Brosha, and F. H. Garzon*
- 3374 Enhancement of Visible-Light-Induced Oxygen Evolution at a  $\text{WO}_3$  Film by Cobalt Ions in an Electrolyte Solution  
*M. Yagi and M. Kajita*
- 3375 Investigation of Carbon Deposition in Three-Dimensionally Ordered Macroporous Ni-YSZ Anode  
*H. Munakata, Y. Katsuki, and K. Kanamura*
- 3376 Phase Analysis and Electrical Conductivity of Mn-doped and Fe-doped Ceria  
*L. Zhao, S. R. Bishop, and K. Sasaki*
- 3377 Sulfonated Polyether Ether Ketone (SPEEK) Membrane for Water Electrolysis  
*R. Venkatkarthick, A. Sankari, S. Meenakshi, S. D. Bhat, P. Sridhar, S. Pitchumani, S. Vasudevan, D. Jonas Davidson, G. Sozhan, and S. Ravichandran*
- 3378 Effects of Sr Doping on Crystallization, Conductivity and Vanadium Reduction of  $\text{La}_{1-x}\text{Sr}_x\text{VO}_3$  Electrode in Reducing Atmosphere  
*K. Fung, C. Liu, C. Ni, and S. Tsai*
- 3379 Effect of Nickel Surface Structure on Urea Electrolysis: An Experimental Study  
*B. Hessler, D. A. Daramola, A. Miller, and G. G. Botte*

- 3380 (Invited) A Bilayer Membrane of Photocatalytic Nanotube Array and Hydrogen Permeable Metal for High-Purity Hydrogen Production  
*K. Noda and M. Hattori*
- 3381 Electrodeposited Pt<sub>100-x</sub>Pbx Alloys and Intermetallics for Direct Formic Acid Fuel Cell  
*S. Hwang, J. Bonevich, J. Kim, and T. Moffat*
- 3382 Characterization of the Electronic and Electrochemical Properties of Cu<sub>2</sub>O and Fe<sub>2</sub>O<sub>3</sub> modified TiO<sub>2</sub> Nanotubes  
*L. Tsui and G. Zangari*
- 3383 Direct Electrodeposition of Porous Platinum  
*L. Jones, A. Ott, T. Junk, and S. Bhargava*
- 3384 The Effect of Surface Modification on the Properties of a Nickel Catalyst: A Theoretical Study  
*D. A. Daramola, B. Hassler, and G. G. Botte*
- 3385 Preparation of Nanostructured Pd Anodes for Alkaline Direct Ethanol Fuel Cells (DEFC) by Electrochemical Milling and Faceting (ECMF)  
*Y. Chen, A. Lavacchi, F. Vizza, A. Marchionni, J. Filippi, M. Bevilacqua, M. Innocenti, and H. Miller*
- 3386 Bringing Conjugated Polymers and Oxide Nanoarchitectures into Intimate Contact: Light Induced Electrodeposition of Polypyrrole and Polyaniline on Nanoporous WO<sub>3</sub> or TiO<sub>2</sub> Nanotube Arrays  
*C. Janaky, N. de Tacconi, W. Chanmanee, and K. Rajeshwar*
- 3387 The Mechanism of Visible-Light-Derived Photocurrent Generation at an Antimony Sulfide / Metal Oxide Electrode  
*A. Shoji, T. Ueno, H. Kabaki, S. Okuyama, and M. Yagi*
- 3388 Carbon-Supported Iron(III)-Corrole as a Non-Precious Metal Catalyst for Fuel Cell Application  
*I. Shown, H. Huang, S. Wang, S. Chang, H. Hsu, H. Du, C. Wang, L. Chen, and K. Chen*
- 3389 Photoelectrochemical Generation of Hydrogen Using p-type CaFe<sub>2</sub>O<sub>4</sub> Photocathodes  
*R. Venkatkarthick, C. Krithiga Devi, L. John Berchmans, S. Vasudevan, D. Jonas Davidson, G. Sozhan, and S. Ravichandran*
- 3390 Development of Electrically Controlled Energetic Materials (ECEM)  
*E. Rozumov, K. Chung, D. Kaminsky, P. Anderson, P. Cooke, K. Griswold, M. Donadio, M. Sussman, J. Laquidara, C. Adam, D. Thompson, T. Manning, J. Wyckoff, V. Panchal, E. Caravaca, W. Sawka, M. McPherson, and T. Buescher*

## **F5 - Magnetic Materials and Devices 12**

*ECS Electrodeposition, ECSJ Magnetic Materials Processes and Devices*

- 3391 Thin Film Magnetic Heads - Early Inventions and Their Ongoing Impact on Magnetic Storage and on Electrochemistry  
*L. T. Romankiw and S. Krongelb*
- 3392 Beyond Perpendicular Magnetic Recording- Alternative Magnetic Storage Technologies  
*N. robertson*
- 3393 Electrodeposition of Magnetic Alloys Used in Fabrication of Recording Heads  
*I. Tabakovic, S. Riemer, J. Gong, V. Venkatasamy, and M. Kautzky*
- 3394 Magnetic Tape Heads and Contact Recording  
*R. G. Biskeborn*
- 3395 Electrochemical Deposition of Magnetic Alloy Films with Large Magnetic Anisotropy  
*D. Liang and G. Zangari*
- 3396 Reversible Change of Magnetism in FePt and CoPt Films by Electrochemical Charging  
*K. Leistner*
- 3397 Resistivity Control in CoFeNiX Magnetic Alloys  
*N. Dole, D. Lee, N. Brockie, A. Papou, W. French, and S. Brankovic*
- 3398 Composition Gradients and Magnetic Properties of 10-100nm NiFe and CoFe Films Obtained by Electrodeposition  
*J. Gong, S. Riemer, V. Venkatasamy, M. Kautzky, and I. Tabakovic*
- 3399 Development of Thin Film Technology for High-Density Magnetic Recording Media  
*M. Futamoto*
- 3400 Electroplated Hardmask for Bit Patterned Media Nanoimprinting Template Fabrication using Block Copolymer Lithography  
*C. Bonhote, G. Siddiqi, J. Lille, and R. Ruiz*
- 3401 Microstructural and Magnetic Studies of Electrodeposited, Equiaatomic Fe-Pt Films  
*D. Liang and G. Zangari*
- 3402 Metastable  $L1_1$  and  $B_h$  Ordered Phase Formation in CoPt Alloy Thin Films Epitaxially Grown on Metal Underlayers  
*M. Otake, D. Suzuki, F. Kirino, and M. Futamoto*
- 3403 Superconformal Electrodeposition of Ni, Co and Fe-Group Alloys  
*T. Moffat, C. Lee, S. Kim, Y. Liu, and D. Josell*
- 3404 Induced Codeposition of NiMo, NiW and CoW Alloys with a Competing Side Reaction  
*S. Sun, T. Bairachna, T. Maliar, H. Cesulic, and E. Podlaha*

- 3405 Electrodeposition of Super Invar into Micro- and Nano- Recesses  
*H. Kim, M. Murphy, S. Soper, and E. Podlaha*
- 3406 Aqueous DC Electrodeposition and Mechanism of Magnetic SmCo Alloys  
*J. Wei, M. Schwartz, and K. Nobe*
- 3407 Developments in Integrated On-Chip Inductors with Magnetic Yokes  
*E. J. O'Sullivan, N. Wang, P. Herget, L. T. Romankiw, B. C. Webb, R. E. Fontana, N. Sturcken, K. L. Shepard, and W. J. Gallagher*
- 3408 A Unique Magnetic Alloy for Integrated Power Systems on a Chip  
*A. Panda, T. Liakopoulos, M. Wilkowski, and A. Lotfi*
- 3409 Magnetic Micro and Nano Actuator Systems  
*H. H. Gatzen*
- 3410 Evaluation of the Effects of Electroplating Conditions on the Material Properties of Iron Cobalt Thick Films using Design of Experiments  
*W. C. Patterson and D. P. Arnold*
- 3411 Nanoporous Alumina Growth in a Magnetic Field  
*A. Ispas, I. Vrublevsky, U. Schmidt, and A. Bund*
- 3412 Investigation of the Crystallization of NiFe81/19 Depending on the Annealing Temperature  
*M. C. Wurz, A. Shaganov, A. Filimonov, and L. Rissing*
- 3413 Integration of Electroplated CoFe in Trench Type Flux Guides for Magnetic MEMS Applications  
*J. Chen, S. Cvetković, and L. Rissing*
- 3414 Microfabrication of High-Performance Thick Co<sub>80</sub>Pt<sub>20</sub> Permanent Magnets for Microsystems Applications  
*O. D. Oniku and D. P. Arnold*
- 3415 Fabrication and Characterization of an Improved Micro Inductosyn® Sensor  
*D. Miletic, J. Flügge, and H. H. Gatzen*
- 3416 Embossing of Soft-magnetic Structures and Influence on Magnetic Properties  
*M. Kaiser, M. C. Wurz, S. Cvetković, R. Schwaiger, and L. Rissing*
- 3417 Magnetic Properties of Ni-Cu Alloy Nanowires Obtained by the Template Method  
*I. Enculescu, E. Matei, M. Toimil Molares, A. Leca, and V. Kuncser*
- 3418 CPP-GMR of Co/Cu Multilayered Nanowires Electrodeposited into Anodized Aluminum Oxide Nanochannels with Large Aspect Ratio  
*N. Goya, Y. Zenimoto, K. Takao, T. Ohgai, M. Nakai, and S. Hasuo*
- 3419 Electroplating of Cu/Sn Layers for Hermetic Encapsulation for Vacuum Applications  
*M. C. Wurz, S. Cvetković, L. Rissing, and F. Bach*

- 3420 Anisotropic Magnetoresistance of Ni-Co-Fe Alloy Nanowires Electrodeposited into Anodized Aluminium Oxide Membrane Thin Films  
*Y. Ikeda, T. Egawa, K. Takao, T. Ohgai, M. Nakai, and S. Hasuo*
- 3421 Current-Induced Magnetization Switching in CPP Junctions based on Fe<sub>3</sub>Si/FeSi<sub>2</sub> Multilayered Films  
*Y. Noda, K. Sakai, T. Sonoda, K. Takeda, and T. Yoshitake*
- 3422 Aligning Superparamagnetic Nanoparticles at Temperatures Much Higher than the Blocking Temperature  
*W. Schwarzacher, J. Eloi, M. Okuda, and S. Ward Jones*
- 3423 Giant Magnetoelectric Effect in Thin Film Composites  
*E. Lage, A. Piorra, C. Kirchhof, E. Yarar, D. Meyners, and E. Quandt*
- 3424 SiGe Spintronics with Single-Crystalline Ferromagnetic Schottky-Tunnel Contacts  
*K. Hamaya, S. Yamada, and M. Miyao*
- 3425 Generation and Detection of a Pure Spin Current Using Co-based Heusler-alloy Spin Injector and Detector: Comparison of Co<sub>2</sub>FeSi and Co<sub>2</sub>MnSi  
*S. Oki, M. Kawano, K. Tanikawa, H. Aoki, S. Yamada, M. Miyao, and K. Hamaya*
- 3426 Electrochemical Synthesis of Ferromagnetic Metal-Metal Oxide Nanocontacts for Magnetic Field Sensor Application  
*J. George, R. Sharma, S. Elhalawaty, R. Carpenter, D. Litvinov, and S. Brankovic*
- 3427 Giantmagnetoimpedance Effect of La<sub>0.6</sub>Bi<sub>0.1</sub>Sr<sub>0.3</sub>MnO<sub>3</sub> at Room Temperature  
*S. K. Barik, R. Katiyar, and R. Mahendiran*
- 3428 Lipid-based Magnetic Nanomedicines for Cancer  
*Y. Namiki, T. Fuchigami, M. Nakagawa, and Y. Kitamoto*
- 3429 FePt Magnetic Hollow Spheres Designed for Nano-Scale Drug Delivery System Targeted to Cancer Tumor  
*T. Fuchigami, M. Nakagawa, Y. Namiki, and Y. Kitamoto*
- 3430 Fabrication of Magnetic Nanoparticle-Assembly with Biodegradable Polymer Core  
*C. Oka, N. Horiishi, and Y. Kitamoto*
- 3431 Development of Specific Delivery of Magnetic Nanoparticles in Cancer Tissue for Hyperthermia and Their Establishment of System for Safety Assessment  
*H. Zhang, T. Nakanishi, and T. Osaka*
- 3432 Separation of Magnetic Nano Beads by Using Soft Magnetic Flux Concentrators  
*M. Kaiser, J. Chen, P. Taptimthong, and L. Rissing*

## **G2 - Synthesis and Engineering General Session**

*ECS Industrial Electrochemistry and Electrochemical Engineering, ECSJ Industrial Electrolysis and Electrochemical Engineering*

- 3433 Electroplated Ni-W-S Alloy Cathode for Alkaline Water Electrolysis  
*D. Suzuki, K. Someya, T. Suzuki, A. Horie, R. Miyamoto, Y. Ishikawa, and S. Yoshihara*
- 3434 Size Control of Hydrogen Nanobubble by Pt-nanoparticle/Ru Electrode  
*K. Kikuchi and T. Okamoto*
- 3435 Degradation of Nickel Anode for Alkaline Water Electrolysis under Potential Cycling  
*H. Ichikawa, K. Matsuzawa, I. Nagashima, A. Manabe, Y. Nishiki, and S. Mitsushima*
- 3436 Water Electrolysis to Produce the Dry Oxygen for the Human Activities under the Closed Environment  
*Y. Sone, S. Masato, Y. Tetsuya, and S. Naoki*
- 3437 Low Voltage Electrochemical Process for Manufacturing Sodium Hydroxide and Halogenated Hydrocarbons  
*B. K. Boggs, S. Gorer, M. Kostowskyj, R. King, J. Miller, and R. Gilliam*
- 3438 Theoretical Study on Pressurized Operation of Solid Oxide Electrolysis Cells  
*M. Henke, C. Willich, C. Westner, F. Leucht, W. Bessler, J. Kallo, and K. Friedrich*
- 3439 Electrolytic Conversion of Sodium Salts in a Kraft Mill  
*J. Cloutier*
- 3440 Scale-up of Low Energy Process for Generation of Alkalinity  
*R. L. King, D. Martinez, J. Miller, S. Gorer, M. Kostowskyj, B. K. Boggs, and R. Gilliam*
- 3441 Design of Rechargeable Air Diffusion Cathode of Metal-Air Battery in Alkaline Solution  
*Y. Takeshita, S. Fujimoto, and M. Sudoh*
- 3442 Development of a High Performance Salt Electrolysis Cell Using Soft-Zero-Gap Method  
*H. Matsui, H. Tanaka, and H. Okido*
- 3443 Electrochemical Processes in Waste Water Treatment: Process Development at Pilot Plant Scale  
*D. Woisetschlaeger, M. Koncar, and M. Siebenhofer*
- 3444 Recycling Electrochemical Machining Electrolyte for Metal Recovery and Elimination of Waste  
*E. J. Taylor, B. Skinn, H. Garich, and M. Inman*
- 3445 Anodic Reactivity of Ferrous Sulfide Particles Generated in Wastewater Treatment  
*E. Mejia Likosova, Y. Poussade, J. Keller, and S. Freguia*

- 3446 Enhanced Electrochemical Oxidation of Rhodamine B by TiO<sub>2</sub>-Coated Granular Activated Carbon  
*X. Li, C. Wang, L. Zhang, Y. Qian, and Y. Wang*
- 3447 A Novel Chlorine Evolution Anode for Electrowinning of Non-ferrous Metals  
*M. Matsuda and M. Morimitsu*
- 3448 Preparation of Shape-Controlled Pt Nanoparticles by Galvanostatic Electrolysis  
*T. Nishimura, T. Nakade, T. Morikawa, and H. Inoue*
- 3449 Development of an Electrolysis-Reversible Hydrogen Electrode (E-RHE)  
*N. Kamiya*
- 3450 Effect of Pt Dissolution on H<sub>2</sub>O<sub>2</sub> Formation by Using RRDE Method  
*K. Ono, N. Takeuchi, K. Sekizawa, T. Yoshida, and M. Sudoh*
- 3451 Characterization and Performance of Non-Iridium Oxide Based Oxygen Evolution Anodes  
*T. Zhang and M. Morimitsu*
- 3452 Mathematical Modeling of Ammonia Electro-Oxidation in a Rotating Disk Electrode (RDE) System  
*L. A. Diaz Aldana, M. Muthuvel, and G. G. Botte*
- 3453 Electrocatalytic Synthesis of Hydrogen Peroxide on Non-Precious Catalysts  
*F. Hasché, T. Fellinger, M. Oezaslan, P. Strasser, and M. Antonietti*
- 3454 Cathodic Characteristic and Structural Analyses of a New Catalyst for Chlorate Electrolysis  
*K. Terada, S. Hatano, K. Hara, A. Kimura, M. Saito, H. Daimon, M. Inaba, and A. Tasaka*
- 3455 TiZO/Ag/TiZO Multilayer Films for the Application of a Very Low Resistance Transparent Electrode  
*G. Heo, Y. Lee, J. Park, J. Oh, D. Shin, and T. Kim*
- 3456 Synthesis and Properties of Pentacenes Having Alkyl-chains at 2, 3, 9, 10-Positions  
*S. Katsuta, C. Ohashi, K. Nakayama, and H. Yamada*
- 3457 Preparation and Characterization of Cathode Active Materials from Spent Lithium Ion Batteries  
*J. Moon, J. Ahn, S. Son, H. Lee, H. Kim, and H. Kim*
- 3458 Enhancement of Electrical Conductivity and Electrochemical Activity of Hydrogenated Amorphous Carbon by Incorporating Boron Atoms  
*H. Naragino, K. Yoshinaga, A. Nakahara, S. Tanaka, and K. Honda*
- 3459 Direct Preparation of Highly Fluorescent Pyrene-Dyes from Non-Fluorescent Precursors Upon Photoirradiation  
*T. Aotake, D. Kuzuhara, and H. Yamada*

- 3460 Two Dimensional Electrochemical-Thermal Coupled Models for Lithium-Ion Battery and Battery Stacks  
*S. De, P. Northrop, S. Santhanagopalan, and V. Subramanian*
- 3461 Experimental Investigation of Two-Phase Electrolysis Under Normal and Zero Gravity  
*P. Mandin, Z. Derhoumi, and H. Roustan*
- 3462 Performance of Acid-doped Polybenzimidazole Membranes for the Hybrid Sulfur Electrolyzer  
*J. Jayakumar, A. Gulledge, J. Staser, B. Benicewicz, and J. Weidner*
- 3463 On A Few Innovations of Chlor-alkali Membrane Process in Japan  
*N. Kawasaki and Y. Nakajima*
- 3464 In-situ Structural Analysis on the Growth Mechanism Pathways of Hydrothermal Synthesized CeO<sub>2</sub> Nanocrystals  
*E. Teo, M. Lin, Z. Fu, S. Ng, J. Tan, and H. Tan*
- 3465 Electrochemical Oxidation of Phenol at Boron-doped Diamond Electrode in Exponential Decay Modulated Current Supply  
*X. Xing, H. Li, and J. Ni*
- 3466 Photooxidation Treatment of Organic Materials on Titanium Dioxide Photoelectrode in Aqueous Solution Containing Sodium Chloride  
*D. Kodama, Y. Kohno, and Y. Maeda*
- 3467 Wear Resistant, Functional Hard Chrome Plated from a Trivalent Bath  
*M. Inman, T. Hall, B. Kagajwala, and E. J. Taylor*
- 3468 Suppression of PbO<sub>2</sub> Deposition on Nano-Structured IrO<sub>2</sub>-Ta<sub>2</sub>O<sub>5</sub>/Ti Anodes in Acidic Solutions  
*K. Kawaguchi, G. Haarberg, and M. Morimitsu*
- 3469 Investigating the Surface Structure of the Ti/SnO<sub>2</sub>-Sb<sub>2</sub>O<sub>5</sub> Anode and the Effect on its Electro-catalysis  
*Q. Ni, D. W. Kirk, and S. Thorpe*
- 3470 Growth Mechanism of WO<sub>3</sub>•0.33H<sub>2</sub>O Hierarchical Structure Prepared by Hydrothermal Method  
*X. He and C. Hu*

## **H1 - Carbon Nanotubes and Graphene: From Fundamental Properties and Processes to Applications and Devices**

*ECS Fullerenes, Nanotubes, and Carbon Nanostructures, ECS Dielectric Science and Technology, ECS Energy Technology, ECS Sensor, CSE*

- 3471 N-type Graphene Induced by Molecular Hydrogen Exposure at Room Temperature  
*B. Kim, S. Hong, S. Baek, H. Jeong, N. Park, M. Lee, S. Lee, J. Lim, Y. Jun, and Y. Park*
- 3472 DFT Calculation for Various Adatom Adsorptions on Graphene for Using Graphene as Substrate  
*A. Ishii, K. Nakada, and T. Torobu*
- 3473 Theoretical Study of a Zigzag Graphene Nanoribbon Field Effect Transistor  
*H. Karamitaheri, M. Pourfath, N. Neophytou, and H. Kosina*
- 3474 Hierarchical Graphene Macroassemblies  
*M. A. Worsley, M. Merrill, M. Suss, J. Lee, S. Kucheyev, C. Valdez, H. Mason, B. Mayer, J. Lewicki, A. Wittstock, M. Stadermann, J. Satcher, J. Biener, and T. Baumann*
- 3475 Nitrogen-Containing Graphene for Electrochemical Oxygen Reduction  
*S. M. Lyth, J. Liu, and K. Sasaki*
- 3476 Graphene Thermal Interface Materials  
*A. A. Balandin*
- 3477 Towards Novel Pillared Nanostructures based on Graphene  
*K. Spyrou, P. Rudolf, D. Gournis, P. Maurizio, L. Kang, and E. Diamanti*
- 3478 Chemically Prepared Reduced Graphene Oxide as Ultra Fast Temperature Sensor  
*S. Sahoo, S. Barik, G. Sharma, G. Khurana, and J. Scott*
- 3479 Comparison of Epitaxial Graphene growth on non-Polar and Polar 6H-SiC  
*L. O. Nyakiti, V. Wheeler, R. Myers-Ward, N. Garces, F. Bezares, J. Caldwell, C. Eddy Jr., and D. Gaskill*
- 3480 Non-Monotonic Size Dependence of Thermal Conductivity of Graphene Ribbons  
*D. Nika, A. Askerov, and A. A. Balandin*
- 3481 Layer by Layer Etching of CVD Graphene for Full Graphene Device Fabrication  
*J. OH, J. Lim, J. Park, and G. Yeom*
- 3482 Wafer-Scale Graphene Synthesis and Tailoring via Segregation Methods Extended to Metals with Low Carbon Solubility  
*A. Zenasni, A. Delamoreanu, and C. Rabot*
- 3483 Study of the Point Defects Induced by Electrochemical Potential in Graphene Monolayers  
*J. J. Velasco-Velez, Y. Zhang, I. Martin-Fernandez, C. Martinez, and M. Salmeron*

- 3484 Interfacing Nanocarbons with Organic and Inorganic Semiconductors - From Extended Tetrathiafulvalenes to Nanocrystals / Quantum Dots  
*D. M. Guldin*
- 3485 Mechanochemical Synthesis of Carbon Nanomaterials by a High-Speed Ball-Milling Process  
*S. Ohara, Z. Tan, K. Yamamoto, and T. Hashishin*
- 3486 Far-Infrared Absorption of Single-Walled Carbon Nanotube Films  
*T. Morimoto, S. Joung, and T. Okazaki*
- 3487 Photosensitized Hydrogen Evolution from Water Using Single-Walled Carbon Nanotube/Fullerodendron/SiO<sub>2</sub> Coaxial Nano hybrid  
*Y. Takaguchi, T. Wada, W. Sakata, and T. Tajima*
- 3488 Electrochemical Property of Well-Coated Multi-Walled Carbon Nanotube with Polyaniline-Cyclodextrin Polymer Composites  
*W. Zhang, M. Chen, X. Gong, and G. Diao*
- 3489 Advantage of Carbon Nanotubes as Catalyst Support in Polymer Electrolyte Membrane Fuel Cells  
*M. Berber, T. Fujigaya, and N. Nakashima*
- 3490 Effect of Charge of Solubilizers on the Electronic States of Single-Walled Carbon Nanotubes  
*Y. Hirana, Y. Niidome, and N. Nakashima*
- 3491 Enlargement of Space Charge Layer by P-N Junction of Multi-walled Carbon Nanotubes Modified with Tin Oxide Nanoparticles  
*T. Hashishin, H. Ikenoko, K. Kojima, and J. Tamaki*
- 3492 Single Molecule Lysozyme Monitoring by a Carbon Nanotube Circuit  
*Y. Choi, P. Sims, I. Moody, T. Olsen, G. Weiss, and P. G. Collins*
- 3493 Application of Carbonaceous Nanomaterials in Biomedicine  
*J. Zhen, Q. Liu, D. Chen, C. Wang, and C. SHU*
- 3494 One-Step Liquid-Phase Synthesis of Carbon Nanomaterials with Carbon Paper  
*K. Yamagawa, Y. Ayato, H. Shiroishi, and J. Kuwano*
- 3495 PVDF/MWCNT Composite Films for Infrared Sensing and Energy Harvesting Applications  
*A. K. Batra, A. Chilvery, and M. Thomas*
- 3496 The Investigation of Partial Reduced Graphene Oxide (GO)/PEDOT:PSS Nanocomposite  
*J. Seo, H. Yun, W. Hong, J. Jung, B. Sohn, J. Lee, and C. Choi*
- 3497 Evaluations of Nonbonding Interactions in Endohedrally and Exohedrally Functionalized Fullerenes  
*N. Mizorogi, T. Akasaka, and S. Nagase*

- 3498 Synthesis and Structural Characterization of Fullerene derivatives Encapsulating Trimetallic Nitride Cluster  
*T. ABE, S. Sato, C. Saito, Z. Slanina, T. Tsuchiya, T. Akasaka, and S. Nagase*
- 3499 Catalytic Synthesis of Carbon Nanotube and Nanofilament Over Oxidized Diamond-Supported Catalysts  
*K. Nakagawa, T. Toriyama, G. Tsujino, T. Ando, and H. Oda*
- 3500 Large-Area Graphene Grown with a Novel rapid Cooling Method  
*M. C. Chen, Y. Huang, C. Chen, S. Hung, C. Cheng, C. Li, H. Hsieh, H. Wu, and G. Chi*
- 3501 Synthesis and Properties of Paramagnetic Metallofullerene/Electron Donor Dyad  
*Y. Kawana, T. Tanaka, T. Tsuchiya, T. Akasaka, N. Mizorogi, and S. Nagase*
- 3502 Complexation Studies of Endohedral Metallofullerene with Concave  $\pi$ -System  
*N. Umekita, T. Tsuchiya, N. Mizorogi, H. Sakurai, N. Martín, D. M. Guldí, S. Nagase, and T. Akasaka*
- 3503 Framework Transformation of Non-IPR Structured Metallofullerene  
*Y. Muto, H. Kurihara, Z. Slanina, T. Tsuchiya, S. Nagase, and T. Akasaka*
- 3504 Thermally Reduced Graphene Oxide as Energy Storage Materials  
*W. Hong, B. Kim, J. Kim, S. Lee, and H. Kim*
- 3505 Soft Lithographic Patterning and Transfer Process of Graphene Sheets  
*H. Kim, M. Jung, D. Jung, S. Lee, J. Lim, J. Lee, and K. An*
- 3506 Novel Growth Process of Carbon Nanotubes in Atmosphere  
*S. Lu and W. Hsu*
- 3507 The Organic Additives Effects during Electroless Nickel and Silver Deposition on Carbon Nanotube  
*T. Saito, Y. Takagi, N. Okamoto, K. Kondo, Y. Kobayashi, and Y. Fujiwara*
- 3508 Integrated Field Emission Diode with a Nano-graphite-diamond-like Emitters Process Development and Its Electrical Characteristics Study  
*N. Zaytsev, S. N. Orlov, S. Yanovich, A. Krasnikov, I. Matyushkin, I. Khomyakov, K. Svechkarev, and R. Yafarov*
- 3509 Multiple Auger Decay at Resonant Photo-Excitation in Carbon Thin Films  
*M. Richter, D. Friedrich, and D. Schmeißer*
- 3510 Photo-Thermo-Voltaic Effects in Carbon Nanotube Films  
*M. Omari, T. Hosseini, and N. Kouklin*

- 3511 Enhancement of Diamond Crystallite Size of Ultrananocrystalline Diamond/Amorphous Carbon Composite Films by Controlling Arc Discharge Energy of Coaxial Arc Plasma Gun  
*K. Hanada, A. Tominaga, T. Sugiyama, K. Sumitani, H. Setoyama, and T. Yoshitake*
- 3512 p-Type Semiconducting Properties of Boron Doped Ultrananocrystalline Diamond/Amorphous Carbon Composite Films Prepared by Coaxial Arc Plasma Deposition  
*Y. Katamune, S. Ohmagari, H. Setoyama, K. Sumitani, Y. Hirai, and T. Yoshitake*
- 3513 Controllable Synthesis of High-Quality Graphene Using Inductively-Coupled Plasma Chemical Vapor Deposition  
*L. Nang, N. Park, Z. Lee, and E. Kim*
- 3514 High Reactive Catalysts Based on Gold Nanoparticles Supported Over Carbon Nanotubes  
*T. M. Abdel-Fattah*
- 3515 Effect of Boric Acid on the Nucleation and Growth of Ni Nanoparticles for CNT Growth  
*J. Vanpaemel, M. van der Veen, C. Huyghebaert, S. De Gendt, and P. Vereecken*
- 3516 The Effect of Carbon-Nanotubes on the Electrochemical Impedance Behavior of Glass and Carbon fibers with AA2024 and AA7075  
*Y. Yoon, K. Lafdi, and M. Bouchard*
- 3517 Carbon Nanotube Enhanced Functional Carbon Fibers from Renewable Resources  
*O. Rios, W. E. Tenhaeff, M. McGuire, P. Menchhofer, A. Johs, K. L. More, and D. White*
- 3518 Highly Conductive, Super Stiff Carbon Nanotube-based Macroassemblies and Their Composites  
*M. A. Worsley, M. Merrill, S. Kucheyev, J. Kuntz, T. Han, J. Satcher, M. Stadermann, A. Hamza, J. Biener, and T. Baumann*
- 3519 Vertically Aligned Carbon Nanofiber Based Electrode for Biosensor Applications  
*D. Suazo, J. Rivera, J. Koehne, M. Meyyappan, and C. Cabrera*
- 3520 Indene-C<sub>60</sub>/C<sub>70</sub> Bisadduct as Acceptor in Polymer Solar Cells  
*Y. Li*
- 3521 Synthesis and Separation Strategies for New Fullerenes Created in Oxidizing Atmospheres  
*S. Stevenson*
- 3522 Design of Robust Functional Structures on Carbon Substrates Using Silyl-Protected Aryldiazonium Electroreduction  
*Y. Leroux and P. Hapiot*
- 3523 Preparation of Hydrophilic Nano-Carbon Particles by Electrolysis and Their Environmental Applications  
*S. Ikeda, S. Kawasaki, Y. Hayashi, S. Kita, A. Nobumoto, H. Ono, and S. Ono*

- 3524 Synthesis and Functions of Hybrid Assemblies Composed of Metallocporphyrin and Heteropolyoxometallates  
*T. Kojima, A. Yokoyama, T. Ishizuka, K. Ohkubo, and S. Fukuzumi*
- 3525 Synthesis and Properties of Acenes Photochemically Prepared from Diketone Precursors  
*H. Yamada, T. Aotake, S. Katsuta, Y. Kaneshige, C. Ohashi, and K. Nakayama*
- 3526 Stability Computations for La@C<sub>76</sub>  
*Z. Slanina, F. Uhlik, T. Akasaka, and S. Nagase*

**I1 - Physical and Analytical Electrochemistry General Session**  
*ECS Physical and Analytical Electrochemistry, ECSJ, CSE, KECS*

- 3527 Electrochemical Measurements in High Magnetic Fields for Energy Storage  
*A. Migliori, C. R. Kreller, R. L. Borup, and F. H. Garzon*
- 3528 The Importance of Electrochemical Surface Potentials in Pressure Solution  
*K. Kristiansen, M. Valtiner, G. Greene, J. Boles, and J. Israelachvili*
- 3529 Surface Intermediates of the Oxygen Evolution Reaction on Iridium as Observed by Surface Interrogation Scanning Electrochemical Microscopy (SI-SECM)  
*N. Arroyo-Curras and A. Bard*
- 3530 SECM Footprint Analysis of Reactive Oxygen Species Produced During Multielectronic O<sub>2</sub> Reduction  
*J. Noel, A. Latus, C. Lagrost, E. Volanschi, and P. Hapiot*
- 3531 New Methods and New Applications of Electrochemiluminescent Analysis  
*G. Xu, L. Hu, L. Zhang, Y. Yuan, T. Yuan, and S. Parveen*
- 3532 Probing The Structure and Composition at the Electrode Interface: Understanding the Importance of Through-Space Interactions  
*M. R. Anderson, M. De La Rosa, M. Tomlinson, and M. Anderson*
- 3533 Surface-Enhanced Raman Spectroscopy Platforms for Studying Electrodeposition and Surface Chemistry of Nanostructured Semiconductors  
*J. Gu and S. Maldonado*
- 3534 Detection of Tetryl by Electrogenerated Chemiluminescence (ECL) quenching of Ru(bpy)3<sup>2+</sup>  
*P. Lindhome and R. L. Calhoun*
- 3535 Simulation of Electrochemical Micromachining with Nanosecond Pulses  
*E. L. Hotoiu, S. Van Damme, and J. Deconinck*
- 3536 Performance Characterization of the Titanium(IV)-Porphyrin Reagent for Determining Hydrogen Peroxide based on Ab Initio Calculations  
*K. Takamura and T. Matsumoto*

- 3537 Quantum Mechanical Analysis on the Effect of Electric Field on the Adsorption of Water and Hydronium on Transition Metal Surfaces  
*A. Huzayyin, J. Chang, F. Dawson, and K. Lian*
- 3538 A Temperature Dependent Multi-Ion Model for Time Accurate Numerical Simulation of the Electrochemical Machining Process  
*D. Deconinck, S. Van Damme, and J. Deconinck*
- 3539 Electroless Deposition of the cylindrical Iron Nanotubes using Anodic Aluminium Oxide Template  
*T. Hussain, A. Shah, and G. Zohra*
- 3540 Extract Metals by a Treated Scallop Shell Powder  
*K. Takeuchi, H. Honda, S. Tamura, T. Ishiguro, Y. Kogo, H. Koyanaka, J. Neufeld, M. Feygenson, and A. Kolesnikov*
- 3541 Preparation and Electrochemical Behavior of Water-Soluble Inclusion Complex of Imidacloprid with  $\beta$ -cyclodextrin Polymer  
*M. Chen, J. Wang, W. Zhang, and G. Diao*
- 3542 Fabrication of Porous Conductive Diamond Hollow Fibers  
*T. Kondo, Y. Kodama, and M. Yuasa*
- 3543 Electroanalytical Performance of Nitrogen-Containing Tetrahedral Amorphous Carbon Thin-Film Electrodes  
*X. Yang, G. DeVivo, L. Haubold, and G. Swain*
- 3544 Synthesis of Pt-Ir Catalysts by Coelectrodeposition: Application to Ammonia Electrooxidation in Alkaline Media  
*S. Le Vot, L. Roué, and D. Bélanger*
- 3545 Electrochemical Study of Ilmenite using Carbon Paste Electrode Under Reducing Condition  
*N. Jabit, G. Senanayake, and M. Nicol*
- 3546 Experiments and Modeling of Electrochemical Impedance Spectroscopy on Pressurized SOFC  
*C. Willich, M. Henke, C. Westner, L. Florian, W. Bessler, J. Kallo, and K. Friedrich*
- 3547 Diffusion Impedance Analyzed by Equivalent Circuit Involving CPE using Microelectrode  
*Y. Hoshi, S. Kawakita, I. Shitanda, and M. Itagaki*
- 3548 Electrochemical Behavior of Samarium and Ytterbium in the 1-(1-Butyl)trimethylammonium Bis(trifluoromethylsulfonyl)imide Ionic Liquid Containing TODGA  
*Y. Pan and C. Hussey*

- 3549 Electrochemical Behavior of Praseodymium and Neo-Dymium in the 1-butyl-3-methylpyrrolidinium bis(trifluoromethylsulfonyl)imide Ionic Liquid Containing Chloride  
*L. Chou and C. Hussey*
- 3550 In-depth Study on Nano-structured Electrode Reaction Mechanism in Lithium-Ion Batteries  
*H. Cho and Y. Meng*
- 3551 Investigation on Polyoxometalates for the Application in Redox Flow Batteries  
*J. Friedl, C. Bauer, R. Al-Oweini, D. Yu, U. Kortz, H. Hoster, and U. Stimming*
- 3552 Electrode Reactions of Dissolved p-Dimethoxybenzene on a Polyaniline-Modified Electrode  
*J. Yano*
- 3553 Equivalent Circuits of Zinc-Air Battery and Analysis of Zinc-Air Battery Oxygen Sensor using the Equivalent Circuits  
*M. Takahashi and M. Yamauchi*
- 3554 The Electrocatalytic Activity of Ligand-Protected Gold Particles: Formaldehyde Oxidation  
*K. Luo, X. Li, and Y. Gong*
- 3555 Nanocomposite Coatings based on the Conductive Polymers and Functionalized Carbon Nanotubes for Obtained of Modified Electrodes  
*V. Branzoi, F. Branzoi, and A. Musina*
- 3556 Solar Driven Hydrogen Production with co-doped Gallium and Nitrogen in Zinc Oxide films prepared by Reactive RF Magnetron Sputtering  
*S. Shet*
- 3557 Comparison between Palladium Electrode and Nanoparticles in the Ethanol Detection to Biosensor and Sensor Applications  
*I. Feliciano, D. Diaz, Y. De la Torre, and C. Cabrera*
- 3558 Preparation of Bismuth Tungstate Nanocrystallites by Ball Milling of Flake-ball Particles and Their Photocatalytic Activity  
*H. Hori and B. Ohtani*
- 3559 Electrochemical Properties of Free-Standing Boron-Doped Heteroepitaxial Diamond Electrode  
*H. Kodama, K. Suzuki, S. Kono, and A. Sawabe*
- 3560 Study on the Effects of Electrochemical Realkalization Method with Alcamines Inhibitors as Electrolyte  
*J. lu, Y. Zhang, J. Zhang, and J. Jiang*
- 3561 Transcutaneous Vein Imaging and Venepuncture System for Blood Test  
*H. Saito, S. Yamamoto, and H. Takagi*

- 3562 Reduction of Perchlorate by Electrochemically Generated Zero-Valent Iron on Conducting Polymer Electrode  
*E. Kim, S. Choi, S. Kim, and K. Paeng*
- 3563 Anomalous Codeposition of Ni-Zn in Acid Solutions  
*Y. ADDI and A. Khouider*
- 3564 Irregular-Stairs Method: A More Precise Method of Measuring the Performance of Dye-Sensitized Solar Cells  
*J. Shimura and K. Noda*
- 3565 Cyclic Voltmogram for HUPD on Pt(111) Calculated from Total Gibbs Energies  
*H. A. Asiri and A. Anderson*
- 3566 Long Term Evaluation of Potentiometric Oxygen Sensors in Molten Lead  
*A. Verdaguer, S. Colominas, and J. Abella*
- 3567 Electrochemical Reduction of Selenite and Selenate Accelerated by Methyl Viologen  
*F. Koshikumo, W. Murata, A. Ooya, and S. Imabayashi*
- 3568 Effect of pH on Absorption and Reductive Desorption Processes for Self-assembled Monolayer of Aromaticthiol Studied by Surface Enhanced IR Spectroscopy  
*K. Nishiyama, A. Kumatabara, H. Ueda, and S. Yoshimoto*
- 3569 Crystalline Composition Analysis of Titanium(IV) Oxide Photocatalyst Particles by X-ray Diffraction Analysis  
*M. SANO and B. Ohtani*
- 3570 Photoelectrochemical Water Splitting with Aluminum and Nitrogen co-doped Zinc Oxide prepared by Sputtering Technique  
*S. Shet*
- 3571 Potentiometric Determination of Potassium Ions in Biodiesel at a Nickel(II) Hexacyanoferrate Modified Electrode Using Microemulsions  
*G. Sedenho, L. Paim, and N. R. Stradiotto*

**12 - Bioelectroanalysis and Bioelectrocatalysis**  
*ECS Physical and Analytical Electrochemistry, ECSJ Bioengineering, CSE*

- 3572 Electrochemical Investigations of Lipid Membranes and Proteins at the Liquid-Liquid Interface  
*R. Kataky*
- 3573 Fabrication of Nanoporous 1- 3 nm Thick Membranes on Nanostructured Microelectrodes for Low nM Detection  
*A. Boateng, F. Irague, and A. Brajter-Toth*
- 3574 Electrochemical Immunoassay of Phosphorylated Proteins  
*D. Du*

- 3575 Intermediate Layers for Immobilization of Biomacromolecules on Various Substrates  
*A. Nowicka, A. Kowalczyk, M. Fau, and Z. J. Stojek*
- 3576 Functional Nanomaterials for Sensitive Bioassay  
*D. Du and Y. Lin*
- 3577 In Vivo Electroanalytical Chemistry: Strategies Based on Surface/Interface Chemistry  
*L. Mao*
- 3578 Development of Nano-Pt/Graphene/Nafion Composite Membrane for Glucose Biosensor  
*H. Leu, K. Chiu, and C. Lin*
- 3579 Electrochemical Techniques as Effective Readout Methods for Aptamer based Biosensors  
*E. Wang*
- 3580 Synthesis Graphene-based Nanocomposites and Apply in Electrochemical Sensors  
*Z. Wang*
- 3581 Electrochemical Surface Plasmon Resonance Sensor based on Nanohole Array Electrode Fabricated by Nanoimprinting Technique  
*O. Niwa, K. Nakamoto, and R. Kurita*
- 3582 Investigation of the Dissimilarity Metal Reduction (DMR) Pathways of *Shewanella* with Spatial Resolution by Scanning Electrochemical Microscopy  
*G. Chen, D. Kimmel, and D. Cliffel*
- 3583 Facilitation of High-Rate NADH Electrocatalysis at Activated Carbon Electrode  
*H. Li, R. Li, R. Worden, and S. Calabrese Barton*
- 3584 Ionic Liquid-Based Electrochemical Biosensors  
*P. Yu and L. Mao*
- 3585 Electrochemical Biosensor and Biofuel Cell Applications of Nanomaterials Modified Electrodes  
*S. Chen, Y. Li, V. Mani, and M. Rajkumar*
- 3586 Direct Electron Transfer and Electrocatalysis of Hemoglobin on ITO Nanoparticle Electrode  
*Y. Ayato, K. Yamagawa, H. Shiroishi, and J. Kuwano*
- 3587 A Third Generation L-fucose Biosensor based on a Novel Dehydrogenase from the Basidiomycete Coprinopsis Cinerea  
*M. Inukai, H. Matsumura, K. Igarashi, M. Samejima, N. Nakamura, and H. Ohno*
- 3588 Characterization of Microbial Fuel Cell Anodic Biofilms Grown on Pure and Mixed Cultures  
*S. R. Higgins, R. Lopez, D. Foerster, M. Cooney, P. Atanassov, C. Lau, S. Minteer, K. Nealson, A. Cheung, O. Bretschger, T. Yan, and E. Pagaling*

- 3589 In Vivo Operating Miniature, Direct Electron Transfer based, Membrane-less Glucose/Oxygen Biofuel Cell  
*M. Falk, V. Andoralov, M. Granmo, D. Suyatin, J. Schouenborg, J. Sotres, R. Ludwig, O. Morozova, Z. Blum, and S. Shleev*
- 3590 Enhanced Electrical Contact of Microbes using Magnetite Particle Coated with Polyelectrolyte onto Multi-Walled Carbon Nanotube Nanohybrid (MaPoNT) in Microbial Fuel Cell  
*I. Park, Y. Heo, P. Kim, and K. Nahm*
- 3591 Ammonia Production at Anabaena variabilis Modified Electrodes  
*T. Paschkewitz and J. Leddy*
- 3592 Solar Bioelectrocatalysis Utilizing Thylakoids  
*S. Minteer*
- 3593 Investigating Separators to Improve Performance of Flat-Plate Microbial Fuel Cells  
*S. Kazemi, K. Fatih, M. Mohseni, and H. Wang*
- 3594 Direct Electron-Transfer Reactions from Solid Electrodes to Chemoautotrophic CO<sub>2</sub> Fixation Microbes  
*T. ISHII, K. Hashimoto, and R. Nakamura*
- 3595 A Novel Recombinant PQQ Alcohol Dehydrogenase as Catalyst for Bioanode: Two-Step Electrochemical Oxidation of Alcohols  
*K. Takeda, H. Matsumura, K. Igarashi, M. Samejima, N. Nakamura, and H. Ohno*
- 3596 Surface Modification of Carbon Black toward Retention of Enzyme Activity in High-Surface-Area Enzymatic Biofuel Cell Electrodes  
*T. Tamaki, H. Fujimoto, H. Ohashi, and T. Yamaguchi*
- 3597 Simultaneous 3-D Impedance Measurement of Whole Biofuel Cell, Anode and Cathode using Porous Carbon Electrode  
*I. Shitanda, H. Yanai, Y. Yoshihata, Y. Hoshi, M. Itagaki, and S. Tsujimura*
- 3598 Polyaniline Nanofiber/Carbon Black Composite as an Air Cathode Material for Microbial Fuel Cells  
*J. Ahmed and S. Kim*
- 3599 Catechol Biosensor based on Polyphenol Oxidase Immobilized by Combining Electropolymerization and Cross-Linking Process  
*S. Wang and J. Kan*
- 3600 A Bioanode for an Ethanol Biofuel Cell Operating at High Temperature  
*A. Kontani, M. Masuda, N. Nakamura, M. Yohda, and H. Ohno*
- 3601 Immobilization of NAD<sup>+</sup> on an Electrode Using Hydrophobic Ionic Liquids  
*M. Masuda, N. Nakamura, and H. Ohno*

- 3602 Investigation of Impedance Spectra of Mediator-type Amperometric Biosensor by Faradaic Impedance Analysis  
*I. Shitanda, Y. Hoshi, and M. Itagaki*

- 3603 The Direct Electron Transfer Reaction of Bilirubin Oxidase in Protic Ionic Liquids  
*R. Ikari, J. Kuwahara, N. Nakamura, and H. Ohno*

### **I3 - Molten Salts and Ionic Liquids 18**

*ECS Physical and Analytical Electrochemistry, ECS Electrodeposition, ECS Energy Technology, ECSJ Molten Salts*

- 3604 Dynamic Atomic Force Microscopy (AFM) Studies to Characterize Multi-Layered Structures at Ionic Liquid/Solid Interfaces  
*W. Zhang, L. Chen, K. Smith, J. J. Sangiovanni, and G. S. Zafiris*

- 3605 Local Structure of Ionic Liquid / Electrode Interfaces Analyzed by Frequency-Modulation AFM and Photoelectron Spectroscopy  
*T. Harada, Y. Kanai, Y. Mino, A. Imanishi, Y. Yokota, and K. Fukui*

- 3606 An Arrhenius Argument to Explain Electrical Conductivity Maxima versus Temperature  
*A. L. East*

- 3607 Electrochemical Investigation of Quinone Complexation by Lewis Acids in a Chloroaluminate Ionic Liquid  
*G. T. Cheek*

- 3608 Effects of the Charge Density of the Anions of Ionic Liquids on the Electrode Kinetics of Ruthenium 2,2'-Bipyridine Complexes  
*Y. Katayama, Y. Toshimitsu, and T. Miura*

- 3609 Voltammetric Studies of Proton Reduction in 1-Butyl-1-methylpyrrolidinium Triflate  
*G. T. Cheek, D. F. Roeper, and W. E. O'Grady*

- 3610 Robust Microelectrodes for Molten Salt Analysis  
*A. Relf, D. Corrigan, C. L. Brady, J. G. Terry, and A. J. Walton*

- 3611 PTFE Bound Activated Carbon - A Quasi Reference Electrode for Ionic Liquids and Its Application  
*D. Weingarth, A. Foelske-Schmitz, A. Wokaun, and R. Kötz*

- 3612 Critical Evaluation of Metallocenes as Internal Reference Scales for Voltammetric Measurements in Ionic Liquids  
*A. A. Torriero and M. Forsyth*

- 3613 Electrochemical Conversion of Carbon Dioxide to Oxygen in Ionic Liquid Media  
*D. Carr, B. Slote, K. Jayne, and M. C. Kimble*

- 3614 Influence of Temperature on the Electrochemical Characteristics of Bi(111) | 1-Butyl-3-Methylimidazolium Tetrafluoroborate Interface  
*L. Siinor, R. Arendi, C. Siimenson, K. Lust, and E. Lust*

- 3615 Fundamental Study on Reduction Rate for Electrolytic Reduction of SiO<sub>2</sub> Powder in Molten CaCl<sub>2</sub>  
*T. Toba, K. Yasuda, T. Nohira, R. Hagiwara, K. Ichitsubo, K. Masuda, and T. Homma*
- 3616 Anodic Reactions on Some Materials in LiCl-KCl Melt  
*T. Takenaka, M. Umebara, D. Araki, and T. Morishige*
- 3617 Properties of Quaternary Phosphonium Fluorohydrogenate Ionic Liquids and Their Derivatives Giving Ionic Plastic Crystal Phases  
*R. Hagiwara, T. Enomoto, and K. Matsumoto*
- 3618 Border between Ionic Liquids and Electrolyte Solutions  
*M. Watanabe*
- 3619 Ion Pairs in Ionic Liquids  
*J. Hallett, I. Villar-Garcia, and T. Welton*
- 3620 Bulk and Interfacial Properties of Ionic Liquids and Their Mixtures with Lithium Salts  
*O. Borodin, J. Vatamanu, L. Xing, G. Smith, and D. Bedrov*
- 3621 Polymorphic Behavior of Alkali Metal Bis(Fluorosulfonyl)Amides  
*K. Matsumoto, T. Oka, T. Nohira, and R. Hagiwara*
- 3622 Effect of Interaction between Cation-Anion on Ionic Conductivity in Room Temperature Molten Fluorides Containing HF  
*A. Tasaka, H. Inoue, T. Isogai, T. Nakai, M. Saito, and M. Inaba*
- 3623 Protic Ionic Liquids as Fuel Cell Electrolytes: Contrast and Similarities between Bulk and Electrochemical Properties  
*M. Miran, T. Yasuda, M. Susan, K. Dokko, and M. Watanabe*
- 3624 Boronium Based Ionic Liquids: Salts of Boron Centered Cations as Promising Salts for Electrochemical Applications  
*J. H. Davis Jr., T. Ruether, and S. C. Dorman*
- 3625 The Structure of Ionic Liquids on the Nanoscale  
*C. J. Margulis, H. Kashyap, H. Annareddy, J. Hettige, E. Castner Jr., C. Santos, and N. Murthy*
- 3626 Physicochemical and Electrochemical Properties of Novel Ionic Liquids Containing Aprotic Heterocyclic Anions Doped with Lithium Salts  
*C. Shi, A. DeSilva, M. Guzman, and J. Brennecke*
- 3627 New Approaches to the Low-melting Inorganic Ionic Liquid Challenge  
*T. G. Tucker and C. Angell*
- 3628 Recent Developments in Low-Temperature Electrolysis of Aluminum  
*A. Redkin, A. Apisarov, A. Dedyukhin, V. Kovrov, Y. Zaikov, O. Tkacheva, and J. Hryn*

- 3629 AlCl<sub>3</sub>/Trimethanyl Hydrochloride Ionic Liquid as an Electrolyte for Electrodepoisiton of Aluminium Wires  
*C. Su, T. Wu, Y. Sun, and I. Sun*
- 3630 Electrodeposition of Lead from Chloride Melts  
*G. Haarberg, L. Owe, B. Qin, J. Wang, and R. Tunold*
- 3631 The Interface Ionic Liquids / Au(111) and nanostructured materials made from ionic liquids  
*F. Endres*
- 3632 Electrodeposition on Tantalum in Alkali Halide Melts  
*J. H. von Barner, A. H. Jensen, and E. Christensen*
- 3633 Electrochemical Deposition of Niobium onto the Surface of Copper Using a Novel Choline Chloride-Based Ionic Liquid  
*A. I. Wixtrom, J. E. Buhler, C. E. Reece, and T. M. Abdel-Fattah*
- 3634 Ta and Nb Electrodeposition from Ionic Liquids  
*S. Krischok, A. Ispas, A. Zühlstorff, A. Bund, and F. Endres*
- 3635 Al-W Alloy Deposition from Lewis Acidic Room-Temperature Chloroaluminate Ionic Liquid  
*T. Tsuda, Y. Ikeda, T. Arimura, A. Imanishi, S. Kuwabata, C. Hussey, and G. Stafford*
- 3636 An Inverted Aluminium Electrolysis Cell Using a High Density Electrolyte and an Inert Anode  
*S. Rolseth, H. Gudbrandsen, and J. Thonstad*
- 3637 Al-Pt Alloy Deposition in AlCl<sub>3</sub>-NaCl-KCl Molten Salt  
*M. Ueda, H. Hayashi, and T. Ohtsuka*
- 3638 Polysaccharide Ecocomposite Materials: Synthesis, Characterization and Application in Removal of Pollutants and Bacteria  
*C. D. Tran and S. Duri*
- 3639 Impact of Anti-Solvents on the Structural Features and Enzyme Digestibility of Regenerated Cellulose from Ionic Liquid Dissolution  
*X. Geng and W. A. Henderson*
- 3640 Electrospinning of Biopolymers from Ionic Liquid - Co-Solvent Systems  
*E. K. Brown, L. M. Haverhals, M. P. Foley, H. De Long, and P. Trulove*
- 3641 Ionic Liquid-based Solvents for Natural Fiber Welding  
*L. M. Haverhals, M. P. Foley, L. Nevin, E. K. Brown, D. Fox, H. De Long, and P. Trulove*

- 3642 Formation of Surface Structures on Biopolymer Substrates Through the Inkjet Printing of Ionic Liquids  
*E. K. Brown, L. M. Haverhals, M. P. Foley, K. Sweely, H. De Long, and P. Trulove*
- 3643 Chitin to Plastic: Utilization of Ionic Liquids for the Depolymerization of Chitin  
*W. M. Reichert, A. Mirjafari, T. Goode, N. Williams, and M. La*
- 3644 Selective Removal and Recovery of Lignin Using Protic Ionic Liquids (PILs) for a Cost-Effective Biomass Pretreatment Method  
*E. C. Achinivu, G. Li, and W. A. Henderson*
- 3645 Electrochemical Behavior of Vanadium Oxides in  $(\text{NH}_2)_2\text{CO}$  - KCl Melt  
*A. V. Savchuk and S. V. Devyatkin*
- 3646 Effect of the Second Coordination Sphere on the Standard Rate Constants of Charge Transfer for the Cr(III)/Cr(II) Redox Couple in Chloride Melts  
*Y. V. Stulov, V. G. Kremenetsky, and S. A. Kuznetsov*
- 3647 Characteristic of Steam-Activated Boron-Doped Diamond Electrode in a Molten  $\text{NH}_4\text{F} \cdot 2\text{HF}$   
*A. Oishi, H. Kazuhiro, M. Uno, T. Nakai, W. Sugimoto, M. Saito, M. Inaba, and A. Tasaka*
- 3648 Corrosion of Nickel-Chromium-Molybdenum Based Alloy in Chloride Melts Containing Transition Metal Ions  
*A. Abramov, V. Karpov, I. B. Polovov, D. Vinogradov, V. A. Volkovich, and O. Rebrin*
- 3649 Electronic Absorption Spectra of Niobium Species in Halide Melts  
*N. Brevnova, I. B. Polovov, M. Chernyshov, V. A. Volkovich, B. Vasin, and T. Griffiths*
- 3650 Corrosion of Ferritic and Ferritic-Martensitic Steels in NaCl-KCl-VCl<sub>2</sub> Melts  
*I. B. Polovov, D. Vinogradov, A. Abramov, A. Shak, V. A. Volkovich, O. Rebrin, and T. Griffiths*
- 3651 Corrosion of Austenitic Steels and Their Components in Vanadium-Containing Chloride Melts  
*A. Abramov, I. B. Polovov, V. A. Volkovich, O. Rebrin, E. Denisov, and T. Griffiths*
- 3652 Evaluation of NaTFSI-TBATFSI Ionic Liquid as an Electrolytic Melt for Na Electrorefining  
*R. Inaba, M. Ueda, and T. Ohtsuka*
- 3653 Induction of Liquid-Crystalline Bicontinuous Cubic Phases into Zwitterions by Addition of Lithium Salts  
*T. Matsumoto, T. Ichikawa, T. Kato, and H. Ohno*

- 3654 Influence of Nonflammable Diluents on Properties of Phosphonium Ionic Liquids as Lithium Battery Electrolytes  
*K. Tsunashima, H. Taguchi, and F. Yonekawa*
- 3655 Absorption and Desorption of Water by 1-Alkyl-3-Methylimidazolium<sup>+</sup> Ionic Liquids, and Studies of Their Electrochemical and Physical Properties  
*J. DeCerbo and V. Katovic*
- 3656 Electrochemical Behavior of Bis(trifluoromethylsulfonyl)imide-based ILs at Gold Single Crystal Electrodes  
*H. Ueda, K. Nishiyama, and S. Yoshimoto*
- 3657 Hysteresis Effects in the in situ SFG and Differential Capacitance measurements on Metal electrode/Ionic Liquids Interface  
*W. Zhou, Y. Wang, R. Yin, and Y. Ouchi*
- 3658 Spatial Distribution of Chemical Species at Ionic Liquid / Electrode Interface Studied by In-situ X-ray Photoelectron Spectroscopy  
*M. Hirogaki, T. Tsuda, S. Kuwabata, K. Fukui, and A. Imanishi*
- 3659 Visualization of Ionic-Liquid/Solid Interfaces by Frequency Modulation Atomic Force Microscopy  
*M. Negami, T. Ichii, K. Murase, and H. Sugimura*
- 3660 Electrochemical Studies of Cyclic Ammonium Based Ionic Liquids with Allyl Substituents  
*T. Wu, C. Su, C. Chen, C. Kuo, and I. Sun*
- 3661 Electrochemical Oxidation of Glucose by Nitroxide Radicals or Gold Nanoparticles in Ionic Liquids  
*A. Konno, M. Abe, and H. Ohno*
- 3662 Characterization of Au Nanoparticles Prepared by X-ray-Induced Reduction in Ionic Liquid at Nanopore  
*T. Arimura, T. Sakamoto, T. Tsuda, S. Kuwabata, K. Fukui, and A. Imanishi*
- 3663 Electrode Kinetics of Oxygen/Superoxide Ion Redox Couple in Some Amide-Type Ionic Liquids  
*T. Nakagawa, Y. Katayama, and T. Miura*
- 3664 Molten Salts as a Promising Medium for the Synthesis of High Active Catalytic Coatings  
*A. R. Dubrovskiy and S. A. Kuznetsov*
- 3665 Synthesis of Carbides Refractory Metal Nanocoatings on Carbon Fibers and Nanoneedles of Silicon in Molten Salts  
*V. S. Dolmatov and S. A. Kuznetsov*
- 3666 Facile Synthesis of Cu-based Semiconductor Nanoparticles by the Oxidation of Cu Metal Sputter-deposited in an Ionic Liquid  
*A. Morimoto, K. Okazaki, S. Kuwabata, and T. Torimoto*

- 3667 Reaction Entropies of some Redox Couples in Ionic Liquids  
*Y. Yamato, Y. Katayama, and T. Miura*
- 3668 Effect of Ion Structures on Phase Behaviors of Hydrophobic and Polar Ionic Liquids after Mixing with Water  
*Y. Fukaya, T. Nakano, N. Nakamura, and H. Ohno*
- 3669 Synthesis of Ionic Liquids as Solvents for Poly(3-Hydroxybutyrate) under Mild Condition  
*H. Mokudai, Y. Fukaya, N. Nakamura, and H. Ohno*
- 3670 Design of Ionic Liquid-Based Polyelectrolytes Showing Dynamic Phase Transition with Water  
*Y. Kohno and H. Ohno*
- 3671 A Design for a Membrane-less Al/Cl<sub>2</sub> Ionic Liquid Flow Battery  
*M. Zhang, T. A. Zawodzinski, P. Trulove, J. Watson, and R. Counce*
- 3672 Electrochemical Behavior of Lithium Metal Electrodes in Ionic Liquid Based Electrolytes  
*A. I. Bhatt*
- 3673 Ionic Liquid Based Electrolytes for Zn-Air and Mg-Air Batteries  
*P. Howlett, A. A. Torriero, T. Khoo, T. Simons, D. MacFarlane, and M. Forsyth*
- 3674 The Solid Oxide-molten Salts Ion Conductors and Multifunctional Nanocomposites for Advanced Fuel Cells  
*B. Zhu*
- 3675 The Kinetics of Electrochemical Alloying in Liquid Mg-Sb  
*J. M. Newhouse, H. Kim, and D. R. Sadoway*
- 3676 Spectroscopic Analysis of Ceria Based Oxide-Carbonate Nanocomposite Electrolyte for Low Temperature Solid Oxide Fuel Cells  
*M. Mizuhata, K. Takeda, R. Raza, and B. Zhu*
- 3677 Measurement of the Diffusion Coefficient of Calcium in the Calcium-Bismuth Liquid Alloy System  
*S. A. Barriga, H. Kim, D. Boysen, and D. R. Sadoway*
- 3678 Electrochemical Properties of Ca-Sb Alloys in Molten Salt Electrolytes  
*T. Ouchi, H. Kim, and D. R. Sadoway*
- 3679 Oxygen Reduction Reaction at LaNiO<sub>3</sub> Supported by Au Ring in Li/Na Eutectic Carbonate with La<sub>2</sub>O<sub>3</sub>  
*K. Matsuzawa, Y. Esaki, K. Watanabe, K. Ota, and S. Mitsushima*
- 3680 EMIHSO<sub>4</sub>-based Polymer Electrolytes and Their Applications in Solid Electrochemical Capacitors  
*S. Ketabi, X. Liu, Z. Le, and K. Lian*

- 3681 Charge and Discharge Properties at Room to Intermediate Temperature of Sodium Secondary Batteries Using Molten NaFSA-MPPyrFSA for the Green Base Transceiver Station (G-BTS)  
*E. Itani, S. Sakai, K. Nitta, S. Inazawa, K. Takeno, and T. Seki*
- 3682 Versatility of Molten Salt Synthesis for the Preparation of Cathode and Anode Electrode Materials for Lithium-Ion Batteries  
*M. Reddy and B. Chowdari*
- 3683 Exploiting the Versatility of Ionic Liquids and Polymeric Ionic Liquids in Chromatographic Separations and Microextractions  
*J. L. Anderson*
- 3684 Separation of Flue Gas Components by Ionic Liquids - Fundamental Chemistry and Industrial Application  
*R. Fehrmann, A. J. Kunov-Kruse, S. L. Mossin, S. Kegnæs, H. Kolding, and A. Riisager*
- 3685 Reactive Separation of H<sub>2</sub>S from Fuel Process Streams Using Ionic Liquids  
*K. Jayne, D. Carr, B. Slote, and M. C. Kimble*
- 3686 Decomposition of CO<sub>2</sub> Gas in CaCl<sub>2</sub>-CaO and LiCl-Li<sub>2</sub>O Molten Salts  
*R. O. Suzuki, K. Otake, T. Uchiyama, H. Kinoshita, and T. Kikuchi*
- 3687 The Use of Ionic Liquids for the Purification of Heavy Metals from Coal Ash  
*T. E. Sutto*
- 3688 Ionic Liquids Technology for Aluminum Deposition  
*T. Naguy, E. Berman, N. Voevodin, P. Brezovec, and M. Miller*
- 3689 Electrode Reactions of Platinum Bromide Complexes in an Amide-Type Ionic Liquid  
*T. Endo, Y. Katayama, and T. Miura*
- 3690 Electronic State Analyses of Redox-Active Molecule Tethered at Ionic Liquid / Electrode Interface by Photoelectron Spectroscopy  
*Y. Kanai, Y. Mino, A. Imanishi, Y. Yokota, and K. Fukui*
- 3691 Electrochemical Deposition of Cobalt onto the Surface of Copper Using a Choline Chloride-Based Ionic Liquid  
*B. T. Damiano, A. I. Wixtrom, and T. M. Abdel-Fattah*
- 3692 Electrochemical Polishing Applications and EIS of a Novel Choline Chloride-based Ionic Liquid  
*A. I. Wixtrom, J. E. Buhler, C. E. Reece, and T. M. Abdel-Fattah*
- 3693 Investigation of Oxidation State of the Electrodeposited Neodymium Metal Related with the Water Contents of Phosphonium Ionic Liquids  
*H. Kondo, M. Matsumiya, K. Tsunashima, and S. Kodama*

- 3694 Electrochemical Formation of Tb-Ni Alloys in a Molten LiCl-KCl-TbCl<sub>3</sub> System  
*H. Konishi, K. Mizuma, H. Ono, E. Takeuchi, T. Nohira, and T. Oishi*
- 3695 Application of Electrochemical Transient Techniques for Studying Niobium Speciation in Chloride Melts  
*G. Fofanov, I. B. Polovov, M. Chernyshov, V. A. Volkovich, O. Rebrin, and T. Griffiths*
- 3696 Complex Formation and Micropassivation at Electrodeposition of Niobium Coatings in Alkali Chloride-Fluoride Melts With Different Cationic Composition  
*E. A. Marenkova and S. A. Kuznetsov*
- 3697 Influence of the Second Coordination Sphere on the Diffusion Coefficients of Niobium Fluoride Complexes in Chloride and Fluoride Melts  
*A. V. Popova, V. G. Kremenetsky, and S. A. Kuznetsov*
- 3698 Electrochemical Behavior and Electrorefining of Vanadium in Melts Containing Titanium Salts  
*O. S. Kazakova and S. A. Kuznetsov*
- 3699 Activity Coefficients and Solubility of Lanthanum and Praseodymium in Gallium-Indium Eutectic Alloy  
*A. Dedyukhin, V. Ivanov, S. Mel'chakov, A. Shchetinskii, V. A. Volkovich, L. Yamshchikov, A. Osipenko, S. Raspopin, and M. Kormilitsyn*
- 3700 Uranium Activity and Solubility in Liquid Ga-In Eutectic Alloy: An Electrochemistry Study  
*V. A. Volkovich, D. Maltsev, L. Yamshchikov, A. Osipenko, S. Raspopin, and M. Kormilitsyn*
- 3701 Precipitation of Rare Earth Phosphates in NaCl-2CsCl Eutectic Based Melts  
*V. A. Volkovich, A. Ivanov, S. Yakimov, I. B. Polovov, B. Vasin, T. Griffiths, A. Chukin, and A. Shtolts*
- 3702 Development of Recycling Process for Rare Earth Magnets by Electrodeposition Using Ionic Liquids Media  
*M. Ishii, M. Matsumiya, and S. Kawakami*
- 3703 Electrochemical Behavior and Solvation Analysis of Rare Earth Complexes in Ionic Liquids Media Investigated by SECM and Raman Spectroscopy  
*N. Tsuda, M. Matsumiya, K. Tsunashima, and S. Kodama*
- 3704 Investigation on the Hydration State of Ionic Liquids toward the Application as a Protein Solvent  
*Y. Nikawa, K. Fujita, and H. Ohno*
- 3705 Dissolution and Stabilization of Proteins in a Hydrophobic Ionic Liquid with Hydrated Zwitterions  
*Y. Ito, Y. Kohno, and H. Ohno*

- 3706 Effect of Carboxylate Anions on Polarity and Water Miscibility of Hydrophobic Ionic Liquids Toward the Matrix for Cellulose Hydrolysis  
*T. Nakano, Y. Fukaya, and H. Ohno*
- 3707 Evaluation of Glucose Oxidase Activity in Ionic Liquids in the Presence of Small Amount of Water  
*K. Nagata, M. Abe, Y. Fukaya, and H. Ohno*
- 3708 HPLC Analysis of Cellulose Dissolved in Ionic Liquids  
*K. Kuroda, Y. Fukaya, and H. Ohno*
- 3709 Ionic Liquid Facilitated Introduction of Functional Materials into Biopolymer Polymer Substrates  
*L. M. Haverhals, E. E. Christman, M. P. Foley, E. K. Brown, H. De Long, and P. Trulove*
- 3710 Direct Dissolution of Wet and Saliferous Microalgae with Ionic Liquids and Isolation of Poly(3-Hydroxybutyrate)  
*D. Kobayashi, K. Fujita, N. Nakamura, and H. Ohno*
- 3711 Preparation of Ionic Liquids Composed of Benzoic Acid Derivatives and Their Phase Behavior with Water  
*T. Ando, Y. Kohno, and H. Ohno*
- 3712 High Temperature Stability of Carbon-Carbonate Mixture in Solid Oxide Electrolyte DCFC  
*B. Chu, K. Kang, K. Kang, and J. Hwang*
- 3713 Task-Specific Room Temperature Ionic Liquids (RT-ILs) for Biological Liquid/Liquid Extraction  
*A. J. McIntosh, S. A. Goodchild, and T. Welton*
- 3714 All That You Wanted to Know About Lanthanide Halides But Were Afraid to Ask  
*M. Gaune-Escard, L. Rycerz, S. A. Kuznetsov, S. Gadzuric, I. Chojnacka, J. Kapala, B. Salamom, M. Berkani, M. Butman, and W. Gong*
- 3715 Behaviour of Cr Species in the Molten System NaF - AlF<sub>3</sub> - (Al<sub>2</sub>O<sub>3</sub>)  
*V. Danielik, P. Fellner, D. Šuleková, and J. Thonstad*
- 3716 Electrochemical Near-Net-Shape Production Via the FFC Cambridge Process --- Dedication to the Special Session for the 2012 Max Bredig Award  
*D. Hu and G. Z. Chen*
- 3717 Deoxidation of Titania Foams  
*E. Krasicka-Cydzik*
- 3718 Towards Sustainable Metals Production by Molten Oxide Electrolysis  
*L. Yin, A. Allanore, and D. R. Sadoway*

- 3719 Synchrotron X-ray Diffraction Monitoring of the Operation of an Inert Anode Utilised in a Cambridge FFC-Cell  
*G. A. Snook, M. R. Rowles, M. J. Styles, K. McGregor, I. C. Madsen, A. J. Urban, N. V. Scarlett, and D. P. Riley*
- 3720 The Development of Ionic Liquid-Based Thermoelectrochemical Cells  
*J. M. Pringle, T. J. Abraham, and D. R. MacFarlane*
- 3721 Room Temperature Ionic Liquid as Electrolyte for Lithium Ion Battery  
*Y. Fung and Y. Yang*
- 3722 Current Status of Technologies for Recycling Rare Earth Metals  
*T. H. Okabe*
- 3723 Extraction of Rare Earth Metals from Nd-based Scrap by Electrolysis from Molten Salts  
*A. Martinez, O. Kjos, E. Skybakmoen, A. Solheim, and G. Haarberg*
- 3724 Separation of Dy and Nd (La) Using Molten Salt and an Alloy Diaphragm  
*H. Konishi, H. Ono, T. Nohira, and T. Oishi*
- 3725 Electrochemical Formation of RE-Ni (RE=Pr, Nd, Dy) Alloys in Molten Halides  
*T. Nohira, S. Kobayashi, K. Kondo, K. Yasuda, R. Hagiwara, T. Oishi, and H. Konishi*
- 3726 Processing Al-Sc Alloys at Liquid Aluminum Cathode in KF-AlF<sub>3</sub> Molten Salt  
*Q. Liu, J. Xue, J. Zhu, Y. Qian, and L. Feng*
- 3727 Electrorefining of Zirconium from Zircaloy-4 Cladding Hulls in LiCl-KCl Molten Salts  
*C. Lee, K. Kang, M. Jeon, C. Heo, and J. Yang*
- 3728 Exploring Novel Uses of Molten Salts  
*D. Fray*
- 3729 The Structure of Nickel Compounds in the Ionic Liquid 1-Ethyl-3-Methyl Imidazolium Chloride/ Aluminum Chloride  
*D. F. Roepke, C. Graham, K. I. Pandya, and W. E. O'Grady*
- 3730 Intercalation Chemistry of Ionic Liquids  
*T. E. Sutto*
- 3731 Dispersion of Organically Modified Layered Silicates in Melt Blended Poly(lactic acid) Composites: Effects of Cation Head Groups and Oxygenated Alkyl Chains  
*D. M. Fox, M. Zammarano, and M. Novy*
- 3732 Ionic Liquids for Controlled Synthesis of Functional Materials  
*P. Fulvio, H. Luo, and S. Dai*
- 3733 Use of Ionic Liquid as a New Medium under Vacuum Conditions  
*S. Kuwabata, A. Imanishi, T. Torimoto, and T. Tsuda*

- 3734 Control of Formation Process of Au Nanoparticles Prepared by Low Energy Quantum Beam Irradiation in Ionic Liquid  
*A. Imanishi, T. Arimura, T. Sakamoto, T. Tsuda, S. Kuwabata, and K. Fukui*
- 3735 Simple Fabrication of Pt Nanoparticle-Carbon Nanotube Composite with Ionic Liquid-Sputtering Method  
*K. Yoshii, T. Tsuda, T. Arimura, A. Imanishi, T. Torimoto, and S. Kuwabata*
- 3736 Fabrication of 3D Polymer Structures from Room-Temperature Ionic Liquid by Quantum Beam Techniques  
*H. Minamimoto, K. Inoue, T. Tsuda, A. Imanishi, S. Seki, and S. Kuwabata*

#### I4 - Electrocatalysis 6

*ECS Physical and Analytical Electrochemistry, ECS Energy Technology, ECS Industrial Electrochemistry and Electrochemical Engineering, ECSJ Interfacial Electrochemistry, CSE*

- 3737 (Invited) Oxygen Evolution Reaction on Minute Amounts of Ru and Ir Catalyst for Application in Fuel Cell Protection  
*R. T. Atanasoski, D. A. Cullen, and L. Atanasoska*
- 3738 ORR Activity Enhancement of MBE-prepared Pt monolayer on Au(111) Single Crystal Substrate  
*Y. Iijima, Y. Takahashi, N. Todoroki, K. Matsumoto, and T. Wadayama*
- 3739 Facile Synthesis of  $Pd_xCo@Pd/C$  Core-Shell Nanoparticles and Pt-Decorated  $Pd_3Co@Pd/C$  as Oxygen Reduction Reaction Electrocatalysts  
*D. Wang, C. Li, and H. D. Abruña*
- 3740 Oxygen Reduction for Fuel Cells and Batteries: Mechanistic Studies and the Design of New Catalysts  
*A. A. Gewirth, C. Tornow, and E. Tse*
- 3741 Surface Modification of PtRu/C by Mono-layered Decoration of Pt, Au, Pd, and Ir for Oxygen Reduction Reaction  
*C. Kuo, L. Chang, Y. Hsieh, P. Wu, and J. Lee*
- 3742 An Excellent Electrocatalysis of Novel Pt-TaOx Composite Electrocatalysts for Oxygen Reduction Reaction  
*Z. Awaludin, T. Okajima, and T. Ohsaka*
- 3743 Carbon Supported Pt-Os Electrocatalysts for Oxygen Reduction Reaction  
*Y. Lee, C. Kuo, Y. Hsieh, P. Wu, and J. Lee*
- 3744 Instantaneous One-Pot Synthesis of Fe-N-codoped Graphene as an Efficient Electrocatalyst for Oxygen Reduction Reaction in Acidic Solutions  
*K. Kamiya, K. Hashimoto, and S. Nakanishi*
- 3745 Strip-Like Nanosized Tungsten Carbide as Catalyst for Oxygen Reduction Reaction  
*S. Kang and P. Shen*

- 3746 In Situ STM Elucidation of the effects of Step Structures on Pt(111) Electrodes for Dissolved CO Oxidation  
*J. Inukai, D. A. Tryk, T. Abe, M. Wakisaka, H. Uchida, and M. Watanabe*
- 3747 High Speed AFM Study on the Potential Dependence of the Dissolution of Shape-controlled Pt Nanoparticles  
*Y. Yamada, C. Yoshida, M. Nakamura, and N. Hoshi*
- 3748 XPS and STEM of the Interface Formation between Ultra-Thin Ru, Ir and Pt Layers and Perylene Red Catalyst Support Whiskers  
*L. L. Atanasoska, D. A. Cullen, A. Hester, and R. T. Atanasoski*
- 3749 Ethanol Electrooxidation on a (2x2)-Sn/Pt(111) Surface Alloy and a SnO<sub>x</sub>/Pt(111) Surface: A Combined Surface Science and In Situ FTIR Study  
*W. Zhou, J. Magee, S. Axnanda, R. R. Adzic, and M. G. White*
- 3750 Electrochemical and ATR-IR Investigation on Decontaminated Shape-Controlled Pd Nanocrystals  
*H. Zhang and W. Cai*
- 3751 Molecular Structures of Fluorinated Self-Assembled Monolayers (SAMs) Constructed on Metal Surfaces Investigated by Surface Vibrational Spectroscopies  
*I. Yagi, K. Nomura, and K. Inokuma*
- 3752 (Invited) Application of Ordered Intermetallic Phases to Electrocatalysis  
*F. Matsumoto and H. Abe*
- 3753 Activation of Noble Metal Centers through Modification with Metal Oxo Species towards Electrocatalytic Oxidation of Alcohols and Formic Acid  
*P. J. Kulesza, I. Rukowska, A. Wadas, D. Marks, K. Klak, and S. Zoladek*
- 3754 Synthesis, Characterization and Electrocatalytic Properties of Electrodeposited Pt Thin Films with Preferential {100} Orientation  
*E. Bertin, S. Garbarino, J. Solla-Gullón, F. Vidal-Iglesia, J. Feliu, A. Ponrouch, M. H. Martin, and D. Guay*
- 3755 Electrode Surface Control by Platinum Nanoparticles Protected by Polyacrylic Acid for Electrocatalytic Hydrogen Generation  
*M. Kajita and M. Yagi*
- 3756 (Invited) Electrochemical Behavior of Pt-Skin Layers on Pt-Co Alloy Single-Crystal Electrodes in Acid Media  
*M. Wakisaka, S. Morishima, Y. Hyuga, H. Uchida, and M. Watanabe*
- 3757 Unique Properties of Reduced SnO<sub>x</sub>: CO Oxidation on Nanostructured SnO<sub>x</sub>/Pt(111)  
*S. Axnanda, W. Zhou, M. G. White, Z. Zhu, and Z. Liu*
- 3758 Clarification of Two-Consecutive Potential Driven Phase Transition Processes of Diphenyl Viologen at a Au (111) Electrode Surface  
*T. Higashi and T. Sagara*

- 3759 Electrooxidation of CO on Epitaxial Bilayer Oxide Formed on Platinum Nanofacets  
*V. Komanicky, D. Hennessy, and H. You*
- 3760 Multiscale Modeling of the H<sub>2</sub> Oxidation Reaction at the Ni/YSZ Interface in the Presence and Absence of Sulfur  
*A. Heyden and S. C. Ammal*
- 3761 Theoretical Investigation of the H<sub>2</sub> Oxidation on the Sr<sub>2</sub>Fe<sub>1.5</sub>Mo<sub>0.5</sub>O<sub>6-δ</sub> (001) Perovskite Surface under Anodic Solid Oxide Fuel Cell Conditions  
*S. Suthirakun, S. C. Ammal, and A. Heyden*
- 3762 Electrochemistry by First-Principles Calculations: Electrochemical Oxidation of Ammonia at Pt(hkl)/Alkaline Solution Interfaces  
*D. Skachkov, C. Venkateswara Rao, and Y. Ishikawa*
- 3763 Density Functional Theory Computation of Electrolyte Competitive Adsorption and Electrochemical Activation Barriers  
*M. J. Janik, K. Yeh, and G. Rostamikia*
- 3764 A DFT Calculation Study of the Hydrogen Electrode Processes on Pt (111) and Pt (100) Surfaces  
*Q. Zhang, J. Chen, and S. Chen*
- 3765 DFT Study of Water Dissociation and Diffusion on Metal Surfaces, Kinks and Step  
*L. Arnadottur*
- 3766 Cost Effective Computational Method for Performing First-Principles Molecular-Dynamics Simulations under Constant Potential Bias  
*N. Bonnet, T. Morishita, O. Sugino, and M. Otani*
- 3767 Vibration Analysis of (Bi)Sulfate Adsorption on Pt (111) Surface in Aqueous Solution from the First Principles Simulation  
*Y. Qian, M. Otani, and T. Ikeshoji*
- 3768 Fundamental Insights on the Electrochemical Water Splitting using Solid Oxide Electrolyzers  
*E. Nikolla*
- 3769 Electrochemically Fabricated Metal Catalysts for Glucose Oxidation in Bio Fuel Cell Application  
*J. Lim, S. Pyo, D. Lee, H. Park, and S. Kim*
- 3770 Redox Catalysis for Dehydrogenation of Liquid Hydrogen Carrier for Fuel Cell Applications  
*E. Deunf, L. Rubin, D. Pete, J. Arnold, and J. Kerr*
- 3771 The Graphene-supported PdSn Nanoparticles as Efficient Catalysts for Ethanol Electrooxidation  
*Y. Kim, S. Choi, E. Lim, S. Lee, and W. Kim*

- 3772 Structural Effects on the Oxygen Reduction Reaction on the High Index Planes of Pt<sub>3</sub>Co  
*Y. Takesue, T. Rurigaki, A. Hototsuyanagi, M. Nakamura, and N. Hoshi*
- 3773 Controlling Diffusion Profile of Electroactive Species for Selective Anodic Stripping Voltammetry of Cd<sup>2+</sup>  
*A. Sugitani, T. Watanabe, and Y. Einaga*
- 3774 Molecular Self-Assembling Control Over the Surface States and Field Effects at N-Gaas (100) Electrodes  
*V. Lazarescu, M. Enache, G. Dobrescu, M. Gartner, C. Negrila, and M. Lazarescu*
- 3775 One-Step Electrodeposition of Multilayered Surfactant/MnO<sub>2</sub> Composite and Its Electrochemistry  
*M. Shamoto, S. Mito, K. Tomono, and M. Nakayama*
- 3776 Tungsten Carbide Promoted Co@Pd Core-Shell Nanoparticles as Highly Active ORR Electrocatalyst  
*Z. Li and P. Shen*
- 3777 Hydrazine Oxidation at {100} Preferentially Oriented Pt Black Surfaces  
*C. Roy, E. Bertin, M. H. Martin, S. Garbarino, and D. Guay*
- 3778 Surface Modification of Diamond Nanoparticle and Its Electrochemical Properties  
*J. Urai, T. Kondo, and M. Yuasa*
- 3779 Electrocatalytic Water Oxidation on a Mesoporous IrO<sub>2</sub> Film Fabricated Using a Triblock Copolymer Template  
*D. Chandra, N. Abe, and M. Yagi*
- 3780 In Situ Observation of Adsorption Behaviors of Nafion Side-Chain Model Compounds on Electrodes by ATR-SEIRAS  
*K. Nomura, N. Ohta, H. Notsu, T. Kondo, and I. Yagi*
- 3781 Electrochemical Activity and Stability of Pt Catalysts Supported on Silica-CNF Hybrid Materials  
*A. Kim, S. Lim, D. Peck, S. Kim, B. Lee, and D. Jung*
- 3782 Intermediates of Ethanol Electro-oxidation on SnO<sub>x</sub>/Pt Catalysts Studied by in situ FTIR Spectroscopy  
*J. Magee, W. Zhou, and M. G. White*
- 3783 Synthesis and Electrocatalytic Activity of Shape Controllable Gold Nanoparticles Enclosed by High-index Facets  
*B. C. Solomon, F. Ke, and X. Zhou*
- 3784 Electrocatalytic Oxidation of Phenol within the Interlayer Space of Surfactant/MnO<sub>2</sub> Multilayer Films  
*M. Nakayama, S. Mito, M. Shamoto, and K. Tomono*

- 3785 Electrochemical Studies of Ternary And Quaternary Pt Based Catalysts for Glycerol Oxidation  
*C. Caliman and J. Ribeiro*
- 3786 Highly Active Pd-based Metallic Glass Nanowires for Alcohol Oxidation in Alkaline Media  
*R. C. Sekol, M. Carmo, G. Kumar, F. Gittleson, K. Sun, J. Schroers, and A. D. Taylor*
- 3787 Influence of Peroxodisulfate Electro-Generation on the Electrochemical Oxidation of Formic Acid on Boron Doped Diamond Electrodes  
*Y. Honda, S. Fierro, C. Comninellis, and Y. Einaga*
- 3788 Effect of pH on Electrooxidation of Formic Acid/Formate on Platinum  
*J. Joo, T. Uchida, A. Cuesta, M. T. Koper, and M. Osawa*
- 3789 Investigation on MEA-performances of Highly Durable Silica-coated Pd/C Electrocatalysts  
*Y. Sato, K. Fujii, M. Ito, S. Takenaka, and M. Kishida*
- 3790 Durable Oxide-Based Catalysts for Application as Cathode Materials in Polymer Electrolyte Membrane Fuel Cells (PEFCs)  
*E. Fabbri, A. Rabis, A. Foelske-Schmitz, D. Kramer, R. Kötz, and T. J. Schmidt*
- 3791 NO Conversion in Porous Cell Stacks  
*R. M. Werchmeister, K. B. Andersen, and K. Kammer Hansen*
- 3792 Photoelectrochemistry Applied to Organic Dye Oxidation and Concomitant Hydrogen Generation  
*M. B. Zanoni and T. Guaraldo*
- 3793 Preparation of Photocatalytic  $\text{TiO}_2/\text{WO}_3$  Hollow Fiber Using Polysulfone as Template  
*K. I. Liu, P. Chen, Y. Hsueh, H. Chen, and T. Perng*
- 3794 Composite Thin Film  $\text{Ir}_{1-x}\text{Nb}_x\text{O}_2$  Electrocatalysts for the Oxygen Evolution Electrode  
*A. Zlotorowicz, F. Seland, and S. Sunde*
- 3795 A Comparative Study of Nickel and Cobalt based Nanoparticles as Electrocatalyst for Alkaline Water Electrolysis  
*A. Patru, F. Favier, and N. Jerez*
- 3796 Chemical Amplitude: A Quantitative Descriptor for the Surface Reactivity of Metals  
*L. Zhuang, B. Huang, L. Xiao, and J. Lu*
- 3797 Nanostructured and Hybrid Carbon Films for Electrocatalytic Reaction with Biomolecules  
*O. Niwa, T. Kamata, D. Kato, A. Ueda, K. Yoshioka, S. Umemura, and S. Hirono*
- 3798 Electrochemical Characterization of Cup-Stacked Carbon Nanofiber-Modified Electrodes and its Application to Biosensing  
*K. Komori, S. Ko, S. Komatsu, T. Tatsuma, A. Sakoda, and Y. Sakai*

- 3799 Large-Scale Self-Assembly of the Nitrogen-Doped Graphene with High Electrocatalytic Activity for Oxygen Reduction  
*C. He and P. Shen*
- 3800 Plasmonic Application of Pt-Group Metal Nanostructures  
*K. Ikeda, S. Uchiyama, and K. Murakoshi*
- 3801 Pit Falls in the Use of Point Electrodes  
*K. Kammer Hansen*
- 3802 Recent Development on Electroanalytical Application of Boron-Doped Diamond Electrodes  
*Y. Einaga*
- 3803 Redox Properties and Catalytic Activity for Oxygen Reduction Reaction of Electropolymerized Aromatic Diamines  
*S. Kishioka*

## I5 - Electrochemical Atomic Layer Epitaxy and Quantum Confinement

*ECS Physical and Analytical Electrochemistry, ECS Electrodeposition*

- 3804 Electrochemical Liquid-Liquid Solid Deposition of Crystalline Semiconductor Materials  
*J. Gu, E. Fahrenkrug, S. Collins, and S. Maldonado*
- 3805 Kesterite Group Materials Thin Films by Elettrodeposition for Photovoltaic Applications  
*M. Innocenti, I. Bencistà, F. Di Benedetto, S. Cinotti, A. De Luca, S. Bellandi, A. Lavacchi, M. Muniz Miranda, F. Vizza, and M. Foresti*
- 3806 New Route for Low Cost Fabrication of Semiconducting Materials for Photovoltaic Applications  
*R. Salazar, S. Sanchez, D. Rouchon, C. Levy-Clement, and V. Ivanova*
- 3807 Electrochemical Atomic Layer Deposition of PV Materials  
*B. Perdue, V. Stickney, J. Stickney, and D. Banga*
- 3808 Characterization of Electrochemical ALD Processes on Bipolar Electrodes Using Confocal Raman Microscopy  
*S. Ndzesse and C. Shannon*
- 3809 Cadmium Telluride Nanowire Electrodeposition for Advanced Photovoltaics  
*E. Menke, L. Reed, and J. Hujdic*
- 3810 Ultra-long Hollow Chalcogen and Chalcogenide Nanofibers by Galvanic Displacement Reaction  
*H. Park, M. Zhang, C. Chang, H. Jung, J. Lim, Y. Choa, and N. Myung*
- 3811 Pulsed Electrodeposition of  $\text{Bi}_2\text{Te}_3/\text{Sb}_2\text{Te}_3$  Superlattices in Flow Cells vs. Single Baths  
*D. Banga, J. Sugar, D. Medlin, V. Stavila, D. B. Robinson, and P. Sharma*

- 3812 Bismuth Thin Films: Growth, Structure and Properties  
*M. Saini, S. Zheng, S. Huang, W. Wang, C. Chien, and S. Morin*
- 3813 Electrochemical Routes to the Reduction of Resistance in Single-Walled Carbon Nanotube Networks  
*D. Asheghali, N. Bhatt, P. Vichchulada, and M. D. Lay*
- 3814 Thermodynamics and Kinetics Aspects of Metal Deposition via Surface Limited Redox Replacement Reaction  
*S. Brankovic*
- 3815 Deposition of Ultra Thin Pt Films via Surface Limited Redox Replacement of UPD Layers on Au  
*N. Vasiljevic, J. Nutariya, M. Fayette, B. Rawlings, and N. Dimitrov*
- 3816 The Electrochemical Atomic Layer Deposition of Pt and Pd Nanoparticles on Ni Foam for the Electro-Oxidation of Alcohols  
*R. M. Modibedi, E. Louw, K. I. Ozoemena, and M. K. Mathe*
- 3817 Electrodeposition of Metals in Catalysts Syntheses: Platinum Monolayer Electrocatalysts for the Oxygen Reduction Reaction  
*M. Vukmirovic, S. Bliznakov, K. Sasaki, J. Wang, and R. R. Adzic*
- 3818 Highly-Active Pt Coated NPG Catalyst for HCOOH Oxidation: Synthesis, SLRR Coating, Activity and Durability  
*N. Dimitrov, M. Kamundi, L. Bromberg, D. McCurry, M. Fayette, and E. Fey*
- 3819 Epitaxial Ag(111) Overlays on Noble Metals  
*K. Soliman and L. A. Kibler*
- 3820 Electrodeposition of Pt Thin Films by Pulsed Potential  
*Y. Liu, D. Gokcen, U. Bertocci, and T. Moffat*
- 3821 NEAR-Surface Equilibrium Phases in Electrochemically Fabricated Low-dimensional Multi-Component Catalysts  
*F. M. Alamgir, R. Rettew, and A. Vitale*
- 3822 Self-Limiting Electroless Deposition of Nanoscale Ruthenium Oxide: Catalyst, Electron/Proton Conductor, Broadband Transparent Oxide  
*D. R. Rolison, C. N. Chervin, J. W. Long, M. Osofsky, J. Melinger, J. Owrusky, F. Rachford, J. Pietron, and M. Pomfret*
- 3823 In Situ Stress Measurement During Pt Deposition Using Surface Limited Redox Replacement  
*G. Stafford, M. C. Lafouresse, Y. Liu, J. Shin, and U. Bertocci*
- 3824 First Principles Studies of Trends in Metal Electrodeposition and Reactivity  
*J. Greeley*

- 3825 Reduction of Nitrate Mediated By Metal UPD on Pd-Modified Au Electrodes In Aqueous Electrolytes  
*A. J. Jebaraj and D. J. Scherson*
- 3826 Preparation of Size-quantized Lead Sulfide Thin Layer on Silver Nanocubes via Electrochemical Atomic Layer Deposition  
*M. Nakano, K. Okazaki, and T. Torimoto*

**J1 - Chemical Sensors 10 - Chemical and Biological Sensors and Analytical Systems**  
*ECS Sensor, ECSJ Chemical Sensor*

- 3827 Phytosensors and Phytoactuators  
*A. G. Volkov, M. I. Volkova, and V. S. Markin*
- 3828 Biofuel Cell Providing a Platform for Self-Powered Biosensors  
*S. Dong*
- 3829 Miniature Enzymatic Biosensors for Tear Glucose Measurement in Capillary Tubes  
*B. Peng, Q. Yan, B. Cohan, T. C. Major, and M. E. Meyerhoff*
- 3830 Real-time and Ultra-sensitive detection of Cancer Marker Using a Novel Silicon Nanobelt Field Effect Transistor  
*Y. Yu, J. Wu, and C. Wu*
- 3831 Graphene Oxide-Based Aptasensor for Heavy Metal Detection  
*M. Li and N. Wu*
- 3832 Time Sensors: Circadian Rhythms in Biologically Closed Electrochemical Circuits of Plants  
*A. Waite, J. Wooten, A. G. Volkov, and V. S. Markin*
- 3833 Immobilization of Enzymes and Redox Proteins and Their Electrochemical Biosensor Applications  
*S. Chen, V. Mani, S. Palanisamy, and Y. Li*
- 3834 Salmonella Typhimurium Detection on Food Surface using Magnetoelastic Biosensors  
*Y. Chai, S. Horikawa, M. Park, S. Li, and B. Chin*
- 3835 Bio-Inspired Autonomous Sentinel System for Screening Invasive Pathogens  
*S. Li, H. Wikle III, Y. Chai, M. Park, S. Horikawa, and B. Chin*
- 3836 New Multimode Sensors based on Nanostructured Materials for Simultaneous Screening of Biological Fluids for Specific Breast Cancer and Hepatitis B Biomarkers  
*R. I. Stefan - van Staden and M. Enachescu*
- 3837 Direct Detection of Salmonella Typhimurium on Tomato and Spinach using a Phage-based Magnetoelastic Biosensor Method  
*M. Park, S. Li, K. Weerakoon, S. Horikawa, Y. Chai, and B. Chin*

- 3838 Development of Electrochemical Cantilever Sensors for DNA Applications  
*X. Quan, Y. Sun, A. Labuda, A. Heiskanen, A. Wolff, J. Jorge Dulanto, P. Grutter, and A. Boisen*
- 3839 Fabrication of Minimally-Invasive Patch Type Glucose Sensors  
*M. Yasuzawa, S. Sato, H. Nakanishi, and K. Edagawa*
- 3840 Flexprint based Glucose Sensors for Continuous Measurement of Glucose Profiles of Diabetic Patients  
*P. D. van der Wal, P. Hadvary, H. Tschirky, and N. de Rooij*
- 3841 Nanodiamond Microelectrode Array with Mesa Structure Fabricated for Bio-Analytical Applications  
*S. Raina, N. Ghosh, and W. Kang*
- 3842 An Electrochemical Probe Technology for a Label-Free, Point-of-Care Biosensor  
*J. Wei, S. Singhal, and H. Liu*
- 3843 Electrical Impedance Sensors for Cancer Cell Study  
*L. Yang*
- 3844 Terahertz Chemical Imaging and Spectroscopy of Molecular Networks in Pharmaceutical and Biomedical Applications  
*K. Ajito, Y. Ueno, H. Song, E. Tamechika, N. Kukutsu, W. Limwikrant, K. Yamamoto, and K. Moribe*
- 3845 (Sensor Division Outstanding Achievement Award Presentation) Ceramic Gas Sensors to Oxide Nanostructures: Opportunities and Challenges  
*S. A. Akbar*
- 3846 The Characteristics of Nanocomposite Chemical Sensors  
*A. K. Batra, J. Stephens, and J. Currie*
- 3847 Diminishing Ethanol Cross-sensitivity via Lamination of Selective Oxidation Catalyst layer on Zirconia-based VOC Sensor  
*T. Sato, M. Breedon, Y. Kugimiya, and N. Miura*
- 3848 Rapid and Simple Immunoassay Based on Negative Dielectrophoresis with Three-Dimensional Interdigitated Array Electrodes  
*T. Yasukawa, H. Shiku, T. Matsue, and F. Mizutani*
- 3849 Bismuth-film electrodes for  $\text{Sn}^{2+}$  Sensing: The Roles of Grain Size, Preferred Orientation Ratio, and Surface Roughness  
*C. H. Lien, K. Chang, C. Hu, Y. Tsai, and D. Wang*
- 3850 High-Throughput Separation Assay for NO Metabolites in Blood using Microfluidic Electrophoresis  
*S. Wakida, T. Miyado, K. Shimazu, Y. Shibutani, T. Mizukami, K. Nose, and A. Shimouchi*

- 3851 Effects of Surface Modification of Noble-Metal Electrodes with Au on the H<sub>2</sub> Sensing Properties of Diode-type Gas Sensors  
*T. Hyodo, T. Yamashita, and Y. Shimizu*
- 3852 Application of Electrospun Carbon Nanofiber and Its Composites in Electroanalytical Chemistry  
*J. Huang, Y. Liu, and T. You*
- 3853 Soluble Polyaniline for a State of Health Sensor  
*M. Kane*
- 3854 Potentiometric YSZ-based Sensors Using Zn-Ta-O-based Sensing Electrode for Selective H<sub>2</sub> Detection  
*S. A. Anggraini, M. Breedon, and N. Miura*
- 3855 Solid Electrolyte Type Ammonia Gas Sensor with High Water Durability  
*S. Tamura, T. Nagai, and N. Imanaka*
- 3856 Low Cost 8 nm Radius Nanoelectrodes Arrays by Sol-Gel Chemistry: To Fundamental Understanding of Mass Transport Toward Direct DNA Hybridization Detection Electrochemical Sensor  
*O. Fontaine, C. Laberty, H. Perrot, and C. Sanchez*
- 3857 Direct Comparison of Anti-Interference Property for Bimetallic PtAu, PtIr, and PtRu Nanoparticle catalysts in Amperometric Detection for H<sub>2</sub>O<sub>2</sub> Based Biosensors  
*M. Janyasupab, Y. Zhang, C. Liu, and C. Liu*
- 3858 A High-Throughput Assay for Evaluation of Embryoid Bodies using Local Redox Cycling-Based Electrochemical Chip Device  
*K. Ino, T. Nishijo, Y. Kanno, H. Shiku, and T. Matsue*
- 3859 Printed Amperometric Gas Sensors  
*M. T. Carter, J. R. Stetter, M. W. Findlay, and V. Patel*
- 3860 Interaction of Water Vapor with SnO<sub>2</sub> Sensor Materials: A Comparison of DRIFTS and Resistance Measurements  
*R. G. Pavelko, K. Grossmann, N. Barsan, and K. Shimanoe*
- 3861 pH Sensing Characteristics and Biosensing Application of Solution-Gated Reduced Graphene Oxide Field-Effect Transistors  
*I. Sohn, D. Kim, J. Jung, O. Yoon, and N. Lee*
- 3862 Development of Micro Hydrogen Gas Sensor Utilizing Polymerized Gel with Ionic Liquid as a Solvent  
*T. Yamauchi*
- 3863 Iridium Oxide pH Sensor Development and Its Application in Corrosion Study  
*F. Huang, Y. Jin, and L. Wen*

- 3864 Surface-enhanced Raman Scattering on Ordered Metal Nanodot Array Obtained Using Anodic Porous Alumina  
*T. Kondo, K. Nishio, and H. Masuda*
- 3865 Enzyme-Encapsulated Quantum Dot Hydrogels in the Development of Biosensors: A Multifunctional Platform for Both Bio-Catalysis and Fluorescent Probing  
*J. Yuan, N. Gaponik, and A. Eychmüller*
- 3866 Adaptive Chemical Sampling Device Inspired by Crayfish  
*R. Takemura, K. Takahashi, T. Makishita, and H. Ishida*
- 3867 Carbohydrate Immobilization on the Surface of Field Effect Transistor Biosensor for Detection of Virus-related Protein  
*S. Hidemitsu, H. Hinou, D. Ebihara, R. Sato, S. Kuroiwa, S. Nishimura, and T. Osaka*
- 3868 Block Co-polymer Enhanced 3D Carbon Nanostructure Electronics  
*S. Guo, A. George, M. Penchev, C. Ozkan, and M. Ozkan*
- 3869 Self-Assembled Monolayers of Oligonucleotides as Receptor Layers for Metal Ions Sensors  
*L. Górska, R. Ziolkowski, and E. Malinowska*
- 3870 Development of Highly-Sensitive Electrochemical Measurement System on Dry Chemistry using Ionic Liquid  
*S. Arimoto, M. Takahashi, A. Kamei, and T. Yoshioka*
- 3871 Chalcogenide Glass Chemical Sensor for Cadmium Detection in Industrial Environment  
*M. Milochova, M. Kassem, and E. Bychkov*
- 3872 Electrochemical Pump Consisting of Cu<sup>2+</sup>-Poly(acrylic acid) Gel  
*K. Takada, N. Yamamura, A. Hayashi, T. Yasui, and A. Yuchi*
- 3873 The pH Sensing Characteristics of Extended-Gate Field-Effect Transistor Base on The Electrode with Copper Oxide Nanowires  
*Y. Huang, H. Lin, H. Li, W. Dai, C. Chou, and H. Cheng*
- 3874 Multiplexed Cantilever Sensors with a Peptide Receptor and Humidity Effects on Binding Kinetics  
*Y. Yoo, M. Chae, J. Kang, K. Hwang, T. Kim, and J. Lee*
- 3875 High Sensitive Amperometric Detection of Glucose using Conductive DLC Electrode in Higher Potential Region  
*K. Honda, H. Naragino, K. Yoshinaga, A. Nakahara, and S. Tanaka*
- 3876 Electrochemical Immunosensor for Diagnostic of Parasitical Human Diseases  
*C. A. Erdmann, J. Inaba, A. G. Viana, C. A. Pessoa, K. Wohnrath, and J. R. Garcia*

- 3877 Characterization and Electrochemical Response of Sonogel Carbon Electrode Modified with Nanostructured TiO<sub>2</sub> and ZrO<sub>2</sub> Film to Detect Common Neurotransmitters  
*M. K. Hughes, N. Vincent, and S. K. Lunsford*
- 3878 A Novel Approach of Pb(II) Determination in Environmental Samples by Lead Selective Electrodes  
*G. Lisak and J. Bobacka*
- 3879 Functionalization of Pyrolyzed Carbon Structures for Bio-nano-electronics Platforms  
*M. Hirabayashi, B. Mehta, S. Kassegne, and A. Khosla*
- 3880 Micromechanical Detection of 2,4-Dinitrotoluene by a Cantilever-based Artificial Olfactory System with Micro-Preconcentrator  
*M. Chae, Y. Yoo, J. Lee, S. Lee, J. Kang, T. Kim, and K. Hwang*
- 3881 Layer-by-Layer Catalytic Interface for Electrochemical Detection of Multiple Substrates Featuring Bio-Functionalized Carbon Nanotubes  
*J. S. Kirsch and A. L. Simonian*
- 3882 Improved Electrocatalytic Performance for H<sub>2</sub>O<sub>2</sub> Detection Based on Bimetallic PtM (M = Pd, Au or Ir) Nanoparticles  
*Y. Zhang, M. Janyasupab, C. Liu, J. Xu, and C. Liu*
- 3883 Superoxide Anion Radical Sensor using GC Electrode Modified with Heparin/PEDOT and Polymerized Iron Porphyrin  
*R. Matsuoka, T. Kondo, and M. Yuasa*
- 3884 Ultra-Sensitive Label-Free Detection of Proteins by Chemically Derived Graphene Based Field-Effect Transistor  
*D. Kim, I. Sohn, J. Jung, O. Yoon, J. Park, and N. Lee*
- 3885 New Application of Produced Pigment from Bacteria to Detect of Ammonia in Combination with Flow Injection for Ammonia Analysis  
*Y. Iida and I. Satoh*
- 3886 Preparation of Fine Implantable Needle Type Biosensors for Blood Vessel Glucose Monitoring  
*K. Edagawa and M. Yasuzawa*
- 3887 CO Sensing Properties of Electrochemical Gas Sensors using an Anion-Conducting Polymer as an Electrolyte  
*T. Goto, T. Hyodo, K. Kaneyasu, H. Yanagi, and Y. Shimizu*
- 3888 Investigation of ZnO-Nanowire-Based Extended-Gate Field-Effect-Transistor pH Sensors  
*C. Li, S. Chang, T. Yang, and S. Chang*
- 3889 NO<sub>2</sub> Sensing Properties of Porous In<sub>2</sub>O<sub>3</sub>-based Powders Preapred by Utilizing Ultrasonic-Spray Pyrolysis Employing PMMA Microsphere Templates: Effects of the Size of the PMMA Microspheres on Their Gas-Sensing Properties  
*E. Fujii, T. Hyodo, K. Matsuo, and Y. Shimizu*

- 3890 Biosensors for Health Monitoring  
*S. Anastasova and P. Vadgama*
- 3891 Redox-Active Alkali Insertion Materials as Inner Contact Layer in All-Solid-State Ion-Selective Electrodes  
*S. Komaba, C. Suzuki, N. Yabuuchi, S. Kanazawa, T. Hasegawa, and T. Akatsuka*
- 3892 Sensing Characteristics of a Fiber Bragg Grating Hydrogen Gas Sensor using Sol-Gel Derived Pt/WO<sub>3</sub> Film  
*S. Okazaki, Y. Maru, and T. Mizutani*
- 3893 Zirconia-based Electrochemical Oxygen Sensor for Accurately Determining Water Vapor Concentration  
*R. E. Soltis*
- 3894 Fabrication of Surface Enhanced Raman Scattering (SERS)-active substrates by using Dip-Pen Nanolithography  
*K. Chao and K. Ou*
- 3895 Application of Commercial Manufacturing Methods to Mixed-Potential NOx Sensors  
*C. R. Kreller, P. K. Sekhar, W. Li, P. Palanisamy, E. L. Brosha, R. Mukundan, and F. H. Garzon*
- 3896 Research on Filter Materials for LP Gas Sensors  
*M. Sai, K. Shinnishi, K. Kaneyasu, T. Suzuki, and M. Takeuchi*

**J2 - Luminescence and Display Materials: Fundamentals and Applications**  
*ECS Luminescence and Display Materials, ECSJ Phosphor Research*

- 3897 Novel Synthesis Methods of Silicate and Silicon Oxynitride Phosphors Using Silicon Monoxide (SiO) as a Raw Material  
*T. Ishigaki, T. Sakamoto, S. Kamei, K. Uematsu, K. Toda, and M. Sato*
- 3898 Synthesis of Nitride and Oxynitride Phosphors Using Fluidized Bed Furnace  
*K. Toda, S. Kamei, K. Uematsu, T. Ishigaki, and M. Sato*
- 3899 Synthesis of Highly Efficient Red Phosphor SrCaSiO<sub>4</sub>:Eu<sup>2+</sup> by Aqueous Solution Method  
*S. Tezuka, K. Hideki, Y. Takatuka, and M. Kakihana*
- 3900 Effects of Preparation Condition for Photoluminescent Properties of White Light Emitting Mesoporous Carbon- $\gamma$ -Silica Nanocomposites  
*Y. Ishii, K. Sato, Y. Ishikawa, and S. Kawasaki*
- 3901 Luminescence Properties of New Thioaluminato Phosphors (Ba<sub>1-x</sub>Sr<sub>x</sub>)<sub>4</sub>Al<sub>2</sub>S<sub>7</sub>:Eu  
*T. Hasegawa, H. Kato, M. Kobayashi, H. Yamane, and M. Kakihana*
- 3902 Anomalous Rare Earth Doping in Nitride and Oxynitride Phosphors  
*T. Takeda, R. Xie, N. Hirosaki, K. Kimoto, and M. Saito*

- 3903 Investigation of Ion Dependence of Electronic Structure for 3d<sup>3</sup> Ions in Mg<sub>2</sub>TiO<sub>4</sub> based on First-principles Calculations  
*M. Novita, H. Yoshida, and K. Ogasawara*
- 3904 Comparison of Simulation and Experimental Results of Crystalline Si Solar Module with YVO<sub>4</sub>:Bi<sup>3+</sup>,Eu<sup>3+</sup> Nanophosphor Spectral Shifter  
*Y. Iso, S. Takeshita, and T. Isobe*
- 3905 Simple-Structure Light-Emitting Diodes Based on a Blend of Nanocrystal Quantum Dots and ZnO  
*J. Kwak, W. Bae, and C. Lee*
- 3906 Optimizing the Synthesis of Europium Dibenzoylmethide Triethylammonium  
*K. Bhat, R. Fontenot, W. A. Hollerman, and M. Aggarwal*
- 3907 Comparison of Hydrothermal and Glycothermal Syntheses of YBO<sub>3</sub>:Ce<sup>3+</sup>,Tb<sup>3+</sup> with Green Fluorescence under Near UV Excitation  
*H. Hara, S. Takeshita, T. Isobe, T. Sawayama, and S. Niikura*
- 3908 Practical Multiplet Energy Level Diagrams for V<sup>2+</sup>, Cr<sup>3+</sup>, Mn<sup>4+</sup> in Oxides and in Fluorides  
*H. Nagoshi, H. Yoshida, and K. Ogasawara*
- 3909 The Influence of Phosphor Decay Time on the Cross-Talk in 3D-PDP  
*J. Yoo, C. Ji, G. Anoop, I. Cho, S. Lee, Y. Cho, W. Kim, and E. Park*
- 3910 Synthesis of InP Multi-Shell Structured Quantum Dot and Their Application for White LEDs  
*K. Kim and S. Jeong*
- 3911 Improved Optical Properties of InP Quantum Dot Through Transition Metal Doping  
*J. No, K. Kim, and S. Jeong*
- 3912 Synthesis and Spectroscopy of Nanoscale Y<sub>2</sub>O<sub>3</sub>:Nd<sup>3+</sup> Phosphors  
*G. Bilir, G. Ozen, J. Collins, and B. Di Bartolo*
- 3913 Preparation and Photoluminescence Property of Praseodymium doped Calcium Titanate Nanocrystals  
*Y. Hakuta, M. Ohara, M. Aoki, K. MInami, K. Sue, and H. Takashima*
- 3914 Effects of Preparing Conditions on the Luminescent Properties of Mn<sup>4+</sup> Ion Doped CaAl<sub>4</sub>O<sub>7</sub> Phosphors  
*J. Park, G. Kim, and Y. Kim*
- 3915 The Luminescent Properties of Eu<sup>2+</sup> Doped Ca<sub>2</sub>SiO<sub>4</sub> Nanopowders Synthesized by a Sol-Gel Method  
*J. Park, J. Lee, and Y. Kim*

- 3916 3D Visualization of 4-Component Relativistic Wave Functions of the Free Ce<sup>3+</sup> Ion and the Ce<sup>3+</sup> Ion in YAG  
*T. Katakami, K. Higashiura, and K. Ogasawara*
- 3917 Low Electric Field Driving Transparent Thin Films Electroluminescence Devices with Perovskite Oxides  
*H. Takashima and I. Mitsuru*
- 3918 Luminescence study of Ca<sub>3-3x/2</sub>(VO<sub>4</sub>)<sub>2</sub>:xEu (0.01≤x≤0.09) Red-Phosphors Prepared by Solution Combustion Method  
*K. Kim, S. Yoon, Y. Shin, and K. Park*
- 3919 Microstructure and Photoluminescence Properties of Sr<sub>2.91</sub>V<sub>2</sub>O<sub>8</sub>:Eu<sub>0.06</sub> Phosphors Prepared by the Solution Combustion Method  
*K. Park, S. Yoon, K. Kim, and Y. Shin*
- 3920 Electroluminescence from Cr<sup>3+</sup> in New Perovskite Thin-Film Phosphors using LaAlO<sub>3</sub> and LaGaO<sub>3</sub> as the Host  
*T. Miyata, Y. Nishi, T. Mori, and T. Minami*
- 3921 Development of Novel Electrochromic Hyperbranched Polymer for Displays  
*S. Kim, A. Tanaka, and T. Nagamura*
- 3922 Electric and Electroluminescence Properties of Ca<sub>0.6</sub>Sr<sub>0.4</sub>TiO<sub>3</sub>:Pr Thin Films Prepared by Sol-Gel Method  
*T. Kyomen, M. Hanaya, and H. Takashima*
- 3923 Optical Phonon Emission of ZnO Thin Films  
*S. Munisamy, S. Kasilingam, T. Rajalingam, and T. Masaki*
- 3924 Synthesis of Sr<sub>2</sub>Si<sub>5</sub>N<sub>8</sub>:Eu<sup>2+</sup> Red-Emitting Phosphor by Induction Heating  
*J. Choi, A. Piquette, M. Hannah, K. C. Mishra, J. B. Talbot, and J. McKittrick*
- 3925 Morphology and Particle Size Dependent Luminescence Properties of Y<sub>2</sub>O<sub>3</sub>:Eu Phosphors Prepared by Various Synthetic Methods  
*Y. Kim, J. Han, J. Talbot, and J. McKittrick*
- 3926 Optoelectronic and Persistent Luminescence Properties in Ce<sup>3+</sup>-Doped Garnet Ceramics  
*J. Ueda, K. Aishima, and S. Tanabe*
- 3927 Ce<sup>3+</sup>-Tb<sup>3+</sup> Energy Transfer in Aluminate Garnets  
*A. Setlur and J. Shiang*
- 3928 Systematic Studies of Structural and Optical Properties of Pure and Doped Pyrochlore Crystals  
*A. Srivastava and M. G. Brik*
- 3929 Experimental and Crystal Field Studies of Spectroscopic Properties of Mn<sup>2+</sup> Ions in Fluoride Crystals in UV-VUV  
*M. G. Brik, M. Kirm, M. True, and G. Zimmerer*

- 3930 Improvement of Luminescence Properties of  $\text{KSrPO}_4:\text{Eu}$  by a Polymerizable Complex Method Employing a Water Soluble Phosphorus Oligomer  
*M. Kim, M. Kobayashi, H. Kato, and M. Kakihana*
- 3931 Relationship between Emission Properties and Host Structure for  $\text{Eu}^{2+}$ -doped Phosphate Investigated by Quantitative Structure Relationship and First Principles Calculation  
*H. Takaba, R. Miura, A. Suzuki, N. Hatakeyama, and A. Miyamoto*
- 3932 Transparent Inorganic Downconverters for Luminescent Solar Concentrators  
*L. Shea-Rohwer, J. Martin, and M. Nyman*
- 3933 Spectroscopy of Pr-doped  $\text{CaTiO}_3$  Nano-particles under Excitation into the Charge Transfer State  
*J. Collins, Y. Tsehay, P. Boutinaud, G. Chadeyron, and R. Boosin*
- 3934 Development of  $\text{YVO}_4:\text{Bi}^{3+},\text{Eu}^{3+}$  Nanophosphor and Its Application as a Spectral Down-Shifter for Solar Cells  
*S. Takeshita and T. Isobe*
- 3935 Liquid Phase Synthesis and Characterization of  $\text{LaPO}_4:\text{Yb}^{3+}/\text{GdPO}_4$  Nanoparticles with NIR Emission under NIR Excitation  
*T. Isobe, T. Shimizu, K. Hara, and S. Takeshita*
- 3936 Photoluminescence of single InAsP quantum dots in InP nanowires  
*P. Poole, D. Dalacu, J. Lapointe, and K. Mnaymneh*
- 3937 Fast Luminescence in Silicon-Germanium Nanostructures  
*D. J. Lockwood, X. Wu, J. Baribeau, N. Modi, and L. Tsybeskov*
- 3938 XANES and XEOL Studies of Luminescent Silicon Carbonitride ( $\text{SiCN}$ ) Thin Films  
*Z. Khatami, P. Wilson, J. Wojcik, and P. Mascher*
- 3939 Design Rule of Ti/Al Ohmic contacts on N-face n-GaN : Solution for Thermal Degradation  
*B. Kim, Y. Song, J. Son, C. Yoo, and J. Lee*
- 3940 Colloidal Synthesis of  $(\text{CuAg})_x\text{In}_{2x}\text{Zn}_{2(1-2x)}\text{S}_2$  Solid Solution Nanocrystals with Tunable Band Gap  
*M. Dai, K. Okazaki, A. Kudo, S. Kuwabata, and T. Torimoto*
- 3941 Core/Shell structured Nanoparticles and Hybrid Electrode Materials for Electrically Tunable Photonic Crystal Display  
*H. Shim, M. Han, J. Lim, C. Heo, H. Jin, C. Shin, S. Jeon, J. Kim, J. Lee, and S. Lee*
- 3942 Enhanced Electrochemiluminescence Light-Emitting Device Driven by Application of AC Voltage and Its Emission Mechanism  
*T. Nobeshima, K. Nakamura, and N. Kobayashi*
- 3943 Efficient Materials for High Quality Light Sources: Present Status and Future Prospects  
*J. Carreras and C. Hunt*

- 3944 Highly Efficient Phosphor-Converted White Light Emitting Diode by Electrophoretic Deposition  
*J. Choi, M. Anc, A. Piquette, M. Hannah, K. C. Mishra, J. B. Talbot, and J. McKittrick*
- 3945 Nano-Pyramids Structure for Enhancement of Light Extraction Efficiency by Nanoimprint Lithography  
*C. Yoo, Y. Song, B. Kim, K. Kim, J. Son, and J. Lee*
- 3946 Highly Reliable Encapsulation Films for OLEDs Composed of SiN<sub>x</sub> and SiO<sub>x</sub>C<sub>y</sub> Prepared Using SWP-CVD  
*S. Ueno, M. Yomogida, M. Suzuki, Y. Konishi, and K. Azuma*
- 3947 Green-Color Selective Organic Photodetector with High Sensitivity for Image Sensor Application  
*K. Lee, D. Leem, K. Park, S. Lim, Y. Jin, S. Lee, K. Kim, and S. Park*
- 3948 Thermo-switchable Emission and Coloration of Composite Material Containing Luminescent Europium(III) Complex and Fluoran Dye  
*K. Nakamura, Y. Kobayashi, K. Kanazawa, and N. Kobayashi*
- 3949 Color tunable organic plasmon-emitting diodes  
*I. Lee, K. Kim, S. Kim, B. Koo, B. Lee, and J. Lee*
- 3950 Electroswitchable Emission of the Luminescent Eu(III) Complex based on Electrochemical Reaction  
*K. Kanazawa, K. Nakamura, and N. Kobayashi*
- 3951 Ultrafine Silver Nanowire Networks as Scattering Core in Organic Light Emitting Diodes  
*B. Lee, K. Kim, S. Kim, I. Lee, B. Koo, and J. Lee*
- 3952 Enhancing Light Outcoupling of Flexible Organic Light Emitting Diodes by Domain Selective-Etching  
*I. Lee, K. Kim, S. Kim, B. Koo, B. Lee, and J. Lee*
- 3953 Triboluminescent Properties of EuD<sub>4</sub>TEA and ZnS:Mn and Their Use for Smart Sensors  
*R. Fontenot, K. Bhat, W. A. Hollerman, and M. Aggarwal*
- 3954 Using Triboluminescence To Detect Ballistic and Hypervelocity Impacts  
*W. A. Hollerman and R. Fontenot*

### **J3 - Materials for Solid State Lighting**

*ECS Luminescence and Display Materials, ECS New Technology Subcommittee, ECSJ Phosphor Research*

- 3955 (Centennial Outstanding Achievement Award Presentation of the LDM Division) Toward Further Breakthroughs in Nitride Phosphors  
*H. Yamamoto*

- 3956 Spatio-Time-Resolved Cathodoluminescence Studies on Freestanding GaN Substrates Grown by Hydride Vapor Phase Epitaxy  
*S. F. Chichibu, Y. Ishikawa, K. Hazu, M. Tashiro, K. Furusawa, H. Namirta, S. Nagao, K. Fujito, and A. Uedono*
- 3957 Electrical Characterization of High-quality InGaN-based Blue Light Emitting Diodes on 8inch Silicon Grown by Metalorganic Chemical Vapor Deposition  
*J. Kim, J. Kim, Y. Tak, J. Kim, H. Hong, S. Chae, M. Yang, J. Lee, H. Choi, J. Park, Y. Park, and U. Chung*
- 3958 Simulation and Design of (In,Ga)N-Based Light Emitting Diodes  
*Z. Liang, E. Stach, T. Sands, and E. García*
- 3959 Tuning of Indium Tin Oxide Work Function with an Ionic Solid Thin Film in Polymer Light-Emitting Diodes  
*Y. Chou and T. Wen*
- 3960 First Principles Investigations of the Electronic Structures and Associated Properties of Solid Solutions of AlN and GaN  
*K. C. Mishra, P. Schmidt, and K. Johnson*
- 3961 Fabrication Semipolar GaN on Nanoscale Pattern C-sapphire by Using Self-Assembled Ni Pattern as Mask  
*C. Chen, C. Hsieh, and Y. Wu*
- 3962 Transparent Electrode for Top Emitting Organic Light Emitting Diodes by Suppression of Surface Plasmons  
*B. Koo, S. Kim, K. Hong, K. Kim, I. Lee, and J. Lee*
- 3963 Growth and Electrical Properties of n-type 4H-SiC Single Crystals  
*X. Xu, Y. Peng, S. Song, X. Chen, and X. Hu*
- 3964 Nanoco's CFQDs for Solid-State Lighting Applications  
*N. Pickett*
- 3965 Fabrication of Efficient, Stable White Light-Emitting Diodes Based on Highly Fluorescent Copper-Indium-Sulfide Quantum Dots  
*W. Song and H. Yang*
- 3966 Glass Matrices Containing Rare-Earth Ions for White Light-Emitting Diodes with High Color Rendering Indices  
*J. Heo and S. Yi*
- 3967 High Color Rendering White LED Based on Silicate/Dye-Bridged Siloxane Hybrid Phosphor Encapsulant  
*B. Bae, S. Kwak, N. Kim, and H. Im*
- 3968 Hybrid Solid-State Lighting Design  
*W. Hertog, C. Hunt, and J. Carreras*

- 3969 Synthesis, Luminescence Mechanism and Application of  $\beta$ -sialon Green Phosphor with Sharp Line-Width  
*K. Takahashi, K. Yoshimura, M. Harada, Y. Tomomura, T. Takeda, R. Xie, and N. Hirosaki*
- 3970 Synthesis and Luminescence of Eu<sup>2+</sup> Activated Yellow Oxynitride Phosphor  
*P. Nammalwar, S. Manepalli, D. Porob, Y. Gao, and A. Setlur*
- 3971 Sr-Containing Sialon Phosphors with High Quantum Efficiencies for White LEDs  
*Y. Fukuda, K. Albessard, A. Okada, T. Sato, R. Hiramatsu, and N. Matsuda*
- 3972 Bandgap Estimates and Ce<sup>3+</sup> Quenching in Cs<sub>3</sub>CoCl<sub>5</sub>-based Phosphors  
*U. Happek and A. Setlur*
- 3973 Single Phase, Highly Efficient Li(Ca<sub>0.99-x</sub>Sr<sub>x</sub>Eu<sub>0.01</sub>)PO<sub>4</sub> Blue Emitting Phosphors for Near UV-Emitting LEDs  
*J. Han, M. Hannah, A. Piquette, J. Talbot, K. C. Mishra, and J. McKittrick*
- 3974 Luminescence Quenching in Highly Doped YAG:Ce  
*A. Setlur, M. Pasricha, M. Perera, G. Levitt, and U. O. Happek*
- 3975 Enhancement of Photoluminescence Properties of Green-Emitting Oxynitride Phosphor using Eu<sub>2</sub>O<sub>3</sub>@B<sub>2</sub>O<sub>3</sub> Core-Shell for White LED Applications  
*D. Yoon*
- 3976 Silica-Overcoated Copper-Indium-Sulfide Quantum Dot-Polymer Composite Plate as a Robust Wavelength Converter of White Light-Emitting Diode  
*W. Song, E. Jang, and H. Yang*
- 3977 Tunable Green-Red- Emitting Ca<sub>14</sub>Mg<sub>2</sub>[SiO<sub>4</sub>]<sub>8</sub>:Eu<sup>2+</sup>,Mn<sup>2+</sup> Phosphor : the Structural and Optical Properties, and Their Application to Near-UV LED-based White LEDs  
*K. Lee and W. Im*
- 3978 The Formation of the Hexagonal Pyramid Facets on Wet Etching Patterned Sapphire Substrate  
*Y. Chen, F. Hsiao, and Y. Wu*
- 3979 High Brightness III - V Light-Emitting Diodes on Diamond/Silicon Composite Substrate  
*T. Chang, J. Hu, Y. Wu, and B. Lin*
- 3980 Organic Light-Emitting Diodes with Contact-Printed Red Emissive Layer  
*S. Peng, J. Jou, S. Chen, and P. Wu*
- 3981 Color Tuning of Red-Emission Eu<sub>1-x</sub>Ba<sub>x</sub>Si<sub>2</sub>O<sub>2</sub>N<sub>2</sub> Phosphors for White-Light-Emitting Diode  
*K. Park, K. Seo, J. Kim, T. Kim, and G. Kim*
- 3982 Blue Excitability of Yellow Zn<sub>1-x</sub>Mn<sub>x</sub>S Phosphor and It's LED Application  
*K. Park, K. Seo, H. Lim, J. Kim, T. Kim, and G. Kim*

- 3983 Green CaSc<sub>2</sub>O<sub>4</sub>: Ce<sup>3+</sup> Phosphor for White-Light-Emitting Diode  
*K. Park, K. Seo, S. Lim, H. Lim, J. Lim, J. Kim, L. Jiang, J. Kim, T. Kim, and G. Kim*
- 3984 Luminescence Properties and Stability Improvement by SiO<sub>2</sub> Coating on Various Phosphors for Near UV-Emitting LEDs  
*J. Han, M. Hannah, A. Piquette, J. Talbot, K. C. Mishra, and J. McKittrick*

**J4 - Microfabricated and Nanofabricated Systems for MEMS/NEMS 10**

*ECS Sensor, ECS Dielectric Science and Technology, ECS Electronics and Photonics, ECS Physical and Analytical Electrochemistry, ECSJ Bioengineering, CSE*

- 3985 Micro-systems and Nanotechnologies in ELISA and Droplet Generation Applications  
*C. Yeh and Y. Lin*
- 3986 A Novel Microdevice for the Treatment of Hydrocephalus  
*J. Oh, F. Kralick, and H. Noh*
- 3987 Wafer Scale Processing of Plasmonic Nanopore Arrays in 200mm CMOS Fab Environment  
*K. Malachowski, R. Verbeeck, T. Dupont, C. Chen, S. Musa, Y. Li, T. Stakenborg, D. Sabuncuoglu Tezcan, and P. Van Dorpe*
- 3988 Tunable Young's Modulus in Carbon MEMS using Graphene-based Stiffeners  
*C. M. Washburn, T. Lambert, J. Blecke, D. Davis, P. S. Finnegan, B. G. Hance, and J. M. Strong*
- 3989 Residue-Free Dry Etching of Polymer Sacrificial Layer for Microelectromechanical-System Device Fabrication  
*K. Takagahara, K. Ono, K. Kuwabara, T. Sakata, H. Ishii, Y. Sato, and Y. Jin*
- 3990 Low Cost UV Laser Direct Write Photolithography System for Rapid Prototyping of Microsystems  
*J. Waynelovich, A. Sepehri, B. Mehta, S. Kassegne, and A. Khosla*
- 3991 The Carbonized SU-8 Electrospun Nano-Fiber for an Electrode in the Energy Storage Device  
*H. Kim, J. Woo, Y. Joo, Y. Chun, and C. Kim*
- 3992 Hydrodynamic Cell Enrichment in Double Spiral Microfluidic Channels  
*J. Sun, M. Li, C. Liu, G. Hu, and X. Jiang*
- 3993 Nanostructured Columnar Thin Films for Biological and Chemical Sensing Applications  
*P. Shah, H. Knachel, A. Sarangan, and K. Hansen*
- 3994 Thermal Conductivity Engineering via Nano Patterning  
*B. Kim, I. El-Kady, and R. H. Olsson III*

- 3995 Photothermal Cantilever Deflection Spectroscopy  
*T. Thundat, M. Bagheri, S. Kim, D. Lee, and S. Jeon*
- 3996 Development of Insulated Conductive AFM Probes for Molecular Electronics  
*Y. Wu, T. Akiyama, P. D. van der Wal, S. Gautsch, and N. de Rooij*
- 3997 All Thin Film Micromachined Cantilever Using PZT/Terfenol-D Multilayer for High Sensitive Magnetoelectric Sensors  
*D. Lee, S. Kim, Y. Yoo, J. Han, W. Jo, and J. Lee*
- 3998 Characterization and Response of Metal Organic Frameworks Based Microcantilever Sensors for the Detection of Volatile Organic Compounds  
*I. Ellern*
- 3999 Manipulation of Micro Condensed Matter by Direct Peeling Method by using Atomic Force Microscope Tip  
*A. Kawai*
- 4000 A MEMS-based Platform for Multi-physics Characterization of Ultra-thin Freestanding Films  
*M. Haque*
- 4001 Effects of Adsorbate Surface Diffusion in Focused Electron-Beam-Induced-Deposition  
*A. Szkudlarek, M. Gabureac, and I. Utke*
- 4002 Electroplating of Microstructured Nickel Phase Gratings for X-Ray Phase Contrast Tomography  
*M. Amberger, K. Bade, J. Meiser, D. Kunka, and J. Mohr*
- 4003 The Defect and Transport Properties of TlBr  
*S. R. Bishop, G. Ciampi, M. Kuhn, H. L. Tuller, W. Higgins, and K. Shah*
- 4004 Microfabricated Systems to Measure Marine Variables  
*S. Aravamudhan*
- 4005 Nanoporous Alumina as a Platform for 3-D Ceramic Microdevices  
*D. Routkevitch*
- 4006 Radiophotoluminescence in Ag<sup>+</sup>-Doped Phosphate Glass Dosimeter  
*T. Ohno, Y. Miyamoto, T. Kurobori, Y. Takei, K. Hirasawa, T. Yamamoto, and H. Nanto*
- 4007 Characterization and Process Optimization of UV Patternable Electrically Conducting SU-8 Silver Nanocomposite Polymer  
*A. Khatri, S. Kassegne, and A. Khosla*
- 4008 Effects of Added Uranium on the Triboluminescent Properties of EuD<sub>4</sub>TEA  
*R. Fontenot, W. Hollerman, K. Bhat, and M. Aggarwal*

- 4009 Micropatternable, Electrically Conducting Polyaniline Photoresist Blends for MEMS Applications  
*C. V. Patel, S. Kassegne, and A. Khosla*
- 4010 Micro-Structures for Electrophoretic Display: Case Studies of the Response Speed/Time and Contrast Ratio Depending on Micro-Structures  
*J. Kim, C. Kim, and K. Suh*